AN AUTOMATIC WEARABLE MULTI-SENSOR BASED GAIT ANALYSIS SYSTEM FOR OLDER ADULTS

Arif Reza Anwary

FACULTY OF SCIENCE AND TECHNOLOGY

BOURNEMOUTH UNIVERSITY

AN AUTOMATIC WEARABLE MULTI-SENSOR BASED GAIT ANALYSIS SYSTEM FOR OLDER ADULTS

By

Arif Reza Anwary

A thesis submitted in partial fulfilment of the requirements of Bournemouth University for the degree of Doctor of Philosophy

October 2018

Abstract

Gait abnormalities in older adults are very common in clinical practice. They lead to serious adverse consequences such as falls and injury resulting in increased care cost. There is therefore a national imperative to address this challenge. Currently gait assessment is done using standardized clinical tools dependent on subjective evaluation. More objective gold standard methods (motion capture systems such as Qualisys and Vicon) to analyse gait rely on access to expensive complex equipment based in gait laboratories. These are not widely available for several reasons including a scarcity of equipment, need for technical staff, need for patients to attend in person, complicated time consuming procedures and overall expense. To broaden the use of accurate quantitative gait monitoring and assessment, the major goal of this thesis is to develop an affordable automatic gait analysis system that will provide comprehensive gait information and allow use in clinic or at home. It will also be able to quantify and visualize gait parameters, identify gait variables and changes, monitor abnormal gait patterns of older people in order to reduce the potential for falling and support falls risk management. A research program based on conducting experiments on volunteers is developed in collaboration with other researchers in Bournemouth University, The Royal Bournemouth Hospital and care homes. This thesis consists of five different studies toward addressing our major goal. Firstly, a study on the effects on sensor output from an Inertial Measurement Unit (IMU) attached to different anatomical foot locations. Placing an IMU over the bony prominence of the first cuboid bone is the best place as it delivers the most accurate data. Secondly, an automatic gait feature extraction method for analysing spatiotemporal gait features which shows that it is possible to extract gait features automatically outside of a gait laboratory. Thirdly, user friendly and easy to interpret visualization approaches are proposed to demonstrate real time spatiotemporal gait information. Four proposed approaches have the potential of helping professionals detect and interpret gait asymmetry. Fourthly, a validation study of spatiotemporal IMU extracted features compared with gold standard Motion Capture System and Treadmill measurements in young and older adults is conducted. The results obtained from three experimental conditions demonstrate that our IMU gait extracted features are highly valid for spatiotemporal gait variables in young and older adults. In the last study, an evaluation system using Procrustes and Euclidean distance matrix analysis is proposed to provide a comprehensive interpretation of shape and form differences between individual gaits. The results show that older gaits are distinguishable from young gaits. A pictorial and numerical system is proposed which indicates whether the assessed gait is normal or abnormal depending on their total feature values. This offers several advantages: 1) it is user friendly and is easy to set up and implement; 2) it does not require complex equipment with segmentation of body parts; 3) it is relatively inexpensive and therefore increases its affordability decreasing health inequality; and 4) its versatility increases its usability at home supporting inclusivity of patients who are home bound. A digital transformation strategy framework is proposed where stakeholders such as patients, health care professionals and industry partners can collaborate through development of new technologies, value creation, structural change, affordability and sustainability to improve the diagnosis and treatment of gait abnormalities.

Contents

Acknowledgement

This thesis would have not been possible without the help and generous support from the kind people around me. I would like to express my gratitude to my principal supervisor, Professor Hongnian Yu. His guidance helped me in all the time of research and writing publications. I again thank him for his tremendous support for academic activities and encouraging my research and for allowing me to grow as a researcher. I would like to thank my supervisor, Dr. Damien Fay for his support and guidance provided during his stay at Bournemouth University. I owe my deepest gratitude to my supervisor, Professor Michael Vassallo for his insightful comments and encouragement, and also for his involvement of my PhD which incented me to widen my research from various perspectives. I would like to thank him drive to success which has motivated me to work hard and aim high. I would like to express my sincere gratitude to my supervisor, Dr. Simant Prakoonwit for his constructive comments and warm encouragement.

My special thanks to Dr. Andrew Callaway (Senior Academic - Sports Performance, Analysis, Dept. of Sport and Physical Activity, BU) for helping me to collect validation study data from Qualisis and Treadmill. Many thanks to the academic staffs Naomi Bailey, Natalie Andrade, Malcolm Green and Karin Ermert for their cooperation and support during my PhD.

I am indebted to all the participants who are involved in this research, without them my work would not have been possible. I would particularly like to thank Doctor Mr Aman, the representatives of Probin Hitoishi Shangha Sher-E-Bangla Nagar, Bangladesh for their support in the participant recruitment and data collection process. Special thanks to Pasha for helping me with long term data collection.

I would like to thank my all friends for their support during my PhD specially Akanda Wahid-ul Ashraf Nuppu, Dr. Sajjad Akbar, Dr. Soumya Kanti Manna, Dr. Ikram Asghar, Dr. Aslam Abdelkader, Dr. Saad Mohamad, Dr. Aboraid Algashami and Dr. Haseeb Ahmad Qureshi.

In conclusion, I recognize that this research would not have been possible without the financial assistance by European Commission funding (ERASMUS MUNDUS FUSION project) and Bournemouth University.

“*It is He who created you from dust, then from a sperm-drop, then from a clinging clot; then He brings you out as a child; then [He develops you] that you reach your [time of] maturity, then [further] that you become elders. And among you is he who is taken in death before [that], so that you reach a specified term; and perhaps you will use reason.*” Surah Ghafir [40:67]

Publications Resulted from This Thesis

1. Arif Reza Anwary, Yu H, Vassallo M, **"Optimal foot location for placing wearable IMU sensors and automatic feature extraction for gait analysis"**, IEEE Sensors Journal, vol. 18, no. 6, pp. 2555-2567, 2018
2. Arif Reza Anwary, Yu H, Vassallo M, **"Automatic gait feature extraction method for identifying gait asymmetry using wearable sensors"**, SENSORS, vol. 18, no. 2, p. 676, 2018
3. Arif Reza Anwary, Yu H, Vassallo M, **"Wearable sensor based gait asymmetry visualization"**, The 24th Americas Conference On Information Systems, AMCIS 2018
4. Arif Reza Anwary, Yu H, Vassallo M, **"Digital Transformation Strategy Framework for Gait Analysis"**, Connected Everything 2018 Conference
5. Arif Reza Anwary, Yu H, Vassallo M, **"Gait Evaluation using Procrustes and Euclidean Distance Matrix Analysis"**, IEEE Journal of Biomedical and Health Informatics, 2018
6. Arif Reza Anwary, Yu H, Callaway A, Vassallo M, **"Validity of an automatic spatiotemporal gait features extraction system using wearable IMUs"**, (Under Review)
7. Arif Reza Anwary, Yu H, Vassallo M, **"Digital Transformation Strategy Framework with a Pilot Study for Gait Analysis"**, (Under Review)

Nomenclature

B_i	Wishart distribution independent of nuisance parameters
$B(X)$	centered inner product matrix
c_i	uniform scaling
D	number of dimensions
E	sum of squares of residuals
E_i	error matrix with Gaussian distribution
$Eu(x)$	matrix of squared distances
$F(X)$	Euclidean distances between all landmarks
G_i	centroid matrix
H	centering matrix
j	unit vector
k	number of dimensions
K	number of landmarks
L	number of pair-wise distances of upper or lower triangle from diagonal
m	number of configurations
M	mean form
O_i	rotation matrix
p	number of landmarks chosen from each configuration
P	number of clusters
R_s	residual sum of squares
S_r	diagonal matrix contains singular values from singular value decomposition
t_i	translation vector
T	transpose of a matrix
$tr(A)$	trace operation of matrix A
$T(\cdot)$	maximal invariant under S space with the group rotation, translation and scaling of configuration

U_r	left singular vector where $U_r^T U_r = I_{r\times r}$ from singular value decomposition
V_r	right singular vector, U_r and V_r are orthogonal where $V_r^T V_r = I_{r\times r}$ from singular value decomposition
X_i	configuration containing landmark information
$\hat{X}_i$	transformations of scaling, rotation and translation
X^c	mean centered of *X*
X^*	rotation, translation of *X*
Y	consensus configuration or the new coordinates of the centroid of the group
Δ	residual, the length of *mp*
δ	Kronecker matrix
Λ	symmetric matrix
λ_{uv}	Lagrange multiplier
μ	population average configuration
$\otimes$	Kronecker product
Σ_K	variance and covariance of landmarks
Σ_D	variance and covariance of the perturbation with respect to the real space coordinate axes
Γ_i	rotation matrix
δ_{lm}	pair-wise Euclidean distance
e_{lm}	squared Euclidean distance between pairs of landmarks
ϕ_{lm}	scaling parameter
σ_{lm}	variance-covariance between pair of landmarks
λ_i	Eigenvalues

Abbreviation

4SST	Four Square Step Test
A	Asymmetry
ANN	Artificial Neural Network
ANOVA	Analysis Based Variance
BBS	Berg Balance Scale
CI	Confidence Interval
CTSIB	Clinical Test Of Sensory Interaction And Balance
DGI	Dynamic Gait Index
EDMA	Euclidean Distance Matrix Analysis
ELGAM	Extra-Laboratory Gait Assessment Method
EMG	Electromyography
Erz	Vertical Energy Ratio
F8W	Figure Of 8 Walk Test
FFT	Fourier Transform
FGA	Functional Gait Assessment
FM	Form Matrix
FMD	Form Difference Matrix
FSR	Force-Sensitive Resistor
GA	Gait Asymmetry
GARS	Gait Abnormality Rating Scale
GMM	Gaussian Mixture Models
GMWT	Groningen Meander Walking Test
Ia	Ratio
ICA	Independent Component Analysis
ICC	Interclass Correlations
ICT	Information And Communications Technology
IMU	Inertial Measurement Unit
ISN	Inertial Navigation System
KSI	Kinematic Symmetry Index
LCC	Lin’s Concordance Correlation
LCEA	Latency Corrected Ensemble Average
LDA	Linear Discriminate Analysis

MSC	Motion Capture System
NMGF	Normal Mean Gait Form
NMGS	Normal Mean Gait Shape
PCA	Principle Component Analysis
PDR	Pedestrian Dead-Reckoning
PIR	Passive Infrared
POMA	Tinetti Performance Oriented Mobility Assessment
PSD	Power Spectral Density
PSSD	Procrustes Size-And-Shape Distance
RAI	Relative Asymmetry Index
RMSD	Root Mean Square Deviation
RSD	Riemannian Shape Distance
RSSD	Riemannian Size-And-Shape Distance
SA	Symmetry Angle
SD	Standard Deviation
SG	Savitzky-Golay
SI	Symmetry Index
SMA	Signal Magnitude Area
SR	Symmetry Ratio
SVM	Support Vector Machines
T25-FW	Timed 25-Foot Walk
TA	Trend Asymmetry
TA	Trend Symmetry
TU&GT	Timed "Up And Go" Test
WEKA	Waikato Environment For Knowledge Analysis
WHO	World Health Organization
ZUPT	Zero-Velocity Update

1. INTRODUCTION

This chapter presents my PhD research project, its area, an overview of the research. It includes a short literature review around the subject in the background and motivation, the worldwide socio-economic impact of gait and balance disorder, the challenges of gait analysis, the necessity of this research, the aim and objective, the contribution and the structure of this thesis.

1.1. Background and motivation

According to the Oxford English Dictionary, gait is defined as "A person's manner of walking". Everyone walks with a distinctive gait and this assumption may assist in identifying someone. The first evidence of identifying someone using gait analysis is conducted in the UK in 2000 where a criminal proceedings in a case of armed robbery, R v. Saunders, heard at The Old Bailey Central Criminal Court in London (Kelly 2000). The evidence included closed-circuit television images which showed the defendant's alleged bow-legged gait. Although, there is limited scientific research to assist a court in deciding whether such evidence is sufficiently reliable and/or of high enough quality to be admitted, the aim of this research is to explore and present the latest scientific research in gait analysis and provide guidance upon how gait analysis can serve as a tool in diagnosing gait abnormalities in individuals and opens the possibilities for home based self-gait assessment.

Human gait is the systematic study of the way, the manor, the style of walking and the ability to maintain balance in an upright posture. It can also be described as an interplay between the two lower limbs, one in touch with the ground, producing sequential restraint and propulsion, while the other swings freely and carries with it the forward momentum of the body (Lovejoy 1988). It relies on complex mechanisms depending upon the closely integrated actions of the musculoskeletal, nervous system (central and peripheral), visual, vestibular, auditory systems leading to the smooth propulsive pattern of movements. Most healthy individuals accomplish walking in a similar manner between the ages of 4 and 8 years because everyone has the same basic anatomic and physiologic makeup (Lovejoy 1988). Gait patterns are highly repeatable both within a subject and between subjects, but clearly each person has a unique walking style. Efficiency of walking depends on mobility of the joints, activity of the muscles, coordination and rhythm of the movements as well as the ability to smoothly move the center of gravity. This rhythmic locomotion is a series of rhythmic alternating movement of arms, legs, and trunk which create forward movement of the body (Murray 1967). The components of gait and balance are

fundamental to physical function. Together, normal gait and balance enable ambulation, also known as mobility which is the primary mode of personal transport.

Gait analysis started in the 19th century (Muro-de-la-Herran et al. 2014), it is a wide area, a search on the Web of Knowledge for scientific articles that include "gait analysis" in the title shows 22,988 in 2018 and it means different things to different domains. The gait analysis title is not protected, hence there is no formal definition of who is, or is not, permitted to do so. Thus, different professional, medical, academic and research groups have focused on different aspects of gait analysis and have therefore attracted the interest of researchers in different disciplines such as clinical gait analysis, biometric gait analysis, forensic gait analysis and running gait analysis etc. This research will be centred and focused to clinical applications on achieving quantitative objective measurements of the different parameters that characterise of gait in order to apply them to various fields such as clinics (Kirtley 2006; Muro-de-la-Herran et al. 2014; Wagner et al. 2018), sports (Lapham and Bartlett 1995; Lees 2002) and rehabilitation (Baker 2006; Patel et al. 2012). It will provide quantitative measurement of locomotion, assessment of human walking and a wide range of spatiotemporal gait information including step, stride, stance, swing, speed, cadence and other information.

Every individual's gait pattern is assumed to be symmetrical where each leg performs identical locomotion. Interestingly every individual has a unique gait pattern and the limb movement of one side is not exactly repeated by the other side. This leads to the difference in the bilateral behaviour of the legs during walking where high differences indicate gait abnormality. Gait analysis provides bilateral locomotive information of gait parameters (e.g., length and period of stride, step, stance and swing), kinematic and kinetic measurements (e.g., angular joint trajectories, angular joint velocities, joint forces, reaction forces), muscular measurements (e.g., muscle contraction, muscle force) and energy expenditure (e.g., oxygen consumption, heart rate) (van der Linde et al. 2004; Muro-de-la-Herran et al. 2014). This has been employed in different domains such health, sports and rehabilitation. Gait changes can be a determinant of recovery in patients with Parkinson's disease (Plotnik et al. 2005), cerebrovascular accidents (Wall and Turnbull 1986), amputees (Skinner and Effeney 1985; Geurts et al. 1992), stroke (Chen et al. 2005; Hodt-Billington et al. 2008; Patterson et al. 2008; How et al. 2013; Lewek et al. 2014), osteoarthritis (Shakoor et al. 2003; Kutilek et al. 2014), spinal deformity (Park et al. 2016), fractures (Larsen et al. 2017), limb-length inequality (Kaufman et al. 1996) and cerebral palsy (Böhm and Döderlein 2012). It can be used to monitor and improve an athlete's performance (Wahab and Bakar 2011) as well as a patient's progress in orthopedics and rehabilitation

(Steultjens et al. 2000). In biometrics and biomedical engineering areas, gait analysis has been used as an assistive tool to characterize human locomotion and has many applications (Bora et al. 2015b). Gait analysis is important in elderly patient fall risk assessment (Hausdorff et al. 2001; Yogev et al. 2007). It is also a predictor of functional and cognitive decline (Plotnik et al. 2011).

Gait change is an indicator of different diseases and disease progression. It results in reduced gait efficiency and activity levels. Therefore, objective assessment of gait is important in the treatment and rehabilitation of patients with various conditions such as falls or orthopaedic surgery. In order to broaden the use of accurate quantitative gait monitoring in clinical application and research and to understand the gait and balance disorder deeply, an affordable automatic gait analysis system is required which can provide comprehensive gait information and allow to use in clinic or at home. It will also allow to identify gait variables and changes, monitor gait and abnormal gait patterns of older people in order to reduce the potential for falling, supporting the future development of a falls risk management system that will aim to improve their quality of life. To achieve this, the main aim of this thesis is to design and develop an automatic affordable lower limb gait analysis system that will provide comprehensive gait information and allow use in clinic or at home for older adults. It will be a portable wireless wearable multi-sensor based personalized gait monitoring system to analyse gait in real-time, monitor gait asymmetry, establish normal range of gait for young and older adults and assess of fall risk in order adults to reduce the potential risk associated with elderly fall. A research programme conducting experiments on volunteers, collaborated with other researchers in Bournemouth University, Bournemouth hospital and care homes are conducted. This system significantly simplifies the monitoring protocols and opens possibilities for home based assessment and supports digital transformation strategies through the development of new technology. This thesis also aims to emphasize how methodological and clinical perspectives that demands related to objective measurements and clinical applicability may be united. In order to achieve the proposed aims, the scope of our research is listed as follows.

- Generally, wearable sensor is placed at different body locations for gait analysis. The foot is the most important part of the body to balance body weight, transmit body weight to the ground and balance posture. It is also responsible for performing locomotion. Thus, investigation on foot movement will provide an initial indication of gait/balance disorder leading to a fall. As the foot is flexible, placing wearable sensor e.g. IMU on different foot locations gives different outputs. The orientation of placing the IMU sensor also

affects sensor output. In order to obtain accurate and reliable data and reduce the sensor variability, an investigation on finding the optimal foot location for placing IMU sensor is essential.

- The research aims to develop a comprehensive lower limb automatic gait features extraction method. Such analysis based on low cost technology to date is not available commercially. Currently available motion capture systems (Qualisys, MotionAnalysis, Vicon, and Shimmer etc) are expensive and require controlled environmental conditions. Gait is generally assessed and reported by physicians, physiotherapists and researchers in clinical settings or in gait laboratories. These are mostly based on visual observation where gait symmetry is frequently reported as present or not. Such reports may not satisfy scientific criteria of reliability and validity. A more objective way of gait assessment tool with low cost solution is required which will automatically extract gait features.
- Visualization of gait information is a common objective in different domains including clinics, sports and research laboratories. The most common approaches for quantification of gait asymmetry provide discrete number in calculation of the symmetry index (SI), symmetry ratio (SR), symmetry angle (SA), trend asymmetry (TA) and other approaches. A real time graphical visualization technique is also required.
- Different gait assessment tools such as the Gait Abnormality Rating Scale (Brach and VanSwearingen 2002), Figure of 8 Walk Test (Hess et al. 2010), Four Square Step Test (Duncan and Earhart 2013), The Functional Gait Assessment (FGA) (Wrisley and Kumar 2010), Groningen Meander Walking Test (Bossers et al. 2014) and Berg Balance Scale (Berg et al. 1992) are used to observe the quality of a patient's gait and balance. The disadvantage of these methods is that they are subjective measurements with a high chance of intra and inter observer variation and human error. This may affect the accuracy of diagnosis, follow-up and treatment of the pathologies (Muro-de-la-Herran et al. 2014). Therefore, a more objective way of automatic gait assessment is required.
- Gait evaluation is also important in the treatment and rehabilitation of patients with different diseases. With an aging population and the increase in chronic illness such as poor mobility and falls there is an increasing drive for new technologies to support treatment of patients at their own home. Longitudinal home based gait assessment system is therefore required to monitor gait abnormalities across a spectrum of diseases. A series of gait feature measurements on a regular basis can identify the progression or recession of changes in gait pattern as well as response to treatment with rehabilitation for these

types of diseases and more. Growing young adults particularly if they have physical disabilities may develop gait abnormalities during puberty growth spurts. Periodic monitoring is becoming essential to make sure that such gait abnormalities are not progressing. Therefore, we will propose an automatic gait evaluation that can be used for such longitudinal monitoring for these cases.

- Gait analysis is a multi-disciplinary research work has diverse research scope.

1.2. Human gait mechanics

Human walking requires significant motor coordination and most people can perform such a complicated task without even thinking about it. Humans are the only animals who characteristically walk upright (Lovejoy 1988). The mechanics of human walking can be described and characterized in the context of a gait cycle. A gait cycle is defined as a sequence of events between two sequential contacts by the same limb which can also be called as a stride. Left and right strides are equal in normal ambulation, but this might not be the case in older adults with gait abnormalities. A stride is the equivalent of a gait cycle made-up of two phases: stance phase and swing phase. The stance phase, which constitutes approximately 60 percent of the normal gait cycle, is the interval in which the foot of the reference extremity is in contact with the ground (Michael and Whittle 2002). This stance phase is comprised of five gait events (initial contact, loading response, mid stance, terminal stance, pre-swing). The swing phase, which makes up the remaining 40 percent of the gait cycle, is the interval in which the reference extremity does not contact the ground (Michael and Whittle 2002). This swing phase is comprised of three gait events (initial swing, mid-swing and terminal swing). Each gait phase and phase events has a functional objective and a critical pattern of selective synergistic motion to accomplish its goal. Stance and swing phases of a gait cycle as described by (Caldas et al. 2017) consist of a total of eight relevant gait events shown in Figure 1.1.

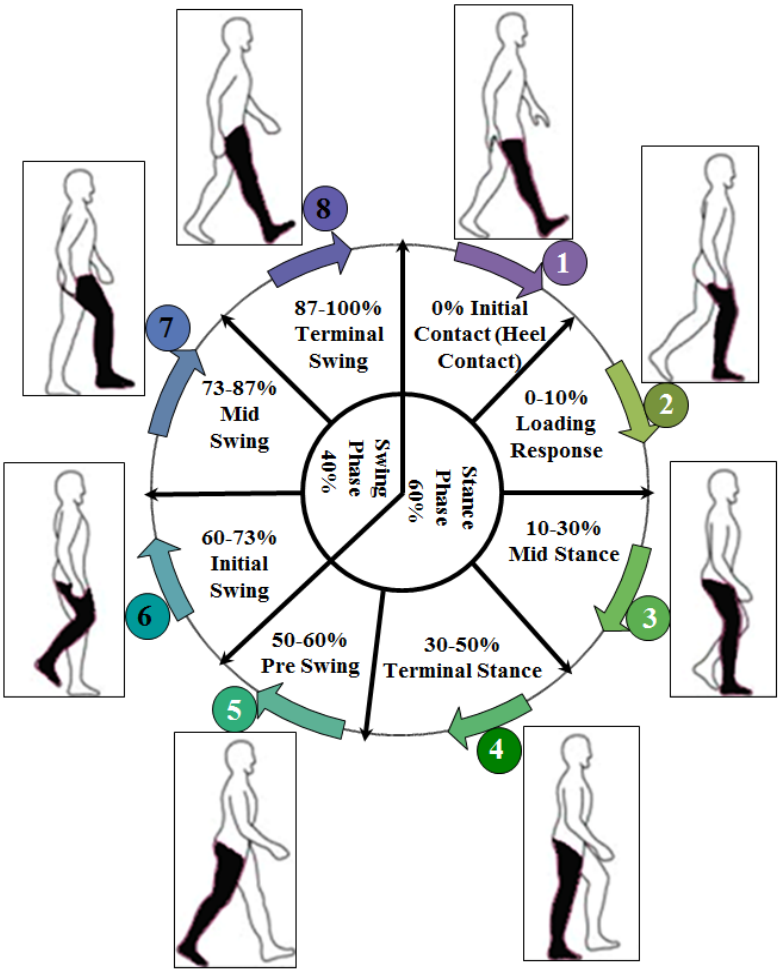

Figure 1.1: Normal human gait phases

There are five gait events of the stance phase. The first event is the initial contact (0%) which starts when the heel contacts the ground and the waist is in its lowest position during the entire step. This marks the beginning of the loading response (0% to 10%) equal to the first period of the stance phase. Toe off with the opposite foot is the end of the double support period known as loading response and the beginning of mid-stance (10% to 30%). There is deceleration of the leg towards the horizontal axis as the velocity moves to zero. Mid-stance is the period of the gait cycle between toe off and heel rise. The time at which the heel begins to lift from the walking surface (heel rise) marks the transition from mid-stance to terminal stance (30% to 50%). The zero velocity remains until the terminal stance phase where the foot is flat on the ground. The next phase is pre-swing (50% to 60%) where the toe is off the ground and starts forward movement demonstrating initial acceleration towards horizontal axis. Toe off (terminal contact) generally occurs at about 60% of the gait cycle separating pre-swing from initial swing (60% to 73%), indicating the point when the stance phase (foot is on the ground) ends and the swing

phase (foot is in the air) begins. The swing phase is when the heel moves off the ground. The time when the swinging leg passes the stance phase leg and the two feet are side by side is called feed adjacent, separating initial swing from mid-swing (73% to 87%). The acceleration interval corresponds to the change from the heel lift to the swing at the height point at mid-swing phase. When the tibia of the swinging leg becomes vertical at about 86% of the gait cycle, the terminal swing (87% to 100%) begins. Deceleration starts during the terminal swing phase from the highest point to the foot back flat on the ground. The gait cycle ends at the next initial contact of the same foot (also known as terminal foot contact). There is zero velocity again in the interval corresponding to the change from a flat foot to a heel lift. A step period is the time measured from an event in one foot to the subsequent occurrence of the same event in the other foot (Michael Whittle 2002). Therefore, a stride or gait cycle consists of two steps. The step period is useful for identifying and measuring asymmetry between the two sides of the body in pathologic conditions. Step length is the distance between one foot in the direction of progression during another step. Cadence refers to the number of steps in a period of time (commonly expressed as steps per minute). The step length, step time, and cadence are fairly symmetric for both legs in normal individuals. These are all useful parameters for conducting gait assessment and the change in these parameters are an indicator of different diseases and disease progression that results in reduced gait efficiency and activity levels for older adults.

1.3. Gait and balance changes in older adults

The ability to walk normally depends on several biomechanical components, including free mobility of joints, particularly in the legs, appropriate timing of muscle action, appropriate intensity of muscle action and normal sensory input, including vision, proprioception and vestibular system. Physical changes associated with aging directly affect an older adult's ability to maintain postural stability and normal gait mechanics (Kang and Dingwell 2008). Aging can lead to several physical changes that affect these basic processes: 1) stiffening of connective tissue; 2) decreased muscle strength; 3) prolonged reaction times; 4) decreased visual acuity; 5) impaired vibratory and proprioceptive sensation, and 6) increased postural sway (Trueblood and Rubenstein 1991). Gait problems can stem from simple age-related changes in gait and balance as well as from specific dysfunctions of the nervous, muscular, skeletal, circulatory and respiratory systems; or from simple deconditioning following a period of inactivity. For older people, muscle strength plus effective motor control to coordinate sensory input and muscle contraction become

weak that results in different kinds of gait disorders and gait pattern changes over the period of time due to natural aging process shown in Figure 1.2.

Figure 1.2: Changes of human gait and balance over time (Captured from OpenSimulator)

This gait disorders encompass a number of issues, including slowing of gait speed and loss of smoothness, symmetry, or synchrony of body movement etc. For living independently, older people need to walk, stand from bed, chair, turn, lean and perform other activities. The common characteristics of gait with aging include an increased stance width, increased time spent in the double support phase (i.e., with both feet on the ground), bent posture, and less vigorous force development at the moment of push off. These changes may represent adaptations to alterations in sensory or motor systems to produce a safer and more stable gait pattern (Salzman 2010). The gait and balance of older people normally changes not only with age but also includes involvement of multiple contributing factors like arthritis, orthostatic hypotension and weak medical condition etc (Salzman 2010). Based on the comprehensive literature study, the medical conditions which may result the change in gait and balance disorder in older adults are presented in Table 1.1.

Table 1.1: Medical conditions that cause gait and balance disorders in older adults (Tinetti et al. 1986; Cunha 1998; Salzman 2010; Bridenbaugh and Kressig 2011; Chen et al. 2016)

Cardiovascular Conditions
Orthostatic Hypotension, Vertebrobasilar Insufficiency, Intermittent Claudiction, Chronic LE Edema, Arrhythmias, Congestive Heart Failure, Coronary Artery Disease, Orthostatic Hypotension, Peripheral Arterial Disease, Thromboembolic Disease
Neurological Conditions
Parkinson's Disease, Stroke, Etat Lacunaire, Peripheral Neuropathy, Dementia, Chronic Subdural Hematoma, Normal Pressure Hydrocephalus, Cerbellar Ataxia, Posterior Column Degeneration, Cervical Spondylosis, Vitamin B_{12} Myelopathy Deficiency, Frontal Lobe Syndrome, Encephalopathy, Progressive Supranuclear Palsy, Peripheral Neuropathy, Spinal Cord Lesions, Cerebellar Dysfunction Or Degeneration, Delirium, Multiple Sclerosis, Myelopathy, Normal-Pressure Hydrocephalus, Vertebrobasilar Insufficiency, Vestibular Disorders
Musculoskeletal Conditions
Osteoarthritis, Osteoarthrosis, Osteomalacia, Status Post-Ortho Surgery, Foot Problems, Unsuspected Fractures, Cervical Spondylosis, Gout, Lumbar Spinal Stenosis, Muscle Weakness Or Atrophy, Podiatric Conditions
Psychological Conditions
Depression, Fear Of Falling, Sleep Disorders, Substance Abuse
Endocrinological Conditions
Hypothyroidism
Sensory abnormalities
Hearing Impairment, Peripheral Neuropathy, Visual Impairment
Other Conditions
General Weakness, Drug Intoxication/Overdose, Benzodiazepines, Tricyclic Antidepressants, Anticonvulsants, Salicylates, Antivertigo Agents, Senile Gait, Idiopathic Gait Disorders, Other Acute Medical Illnesses, Recent Hospitalization, Recent Surgery, Use Of Certain Medications (i.e., antiarrhythmics, diuretics, digoxin, narcotics, anticonvulsants, psychotropics, and antidepressants; especially four or more)

1.4. Falls in older adults due to gait and balance disorder

Human gait is a cyclical activity and the basic assumption is that one step is essentially the same as the next step. Normal human gait pattern is described as a succession of repetitive events where one complete gait cycle is the period between two consecutive gait events and contains both a stance phase and a swing phase. Normal human walking speed known as gait velocity remains stable until about age 70. It then declines about 15% per decade for usual gait and 20% per decade for fast walking. Gait velocity is a powerful predictor of mortality—as powerful as an older person's number of chronic medical conditions and hospitalizations. At age 75, slow walkers die ≥ 6 year earlier than normal velocity walkers and ≥ 10 years earlier than fast velocity walkers (Wolfson 2001). Gait velocity slows because older people take shorter steps at the same rate termed as cadence. The most likely reason for shortened step length which is the distance from one heel strike to the next is weakness of the calf muscles, which propel the body forward and calf muscle strength is substantially decreased in older people. However, older people seem to compensate for decreased lower calf power by using their hip flexor and extensor muscles more than young adults (Judge 2016). Although the causes of falls in older adults are associated with multiple contributing factors, gait and balance disorders are the second major cause of these falls (Hausdorff and Alexander 2005). Therefore, physicians caring for older patients recommend or examine gait assessment at least once annually to understand the contributing factors and targeted interventions for the management of fall risk. For older adults who report a fall, physicians conduct gait assessment and observe for any gait or balance dysfunctions. Early identification of gait and balance disorders and appropriate intervention may prevent dysfunction and loss of independence (Whitney et al. 2012). A clear understanding of insight into effect of aging on gait and balance is important for therapeutic planning, management, clinical decision making and rehabilitation. The worldwide scenario of these users and care cost is described in the next section.

1.5. Worldwide socio-economic impact of gait and balance disorder

Gait and balance disorders are multifactorial problem associated with intrinsic mental or physical health, environment and aging problem etc. There may be other independent reasons for gait and balance disorder including affliction, as well as several issues undermining posture and ambulation. The effects of aging, deterioration caused by disease and alterations due to

medication all are contributing factors. People get old in natural aging process with loss of functional independence, unsteady, frailer, unconscious and impairment may result fall. Falls in older adults is a major global concern for health and social care providers all over the world. Sometime this falls results in different severe injuries, functional disorder, short/long-term care, disability and even can lead to death. It is broadly associated with gait/balance disorder, intrinsic mental or physical health problem and environment problem. Literature shows that gait and balance disorders among older adults are the major cause of fall.

Demographic projections suggest that the populations of all countries are ageing, which will have wide-ranging effects on social, economic, and health systems (Chatterji et al. 2015). Healthcare centers across the world are providing various long and short time services including primary, behavioural, medical and special care to improve the quality of life. The world's population aged 60 years old and older is set to rise from 841 million in 2013, to over 2 billion by 2050 (Nations 2013). By 2050, 21.1% of the world population will be 60 years old or older, and 80% of this demographic group will live in low-income and middle-income countries, compared with about two-thirds at present. During the same period, global life expectancies are predicted to rise, reaching 83 years in high-income regions and 75 years in low-income and middle-income regions by 2045 to 50 (Nations 2013). According to WHO (Organization 2007), approximately 28-35% of world population aged of 65 and over fall each year increasing to 32-42% for those over 70 years of age. In 2016, 3.7 million (15%) of Australian (Welfare 2017) and 49.2 million (15%) United States (Jonathan Vespa et al. 2018) people were 65 and over. The older adult fall scenario in USA is presented in Figure 1.3.

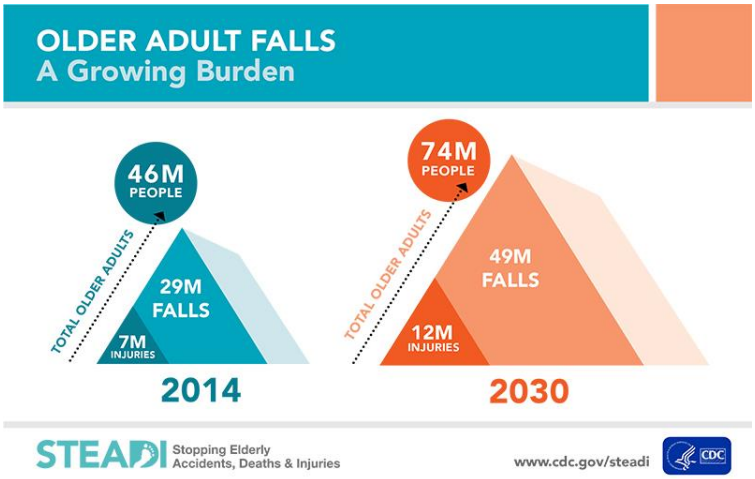

Figure 1.3: Fall scenario in USA outlined by (CDC) (Anon. 2017)

About 30-50% of people living in long-term care institutions fall each year, and 40% of them experienced recurrent falls (Organization 2007). Research (R. Craven and P. Bruno 1986; Eakman 2002) has shown that more than 1/3 of accidental deaths occur in adults over the age of 65 results from falls. It has been also found that those older adults who fall two to three times more likely to fall again. 53% of the older adults who are discharged for fall-related hip fractures will experience another fall within six months (Aging January 2013). According the NHS first year treatment costs in the UK for older adults' fall in home is shown that falls on stairs is £207 million, falls on the level is £128 million, falls between levels is £84 million and falls associated with baths is £16 million (ageUK 2015). In 2009, 2.2 million fall-related injuries among adults aged 65 years or older were treated in emergency departments, and more than 581,000 of the patients involved were hospitalized (Prevention 2015) and in 2011, due to poor housing more than £1.4 billion were expended for NHS treatment (ageUK 2015). In 2012, there were 24,190 fatal and 3.2 million medically treated non-fatal fall related injuries in the US, direct medical costs total of $616.5 million for fatal and $30.3 billion for non-fatal injuries in 2012 and rose to $637.5 million and $31.3 billion, respectively in 2015 (Burns et al. 2016); and this cost are projected to increase $240 billion by year 2040 (Organization 2007). Although the enhancement in life expectancy offers new opportunities, it also creates challenges for future fall in older adults' care facilities. The rapid increased in the number of older adults around the world has created an unprecedented demographic revolution which has tremendous impact on socio-economic development of a country. Consequently, creating comfort living for the older adults and ensuring better healthcare, living independently without any attendant with constant remote and local health monitoring including prevention of falls in older adults has become a challenging task.

Falls in older adults and the economic impact are now one of the major concerns for healthcare providers. To address falls risk researchers used various wearable and ambient sensors for fall detection with high accuracy. Fall prediction using long term data aiming to take protective actions that prevent falls occurrence is still challenging and limited research has been conducted in this area. Technology to help increase mobility and monitor and improve the health of older people at home is very much needed. There is also a need to take advantage of the opportunities that ICT offer older adults, carers and healthcare professionals. This presents new technological challenges as it requires the development of new portable and affordable technologies to deliver diagnostic and therapeutic interventions in the patients' own home within

environmental and financial constraints. One area is to develop personalized automatic monitoring of gait for older. This will enhance the entire healthcare service-delivery chain from diagnosis to post-care while improving the relationship between patients, caregivers, healthcare professionals and other leveraged partners. New technologies need to be user friendly and relatively inexpensive to deliver more value for money and greater productivity in the provision of services. Therefore, the objective assessment of gait and understanding the gait changes has many potential uses.

1.6. Challenges of gait analysis (Problem Statement)

1.6.1. Gait assessment

The tools and methodologies used to assess human gait are often arbitrary and often studied in artificial controlled conditions. Gait abnormalities are generally assessed and reported by physicians, physiotherapists and researchers in clinical settings or in gait laboratories. Clinical scales used to analyse gait parameters are subjective or semi-subjective and a poor replacement to laboratory based methods for identifying changes in gait asymmetry. There are ground reaction forces (Su et al. 2015), dynamic electromyography (Bervet et al. 2013), instrumented walkways (Williams et al. 2013) and camera (Shorter et al. 2008; Auvinet et al. 2017; Cabral et al. 2017; Polk et al. 2017) based methods for gait assessment in laboratory environment which are often carried out by technical or clinical staff. These advanced, accurate gait estimations, time consuming and sometime very expensive methodologies are not applicable for practical use in clinics due to complexity, labour and costing. The conventional scales used to analyse gait parameters in clinical assessment are mainly subjective or semi-subjective. Different assessment tools such as the Gait Abnormality Rating Scale (Brach and VanSwearingen 2002), Figure of 8 Walk Test (Hess et al. 2010), Four Square Step Test (Duncan and Earhart 2013), The Functional Gait Assessment (Wrisley and Kumar 2010), Groningen Meander Walking Test (Bossers et al. 2014) and Berg Balance Scale (Berg et al. 1992), are used to observe the quality of patient's gait and balance. These are mostly based on visual observation, sometime provide scoring based on clinical expertise and sometime abnormality reported as present or not. Such reports may not satisfy scientific criteria of reliability and validity (Archer et al. 2006), which may affect the accuracy of diagnosis, follow-up and treatment (Muro-de-la-Herran et al. 2014). Again, there is no commonly accepted guideline, preferred methodology or protocol for gait changes evaluation.

The European GAITRite Network Group, developed Guidelines for Clinical Applications of Gait Analysis (Kressig and Beauchet 2006), with the intention to facilitate collaboration and provide guidance to clinicians who wish to implement spatiotemporal gait analysis to their clinic. Two issues addressed in the guideline are 1) environmental conditions and safety issues which describe factors such as lighting, noise, visual distraction, clothing, footwear and safety; and 2) measurement procedures which describe steady-state gait at different velocities, standardized walking instructions, assistive devices, stride-to-stride variability, and gait analysis in association with simultaneous cognitive tasks. In order to evaluate stride-to-stride variability, the guideline recommends the highest possible number of gait cycles from a practical standpoint, with a minimum of three consecutive gait cycles for both left and right sides i.e. a total of six gait cycles. There are many issues mentioned which are relevant in gait assessment, however there is no recommended systematic procedure in the guideline. Although there are many approaches for assessment of gait, there is little research conducted on objective gait assessment system. Therefore, a more objective way of assessing gait is required.

1.6.2. Automatic extraction of gait parameters

There are a variety of wearable sensors including an accelerometer, gyroscope, magnetometer, foot pressure sensor, inclinometer, and goniometer (Agostini et al. 2015; Urbanek et al. 2017) that are generally used to measure various characteristics of human gait. IMUs have been used in different gait asymmetry techniques such as monitoring of post-operative gait abnormalities (Hanly et al. 2016), stride variability (Urbanek et al. 2017), measurement of gait asymmetry (Esser et al. 2012), fall-related gait characteristics measured on a treadmill in daily life (Rispens et al. 2016), nature of parkinsonian gait (Okuda et al. 2016) and human waking foot trajectory (Kitagawa and Ogihara 2016). Therefore, the use of IMU sensor in gait analysis has become increasingly popular as it is easily adopted to clinical settings as well as to patients' homes or elsewhere in the community where ambulation normally take place. Research into accelerometer based gait parameters such as times of stance, swing, single support and double (Lee et al. 2007); stride length and stance phase (Chung et al. 2012); gait velocity, stride duration, cadence and step length (Kavanagh 2009); step number, moving distances, every step instant speed and average speed (Song et al. 2007); step counting (Foster et al. 2005; Mladenov and Mock 2009; Brajdic and Harle 2013); times of heel strike, toe strike, heel-off, and toe-off (Boutaayamou et al. 2015); stride length and duration (Rebula et al. 2013); walking distance, time and speed (Brandes et al.

2006) are investigated. Researchers also used portable gait analysis system based on force-sensitive resistor (FSR) placed in insoles to detect ground contact and estimate stance time for gait asymmetry (Afzal et al. 2015), Microsoft Kinect based gait asymmetry (Auvinet et al. 2017), IMU and pressure sensitive shoe insole based gait onset and toe-off detection (Novak et al. 2013), IMU-based knee flexion/extension angle measurements (Seel et al. 2014) and gait asymmetry using gyroscopes (Gouwanda and Arosha 2011). Although, IMU sensor based gait analysis methods are available, automatic gait assessment was actually found in only a few studies without fully automatic system including data collection, feature extraction and quantitative measurement where both limbs are evaluated. Many investigations carried out using a single gait parameter or applying simple statistical methods for comparisons, are additional limitations of these studies and there are not enough studies where a substantial number of participants took part in the study. In order to use accurate quantitative gait monitoring in clinical screening and research, low cost gait assessment tool is required which will provide facility to measure in clinic and home. Again, the use of fused accelerometer and gyroscope based automatic gait features extraction to identify gait assessment has not been reported.

1.6.3. Evaluation of gait parameters

Automated recognition of gait changes has many advantages including, early identification of at-risk gait and monitoring the progress of treatment outcomes. The available common approaches for gait quantification of temporal and spatial gait pattern, symmetry deviations, symmetric indices and symmetry ratios are SI (Robinson et al. 1987), SR (Seliktar and Mizrahi 1986), Ratio (Vagenas and Hoshizaki 1992), symmetry index (Agrawal et al. 2009) and GA (Plotnik et al. 2005; Plotnik et al. 2007). The advantages and disadvantages of these approaches are discussed in (Sadeghi et al. 2000). The commonly used SI needs to be normalized to a reference value (Zifchock et al. 2008; Błażkiewicz et al. 2014) and there is potential influence for artificial inflation as the normal values for young and older patients are not the same (Herzog et al. 1989). Sometimes the mean value calculation used for quantifying gait asymmetry may lead to erroneous results as the mean measurements from two abnormal limbs may appear normal. For example, in a situation where a patient has asymmetry in the opposite direction of gait, the true magnitude of asymmetry for affected or unaffected limbs may be very small. The effect of the direction of gait asymmetry may be eliminated by the use of absolute values in the symmetry indices (Zifchock et al. 2008). There are methods (Miller et al. 1996; Crenshaw and Richards

2006; Sant'Anna et al. 2011) which do not make it possible to identify the point during the gait cycle at which deviations occur. There are other approaches (Sadeghi et al. 2000; Carpes et al. 2010) including principal component analysis (Sadeghi 2003), regions of deviation analysis (DiBerardino III et al. 2012), and paired *t*-test (Shorter et al. 2008) to quantify gait symmetry. However, the number of test subjects and experiments are important for these methods. These methods may also need normative data from able-bodied subjects as a reference (Błażkiewicz et al. 2014). Although gait abnormality is frequently reported as present or not present which may not satisfy scientific criteria of reliability and validity (Archer et al. 2006), an arbitrary cut-off value of 10% deviation from perfect symmetry has been used as a criterion of abnormality in gait assessment (Robinson et al. 1987; Balasubramanian et al. 2009). This is later criticized due to its non-parameter specific nature (Herzog et al. 1989). Other previously used criteria to describe the absence or presence of gait abnormality include sensitivity and specificity of parameter measurement (Leddy et al. 2011), the use of 95% confidence interval (CI) where gait abnormality within the limits of a 95% CI obtained in a healthy population would define able-bodied gait, while gait abnormality outside the 95% CI would define pathologic gait (Herzog et al. 1989), and significant limbs difference (Sadeghi et al. 2000) etc. Although there are many approaches for quantifying gait, there is little research conducted on a gait evaluation method based on overall gait features. To date, research on comprehensive understanding of gait quantification based on overall gait features to allow assessment and monitoring of gait changes from young and older adults has received little attention. Therefore, automatic gait evaluation is required.

1.7. Necessity of this research

Gait analysis is important for fall risk assessment of elderly patients (Hausdorff et al. 2001) as well as the prediction (Maki 1997), detection (Bianchi et al. 2008) and prevention of falls (Bridenbaugh and Kressig 2011). It is also a predictor of functional and cognitive decline (Marquis et al. 2002; Verghese et al. 2007). Gait disorders are common in older people due to physiological age related changes in the musculoskeletal system as well as increased prevalence of several diseases promoting postural instability such as arthritis of the leg or foot, other foot conditions (such as a callus, corn, ingrown toenail, wart, pain, skin sore, swelling, or spasms), fractures, psychological disorders (Shelat 2/3/2015) and several others. Importantly, gait disturbances may also be a marker of the development of Parkinson's disease (van Nuenen et al. 2008), cardiovascular disease (Bloem et al. 2000), diabetic neuropathy (Tahir Khan August 2012)

and dementia (Snijders et al.; Verghese et al. 2007). Research investigations also show that gait changes as a determinant of recovery in patients with Parkinson's disease (Plotnik et al. 2005), cerebrovascular accidents (Wall and Turnbull 1986), amputees (Skinner and Effeney 1985; Geurts et al. 1992), stroke (Chen et al. 2005; Hodt-Billington et al. 2008; Patterson et al. 2008; How et al. 2013; Lewek et al. 2014), osteoarthritis (Shakoor et al. 2003; Kutilek et al. 2014), spinal deformity (Park et al. 2016), fractures(Larsen et al. 2017), limb-length inequality (Kaufman et al. 1996) and cerebral palsy (Böhm and Döderlein 2012). In biometrics and biomedical engineering areas, gait analysis has been used as a fundamental method and assistive tool to characterize human locomotion and has many applications (Bora et al. 2015b). Finally, gait disorders are associated with a reduced quality of life, falls and mortality. Gait analysis has therefore attracted the interest of researchers in different disciplines.

Older adults in number are growing all over the world and about a third of people with age over 65 years fall each year and over half of seniors aged 80 years fall annually. UK statistics show that falls and fractures in people aged over 65 account for over 4 million hospital bed days each year in England alone, and the healthcare cost associated with fragility fractures is estimated at £2 billion a year (England 2017b). Considering all these factors there is a national imperative to develop new more cost-effective models of care underpinned by new technologies that are less expensive to develop and run to help increase the mobility and monitor the health of older people at home is very much needed. This needs to adapt to take advantage of the opportunities that science and technology offer patients, carers and health care professionals. This presents new technological challenges as it requires the development of new portable technologies to deliver diagnostic and therapeutic interventions in the patient's own home. This need to develop new technologies also need to take place in an environment that is financially stringent New technologies need to be user friendly and relatively inexpensive to deliver more value for money and greater productivity in the provision of services. Our proposed research therefore is timely in addressing various of these requirements set in this national agenda.

Therefore, an automatic gait analysis system is proposed in this research. It starts with exploring the optimal location of placing the sensors on different foot locations to maximize the interpretable information for gait analysis. An automatic time and distance based gait features (stride number, distance, speed, length and period of stride, stance and swing) extraction method is proposed with the aim to identify gait asymmetry and monitor abnormal gait pattern changes over time. Four spatiotemporal gait visualization approaches are proposed to provide automatic

graphical visualizations of information about gait. Next, validation study is conducted with the aims to determine the concurrent validity of spatiotemporal gait extracted features from proposed system against Motion Capture System e.g. Qualisys and Treadmill measurements in young and older adults and to compare the levels of agreement for average spatiotemporal gait parameters. Finally, a gait evaluation system is proposed using Procrustes and Euclidean distance matrix analysis based on overall gait features. While there are systems to analyse gait and balance to our knowledge, but this is one of the first body warn low cost systems to collect synchronous data from sensors intended to do this. The system will have the potential to be used in assessment of gait, gait change monitoring, gait asymmetry and clinical use associated with gait pattern. This has considerable potential to identify long time gait pattern changes based on these automatic gait features and explore ways how these features can be useful to classify gait changes over time and identify abnormal gait patterns for the assessment of elderly fall risk, rehabitation and sports applications. Older adults in home could use this system to decide their health condition for admission to hospital.

1.8. Aim and objective

Falls in older adults are one of the major health care concerns. Due ageing populations the frequency of falls is increasing and the health economic burden of this is of concern. Considerable research in the area of balance and gait disorders associated with falls is required. To address this challenge, a comprehensive investigation of gait and balance deficits that increase fall risk is required. The association between gait pattern changes over a period of time and falls requires further study to determine which aspects of balance are most predisposing to falls.

Nevertheless, at present no affordable automatic objective gait assessment system exists in clinics and research laboratories that can be applied reliably across different settings to quantify, monitor and identify gait abnormalities. Among the available existing tools, only few have been validated in different settings. Thus, the main aim of this thesis is to design and develop an automatic affordable lower limb gait analysis system that will provide comprehensive gait information and allow use in clinic or at home for older adults. The system will continuously monitor user's gait information, quantify, monitor and identify gait abnormalities through sensors in order to reduce the potential risk associated with elderly fall so that older people could lead quality of life. The specific research objectives of this research are following.

1. To conduct a literature review of available wearable sensors and its application for gait analysis to identify research gap (Chapter 2).
2. To design and develop a data collection platform, sensor selection, design and development of sensor protection system, design and development of an android app, synchronous data collectionplatform and the proposed multi-sensor based gait analysis framework (Chapter 3, Section 3.2.2 to 3.2.7).
3. To find the optimal foot location of placing IMU sensors in order to obtain accurate, reliable and robust sensor output to maximize the highest possible interpretable information for gait analysis. This also investigates the influence of parametric uncertainties for extracting automatic features from gait parameters with the aim of improving the quality of IMU sensor output (Chapter 3).
4. To design and implement a wireless wearable automatic gait feature extraction method (Chapter 4.2) and collect data from both young and older adults. To determine the effect of young and older adults walking condition on major descriptive gait statistical features in terms of total distance, total time, total velocity, stride, step, cadence, step ratio, stance, and swing.
5. To demonstrate a tool for visualizing, quantifying, monitoring and accessing gait cycle with comprehensive gait symmetry information for users, clinical use and rehabilitation (Chapter 4.3).
6. To determine the concurrent validity of spatiotemporal automatic gait extracted features with “gold standard” measurements in young and older adults and to compare the levels of agreement for average spatiotemporal gait parameters (Chapter 4.4).
7. To allow assessment and monitoring of gait changes based on overall gait features for comprehensive understanding of gait from young and older adults in both a clinic and at home which increases the availability and affordability of gait assessment (Chapter 5).
8. To propose a hypothetical digital transformation strategy framework for gait analysis based on the development and the possible use of new technology, changes to value creation, structural change, affordability and sustainability (Chapter 6.5).

1.9. Ethics and participant evaluation

This research involves studies with young and older adult participants, ethical issues regarding human participation are taken into consideration. I have studied thoroughly and understood the

Helsinki Declaration. An online course of "*Ethics1: Good Research Practice"* is completed with a certificate. An ethical approval is permitted from *Bournemouth University ethical review committee* to conduct this research. This research considered young and older adult participants' safety and emergency aids. A *Participant Information Sheet* and signed an informed *Participant Agreement Form* are prepared for young and elderly participants. Before the data collection sessions, the participants are given brief introduction about the study and an explanation about the data collection processes by reading the *Participant Information Sheet* and *Participant Agreement Form* written informed consents are obtained from all participants and they are informed they could withdraw at any time from the study. The certificate of "*Ethics1: Good Research Practice", Participant Information Sheet* and *Participant Agreement Form* are presented in Appendix A.

1.10. Contribution

The major contributions of this research are the following

1) Finding the optimal location from five anatomical foot locations for placing IMU sensors for the analysis of gait
2) Developing an automatic gait feature extraction method (a stride detection technique, a stance and swing detection technique, and a method for estimating travelled distance) to monitor gait asymmetry
3) Demonstrating four visualization approaches for monitoring gait asymmetry to provide automatic graphical visualizations of information about gait
4) Determining the concurrent validity of spatiotemporal IMU gait extracted features against Motion Capture System and Treadmill measurements in young and older adults and comparing the levels of agreement for average spatiotemporal gait parameters
5) Developing a novel gait evaluation method using Procrustes and Euclidean distance matrix analysis
6) Proposing a digital transformation strategy framework for gait analysis based on the development and use of new technology, changes to value creation, structural change, affordability and sustainability
7) Designing and developing an android app to collect real time synchronous IMU data

8) Creating a data set for each study using our developed app and designed sensor protection system (MetaWear casing, Velcro elastic belt, and buckles) for validating the designed app and the proposed methods

The detailed discussion of these contributions is provided in the upcoming chapters and is summarized below.

Chapter 2: An extensive literature review has been conducted on wearable sensor based gait analysis, available gait assessment procedures and its application in clinics and at home. The lack of empirical studies of the currently available systems for gait analysis are identified. Addressing the research gaps to propose framework for automatic gait assessment.

Chapter 3: The details of designing a sensor casing using 3D printer, Velcro elastic belt, and buckles for data collection are described. The details research approach is also described. An investigation of placing the IMU sensor on five different foot locations is conducted. The investigation results give indication to find the best foot location for placing an IMU sensor as it delivers the most accurate output signal. A gait features extraction method is also proposed. This chapter is published in IEEE Sensors Journal.

> Anwary A R, Yu H, Vassallo M, **"Optimal foot location for placing wearable IMU sensors and automatic feature extraction for gait analysis"**, IEEE Sensors Journal, vol. 18, no. 6, pp. 2555-2567, 2018, (Impact Factor: 2.617)

Chapter 4: In this chapter, we propose an automatic gait feature extraction method (a novel stride detection technique, a stance and swing detection technique, and a method for estimating travelled distance). The Section 4.2 is published in Sensors.

> Anwary A R, Yu H, Vassallo M, **"Automatic gait feature extraction method for identifying gait asymmetry using wearable sensors"**, SENSORS, vol. 18, no. 2, p. 676, 2018, (5-Year Impact Factor: 3.014)

We propose a tool for visualizing, quantifying, monitoring and accessing gait cycle with comprehensive gait symmetry information for users in Section 5.3. The section is published in The 24th Americas Conference On Information Systems (AMCIS 2018). This is Rank A conference through http://portal.core.edu.au/conf-ranks/115/.

Anwary A R, Yu H, Vassallo M, **"Wearable sensor based gait asymmetry visualization"**, The 24th Americas Conference On Information Systems, AMCIS 2018

We conduct a concurrent validity of spatiotemporal automatic gait extracted features with "gold standard" measurements under three experiments in young and older adults in Chapter 4.4. The section is under review in the Journal of Biomechanics.

Anwary A R, Yu H, Callaway A, Vassallo M, **"Validity of an automatic spatiotemporal gait features extraction system using wearable IMUs"**, (Under Review)

Chapter 5: We propose a novel gait evaluation method using Procrustes and Euclidean Distance Matrix Analysis. The study is published in the IEEE Journal of Biomedical and Health Informatics.

Anwary A R, Yu H, Vassallo M, **"Gait Evaluation using Procrustes and Euclidean Distance Matrix Analysis"**, IEEE Journal of Biomedical and Health Informatics, 2018 (Impact Factor:3.85)

Chapter 6: We design a novel digital transformation strategy framework for gait analysis based on the development and use of new technology, changes to value creation, structural change, affordability and sustainability. The initial concept of digital strategy framework is published in Connected Everything 2018 Conference.

Anwary A R, Yu H, Vassallo M, **"Digital Transformation Strategy Framework for Gait Analysis"**, Connected Everything 2018 Conference

The extended concept of proposing digital transformation strategy framework is under review in the Business & Information Systems Engineering.

Anwary A R, Yu H, Vassallo M, **"Digital Transformation Strategy Framework with a Pilot Study for Gait Analysis"**, (Under Review)

1.11. Thesis outline and organization

In this thesis, five thematically related studies are presented to accomplish the objectives presented in Section 1.8. Each study is presented as an independent publication. Chapter 2 discusses the literature review on available gait assessment systems in clinics and laboratory (Objective 1). It also discusses about wearable sensor placing location and research gap and

research design. The optimal location of placing IMU sensors is studied in Chapter 3. Chapter 3 address Objective 3 and is accepted for publication in IEEE Sensors Journal. The findings of these two chapters provide evidence for placing IMU sensors at the best foot location to collect data for automatic gait analysis. In response to current challenges in analysing multivariate spatiotemporal gait feature extraction generated by quantitative objective measures, Section 4.2 describes a novel wireless wearable automatic gait feature extraction method. Section 4.2 addresses Objective 4 and is accepted for publication in Sensors. Section 4.3 describes real time based gait spatiotemporal visualization tool that addresses Objective 5 and is accepted in The 24th Americas Conference On Information Systems (AMCIS 2018). Section 4.4 describes the concurrent validity of spatiotemporal automatic gait extracted features with "gold standard" measurements in young and older adults and to compare the levels of agreement for average spatiotemporal gait parameters. This section addresses Objective 6 and is under review. Chapter 5 describes a novel assessment and monitoring of gait changes method based on overall gait features for comprehensive understanding of gait from young and older adults in both a clinic and at home which increases the availability and affordability of gait assessment. This chapter addresses Objective 7 and is accepted for publication in the IEEE Journal of Biomedical and Health Informatics. The digital transformation strategy framework for gait analysis is described in Chapter 6 and is accepted at Connected Everything 2018 Conference. The extended version of the concept is under review.

This thesis has six chapters and five appendixes. The chapters are organized in the framework shown in Figure 1.4.

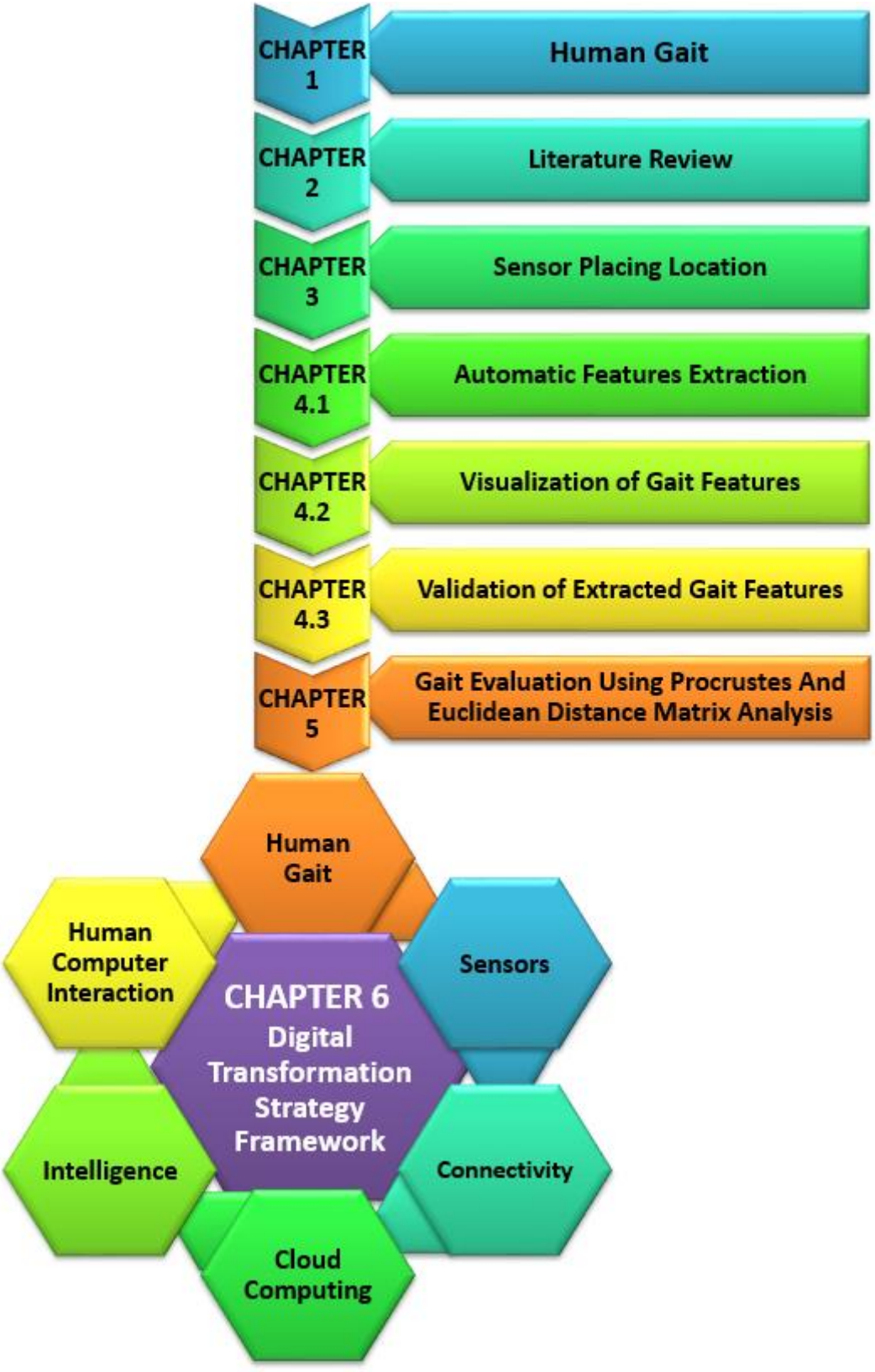

Figure 1.4: The proposed multi-sensor based gait analysis framework

1.11.1. Chapter 1 (current chapter)

Chapter 1 presents the statement of problem and motivation. It also provides a brief introduction of the gait related terms and scope. Finally, it discusses the objective and contribution of this thesis.

1.11.2. Chapter 2

Gait analysis is currently carried out in three very different ways. One is based on visual observation available in clinical settings. A second analysis modality is conducted in a motion laboratory and third is based on wearable technology. In this chapter, a comprehensive literature review of current research covering these major three areas including a history of wearable sensors, current state of art and methodology for gait analysis is presented. Initially, a systematic approach is used for literature review. The gait analysis scope in older adults is reviewed. Next, the conventional gait analysis methods are presented. Then, the available wearable sensors for gait analysis such as accelerometer, gyroscope and magnetometer etc are reviewed. The methods for extracting commonly used gait features such as stride, step, stance, and swing related information etc. are reviewed.

1.11.3. Chapter 3

Finding the optimal location for placing sensors and the influence of parametric uncertainties for extracting automatic gait features are important to improve the quality of an IMU sensor output to maximize the highest possible interpretable information for gait analysis. In this Chapter 3, we investigate to find the optimal location of placing an IMU sensor on the barefoot and the parameters that influence the automatic extraction of gait features. Sensors are generally worn or attached directly or indirectly to different body locations such as foot, wrist, chest and head, and sometime attached using belts, clips or other accessories (Matthews et al. 2012). Various factors can affect the signal input and output. For example during locomotion, movement of clothes can cause interference with accelerometer output (Bouten et al. 1997). There can be vibration or momentum noise if the sensor is not attached properly. Again, attaching the sensor with a belt or keeping in a pocket can induce relative motion interference (Plasqui and Westerterp 2007). The placement and orientation of IMU sensor also have an influence on sensor output (Intille et al. 2012). To address these issues, the aim of this chapter is to determine the sensor orientation and

optimal location for sensor placement to extract automatic feature information from accelerometer and gyroscope data when attached to different areas of the foot. The proposed positions for finding the optimal location are our novel approach in this gait analysis research area and has not been explored before to our best knowledge.

Research into accelerometer based gait parameters such as times of stance, swing, single and double support (Lee et al. 2007); stride length and stance phase (Chung et al. 2012); gait velocity, stride duration, cadence and step length (Kavanagh 2009); step number, moving distances, instant step speed and average speed (Song et al. 2007); step counting (Foster et al. 2005; Mladenov and Mock 2009; Brajdic and Harle 2013); times of heel strike, toe strike, heel-off, and toe-off (Boutaayamou et al. 2015); stride length and duration (Rebula et al. 2013); walking distance, time and speed (Brandes et al. 2006) are investigated. However, a low cost multi-sensor based synchronous data collection system for a comprehensive physical gait analysis totalling ten parameters has to our knowledge not been reported so far. Our android app is used for collecting synchronous information and an automatic gait features extraction method is applied to extract features on stride number, total distance, total speed, stride length, stride period, stance length, stance period, swing length, swing period and ratio of stance and swing events, using low cost wearable IMU sensors. It covers the strategy for selecting wearable sensor, design and development of sensor protection system, design and development of Android App, synchronous data collection and the proposed multi-sensor based gait analysis framework. It describes output differences of placing the sensor in different body locations and available methods of extraction gait features. It also investigated for finding the optimal location to place the sensor. The details result of this study is presented in Appendix B.

1.11.4. Chapter 4

In order to broaden the use of accurate quantitative gait monitoring in clinical screening and research, an affordable gait analysis tool is required which can be used in clinic or home. This study aims to design and implement an automatic lower limb gait features extraction method based on accelerometer and gyroscope data to increase the reliability and validity of gait monitoring. We set out to develop an affordable multi-sensor based synchronous data collection system for a comprehensive physical gait analysis extracting 24 commonly reported gait features. We use our android app for collecting synchronous accelerometer and gyroscope data from both legs. Features include total distance, total time, total velocity, stride, step, cadence, step ratio,

stance, and swing. We also estimate the mean, standard deviation, variance, minimum and maximum values. This chapter describes available gait assessment methods and tools currently being used in clinics and other applications. It also proposed systematic methods to extract automatic gait features for monitoring gait variability. The details analysis results of automatic gait features are presented in Appendix C. It presents four spatiotemporal real time gait visualization approaches: 1) Real time dial visualization; 2) Visualization of individual leg time variation; 3) Visualization of both legs asymmetry; and 4) Boxplot-based visualization. Real time dial visualization shows the instantaneous gait asymmetry of both legs from distance and time of stride, step and swing phases of each gait cycle using a dial and an indicator. It also showed instantaneous distance and time of stride, step and swing values in a seven segment display. Individual leg variation visualization showed the variation in stride, stance and swing phases in time. Both legs asymmetry visualization showed the asymmetry between two legs for strides and steps. Boxplot-based visualization showed the overall stride, step, stance and swing phases distribution. These methods are user friendly and easy to interpret and have the potential of helping professionals detect and interpret gait asymmetry. It also describes with the aims to determine the concurrent validity of spatiotemporal IMU gait extracted features with Motion Capture System (MCS) and Treadmill measurements in young and older adults and to compare the levels of agreement for average spatiotemporal gait parameters. 48 subjects (28 young and 20 older adults) participate in the study. We validate our system using three experiments; 1) Treadmill at various walking paces vs MCS, 2) Self-selected (free) walking vs MCS, and 3) Self-selected (free) walking vs Digital tape for distance. The details validation results are presented in Appendix D.

1.11.5. Chapter 5

Quantification of gait variabilities, kinematic and kinetic measurements, muscular measurements and energy expenditure, provide comprehensive locomotive gait information (Muro-de-la-Herran et al. 2014). Gait quantification information is used to 1) distinguish the type of gait impairments and suggest possible diagnoses; 2) measure and monitor the severity of an injury or a disease and determine the most appropriate treatment (Baker 2006); 3) be a determinant of progression in patients with medical conditions causing gait disorders (Böhm and Döderlein 2012; Lewek et al. 2014) monitor response to treatment in orthopaedic rehabilitation (Steultjens et al. 2000); 4) monitor and improve an athlete's performance (Wahab and Bakar 2011); and 5) in

biometrics and biomedical engineering areas, be an assistive tool to characterize human locomotion and have many applications (Bora et al. 2015a). Gait quantification information is important in elderly patient fall risk assessment (Yogev et al. 2007) and also a predictor of functional and cognitive decline (Plotnik et al. 2011). Therefore, the objective evaluation of gait and understanding the gait changes has many potential uses.

Although there are many approaches for quantifying gait, there is little research conducted on a gait quantification method based on overall gait features. In order to provide comprehensive gait information and evaluation in clinical screening and research, an affordable gait evaluation system is required which will provide the facility in clinic or a home. Considering all the various parameters that constitute the gait cycle, we propose a gait evaluation system using Procrustes and Euclidean distance matrix analysis which may offer a simple and easily interpretable assessment of gait with good accuracy and comprehensive features. An alignment technique to better express the normal mean gait shape (NMGS) using Procrustes superimposition (Bookstein 1991; Goodall 1991) is applied. Our technique can also find the shape and size difference between the NMGS and individual gaits. Four shape and size comparison techniques (Riemannian shape distance (RSD) (Kendall 1984), Riemannian size-and-shape distance (RSSD) (Le 2016), Procrustes size-and-shape distance (PSSD) (Dryden and Mardia 1998) and Root mean square deviation (RMSD) (Dryden and Mardia 1998)) are applied to quantify individual gait based on all gait features. We also investigate how each feature impacts on a gait using EDMA. We estimate a mean form, inter-feature distances and mean form difference from all young subjects using EDMA. The mean form estimated from all young is considered as a standard normal mean gait form (NMGF). The degree of abnormality of individual features for form difference between the NMGF and each gait is estimated. A high value indicates high degree of feature difference in the gait and low value indicates close to normal gait. To date, research on comprehensive understanding of gait quantification based on overall gait features to allow assessment and monitoring of gait changes from young and older adults has received little attention. Our method provides the facility to quantify gait and gait changes in both a clinic and at home which increases the availability and affordability of gait assessment. The details analysis results are presented in Appendix E.

1.11.6. Chapter 6

In this research, a multiple IMU based automatic gait analysis system is proposed for older adults to support assisted living applications. The average age and number of co-morbidities per person has rapidly increased worldwide over the past decades. This has a major effect on health care where issues such as a rise in care cost, high demand in long-term care, burden to carers, and insufficient and ineffective care are likely to occur. Our automatic gait analysis system can be used as the key part of intelligent systems to allow older adults to monitor their gait at home to live independently, reduce care cost and burden to the carers, provide ensuring for the families, and promote better care. Through our comprehensive literature on gait analysis and wearable gait analysis, it is found that gait abnormalities are very common in clinical practice and there is an increasing need to improve technology for its analysis. Such abnormalities lead to serious adverse consequences such as falls and injury resulting in increased cost. There is therefore a national imperative to address this challenge. Currently assessment is done using standardized clinical tools dependent on subjective evaluation. More objective gold standard methods to analyse gait rely on accessing to expensive complex equipment based in gait laboratories. These are not widely available for several reasons including requirement for expensive equipment, need for technical clinical staff, need for patients to attend in person, complicated time consuming procedures and overall expense. Improving opportunities for gait analysis to increase accessibility requires a development of an automatic gait analysis system using of new and affordable technologies for diagnosis and monitoring of gait using digital technology, nevertheless with population ageing it will soon be a huge market and in order to compete in such market, the cost will be a vital factor. There remain many issues and challenges in developing gait analysis systems including user acceptance, usability, privacy, visibility, systems accuracy, lack of human and social interaction and cost. Therefore, in this research, an automatic gait analysis system is proposed and developed considering both practical and technical aspects using wearable, inexpensive wireless sensors so that the acceptance and usability are increased allowing the system to be used in reality.

2. LITERATURE REVIEW

This chapter has four major sections that critically review the relevant literature to get a clear picture of available techniques in gait analysis (Section 2.2), wearable sensor based gait analysis (Section 2.3), user requirement (2.4) and research gap identification (Section 2.5). A summary is presented in Section 2.6.

2.1. Literature search strategy

In this research, we choose carefully what criteria are to be included in this study because these criteria determine the quality of the study; therefore, in the search only the most relevant articles are chosen for this research. Therefore, in the initial of review demands a formation of research questions that need to be considered in order to fully cover the research area of conventional gait assessment techniques and wearable sensors for gait analysis. The answers to the following questions are provided through this review paper relying on the proposed review process:

- What are the conventional gait analysis systems used in clinics?
- How is it possible to assess gait of a user by the way he walks relying on data acquired by wearable single, multiple and fusion sensors?
- What are the methodological constraints and how are those addressed?
- What are the gait related constrains and how are those addressed?
- How is the monitoring procedure of gait analysis and what are the relevance validation procedure and results?
- What is the performance and reliability of the most practical approach and how efficient are those approaches?
- What is the potential for the general use in real world circumstances for clinic and home use?
- What are the underlying problems and in which direction the further development is aimed?

For the study to be more reliable, it is also necessary to exclude some criteria just as it is crucial to include some criteria. Any article that does not fall within the subject of the study is not considered. A general list of inclusion and exclusion criteria is shown in following Table 2.1.

Table 2.1: Inclusion and exclusion criteria for searching literature

Inclusion criteria	Exclusion criteria
1. Articles directly related with gait and mobility analysis or assessment, wearable feedback used to either assess, train human gait or wearable sensors to detect balance and provided instant biofeedback based on the detected information 2. Articles that included healthy adults, as well as patients with balance disorders 3. Articles that are available to us 4. Articles available in full text 5. Articles from engineering, technology, medical, bio-technology, and rehabilitation areas 6. Articles from peer reviewed impact factor journals 7. Articles of most recent work	1. Articles that are not relevant of our study domain 2. Articles of movement analysis other than gait domain 3. Articles not related with human movement 4. Articles without any abstract 5. Articles require charge 6. Articles not written in English

Based on the inclusion and exclusion criteria for searching literature in Table 2.1, a systematic literature search is conducted to find related works to the research area related to engineering, computing and medicine etc. Eight major databases on biomedical engineering, computing and medicine are searched up to May, 2018: Web of Science, ScienceDirect, IEEE Xplore, ACM Digital Library, EBSCO, PubMed, SCOPUS and Cochrane Library for selecting relevant publications. Figure 2.1 shows the review process and criteria and it also shows a glimpse the distribution of research efforts in gait analysis using wearable sensors. Overall, gait analysis has already become an established field, given that over 600000 papers from the eight databases are associated with gait analysis. For this systematic search, the search terms are defined as (gait OR walking OR locomotion) AND (analysis OR evaluation OR assessment) AND (wearable OR inertial OR inertial measurement unit OR accelerometer OR gyroscope OR magnetometer OR sensors) AND (artificial intelligence OR machine learning OR adaptive OR intelligent

algorithm). In the first phase of the review process, these keywords are passed to search engines databases and digital libraries. The results are shown in Figure 2.1. The selection of these specific datasets stems from their significance in the field of engineering, as well as in biomechanics, medicine, and biometry etc. Studies evaluating kinematic of gait parameters e.g. stride, stance, swing etc gait phases or spatiotemporal features of healthy, older adults or impaired subjects are included with artificial intelligence for processing data collected using IMUs, accelerometers or gyroscopes etc. Next, these papers (i.e., searched by the key words "inertial sensor gait") are manually screened to eliminate work that has not yet been applied to patient studies or not relevant to research interest. After the careful consideration of all abstracts, the papers that are insignificant or are not directly related to wearable sensor based gait analysis are omitted. Finally, all of the manually screened papers from all eight databases are selected again to eliminate duplication, papers that have not provided enough insight into gait pathologies and papers fulfill the criteria presented in Table 2.1. In this manner, a total of 162 papers that cover the reviewed topic are obtained.

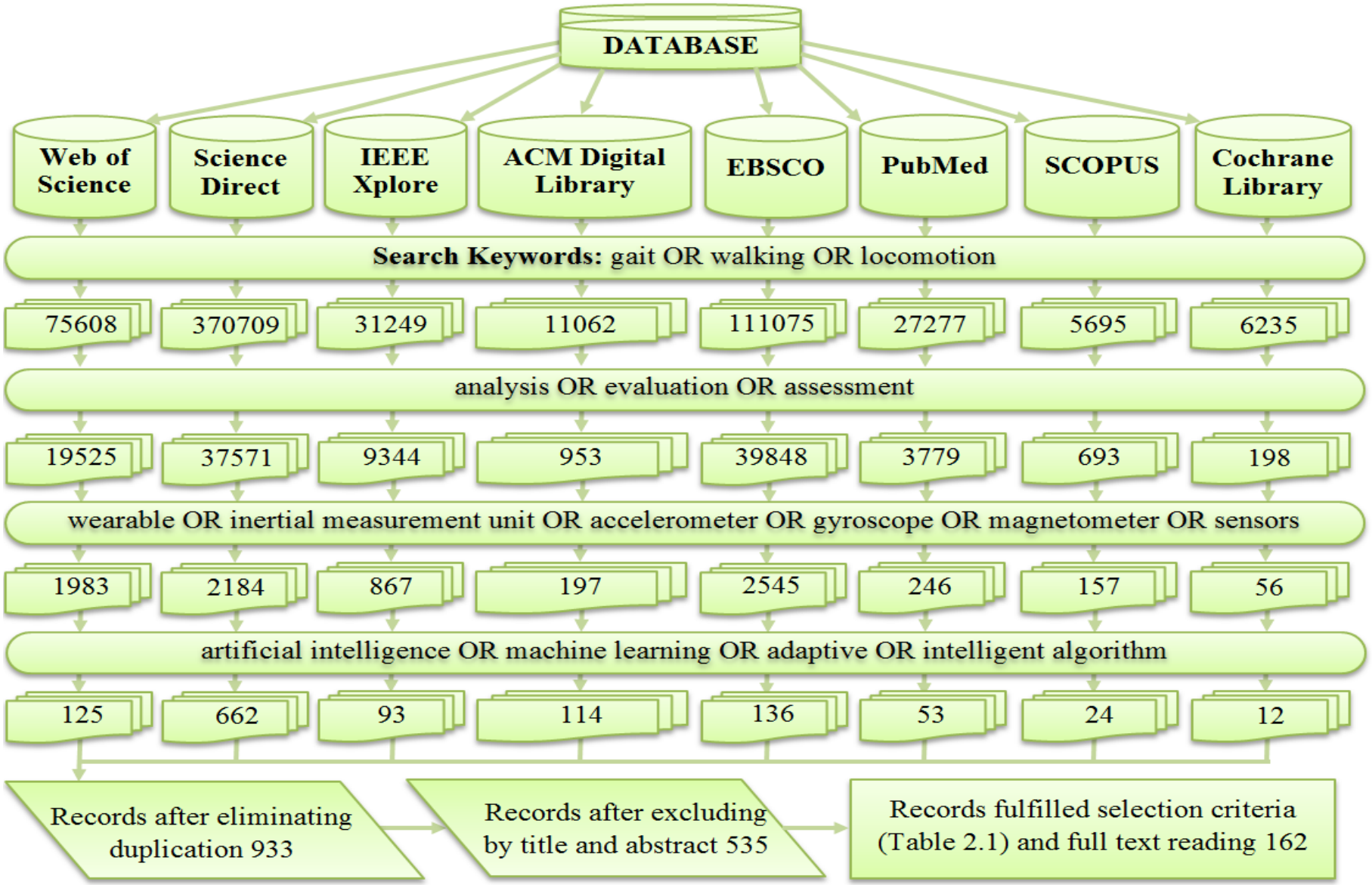

Figure 2.1 Systematic search for current research on wearable gait analysis (up to May 2018)

After careful review of a total of 162 papers, 30 papers that reflect the most significant contribution for conventional gait assessments, 62 papers that reflect on the sensor selection, 33 papers that reflect sensor placing locations, 13 papers that reflect on sensor fusion, 33 papers that reflect on feature selection, 27 papers that reflect on quantification and visualization, 10 papers that reflect on feature selection methods, 22 papers that reflect on feature classification and 10 papers that reflect on validation topic are selected. Majority of these papers are published in recognised high impact factor journals while some of them are published in proceedings of significant conferences. There are many patents available for gait analysis, however objective gait assessment for older adults using affordable system are found in few studies. This area will be explored in our future study at the time of designing the system for commercialization.

2.2. Current state-of-the-art on gait analysis

Analysis of gait and balance is a useful clinical tool in the management of walking and movement problems for patients with different gait abnormalities since the later part of the twentieth century. Technology related to gait analysis in clinical assessment and management are improved significantly in recent years. The following describes the currently available assessment systems of gait and balance.

2.2.1. Clinical gait assessment

Clinical gait assessment is the process by which quantitative information is collected to aid in understanding the quality of patient's gait and balance abnormalities and in treatment decision-making. The conventional scales used to analyse gait parameters in clinical assessment are mainly subjective or semi-subjective. These methods usually consist of analyses carried out in clinical conditions by a clinician. The various gait-related parameters of the patient are observed and evaluated while the patient walks on a pre-determined circuit. The following describes the most common subjective or semi-subjective gait analysis techniques.

2.2.1.1. Gait abnormality rating scale

Gait Abnormality Rating Scale (GARS) instrument incorporates evaluations of total of 16 facts. It is a screening tool to identify patients at risk for injury from falls. The screening tool has a scale that comprises of three categories: five general facts, four lower extremity facts and seven trunks, head and upper extremity facts. Each fact is scored range from 0 (good) to 3 (poor) that

mark characteristics of abnormal gaits (Wolfson et al. 1990). A modified version is published later GARS-M (VanSwearingen et al. 1996).

2.2.1.2. Timed 25-foot walk

Timed 25-Foot Walk (T25-FW) is also known as the 25 foot walk test. A standardised quantitative evaluation instrument consisting of three parts for use in clinical studies, particularly clinical tests on multiple sclerosis (Cutter et al. 1999). A specialist measures the time it takes the subject to walk a distance of 7 and a half meters in a straight line in the test.

2.2.1.3. Clinical test of sensory interaction and balance

Clinical Test of Sensory Interaction and Balance (CTSIB) (Shumway-Cook and Horak 1986) is developed to assess the contribution of the visual, somatosensory, and vestibular systems to postural control. The test evaluates static postural stability in 6 distinct standing conditions with eyes open, with eyes closed, and with the use of a dome to alter visual input on both firm and foam surfaces. This test has been modified to include eyes open and eyes closed on both firm and foam surfaces, given the finding that altered visual inputs from the dome are not different from those in the eyes closed condition (Cohen et al. 1993).

2.2.1.4. Tinetti performance oriented mobility assessment

Tinetti Performance Oriented Mobility Assessment (POMA) assessment tool is an easily administered task-oriented test that measures an older adult's gait and balance abilities. Patient is required to walk forward at least 3 meter, turnaround of 180° and then walk quickly back to the chair (Tinetti 1986). Patients use their habitual walking stick or walker aid. The assessment on balance disorders is based on 13 parameters organized in three levels and the study of the human gait is based on nine additional parameters classified in four levels. This assessment makes it possible to accurately evaluate elderly persons' balance and gait disorders in everyday situations. However, the test requires a great deal of time with active participation from the subjects.

2.2.1.5. Timed "Up and Go" test

Timed "Up and Go" Test (TU&GT) test is a timed test that requires patients to get up from a sitting position, walk a short distance, turn around, walk back to the chair and sit down again (Mathias et al. 1986). It is widely employed in the examination of elders for basic mobility skills

including a sequence of functional manoeuvres used in everyday life, but definitive normative reference values are lacking.

2.2.1.6. Figure of 8 walk test

Figure of 8 Walk Test (F8W) (Hess et al. 2010) test is designed to assess motor skill (speed, amplitude and accuracy of movement) through curved-path as well as straight-path walking for daily life in older people with walking difficulties. Participants walk a figure-of-eight at their self-selected usual pace around 2 cones placed 5 ft apart.

2.2.1.7. Four square step test

Four Square Step Test (4SST) (Duncan and Earhart 2013) is a quick and simple test of multidirectional stepping which is useful in predicting falls in people with Parkinson disease.

2.2.1.8. Extra-laboratory gait assessment method

Extra-Laboratory Gait Assessment Method (ELGAM) (Fried et al. 1990) evaluates gait in the home or community to identify of risk factors for fallers among elderly. The parameters study includes step length, speed, initial gait style, ability to turn the head while walking and static balance. Low speed (under 0.5 m/s), short steps, difficulty turning the head and lack of balance are significantly linked to unstable gait.

2.2.1.9. Functional gait assessment

Functional Gait Assessment (FGA) (Wrisley and Kumar 2010) is a 10-item gait assessment based on the dynamic gait index (DGI) (Vander Linden 1996). It comprises 7 of the 8 items from the original DGI and 3 new items, including “gait with narrow base of support,” “ambulating backwards,” and “gait with eyes closed”.

2.2.1.10. Groningen meander walking test

Groningen Meander Walking Test (GMWT) (Bossers et al. 2014) measures dynamic walking ability by walking over a meandering curved line, with an emphasis on walking speed and stepping accuracy while changing direction specifically for people with dementia.

2.2.1.11. Berg balance scale

Berg Balance Scale (BBS) (Berg et al. 1992) is a widely used clinical test that measures balance among older people with impairment in balance function by assessing the performance of functional tasks. It is a 14 item list qualitative measure that assesses balance via performing functional activities such as reaching, bending, transferring, and standing that incorporates most components of postural control: sitting and transferring safely between chairs; standing with feet apart, feet together, in single-leg stance, and feet in the tandem Romberg position with eyes open or closed; reaching and stooping down to pick something off the floor. Each item is scored along a 5-point scale, ranging from 0 to 4, each grade with well-established criteria. Zero indicates the lowest level of function and 4 the highest level of function. The total score ranges from 0 to 56. It takes approximately 20 minutes to complete. However, it does not include the assessment of gait.

These subjective or semi-subjective methods usually consist of analyses carried out in clinical conditions by a specialist and abnormalities are generally assessed and reported by physicians, physiotherapists and researchers in clinical settings or in gait laboratories, where assessment time is limited, using visual observation, questionnaires or functional assessment to determine abnormalities in spatiotemporal gait parameters etc. These gait assessments are highly dependent on assessors' experience and judgment. Such visual assessments may not satisfy scientific criteria of reliability and validity (Archer et al. 2006), which may affect the accuracy of diagnosis, follow-up and treatment (Muro-de-la-Herran et al. 2014). Again, there is no commonly accepted guideline, preferred methodology or protocol for gait changes evaluation. Therefore, a more objective gait assessment supporting tool is required.

2.2.2. Laboratory gait assessment

There are also "gold standard" methodology for assessment of gait parameters e.g. three-dimensional kinematic analysis using a marker based motion capture system such as Vicon Motion Systems Ltd (www.vicon.com), Qualisys Motion Capture Systems (www.qualisys.com), Motion Analysis Corporation (www.motionanalysis.com), Northern Digital Inc (www.ndigital.com), OptiTrack Motion Capture Systems (https://optitrack.com), and Codamotion (www.codamotion.com), force plate and pressure activated sensors (Bilney et al. 2003; Moeslund et al. 2006; Beauchet et al. 2008; Zammit et al. 2010), ground reaction forces (Su et al. 2015), dynamic electromyography (Bervet et al. 2013), instrumented walkways

(Williams et al. 2013) and camera (Shorter et al. 2008; Auvinet et al. 2017; Cabral et al. 2017; Polk et al. 2017). These methods provide accurate gait parameters, high measurement resolution, very low marker jitter, sometimes do not require the user to wear wires or electronic equipment, capacity of multiple performance capture and high capture frequency etc. These methods for gait assessment are conducted in specialized locomotion laboratory environment which are often carried out by technical or clinical staff. However, these current available technologies are expensive, lengthy set up and post-processing times, sometime limited to capture small gait cycles, extensive post-processing, markers can be blocked by body parts or clothes, and laboratory based which reduce their feasibility to be used at home and in clinics. Moreover, limitations in terms of the moving area and gait cycles for the observed subject/patient have been observed (Tao et al. 2012). Therefore, an inexpensive, portable and easy to use gait assessment supporting tool is required.

2.2.1. Other gait assessment

Along with the wide application of wearable sensors in gait analysis, some commercialized wearable sensors are commercially available in the market. Xsens 3D motion tracking (www.xsens.com) uses sensors fusion and provides information of six degrees of freedom, force and moment to estimate joint moments and powers of the ankle. The 3D displacements of center of mass during gait are calculated using measurements of the sensor system (Schepers et al. 2009). Other commercially available systems are Shimmer Sensing (www.shimmersensing.com), iSen (www.stt-systems.com), Synertial Motion Capture (www.synertial.com), Rokoko (www.rokoko.com), Trivisio (www.trivisio.com), Polhemus (https://polhemus.com), Inertial Labs (https://inertiallabs.com), Eliko (www.eliko.ee), Motion Shadow (www.motionshadow.com), LaiTronic (http://www.laitronic.com) and Perception Neuron (https://neuronmocap.com) etc. These are also expensive, restricted movement, predefined marker configuration and capture smaller area. Although several low cost instruments e.g. Kinect (Auvinet et al. 2017) and camera (Krishnan et al. 2015) are appealing, they are restricted to a small capture volume, lead to a lack of privacy and only a few gait parameters can be analysed. Therefore, an affordable, user-friendly, portable multi-sensor based gait analysis system which is able to capture long time data and allow comprehensive gait information are potentially important for users at home and in clinics.

2.3. Survey on wearable sensor based gait analysis

The primary purpose of this chapter is to review the current status of gait analysis technology based on wearable sensors. Therefore, this research is centred and focused to clinical applications on achieving qualitative objective measurements of the different parameters that characteristics of gait using wearable sensors. Hence, the literature covers every step for developing an automatic gait assessment system from sensor input to evaluation. As the literature review on this area is vast, therefore much attention has been given to wearable sensors.

2.3.1. Sensor selection

The sensor selection is typically used as a starting point of any data analysis system. For an automatic gait assessment system, a variety of wearable, ambient, camera and remote sensors are available and many of them are integrated into the garment's fabric, simultaneously collecting signals in a non-invasive and unobtrusive way. There are most commonly used wearable sensors such as accelerometer, gyroscope, magnetometer sensors, ultrasonic sensors, flexible goniometer, electromagnetic tracking system, sensing fabric, force sensor, strain gauges, inclinometers, electromyography so on are used for gait analysis (Tao et al. 2012; Muro-de-la-Herran et al. 2014; Agostini et al. 2015; Mukhopadhyay 2015; Chen et al. 2016). Many of these sensors information is used to perform the gait analysis e.g. the temporal characteristics of gait are collected and estimated from body-worn accelerometers and pressure sensors inside footwear (Lee et al. 2007; Khan et al. 2010; Rodríguez-Martín et al. 2013; Okuda et al. 2016). The goniometric measurements at the hip, knee, and ankle joints are used to detect five different gait phases (Chizeck 1997). The three-dimensional ground reaction forces are estimated from the insole based on foot pressure data (Cordero et al. 2004). With the development of motion-sensing technology, an increasing number of wearable sensors will be developed for gait analysis in the future (Tao et al. 2012). Therefore, gait analysis using wearable sensors are becoming popular and widely used in the clinical field. Different sensors characteristics, application, accuracy and price is studied in (Muro-de-la-Herran et al. 2014).The basic principles and features of these most commonly used sensors are described in the following.

2.3.1.1. Inertial measurement unit

IMUs are electronic devices that measure an object's velocity, acceleration, orientation, and gravitational forces, using a combination of accelerometers and gyroscopes and sometimes magnetometers (Morrison 1987). IMU has a 3-axis accelerometer, a 3-axis gyroscopes and a 3-axis magnetometer. IMU has been used in different spatiotemporal and kinematic assessments of gait such as monitoring of post-operative gait abnormalities (Hanly et al. 2016), stride variability (Urbanek et al. 2017), measurement of gait asymmetry (Esser et al. 2012), fall-related gait characteristics measured on a treadmill in daily life (Rispens et al. 2016), nature of parkinsonian gait (Okuda et al. 2016) and human walking foot trajectory (Kitagawa and Ogihara 2016). IMUs are relatively inexpensive with low power consumption which allows long time data collection (virtually unlimited number of steps to be evaluated), and Bluetooth™ embedded within IMU enables portability, and provides the ability to evaluate gait and movement disorders outside the constrained environments of the clinic and research laboratory. Therefore, the use of IMU sensor in gait analysis has become increasingly popular as it is easily adopted to clinical settings as well as to patients' homes or elsewhere in the community where ambulation normally takes place. Although, IMU sensor based gait analysis methods are available, the specific objective of gait analysis for users at home and in clinical areas is actually found in only a few studies. Many investigations are carried out using a single gait parameter or applying simple statistical methods for comparisons. Studies also include a small number of participants.

2.3.1.2. Accelerometer

Accelerometer is an electronic device for measuring the acceleration of a moving object or vibration of a body. Three common types of accelerometers are available, namely, piezoelectric, piezoresistive, and capacitive accelerometers (Westbrook 1994). It consists of different parts and works in many ways. The piezoelectric effect is widely used form of accelerometer which uses microscopic crystal structures that become stressed due to accelerative forces. These crystals create a voltage from the stress, and the accelerometer interprets the voltage to determine velocity and orientation.

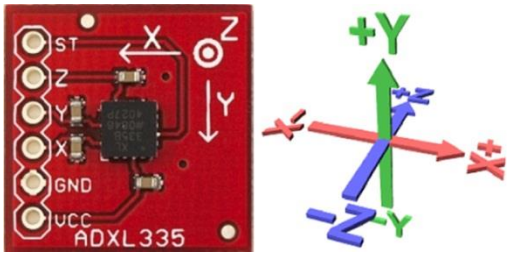

Figure 2.2: ADXL 335 Accelerometer Device (Anon. Accessed on 27/01/2016)

Again, the capacitance accelerometer senses changes in capacitance between microstructures located next to the device. If an accelerative force moves in one of these structures, the capacitance will change and the accelerometer will translate that capacitance to voltage for interpretation which means measuring of the change in velocity or speed divided by time. The movement data towards three dimensional coordinates *x*, *y* and *z* are generated by accelerometer is measure the motion status in the human gait (Urbanek et al. 2017). There are many wearable accelerometer sensor manufactures around the world and among them Actismile (http://www.actismile.ch/index.php/en/), Activinsights (http://www.geneactiv.org/), Alpenheat (http://alpenheat.com/) and Adafruith (http://cpc.farnell.com/adafruit-industries) are based in UK.

2.3.1.3. Gyroscope

Gyroscope is a device consisting of a wheel or disc mounted so that it can spin rapidly about an axis which is free to alter in direction. The orientation of the axis is not affected by tilting of the mounting, so gyroscopes can be used to provide stability or maintain a reference direction in navigation systems, automatic pilots, and stabilizers (Anon. 2016).

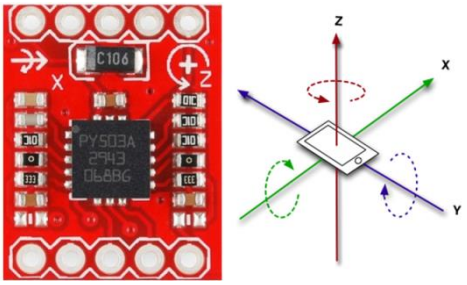

Figure 2.3: Gyroscope Device (Anon. Accessed on 27/01/2016)

Gyroscope gives angular velocity which changes in rotational angle per unit of time termed degrees per second. The working principal is based on the concept of measuring the Coriolis force, which is an apparent force proportional to the angular rate of rotation in a rotating

reference frame. By detecting the linear motion from the Coriolis effort and performing an integration of the gyroscopic signal, the angular rate can be obtained (Tao et al. 2012). Gyroscope is used for the measurement of the motion and posture of the human segment in gait analysis (Tong and Granat 1999; Greene et al. 2010a). Although, gyroscope based motion and posture of the human segment in gait analysis methods are available, the specific objective of gait analysis for users at home and in clinical areas is actually found in only a few studies. It is mentioned earlier that gait change is multi-contributing factors, only one sensor information is not sufficient for addressing objective gait assessment.

2.3.1.4. Magnetometer

A magnetometer measures magnetic fields as the earth has two magnetic poles, it can be used as a compass to determine absolute orientation in the NESW plane. If a magnetic flux (magnetic field) is not applied, the current flows straight through a plate. A Lorentz force proportional to the magnetic flux density will deflect the current path if a magnetic flux is applied. As the current path is deflected, the current flows through the plate for a longer distance, causing the resistance to be increased. That is, the magneto resistive effect refers to the change in the resistivity of a current carrying ferromagnetic material resulting from a magnetic field, with the resistance change proportional to the tilt angle in relation to the magnetic field direction (Graham et al. 2004). The magnetic North or the vertical axis of a body segment in relation to in the gait analysis can be estimated based on the magneto resistive sensors information (O'Donovan et al. 2007; Choi et al. 2008). Although, magnetometer based orientation changes of the human body segment in gait analysis methods are available, the specific objective of gait analysis for users at home and in clinical areas is actually found in only a few studies. It is mentioned earlier that gait change is multi-contributing factors, only one sensor information is not sufficient for addressing objective gait assessment.

2.3.1.5. Barometric pressure

Barometric pressure is the measurement of air pressure in the atmosphere, specifically the measurement of the weight exerted by air molecules at a given point on earth. Researchers (Nam and Park 2013; Moncada-Torres et al. 2014) used acceleration and barometric pressure information from different body locations for activity classification. Barometric pressure changes

constantly and is always different depending on where the reading takes place. Not many research has been conducted for gait analysis using barometric pressure.

2.3.1.6. Pressure and force sensors

Force sensors measure the ground reaction force under the foot and return a current or voltage proportional to the pressure measured. Pressure sensors measure the force applied on the sensor without taking into account the components of this force on all the axes. The most widely used models of this type are capacitive, resistive piezoelectric and piezo resistive sensors. This type of sensor is small and can be integrated into instrumented shoes (Howell et al. 2013; Rösevall et al. 2014; Rosa et al. 2015). Such shoe where an insole containing 12 capacitive sensors shows a high correlation to the simultaneous measurements from a clinical motion analysis laboratory (Howell et al. 2013). Another shoe is developed that is sensitive to normal and shear loads and uses reflected light intensity to detect the proximity of a reflective material (Lincoln et al. 2012).

2.3.1.7. Summary of wearable gait analysis sensors

Based on the literature review, a list of wearable gait analysis sensors is presented in a Table 2.2

Table 2.2: Wearable sensors for gait analysis

Index	Sensor	Parameters	Reference
1.	Accelerometer	X, Y and Z axes	(Foster et al. 2005; Brandes et al. 2006; Lee et al. 2007; Song et al. 2007; Kavanagh 2009; Mladenov and Mock 2009; Chung et al. 2012; Brajdic and Harle 2013; Rebula et al. 2013; Boutaayamou et al. 2015; Urbanek et al. 2017)
2.	Gyroscope	Rotation along X, Y and Z axes	(Tong and Granat 1999; Greene et al. 2010a; Tao et al. 2012)
3.	Magnetometer	Magnetic field along X, Y and Z axes	(Graham et al. 2004; O'Donovan et al. 2007; Choi et al. 2008)
4.	IMU	3-axis accelerometer, 3-axis gyroscopes and 3-axis magnetometer	(Esser et al. 2012; Hanly et al. 2016; Kitagawa and Ogihara 2016; Okuda et al. 2016; Rispens et al. 2016; Urbanek et al. 2017)
5.	Barometric pressure	Atmospheric air pressure	(Nam and Park 2013; Moncada-Torres et al. 2014)
6.	Pressure and Force Sensors	Force per unit area	(Lincoln et al. 2012; Howell et al. 2013; Rösevall et al. 2014; Rosa et al. 2015)

7.	Electromyography (EMG)	Electrical impulse	(Erni and Colombo 1998; Rainoldi et al. 2004; Frigo and Crenna 2009)
8.	Goniometers	Relative rotation	(Donno et al. 2008; Laskoski et al. 2009; Domínguez et al. 2013)
9.	Global Positioning System	Location API	(Cavallo et al. 2005; Terrier and Schutz 2005)
10.	Microphone	Audio	(Li et al. 2012)
11.	Radar	Feedback signal	(Otero 2005; Liang et al. 2011; Liang et al. 2014; Wu et al. 2015)
12.	Electrocardiogram (ECG)	Electrical impulse	(Heck and van Dongen 2008)
13.	Ultrasonic Sensors	Sound reflection	(Wahab and Bakar 2011; Maki et al. 2012)
14.	Sensing Fabric	Fabric flexibility	(Scilingo et al. 2003; Tognetti et al. 2007)
15.	Photoplethysmographic	Physical information	(Shaltis et al. 2006; Wood and Asada 2007)
16.	Radio-frequency identification (RFID)	Electromagnetic field	(Chen and Lin 2010; Krigslund et al. 2013)

2.3.2. Sensor placing location

Studies in wearable sensor based gait analysis have been carried out investigating the use of sensors on different body locations. The locations where the sensors are placed and how the sensors are attached to those locations are important for collecting accurate reliable robust data. Wearable sensors can be placed on different body locations whose movements are being studied. It also depends on the interest for the purpose of data collection, for example, in many cases sensors are commonly placed on the sternum (Najafi et al. 2003) lower back (Meijer et al. 1991), waist (Karantonis et al. 2006) to measure the whole-body movement and other locations presented in (Jarchi et al. 2018). Many studies show that the sensors are mounted at waist because of the fact that the waist is close to the center of mass of a whole human body and the torso occupies the most mass of a human body (Yang and Hsu 2010). This implies that the user movement measured by a single sensor at this location can better represent the major human motion. Therefore, the sensors are attached to or detached from a belt around waist level. Hence, sensors placement at the waist causes less constraint in body movement and discomfort can be minimized as well. A range of basic daily activities, including walking, postures and activity transitions can be classified according to the accelerations measured from a waist-worn accelerometer (Karantonis et al. 2006; Yang and Hsu 2010). The ergonomic guideline of "wearability" that the interaction between the human body and wearable objects is described in

(Gemperle et al. 1998). The proper locations of a human body for unobtrusive sensor placement is generalized using "wearability map". These locations include collar area, rear of upper arm, forearm, front and rear sides of ribcage, waist, leg, arm, wrist, upper arm, upper torso, shoulder, hip, ankle, chest, hand, thigh, trunk, shank, shin, feet, abdominal, lower back and top of the foot. Current research on different body locations of placing sensors for gait analysis is presented in Table 2.3.

Table 2.3: Location of placing wearable sensors for gait analysis

Sensor	Locations	Parameters	Application	Reference
IMU	Thigs, shanks, feet	Flexion or extension angle, gait cycle, balance level measured by joint angle at particular gait events	Balance and knee extensibility of hemiplegic gait	(Guo et al. 2013)
IMU, geo-magnetic	Barefoot soles, ankles, knees, hip joints	Joint kinematics, shank angular velocity, toe trajectory, spatiotemporal parameters	reconstructed joint kinematics difference between normal and overweight/ obese subjects	(Agostini et al. 2017)
IMU	Top of feet	Stance time, swing time, turning rate, stride length, clearance, cycle time, cadence, speed	non-hospital settings for neurological disorders	(Tunca et al. 2017)
IMU	Wrists, both shanks and waist	Temporal features, gait complexity, gait	Assessment of multiple sclerosis	(Chen 2013)

		stability, gait speed		
IMU	Right thigh, right shank and both feet	Cadence, step length, thigh and knee angle of right leg, gait events	Gait phase detection for dementia patients	(Meng et al. 2013)
gyroscopes	Both shanks and both wrists	Symbolic symmetry index	Movement symmetry detection in early Parkinsonian gait	(Sant'Anna et al. 2011)
IMU and Kinect	forearms, arms, thighs, shanks, chest	Knee flexion, joint position and angle	Whole body tracking	(Destelle et al. 2014)
IMU and Kinect	Thigh, shank	knee flexion angles	functional rehabilitation movements	(Tannous et al. 2016)
IMU	Bilateral shanks, feet	Ankle joint angle, range of motion	Assessing efficacy of ankle-foot orthoses for children with cerebral palsy	(Chen et al. 2011)
Accelerometer, gyroscope	Shoes, waist	No of strides, walking time, stride length, cadence, swing time, stance time	Gait and balance test for patients with Alzheimer' disease	(Hsu et al. 2014)
IMU	Back	Step and stride length, gait speed, stride duration, stance and swing time,	Assessing the potential benefit of ankle-foot orthoses for patients with	(Benedetti et al. 2011)

		double support time, stride length and height ratio, cadence, symmetry	hemiplegia	
IMU	Both shoes	Reconstructed gait trajectory, walking speed, stride length, foot swing time, stance time	Characterizing hemiplegic gait in post-stroke patients	(Wang et al. 2013)
Accelerometer, gyroscope	Wrists, shanks, waist	Cadence, double stance time, gait speed, gait stability	Differential diagnosis for normal pressure hydrocephalus	(Chen et al. 2012)
IMU	Shank	Cadence, step length, symmetry of strides	Detection of freezing of gait episode in Parkinson's desease	(Azevedo Coste et al. 2014)
Accelerometer, gyroscope	pelvis	Speed, cadence, step time, step length, step irregularity, step asymmetry, range of motion	Gait, sit-to-stance transfers and step-up transfers in patients after knee operations	(Bolink et al. 2012)
Accelerometer, gyroscope	Dorsal spine	Autocorrelation coefficient, walking speed	Walking speed and symmetry assessment after hip arthroplasty	(Gong et al. 2015)
Accelerometer	Lower back	Improved local dynamic stability	Stability to differentiate	(Ihlen et al. 2016)

			fallers and non-fallers	
Plantar force sensors	Planter surface of the foot	Vibrotactile	Provide simultaneous vibration based on the detected gait phase transitions	(Crea et al. 2015)
IMU	Feet	ankle joint clearance	robust foot clearance estimation	(Benoussaad et al. 2015)
Goniometer, accelerometer	Thigh, shank	flexion-extension angles	Daily Life	(Tognetti et al. 2015)
force-sensitive resistors, IMU	Insoles	gait phases, loading response time, mid-stance time, terminal stance time, pre-swing time, swing time	healthy ambulatory system	(González et al. 2015)
IMU	T4 position at back	Voltage	patients with balance disorders vs. normal subjects	(Nukala et al. 2016)

These locations have common characteristics of similar area for men and women, a relatively larger continuous surface, and low movement and flexibility. The output of a wearable sensor depends on the position at which it is placed, its orientation, posture, and activity being performed (Merryn et al. 2004). Summary of wearable sensor placing location and accuracy is presented details in (Moncada-Torres et al. 2014). Various factors can affect the signal input and output. For example, during locomotion, movement of clothes can cause interference with accelerometer output (Bouten et al. 1997). There can be vibration or momentum noise if the sensor is not attached properly. Attaching the sensor with a belt or keeping in a pocket can also

induce relative motion interference (Plasqui and Westerterp 2007). To increase the reliability and validity of automatic feature extraction from gait parameters for gait analysis, the influence of sensor location and attachment has to be determined. Further study on the best location for sensor placement is therefore required (Intille et al. 2012). Therefore, an investigation for placing the sensor on different foot locations is conducted to find the optimal location of placing the sensor for collection accurate, reliable and robust data described in Chapter 3.

2.3.3. Sensor fusion

Sensor fusion is the technique to combine multiple sensor information for the purpose of improving performance of the system. Combining data from multiple sensors corrects for the deficiencies of the individual sensors to calculate accurate position and orientation information (Kramer 1997). The technique of sensor fusion can be a simple idea like concatenate all sensor information together and treat it as one single source or more complicated by associating different sources using probability theory. The details of sensor data fusion is presented in (Llinas and Hall 1998) where wearable sensor based gait analysis use more than one sensor to obtain movement and orientation information (Casamassima et al. 2014; Agostini et al. 2015; Mukhopadhyay 2015; Cornacchia et al. 2017). A list of sensor fusion algorithm is presented in Table 2.4.

Table 2.4: Sensors fusion algorithm, fusion output and application

Sensors Fusion	Algorithm	Fusion output	Application	Reference
IMU, Kinect	Weighted averaging	Joint position and angle	body tracking	(Glonek and Wojciechowski 2016)
IMU, Kinect	Kalman filter	Joint position and angle	body tracking	(Tian et al. 2015)
IMU, Kinect	Linear Kalman filter	Joint position	body tracking	(Kalkbrenner et al. 2014)
IMU, Kinect	Multi-rate linear Kalman filter	Joint position	Hand tracking	(Feng and Murray-Smith 2014)
IMU, Kinect	Separate	Joint position	body	(Destelle et al. 2014)

		and angle	tracking	
IMUs	neural networks and the hidden Markov models	Transitional and displacement activities	elderly daily activity classification	(Zhu and Sheng 2009)

For feature fusion, data from different wearable sensors are combined together and pass through a single classifier. Such approach has advantage that more information is obtained thus recognition accuracy may be improved. However, research (Gunatilaka and Baertlein 2001) shows that sensor fusion at feature level may be difficult to perform for non-commensurate data i.e. data that are not comparable. Sensor information from different sensors are different in form and size. For example, captured image from camera represents in pixel information and accelerometer provides movement information respective to *x, y* and *z* axis. Again, different sampling rate or deployment in different platform makes the fusion more complicated. Therefore, an appropriate pre-processing technique e.g. data normalisation and feature reduction or selection needs to be carried out to normalise and reduce the size of the feature space. This approach is normally employed due to its simplicity. Again, the use of fused multi-sensor based synchronous data collection for automatic gait features extraction of gait assessment has not been reported. In order to use accurate quantitative gait monitoring in clinical screening and research, multi-sensor based synchronous data collection platform for gait assessment is required which will provide facility to measure in clinic and home.

2.3.4. Feature selection

After collecting raw data from different sensors, pre-processing of collected data is essential to minimize the occurrence of different noise, motion artefact and sensor errors. Pre-processing involves filtering unusual data to remove artefacts and remove high frequency noise (Daby et al. 2013). There are statistical tools like mean, standard deviation, peak-to-peak amplitude, fast Fourier transform (FFT) coefficients, wavelet features, power spectral density (PSD), and low-pass or high-pass filtering etc commonly used for raw data processing. When the data is collected from different wearable and ambient sensors, normalization and synchronization of sensory data is also important. The appropriate selection of the pre-processing for input data depends on the

data set and type of noise in the data set. Michael Marschollek et al. (Marschollek et al. 2008) used Waikato Environment for Knowledge Analysis (WEKA) toolkit in R to filter raw accelerometer data with a 0.25-4 Hz band-pass Butterworth filter for gait patterns of elderly persons. Accelerometer data is collected where the raw data includes acceleration due to body movement, gravitational acceleration, external vibrations, not produced by the body itself (e. g. , resulting from vehicles) and accelerations due to bouncing of the sensor against other objects, eventually resulting in mechanical resonance (Yi et al. 2012). The first and second sources are directly related to intentional movement of the body and third and fourth are considered as noise which are attenuated by using a median filter with n=3 results a nice smoothing effect. Accelerometer data is collected and applied a linear interpolated to match 20 Hz on each 10 second clips (Albert et al. 2012). Researcher (Popescu et al. 2008) used acoustic data recorded on a laptop using a National Instruments data acquisition card NI 9162 and applied Wiener filter to minimize noise. The pre-processing techniques from different sensors are almost similar in different areas like bio-data, medical data and environmental data. Researchers (Daby et al. 2013; Hadi et al. 2013) addressed the detail challenges of pre-processing area in healthcare including formatting, normalization and synchronization of sensory collected data. Moreover, there is no real time detailed scenario data based on these challenges presented. After the pre-processing, post-processing is the next step to reduce the number of features by applying feature selection/extraction and dimensionality reduction techniques.

Discovering the most important characteristics that identically represent the originality of that sensor from pre-processed dataset is another important task for automatic gait assessment. Due to the magnitude and complexity of raw data from wearable or ambient sensors, the feature extraction provides a meaningful representation of the sensor data which can formulate the relation of the raw data with the expected knowledge for decision making. A summary table is shown for the most commonly used features of each wearable sensor (Hadi et al. 2013). General measurement of gait features includes cadence, stride length and gait velocity (Michael and Whittle 2002), alone or in combination with other outcome measures such as stride to stride variability assessed by an accelerometer, gyroscope and magnetometer (Novak et al. 2013; Afzal et al. 2015; Boutaayamou et al. 2015; Urbanek et al. 2017). Researchers presented a set of 31 gait variables in (Thingstad et al. 2015) and 16 variables were investigated. Stride-to-stride variability (Hausdorff et al. 1998) is commonly used to quantify walking consistency which is strongly associated with motor ability (Zeni and Higginson 2010), mild cognitive impairment (Beauchet et

al. 2013), dementia (IJmker and Lamoth 2012) and stroke (Balasubramanian et al. 2009). Research into accelerometer based gait parameters such as times of stance, swing, single support and double (Lee et al. 2007); stride length and stance phase (Chung et al. 2012); gait velocity, stride duration, cadence and step length (Kavanagh 2009); step number, moving distances, every step instant speed and average speed (Song et al. 2007); step counting (Foster et al. 2005; Mladenov and Mock 2009; Brajdic and Harle 2013); times of heel strike, toe strike, heel-off, and toe-off (Boutaayamou et al. 2015); stride length and duration (Rebula et al. 2013); walking distance, time and speed (Brandes et al. 2006) were investigated. Researchers also used portable gait analysis system based on force-sensitive resistor (FSR) placed in insoles to detect ground contact and estimate stance time for gait asymmetry (Afzal et al. 2015), Microsoft Kinect based gait asymmetry (Auvinet et al. 2017), IMU and pressure sensitive shoe insole based gait onset and toe-off detection (Novak et al. 2013), IMU-based knee flexion/extension angle measurements (Seel et al. 2014) and gait asymmetry using gyroscopes (Gouwanda and Arosha 2011). The current gait features and disorder type for different applications is presented in Table 2.5.

Table 2.5: Current research on gait features and disorder type for different applications (Esser et al. 2013; Muro-de-la-Herran et al. 2014; Chen et al. 2016; Mikos et al. 2017)

Gait feature	Disorder type	Application
Stride time	Gait stability	Clinics, sports, research
Stride length	Parkinson's disease freezing of gait	Clinics, sports, research
Stride velocity	Stability	Clinics, sports, research
Stance time	Antalgic gait, hesitation	Clinics
Swing time	Difficulty in clearing off at toe off, difficulty in swinging	Clinics
Swing length	Stability	Clinics
Step length	Parkinson gait, small steps, gait with little steps	Clinics
Step width	Cerebellar gait (ataxic gait), wide base, extremely narrow base	Clinics

Step height	Peripheral neuropathic gait, foot drop, high stepping gait	Clinics
Gait speed	Slow walking	Clinics
Cadence	Slow walking, gait efficiency	Clinics
Stride-stride variability	Abnormal rhythm of gait	Clinics
Knee joint angle	Crouch gait, drop foot, equine gait, stiff knee	Clinics
Ankle joint angle	Equine gait, crouch gait	Clinics
No. of steps during turning	Difficulty with turning	Clinics
Hip flexion	Myopathic gait, waddling gait, excessive hip sway, drop of pelvis	Clinics
Heel-strike amplitude, ground reaction forces	Sensory gait, stomping, stamping	Clinics
Motion signal distribution	Tremor	Clinics, sports
Double support time	Steadiness	Clinics, sports, research
Bilateral sensor comparison	Gait asymmetry	Clinics, sports, research
Muscle force from EMG	Muscle weakness, abnormal muscle activity	Clinics, sports, research

2.3.5. Quantification and visualization

The available common approaches for quantifying the temporal and spatial of gait are presented in Table 2.6.

Table 2.6: Equations used to calculate and quantify gait

Index	Formula name	Equation
1.	Symmetry index (SI) (Robinson et al. 1987)	$SI(\%)=\frac{RightLeg-LeftLeg}{0.5(RightLeg+LeftLeg)}*100$

2.	Symmetry ratio (SR) (Seliktar and Mizrahi 1986)	$SR(\%)=\frac{RightLeg}{LeftLeg}*100$
3.	Ratio (Ia) (Vagenas and Hoshizaki 1992)	$Ia(\%)=\frac{LeftLeg-RightLeg}{\max(LeftLeg,RightLeg)}*100$
4.	Symmetry index (Agrawal et al. 2009)	$SI(\%)=100-\left\|100*\left(\frac{\|W_I\|-\|W_P\|}{\|W_I\|+\|W_P\|}\right)\right\|$ W_I=Work done by intact limb W_P=Work done by prosthetic limb
5.	Gait asymmetry (GA) (Plotnik et al. 2005; Plotnik et al. 2007)	$GA=\left\|\ln\left\{\frac{\min(RightLeg,LeftLeg)}{\min(RightLeg,LeftLeg)}\right\}\right\|$
6.	Symmetry angle (SA) (Zifchock et al. 2008)	a) $SI_{left}=\frac{\|(LeftLeg-RightLeg)\|}{LeftLeg}*100\%$ b) $SI_{right}=\frac{\|(LeftLeg-RightLeg)\|}{RightLeg}*100\%$ c) $SI_{left}=\frac{LeftLeg-RightLeg}{avg(LeftLeg,RightLeg)}*100\%$ d) $SA(\%)=\frac{(45^\circ-\arctan(LeftLeg/RightLeg))}{90^\circ}*100\%$
7.	Trend symmetry (TA) (Crenshaw and Richards 2006)	$TA=100*mean_n\left\{\frac{\text{var}(Xrot_L^n)}{\text{var}(Xrot_R^n)}\right\}$ where $Xrot_L^n=Xm_L^n\cos(\theta)-Xm_R^n\sin(\theta)$ $Xrot_R^n=Xm_R^n\cos(\theta)+Xm_L^n\sin(\theta)$ θ is the angle between the first eigenvector of

		$M = \left[Xm_R^n, Xm_N^n\right]$ and the horizontal axis, $Xm_{R(L)}^n = X_{R(L)}^n - mean(X_{R(L)}^n)$, and $Xm_{R(L)}^n$ is the signal from the right (left) side for cycle *n*
8.	Latency corrected ensemble average (LCEA) (Miller et al. 1996; Sant'Anna et al. 2011)	LCEA=$100 * \max\left\{\frac{\rho_{RL}}{\sqrt{\rho_{RR} * \rho_{LL}}}\right\}$ where ρ_{RL} is the cross-correlation between $LCEA_R$ and $LCEA_L$, $\rho_{RR(LL)}$ is the autocorrelation of $LCEA_{R(L)}$, $LCEA_{R(L)}$ is the column-wise average of *LxN* matrix $S_{R(L)}$ and each row of $S_{R(L)}$ contains the signal for once cycle of the data, normalized to *L* samples. *N* is the total number of cycles in the dataset for the right (left) side
9.	Relative asymmetry index (RAI) (Forczek and Staszkiewicz 2012)	RAI= $\frac{\overline{X}}{Y} * 100\%$ where $\overline{X} = \frac{\sum_{i=1}^{i=n} \lvert R_i - L_i \rvert}{\%GC}$ $\overline{X}$ is the average difference between the values noted from the right and left limbs in a given phase of the gait cycle. Y is total range of motion of the angular changes in the given phases. *R*, *L* instantaneous value of the angle individual joints in the right and left lower limb, *%GC* relative duration of the given phase in the gait cycle.
10.	Asymmetry (A) (Carabello et al. 2010)	A(%)= $\frac{\lvert WeakLegValue - StrongLegValue \rvert}{StrongLegValue} * 100$

11.	Vertical energy ratio (ERz) (Audigié et al. 2002)	ERz(%)= $\left(\frac{amp2^2}{amp1^2}+amp2^2\right)$*100% where amp2 is the symmetrical component and amp1 is the asymmetrical component estimated using Fourier analysis.
12.	Kinematic symmetry index (KSI) (Pourcelot et al. 1997)	KSI= $\overline{X}=\frac{\sum\left\|\left(R_j-MeanR\right)*\left(L_j-MeanL\right)\right\|^2}{\sum\left(R_j-MeanR\right)^2*\sum\left(L_j-MeanL\right)^2}$ where R_j and L_j represent right and left displacement values at frame number *j*. *MeanR* and *MeanL* are the mean displacement values across the stride.
13.	Symmetry indices (Hodt-Billington et al. 2011)	$SI=\left\|1-\frac{Unaffected\,Limb}{Affected\,Limb}\right\|$
14.	Symmetry indices (Brandstater et al. 1983)	$SI=\left\|1-\frac{Affected\,Limb}{Unaffected\,Limb}\right\|$
15.	Symmetry indices (Hodt-Billington et al. 2011)	$SI=\left\|1-\frac{LimbWithLowerValue}{LimbWithHigherValue}\right\|$

However, each approach has advantages and disadvantages (Sadeghi et al. 2000). Gait abnormality is frequently reported as present or not present which may not satisfy scientific criteria of reliability and validity (Archer et al. 2006). Thus, an arbitrary cut-off value of 10% deviation from perfect asymmetry has been used as a criterion of asymmetry in gait assessment (Robinson et al. 1987; Balasubramanian et al. 2009) This was later criticized due to its non-parameter specific nature (Herzog et al. 1989). Other previously used criteria to describe the absence or presence of gait asymmetry include sensitivity and specificity of measurements of what? (Leddy et al. 2011), the use of 95% confidence intervals where gait asymmetry within the limits of a 95% CI obtained in a healthy population would define able-bodied gait, while gait asymmetry outside the 95% CI would define pathologic gait) (Herzog et al. 1989), and significant

limbs difference (Sadeghi et al. 2000) etc. Although, there are many approaches for quantifying gait symmetry, a user friendly visualization of gait asymmetry is not readily available. Researchers (Manal and Stanhope 2004) proposed a visual representation of examining gait change behavior where the method are presented in the context of clinical gait analysis and displayed movement pattern deviations relative to normative data by color-coding the magnitude and the direction of the deviation. This approach provides a single-page summary of all the deviation magnitudes and can be displayed simultaneously in a manner of concise, visually effective and reduces complexity. However, quantitative information of the gait quantification for the comparison and analysis of complex movement patterns are missing and it does not examine changes in symmetry of bilateral parameters. Common approaches for the quantification of gait give the numerical values of parameters such as symmetry index, symmetry ratio, symmetry angle etc. It may be difficult for users to understand those numerical values. In order to conveniently use quantitative gait monitoring for users, an affordable visualization tool is useful to provide a facility for their use in clinic and at home. This will provide the facility to measure gait asymmetry in both a clinic and at home. To date, an automatic real time gait symmetry visualization technique based on fused accelerometer and gyroscope data has not been reported. After gait quantification, validation of those features are important for accuracy, reliability and robustness.

2.3.6. Feature selection methods

There are many approaches for dimensionality reduction are principle component analysis (PCA), independent component analysis (ICA), linear discriminate analysis (LDA), threshold based rule, analysis based variance (ANOVA), and Fourier transformations (Achmad and Bo-Suk 2007). Due to easy interpretation, simple logistic regression algorithm is applied for classifier using a combined machine learning algorithms WEKA Workbench (Waikato Environment for Knowledge Analysis, version 3.4.7) (Marschollek et al. 2008). Signal Magnitude Area (SMA) is applied to distinguish between periods of user activity and rest which characterizes the degree of change of human movement as the high value indicates violent motion state changes (Yi et al. 2012). The current feature selection methods of gait analysis are summarised in Table 2.7.

Table 2.7: Current feature selection methods of gait analysis

Features	Method	Procedure	Result	Reference
Ground-reaction force	Genetic algorithm	Verify the combination of genetic algorithm with artificial neural network against the back-propagation algorithm for more accurate in classification of the gait patterns of patients with ankle arthrodesis and healthy subjects	Genetic algorithm with artificial neural network model classified with accuracy up 98.7%, due to selection of the 5 most relevant features from 9 features, while the back-propagation algorithm (without feature selection method) presented recognition rates of 89.7%	(Su and Wu 2000)
Spatiotemporal parameters of the segment motion	principal component analysis	Select the spatial and temporal information more relevant in the classification of distinct gait patterns (elderly and young healthy subjects)	Maximum accuracy (95.8%) was reached when using 36 to 39 PCs. The worst distinction between elderly and young gait patterns had an accuracy of 58% using only 10 PCs	(Eskofier et al. 2013)
Minimum toe clearance values	Hill-climbing	Computational cost reduction using the classification with SVM and extract the most significant features in the	An accuracy of 100% when 512, 256, 128 64 and 32 features combined. The worst accuracy of classification	(Lai et al. 2008)

		distinction between tripping patterns from healthy patterns of adults	was 52.17% when are only used 8 features	
biomechanical features that best characterize the differences between knee osteoarthritis and control groups	principal component analysis	Magnitude of flexion angle, range of motion, phase shift of flexion angle, magnitude of flexion moment during stance, amplitude of flexion moment, phase shift of flexion moment, magnitude of adduction moment during stance, magnitude of adduction moment in first half of stance of the knee	Differences in the gait patterns of patients with knee osteoarthritis and healthy subjects are characterized by 4 PCs from 8 features. The distinction of the both gait patterns with 4 PCs resulted in an accuracy of 92%	(Deluzio and Astephen 2007)
Cadence, symmetry and step regularity in vertical and anterior-posterior directions, root mean square, integral of power spectral density and stride regularity in vertical, medio-lateral, anterior-posterior directions	Hill-climbing	Assess the use of hill-climbing method leads to a smaller subset of features to distinguish the difference between younger and older adults locomotion by means of support vector machine, multilayer perceptron, Naïve	Hill-climbing shows increasing the accuracy from 82.9% to 84.9% due to dimensional reduction of 14 to 10 gait features	(Chan et al. 2013)

		Bayes and decision tree classifiers		
Pulse rate, respiration rate, skin conductance level, skin conductance response, skin temperature	principal component analysis	Possibility of reducing number of features in the evaluation of distinct machine learning approaches in the estimation of physiological states in a robot-assisted training	Best classification (91.3% of accuracy) is achieved using the 3 PCs (using feature extraction) and 5 PCs (no feature extraction) in the support vector machine classifier, meanwhile the worst classification (49.52% of accuracy) was performed by Naïve Bayes with 1st PC	(Badesa et al. 2014)
Stride length, stride duration, gait velocity, single support duration, stance duration, swing duration, gait cadence, and hip, knee and ankle angles and angular range of motion during the stance phases, swing phases and three intervals (heel contact to toe contact, toe contact to heel rise,	principal component analysis and kernel based principal component analysis	Evaluate the principal component analysis and kernel based principal component analysis for extracting more significant gait features than only principal component analysis in the classification of young-elderly gait patterns	The combination of principal component analysis and kernel based principal component analysis; and support vector machine achieved best performance (accuracy of 91%) than the combination of principal component analysis with support vector machine (accuracy of 87%),	(Wu et al. 2007)

and heel rise to toe-off			have been selected 17 and 14 PCs from the 36 gait features, respectively. No implementation of principal component analysis and principal component analysis and kernel based principal component analysis resulted in an support vector machine performance of 85%	

2.3.7. Feature classification

A large number of data is accumulated from different sensors and features are identified mentioned in the Section 2.4.3 and 2.4.4. This data from different sensors is multivariate with possible dependencies. In order to make sense of the data, appropriate data processing techniques are essential for objective gait assessment. Threshold, machine learning, context-awareness and other algorithm based methods have been implemented in wearable gait analysis. The common techniques of feature classification are described in the following.

Support Vector Machines (SVM) is based on the concept of decision planes that define decision boundaries. It can classify unseen information by deriving selected features and constructing a higher dimensional place to separate the data points into two classes in order to make a decision model. SVM is applied for the automatic recognition of young-old gait types from their respective gait-patterns (Begg et al. 2005). The effectiveness of a wavelet based multi-scale analysis is used of a gait variable for developing a model using SVMs for screening of balance impairments in the elderly (Khandoker et al. 2007). SVM methods are also used for ECG, HR and SpO2. SVM classifier is used for congestive heart failure from ECG signals (Ken Ying-Kai Liao et al. 2015). SVM methods are generally proposed for anomaly detection and

decision making tasks in healthcare services. However, SVM is not an appropriate method to integrate domain knowledge in order to use metadata symbolic knowledge seamlessly with the measurements from the sensors and like other classifiers, SVM could not be applied to find the unexpected information from unlabelled data (Hadi et al. 2013).

Artificial Neural Network (ANN) is widely used for classification and prediction. The method train the data by learning the known classification of the records and comparing with predicted classes of the records in order to modify the network weights for the next iteration of learning and due to admissible predictive performance of neural network, it is presently the most popular data modelling method used in different domains (Mussarat Yasmin et al. 2013). Linear-discriminant analysis and ANNs are applied to recognize three states and 15 activities with an average accuracy of 97.9% using only a single tri-axial accelerometer attached to the subject's chest (Khan et al. 2010). An assessment is proposed using a neural network to distinguish 'healthy' from 'pathological' gait (Holzreiter and Köhle 1993). A framework is proposed to recognize heart rate variability pattern using ECG and Accelerometer sensors (Thi Hong Nhan Vua et al. 2010). A three layer ANN is used to incrementally learn the extracted patterns and classify them. Three classifications of data for location, activity and heart status are performed by the three nodes in the output layer. The ANN is commonly used in clinical conditions with large and complicated data sets for decision making. As the modelling process in ANN is a black box process, ANN method needs to justify for each input data (Hadi et al. 2013). There are other methods like Hidden Markov Models (Rabiner and Juang 1986), Rule Based Methods (Ahmad A. Al-Hajji March 2012) and Statistical Tools (Apiletti 2009) etc.

Decision Tree is a way of learning to provide an efficient representation of rule classification and it a reliable technique to use a different areas of medicine domain in order to take a right decision (Vili et al. 2002). Fuzzy based decision trees are used for linking clinical measurements and kinematic gait patterns of toe-walking to increase understanding of gait deviation, and could help clinicians plan treatment (Armand et al. 2007).

Gaussian Mixture Models (GMM) is statistical model used for classification, pattern recognition and proposed a GMM method using inter-pulse interval (IPI) signals of ECG in order to make the secure body sensor communication (Wei et al. 2011). GMM is able to detect unseen information in physiological data and it has been used for prediction tasks (Hadi et al. 2013). GMM system is used to allow better detection of short-duration movements and achieve a mean

accuracy of 91.3%, distinguishing between three postures (sitting, standing and lying) and five movements (sit-to-stand, stand-to-sit, lie-to-stand, stand-to-lie and walking), compared to 71.1% achieved by the Heuristic system (Allen et al. 2006). The summary is presented in Table 2.8 on current features classification methods of gait analysis.

Table 2.8: Current feature classification methods of gait analysis

Classifier	Objective	Features	Cross validation	Result	Reference
Support vector machine with a linear Kernel	Gait patterns classification of younger and elderly subject	Spatial and temporal Parameters	Leave-one-out	Support vector machine distinguished the two patterns with an accuracy of 95.8%	(Eskofier et al. 2013)
Support vector machine with linear, Polynomial and radial basis function Kernels	Recognition of gait patterns during lower extremity muscular fatigue and no-fatigue	Step width, step length, stride duration, heel contact velocity, stance time	5-fold cross-validation scheme	Support vector machine with linear and radial basis function Kernels recognized the fatigued and no-fatigued gait With an accuracy of 96%	(Zhang et al. 2014)
Support vector machine with linear, Polynomial and radial basis function	Automatic recognition of gait patterns related to balance impairments	Minimum foot clearance data from the first 512 continuous gait cycles of each subject	Leave-one-out	Polynomial kernel performed better (accuracy of 100%) than linear (accuracy of 86.95%) and	(Khandoker et al. 2007)

kernels				radial basis function (accuracy of 86.95%) kernels	
Multilayer perceptron, support vector machine with Polynomial kernel, Naïve Bayes and decision tree	Gait patterns classification of young and older individuals	Root mean square, integral of power spectral density, cadence, stride and step in vertical, medio-lateral and anterior-posterior directions	10-fold cross-validation scheme	Multilayer perceptron achieved the best accuracy (80.6%) to discriminate young and elderly gait patterns	(Chan et al. 2013)
Support vector machine (linear, polynomial and radial basis function kernels)	Classification of gait patterns of young and elderly subjects	Spatiotemporal, kinematic and kinetic parameters	6-fold cross-validation scheme	Support vector machine with linear, polynomial and radial basis function kernel achieved the same accuracy (91.7%)	(Begg and Kamruzzaman 2005)
Artificial neural networks (three-layer) and Support vector	Classification of gait patterns of young and elderly subjects	Minimum, maximum, median, 1st and 3rd quartile values of minimum foot clearance	3-fold cross-validation scheme	The best distinction of both gait patterns was achieved with support vector machine using	(Begg et al. 2005)

machine (linear, Polynomial and radial basis function Kernels)				linear kernel (accuracy of 83.3%), while the artificial neural networks showed the worst accuracy (75%)	
Five-class classification with support vector machine, decision tree, K-nearest neighbours, Naïve Bayes and artificial neural networks	An early automatic recognition tool of distinct abnormal gait patterns	Angles, spatiotemporal parameters from shoulders, elbows, hips, knees and ankles	10-fold cross-validation scheme	Accuracy of 97.9%, 90.1%, 100%, 97.2%, 100% for support vector machine, decision tree, K-nearest neighbours, Naïve Bayes, and artificial neural networks, respectively	(Pogorelc et al. 2012)
Support vector machine	Distinguish the gait patterns of an osteoarthritis patient from a control subject	Features extracted from 3d kinematics	5-fold cross-validation scheme	Support vector machine distinguished the gait patterns of osteoarthritis and healthy participants with an accuracy of 88%	(Laroche et al. 2014)
K-nearest	Automatic	Features based	Leave-	K-nearest	(Alaqtash et

neighbours and artificial neural networks	classification of pathological gait patterns (cerebral palsy and multiple sclerosis) from healthy walking	on amplitude and temporal parameters of ground reaction forces	one-out	neighbours were more accurate than artificial neural networks (accuracy of 85% against 80%) in the classification of 3 gait patterns through ground reaction forces data	al. 2011)

2.3.8. Validation

Validity in research is concerned with the accuracy and truthfulness of scientific findings (LeCompte and Goetz 1982). Thus it refers to the credibility or believability of the research. A validity study demonstrates what actually exists and a valid instrument or measure actually measure that it is supposed to measure (Brink 1993). It is a discussion that how the chosen research methodology can achieve validity forms an integral part of any rigorous research effort. However, few scientific techniques have been developed to address the scientific worth and rigour of qualitative research, in particular case study research (De Ruyter and Scholl 1998). Six specific criteria to judge the validity and reliability of case study research within the realism paradigm are presented in (Healy and Perry 2000). Although they presented six specific criteria, a thorough comparison and discussion on theoretical paradigms and philosophical foundations concluding that the realism perspective appears to be the most appropriate one for marketing researchers etc, it does not conclude as to what "really needs to be done" to establish validity and reliability in case study research. There are many validation studies of gait analysis available. A concurrent validity of a real time temporal gait parameters of (gait cycle time, single limb support time, and double limb support time) is conducted derived from Noise-Zero Crossing algorithm against parameters measured by an instrumented walkway (Allseits et al. 2017). Four consecutive fundamental events of walking heel strike, toe strike, heel off and toe off gait phases are validated in seven healthy volunteers against reference data provided by a force place, a kinematic 3D

analysis system and video camera (Boutaayamou et al. 2015). There are many studies conducted for validating gait parameters (Bilney et al. 2003; Ghoussayni et al. 2004; Leddy et al. 2011; Washabaugh et al. 2017). A validity of our developed gait assessment system is conducted to determine the concurrent validity of spatiotemporal IMU gait extracted features with Qualisys and Treadmill measurements in young and older adults and to compare the levels of agreement for average spatiotemporal gait parameters. We validate our system using three experiments; 1) Treadmill at various walking paces vs 3D camera system, 2) Self-selected (free) walking vs 3D camera system, and 3) Self-selected (free) walking vs Digital tape for distance (details in Chapter 6).

2.4. User requirement

At the beginning of this research, the current clinical methods of analysing gait are investigated. We have visited Royal Bournemouth Hospital and Agargaon Probin Hitoishi Sangha hospital (Dhaka, Bangladesh) to study their available gait assessment tools. We have discussed with medical doctors (Professor Mike Vassallo, Royal Bournemouth Hospital; Dr. Azizur Rob and Dr. Aman, Agargaon Probin Hitoishi Sangha hospital, Bangladesh), and experts in biomedical engineering and physiotherapy (Dr. Jonathan Williams, Principal Academic in Physiotherapy, Bournemouth University and Dr. Osman Ahmed, Physiotherapy in the Faculty of Health and Social Sciences, Bournemouth University) regarding methodology for gait and fall risk assessment of older adults. We have directly talked with older adults in two different elderly care homes (Agargaon Probin Hitioshi Shongho and Old Rehabilitation Centre (বয়স্ক পুনর্বাসন কেন্দ্র), Dhaka, Bangladesh) to get their requirements. We have studied older adult's needs and requirements, recommendations from clinical perspective and available technologies. Several meeting with caregivers, medical doctors, therapists, geriatricians, assistive technology experts and older adults (both living in care home and living home independently) are conducted. Current clinical methods of analysing gait fall into two extremes. The first is based on observational gait analysis which is inexpensive but qualitative. The second is analysis in a motion laboratory which is quantitative but expensive. In both methods, the subject is very aware of being observed and analysed which is likely to affect the gait of the subject. In the first method, gait abnormalities are generally assessed and reported by physicians, physiotherapists and researchers in clinical settings. Clinical scales used to analyse gait parameters are subjective or semi-subjective and a poor replacement to laboratory based methods for identifying changes in gait.

Sometime these methods provide scoring based on clinical expertise and sometimes abnormalities are reported as present or not which may affect the accuracy of diagnosis, follow-up and treatment. In the second method, the motion laboratory based gait analysis is considered as "gold standard". However, the current available "gold standard" methods are expensive, time consuming, limited to a single gait cycle and laboratory based which reduce their feasibility to be used at home and in clinics. A clear understanding of the gait abnormality is important for therapeutic planning, management, clinical decision making and rehabilitation. There is no such system available which is inexpensive, easy to use and easy to interpret results based gait analysis system available in current clinical applications. Therefore, a high demand of automatic objective gait analysis system is appealing from therapists, geriatrics and doctors for gait monitoring and rehabilitation.

On the other hand, older adults with mobility problem need to go through a regular visit to hospital for health check-up. A self-assessment gait analysis system will help them to monitor gait abnormality in their own home which will reduce their burden of visiting hospital. It will also enable older adults to live longer in their preferred environment, to enhance the quality of lives and to reduce costs for society and public health system. Especially with the population ageing, an automatic gait analysis system will be the key component of monitoring mobility problems and reduce potential risk of falls. Therefore, an inexpensive, wireless, portable, simple and easily to use and visualize results, multi-sensor based synchronous gait analysis system is necessary for users at home and in clinics. The system will provide the facility to quantify gait and gait changes both in clinic and at home which increases the availability and affordability of gait assessment. It will also allow identifying gait variables and changes, monitor of gait and abnormal gait patterns of older people in order to reduce the potential for falling support falls risk management aiming to improve their quality of life. It will significantly simplify the monitoring protocol and opens the possibilities for home and clinics based assessment.

2.5. Research gap identification

This section discusses and identifies the gaps attained from the analysis of literature reviews in wearable sensor based gait analysis for gait assessment in clinics and at home. It also discusses how the research is different from previous studies.

2.5.1. Challenges of current gait assessments

A clear understanding of the gait abnormality is important for therapeutic planning, management, clinical decision making and rehabilitation for patients. As the literature shows that the conventional approaches of gait abnormality assessment in clinics are based on visual observation. The assessment is conducted and reported by physicians, physiotherapists and researchers in clinical settings or in gait laboratories where the assessment time is limited, using visual observation, questionnaires or functional assessment to determine abnormalities in spatiotemporal gait parameters etc. These gait assessments are highly dependent on assessors' experience and judgment. Such visual assessments may not satisfy scientific criteria of reliability and validity (Archer et al. 2006), which may affect the accuracy of diagnosis, follow-up and treatment (Muro-de-la-Herran et al. 2014). Again, there is no commonly accepted guideline, preferred methodology or protocol for gait changes evaluation. There are "gold standard" technologies for assessment of gait parameters e.g. three-dimensional kinematic analysis using a motion capture system, force plate and pressure activated sensors. However, the current available technologies are expensive, time consuming, limited to a single gait cycle and laboratory based which reduce their feasibility to be used at home and in clinics. Although several low cost instruments e.g. Kinect (Auvinet et al. 2017) and camera (Krishnan et al. 2015) are appealing, they are restricted to a small capture volume, lead to a lack of privacy and only a few gait parameters can be analysed. Therefore, an affordable, user-friendly, portable multi-sensor based objective gait analysis system which is able to capture long time data and allow comprehensive gait information are potentially important for users at home and in clinics.

2.5.1.1. Sensor selection

Several comprehensive reviews about the subject of gait analysis with wearable sensors have been previously presented in the literature. Although, many wearable sensors based gait analysis methods are available, the specific objective of gait analysis for users at home and in clinical areas is actually found in only a few studies. These studies do not demonstrate a fully automatic system including data collection, feature extraction and quantitative measurement where both limbs are evaluated. Many investigations are carried out using a single gait parameter or applying simple statistical methods for comparisons. Studies also include a small number of participants. Again, research on comprehensive understanding of gait quantification based on overall gait

features to allow assessment and monitoring of gait changes from young and older adults has received little attention.

Using IMUs for gait analysis has been well explored in the literature with promising results. IMUs are relatively inexpensive with low power consumption which allows long time data collection (virtually unlimited number of steps to be evaluated), and sometimes Bluetooth™ embedded within IMU enables portability, and provides the ability to evaluate gait and movement disorders outside the constrained environments of the clinic and research laboratory. However, the majority of the existing work does not consider realistic conditions where data collection and sensor placement imperfections are imminent. Moreover, some of the underlying assumptions of the existing work are not compatible with pathological gait that decreases the accuracy. Again, accelerometer, gyroscope and magnetometer sensors in IMU are susceptible to noise in practical application and other small errors, which cause significant drift when the raw measurements are integrated. The drift errors due to integration result in a linearly-growing error in angle and position. Other sources of errors from IMU sensors are described details in (Lan and Shih 2013; Ilyas et al. 2016). Some of these challenges can be overcome by the state of the art proposals in the literature, while some of them are not yet addressed or solved. Hence, there is a need for additional domain knowledge to estimate and eliminate drift periodically.

2.5.1.2. Sensor placing location

The output of sensors depend on the position at which it is placed, its orientation, posture, and activity being performed (Merryn et al. 2004). The signal also varies depending on the position on the foot (Markowitz and Herr 2016). Various factors can affect the signal input and output. For example, during locomotion, movement of clothes can cause interference with accelerometer output (Bouten et al. 1997). Factors such as location of the sensor, number of sensors are linked with the acceptance and usability level of an automatic gait assessment system. Certain sensors location or multiple sensor locations may prevent elderly people from performing activities normally or may cause discomfort. Also, some sensor types may be perceived as stigmatisation or too complicated to use resulting in low acceptance. Again, a system solely consisting of wearable sensors, without the aid of infrastructural system elements, rarely achieves completeness in terms of gait metrics. The literature still lacks a complete system that can be easily used by non-professionals in clinics or at home. To increase the reliability and validity of automatic feature extraction from gait parameters for gait analysis, the influence of sensor

location and attachment has to be determined. Further study on the best location for sensor placement is therefore required (Intille et al. 2012).

2.5.1.3. Sensor fusion

Many gait analyses use a single sensor of user information. Since many wearable sensor applications require sophisticated signal processing techniques and algorithms (Tognetti et al. 2015), their design and implementation remain a challenging task still today. Sensor's streaming data collection, processing and transmitting remotely by means of wearable devices with limited resources in terms of energy availability, computational power, and storage capacity are crucial. Although, sensor fusion technology combines sensor outputs to maximum accuracy and efficiency, as well as minimal noise and power consumption, a lot of sensors come with specific constraints in terms of power efficiency, frequency, latency and plays a crucial part in efficient sensor-fusion designs. The details of wearable sensor fusion challenges are described in (Gravina et al. 2017). There are many studies conducted with sensor fusion, however only a limited number of studies are found for collecting synchronous data from multiple sensors for gait analysis.

2.5.1.4. Quantification and visualization

The most common approaches for the quantification of gait give the numerical values of parameters such as symmetry index, symmetry ratio, symmetry angle etc. It may be difficult for users to understand those numerical values. However, there are often difficulties in how to interpret results and number of test subjects and experiments are low. Although, there are many approaches for quantifying gait symmetry (described in Section 2.3.5), a user friendly visualization of gait information is not readily available. Researchers (Manal and Stanhope 2004) proposed a visual representation of examining asymmetric behavior where the method is presented in the context of clinical gait analysis and displays movement pattern deviations relative to normative data by color-coding the magnitude and the direction of the deviation. This approach provides a single-page summary of all the deviation magnitudes and can be displayed simultaneously in a manner of concise, visually effective and reduces complexity. However, quantitative information of the gait for the comparison and analysis of complex movement patterns are missing and it does not examine changes in symmetry of bilateral parameters.

2.5.1.5. Feature selection

There is no commonly accepted superior guideline, preferred methodology or protocol for gait feature selection. To evaluate stride-to-stride variability, European GAITRite Network Group developed Guidelines for Clinical Applications of Gait Analysis (Kressig and Beauchet 2006) recommend the highest possible number of gait cycles from a practical standpoint, with a minimum of three consecutive gait cycles for both left and right sides (i.e., a total of six gait cycles) (Kressig and Beauchet 2006). Although most of the proposed frameworks in the gait analysis contain feature extraction/selection phases, the main challenge still is to balance between the optimum feature extraction/selection methods and their costs for the system. Researchers (Daby et al. 2013; Hadi et al. 2013) addressed the detail challenges of feature extraction area including formatting, normalization and synchronization of sensory collected data. The optimal feature selection for gait analysis of older adults is still challenging to balance between the optimum feature extraction or selection methods and their cost for the system.

2.5.1.6. Feature classification

There are different machine learning algorithms used for classification of human gait phases using threshold, context-awareness, multi-layer perceptron SVM, Decision tree, Genetic Algorithm and other algorithms can be seen from (Igual et al. 2013). Current research work shows that most of the work on gait phase detection has mainly focused on simplified use one accelerometer sensor data involving single-user. In the real world, gait phases and events are often in complex manner. Thus, high level activity real time detection is a complex process due to manipulation with huge sensory data. The challenging task is to develop algorithm which will need less supervision for high-level gait phases and events detection.

Through the comprehensive literature on gait analysis and wearable gait analysis, it is found that gait abnormalities are very common in clinical practice and there is an increasing need to improve technology for its analysis. Such abnormalities lead to serious adverse consequences such as falls and injury resulting in increased cost. There is therefore a national imperative to address this challenge. Currently assessment is done using standardized clinical tools dependent on subjective evaluation. More objective gold standard methods to analyses gait rely on access to expensive complex equipment based in gait laboratories. These are not widely available for several reasons including requirement for expensive equipment, need for technical clinical staff,

need for patients to attend in person, complicated time consuming procedures and overall expense. Improving opportunities for gait analysis to increase accessibility requires a development of an automatic gait analysis system using of new and affordable technologies for diagnosis and monitoring of gait using digital technology, nevertheless with population ageing it will soon be a huge market and in order to compete in such market, the cost will be a vital factor. There remain many issues and challenges in developing gait analysis systems including user acceptance, usability, privacy, visibility, systems accuracy, lack of human and social interaction and cost. Therefore, in this research, an automatic gait analysis system is proposed and developed. In broad aspect, there are two main gaps identified based on comprehensive literature on wearable gait analysis. The first is related with practical aspect which includes user acceptance, usability, cost and privacy. The second aspect is the technical issues. The identified technical issues in wearable sensor based gait analysis system for users at home and in clinics are listed following.

1. Investigation of the effect for placing sensors on different anatomical foot locations are not available to collect accurate and reliable data
2. Multi-sensor fused and synchronous data collection for gait analysis is found only few papers
3. Automatic comprehensive gait features extraction methods are not available for objective gait assessment to monitor and identify gait abnormalities over time
4. Visualization of spatiotemporal gait parameters in real time is not available for monitoring and rehabilitation program
5. Validation of extracted gait features against gold standard systems in different settings with young and older adults are found only in few studies
6. Evaluation of gait based on all gait features using morphological techniques are not available.

2.6. Summary

This literature review covers the state-of-the-art on conventional gait analysis approaches, wearable sensors based gait analysis including sensor selection, sensor placing location, sensor fusion, feature selection, quantification and visualization, feature selection methods, feature classification and validation. From this literature analysis, we verify that proper and reliable wearable sensors based gait analysis system should involve several phases. The sensor selection

phase is to collect movement data. Sensor should be an inexpensive, wireless, portable, low powered, simple and easy to use. Location of placing sensor is important to maximize the interpretable sensor data information. Feature extraction/selection should be normalized to achieve the most significant features to distinguish the classes based on dependence of classifier performance of features for more robust gait events. Quantification and visualization should be used to easily interpret gait information for monitoring. Feature classification methods should be applied to form the training and testing datasets to prevent over-fitting and generalize the classifier performance. Sixth, evaluation of gait information should be used for monitoring and rehabilitation. Therefore, in this research, considering all the various aspects described above, an inexpensive, wireless, portable, simple and easily to use, multi-sensor based synchronous gait analysis system should be designed and developed for users at home and in clinics.

The detail research gap is described in Section 2.5. There are two main aspects of the research gaps in wearable sensor based gait analysis system. The first gap is related to practical aspects including cost, user acceptance, usability and privacy. The other gap is related to technical aspects described in Section 2.5.2. To overcome these limitations, an affordable wearable multi-sensor based gait analysis system is developed. The developed gait analysis system significantly simplifies the monitoring protocol and opens the possibilities for home based assessment. This section discusses the research design for developing the automatic gait analysis system. Older people generally walk slow and sensitive sensors are necessary to transfer locomotive information to electric signals. From the literature, it is found that an IMU is an electronic device that measures an object's velocity, acceleration, orientation, and gravitational forces, using a combination of accelerometers, gyroscopes and sometimes magnetometers. Due to low cost and small size, researchers use it in different areas for movement analysis. An accelerometer is used for measuring the acceleration of a moving body and a gyroscope is used for measuring or maintaining orientation and angular velocity. Therefore, it is decided that fused accelerometer and gyroscope in IMU will be used for collecting movement data from older adults. From the literature, the optimal placing of IMU sensors on different foot locations are not available. Therefore, the effect of IMU sensor output on different anatomical foot locations needs investigation to maximize the interpretable information for gait analysis. It is also important to understand the parameters that influence the extraction of automatic gait features. The next step is to perform an analysis to bring out meaningful information from collected data from IMU sensors. From the literature, researchers used a variety of methods (Brajdic and Harle 2013) for

gait phases detection using IMU sensors. However, difficulty arises to find the automatic selection of the threshold value which can vary between users, surfaces and shoes (Gafurov and Snekkenes 2008). Most of these studies were carried under laboratory conditions (Rebula et al. 2013) and tested on a relatively small number of subjects (Brajdic and Harle 2013). Therefore, an automatic gait features extraction method is developed for comprehensive understanding of gait. These automatic extracted features then need to be displayed in a user friendly way to enable users to understand the information easily. From the literature, the most common approaches for the quantification of gait give the numerical values of parameters such as symmetry index, symmetry ratio, symmetry angle etc which may be difficult for users to understand. Therefore, an easy visualization tool is useful to provide a facility for their use in clinic and at home. Next comes the validation of the developed automatic gait feature extraction method. The validation is conducted for both young and older adult's data in different environment against a gold standard system. The final phase is to provide an automatic gait assessment system based on all features where the assessment will be conducted by users automatically without the intervention of a physician or expert. For developing the above mentioned system, tools including MATLAB, R and Android Studio are used for data collection, analysis, and model evaluations. SolidWorks is used for designing sensor casing and printed using 3D printer. MATLAB is a popular platform which can be used for exploring, visualising, and modelling data; R is a popular platform for statistical analysis and Android Studio is the official integrated development environment for Google's Android operating system. Android Studio has built on JetBrains' IntelliJ IDEA software and it is designed specifically for Android mobile phones. The choices of techniques used and investigated in the research are selected based on literature reviews e.g. techniques that are successfully applied and popularly used in related problems. As part of this research is concerned on the practicality of the automatic gait analysis system, the validation and evaluation are carried out such that issues such as cost, usability, privacy, and acceptance are considered.

3. OPTIMAL LOCATION OF PLACING IMU SENSOR

The chapter is organized in the following sections. Section 3.1 presents methods includes the participant selection, sensor selection, design and develop sensor protection system, design and develop android app, sensor placing location, data collection, raw data processing, velocity and distance calculation, stride event detection, stance and swing events detection and gait features extractions. Section 3.2 delivers the experimental results for 15 participants to demonstrate the proposed method, and the discussions. The conclusion is given in section 3.3.

3.1. Methods

The experimental materials and methods used for the development of this work are described in the following subsections.

3.1.1. Participants selection

A convenience sample of 15 young subjects are recruited: 10 male and 5 female participants (mean age: 25.3 years (19 to 35), weight: 60.7 kg and height: 1.658 meter). The subjects are selected with no signs of gait, balance or walking abnormalities. The exclusion criteria for selecting these young subjects are recent ligament major injury, abnormal gait pattern, musculoskeletal or neurological pathology, contraindication to exercise, recent surgery, fracture or muscle injury, impairment attributable to other cause by history or other health conditions that may adversely impact the outcomes of the study. In this initial part of our study and development we purposefully select young subjects with normal gait to find the optimal location for placing an IMU sensor. We want to maximize the highest possible interpretable information for gait analysis in this normal group of subjects. We have no reason to believe that this optimal location will be different in young and older subjects but in future research we will aim to demonstrate whether this is the case or not. Gait abnormalities are common in older adults and IMU sensor output from this group might affect sensor output but will aim to explore this in future research.

3.1.2. Sensor selection

The accelerometer measures the acceleration while the gyroscope measures the angular rotation of the reference object. This sensor array is known as IMU. When an object changes its position with respect to gravity, or goes through the inclination or gets tilted, the movement is rather

slowly interpreted as compared to the vibrations and shock the device goes through. Due to this, the sensing range varies from low g to high g today, to facilitate the bandwidth capability associated with the potential applications of device for sensing human locomotion. This research involves the use of multiple IMU sensors to detect gait information. Chapter 2 describes available sensors for gait analysis. There are wearable wireless IMU sensors commercially used for health rehabilitation, movement monitoring, sports tracking or research. A wireless wearable Bluetooth, long autonomy, minimum consumption, multiple synchronised data transmission supported IMU senor with low cost is important for our investigation. More specifically, since our later investigation is to identify older adults gait pattern changes over long time, the IMU device is required to last approximately a week or more with low price. Selecting a sensor should also have generic considerations such as protection from pressure, water and temperature; and the battery life etc. Therefore, the following criteria are set in order to select the suitable sensors that meet the research aim.

- Human gait provides locomotive information and the sensors need to capture that locomotive information
- The sensors need to be inexpensive, wireless, portable, low powered, simple and easily to use and easy to acquire (preferably off-the-shelf)
- The sensors need to fulfil criteria for user acceptance, usability and privacy
- The sensors need be easy to implement and/or develop and/or integrate and/or extend on an existing sensor board or system
- The sensors need to allow fusion and synchronous data collection platform

A variety of sensors have been investigated in wearable sensor based gait analysis research (Patel et al. 2012; Mukhopadhyay 2015). For collecting human locomotive information, we conduct investigation using passive infrared (PIR), 3-Space™ (Inc 2015), SensorTag CC2650STK (Instruments) and MetaWearCPro (MbientLab (accessed on 03/08/2016)). Other miniature sensors such as tri-axis accelerometer (ADXL 335, ADXL 345, LIS331), tri-axis gyroscope (L3G4200D, ITG-3200), 6 DOF Digital Combo, 9 DOF IMU (Razor, LSM9DSO, AltIMU10, MiniIMU9) are also investigated. These sensors need to combine with wireless data transmission module and power supply to make it wearable user-friendly. Therefore, we search for an integrated low powered device to serve our purpose. The PIR sensor has two slots and each slot is made of a special material sensitive to infrared. The first slot (one half of the PIR sensor) intercepts when a warm body like a human passes results a positive differential change between

the two halves. The reverse happens when the warm body leaves the sensing area and the sensor generates a negative differential change. These change pulses are indicators of human movement. This is an ambient type sensor which needs to install in environment and hence, not good to serve our purpose. The Yost Labs 3-Space™ Sensor Wireless integrates a miniature, IMU with a 2.4GHz DSSS communication interface and a rechargeable lithium-polymer battery. The battery lasts up to 5 hours after a full research. Unit price is $265.00. Due to short battery last, cost and size of the device, it is not suitable for our research. Texas Instruments' the SensorTag (CC2650STK) is based on Bluetooth low energy offers 75% lower power consumption and years of battery lifetime from a single coin cell battery. However, the data sampling rate is 10 Hz which is low for human gait analysis and not suitable for our research. Based on the criteria mentioned above, literatures and with considering all aspects of our research, the MetaWearCPro sensor is found the most suitable for our research.

This sensor, introduced by MbientLab, Portola, San Francisco, CA, 94134 USA, is used to collect accelerometer and gyroscope data. It is sensitive to acceleration and rotatory movements that occur during normal human locomotion (Figure 3.1). It has a 32-bit ARM Cortex-M0 SOC - nRF51822 CPU, Embedded 2.4GHz BLE transceiver, radio-peak currents below 10 mA 3V, and powered by a coin-cell battery. It has internal 256K FLASH /16K RAM, BOSCH BMI160 accelerometer + gyroscope, BOSCH BMP280 barometer + temperature, Lite-On LTR329 light sensor, BOSCH BMM150 magnetometer, temperature sensor, indicator LEDs, and GPIOs / I2C. The board is 24mm diameter x 7.0mm height. Sensor data can stream at up to 100Hz using the Bluetooth Low Energy link and log up to 10K entries of sensor data at 800Hz in the MetaWear memory. The price was $30.00.

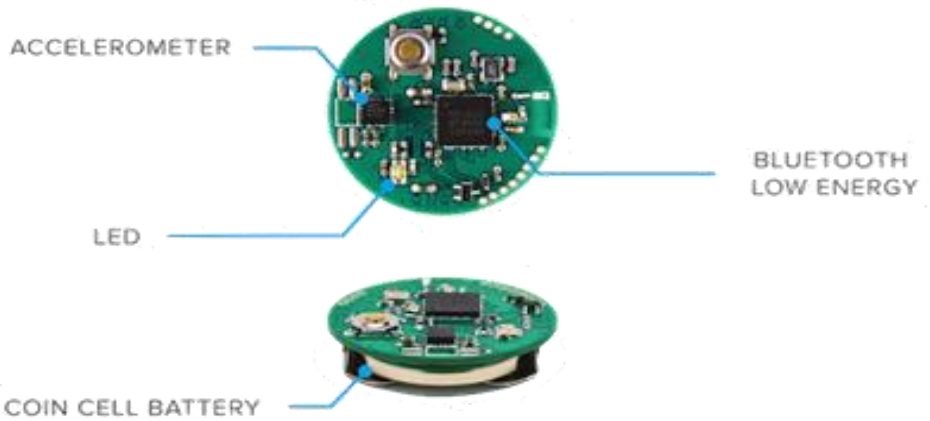

Figure 3.1: IMU sensor MetaWearCPro (MbientLab (accessed on 03/08/2016))

The sensor has a high accurate BOSCH BMI160 component which is a 6-axis IMU comprised of a 16-bit accelerometer and an ultra-low power gyroscope with an amplitude up to ±16g (S_{8g} sensitivity 4096 LSB/g) and a range of 2000 degrees/sec (R_{FS500} sensitivity 65.6 LSB/deg/sec) with a frequency up to 1600Hz (Figure 3.1). It can achieve 99% accuracy. Investigation showed that IMU based sensors are sampled at a frequency range of 20Hz to 200Hz (Hegde et al. 2016). In practice, a low sampling rate for the accelerometer possibly produces excellent recognition and accuracy in posture and activity classification (Aminian et al. 1994; Sazonov et al. 2011). In (Aminian et al. 1994) acceleration data are sampled at 25Hz, in (Hikihara et al. 2014) data are sampled at 32Hz and in (Truong et al. 2016) at 50Hz. For this study, the accelerometer range is set to ± 8 m/s^2 and gyroscope range is set to ± 500 degs/s. The sampling rate of data collection is set to 50Hz. The power consumption of our sensor is low during sleep mode and high during operation mode. The sensor is in an active state when connected by Bluetooth to our android device and only goes to sleep mode once it is disconnected.

3.1.3. Design and development of sensor protection system

Once the sensor is selected, it is necessary to design the sensor protection system. Sensor protection is a very important infrastructure for lower limb gait analysis. The system will ensure that the sensor is protected from pressure, water and temperature etc. Due to damage of the protection system may directly affect the sensor output and its economic benefit. Therefore, case damage is a serious problem to be considered during the design and development of the casing system, and in general, sensor casing damage are caused due to material stress factors, engineering technique factors and corrosion factors during body movement. Considering all issues, the goal is to design a sensor casing that is physically robust, simple, and easy to construct. The fundamental design parameters addressed during the development of the sensor casing are based on size, simplicity, cost, adaptability, scalability, wearable, flexible for attachment with body and should not move or change orientation during movement. SolidWorks (SolidWorks 2002) is used to design the case for the sensors and printed using 3D printer. Acrylonitrile Butadiene Styrene material is used in the 3D printer for developing the sensor casting. This material is one of the first plastics to be used with industrial 3D printers and it is still a very popular material due to its low cost and good mechanical properties. It is known for its toughness and impact resistance, allowing to print durable parts that will hold up to extra usage and wear. LEGO building blocks are therefore made from this material for that same

reason. It also has a higher glass transition temperature, which means the material can withstand much higher temperatures before it begins to deform. All these characteristics make a great choice of using this material for indoor or outdoor applications. The sensor casing securely holds the IMU sensors and provides protection. A Velcro elastic belt and buckles are used to adjust and attach the sensor. In Figure 3.2: (1) Buckle and Elastic Belt: the buckle is sewn onto an elastic belt for fastening to Velcro; (2) Bottom case which keeps the sensor safe from pressure, temperature and water; (3) Lock Open Edge which helps to open the cover from bottom case; (4) Sensor Lock Mechanism: The four locks keep the sensor sideways movement and orientation; (5) Cover Lock Mechanism which tightly locks with the case; (6) Velcro-Elastic Joint: The elastic belt is sewed with Velcro; (7) Velcro which adjusts and tighten when the sensor is attached; and (8) IMU sensor and Coin Cell battery.

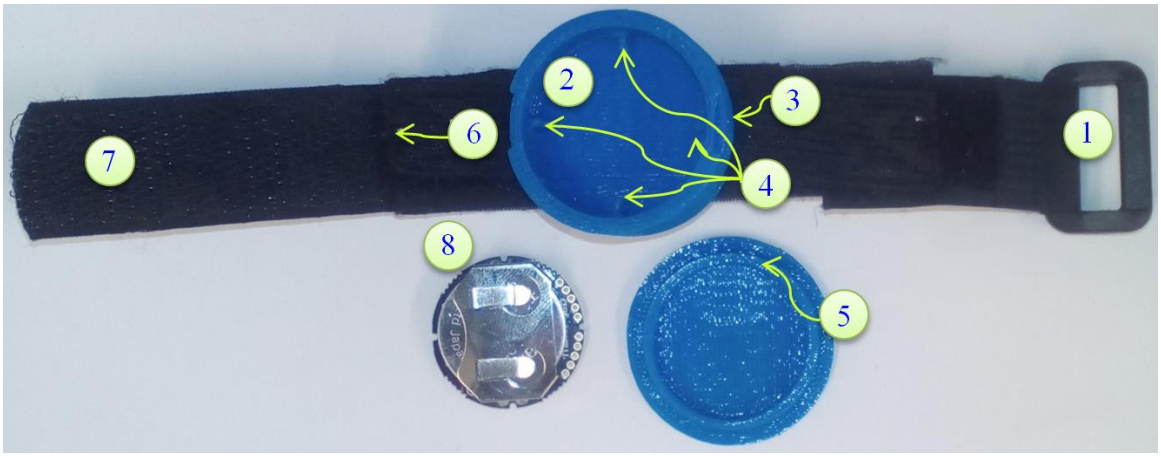

Figure 3.2. Proposed MetaWear casing, Velcro elastic belt, buckles and IMU sensor

3.1.4. Design and development of Android App

The MetaWear CPro sensor provides an Android API library for interacting with the MetaWear board on an Android mobile phone. A minimum of Android 4.3 (SDK 19) is required to use this library, however some features will not function properly due to the underlying Bluetooth LE (BLE) implementation. To get the best results, it is recommended to use an Android 4.4 (SDK 19) or higher. MetaWear CPro uses BLE 4.0. The app is designed through the following.

- Requirement: Requirement analysis is conducted through the literature review, discussion with the expert and users.
- Market availability: The market available mobile software development platforms are reviewed. Mobile platforms and supporting devices are selected considering hardware

performance, battery life, ruggedness, required peripherals, device coverage, device support and performance.

- Initial design: Activity classes are reviewed including SplashActivity, MenuActivity, PlayActivity and HelpActivity etc. A very basic design is implemented using Android Studio 2.2.
- Testing and debugging: The app is tested and users' feedbacks are recorded. All issues are addressed, the app is improvement and documented.
- Multi-sensor synchronous data collection: The app is designed to collect up to 7 IMU sensors data synchronous through Bluetooth LE 4.1.

The Android app is developed to collect real time data from the MetaWear sensor. The HTC M9 mobile phone which has BLE 4.1 is used to connect to multiple MetaWear Cpro sensors. This mobile phone supported up to 7 MetaWear Cpro devices and it is able to collect synchronous data. The app collected accelerometer and gyroscope data, and stored data on an external SD card as a csv file. The data storing format in the csv file is date (*dd/mm/yyyy*), time (*HH:MM:SS.ss*), system clock (Millisecond), accelerometer (*X, Y, Z*) and gyroscope (*X, Y, Z*). The screenshot of the android app is shown in Figure 3.3.

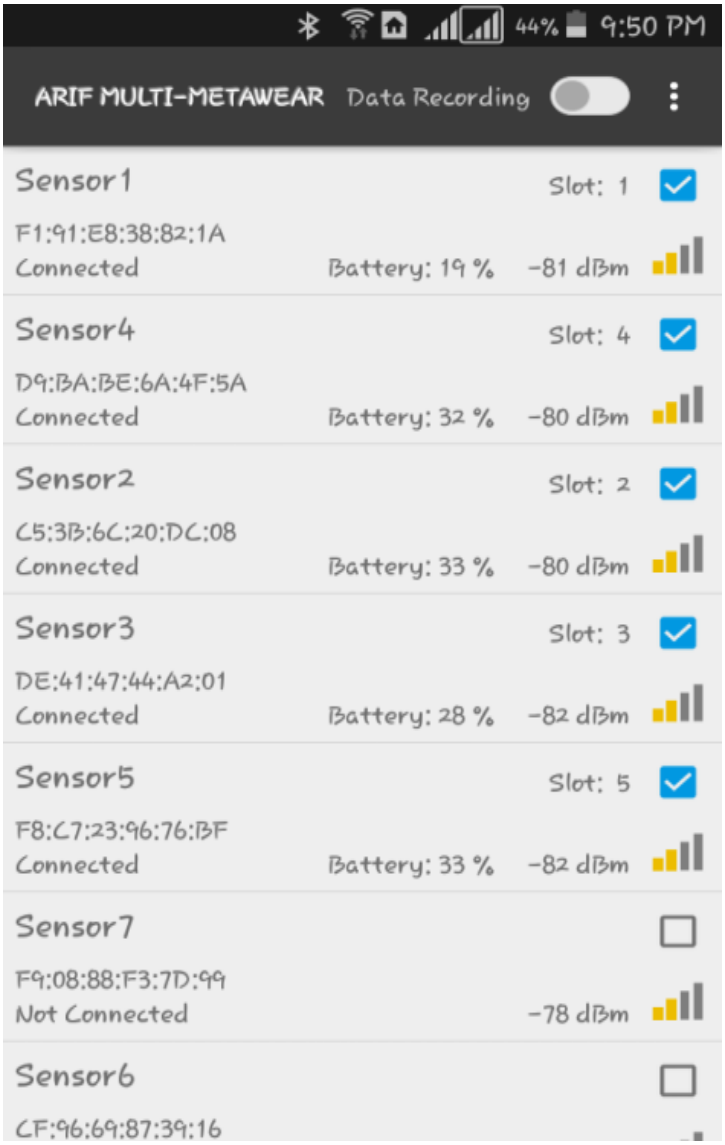

Figure 3.3 Proposed android app to collect data from MetaWear CPro.

Initially the SCAN button on the app is pressed to find all the MetaWear CPro devices available for data collection. The order of data collection is selected by the Slot number. Each sensor then automatically connects with the corresponding mac address by showing "CONNECTED". Once the DATA RECORDING switch is pressed, a dialog box appeared prompting for a file name. Data collection starts when the "OK" button was pressed. When the "STOP" button is pressed, the collected data is stored as a CSV file.

3.1.5. Synchronous data collection

The MetaWear CPro transfers the measurements from 3-axis accelerometer and 3-axis gyroscope sensors information through Bluetooth LE to Mobile phone. The algorithm in (MbientLab

(accessed on 03/08/2016)) fuses the raw data in an intelligent way to improve each sensors output. The HTC M9 mobile phone which has BLE 4.1 is used for collecting MetaWear Cpro data. The developed Android app supports up to 7 MetaWear Cpro devices concurrent connection and it is able to collect synchronous data.

3.1.6. Sensor placing location

Initially the sensor placing effect is explored by placing two sensors once with loosely fitted and another with tightly fitted with Velcro elastic belt. The data output from the loose fit is poor output with high relative motion noise and the accuracy of tightly fitted result is high. The output of an accelerometer depends on the position at which it is placed, its orientation, posture, and activity being performed (Merryn et al. 2004). The signal also varies depending on the position on the foot (Markowitz and Herr 2016). We find that placing a sensor in different foot locations give different signal patterns and affect sensor output. A Velcro elastic belt and buckles are used to adjust and attach the sensor (Figure 3.4).

Figure 3.4: Proposed MetaWear casing, Velcro elastic belt, buckles and sensor placement on foot.

We also observe that the orientation of the sensor has a significant effect on output data and placing the sensor in different locations gives a different shape in data. If data are to be collected regularly, the position and orientation of the sensor is crucial as changes in position through human error may give different data patterns which might be difficult to interpret. This highlights the importance of properly fixing the sensor to the optimal location to avoid inaccuracies. The orientation of the sensor at placing time is also important. Other possible areas of error may arise from frictional noise and relative movement of clothing and shoes of the sensor. The placing of sensor on foot locations requires other generic considerations. There is a need to try to extend the

battery life as much as possible. The power consumption of our sensor is low during sleep mode and high during on operation mode. As there is no switch in the sensor, it is always in active state, if the sensor is disconnected from the Bluetooth android, it goes to sleep mode automatically after a short delay. The sensor output can vary due to relative movement between foot, shoe and sensor (Gafurov and Snekkenes 2008). In order to increase the sensor output accuracy and reliability, and reduce the variability, all sensors are fitted tightly to the barefoot. We chose the barefoot rather than sensors attached to a shoe because wear and tear in the shoe can affect the position of the sensor and accuracy of the data output. The plantar aspect is not covered as this is the part of the foot in contact with the floor and is not practical for the subject to walk on the sensor. Our subjects walk barefoot and it is not possible to wear a shoe over the sensor as this would have caused discomfort. However, our work has established our method for finding optimal location and extracting automatic gait features. Indeed, we agree that for future development and for widespread use the sensor needs to be incorporated into a shoe. Reaching this final goal is however a process that needs to happen in several stages. After this study, we now know how the best signal can be extracted from the bare foot. The next step is therefore to incorporate the sensors into a shoe and compare the output to our barefoot readings. This will ensure that the best possible signal from a shoe based sensor can be achieved. The proposed positions are our novel approach in this gait analysis research area and has not been explored before to our best knowledge.

The sensors do not need to be worn in a perfectly upright position as this is not user-friendly and very hard to achieve. Any discrepancy between the sensor, foot and earth frame, is compensated using transformation of the sensor frame to earth frame assuming that the relative movement between the sensor frame and foot frame is negligible.

Accelerometer and gyroscope data are collected by placing the sensors in five selected foot locations that covers all of the regions of the barefoot (Figure 3.5): the positions are chosen to include the medial, lateral, anterior dorsal, posterior dorsal and posterior of the foot.

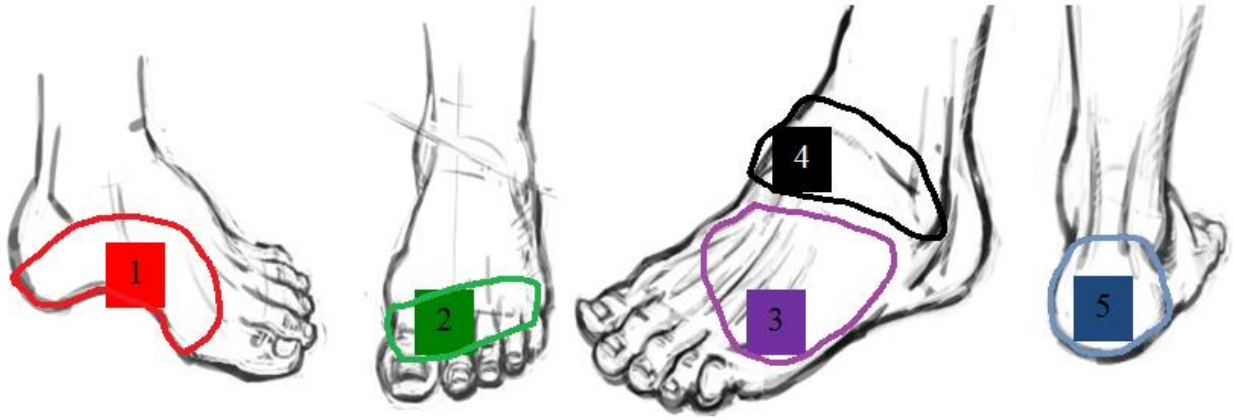

Figure 3.5: Proposed IMU sensor placement of participants to five barefoot locations 1) metatarsal, 2) proximal phalange, 3) side metatarsal, 4) talus and 5) Achilles tendon

Location 1 - Medial aspect of foot over the bony prominence of the first cuneiform: This location is chosen to provide stability to the sensor and minimize its movement during motion of the foot.

Location 2 – Anterior dorsal aspect of foot over the second Metatarso pharyngeal joint: It is a flexible part of the foot during motion.

Location 3 - lateral aspect of foot over the base of the 5th metatarsal: The location is a flexible part of the foot during motion.

Location 4 – Posterior dorsal over the Talar dome anterior to the ankle joint: It is a mobile part of the foot.

Location 5 - Achilles tendon: over the insertion of the Achilles tendon into the calcaneum, evaluates sensor data from the posterior aspect of the foot. As the sensor is placed over the calcaneum it is considered a relatively stable part of the foot during motion.

3.1.7. Experimental protocol and calibration

The experiment is performed in a straight corridor. All subjects perform a trial in a straight corridor comprising 25 strides of normal walking, a turn-around and another 25 strides. Accelerometer and gyroscope data from sensors attached on two foot locations are recorded in a database synchronously using our Android app. The distance carried out by walking on the

corridor is measured by a tape. Calibration is performed individually where the distance travelled is measured manually and the result compared to the output from the sensor.

3.1.8. Data collection

In natural walking the head, torso and hips are synchronized in a smooth bouncing vertical motion with each step. This vertical motion is in the same direction as the earth's gravitational force. Legs do most of the work during walking as the joints produce greater ranges of motion to move the body forward in the horizontal direction. This repetitive movement involves steps and strides known as the gait cycle. This horizontal movement produces high acceleration and this is the movement investigated in this study. An accelerometer and a gyroscope are used to collect this horizontal movement information and then data are analyzed using our proposed method to find strides, stance and swing event information. The raw data from the accelerometer and gyroscope for location 1 to location 5 is presented in Figure 3.6 and will be analyzed in Section 3.3.

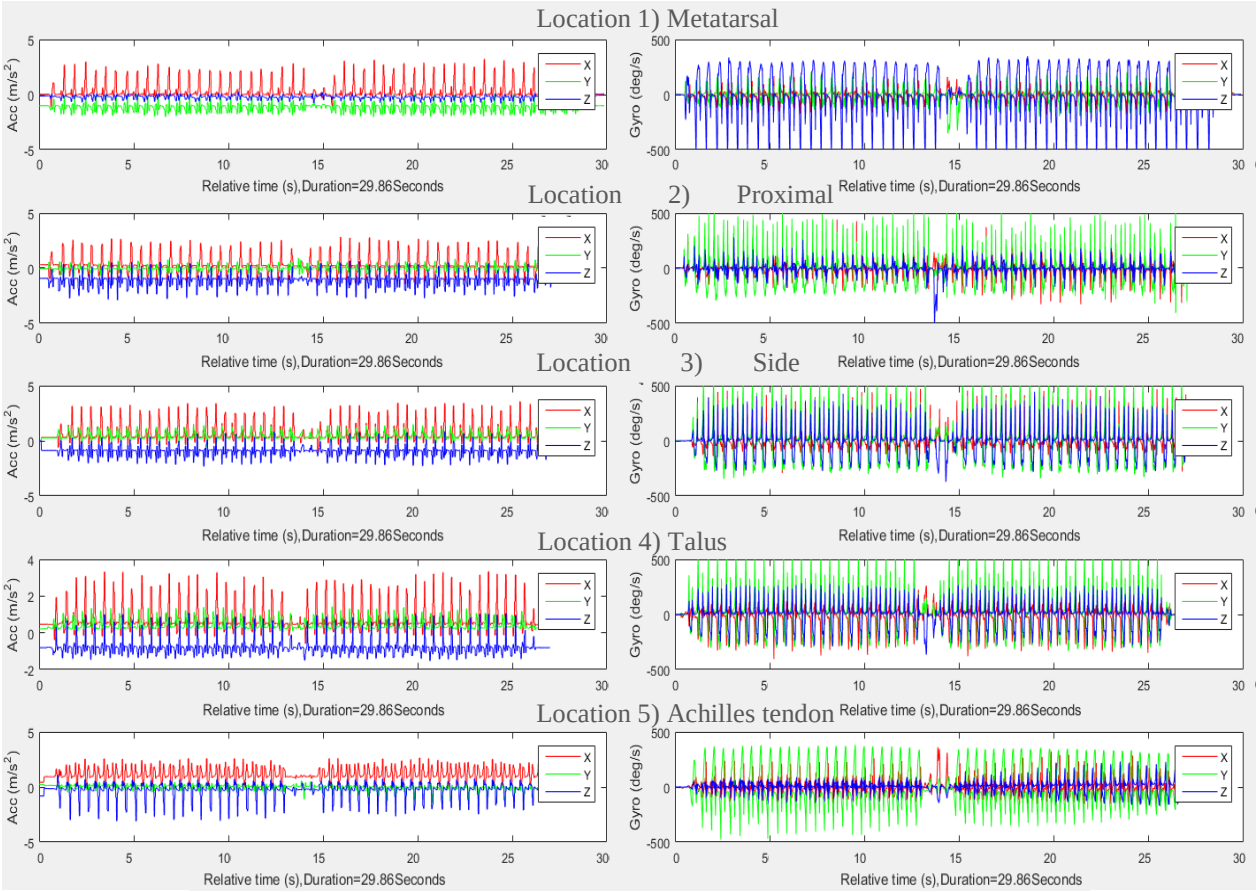

Figure 3.6: Raw accelerometer and gyroscope data from test subject 1 for five locations

3.1.9. Gait features extraction

3.1.9.1. Raw data processing

It is noted that accelerometers are sensitive to altitude and impact forces, while gyroscopes are sensitive to temperature changes and suffer from a low-changing bias. Consequently accelerometers have poor dynamic features and gyroscopes have poor static features (Zhi 2016). IMU sensor produces some noise (such as constant bias, flicker noise, temperature effects and calibration errors) which are described details in (S Flenniken et al. 2017). One way of reducing noise is to apply advanced optimal recursive filter techniques such as Kalman filter (Yun and Bachmann 2006). It (Kalman 1960) is a filtering algorithm which can remove noise from a signal while retaining the useful information. It uses a feedback control mechanism in order to estimate a process. Noisy measurements are taken as feedback and using them, the process is estimated. The recursive approach for minimizing errors ensures that estimated state from previous step and current measurement are used to estimate the current state, therefore no history of previous measurements is required. MetaWear CPro uses Kalman filter fusion to reduce noise, provide distortion-free and refined orientation vectors (MbientLab (accessed on 03/08/2016)). The IMU sensor gives three dimensional accelerometer data $A=[a_x, a_y, a_z]$ and gyroscope data $G=[g_x, g_y, g_z]$ with respect to time t. As the accelerometer is sensitive to linear acceleration due to movement and the local gravitational force, the input data consists of user acceleration and gravitational acceleration. The user movement will result in positive data towards the a_x, a_y, and a_z axis of the sensor and, by convention, these are defined so that a linear acceleration aligned in the direction of these axes will give a positive acceleration output. Again a gravitational force component aligned along the same axes directions will, however, result in a negative reading on the accelerometer.

In this study, there are three coordinate systems: the foot frame, the sensor frame and the earth frame. Since the sensor is attached to the foot tightly, the sensor does not slip or move during walking time. The relative movement between the sensor frame and foot frame is assumed to be negligible; hence the foot frame and sensor frame are treated as a same frame. The sensor frame and the earth frame are the two coordinates and the sensor frame should be transferred to the earth frame and remove gravitational component. The A_x axis is aligned along the foot axis of the IMU sensor, the A_z axis points downwards so that it is aligned with gravity and the A_y axis is

aligned at right angles to both A_x and A_z axes so that the three axes from a right handed coordinate system are shown in Figure 3.7.

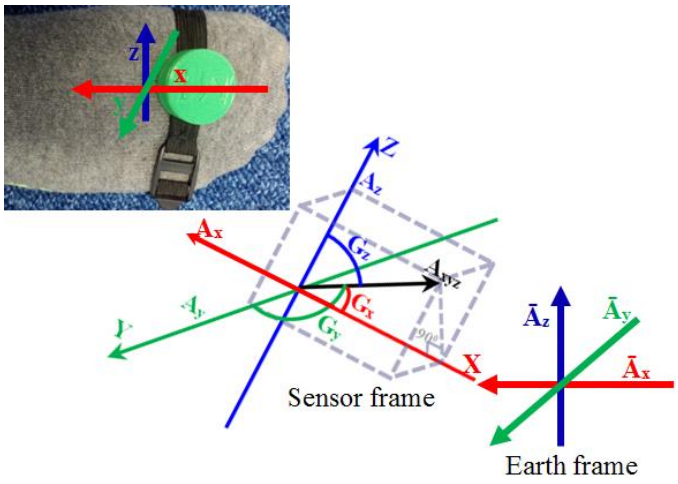

Figure 3.7: Three dimensional IMU axes (*XYZ* is the foot coordinate; $\bar{A}_x\bar{A}_y\bar{A}_z$ is the earth coordinate)

There are many conventional methods to split the gravitational component from accelerometer data and three of them (Mizell 2003; Mahony et al. 2008; Madgwick 2010) are investigated. The method developed by (Mizell 2003) is used to estimate the vertical component and the magnitude of the horizontal component of the user's motion. This method is applied as it is simple and easy to understand. The average initial gravity component on each axis is estimated at standing position before starting to walk.

$$\bar{A} = [\bar{a}_x, \bar{a}_y, \bar{a}_z] = \frac{1}{n}\sum_{i=1}^{n}[a_{xi}, a_{y_i}, a_{zi}] \tag{3.1}$$

Thus the initial gravity acceleration vector $[\bar{a}_x, \bar{a}_y, \bar{a}_z]$ consisted of the average magnitude of *n* samples of accelerometer data and is estimated using equation (3.1),where *i=1,2,3,…,n* and *n=10.* It is noted that initially the earth frame and the foot frame are the same. Here $\bar{A}$ is used as the acceleration under the earth frame.

$$A_d = [d_x, d_y, d_z] = [a_x - \bar{a}_x, a_y - \bar{a}_y, a_z - \bar{a}_z] \tag{3.2}$$

The dynamic component of the acceleration estimated using equation (3.2) is due to user motion rather than gravitational force, where A_d is the acceleration under the foot frame.

$$A_P = \left(\frac{A_d \bullet \overline{A}}{\overline{A} \bullet \overline{A}} \right) \overline{A} \tag{3.3}$$

The projection A_p of A_d on the axis $\bar{A}$ using equation (3.3) (Mizell 2003). In equation (3.3), A_p is the projection component of the dynamic acceleration vector A_d on $\bar{A}$.

$$A_h = A_d - A_p \tag{3.4}$$

As a three-dimensional vector consists of its vertical and horizontal components, the horizontal component A_h of the dynamic acceleration is computed using equation (3.4). The conversion of the accelerometer from gravitational force g to user acceleration of movement (AM) m/s^2 is $AM_{xyz}=A_h*9.81$ where $AM_{xyz}=[am_x, am_y, am_z]$. The three axis data are transformed due to the fact that mapping at specific axes is sensitive to the sensor orientation (Starlino 2009). If the data are mapped on each axis individually, small changes in orientation or attached location may erroneously be flagged as a change in movement. The sensor orientation and attachment are maintained using a small casing and Velcro elastic buckles, every time the sensor is attached. We aim to put in the same orientation even though a different orientation would have given similar results.

$$\left| A_{xyz_i} \right| = \sqrt{am_{x_i}{}^2 + am_{y_i}{}^2 + am_{z_i}{}^2} \tag{3.5}$$

$$\left| G_{xyz_i} \right| = \sqrt{g_{x_i}{}^2 + g_{y_i}{}^2 + g_{z_i}{}^2} \tag{3.6}$$

The acceleration of total A_{xyz} and gyroscope G_{xyz} towards three axes x, y and z directions are estimated by using equations (3.5) and (3.6) where $i=1,2,3,\ldots,n$. The preliminary experimental data are collected in this section from one male subject age 35 years old, height 1.72m and weight 73kg to develop and demonstrate our method. At this stage of the experiment the aim is to prove the concept and that data can be collected and analyzed. It is not intended to generate conclusions about the optimal location for placing sensors. The total walking distance is measured offline and then compared with the calculated distance. The wearable MetaWear CPro sensors are placed in five different locations on the right foot. The subject performed a trail in a straight corridor walking on a hard floor. The trail comprised of 25 strides of normal walking, a turn-around and another 25 strides. The distance is measured by a tape and the Android app is used to record the

time. For example, for the data from this subject, total acceleration $|A_{xyz_i}|$ and gyroscope $|G_{xyz_i}|$ signals are shown in Figure 3.8. From $|A_{xyz_i}|$ and $|G_{xyz_i}|$, we found that data are normally distributed.

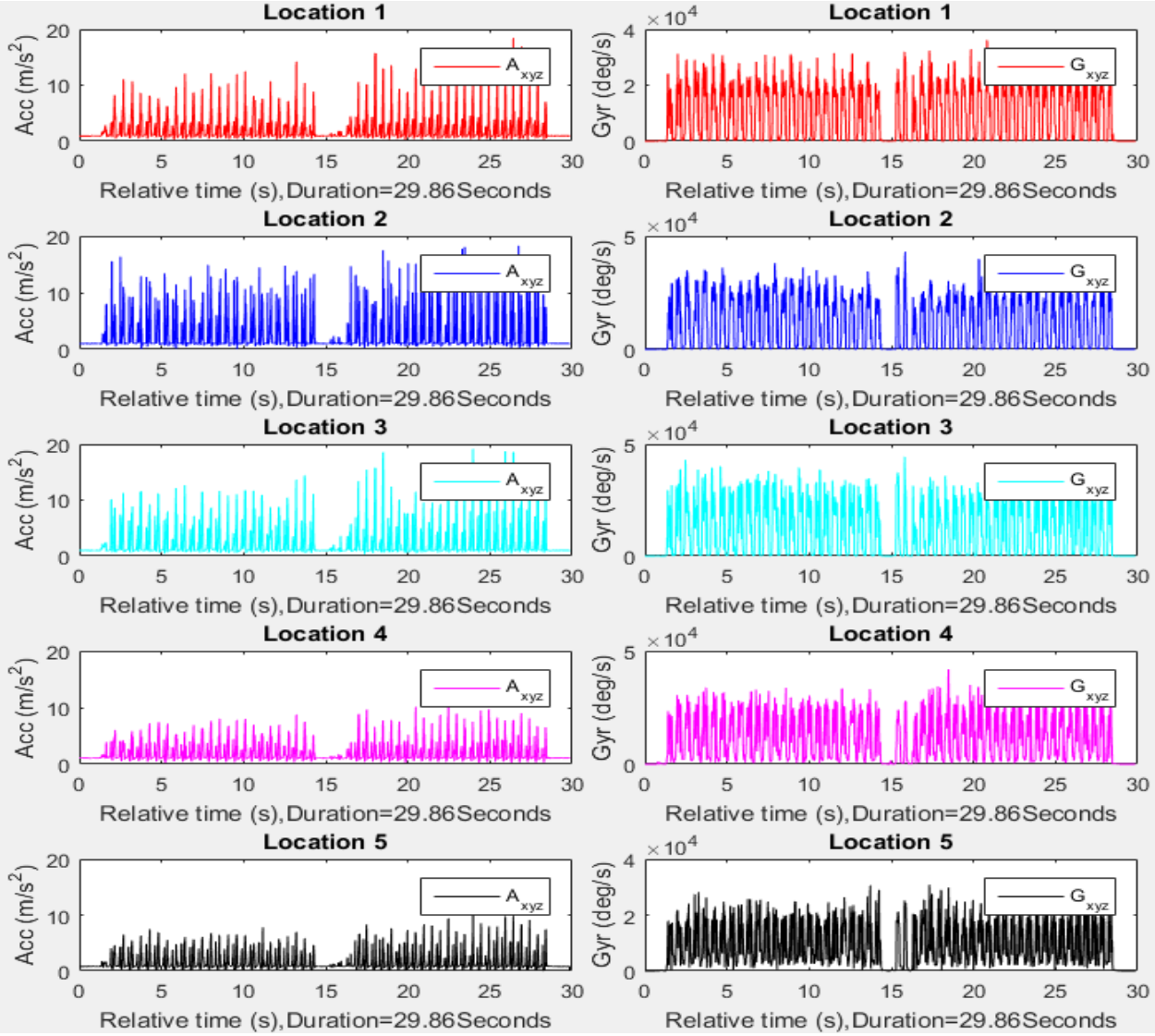

Figure 3.8: Total acceleration A_{xyz} and gyroscope G_{xyz} towards three axes *x*, *y* and *z* directions from Location 1 to 5

The A_{xyz} and G_{xyz} signals are then filtered by the *Savitzky-Golay* (*SG*) filter (Orfanidis 1996) to get A_{sg} and $G_{sg.}$ This filter tends to filter out a significant portion of the original signal's high frequency content along with the noise and minimized the error by fitting a polynomial to frames of noisy data. A_{xyz}, G_{xyz}, A_{sg} and G_{sg} are then shifted to the center shown in Figure 3.9.

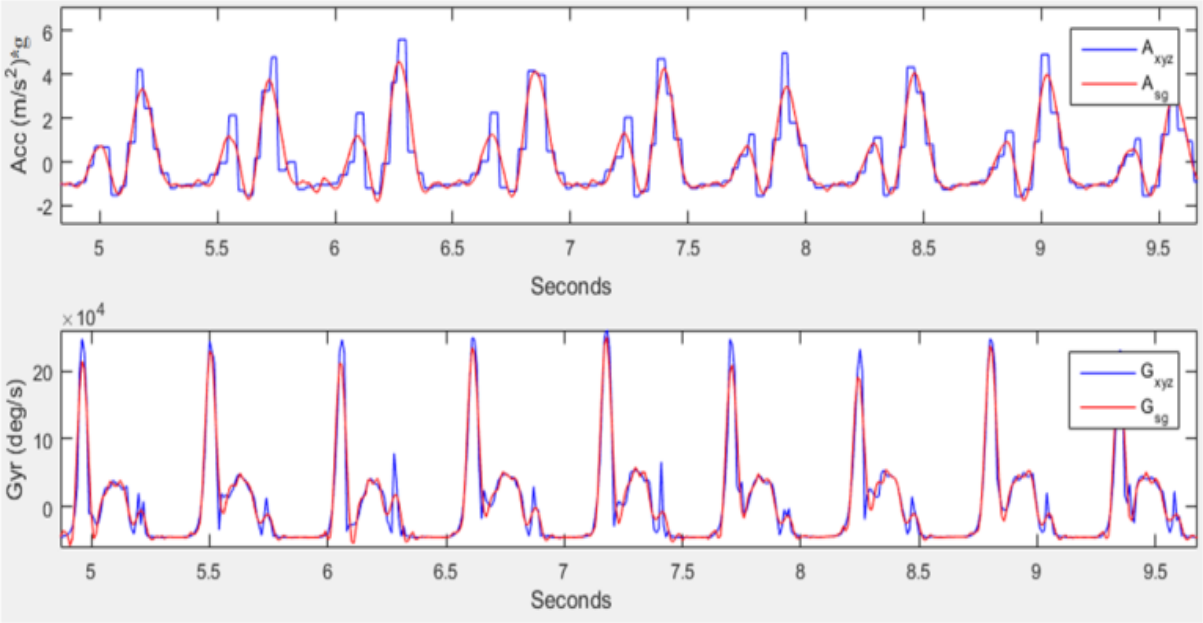

Figure 3.9: Original (A_{xyz} and G_{xyz}) and filtered (A_{sg} and G_{sg}) acceleration and gyroscope data using Savitzky-Golay

3.1.9.2. Velocity and distance calculation

The accelerometer gives information about acceleration, velocity and position. In an ideal world, the position can be estimated by applying double integration formula to the acceleration signal captured from the sensor after removing the gravity component. First integration is applied to obtain velocity vector using equation (3.7). This velocity vector is then integrated second time to obtain the distance using equations (3.8).

$$v(t) = v(t_0) + \int_{t_0}^{t} a(\tau) d\tau \tag{3.7}$$

$$s(t) = s(t_0) + \int_{t_0}^{t} v(\tau) d\tau \tag{3.8}$$

where $v(t)$ is the velocity vector, $a(\tau)$ is the acceleration vector, $s(t)$ is the distance, t_0 is the initial time and $v(t_0)$ is the initial velocity, which is a constant. These equations are applicable for continuous data that is used after measurement. However, our IMU requires real time displacement updates and uses discrete input values. Therefore, trapezoidal integration formula (Slifka 2004) is applied for this study. There are some discrete integration methods available to

perform numerical integration and a list of distance estimation approaches can be seen in (Truong et al. 2016).

$$y(n) = y(n-1) + \frac{1}{2f_s}[x(n-1) + x(n)], \quad n = 1,2,3... \tag{3.9}$$

Trapezoidal integration is a discrete method that uses the current and previous measurement to determine the integrand shown in (3.9). In this equation $y(n)$ is the integrated output, $y(n-1)$ is the previous output, f_s is the sampling frequency, $x(n-1)$ is the previous input $x(n)$ is the current input. This integration method is applied first to the acceleration and second to the velocity to obtain the distance. Using the trapezoidal integration method will work for noise-less data that does not come from IMU accelerometers. Low-cost accelerometers do not have the required precision, and there are many errors sources associated with IMUs (S Flenniken et al. 2017). Two problems are important that need to be addressed when performing a double integration (Slifka 2004). First problem is the unknown initial conditions. Integration requires a known initial condition, whether it is initial velocity or position. Second problem is the drift in an accelerometer signal. Both can lead to serious integration errors if not corrected. To address those, each filtering step applied will result losing the ability to track a certain kind of motion. Related work in this field processes the signal in the frequency domain (Ribeiro et al. 2001; Slifka 2004).

The first problem of double integration on an acceleration signal is the lack of initial conditions where for proper integration, both initial velocity and initial position must be known from a direct measurement. If acceleration signal is integrated for an integer number of periods, the velocity function will have no DC component and therefore, there would be no need to add an initial condition (Slifka 2004). The second problem is acceleration drift that is an unwanted phenomenon caused by a small DC bias generally occurs in the acceleration signal (Ribeiro et al. 2001; Thong et al. 2004), because integrating a constant gives a slope and the second integration will give an exponential function, quickly making the output data unusable. To prevent this a high-pass filter must be applied to the input data, to correct this even better a high-pass filter should be implemented between every integration step as well (Thong et al. 2004).

During walking, horizontal distance can be obtained by integrating the acceleration. In this analysis, the distance travelled by walking is obtained principally from the trapezoidal double

integration method of the user movement accelerometer signal A_{xyz} in the walking direction. As the displacement signal emphasizes the low frequency data more than the acceleration signal, the input A_{xyz} data are passed through a high-pass filter to remove the DC component of the acceleration signal. The double integral process is shown in Figure 3.10 for calculating travelled distance. The Figure 3.10 is prepared based on the concept by (Thong et al. 2004).

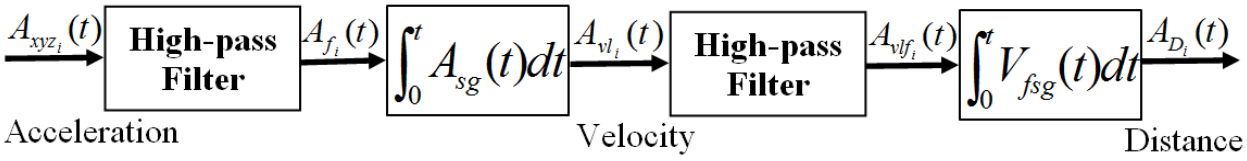

Figure 3.10: Double integral process

In order to obtain the velocity and distance in time series, two stages of integration and two stages of high-pass filtering are applied. A second-order *od=2* Butterworth high-pass filter is designed with sampling frequency *fs=50 Hz*, cut off frequency *fc=0.001 Hz*. The Butterworth filter is used with *fc* and *od* which have a magnitude response that is maximally flat in the band-pass and monotonic overall. This smoothness comes at the price of decreased roll off steepness. The output from Butterworth filter is then passed to *filtfilt* filter. The *filtfilt* corrected for phase distortion introduced by a one-pass filter, though it does square the magnitude response in the process (Oppenheim 1989). The first integral operation is applied on A_f data with respect to time *t* that gives the A_{vl} velocity (Figure 3.11).

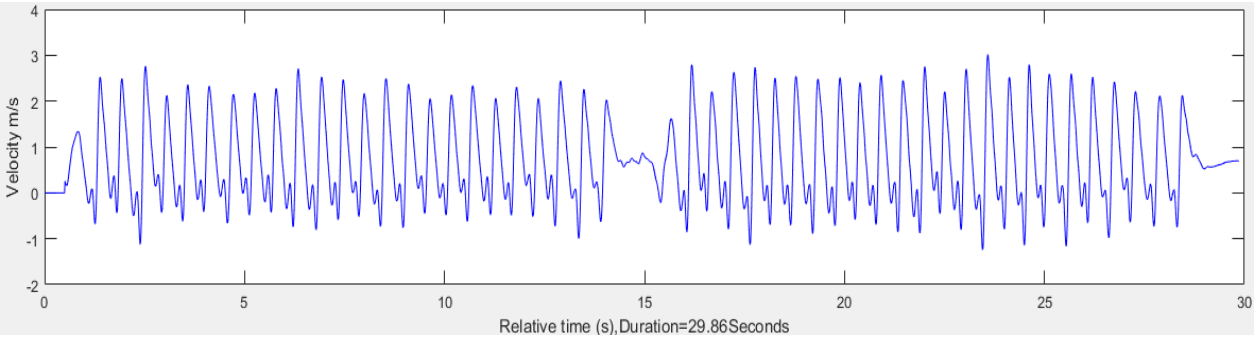

Figure 3.11: Velocity A_{vl} after first integral

Linear trends are removed using *detrend* function by computing the least-squares fit of a straight line to the data and subtracted the resulting function from the data. A_{vl} is then passed through the high-pass filter for the second time and then the distance A_D is estimated after a second integral operation that is shown in Figure 3.12.

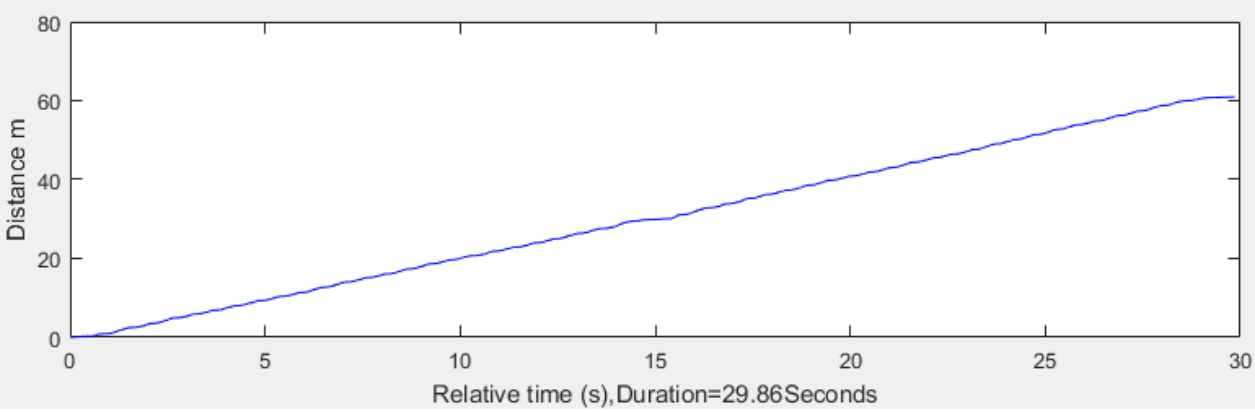

Figure 3.12: Distance A_D after second integral

The double integral process shown in Figure 3.10 and equation 3.9 are applied to estimate the walking distance. The result is presented in Table 3.1.

TABLE 3.1
Distance and Speed calculation

SL	RD (m)	ED (m)	Accuracy (%)	Period (s)	ES (m/s)
1	60.96	60.38	99.05	29.86	2.02
2	60.96	55.11	90.40	29.86	1.85
3	60.96	68.24	88.06	29.86	2.29
4	60.96	40.46	66.37	29.86	1.35
5	60.96	61.35	99.36	29.86	2.05

RD=Real Distance, ED=Estimated Distance, ES=Estimated Speed

The highest accuracy 99.36% is found at location 5. The second best accuracy is found at location 1 (99.05%) followed by location 2, location 3 and location 4. The period of walking is recorded using the android app. The estimated walking speed varied from 1.35 m/s to 2.29 m/s depending on the location. These results are consistent with human walking speed 1.5m/s to 2.5m/s previously documented in (Minetti 2000; Mohler et al. 2007).

3.1.9.3. Stride event detection

Human walking can be described and characterized in the context of a gait cycle and the details are described in Section 1.2. The period from the initial contact to pre-swing composes about 60% and initial swing and terminal swing composes about 40% of the gait cycle shown clearly in Figure 3.13. As each stride consists of stance and swing events, thus the initial contact and the border between pre-swing and initial swing are detected to get stance and swing information.

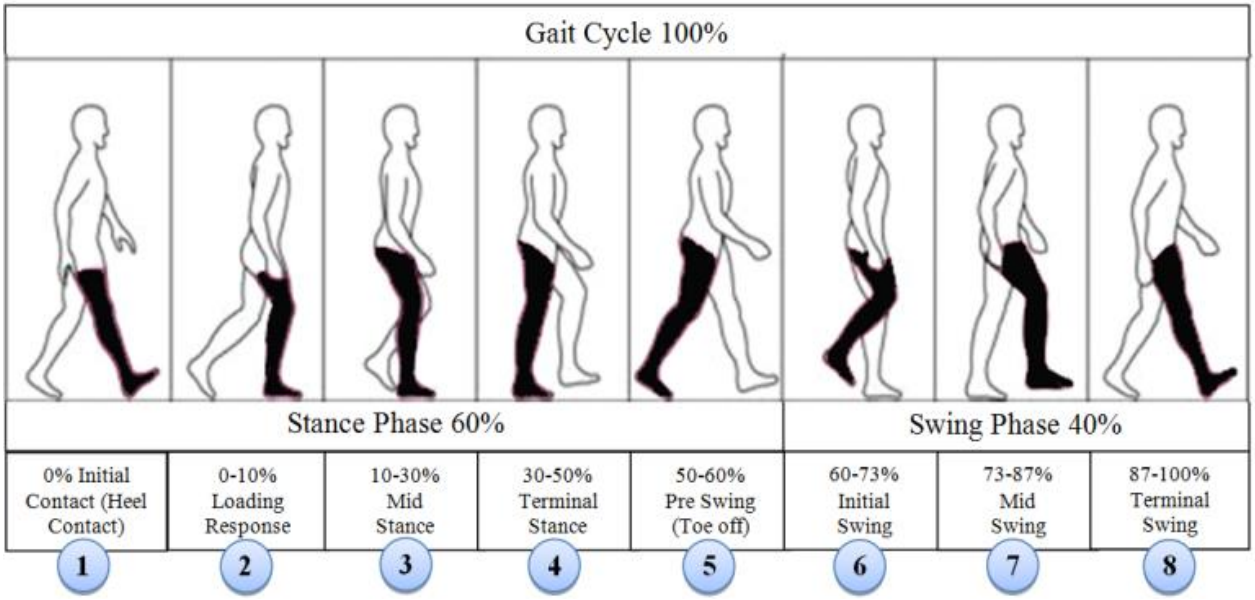

Figure 3.13. Normal human gait phases (Liu et al. 2016)

These different phases of gait cycle are identifiable from IMU acceleration data (Figure 3.14a). The gait cycle signal patterns from literature accelerometer data (Patterson et al. 2014; Liu et al. 2016) and literature gyroscope data (Greene et al. 2010b; Casamassima et al. 2014) are compared to our gait cycle signal patterns i.e. the different phases labelled in Figure 3.13 with the corresponding accelerometer data are shown in Figure 3.14a.

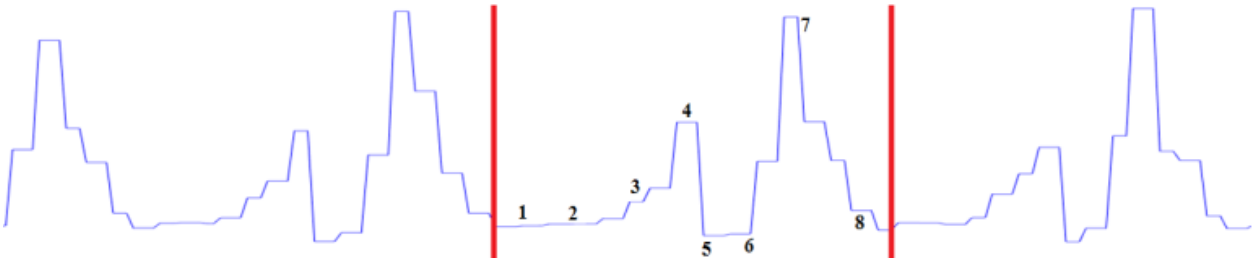

(a)

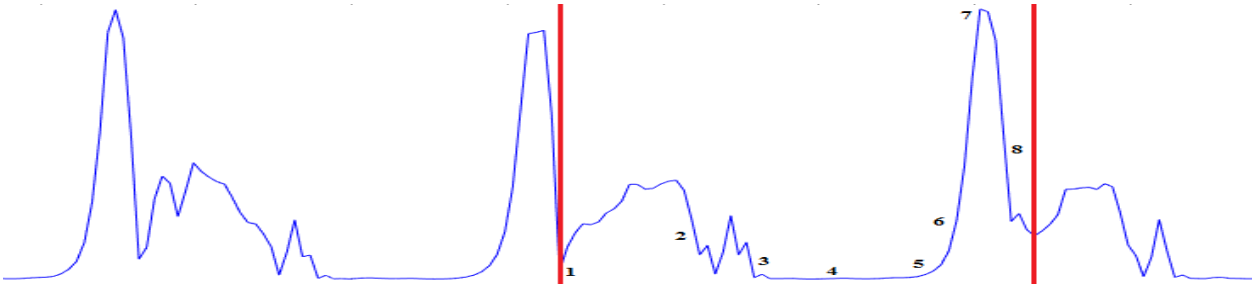

(b)

Figure 3.14: Eight different phases of a gait cycle from (a) accelerometer data and (b) gyroscope data

As we can see from Figure 3.14 that the mid-swing phase in accelerometer and gyroscope data is a reliable indicator for the performance of the gait cycle, we select this mark for counting the number of strides. The number of mid-swing phases in the accelerometer data is therefore equal to the number of strides.

Researchers used a variety of methods (Brajdic and Harle 2013) for stride event detection from IMU sensors. During human walking, a consistent sequence of motions is performed at each stride that results in a maximum peak value in the mid-swing phase. This mid-swing phase appears when the person lifts up his/her foot, shortening the limb to clear the ground, releasing the foot until it is again in contact with the ground. A particular threshold value is set to detect these characteristics for (HenkMuller 2003; Kim et al. 2004; Goyal et al. 2011). A disadvantage of these methods is that any motion with a similar periodicity of walking will trigger off a false stride event. Difficulty arises to find the automatic selection of the threshold value which can vary between users, surfaces and shoes (Gafurov and Snekkenes 2008). Most of these studies are carried under laboratory conditions (Rebula et al. 2013) and tested on a relatively small number of subjects (Brajdic and Harle 2013).

From Gyroscopic data the highest peak occurs at the mid-swing at the 7^{th} phase (Figure 3.14b). Figure 3.8 shows that terminal stance and mid-swing events have very similar amplitudes. Applying a threshold based method to detect the stride number has a low accuracy as it detects two strides instead of single stride.

The main idea behind stride detection is identifying the characteristics of local maximal prominences of A_{sg} and G_{sg} signals that correspond to a single stride phase shown in Figure 3.14 (a). The prominence of a peak measures how much the peak stands out due to its intrinsic height and its location relative to other peaks. Measurement of the prominence of a peak requires three steps. First a marker is placed on the peak. One way of marking the peaks is to make use of the fact that the first derivative of a peak has a downward-going zero-crossing at the peak maximum. Second, a horizontal line from the trough is extended to the left and right side until the line crosses the signal or reaches the left or right end of the signal. Third calculate the maximum perpendicular distance from the peak to the horizontal line. This is defined as the maximum prominence of the peak. Figure 3.15 demonstrates an example of these three steps. Each peak is assigned to a marker labelled *1* to *3* (peak) and *a* to *c* (trough). A horizontal line from each through is extended to right and left side. The line from marker *a* reaching to the left end. The

maximum perpendicular distance is then estimated between the marker *a* and the endpoint. The similar procedure is followed for finding the maximal prominence of the peak.

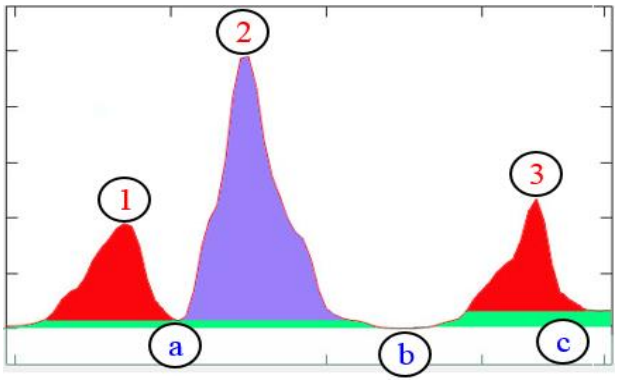

Figure 3.15: Finding the maximum prominence of the peak

To perform the analysis, the characteristics of local maximal prominences of A_{sg} and G_{sg} are estimated through to a MATLAB built-in function *findpeaks* (The MathWorks Inc 2016). The *findpeaks* finds local peaks in the data vector and ignores small peaks that occur in the neighbourhood of a larger peak. It returns two vectors with the peaks (local maximal) and locations at which the peaks occur. A local peak is a data sample that is either larger than its two neighbouring samples or is equal to *Inf*. If a peak is flat, the function returns only the point with the lowest index. The outputs of these steps are shown in Figure 3.16. The blue triangles show mid-swing phases for accelerometer (upper plot) and gyroscope (lower plot) in each stride.

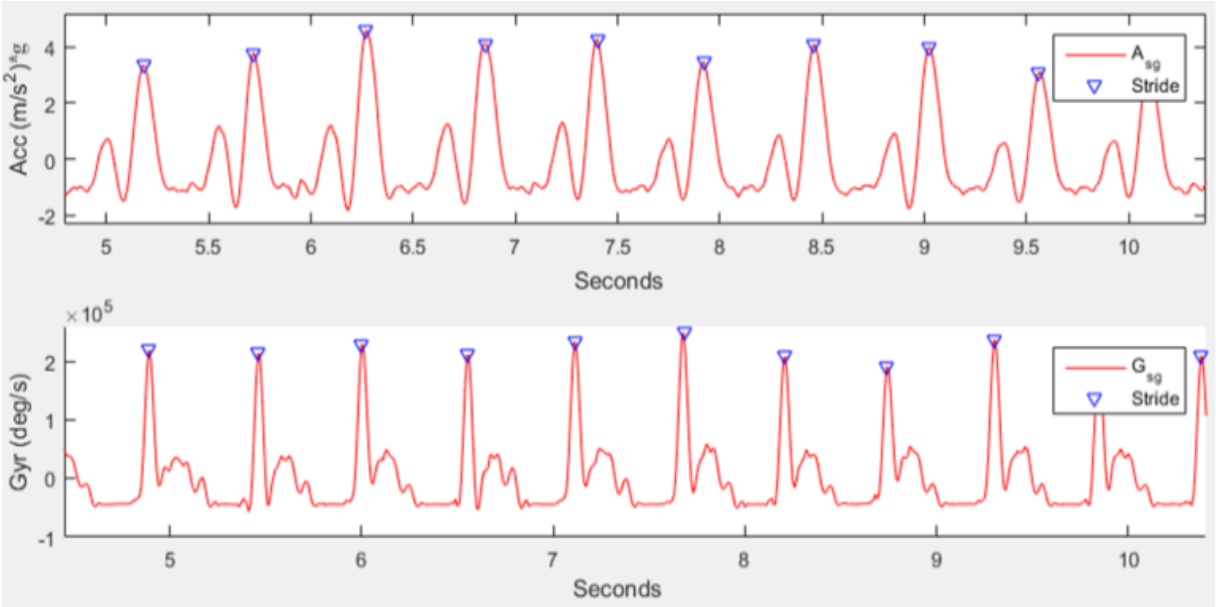

Figure 3.16: Strides detection from accelerometer and gyroscope data

These strides contain two arrays, one containing amplitude A_P, G_P in m/s^2 (peaks) and the time of those amplitudes A_L, G_L in *Time(t)* (locations) for corresponding accelerometer and gyroscope data. The number of A_P and G_P give the number of strides.

$$Accuracy = \begin{cases} \dfrac{StrideNumber_{Acc}}{ActualStride} \times 100\% & if\ (ActualStride \geq StrideNumber_{Acc}) \\ \dfrac{100 - StrideNumber_{Acc}}{ActualStride} \times 100\% & Otherwise \end{cases} \tag{3.10}$$

The accuracy of the stride number estimated from five locations is computed using equation (3.10) and compared to the offline measured values shown in Table 3.2. The accuracy for both accelerometer and gyroscope data is estimated using equation (3.10) where *ActualStride* = 50.

TABLE 3.2
Stride detection accuracy from accelerometer and gyroscope data

Stride Number Estimation				
SL	SN_{Acc}	$Accuracy_{Acc}$	SN_{Gyr}	$Accuracy_{Gyr}$
1	48	96%	50	100%
2	43	86%	46	92%
3	48	96%	49	98%
4	48	96%	48	96%
5	50	100%	50	100%

SL=Sensor Location, SN=Stride Number

From Table 3.2, the highest detection is 100% from both acceleration and gyroscope data at location 5 which is over the insertion of the Achilles tendon into the calcaneum. The sensor orientation is also at a phase of 90 degrees with the earth frame that gave significant information of each stride. The second best result is 96% from accelerometer and 100% from gyroscope data at location 1 (medial aspect of foot over the bony prominence of the first cuneiform). The sensor orientation and location of this place is the most stable as it is over a bone and relative movement is low. The third and fourth best locations are location 3 and 4 where the sensor orientation is tilted and the relative movement is high. The stride information of test subject 1 is presented in Table 3.3.

TABLE 3.3
Stride length and period for subject 1

Stride Information				
	Length (m)		Period (s)	
SL	M	SD	M	SD
1	1.042	0.134	0.509	0.077
2	1.543	0.313	0.485	0.098
3	0.541	0.166	0.434	0.133
4	0.917	0.163	0.476	0.085
5	0.904	0.247	0.453	0.124

M=Mean, SD=Standard Deviation

The standard deviations of the mean length and the mean period from location 1 are the lowest compared to location 2 to 5. Location 1 is therefore the more consistent and stable location. Location 2 has the highest standard deviation for mean length and location 3 for mean period indicating that these locations has more variation and poorer reliability.

3.1.9.4. Stance and swing events detection

The stance and swing events are then detected by finding the local minima prominences before and after each mid-swing from A_P, and A_L using function *findpeaks*. A loop from 1 to total stride number is used to find each stance and swing events for each stride. The output to extract stance and swing phases is shown in Figure 3.17.

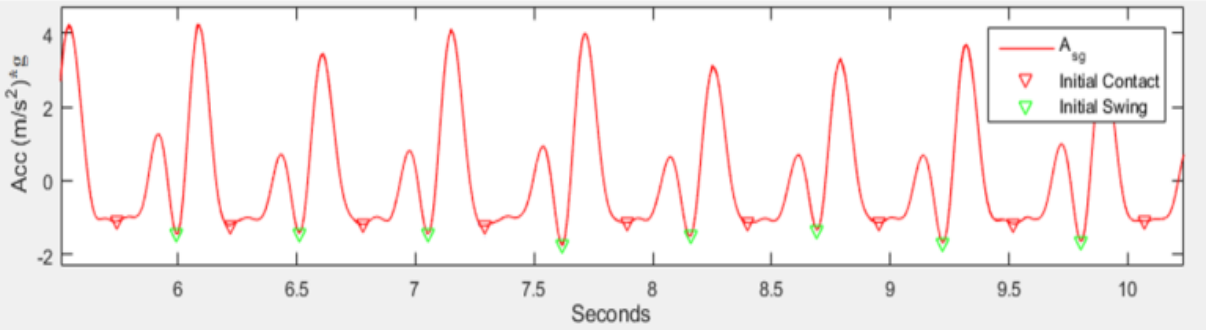

Figure 3.17. Stance and swing phases

In natural walking, the foot is on the ground for a little more than 60% of the total gait cycle referred as stance phase. A stance length is the distance between the heel contact and pre-swing phases and stance period is the interval of stance length. The stance information of test subject 1 is presented in Table 3.4. During the remainder of the gait cycle which is around 40%, the foot is off the ground as the limb is swung forward to begin the next stride referred as the swing phase. A swing length is the distance between the initial swing and terminal swing phases

and the swing period is the interval of swing length. The swing information of test subject 1 is presented in Table 3.5.

Using the stride and distance data, our method is used to estimate stance and swing phase movement information shown in Tables 3.4-3.5.

TABLE 3.4

Stance length, period and ratio for subject 1

Stance Information					
	Length (m)		Period (s)		% of Stride
SL	M	SD	M	SD	
1	0.555	0.011	0.271	0.057	53.214
2	0.560	0.012	0.176	0.038	36.292
3	0.196	0.054	0.157	0.044	36.178
4	0.534	0.010	0.278	0.053	58.309
5	0.526	0.014	0.264	0.074	58.245

M=Mean, SD=Standard Deviation

TABLE 3.5

Swing length, period and ratio for subject 1Swing Information

	Length (m)		Period (s)		% of Stride
SL	M	SD	M	SD	
1	0.488	0.010	0.238	0.051	46.786
2	0.983	0.025	0.309	0.079	63.708
3	0.345	0.012	0.277	0.098	63.822
4	0.382	0.008	0.198	0.042	41.691
5	0.377	0.010	0.189	0.051	41.755

M=Mean, SD=Standard Deviation

Stance is the first part of a stride. The standard deviations of length and period for stance and swing are low (Table 3.4). The highest % of stride is found at location 5 and location 4. According to the literature the stance and swing ratio is 60:40% of the stride location 5 and 4 are close to 60:40 % split of the stride for this subject. Although location 5 shows close to 60% of the stride for this subject, statistical analysis for this will be conducted in Section 3.3 experiment and discussion.

3.1.9.5. Summary of gait features extraction

Number of stride, travelled distance, speed, stride length, stride period, stance length, stance period, swing length and swing period and the ratio of stance and swing are estimated from the method described above. To summarize the above discussion, our proposed gait features extraction method is shown in Figure 3.18.

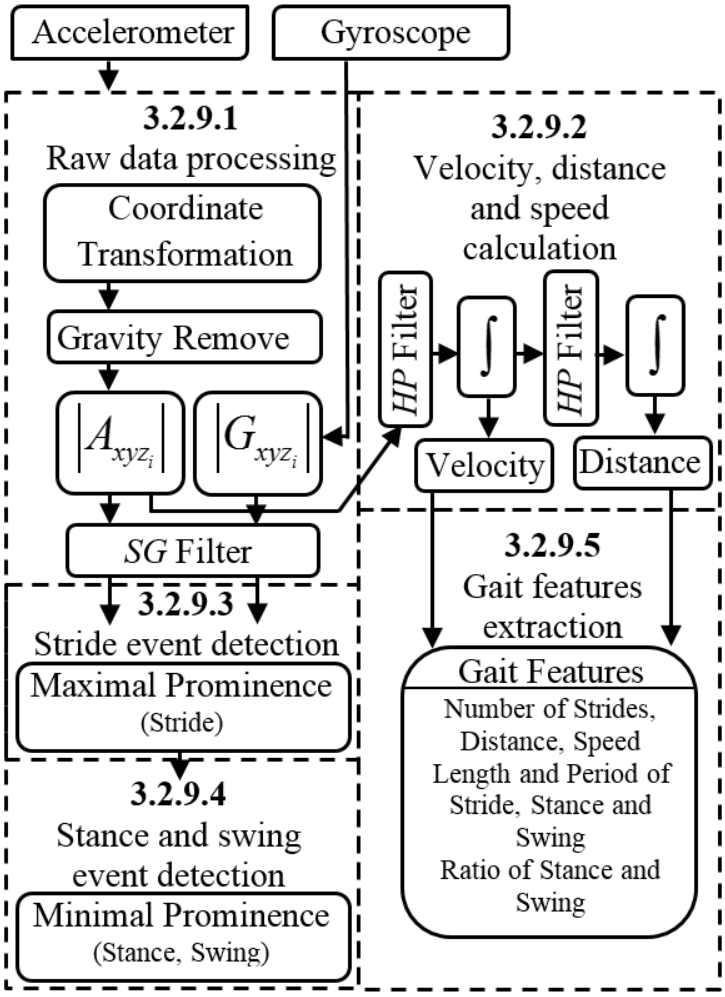

Figure 3.18: The process diagram of the automatic features extraction from accelerometer and gyroscope

3.2. Experiments and discussion

In this section, we apply the method developed in Section 3.2 from one participant to 15 participants. We present the results to demonstrate our proposed method statistically and the discussion.

3.2.1. Experiments

The procedure for gait features extraction is conducted for a total of 10 male and 5 female participants.

TABLE 3.6

Stride detection accuracy for 15 subjects

Average Stride Number Estimation				
SL	SN_{Acc}	$Accuracy_{Acc}$	SN_{Gyr}	$Accuracy_{Gyr}$
1	47.73	95.47%	46.80	93.60%
2	45.07	90.13%	46.33	92.66%
3	44.93	89.87%	46.40	92.80%
4	47.00	94.00%	46.53	93.06%
5	47.40	94.80%	46.60	93.20%

SL=Sensor Location, SN=Stride Number

Table 3.6 shows the average stride number detected for 15 participants. The highest accuracy for the detection of stride count from accelerometer and gyroscopic data is in location 1 closely followed by locations 5 and 4. Although, location 5 gave the highest accuracy during the method development in Section 3.2, with more participants location 1 shows the best result in being the closest to correlate estimated distance travelled to measured (actual) distance travelled (Table 3.7) and is also closest to the 60:40% split for average stride, stance and swing information (Table 3.8).

TABLE 3.7

Swing length, period and ratio for subject 1

SL	ED (m)	95% Confidence		Period (s)	95% Confidence	
1	58.45	56.05	60.84	1.40	1.24	1.56
2	60.10	58.12	62.09	1.46	1.27	1.65
3	56.46	52.95	59.98	1.37	1.17	1.58
4	56.68	53.68	59.67	1.38	1.20	1.56
5	56.01	53.65	58.37	1.35	1.18	1.52

ED=Estimated Distance

We checked the data for statistical errors and assessed whether the estimated values are reasonable. A boxplot of stride number estimation and accuracy of detection from accelerometer and gyroscope data for location 1 to location 5 from 15 participants is presented in Figure 3.19.

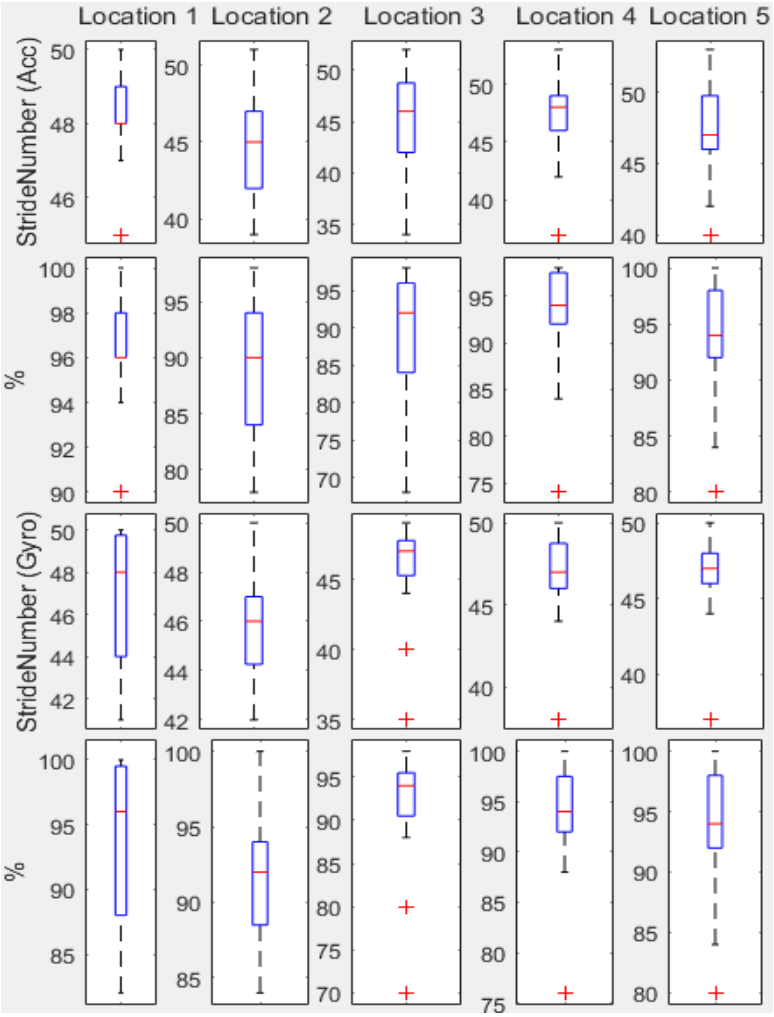

Figure 3.19: Boxplot of Stride number estimation and accuracy of detection from Accelerometer and Gyroscope data for location 1 to location 5 from 15 participants

It is to be noted that the observations identified by the boxplots are not especially extreme. Our method to detect the stride number from location 1 to location 5 shows about 45±5 strides with accuracy of about 90±5% for accelerometer and accuracy of about 90±10% for gyroscope data. The highest value of the average stride number estimation from the gyroscope is in location 1 but the data distribution is wider than other locations. The overall mean values of stride detection show that the IMU data collected from five different foot locations do not have a high variation from accelerometer data. However, the accelerometer data distribution of location 1 is more stable compared to the gyroscope data distribution showing it to be more reliable for gait analysis. Location 5 of gyroscope data shows a good data capture. Based on these observations, location 1 appeared to be the most stable to collect reliable and quality data from an accelerometer for lower limb gait analysis.

The average actual and estimated distance travelled by 15 participants, their accuracy, period of walking and estimated speed information with confidence intervals from location 1 to location 5 are presented in Table 8. The average estimated walking speed from young participants varies from 1.35m/s to 1.46m/s. The highest accuracy of distance estimation is found from location 1 with an accuracy of 95.24% followed by location 5, location 2, location 3 and location 4.

TABLE 3.8

Accuracy and confidence interval of distance and speed for 15 subjects

Average Distance and Speed calculation									
SL	AD (m)	ED (m)	(%)	95% CI		P(s)	ES (m/s)	95% CI	
1	59.21	58.45	95.24	56.05	60.84	41.22	1.40	1.24	1.56
2	59.21	60.10	85.95	58.12	62.09	41.22	1.46	1.27	1.65
3	59.21	56.46	85.87	52.95	59.98	41.22	1.37	1.17	1.58
4	59.21	56.68	85.06	53.68	59.67	41.22	1.38	1.20	1.56
5	59.21	56.01	90.85	53.65	58.37	41.22	1.35	1.18	1.52

AD=Actual Distance, ED=Estimated Distance, (%) =Accuracy, P=Period, ES=Estimated Speed, CI=Confidence Intervals

The total actual and estimated distances for performing 25 strides of normal walking, a turn-around and another 25 strides, traveling period and speed summary are presented in Figure 3.20.

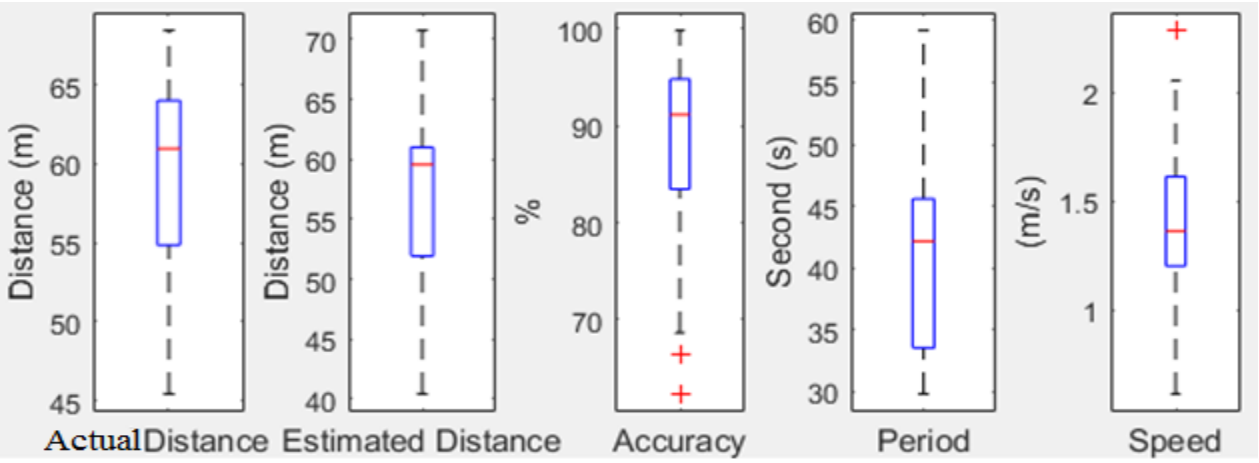

Figure 3.20: Boxplot of actual and estimation distance, their accuracy, period and speed from accelerometer data for location 1 to location 5

Due to different age groups, height and walking style, participants walks from 45m to 70m to complete a total of 50 strides. The actual distance and the estimated distance are very close in the dataset with average accuracy is more than 90%. The average stride, stance and swing phase information for 15 participants are presented in Table 3.9.

TABLE 3.9

Stride, stance and swing information for 15 subjects

SL	Average Stride		Average Stance			Average Swing		
	L (m)	P (s)	L (m)	P (s)	% S	L (m)	P (s)	% S
1	1.104	0.503	0.649	0.259	59.501	0.455	0.244	40.499
2	1.304	0.460	0.659	0.229	63.705	0.413	0.228	48.169
3	1.251	0.468	0.614	0.228	56.438	0.465	0.238	51.013
4	0.971	0.512	0.499	0.261	82.399	0.372	0.247	47.225
5	1.223	0.503	0.621	0.255	49.907	0.590	0.244	48.782

L=Length, P=Period, % S=% of Stride

The calculated average stride is based on heel to heel contact. The length and period from location 1 to 5 varies low and for normal walking, the stride length varies from person to person. Location 1 is closest to the 60:40% split for stance : swing that agrees with the literature (Iosa et al. 2013; Liu et al. 2016). The individual participant information including anthropometric characteristics is provided in Appendix B.

3.2.2. Discussion

From the above results, this study has shown that placing an IMU sensor at location 1 located on the medial aspect of foot over the bony prominence of the first cuneiform maximizes the accuracy of the collected accelerometer and gyroscope data. In this location the sensor offers the best performance to identify the stride count, calculated distance and average stride, stance and swing information. Location 1 is closely followed by locations 4 and 5. This may well be because it is easier to secure the sensor at these locations. Sensor locations 1 and 5 have less relative movement; locations 4 and 3 have slight movement during walking time while location 2 has movement due to expansion and squeezing of the foot during step movement. Location 3 also has an angular orientation when the sensor is placed that cancels the prominent data.

We have identified that placing the sensor on different locations of the foot parts affects sensor output. It is also noted that the orientation of the sensor has a significant effect on output data and placing the sensor in different locations gives a different pattern to the data. If data are to be collected regularly, the position and orientation of the sensor are crucial as changes in position through human error may give different data patterns which might be difficult to interpret. This highlights the importance of properly fixing the sensor to the optimal location to avoid inaccuracies.

Other possible areas of error may arise from frictional noise and the relative movement of clothing and shoes to the sensor. The placing of sensors on foot locations requires other generic considerations such as battery life and android device that is BLE enable to pick up sensor data.

In order to track the position in a virtual environment, several navigation methods (Hasan et al. 2009) are available to derive pose estimates from electrical measurements of mechanical, inertial, acoustic, magnetic, optical, and radio frequency sensors. Each approach has advantages and limitations including modality-specific limitations related to the physical medium, measurement-specific limitations imposed by the devices, associated signal-processing electronics, and circumstantial limitations that arise in a specific application (Welch and Foxlin 2002).

Our distance estimation method is based on results of a double integral of acceleration data and removes linear trend from the signal to estimate distance. We used the simplest technique of trapezoidal rule for estimating distance for our collected data and our estimated distance results are close to the actual distance. There are many other types of numerical integration schemes available which are much more involved and with the potential for more accuracy. However, the trapezoidal rule is the simplest technique of an entire class of numerical integration schemes which is known as the *Newton-Cotes Formulas* (Weisstein 2004) and which we have adopted. Our future plan is to investigate other methods with our collected data.

Our proposed method for detecting stride information is based on local maxima, stance and swing event information is based on local minima prominence characteristics instead of conventional threshold based detections mentioned in section 3.2.9.3. We found that that when turning or when stopping there is a poor acceleration signal. For this reason, we used local maxima or minima prominence characteristics to detect different events to avoid these crucial phases. We have shown that it is possible to detect stride, stance and swing event but further analysis of the eight events in a gait cycle is necessary to provide more accurate information of gait pattern. Automatic gait features (stride number, distance, speed, length and period of stride, stance and swing) extracted from accelerometer and gyroscope data can be used to identify and monitor abnormal gait patterns changes over time. They can provide real time monitoring of patients. This has considerable potential for future developments to identify long time gait pattern changes and explore ways how these features can be useful for fall risk assessment in an elderly population. This study has shown that this is possible.

The number of subjects is small (10 male and 5 female) which is a limitation of this study. There is also potential of a Type 1 error in detecting an effect that is not there. In addition, our subjects are walking barefoot and it is not possible to wear a shoe over the sensor as this would have caused discomfort.

We have shown that our method is capable of extracting these automatic features and has the potential to be used in assessment of gait, gait change monitoring, gait asymmetry and clinical use associated with gait pattern. Gait with slow velocity is common in elderly people (Brach and VanSwearingen 2013) and gait analysis where the gait cycle is relatively slower compared to young adult. Our low cost portable personalized proposed solution could bring out automatic gait features for monitoring longitudinal gait changes or abnormalities. In future works, we plan to use our automatic extracted gait features information to classify gait changes over time to identify abnormal gait patterns for the assessment of elderly fall risk, rehabitation and sports applications.

3.3. Conclusion

In our study we have found the optimal or best location on the foot for placing an IMU sensor for interpreting human locomotion. We have developed a mobile phone app for synchronized data collection from a low cost MetaWear CPro sensor. We also propose a method for automatic gait features and present our own real time physical data.

The influence of IMU sensor orientation and sensor placement on different foot locations had been investigated to improve the accuracy for gait analysis. The IMU accelerometer and gyroscope data had been analysed using our method to extract ten automatic features: Number of Strides, Distance, Speed, Stride Length, Stride Period, Stance Length, Stance Period, Swing Length, Swing Period and ratio of stance and swing. The trapezoidal rule based double integrating technique is applied on acceleration data to estimate the horizontal displacement of the foot and compared the result with actual distance in the real world. Our study shows that the sensor orientation and small changes of sensor location influence the sensor output. The results show that location 1 over the bony prominence of the first cuboid bone is the best place for placing a sensor as it delivers the most accurate data. This location is also the centre point of foot length. The sensor is attached with a Velcro elastic belt and buckles to adjust the fitting. As the sensor is attached on bone the relative movement between the sensor frame and foot frame is

assumed to be zero. Currently, the proposed method is only applied on estimating distance of normal walking on ground level and this method will be extended to assessment of gait, gait change monitoring, gait asymmetry and clinical use associated with gait pattern. The comparison between the real and estimated distance and speed shows a good agreement with low errors which shows that these features could be used for gait analysis in a normal daily living environment. Our future work aims to use the optimal foot location for placing IMU sensors and analyze to classify long term gait pattern changes for identifying abnormal gait patterns for the assessment of elderly fall risk, rehabilitation and sports applications.

4. GAIT FEATURE EXTRACTION, VISUALIZATION AND VALIDATION

This chapter is organized in the following sections: Section 4.1 presents the design and the method of the proposed automatic gait features extraction. Section 4.2 presents visualization of gait features information. Section 4.3 presents concurrent validation of the extracted gait features. The conclusion is given in Section 4.4.

4.1. Gait feature extraction methods

4.1.1. Participants selection

We recruit a convenience sample of 20 subjects with 10 healthy young subjects (9 male, mean age 25.3 years, standard deviation 4.64, range 19–35 years), and 10 older subjects (9 male, mean age 69.4 years, standard deviation 7.28, range 62–86 years). Older subjects 1, 3, 5, 6, 9 and 10 do not have any known health problem. Subject 2 has a right foot drop and drags the foot and toes. Subject 4 has pain in the right leg lower muscle and walks without any support. Subject 7 has pain in the lower part of his left leg and uses a crutch during walking. Subject 8 has pain in both ankles and walks with support of a walker. According to World Health Organization (WHO), the life expectancy at birth is 71 years in Bangladesh (Paranietharan 2017). Therefore, 65+ is considered old age in Bangladesh although would be viewed as young old in the Western countries. The subjects are purposefully chosen for this study to provide a variety of gaits for evaluation.

4.1.2. Experimental protocol and calibration

The experiment is performed in two different locations for young and older. The older subjects are residents in a care home. All subjects perform a walk in a straight corridor comprising of 15 strides of normal forward walking, a turn-around and another 15 strides. Accelerometer and gyroscope data from sensors attached on two foot locations are recorded in a database synchronously using our Android app. The distance carried out by walking on the corridor is measured by a tape. The several older subjects perform less than 15 strides. Calibration is performed individually where the distance travelled is measured manually and the result compared to the output from the sensor.

4.1.3. Sensor placing location

It is observed that the orientation of the IMU sensor has a significant effect on output data. In order to increase the sensor accuracy and reliability, and reduce the variability, all sensors are fitted tightly to the barefoot. From our investigation in Chapter 3, it is found that placing a sensor in different foot locations gives quite different signal patterns. In this study, the sensors are placed at metatarsal foot locations of both legs (Figure 4.1) for collecting data since the best performance can be achieved (according to the results presented in Chapter 3).

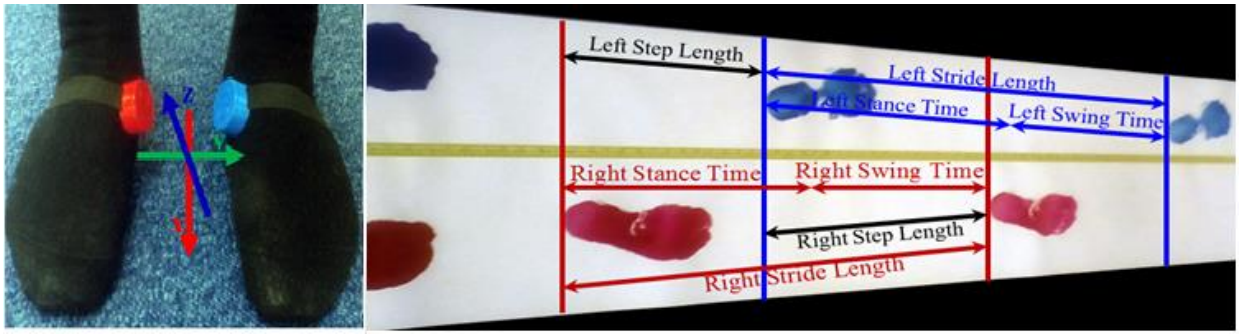

Figure 4.1: IMU sensors placement in right and left metatarsal foot locations of the barefoot.

This horizontal movement produces high acceleration during walking and this movement is the subject of investigation in this study for gait monitoring. The data with the horizontal movement information from the feet are analysed using our method to find gait information. Figure 4.2 shows the raw data of accelerometer and gyroscope collected from both right and left legs.

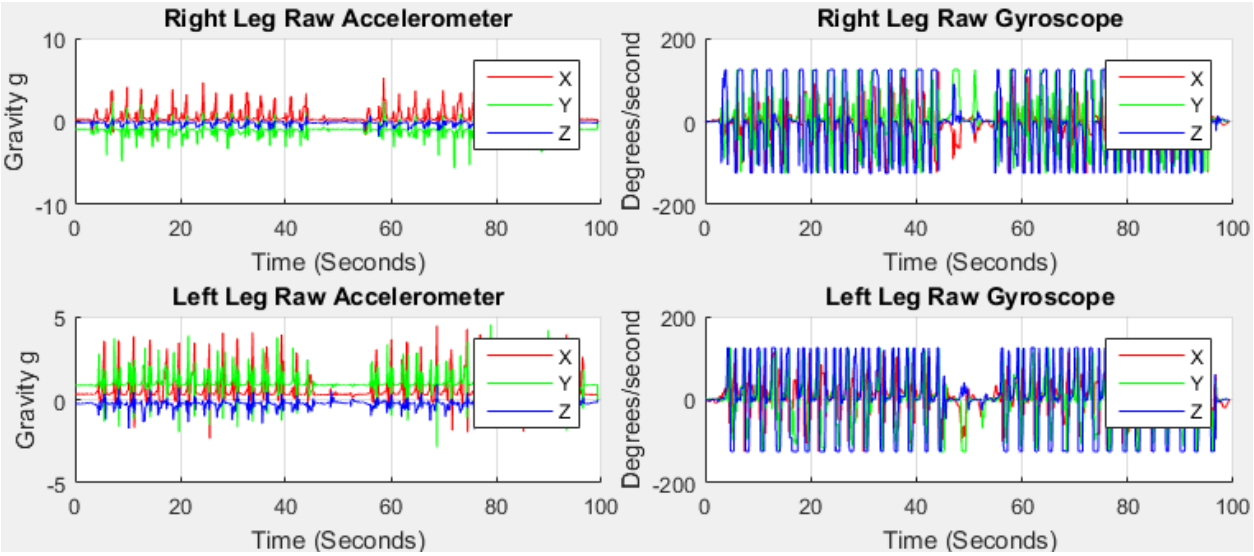

Figure 4.2: Raw accelerometer and gyroscope data from right and left feet of older subject 1.

The red, green and blue lines in Figure 4.2 stand for accelerometer readings on *x*, *y* and *z* axis, respectively, with *g* units (9.81 m/s^2) in the sensor frame. We can observe from the raw data that the accelerometer reading on *x* is the highest and *z* is the lowest before the commencement of walking for right leg indicative of the initial gravitational force. Similarly, the accelerometer reading on *y* is the highest and *z* is the lowest before the commencement of walking for left leg. The initial data is not aligned to zero means that the sensors are not placed perfectly upright position with the earth frame in the foot locations due to the initial gravity part of *y* and *z*. For this study, the sensors do not need to be perfectly upright which in any case is not user-friendly and impossible. The discrepancy between the sensor frame, the foot frame and the earth frame are compensated for in this study.

4.1.4. Raw data processing

To provide a robust absolute orientation vector in the form of quaternion or Euler angles, the MetaWear CPro IMU sensor combines the measurements from 3-axis accelerometer and 3-axis gyroscope sensors. The IMU sensor provides accelerometer $A(a_x, a_y, a_z)$ and gyroscope $G(g_x, g_y, g_z)$ with respect to time *t*. As the accelerometer is sensitive to acceleration due to movement and the local gravitational force, the input data consists of the user acceleration and gravitational acceleration.

4.1.5. Coordinate systems

In this study, there are three coordinate systems, the foot frame describing the foot rotation, the sensor frame describing the motion of the sensor and the global or Earth frame. Since the sensor is attached to the foot tightly using an elastic Velcro belt, we assume that the sensor does not slip or move during walking time. Therefore, we consider that the foot frame and sensor frame are the same. Our approach is to transfer the sensor frame to the Earth frame and then to remove the gravitational component. The high gravitational force of the Earth frame is downward towards Earth. The A_x axis is aligned along the foot axis of the IMU sensor, A_z points downwards so that it is aligned with gravity so that the three axes from a right handed coordinate system shown in Figure 4.3a.

4.1.6. Quaternion

Quaternion is a concept related to the foundations of algebra and number theory. While the accelerometer and gyroscope sensors enable the tracking of translational and rotational movements, the accurate measurement of the sensor orientation is important to interpret sensor information. Quaternions are a mathematical construct that consist of four individual numeric complex number components that can be used to represent the orientation of a ridged body or coordinate frame in a three dimensional space. Many quaternions are available to estimate the orientation from accelerometer, gyroscope and magnetometer data. We use the technique (Madgwick 2010) which fuses accelerometer, gyroscope and magnetometer for estimating quaternion. An arbitrary orientation of frame S relative to frame E can be achieved through a rotation of angle θ around an axis of S_{xyz} defined in frame E shown in Figure 4.3b where the mutually orthogonal unit vectors S_x, S_y, S_z and E_x, E_y, E_z define the principle axis of coordinate frames S and E, respectively.

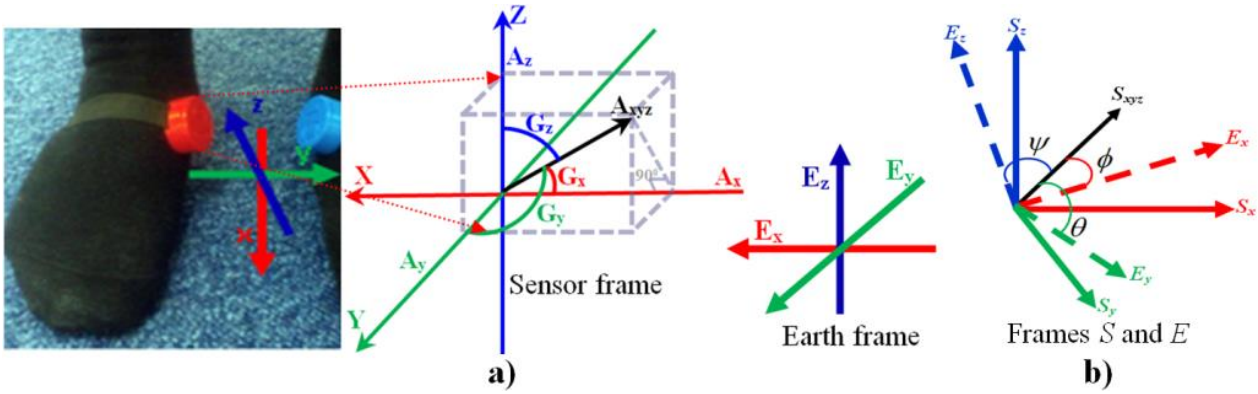

Figure 4.3: (a) Sensor frame and earth frame of accelerometer and gyroscope axes; (b) The orientation of frame E is achieved by a rotation, from alignment with frame S, of angle of φ, θ, and ψ around the axis S_{xyz}.

S_x, S_y and S_z define the components of the unit vector S_{xyz} in the three dimensional x, y and z axes of the frame S respectively.

$$ {}^{S}_{E}\hat{q} = \begin{bmatrix} q_1 & q_2 & q_3 & q_4 \end{bmatrix} = \begin{bmatrix} \cos\frac{\theta}{2} & -S_x \sin\frac{\theta}{2} & -S_y \sin\frac{\theta}{2} & -S_z \sin\frac{\theta}{2} \end{bmatrix} \qquad (4.1) $$

To denote the relative frames of orientations and vectors, ${}^{S}_{E}\hat{q}$ in equation (4.1) represents the orientation of frame E relative to frame S and S_{xyz} is a vector described in frame S (Madgwick

2010). Quaternion arithmetic often requires that a quaternion describing an orientation is first normalised which is therefore conventional for all quaternions describing an orientation to be of unit length (Madgwick 2010).

$$ {}^{S}_{E}\hat{q}^{*} = {}^{E}_{S}\hat{q} = \begin{bmatrix} q_1 & -q_2 & -q_3 & -q_4 \end{bmatrix} \tag{4.2} $$

Equation (4.2) shows the conjugate of ${}^{S}_{E}\hat{q}$. The quaternion product denoted by $\otimes$ can be used to define compound orientations. For example, two orientations described by ${}^{S}_{E}\hat{q}$ and ${}^{E}_{F}\hat{q}$, the compounded orientation ${}^{S}_{F}\hat{q}$ are defined as

$$ {}^{S}_{F}\hat{q} = {}^{E}_{F}\hat{q} \otimes {}^{E}_{S}\hat{q} \tag{4.3} $$

$$ E_v = {}^{S}_{E}\hat{q} \otimes S_v \otimes {}^{E}_{S}\hat{q}^{*} \tag{4.4} $$

A three dimensional vector can be rotated by a quaternion using the relationship described in equation (4.4) (Kuipers 2002) where S_v and E_v are the same vector described in frame S and frame E respectively and each vector contains a 0 inserted as the first element to make them four element row vectors.

$$ {}^{S}_{E}R = \begin{bmatrix} 2q_1^2 - 1 + 2q_2^2 & 2(q_2q_3 + q_1q_4) & 2(q_2q_4 - q_1q_3) \\ 2(q_2q_3 - q_1q_4) & 2q_1^2 - 1 + 2q_3^2 & 2(q_3q_4 + q_1q_2) \\ 2(q_2q_4 + q_1q_3) & 2(q_3q_4 + q_1q_2) & 2q_1^2 - 1 + 2q_4^2 \end{bmatrix} \tag{4.5} $$

The orientation described by ${}^{S}_{E}\hat{q}$ can be represented as the rotation matrix ${}^{S}_{E}R$ defined by equation (4.5).

$$ \phi = S\tan 2(2q_2q_3 - 2q_1q_4, 2q_1^2q_2^2 - 1) \tag{4.6} $$

$$ \theta = -\sin^{-1}(2q_2q_4 + 2q_1q_3) \tag{4.7} $$

$$ \psi = S\tan 2(2q_3q_4 - 2q_1q_2, 2q_1^2 + 2q_4^2 - 1) \tag{4.8} $$

The three Euler angles roll (ϕ), pitch (θ) and yaw (ψ) are known aerospace sequence (Kuipers 2002) that describe an orientation of frame E achieved by the sequential rotation to

alignment with frame *S*, of ϕ around E_x, θ around E_y and ψ around E_z. The Euler angles represented by ${}^{S}_{E}\hat{q}$ are presented in equations (4.6), (4.7) and (4.8).

4.1.6.1. Orientation from angular rate

A three dimensional gyroscope measured the angular rate about the *x*, *y* and *z* axes of the sensor frame defined as ω_x, ω_y and ω_z respectively.

$$ {}^{S}\omega = \begin{bmatrix} 0 & \omega_x & \omega_y & \omega_z \end{bmatrix} \tag{4.9} $$

$$ {}^{S}_{E}\dot{q} = \frac{1}{2} {}^{S}_{E}\hat{q} \otimes {}^{S}\omega \tag{4.10} $$

The quaternion derivative describing the rate of change of orientation of the earth frame relative to the sensor frame ${}^{S}_{E}\dot{q}$ can be calculated by the parameters ω_x, ω_y and ω_z in rads^{-1} arranged into the vector ${}^{S}\omega$ defined by equations (4.9) and (4.10) (Madgwick 2010).

$$ {}^{S}_{E}\dot{q}_{\omega,t} = \frac{1}{2} {}^{S}_{E}\hat{q}_{est,t-1} \otimes {}^{S}\omega_t \tag{4.11} $$

The orientation of the earth frame relative to the sensor frame at time *t*, ${}^{S}_{E}\dot{q}_{\omega,t}$, can be computed by numerically integrating the quaternion derivative ${}^{S}_{E}\dot{q}_{\omega,t}$ as described by equations (4.11) and (4.12) provided that initial conditions are known.

$$ {}^{S}_{E}q_{\omega,t} = {}^{S}_{E}\hat{q}_{est,t-1} + {}^{S}_{E}\dot{q}_{\omega,t}\Delta t \tag{4.12} $$

where ${}^{S}\omega_t$ is the angular rate measured at time *t*, Δt is the sampling period and ${}^{S}_{E}\hat{q}_{est,t-1}$ is the previous estimation of the orientation. The subscript ω indicates that the quaternion is calculated from angular rate.

4.1.6.2. Orientation from vector observations

An accelerometer sensor measures the magnitude and the gravitational force of the direction in the sensor frame compounded with linear accelerations due to motion of the sensor. In this application of gait asymmetry, it may be acceptable to use a Euler angle representation allowing

an incomplete solution to be found as two known Euler angles. However, a quaternion representation requires a complete solution to be found which may be achieved through the formulation of an optimization problem where an orientation of the sensor, ${}^{S}_{E}\hat{q}$, is that which aligns a predefined reference direction of the field in the earth frame, ${}^{E}\hat{q}$, with the measured direction of the field in the sensor frame ${}^{S}\hat{s}$, using the rotation operation described by equation (4.4) (Madgwick 2010).

$$\min_{{}^{S}_{E}\hat{q} \in \Re^4} f({}^{S}_{E}\hat{q}, {}^{E}\hat{d}, {}^{s}\hat{s}) \tag{4.13}$$

$$f({}^{S}_{E}\hat{q}, {}^{E}\hat{d}, {}^{s}\hat{s}) = {}^{S}_{E}\hat{q} * \otimes {}^{E}\hat{d} \otimes {}^{S}_{E}\hat{q} - {}^{s}\hat{s} \tag{4.14}$$

$${}^{S}_{E}\hat{q} = \begin{bmatrix} q_1 & q_2 & q_3 & q_4 \end{bmatrix} \tag{4.15}$$

$${}^{E}\hat{d} = \begin{bmatrix} 0 & d_x & d_y & d_z \end{bmatrix} \tag{4.16}$$

$${}^{S}\hat{s} = \begin{bmatrix} 0 & s_x & s_y & s_z \end{bmatrix} \tag{4.17}$$

Therefore ${}^{S}_{E}\hat{q}$ may be found as the solution to equation (4.13) where equation (4.14) defines the objective function. The components of each vector are defined in equations (4.15) to (4.17) (Madgwick 2010).

$${}^{S}_{E}q_{k+1} = {}^{S}_{E}\hat{q}_k - \mu \frac{\nabla f({}^{S}_{E}\hat{q}_k, {}^{E}\hat{d}, {}^{s}\hat{s})}{\left\| \nabla f({}^{S}_{E}\hat{q}_k, {}^{E}\hat{d}, {}^{s}\hat{s}) \right\|}, k = 0,1,2,...n \tag{4.18}$$

$$\nabla f({}^{S}_{E}\hat{q}_k, {}^{E}\hat{d}, {}^{s}\hat{s}) = J^T({}^{S}_{E}\hat{q}_k, {}^{E}\hat{d}) f({}^{S}_{E}\hat{q}_k, {}^{E}\hat{d}, {}^{s}\hat{s}) \tag{4.19}$$

$$\nabla f({}^{S}_{E}\hat{q}_k, {}^{E}\hat{d}, {}^{s}\hat{s}) = \begin{bmatrix} 2d_x(\frac{1}{2} - q_3^2 - q_4^2) + 2d_y(q_1q_4 + q_2q_3) + 2d_z(q_2q_4 - q_1q_3) - s_x \\ 2d_x(q_2q_3 - q_1q_4) + 2d_y(\frac{1}{2} - q_2^2 - q_4^2) + 2d_z(q_1q_2 + q_3q_4) - s_y \\ 2d_x(q_1q_3 + q_2q_4) + 2d_y(q_3q_4 - q_1q_2) + 2d_z(\frac{1}{2} - q_2^2 - q_3^2) - s_z \end{bmatrix} \tag{4.20}$$

$$J({}^{S}_{E}\hat{q}_k, {}^{E}\hat{d}) = \begin{bmatrix} 2d_y q_4 - 2d_z q_3 & 2d_y q_3 + 2d_z q_4 & -4d_x q_3 + 2d_z q_3 - 2d_z q_1 & -4d_x q_4 + 2d_y q_1 + 2d_z q_2 \\ -2d_x q_4 + 2d_z q_2 & 2d_x q_3 - 4d_y q_2 + 2d_y q_1 & 2d_x q_2 + 2d_z q_4 & -2d_x q_1 - 4d_y q_4 + 2d_z q_3 \\ 2d_x q_3 - 2d_y q_2 & 2d_x q_4 - 2d_y q_1 - 4d_z q_2 & 2d_x q_1 + 2d_y q_4 - 4d_z q_3 & 2d_x q_2 + 2d_y q_3 \end{bmatrix} \tag{4.21}$$

The gradient descent algorithm is one of the simplest to both implement and compute presented in equation (4.18) that describes the gradient descent algorithm for *n* iterations resulting in an orientation estimation of ${}^{S}_{E}\hat{q}_{n+1}$ based on an 'initial guess' orientation ${}^{S}_{E}\hat{q}_0$ and a step-size μ and equation (4.19) computes the gradient of the solution surface defined by the objective function and its Jacobian which is simplified to the 3rd row vectors defined by equations (4.20) and (4.21) respectively (Madgwick 2010). Equations (4.18) to (4.21) describe the general form of the algorithm applicable to a field predefined in any direction. However, if the direction of the field can be assumed to only have components within 1 or 2 of the principle axis of the global or earth coordinate frame then the equations simplify.

$${}^{E}\hat{g} = \begin{bmatrix} 0 & 0 & 0 & 1 \end{bmatrix} \tag{4.22}$$

$${}^{s}a = \begin{bmatrix} 0 & a_x & a_y & a_z \end{bmatrix} \tag{4.23}$$

$$f_g({}^{S}_{E}\hat{q}, {}^{s}\hat{a}) = \begin{bmatrix} 2(q_2 q_4 - q_1 q_3) - a_x \\ 2(q_1 q_2 + q_3 q_4) - a_y \\ 2(\frac{1}{2} - q_2^2 - q_3^2) - a_z \end{bmatrix} \tag{4.24}$$

$$J_g({}^{S}_{E}\hat{q}) = \begin{bmatrix} -2q_3 & 2q_4 & -2q_1 & 2q_2 \\ 2q_2 & 2q_1 & 2q_4 & 2q_3 \\ 0 & -4q_2 & -4q_3 & 0 \end{bmatrix} \tag{4.25}$$

An appropriate convention would be to assume that the direction of gravity defines the vertical z axis as shows in equation (4.22) then substituting ${}^{E}\hat{g}$ and normalized accelerometer measurement ${}^{E}\hat{a}$ for ${}^{E}\hat{d}$ and ${}^{s}\hat{s}$ respectively in equations (4.20) and (4.21) yields equations (4.24) and (4.25) (Madgwick 2010).

$$f_{g,b}({}^{S}_{E}\hat{q}, {}^{s}\hat{a}, {}^{E}\hat{b}) = \begin{bmatrix} f_g({}^{S}_{E}\hat{q}, {}^{s}\hat{a}) \\ f_b({}^{S}_{E}\hat{q}, {}^{E}\hat{b}, \end{bmatrix} \tag{4.26}$$

$$J_{g,b}({}^{S}_{E}\hat{q}, {}^{E}\hat{b}) = \begin{bmatrix} J_g^T({}^{S}_{E}\hat{q}) \\ J_b^T({}^{S}_{E}\hat{q}, {}^{E}\hat{b}) \end{bmatrix} \tag{4.27}$$

The solution surface created by the object function in equations (4.25) and (4.26) has a minimum defined by a line and the measurements and reference directions of both fields may be combined as described in equations (4.27) and (4.28) (Madgwick 2010). A conventional approach to optimize would require multiple iterations of equation (4.18) to be computed for each new orientation and corresponding sensor measurements and an efficient algorithm would also require the step-size μ to be adjusted each iteration to an optimal value which usually obtain based on the second derivative of the objective function called the Hessian in (Madgwick 2010).

$${}^{S}_{E}q_{\nabla,t} = {}^{S}_{E}\hat{q}_{est,t-1} - \mu_t \frac{\nabla f}{\|\nabla f\|} \tag{4.28}$$

$$\nabla f = \begin{Bmatrix} J_g^T({}^{S}_{E}\hat{q}_{est,t-1}) f_g({}^{S}_{E}\hat{q}_{est,t-1}, {}^{s}\hat{a}_t) \\ J_{g,b}^T({}^{S}_{E}\hat{q}_{est,t-1}, {}^{E}\hat{b}) f_{g,b}({}^{S}_{E}\hat{q}_{est,t-1}, {}^{s}\hat{a}, {}^{E}\hat{b}) \end{Bmatrix} \tag{4.29}$$

However, these requirements considerably increase the computational load of the algorithm and are not necessary in this application and it is acceptable to compute one iteration per time sample provided that the convergence rate governed by μ_t is equal or greater than the physical rate of change of orientation presented in equation (4.28) that calculates the estimated orientation ${}^{S}_{E}q_{\nabla,t}$ computed at time *t* based on a previous estimate of orientation ${}^{S}_{E}\hat{q}_{est,t-1}$ and the objective function gradient ∇f defined by sensor measurements of ${}^{S}\hat{a}_t$ sampled at time *t* described in (Madgwick 2010) where the form of ∇f is chosen according to the sensors in use shown in equation (4.29) and the subscript ∇ indicates that the quaternion is calculated using the gradient descent algorithm.

$$\mu_t = \alpha \left\| {}^{S}_{E}\dot{q}_{\omega,t} \right\| \Delta t, \quad \alpha > 1 \tag{4.30}$$

An optimal value of μ_t can be defined as that ensures the convergence rate of ${}^{S}_{E}q_{\nabla,t}$ is limited to the physical orientation rate as this avoids overshooting due to unnecessarily large step size and therefore μ_t can be calculated using equation (4.30) from (Madgwick 2010) where Δt is the sampling period and ${}^{S}_{E}\dot{q}_{\omega,t}$ is the physical orientation rate measured by gyroscopes and α is an augmentation of μ to account for noise in accelerometer measurements.

4.1.6.3. Accelerometer and gyroscope filter fusion algorithm

An estimated orientation of the sensor frame relative to the earth frame ${}^{S}_{E}\dot{q}_{\omega,t}$ is obtained through the fusion of the orientation calculations ${}^{S}_{E}q_{\omega,t}$ and ${}^{S}_{E}q_{\nabla,t}$ calculated using equations (4.12) and (4.28) respectively.

$$ {}^{S}_{E}q_{est,t} = \gamma_t {}^{S}_{E}q_{\nabla,t} + (1-\gamma_t){}^{S}_{E}q_{\omega,t} \quad 0 \le \gamma_t \le 1 \tag{4.31} $$

The fusion ${}^{S}_{E}\hat{q}_{\omega,t}$ and ${}^{S}_{E}q_{\nabla,t}$ is described by equation (4.31) where γ_t and $(1-\gamma_t)$ are weights applied to each orientation calculation (Madgwick 2010).

$$ (1-\gamma_t)\beta = \gamma_t \frac{\mu_t}{\Delta t} \tag{4.32} $$

$$ \gamma_t = \frac{\beta}{\frac{\mu_t}{\Delta t} + \beta} \tag{4.33} $$

An optimal value of γ_t can be defined that ensures the weighted divergence of ${}^{S}_{E}q_{\omega}$ is equal to the weighted convergence of ${}^{S}_{E}q_{\nabla}$ represented in equation (4.32) where $\frac{\mu_t}{\Delta t}$ is the convergence rate of ${}^{S}_{E}q_{\nabla}$ and β is the divergence rate of ${}^{S}_{E}q_{\omega}$ expressed as the magnitude of a quaternion derivative corresponding to the gyroscope measurement error with rearranging of equation (4.32) to define γ_t in equation (4.33) (Madgwick 2010). Equations (4.32) and (4.33) ensure the optimal fusion of ${}^{S}_{E}q_{\omega,t}$ and ${}^{S}_{E}q_{\nabla,t}$ assuming that the convergence rate of ${}^{S}_{E}q_{\nabla}$ governed by ${}^{S}_{E}q_{\omega,t}$ and α is equal or greater than the physical rate of change of orientation. Therefore α has no upper bound.

$$ {}^{S}_{E}q_{\nabla,t} \approx -\mu_t \frac{\nabla f}{\|\nabla f\|} \tag{4.34} $$

If α is assumed to be very large then μ_t defined by equation (4.30) also becomes very large and the orientation filter equations simplify and a large value of μ_t used in equation (4.28) means that ${}^{S}_{E}\hat{q}_{est,t-1}$ becomes negligible and the equation can be rewritten as equation (4.34) (Madgwick 2010).

$$ \gamma_t \approx \frac{\beta \Delta t}{\mu_t} \tag{4.35} $$

The definition of γ_t in equation (4.33) also simplifies as the β term in the denominator becomes negligible and the equation can be rewritten as equation (4.35) (Madgwick 2010) assuming that $\gamma_t \approx 0$.

$$ {}^{S}_{E}\hat{q}_{est,t} = \frac{\beta \Delta t}{\mu_t}\left(-\mu_t \frac{\nabla f}{\|\nabla f\|}\right) + (1-0)\left({}^{S}_{E}\hat{q}_{est,t-1} + {}^{S}_{E}\dot{q}_{\omega,t}\Delta t\right) \tag{4.36} $$

$$ {}^{S}_{E}q_{est,t} = {}^{S}_{E}\hat{q}_{est,t-1} + {}^{S}_{E}\dot{q}_{est,t}\Delta t \tag{4.37} $$

$$ {}^{S}_{E}\dot{q}_{est,t} = {}^{S}_{E}\dot{q}_{\omega,t} - \beta {}^{S}_{E}\dot{\hat{q}}_{\in t,t} \tag{4.38} $$

$$ {}^{S}_{E}\dot{\hat{q}}_{\in t,t} = \frac{\nabla f}{\|\nabla f\|} \tag{4.39} $$

Substituting equations (4.12), (4.34) and (4.35) into equation (4.30) directly yields equation (4.36) (Madgwick 2010) by noting that in equation (37), γ_t has been substituted as both as equations (4.34) and 0. Equation (4.36) can be simplified to equation (4.37) where ${}^{S}_{E}\dot{q}_{est,t}$ is the estimated rate of change of orientation defined by equation (4.38) and ${}^{S}_{E}\dot{q}_{\in,t}$ is the direction of the error of ${}^{S}_{E}\dot{q}_{est,t}$ defined by equation (4.39) (Madgwick 2010). It can be seen from equations (4.37) and (4.39) that the filter calculates the orientation ${}^{S}_{E}q_{est}$ by numerically integrating the estimated orientation rate ${}^{S}_{E}\dot{q}_{est}$ and the filter computes ${}^{S}_{E}\dot{q}_{est}$ as the rate of change of orientation measured by

the gyroscope ${}^{S}_{E}\dot{q}_{\omega}$ with the magnitude of the gyroscope measurement error β removed in the direction of the estimated error ${}^{S}_{E}\dot{\hat{q}}_{\epsilon}$ computed from accelerometer measurement.

Any practical implementation of an IMU must also address the gyroscope zero bias drift over time with temperature and motion. Therefore, gyroscope bias drift may be compensated for any simpler orientation filters through the integral feedback of the error in the rate of change of orientation (Mahony et al. 2008).

$$ {}^{S}\omega_{\epsilon,t} = 2\,{}^{S}_{E}\hat{q}^{*}_{est,t-1} \otimes {}^{S}_{E}\dot{\hat{q}}_{\epsilon,t} \tag{4.40} $$

We use the approach similar in (Madgwick 2010) to normalize the direction of the estimated error in the rate of change of orientation ${}^{S}_{E}\dot{\hat{q}}_{\epsilon}$ by expressing the angular error in each gyroscope axis using equation (4.40) derived as the inverse to the relationship defined in equation (4.10).

$$ {}^{S}\omega_{b,t} = \varsigma \sum_{t} {}^{S}\omega_{\epsilon,t} \Delta t \tag{4.41} $$

$$ {}^{S}\omega_{c,t} = {}^{S}\omega_{t} - {}^{S}\omega_{b,t} \tag{4.42} $$

The gyroscope bias ${}^{S}\omega_{\epsilon}$ is represented by the DC component of ${}^{S}\omega_{\epsilon}$ and so may remove as the integral of ${}^{S}\omega_{\epsilon}$ weighted by an appropriate gain ς which yield the compensated gyroscope measurements ${}^{S}\omega_{c}$ as shown in equation (4.41) and (4.42) where the first element of ${}^{S}\omega_{c}$ is always assumed to be zero (Madgwick 2010). The compensated gyroscope measurement ${}^{S}\omega_{c}$ then be used in place of the gyroscope measurements ${}^{S}\omega$ in equation (4.10) where the magnitude of the angular error in each axis ${}^{S}\omega_{\epsilon}$ is equal to a quaternion derivative of unit length and then the integral gain ς directly defines the rate of convergence of the estimated gyroscope bias ${}^{S}\omega_{b}$ expressed as the magnitude of a quaternion derivative (Madgwick 2010). The complete orientation of ${}^{S}_{E}\hat{q}_{est,t}$ is achieved and Figure 4.4 shows a block diagram representation of the complete orientation filter implemented for an IMU.

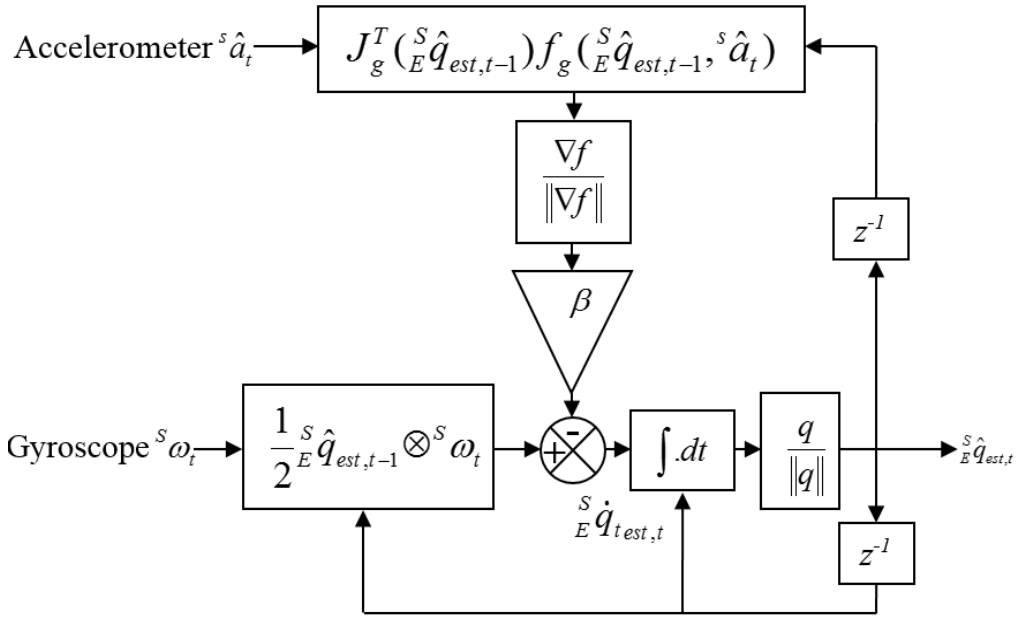

Figure 4.4: The process diagram of the complete orientation filter for an IMU.

We apply the technique shown in Figure 4.4 to our collected data for body acceleration to the Earth frame with a sampling frequency of 50 Hz, β gain of 0.1. The gravity components are removed and the conversion of the accelerometer from gravitational force g to user acceleration of movement (AM_{xyz}) m/s^2 is achieved by multiplying 9.81. The three axis data are transformed due to the fact that looking at specific axes is sensitive to the sensor orientation (Starlino 2009). Figure 4.5 shows the acceleration due to user movement AM_{xyz} = [am_x, am_y, am_z] for both feet of older subject 1.

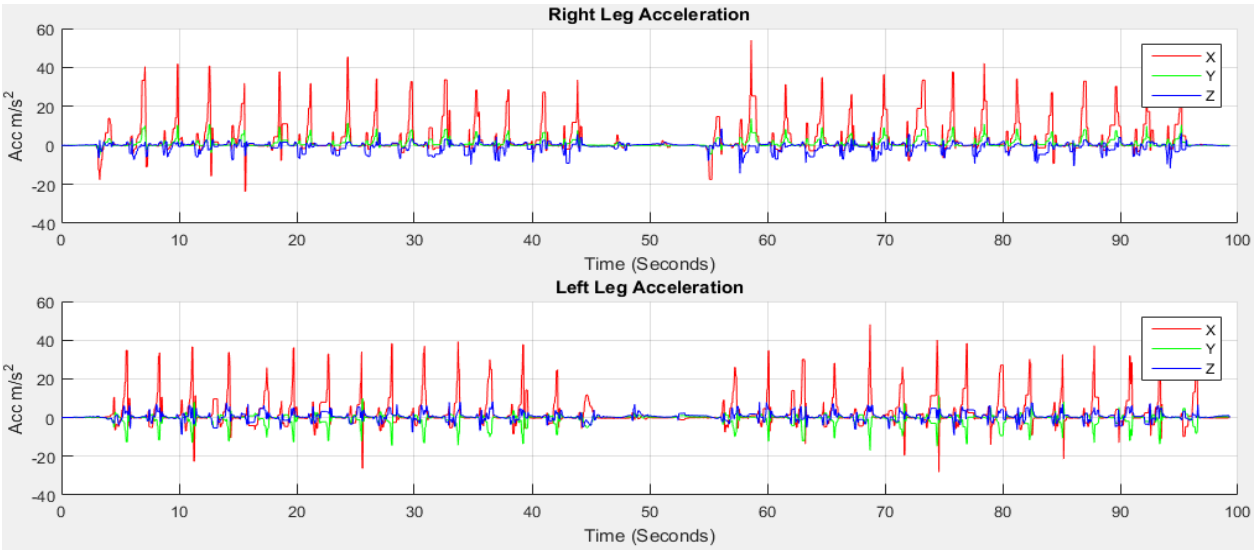

Figure 4.5: Acceleration due to user movement AM_{xyz} after removing gravity component.

Figure 4.6 shows the acceleration of total AT_{xyz} and gyroscope GT_{xyz} towards *x*, *y* and *z* directions estimated using equation (4.43):

$$\left|AT_{xyz_i}\right| = \sqrt{am_{x_i}{}^2 + am_{y_i}{}^2 + am_{z_i}{}^2} \text{ and } \left|GT_{xyz_i}\right| = \sqrt{g_{x_i}{}^2 + g_{y_i}{}^2 + g_{z_i}{}^2} \quad (4.43)$$

Statistical information of acceleration $\left|AT_{xyz_i}\right|$ and gyroscope $\left|GT_{xyz_i}\right|$ are investigated and found that data are normally distributed.

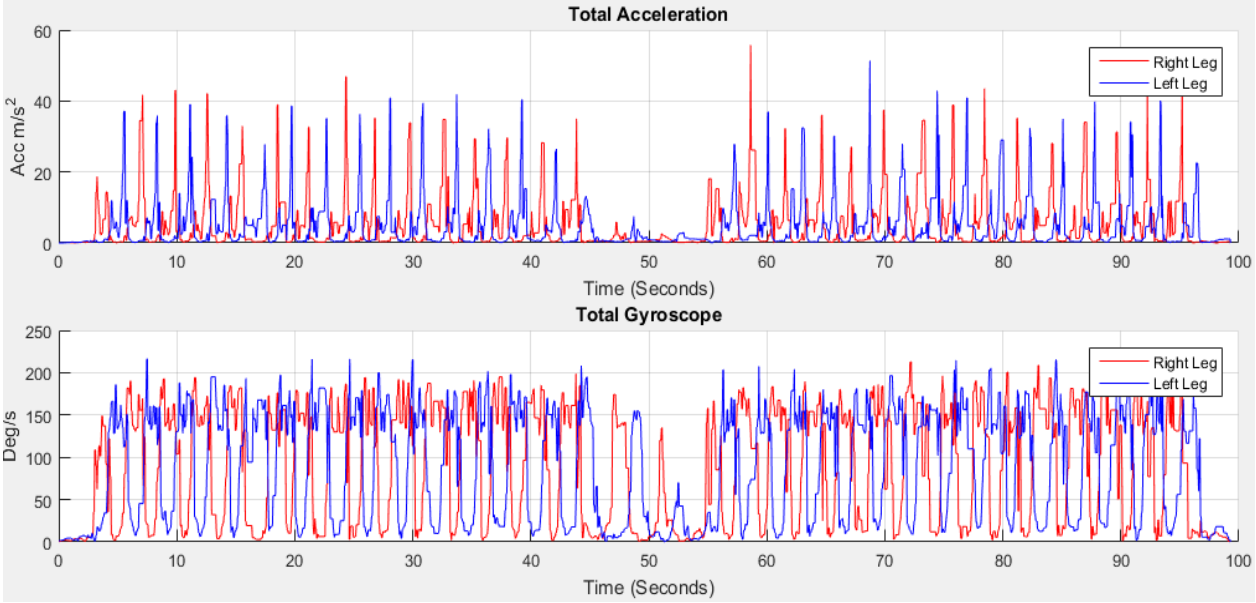

Figure 4.6: The total acceleration AT_{xyz} and gyroscope GT_{xyz}.

4.1.7. Stride, stance, swing and step events detection

The first phase starts when the heel contacts the ground and the waist is in its lowest position during the entire step. There is deceleration of the leg towards the horizontal axis as the velocity moves to zero. The zero velocity remains until the terminal stance phase where the foot is flat on the ground. The next phase is pre-swing where the toe is off the ground and starts forward movement demonstrating initial acceleration towards horizontal axis. The swing phase is when the heel moves off the ground. The acceleration interval corresponds to the change from the heel lift to the swing at the height point at mid-swing phase. Deceleration starts during the terminal swing phase from the highest point to the foot back flat on the ground. There is zero velocity again in the interval corresponding to the change from a flat foot to a heel lift. These different phases of gait cycle presented in Figure 10 are identifiable from the IMU acceleration signal. The same phenomenon of human limb kinematic with accelerometer signal output during a typical

walking cycle has been identified in the literature. Our gait cycle accelerometer signal AT_{xyz} (Figure 4.10) agrees with the signal pattern in (Patterson et al. 2014; Liu et al. 2016). The different phases of the gait cycle (Figure 3.13) with corresponding accelerometer signal are shown in Figure 3.14 in Section 3.2.9.3.

Many algorithms (Brajdic and Harle 2013) are available for stride event detection from IMU sensors. During human walking, a consistent sequence of motions is performed at each stride that results in a maximum peak value that lies in the mid-swing phase. This mid-swing phase appears when a user pushes off this foot and shortens the limb to clear ground thus releasing the foot from the ground until it again contacts with ground as shown in Figures 3.13 and 3.14. A particular threshold value is set to detect these characteristics for detecting stride (Mladenov and Mock 2009; Chon et al. 2012). One disadvantage of these algorithms is that any motion with a similar periodicity of walking will trigger for a false stride event. In addition, difficulty arises in finding the automatic selection of the threshold value which can vary between users, surfaces and shoes (Gafurov and Snekkenes 2008). The variation in the peak magnitude gets larger for faster human waking velocities (Lee et al. 2015) and a window based threshold calculation (Chon et al. 2012) is used to obtain an acceptable level of accuracy for a larger window size. However increasing the window size may degrade the step detection accuracy during the translation of step mode because the threshold calculated from a larger window may not be able to effectively handle the variation in the recent statistics (Lee et al. 2015). Due to peak magnitude variation, the threshold value also varies based on individuals walking style and even differs from left to right leg as shown in Figure 4.7.

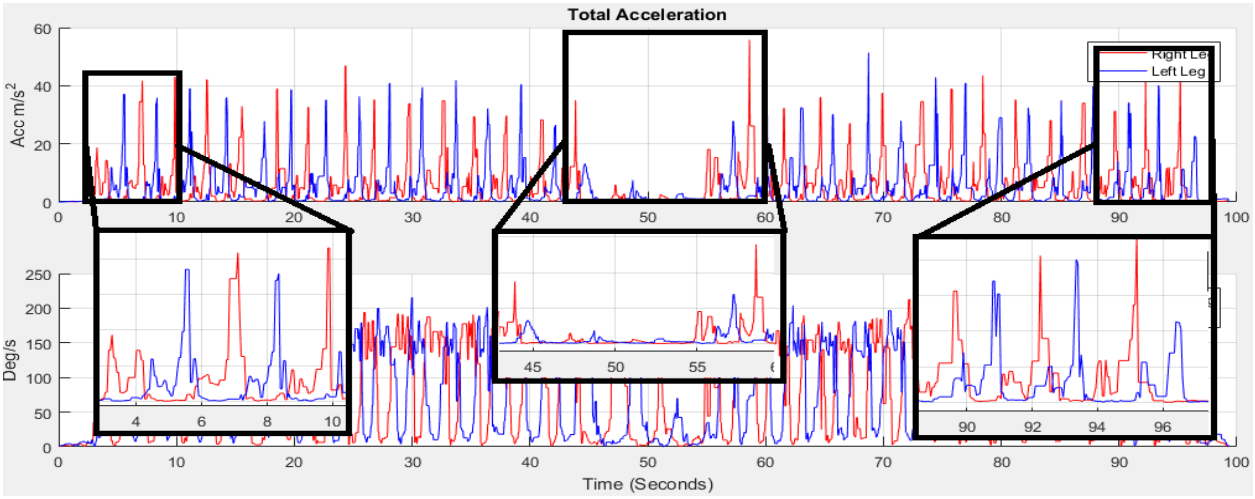

Figure 4.7: Peaks magnitude variation from Figure 4.6.

The different threshold may result in a different output of detecting steps. From our experience, we observe that older adults gait speed is slow and foot goes up a little during normal walking. Therefore, threshold based detection is not suitable for our research. Another important point is that when a subject begins walking from a standing state, stops walking for a turnaround or stops, there is poor acceleration and it is crucial to detect the gait cycle in these situations. For this reason the 1st stride is not considered for gait analysis by researchers (Truong et al. 2016). We take this in consideration to address this point in this study. As the mid-swing phase in accelerometer data is a good indicator for performing a complete gait cycle, thus for counting the number of strides, the number of mid-swing phase in accelerometer data is analysed as walking strides are equal to the number of mid-swing phases. The highest peak occurs at the push off phase starting from the terminal stance at the 4th to pre-swing at 5th phases shown in Figure 4.10b for gyroscope data. We apply threshold based algorithms obtaining low accuracy to detect the stride number for our collected accelerometer and gyroscope dataset. As the peaks at terminal stance phase are more prominent than the mid-swing phase, the threshold based algorithm detects two strides instead of single stride. We also investigate the maximum provenance of the peak for detecting strides in Section 3.2.9.3. To improve our previous study and to avoid the above problems, a novel stride detection technique is proposed based on the local minimal prominence characteristics of strides (minimal prominence of stance phase in Figure 3.14b) associated with the time-varying magnitude of acceleration shown in Figure 4.8. Our investigation shows that the minimal prominence has less variation than the peak of maximal prominence. Therefore, the minimal prominence of stance phase (phase 1 and 2 in Figure 3.14b) and swing phase (phases 5 and 6 in Figure 3.14b) are detected. The technique consists of designing a high-pass filter, computing the absolute value, designing a low-pass filter, shifting data to centroid and finding the strides from minimal prominence of the signal. To measure the prominence of a peak requires three steps described in Section 3.2.9.3. For implementing to find the minimal prominence of the signal, *findpeaks* (The MathWorks Inc 2016) function is used.

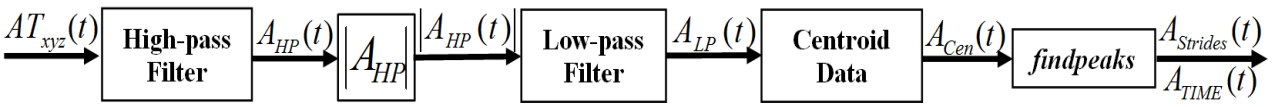

Figure 4.8: The proposed step detection technique.

The accelerometer converts acceleration to an electrical signal and in the process, unwanted constant bias in acceleration becomes a linear error called drift. Thus the 2nd order Butterworth

digital high-pass filter with a sampling rate *fs* = 50 Hz and cut off frequency *fc* = 0.001 Hz is applied to AT_{xyz} to remove the linear DC component of the acceleration signal. The smoothness is achieved at the price of decreased roll off steepness. The phase response of this filter is not linear that means if a signal is passed through this filter, then different frequency components of this signal will be delayed by different lengths of time, causing distortion (Thong et al. 2004). To linearize the phase, we filter the signal, time reverse the signal, and filter it again with the same filter (Thong et al. 2004). The second time through the filter corrects the phase response. The phase distortion after the digital high-pass filter is corrected by applying a zero phase *filtfilt* delay filter (Oppenheim 1989).

$$A_{Cen} = A_{LP} - mean(A_{LP}) \tag{4.44}$$

The output of *filtfilt* filter then is passed through a low-pass filter with *fc* = 5 Hz for smoothing to obtain A_{LP} which is shifted to centroid using equation (4.44). To find the local minima prominences, A_{Cen} is passed through a *findpeaks* function which finds local peaks in the data vector and ignores small peaks that occur in the neighbourhood of a larger peak. A local peak is a data sample that is either greater than its two neighbouring samples or is equal to Inf. If a peak is flat, the function returns only the point with the lowest index. The *findpeaks* function detects the stationary periods when the foot touches the ground the point of minimal prominence during walking. The function returns two vectors containing the minimal local peaks $A_{Strides}$ and the locations A_{TIME} at which the peaks occur. The number of strides is the same as the length of $A_{Strides}$ vector. Again, as each stride consists of stance and swing events, thus the initial contact and the transition between pre-swing and initial swing (4th and 5th phases in Figure 3.14b) are detected using steps in Figure 4.9 to get stance and swing information.

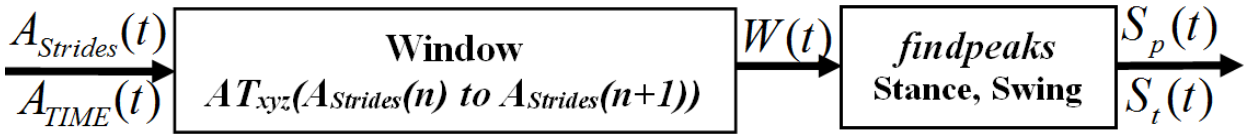

Figure 4.9: Proposed stance and swing detection technique.

A *window* is prepared whose size is the difference between a pairwise consecutive strides from $A_{Strides}$. Each *window* is then passed through *findpeaks* function as there is only one local maximum in each stride located between 4th and 5th phases (Figure 3.12). A loop from 1 to total detected strides number is used to find the stance and swing event for all strides. The detected *Start* (purple circle), *SS* (cyan triangle) and *End* (black rectangle) information of each stride are

shown in Figure 4.10 for right and legs where the stance phase information is provided by the difference between *Start* and *SS*; and the swing information is the difference between *SS* and *End*.

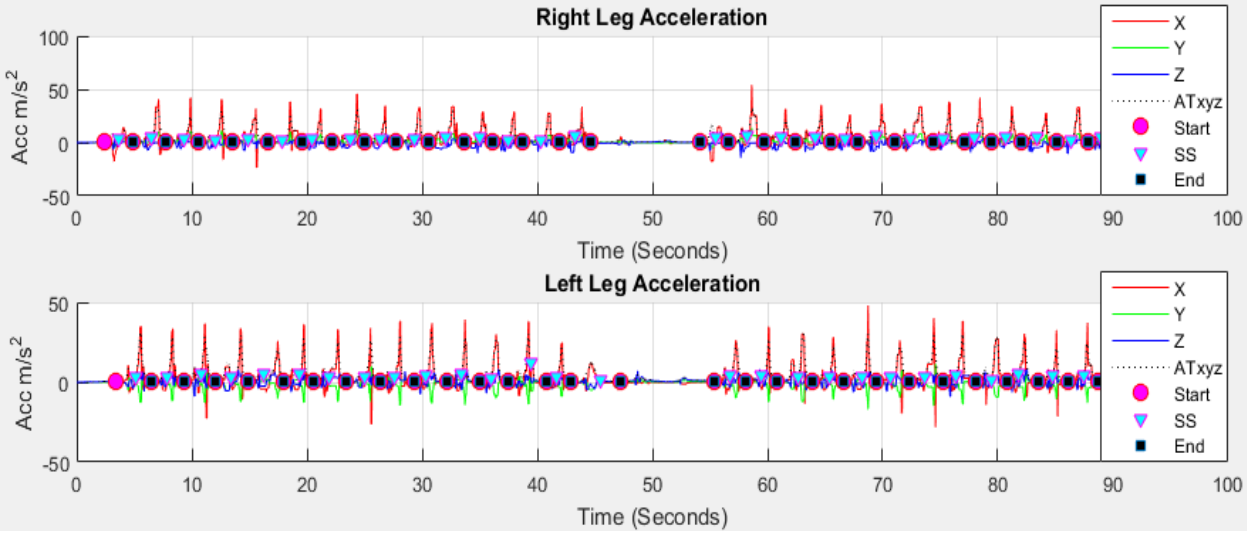

Figure 4.10: Result of stride, stance and swing event detection using proposed method.

A step is the sequence of events between the contact of one foot and the next contact of the opposite foot. At the beginning of the stance phase, the initial contact of the foot contacts with ground of the one leg. The loading response begins at the initial contact and ends when the toe of opposite leg leaves the ground, mid-stance then begins and finishes when the center of gravity is over the same foot. The terminal stance begins when the center of gravity is over the supporting foot and ends when the opposite leg contacts the ground. The strides, stance and swing event are detected from right and left legs. The step event is then detected between the heel of two subsequent feet shown in Figure 4.11.

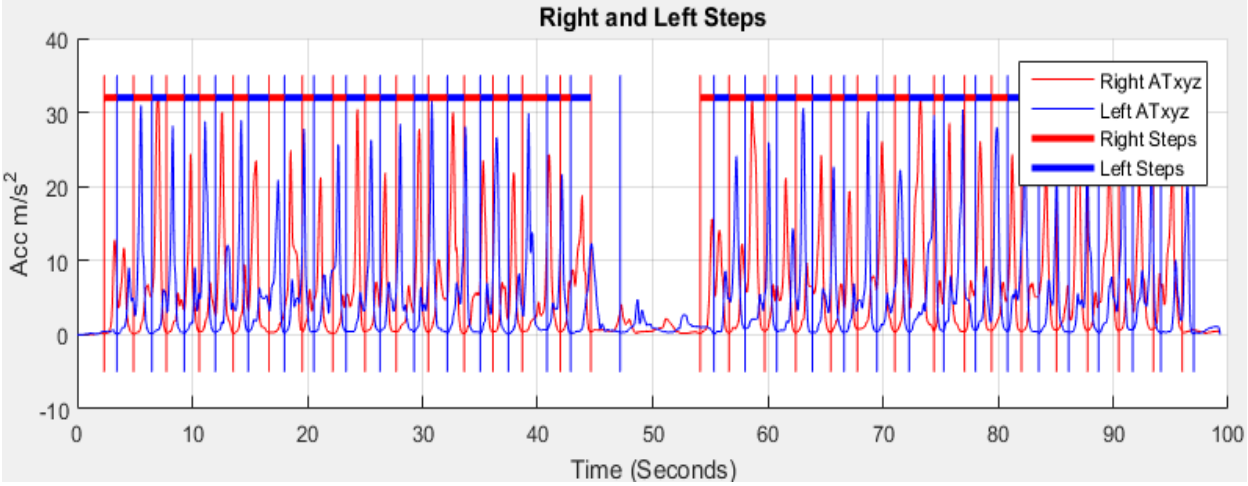

Figure 4.11: Result of step event detection using proposed method.

4.1.8. Velocity and distance estimation

We consider the walking constrains of a user with an IMU fitted on the both right and left legs. We apply appropriate methods to detect the movement of the leg, changes in position and compute its velocity and travelled distance from the initial location by means of the data collected from the accelerometers. The basic approach lies on the double integral of the accelerometer data where the first applying integration retrieves the current velocity and then the second applying integration computed on the velocity provides the distance travelled. Distance travelled is obtained principally from trapezoidal double integration (Thong et al. 2004) of the user movement signal on each stride detected in the direction of travel as mentioned in Section 4.3.4. However, there are two main problems for performing a double integration of the acceleration signal, unknown initial condition and drift. The unknown initial condition problem means integration requires a known initial condition. Drift means IMU sensors are subject to errors in acceleration that when integrated in to velocity and distance, leads to drastic integration error. This can be unbound over time if the acceleration signal is integrated without filtering (Thong et al. 2004; Foxlin 2005; Sukumar and Hazas 2012; Lan and Shih 2013; Ilyas et al. 2016). The integration works properly with known initial conditions. Thus, to calculate the actual displacement, integration errors must be minimized. A method known as zero-velocity update (ZUPT) (Fang et al. 2008; Lan and Shih 2013; Ilyas et al. 2016) is often used to correct for drift and is often used to aid in autonomous inertial pedestrian navigation. ZUPT uses the fact that during human walking time, one foot is always stationary on the ground. When a stationary period of the acceleration is detected the assumption is made that the foot is on the ground and the velocity at that time is set to 0. In this way, the drift is greatly reduced. However, ZUPT assumption implies that the angular rate is 0 as well and consequently if the accelerometer is moving at a constant velocity, the algorithm would misjudge the motion as stationary. ZUPT therefore cannot reduce all errors (Ilyas et al. 2016; Zhi 2016). Based on our experience, an accelerometer is very sensitive to movement and walking is a complex course of acceleration and deceleration. The detection of zero velocity does not fail due to misjudgment, but adjusting the threshold value for motion detection plays an important role in that misjudgment when motion detection is not properly set (discussed and showed in Section 4.2.7).

In addition, this issue may not be relevant to this study as the “foot stationary event” is already detected based on local minimal prominence as described in Section 4.2.7. The stationary

period remains in the stance phase and the movement period remain in the swing. As IMU sensors are mounted on each foot, the acceleration is high in the swing phase due to the movement of the leg during walking. The zero-velocity in non-stationary period of stance phase is used in the ZUPT scheme to reduce the drift. The ZUPT based on local minimal prominence to detect the swing phase is shown in Figure 4.12.

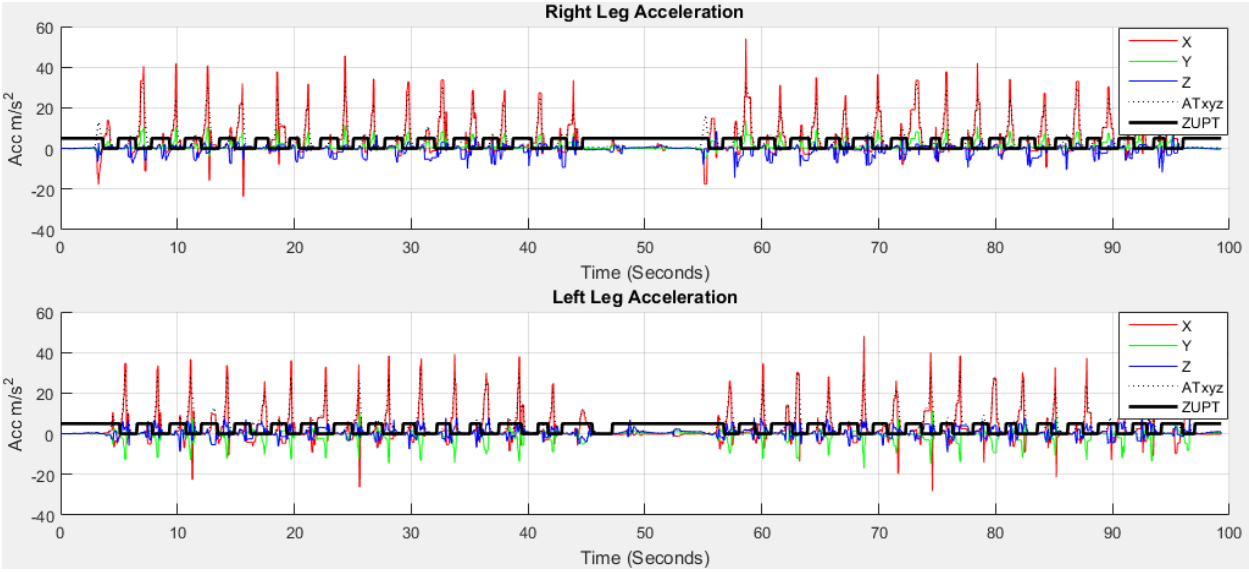

Figure 4.12: Zero-velocity update (ZUPT) from $|AT_{xyz_i}|$

Another concern regarding the double integration is that the displacement signal emphasizes the low frequency data more than the acceleration signal, a low-pass filter effect of the integrator. Therefore, the input data are passed through a high-pass filter to remove the direct component of the acceleration signal. Considering these issues, a double integral method shown in Figure 4.13 is proposed for calculating travelled distance.

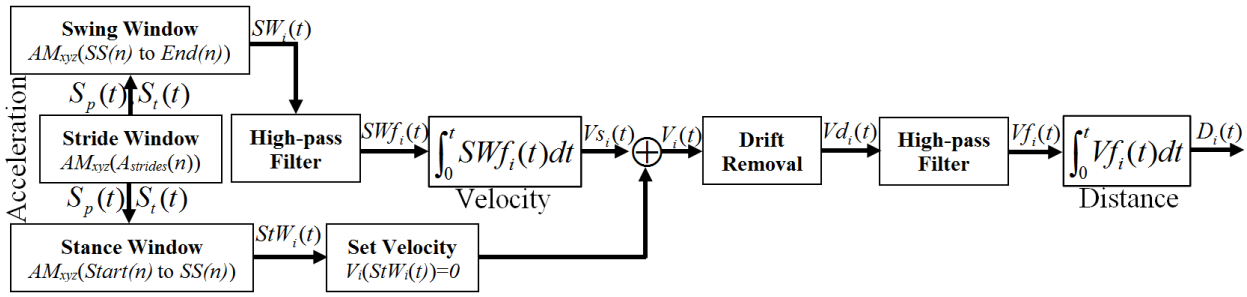

Figure 4.13: Proposed method for estimating travelled distance

In order to obtain the velocity and distance in time series, two stages of integration and two stages of high-pass filtering are applied. A stride window is prepared from $A_{Strides}$ and AM_{xyz}. The swing and stance windows are brought out from the corresponding stride window using *Start*, *SS*

and *End* mentioned in Section 4.3.4. A 1st order Butterworth high-pass filer is designed with fs = 50 Hz and fc = 0.001 Hz. The integration procedure is described in Section 4.2.5.2. The 1st integral operation is applied on SWf_i with respect to time t that gives the $Vs_i(t)$ velocity for the 1st swing phase. The ZUPT is applied on stance phase to set the stationary velocity to 0. The non-stationary period of swing velocity and stationary period of stance zero velocity are then combined to obtain $V_i(t)$ shown in Figure 4.14.

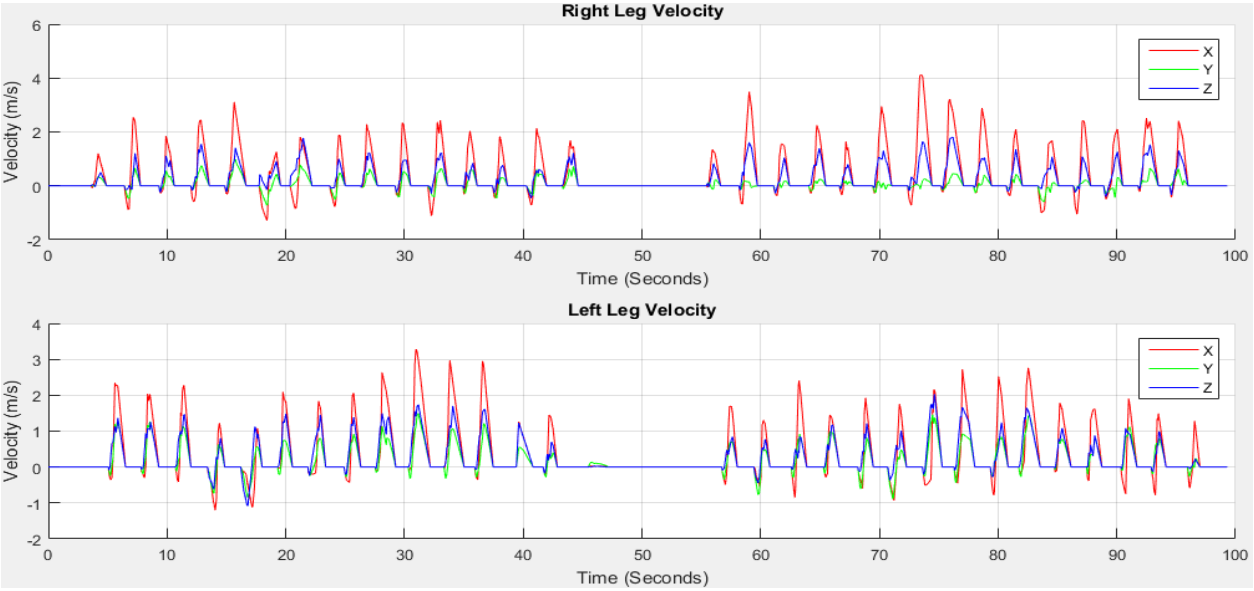

Figure 4.14: First integral operation to get velocity $V_i(t)$.

As the stationary period in stance phase velocity is set to zero, the integral constant from non-stationary period in swing phase exists in $V_i(t)$. Therefore, it is important to remove the drift caused by integration from $V_i(t)$. To remove the integral drift (Zhi 2016), the velocity difference between the initial and end of a non-stationary period is estimated. The velocity difference is then divided by the number of samples during this non-stationary period to get the drift rate. The drift rate is multiplied with the corresponding data index to estimate the drift value at that certain point. The drift value is then subtracted from the calculated velocity $V_i(t)$ to obtain the error free velocity $Vd_i(t)$. $Vd_i(t)$ is then passed through the high-pass filter for the 2nd time and the distance $D_i(t)$ is estimated after 2nd integral operation. $D_i(t)$ consists of the distance towards x, y and z coordinates. Repeat the same procedure for all strides to calculate velocity and distance. Then estimate the travelled distance using equation (4.45):

$$TD_{xyz_i} = \sqrt{D_{x_i}^{\ 2} + D_{y_i}^{\ 2} + D_{z_i}^{\ 2}} \tag{4.45}$$

Figure 4.15 shows the estimated distance $D_i(t)$ towards x, y and z and travelled distance TD_{xyz}.

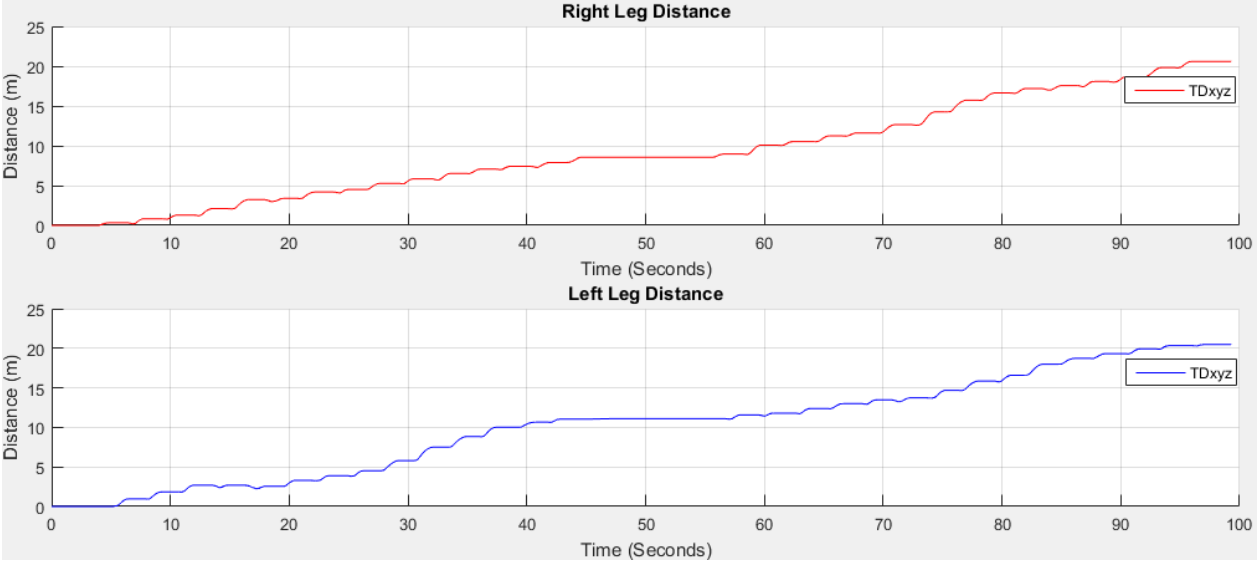

Figure 4.15: 2nd integral operation to get distance $D_i(t)$.

4.1.9. Selection of gait asymmetry variables

In our study, a set of 24 commonly reported physical gait variables are initially considered for this analysis from both right and left legs. Figure 4.16 shows the gait variables.

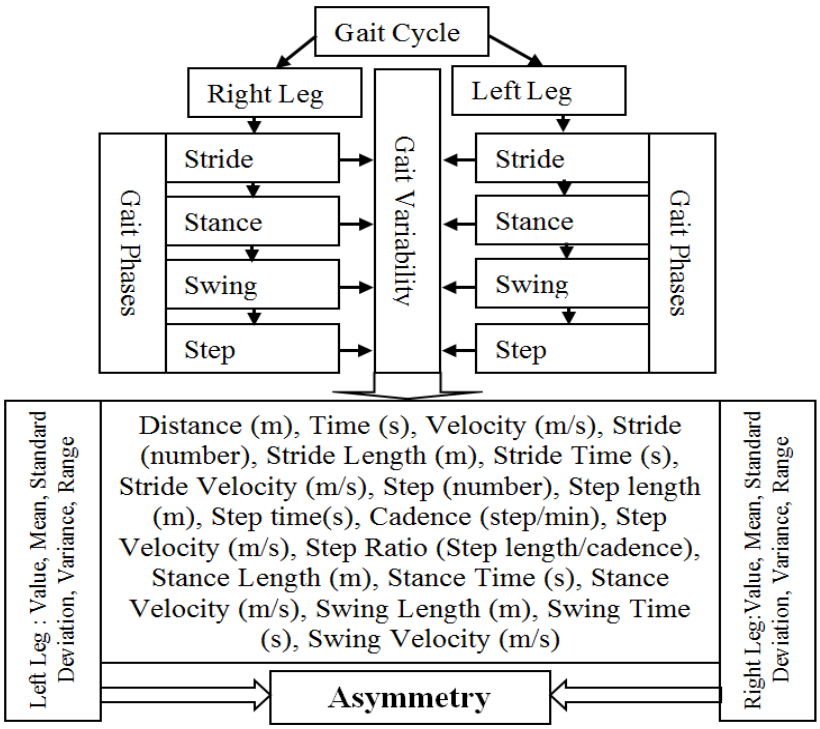

Figure 4.16: Proposed variability monitoring for GA.

4.1.10. Experimental Results

4.1.10.1. Results of gait features extraction

Initial experimental results from older subject 1 (male, age 67, height 1.52 m and weight 68 kg) are presented. We extract automatic GA features based on the data collected from both feet.

4.1.10.2. Results of older Subject 1

Table 4.1 shows the accuracy of the distance travelled and estimated, detecting stride and step number from both legs.

Table 4.1. Velocity, distance, stride and step information

Older subject 1	**Age**	**Height (m)**	**Weight (Kg)**	**Gender**	
	67	1.57	68	Male	
Total Time (s)	99.3				
	Actual *	Right Leg **	Accuracy (%)	Left Leg **	Accuracy (%)
Total Distance (m)	21.03	20.59	97.91	20.47	97.34
Estimated Velocity (m/s)	0.21	0.21	97.91	0.21	97.34
Detected Stride Number	30	30	100	30	100
Detected Step Number	30	30	100	30	100

*ActualValue, ** EstimatedValue.

$$Accuracy = \left(100 - \left|\frac{ActualValu\,e - EstimatedValue}{ActualVale}\right| \times 100\right)\% \qquad (4.51)$$

The accuracy is estimated using equation (4.51). The actual distance travelled is 21.03 m measured using manual tape with 99.3 s walking time. The estimated both legs travelled distances are 20.59 m and 20.47 m. The actual and estimated distances are very close. Normal human walking velocity may vary from 1.5 to 2.5 m/s (Mohler et al. 2007) and the walking velocity for this subject is 0.21 m/s which is slow. The accuracy of stride and step event detection are 100%. Table 4.2 shows the summery of average gait variability.

Table 4.2. Gait Asymmetry Variability

	Right Leg					**Left Leg**				
Gait Features	**Mean**	**Std**	**Var**	**Min**	**Max**	**Mean**	**Std**	**Var**	**Min**	**Max**
Stride Length (m)	0.69	0.07	0.00	0.56	0.84	0.69	0.09	0.01	0.49	1.05
Stride Time (s)	2.80	0.28	0.08	2.30	3.40	2.85	0.37	0.13	2.05	4.30
Stride Velocity (m/s)	0.25					0.24				
Step length (m)	0.27	0.06	0.00	0.14	0.46	0.32	0.05	0.00	0.23	0.46
Step time(s)	1.28	0.30	0.09	0.65	2.15	1.52	0.26	0.07	1.10	2.15
Step Velocity (m/s)	0.25					0.24				
Cadence (step/min)	18.13					18.13				
Step Ratio (Step length/cadence)	0.02					0.02				

Stance Time (s)	1.65	0.23	0.05			1.67	0.35	0.12		
Swing Length (m)	0.69	0.35	0.12			0.69	0.44	0.19		
Swing Time (s)	1.16	0.23	0.05			1.18	0.21	0.04		
Swing Velocity (m/s)	0.59					0.58				

Std = Standard Deviation, Var = Variance, Min = Minimum and Max = Maximum

We can observe from Table 4.2 that the mean stride lengths of both legs are the same. Although, the standard deviations are low and the right leg's value is lower indicating that the left stride length has more variation compared to the right stride length. The highest stride length is found at the 15th stride (last stride) on the left leg which is before turning. The mean stride times are close for both legs. Although, the right and left leg stride length, time and velocity difference is low, Figure 4.17 shows that a little stride asymmetry is noticeable in right and left strides time and distance. The difference of other parameters between the legs is also low. However, it is noted from Figure 4.18 that step asymmetry is more prominent than stride asymmetry which may result in an inconsistent gait.

4.1.10.3. Results of young and older Subjects

Table 4.3 shows the gait data from the 10 young subjects and shows that the accuracy of estimating the total distance compared with the actual distance is also high for both legs. The detected stride and step number using the proposed method is excellent. For all young subjects, the accuracy of detecting stride number using proposed method is 100%. The accuracy of estimating travelled distance using proposed method is 97.73% for right and 98.82% for left legs.

Table 4.3. Velocity, distance, stride and step results for young subjects.

AVERAGE	**Age**	**Height (m)**	**Weight (Kg)**	**Gender**	
	25.30	**1.61**	**61.90**	**9 M, 1 F**	
Total Time (s)	**51.85**				
	Actual *	**Right Leg ****	**Accuracy**	**Left Leg ****	**Accuracy**
Total Distance (m)	37.77	37.19	97.73	37.81	98.82
Estimated Velocity (m/s)	0.73	0.72	97.73	0.73	98.82
Detected Stride Number	30.00	30.00	100.00	30.00	100.00
Detected Step Number	30.00	30.00	100.00	30.00	100.00

* ActualValue, ** EstimatedValue.

Table 4.3 shows the details of both legs asymmetry variables information. The stride lengths of legs are the same for young subjects. The overall difference between legs is low for young subjects. In natural walking, the foot is on the ground for about 60% of the total gait cycle during stance phase and 40% during swing phase. The ratio of stance and swing is found closest to the 60:40% split for average stride, stance and swing information (Table 4.4) for young subjects.

Table 4.4 Right and left legs asymmetry of young subjects.

	Right					Left				
Gait Features	**Mean**	**Std**	**Var**	**Min**	**Max**	**Mean**	**Std**	**Var**	**Min**	**Max**
Stride Length (m)	1.17	0.17	0.03	0.91	1.65	1.17	0.17	0.03	0.89	1.61
Stride Time (s)	1.41	0.20	0.04	1.10	1.97	1.39	0.19	0.04	1.07	1.91
Stride Velocity (m/s)	0.83	0.83	0.83			0.84	0.84	0.84		
Cadence (step/min)	34.93					34.93				
Step Velocity (m/s)	0.83	0.85	0.75			0.84	0.86	0.77		
Step length (m)	0.50	0.14	0.02	0.15	0.84	0.54	0.18	0.04	0.24	1.10
Step time(s)	0.68	0.19	0.04	0.21	1.14	0.74	0.24	0.07	0.33	1.48
Step Ratio (Step length/cadence)	0.01					0.01				
Stance Time (s)	0.84	0.16	0.03			0.83	0.13	0.02		
Swing Length (m)	1.17	0.68	0.49			1.17	0.94	1.14		
Swing Time (s)	0.58	0.12	0.02			0.57	0.15	0.02		
Swing Velocity (m/s)	2.07	1.80	1.80			2.10	1.83	1.83		

Table 4.5 shows that the accuracy of estimating the total distance compared with the actual distance is high for both legs of 10 older subjects. For all older subjects the accuracy of detecting stride number using the proposed method is 92.67%. The accuracy of estimating the travelled distance using the proposed method is 88.71% for the right and 89.88% for the left legs. The detected stride and step number using the proposed method is also high. However, comparing to results in young subjects (Table 4.4), the accuracy is lower for older subjects. This is likely to be due to older people walking slowly resulting in a poorer signal output. Table 4.6 shows the details of both legs asymmetry variables for older subjects. Overall the stride lengths of both legs are similar. The overall difference between legs is very low.

Table 4.5. Velocity, distance, stride and step results for older subjects.

Average	**Age**	**Height (m)**	**Weight (Kg)**	**Gender**	
	69.40	**1.52**	**63.40**	**9 M, 1F**	
Total Time (s)	**80.26**				
	Actual *	**Right Leg ****	**Accuracy**	**Left Leg ****	**Accuracy**
Total Distance (m)	22.49	22.21	88.71	21.19	89.88
Estimated Velocity (m/s)	0.31	0.29	88.71	0.27	89.88
Detected Stride Number	30	27.80	92.67	27.80	92.67
Detected Step Number	30	27.80	92.67	27.80	92.67

*ActualValue, **EstimatedValue

We check the data for statistical errors and assessed whether the estimated values are reasonable. Figure 4.17 shows the boxplot of travelled distance from young and older subjects. It is noted that the observations identified by the boxplots are not especially extreme. The young subjects' travelled distance for 30 strides has a wider range and is significantly different than older ones. On average young subjects travelled distance is 37.77 (95% CI ± 3.57) m and in older ones is 22.50 (95% CI ± 2.34) m. Similarly, the legs stride and step variation is low for older ones than

young ones. Older one's gait is slow and results in a low variation in walking comparing with young ones. The step length has more variation then stride length. Based on the total travelled distance, stride and step information, it can be seen that young and older subjects are distinguishable.

Table 4.6. Right and left legs asymmetry of older subjects.

	Right					Left				
Gait Features	**Mean**	**Std**	**Var**	**Min**	**Max**	**Mean**	**Std**	**Var**	**Min**	**Max**
Stride Length (m)	0.74	0.14	0.02	0.54	1.16	0.74	0.13	0.02	0.55	1.09
Stride Time (s)	2.47	0.46	0.24	1.84	3.88	2.44	0.39	0.16	1.80	3.47
Stride Velocity (m/s)	0.32	0.32	0.32			0.33	0.32	0.32		
Cadence (step/min)	24.34					24.34				
Step Velocity (m/s)	0.32	0.33	0.13			0.33	0.33	0.13		
Step length (m)	0.22	0.23	0.06	0.22	0.63	0.35	0.18	0.04	0.04	0.57
Step time(s)	0.54	0.86	1.02	1.02	2.07	1.13	0.73	0.81	0.18	2.20
Step Ratio (Step length/cadence)	0.007					0.014				
Stance Time (s)	1.39	0.30	0.10			1.37	0.28	0.08		
Swing Length (m)	0.74	0.78	0.73			0.74	0.76	0.66		
Swing Time (s)	1.09	0.30	0.10			1.07	0.23	0.05		
Swing Velocity (m/s)	0.78	0.68	0.68			0.78	0.65	0.65		

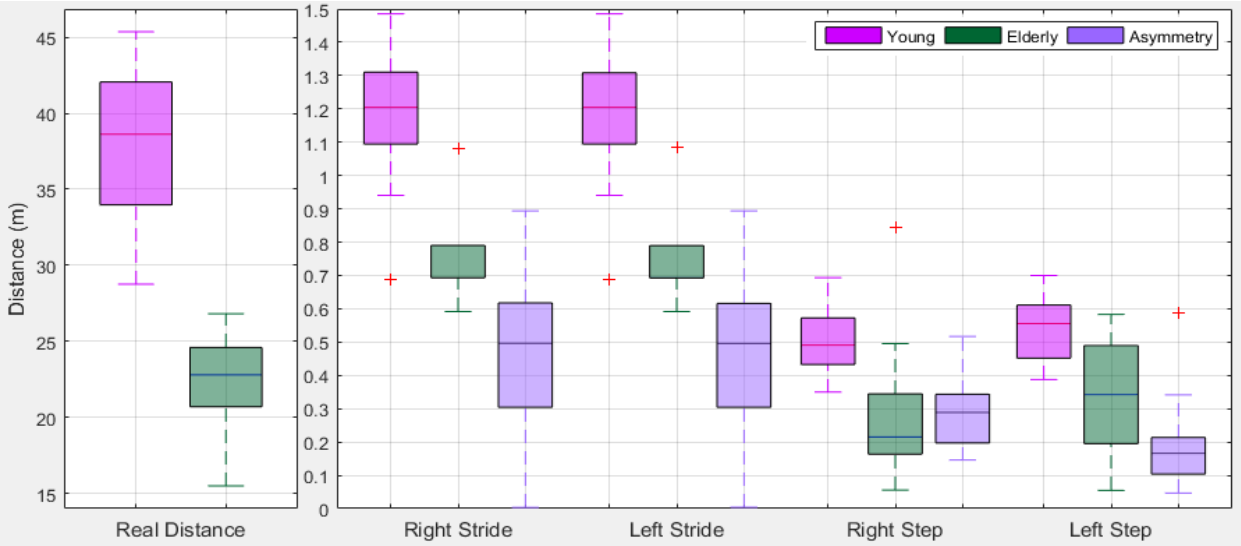

Figure 4.17: BoxPlot of stride and step asymmetry in distances from right and left legs.

Figure 4.18 shows a boxplot of total time from young and older subjects with their difference. The total time for performing a total of 30 strides is lower for young subjects than older ones. On average the young subjects travelled time is 51.85 (95% CI ± 3.08) s and older ones is 84.02 (95% CI ± 9.98) s. Young subjects show low leg variation with a lower range than older ones. Based on the total time, stride and step timing information, it can be seen that young subjects and older ones are distinguishable. The detailed results of the 20 subjects are presented in Appendix C.

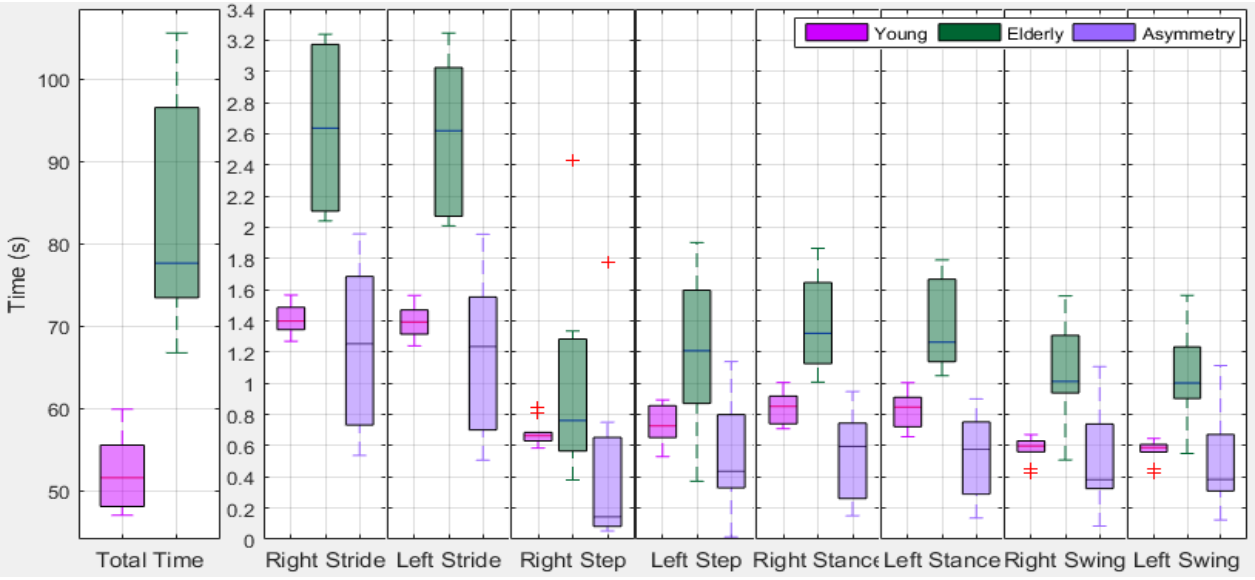

Figure 4.18: Box Plot of stride and step asymmetry in times from right and left legs.

4.1.11. Discussion

In this research we show that in a clinical setting outside of a gait laboratory it is possible to collect information about gait using IMU sensors. From Figure 4.10, we can see that our gait cycle accelerometer signal AT_{xyz} is agreed with the signal pattern in (Patterson et al. 2014; Liu et al. 2016). We demonstrate the systematic steps of an automatic gait features extraction method that we deployed. Our research enriches the current literature in gait assessment. It is possible to evaluate walking distance using a multi-sensor approach. Current methods however rely on the threshold based detection of the spike (Mladenov and Mock 2009; Chon et al. 2012; Boutaayamou et al. 2015; Truong et al. 2016). Our method uses minimal prominence characteristics for detecting gait phases. The former relies on generating a movement of sufficient magnitude to generate the spike and therefore has limited utility in people with slow gait. Our method therefore has the potential for broader use as it can be used in people with slower gaits such as older adults. We demonstrate that our method can deliver accurate results of stride detection and distance travelled similar to accuracy levels demonstrated by other authors (Boutaayamou et al. 2015; Truong et al. 2016). We believe that there are advantages to using the minimal prominence approach as it can be used in a wider population people with different gait patterns.

For this study, the number of subjects is still relatively small (20). There is potential of a Type 1 error (false positive) in detecting an effect that is not there. IMU calibration is an essential

part for distance estimation. Although in our methods we try to minimize errors, as gait features are intrinsically variable from person to person, any such algorithm should involve a degree of calibration and error in the measurements. Individual quirks, heel strike, significant body up-down movement and other factors can affect the results. However, we have established our method for extracting automatic gait features. There are several other possible sources of errors (S Flenniken et al. 2017) that may arise from the use of IMU sensors including errors of repeatability, stability and drift. Although IMU sensors performance has been ramped up dramatically, the errors in measurement are unavoidable, especially for miniature micro-electro-mechanical (MEMS) sensors. Future developments should focus on MEMS sensor error modelling and accommodation to further improve parameter estimation accuracy (Yang et al. 2012). Other possible areas of error may arise from frictional noise and the relative movement of clothing and shoes to the sensor. However, we have tried to making the effect of such errors minimal.

To achieve our goal, data are collected from two sensors placed on the barefoot at the medial aspect of foot over the bony prominence of the first metatarsal. It is noted that the orientation of the sensor has a significant effect on output and placing the sensor in different locations gives a different pattern to the data. The position and orientation of the sensor are crucial as changes in position through human error may give different data patterns which might be difficult to interpret. This highlights the importance of properly fixing the sensor to the optimal location to avoid inaccuracies. The placing of sensors on foot locations requires other generic considerations such as battery life and Android device that is BLE enabled to pick up sensor data.

To estimate the orientation of the IMU sensors, we apply (Madgwick 2010) technique for our collected data but not the magnetic field parameter. The technique is developed assuming that the acceleration would only measure gravity. In practice, accelerations due to motion will result in an erroneous observed direction of gravity and the distortion will present for only short periods of time. Therefore, the magnitude of the filter gain β (Section 4.2.6) is chosen low enough that the divergence caused by the erroneous gravitational observations is reduced to an acceptance level over the period. In future, an investigation of dynamic values of gain β will be conducted to reduce errors.

A threshold is used for detecting steps (Boutaayamou et al. 2015; Truong et al. 2016) and different value may result in a different output. It is crucial to detect the 1st and last strides of gait cycle when a person starts and stop walking. Thus, the 1st stride is not considered by researchers (Truong et al. 2016). Our proposed method for detecting the stride information is based on the local minimal prominence which starts when the heel contacts the ground resulting in the stationary period and estimated the total number of strides. We also confirm these results obtained by counting the highest peak in the mid-swing phase as it also is a good indicator for a complete gait cycle. From each stride, the local minimal prominence which is the transition between pre-swing and initial swing (4th and 5th phases in Figure 3.13) is detected. We find that that when turning or when stopping there is a poor acceleration signal. As gait of older subjects is much slower, it is crucial to detect strides, stance and swing phases from the gait cycle. However, the stationary stance phase is prominent for both young and older subjects. For this reason, we use the local minimal prominence characteristics to detect different events to avoid these crucial phases. We have shown that it is possible to detect, stride, stance and swing events but further analysis of the eight events including single and double support phases in a gait cycle is necessary to provide more accurate information for gait asymmetry analysis.

In order to track the position in a virtual environment, several navigation methods (Hasan et al. 2009) are available to derive pose estimates from electrical measurements of mechanical, inertial, acoustic, magnetic, optical, and radio frequency sensors. Each approach has advantages and limitations including modality-specific limitations related to the physical medium, measurement-specific limitations imposed by the devices, associated signal-processing electronics, and circumstantial limitations that arise in a specific application (Welch and Foxlin 2002). Our velocity and distance estimation is based on results of a double integral with ZUPT. We apply the high pass filter on acceleration data that removes linear trend from the signal and then remove drift to estimate distance. We use the simplest technique of trapezoidal rule for estimating distance for our collected data and our estimated distance results are close to the actual distance. There are many other types of numerical integration schemes available which are much more involved and with the potential for more accuracy. However, the trapezoidal rule is the simplest technique of an entire class of numerical integration schemes which are known as the Newton-Cotes formulas (Weisstein 2004) and which we have adopted. Our future plan is to investigate other methods with our collected data.

The results show that our method is capable of automatic extracting gait features and has the potential to be used in gait assessment and gait change monitoring for home and clinical use. Gait with slow velocity is common in older adults (Brach and VanSwearingen 2013) and an automatic system sensitive enough to detect gait features in these circumstances is required. Our low cost portable personalized proposed solution could bring out automatic gait features for monitoring longitudinal gait changes or abnormalities. In future work, we plan to use our automatic extracted gait features information to classify gait changes over time to identify abnormal gait patterns for the assessment of elderly fall risk, rehabitation and sports applications.

4.2. Visualization of spatiotemporal gait features

We describe the materials and methods used for the development of this work in the following subsections.

4.2.1. Data and statistical analysis

We obtain values for ten spatial-temporal gait parameters separately from the right and left lower limbs that include stride length (m), stride time (s), stride velocity (m/s), step length (m), step time (s), step velocity (m/s), stance time (s), swing length (m), swing time (s) and swing velocity (m/s). The asymmetry factors SI (Robinson et al. 1987), SR (Seliktar and Mizrahi 1986), Ia (Vagenas and Hoshizaki 1992), GA (Plotnik et al. 2005; Plotnik et al. 2007) and SA (Zifchock et al. 2008) are calculated for each parameter using equations (4.46) to (4.50). These are chosen because they are very commonly used approaches of evaluating gait asymmetry (Patterson et al. 2010).

SL1 - SI (Robinson et al. 1987):

$$SI(\%)=\frac{RightLeg-LeftLeg}{0.5(RightLeg+LeftLeg)}*100 \quad (4.46)$$

SL2 - SR (Seliktar and Mizrahi 1986):

$$SR(\%)=\frac{RightLeg}{LeftLeg}*100 \quad (4.47)$$

SL3 - Ia (Vagenas and Hoshizaki 1992):

$$Ia(\%)=\frac{RighttLeg-LefttLeg}{\max(RightLeg,LeftLeg)}*100 \quad (4.48)$$

SL4 - GA (Plotnik et al. 2005; Plotnik et al. 2007):

$$GA = \left| \ln \left\{ \frac{\min(RightLeg, LeftLeg)}{\min(RightLeg, LeftLeg)} \right\} \right| \tag{4.49}$$

SL5 - SA (Zifchock et al. 2008):

$$SA(\%) = \frac{(45^{\circ} - \arctan(RightLeg / LeftLeg))}{90^{\circ}} * 100\% \tag{4.50}$$

SL1 is based on percentage assessment of the difference between the kinematic and kinetic parameters for both legs during walking. SI=0 indicates that there is no asymmetry and SI ≥ 100% indicates high asymmetry. SL2 indicates the highest value results asymmetries. SR=100 indicates no asymmetry, SR > 100 indicates right leg value is higher than left leg and SR<100 indicates that left leg value is higher. SL3 is based on kinematic asymmetry of the lower limbs. Ia=0 indicates no asymmetry. Ia = ±0, the higher the value indicates the higher level of asymmetry. SL4 is based on logarithmic transformation of right and left leg's ratio of gait asymmetry. GA=0 and GA=1 denote no asymmetry and highest asymmetry respectively. SL5 is the symmetry angle calculated for the angle of the vector plotted from the right and left values of discrete gait parameters. SA shows absolute value of right and left leg's ratio in percentage. SA=0 indicates no asymmetry and SA≥100% indicates asymmetry.

Pearson's linear correlation coefficients are calculated. The correlation between the experimental results and linear least square regression is analyzed. Although the available asymmetry factors SI (Robinson et al. 1987), SR (Seliktar and Mizrahi 1986), Ia (Vagenas and Hoshizaki 1992), GA (Plotnik et al. 2005; Plotnik et al. 2007) and SA (Zifchock et al. 2008) provide a numerical indication of the degree of asymmetry they are not easily interpretable to users. These rely on the computation of complex equations as well as knowledge to interpret the results. This may affect the accuracy of use. Therefore, in order to conveniently use quantitative gait asymmetry monitoring, an easy to interpret and affordable gait symmetry visualization tool is required to provide a facility for use in clinic and at home. This section mainly presents the gait asymmetry visualization to the users, not give the cause of gait asymmetry. The cause of gait asymmetry is an important topic to conduct research in future.

4.2.2. Spatiotemporal gait visualization

We purposely show the visualizations from a single subject as there is no point in showing an aggregate of the results from our 20 subjects. Individual visualizations for all are shown in Appendix B and C. This section presents four novel gait asymmetry visualization approaches aimed to show the various aspects of gait symmetry analysis and make the results accessible and useful to both patients, for self-directed care, and therapists: **1) Real time dial visualization:** this is intended for patient use by providing a spatiotemporal gait information to the patient who can then identify and make attempts to rectify gait asymmetry; **2) Visualization of individual leg time variation:** this is intended for therapists assessing gait by giving an overall picture of time asymmetry over a series of strides. In normal human gait the period from the initial contact to pre-swing composes about 60% of the time and initial swing and terminal swing composes about 40% of the time in the gait cycle shown in Figure 2a. This visualisation provides the therapists the opportunity easily identifies any deviation from this 60:40 split; **3) Visualization of both legs asymmetry:** this visualization shows both time and distance for stride and step for both right and left legs. As they are comparing both legs then they would be expected to be as near to equal as possible and any difference is asymmetry; This will also indicate which of the legs is most affected and helps therapists' direct attention to the legs with most abnormality; and **4) Boxplot-based visualization:** this visualization provides an overall summery of the results obtained through the above and therefore can be used to monitor progress with therapy.

4.2.2.1. Real time dial visualization

The stride, step and swing information is considered for visualization. We extract stride, stance, swing and step features of gait. The stance is a stationary phase of a gait cycle and the distance travelled in the stationary phase is zero. Initially we estimate the maximum (*max*), minimum (*min*), and confidence interval (*CI*) of each feature. We draw a circle from θ=0 to 2π of duration of 0.01 using $x = \sin(\theta), y = \cos(\theta)$. We define the interval α=50 and the value of each step increment (δ) is computed by $\delta = (\max - \min)/\alpha$. The interval angle ω is estimated using $\omega = \lambda * \pi / \alpha$ with λ =1.25. The scale is represented from 0 to α using $\gamma = -\lambda * \pi / i * n + \lambda * \pi$, for n= 0 to α.

The small scale line is then drawn using $x = \sin(\gamma), y = \cos(\gamma)$. The minimum and maximum values of the scale are the lower *CI* and upper *CI* respectively. The indicator line (β) is

then set with the instantaneous difference between left and right value of the feature (η) using $\beta = -\omega * (\eta - \min) / \delta + \lambda * \pi$. The indicator line is drawn from 0 to β. We draw gradient colors to make it colorful looking. The instantaneous feature value is displayed at the bottom of each dial with seven segment display. The same procedure is followed for displaying instantaneous distance and time from stride, step and swing information.

When the app is run for the first time, there is an option to input a number of last performed strides. By default, the value is set as 30. It will then detect phases and display corresponding information on to dial. Every time it starts, it will restore the last calculated *CI* for scaling and it will update automatically after each 30 or specified numbers of strides. There is an option to change the scaling factor according to SI (Robinson et al. 1987), SR (Seliktar and Mizrahi 1986), Ia (Vagenas and Hoshizaki 1992), GA (Plotnik et al. 2005; Plotnik et al. 2007) and SA (Zifchock et al. 2008) format.

4.2.2.2. Visualization of individual leg time variation

Each stride is composed of stance and swing phases. The stride time is composed of stance time and swing time. To visualize the individual legs variation, we estimate the maximum and minimum values of each feature. We draw an outline rectangle using blue color towards vertical line to represent right of the first stride value with aspect ratio of the maximum value. A cyan color rectangle of stance time is drawn on that stride rectangle and a yellow color rectangle of swing time is drawn at the top of the stance rectangle. All rectangles are followed the aspect ratio with the maximum value. This process is conducted for all stored strides.

4.2.2.3. Visualization of both legs asymmetry

Each stride and step feature has distance and time information. Initially we calculate the maximum and minimum of features. A red color rectangle is drawn which height is the first right stride distance with aspect ratio of the maximum value. A blue rectangle is drawn which height is the left stride distance at the side of right rectangle. We follow this procedure for both strides and step asymmetry visualization of all stored strides considering the aspect ratio with the maximum value.

4.2.2.4. Boxplot-based visualization

We estimate median, upper-quartile, lower quartile and whisker values from features and plot a Boxplot. This is a simple representation of descriptive statistics to understand each features distribution, non-normal/unusual level, outliers, symmetry and overall gait asymmetry information.

4.2.3. Results of visualization of spatiotemporal gait features

The total time taken to travel 33.38 meters is 22.21 seconds. The estimated legs travelled distances are 33.35 meters and 32.87 meters with accuracy of 99.92% and 98.48%. The actual and estimated distances are very close. The accuracy of stride and step event detection is 100%. Table 4.7 shows the average gait variability and quantifying gait asymmetry using five techniques.

Table 4.7: Gait variability and asymmetry factors (SI, SR, Ia, GA and SA)

	Right Leg		**Left Leg**		**SL1**	**SL2**	**SL3**	**SL4**	**SL5**
Gait Features	**Mea**	**95%**	**Mean**	**95% CI**	SI	SR	Ia	GA	SA
Stride Length (m)	1.112	0.225	1.096	0.230	1.45	101.46	-1.44	0.01	0.46
Stride Time (s)	0.595	0.027	0.588	0.026	1.13	101.13	-1.12	0.01	0.36
Stride Velocity	1.823	0.308	1.855	0.371	-1.73	98.29	1.71	0.02	-0.55
Step length (m)	0.507	0.041	0.387	0.043	26.68	130.79	-23.54	0.27	8.44
Step time(s)	0.258	0.028	0.337	0.027	-26.58	76.53	23.47	0.27	-8.41
Step Velocity (m/s)	2.185	0.337	1.256	0.223	53.98	173.94	-42.51	0.55	16.78
Stance Time (s)	0.315	0.018	0.278	0.021	12.36	113.17	-11.64	0.12	3.93
Swing Length (m)	1.009	0.202	0.990	0.207	1.88	101.90	-1.86	0.02	0.60
Swing Time (s)	0.280	0.019	0.310	0.021	-10.18	90.31	9.69	0.10	-3.24
Swing Velocity	1.729	0.248	1.537	0.248	11.79	112.53	-11.13	0.12	3.75

From Table 4.7 we can see that the mean stride lengths and times of both legs are very close. However, high asymmetry is found in step length, time and velocity. The estimated asymmetry factors show numerical values that indicate differences both between the features and between the indicators. The lowest gait asymmetry is observed during the stride phase and the highest is found during the step event. Using the Shapiro-Wilk test, most of the parameters show normal distribution for 20 participants. Additionally, the lowest confidence intervals are observed for most of the parameters indicating consistent data.

The analysis of Pearson linear correlation coefficients between the SL1, SL2, SL3, SL4 and SL5 factors indicates a very strong association ($p<0.001$) for most of the cases excluding SL4. As

such, it is more useful to analyze the compatibility of the results for individual factors in the assessment of the symmetry of the factors indicating high symmetry. The coefficient ordered rank also agrees for most of the cases. The linear least square regressions show very high correlations. It is important for clinical practice to evaluate the impact of individual factors resulting high gait symmetry and the interpretation of these numerical values provide limited information. Therefore, a visual representation of these values with interpretation would provide much more user friendly information.

4.2.4. Results of spatiotemporal gait visualization

Next, we show the results of the four gait asymmetry visualizations.

4.2.4.1. Real Time Dial Visualization

Figure 4.19 demonstrates spatiotemporal measurements in a dial fashion taken from one subject. Both legs should theoretically give identical results and therefore perfect asymmetry should give dial indicator readings of zero. The first dial is an asymmetry display for stride length and time comparing both legs. The second dial displays the real time measurement of step length and time. It is noted that there is a difference in the level of asymmetry. The third dial shows the swing phase distance and time. Similarly, there is little asymmetry between two legs. The scales on all three dials represent the confidence intervals and the pointer represents the instantaneous real time difference between two legs. For example, in this case although the dials for stride and swing show near perfect symmetry, measurements relating to step are not. Step measurement entails information on distance and time. The distance dial shows that the right leg is travelling longer (0.51m) than the left leg (0.39m). The patient therefore needs to shorten the distance travelled by the right leg and/or make the left step longer. The time dial demonstrates that the right leg travels the longer distance in a shorter time (0.26s) compared to the left leg (0.34s). The digital number below the dial is showing the absolute measure for all three markers.

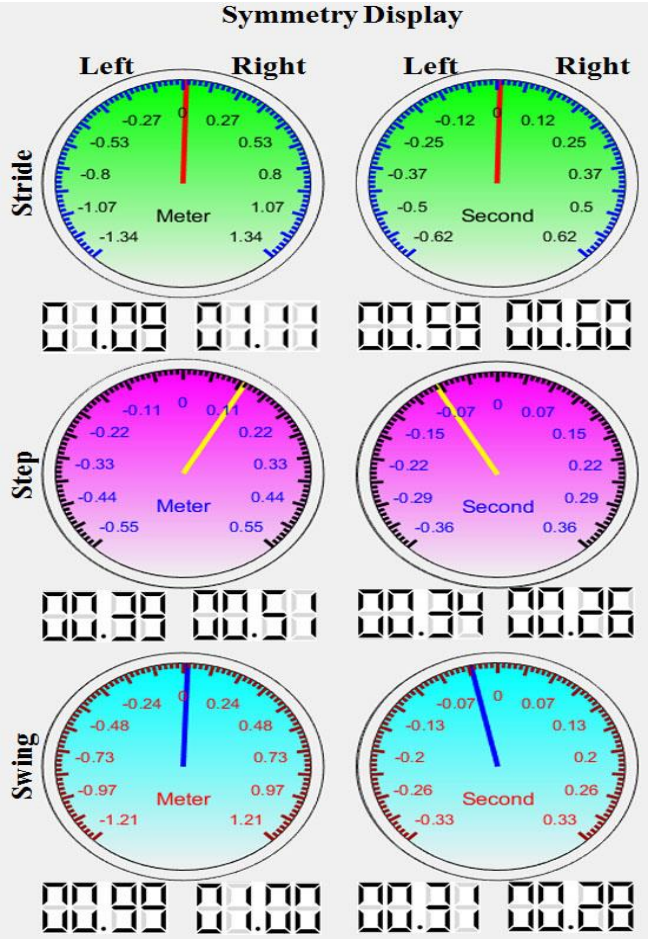

Figure 4.19: Real time gait asymmetry visualization

4.2.4.2. Visualization of Individual Leg Time Variation

30 strides are performed and the time of stride, stance and swing phases is presented in Figure 4.20 where each bar shows the stride time.

Figure 4.20: Time of stride, stance and swing phases from right and left legs

The cyan and yellow colors represent the time of stance and swing phases respectively. There is a small variation of stance and swing phase timing. This visualization clearly represents the variability of stance and swing phases in each stride of the legs. The ratio of stance and swing is found closest to the 60:40% split for average stride, stance and swing information (Figure 4.20).

4.2.4.3. Visualization of Both Legs Asymmetry

In this visualization the stride and step asymmetry information for both time and distance from both legs are presented in Figure 4.21. We can see that while there is good symmetry in the stride there is strong variation in the step phases.

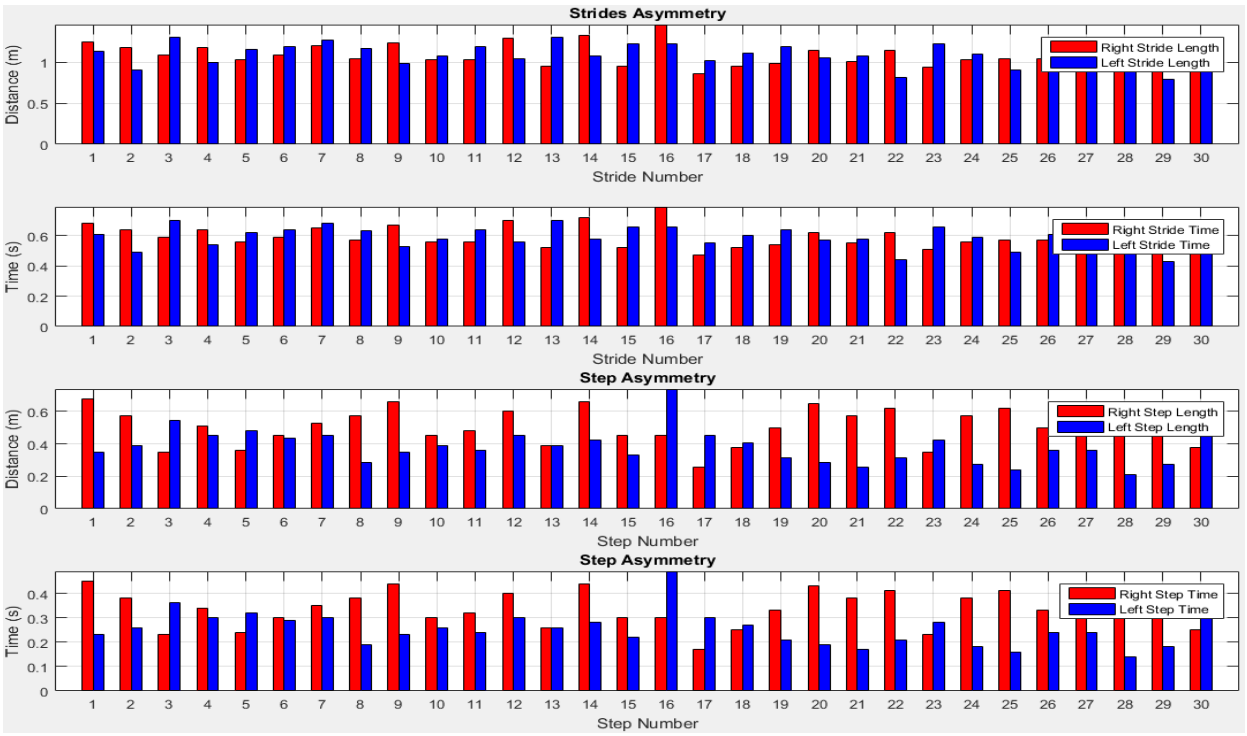

Figure 4.21: Gait asymmetry of stride and step phases from right and left legs

4.2.4.4. Boxplot-Based Visualization

Figure 4.22 shows a boxplot of the distribution of values for individual factors where the mean values obtained for stride and step for both legs. The quartile ranges are identified in the boxplot and show low variation for the stride. The first box plot shows higher variation in the step length on the left leg than on the right. This demonstrates that although the stride length is similar on the right and left there can be a higher variation in the step length. The boxplots for time indicate that variation is low for both legs.

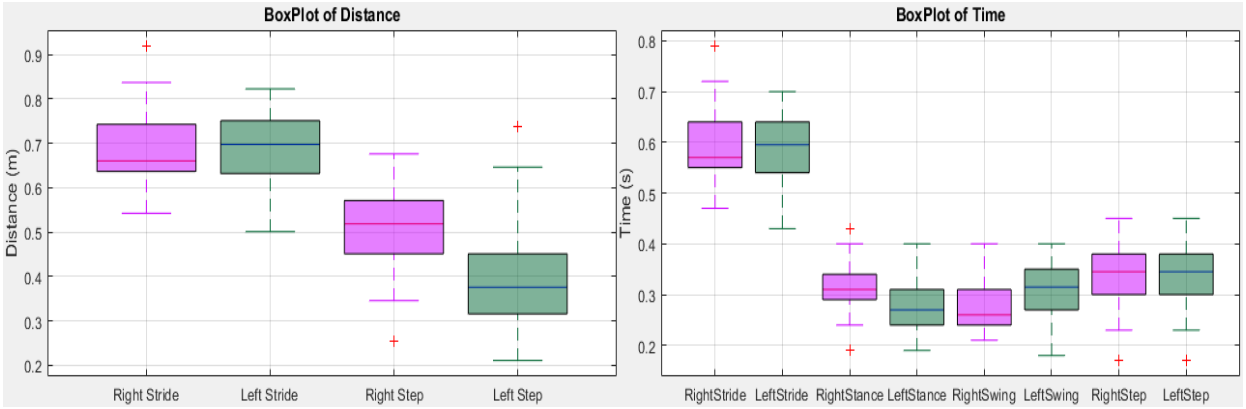

Figure 4.22: Boxplot of stride, stance and swing information

If we exclude the first and last stride of each walking on the corridor, the asymmetry is not that high. Those phases consist of more variation due to initial acceleration and ending momentum. It is noted that the observations identified by the boxplots are not especially extreme.

4.2.5. Discussion

This study adds to current literature by demonstrating a new visual method of demonstrating gait asymmetry that increases the reliability and validity of monitoring gait abnormalities. In addition, our sensors are wearable and can be used in different clinical setting and the patient's home and do not rely on complex equipment. This has the potential of a significant advance. As, gait asymmetry has been shown to be a determinant of recovery in patients suffering from several conditions with stroke (Hodt-Billington et al. 2008), lower limb amputations (Skinner and Effeney 1985), osteoarthritis (Shakoor et al. 2003) and cerebral palsy (Winiarski) such equipment may have a role in the evaluation of such patients. It can also be used to monitor patient progress in orthopedics and rehabilitation (Steultjens et al. 2000). There is also a potential use in sports training where running as close as possible to zero asymmetry may improve an athlete's performance (Wahab and Bakar 2011).

Our proposed real time dial based visualization tools offer an easy and user friendly way to visualize and monitor gait asymmetry. Our visualization techniques offer several advantages: 1) it shows real time gait features using graphical visualization which it is easy to interpret; 2) it does not require complex set up and equipment with segmentation of body parts required in a gait lab 3) it provides compressive longitudinal gait information for clinical use; and 4) its versatility has the potential to increase its usability at home supporting inclusivity of patients who are home bound. Therefore, our proposed gait information visualization approaches can be used for

different applications at home as well as in clinics for gait monitoring and rehabilitation. This has the potential of making gait asymmetry analysis more widely available for use.

4.3. Validation of extracted gait features

In order to use accurate quantitative gait monitoring in clinical applications, a low cost gait assessment tool is required which can provide the facility to analyse gait in clinic and at home. To address these issues, primarily we developed an affordable, wireless, wearable, simple and easy to use automatic spatiotemporal gait features extraction system that allows the subject to measure in indoor and outdoor (Anwary et al. 2018). This study has two main purposes: 1) to determine the concurrent validity of spatiotemporal automatic gait features collected using (Anwary et al. 2018) with the Motion Capture System (MCS) and Treadmill in both young and older adults, and 2) to compare the levels of agreement for average spatiotemporal gait parameters. We validate our proposed method using three experiments; 1) Treadmill at various walking paces vs MCS, 2) self-selected (free) walking vs MCS, and 3) self-selected (free) walking vs Digital tape for distance.

Three experimental materials and methods used for the development of this work are described in the following subsections.

4.3.1. Common experimental setup

Motion data are collected using a 10 camera Qualisys MCS operating at 100Hz (Qualisys Motion Capture). The data from these markers are processed for signal smoothing and stored in a data file with a C3D format. The data collected using IMU sensors are stored in another data file with a CSV format.

4.3.2. Experiment 1: Participants

A convenient set of 8 young subjects (7 males and 1 female, age 33.5 ± 5.06 years, weight 78.68 ± 16.51 kg, height 1.73 ± 0.6 m, BMI 26.14 ± 4.30 kg/m^2) are selected for this experiment. The subjects are selected with no signs of gait, balance or walking abnormalities. The exclusion criterion for selecting young subjects are recent ligament major injury, abnormal gait pattern, musculoskeletal or neurological pathology, contraindication to exercise, recent surgery, fracture

or muscle injury, impairment attributable to other cause by history or other health conditions that may adversely impact the outcomes of the study.

4.3.2.1. Experimental setup and protocols

Two reflective marks are placed on proximal phalange and ankle locations on both legs. Each subject walked on the treadmill with different speed settings at 0.6, 1.0, 1.4, 1.8, 2.0, 2.2 and 2.5 m/s, respectively. The subjects perform a walk on single belt treadmill (Woodway, model ELG) comprising of 30 strides.

4.3.3. Experiment 2: Participant selection

A convenient set of 10 young subjects (All males, age 27.55 ± 3.54 years, weight 62.56 ± 6.75 kg, height 1.59 ± 0.2 m, BMI 25 ± 3.8 kg/m2) are recruited for this experiment. The exclusion criterion for young subjects mentioned in Section 4.4.2 is followed.

4.3.3.1. Experimental setup and protocol

Two reflective marks are placed on proximal phalange and ankle locations on both legs. Each subject walked in a straight line for 10 m at a self-selected (free) walking pace.

4.3.4. Experiment 3: Participants

A convenience sample of 30 subjects are recruited: 10 healthy young subjects (9 males and 1 female, age 25.3 ± 4.64 years, weight 61.9± 4.61 kg, height 1.61 ± 0.1 m, BMI 24.45 ± 5.77 kg/m2); 20 older adults (19 males and 1 female, age 71.86 ± 8.55 years, weight 63.4 ± 3.03 kg, height 1.52 ± 0.1 m, BMI 28.14 ± 6.07 kg/m2). The exclusion criterion for young subjects mentioned in Section 4.4.2 is followed. The older adults are resident in a care home. Several of the older adults have problems with their gait. The subjects are purposefully chosen for this study to provide a variety of gaits for evaluation.

4.3.4.1. Experimental setup and protocol

Young subjects walk in a straight line along a corridor comprising of 15 strides at a self-selected (free) walking pace, a turn-around and another 15 strides. The distance travelled is measured by a digital tape. Older adults are also asked to perform a trail in a straight corridor comprising 15 strides of their walking, turn-around and another 15 strides. Several of the older participants

perform less than 15 strides. The distance carried out by walking on the corridor is then measured by a digital tape.

For experiments 1 and 2, the data collected from Qualysis is the 3D positions of the reflective markers from both legs. The position signals along the three coordinates are analysed to obtain the total distance, total time, stride (number, length, and time) and speed.

4.3.5. Statistical analysis

The data analysis is performed using SPSS (IBM Corp 2016) and R statistical software (R Development Core Team 2018). The gait features extracted from IMU using (Anwary et al. 2018) are validated against the data collected from either the treadmill and/or MCS. The treadmill and MCS are considered to be either gold or clinical standards. The treadmill gives information of speed and the MCS gives information of total distance, total time, stride number, stride length, stride time and speed. The collected gait features are explored for normality using the Shapiro-Wilk test. A series of statistical tests are applied, some of which may seem redundant in order to provide a complete representation of the system's validity. The level of absolute agreement between the extracted gait features and the MCS are analysed with Interclass correlations (ICC) by ICC(2,1) (Shrout and Fleiss 1979) for consistency (two-way mixed). Lin's concordance correlation coefficients (Lin 1989) (LCC - an index of how a new test reproduces a "gold standard" test) is applied to validate IMU gait features and MCS. LCC captures any subtle deviations in agreement between the measured variables and the reference criteria. Pearson's correlation coefficients (r) are applied to measure the linear strength of association between IMU gait features and MCS. This correlations are a poor indicator of validity since they do not account for absolute agreement, but they indicate if measurements can be fixed with recalibration (i.e., if a variable has a high PCC, a scaling or offset can be applied to allow absolute agreement) (Washabaugh et al. 2017). Means, SDs and CI for both systems are calculated. Bland-Altman plots are produced to provide a visual representation of heteroscedasticity by plotting the individual subject difference between the two systems against the individual mean of the two systems (Bland and Altman 1999). *T*-tests are also used to identify differences in IMU gait extracted features and MCS measurements.

4.3.6. Results of validation of extracted gait features

We present the validation results between automatic IMU gait extracted features with MCS and Treadmill measurements in the following sections.

4.3.6.1. Experiment 1: Using Treadmill and MCS

Table 4.8 shows the MCS and IMU gait features information where the treadmill speed is set to 0.6 m/s. The MCS estimation is considered as 'gold standard'/ 'clinical standard' and the accuracy of IMU gait features are estimated. The results for the treadmill speed settings at 1.0, 1.4, 1.8, 2.0, 2.2 and 2.5 m/s are provided in Appendix D. On the treadmill each participant walks for a total of 30 strides with a constant speed set to 0.6 m/s. The sample size is 1680 strides (8 subjects walk for 30 strides with 7 different speeds in total of 8x30x7 strides). The total distance travelled and the total time of each participant are recorded from both right and left legs concurrently by IMU and MCS. The speed is then obtained from distance and time information.

Table 4.8: IMU gait extracted features accuracy with MCS and Treadmill

Subjects	Treadmill Speed = 0.6 m/s																	
	QUALISYS						IMU						Accuracy (%)					
	Right Leg			Left Leg			Right Leg			Left Leg			Right Leg			Left Leg		
	D(m)	T(s)	S(m/s)	D(m)	T(s)	S(m/s)	D(m)	T(s)	S(m/s)	D(m)	T(s)	S(m/s)	D(m)	T(s)	S(m/s)	D(m)	T(s)	S(m/s)
1	26.34	38.66	0.68	25.51	37.61	0.68	26.60	38.47	0.69	24.63	37.45	0.66	98.99	99.49	98.48	96.54	99.57	96.95
2	19.75	32.92	0.60	19.73	32.88	0.60	20.39	32.89	0.62	20.12	32.96	0.61	96.77	99.91	96.68	97.99	99.75	98.24
3	31.96	49.69	0.64	31.96	50.31	0.64	32.26	49.84	0.65	31.94	50.20	0.64	99.05	99.70	99.35	99.96	99.79	99.84
4	40.44	67.40	0.60	40.42	67.37	0.60	42.61	67.48	0.63	41.38	67.20	0.62	94.65	99.89	94.76	97.63	99.76	97.38
5	15.38	25.63	0.60	15.32	25.53	0.60	15.12	25.66	0.59	15.03	25.57	0.59	98.33	99.92	98.25	98.08	99.87	97.96
6	15.32	25.53	0.60	15.35	25.59	0.60	15.01	25.54	0.59	14.70	25.60	0.57	97.99	99.97	97.96	95.75	99.94	95.70
7	36.98	61.64	0.60	38.19	62.32	0.61	40.78	61.51	0.66	38.30	62.19	0.62	89.75	99.80	89.52	99.72	99.78	99.50
8	19.45	32.42	0.60	19.48	32.47	0.60	22.28	32.40	0.69	20.22	32.50	0.62	85.48	99.92	85.38	96.23	99.91	96.32

D=Distance, T=Time, S=Speed

The accuracy is estimated using equation (4.51). The stride to stride information is analysed and the accuracy of IMU gait extracted features distance, time and speed are very high, indicating that the measurements are significant comparing with MCS. From the time column of Table 4.8, we can see that the accuracy of walking time is good comparing with the distance as it is recorded directly from the signal. The distance is obtained from accelerometer signal with mathematical analysis. The speed is also estimated based on distance and time information. Therefore, the accuracy of distance and speed are lower comparing with the time accuracy. The relative accuracy of our IMU sensors is between 85.48% - 99.96% for travel distance and 99.49%-99.97% for Time measurement. The lowest accuracy is 85.48% found in the travelled distance

from the right leg of subject 8. Actually the speed of 0.6 m/s is low comparing with normal human walking and subjects needed to adjust with the speed. However, the overall accuracy for all speeds is high. The distance and time of IMU and MCS are found normally distributed. The ICC(2,1), LCC and Pearson's correlation (r) are shown in Table 4.9.

Table 4.9: Validity of the IMU gait features and MCS

Subjects	Interclass correlations				Lin's correlation coefficients				Pearson's correlation coefficients			
	Right Leg		Left Leg		Right Leg		Left Leg		Right Leg		Left Leg	
	Dis	Tim	Dis	Tim	Dis	Tim	Dis	Tim	Dis	Tim	Dis	Tim
	ICC	ICC	ICC	ICC	LCC	LCC	LCC	LCC	r	r	r	r
1	0.88	0.97	0.88	0.97	0.79	0.94	0.78	0.93	0.81	0.94	0.81	0.93
2	0.99	1.00	0.99	1.00	0.98	1.00	0.98	1.00	0.98	1.00	0.99	1.00
3	0.98	1.00	0.98	0.99	0.96	1.00	0.96	0.99	0.96	1.00	0.96	0.99
4	0.93	1.00	0.96	1.00	0.83	1.00	0.91	1.00	0.88	1.00	0.93	1.00
5	1.00	1.00	1.00	1.00	0.99	1.00	0.99	1.00	0.99	1.00	0.99	1.00
6	0.99	1.00	0.99	1.00	0.97	1.00	0.98	1.00	0.98	1.00	0.99	1.00
7	0.94	1.00	0.97	1.00	0.89	1.00	0.93	1.00	0.89	1.00	0.94	1.00
8	0.97	1.00	0.99	1.00	0.94	1.00	0.97	1.00	0.94	1.00	0.98	1.00

Dis=Distance, Tim=Time, r (Pearson's correlation coefficient)

The level of agreement using ICC(2,1), LCC and r between IMU gait extracted features and MCS for each gait variable of distance and time at different speed levels from right and left legs from all subjects is good (from 0.78 to 1). The mean, standard deviation and 95% confidence interval (CI) are provided in Appendix D. The Bland-Altman plots of subject 1 are shown in Figure 4.23 and plots for other subjects are provided in Appendix D.

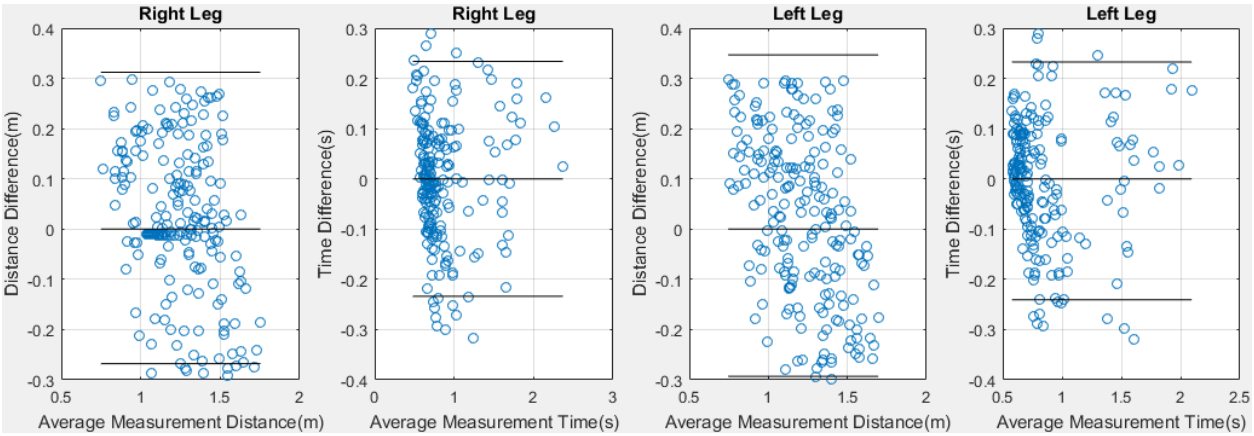

Figure 4.23: Bland-Altman plots for validity of distance and time measured for right and left legs with IMU and MCS from subject 1.

The plots in Figure 4.23 show the validity of gait extracted features as measured with the IMUs against the MCS measurement for subject 1. The *y*-axis of the plot corresponds to the difference between the two measurement systems, while the *x*-axis is the average of the two measurements. The line at the middle passes through zero axis is the average difference for the whole sample, while the upper and lower lines correspond to the 95% limits of agreement. It is observed from Figure 1 that the mean difference of the two estimations is zero and the most of the difference lies in between the 95% limits of agreement.

4.3.6.2. Experiment 2: MCS

Table 4.10 shows the accuracy of the IMU gait extracted feature and MCS measurements. The average accuracy of the result is 97.57% with 95% confidence interval ±1.327 for the estimated distance and 99.01% with 95% confidence interval ±0.266 for the Time.

Table 4.10: Validation of IMU gait extracted features with MCS

Subjects	Leg	Qualisys	IMU		Qualisys	IMU	
		Distance (m)		Accuracy (%)	Time (s)		Accuracy (%)
1	Right	7.650	7.607	99.435	12.670	12.510	98.740
	Left	7.522	7.459	99.159	12.330	12.330	100.000
2	Right	7.402	7.155	96.664	12.670	12.830	98.740
	Left	7.456	7.327	98.270	12.330	12.280	99.590
3	Right	8.181	8.126	99.330	8.720	8.740	99.770
	Left	7.984	7.747	97.034	8.280	8.150	98.430
4	Right	7.978	7.806	97.848	8.720	8.880	98.170
	Left	8.121	8.061	99.259	8.280	8.180	98.790
5	Right	7.735	7.699	99.531	9.780	9.750	99.690
	Left	7.842	7.791	99.345	9.720	9.640	99.180
6	Right	7.564	7.493	99.066	9.780	9.710	99.280
	Left	7.481	7.518	99.505	9.720	9.830	98.870
7	Right	7.693	6.784	88.181	7.380	7.250	98.240
	Left	7.626	7.197	94.377	7.030	7.130	98.580
8	Right	7.422	6.939	93.497	7.380	7.310	99.050
	Left	7.144	6.669	93.344	7.030	7.140	98.440
9	Right	7.769	7.744	99.678	7.940	7.910	99.620
	Left	7.755	7.626	98.331	7.870	8.000	98.350
10	Right	7.508	7.485	99.698	7.940	7.960	99.750
	Left	7.623	7.613	99.870	7.870	7.800	99.110

The *t*-test shows that there is no difference in means (p = 0.094) between MCS (μ_1 = 7.67, $\sigma 1$ = 0.26) and Estimated Distance ($\mu 2$ = 7.49, $\sigma 2$ = 0.39). Pearson's correlation coefficient (r = 0.81) indicates a strong correlation.

4.3.6.3. Experiment 3: Digital tape

Table 4.11 shows the average IMU gait extracted features information for both right and left legs from 10 young subjects.

Table 4.11. Validation of IMU gait features with digital tape for young subjects

AVERAGE	Age(y)	Height (m)	Weight (Kg)	Gender	
	25.30	1.61	61.90	9 M, 1 F	
Total Time (s)	57.85				
	Actual *	Right Leg **	Accuracy	Left Leg **	Accuracy
Total Distance (m)	37.77	37.19	97.73	37.81	98.82
Estimated Velocity (m/s)	0.73	0.72	97.73	0.73	98.82
Detected Stride Number	30.00	30.00	100.00	30.00	100.00
Detected Step Number	30.00	30.00	100.00	30.00	100.00

* ActualValue = recorded using digital tape, ** EstimatedValue = using IMU gait extracted features measurements

Table 4.12. Gait features information from young subjects

	Right Leg					Left Leg				
Gait Features	**Mean**	**Std**	**Var**	**Min**	**Ma**	**Mean**	**Std**	**Var**	**Min**	**Max**
Stride Length (m)	1.17	0.17	0.03	0.91	1.65	1.17	0.17	0.03	0.89	1.61
Stride Time (s)	1.41	0.20	0.04	1.10	1.97	1.39	0.19	0.04	1.07	1.91
Stride Velocity (m/s)	0.83	0.83	0.83			0.84	0.84	0.84		
Step length (m)	34.93					34.93				
Step time(s)	0.83	0.85	0.75			0.84	0.86	0.77		
Step Velocity (m/s)	0.50	0.14	0.02	0.15	0.84	0.54	0.18	0.04	0.24	1.10
Cadence (step/min)	0.68	0.19	0.04	0.21	1.14	0.74	0.24	0.07	0.33	1.48
Step Ratio (Step	0.01					0.01				
Stance Time (s)	0.84	0.16	0.03			0.83	0.13	0.02		
Swing Length (m)	1.17	0.68	0.49			1.17	0.94	1.14		
Swing Time (s)	0.58	0.12	0.02			0.57	0.15	0.02		
Swing Velocity (m/s)	2.07	1.80	1.80			2.10	1.83	1.83		

Std = Standard Deviation, Var = Variance, Min = Minimum and Max = Maximum

The accuracy is estimated using equation (4.51). The distance travelled by each young subject is measured using a digital tape and the average travelled distance is 37.77 m. The average estimated travel distance is 37.19 m for right leg and 37.81 for left leg. The accuracy of estimating average distance compared with the average actual distance is high for both legs. The accuracy of detected stride and step number achieves 100%. The accuracy of estimating travelled distance is 97.73% for right and 98.82% for left legs. Normal human walking velocity may vary from 1.5 to 2.5 m/s (Mohler et al. 2007) and the estimated average speed is 1.53 m/s which agrees with the literature. The stride lengths of legs are the same and the overall difference between legs is low. In natural walking, foot is on the ground for about 60% of the total time of

gait cycle during stance phase and 40% during swing phase. The ratio of stance and swing is found closest to the 60:40% split for average stride, stance and swing information (Table 4.12) for young subjects.

The accuracy of estimating the total distance compared with the actual distance is high for both legs for older adults shown in Table 4.13. The accuracy of detecting stride and step number is 92.67%. The accuracy of estimating the travelled distance is 88.71% for right and 89.88% for left legs. However, comparing to results in young subjects (Table 4.12), the accuracy is lower for older subjects with less than 9%. This may be due to older people walking slowly resulting in a poorer signal output. We will investigate this in our future work.

Table 4.13. Validation of IMU gait features with digital tape for older subjects

Average	Age	Height (m)	Weight (Kg)	Gender	
	72.15	1.53	63.55	28 M, 2F	
Total Time (s)	86.71				
	Actual *	Right Leg **	Accuracy	Left Leg **	Accuracy
Total Distance (m)	21.74	21.48	89.09	20.47	89.94
Estimated Velocity (m/s)	0.26	0.26	89.09	0.24	89.94
Detected Stride Number	30	28.4	91.48	29.33	91.2
Detected Step Number	30	28.4	91.48	29.33	91.2

Table 4.14. Gait features information from older subjects

	Right					**Left**				
Gait Features	**Mean**	**Std**	**Var**	**Min**	**Max**	**Mean**	**Std**	**Var**	**Min**	**Max**
Stride Length (m)	0.74	0.17	0.03	0.51	1.29	0.74	0.15	0.03	0.53	1.16
Stride Time (s)	2.72	0.62	0.5	1.91	4.75	2.69	0.51	0.32	1.85	4.02
Stride Velocity (m/s)	0.28	0.28	0.28			0.28	0.3	0.3		
Cadence (step/min)	24.34					24.34				
Step Velocity (m/s)	0.33	0.28	0.13			0.34	0.3	0.1		
Step length (m)	0.28	0.25	0.06	0.22	0.63	0.28	0.22	0.07	0.04	0.57
Step time(s)	0.2	1.01	1.02	1.02	2.07	0.32	0.93	1.42	0.18	2.2
Step Ratio (Step length/cadence)	0.01					0.01				
Stance Time (s)	1.39	0.51	0.17			1.37	0.46	0.52		
Swing Length (m)	0.74	0.8	0.76			0.74	0.9	0.98		
Swing Time (s)	1.09	0.41	0.21			1.07	0.32	0.14		
Swing Velocity (m/s)	0.78	0.6	0.6			0.78	0.59	0.59		

*ActualValue, **EstimatedValue

Table 4.14 shows the details of both legs gait variables for older subjects. Overall the stride lengths of both legs are similar for older adults. The overall difference between legs is very low. We check the data for statistical errors and assess whether the estimated values are reasonable. The young subjects' travelled distance for 30 strides has a wider range and is significantly different than older ones. On average young subjects travelled distance is 37.77 (95% CI ± 3.57) m and the distance of older ones is 22.50 (95% CI ± 2.34) m. Similarly, the legs stride and step

variation is low for older ones than young ones. Older one's gait is slow and results in a low variation in walking comparing with young ones.

4.3.7. Discussion

This study evaluates the validity of an automatic spatiotemporal gait features extraction system using wearable IMUs from young and older subjects so that clinicians and researchers can better interpret gait information. Based on the three experiments, the findings of this study indicate that our automatic IMU gait extracted features are accurate for measuring comprehensive spatiotemporal gait features comparing with 'gold standard' MCS and Treadmill.

In Experiment 1, the use of a treadmill condition allows us to select different walking speeds and tease out the true instrumentation error from the measurement error due to biological variation (i.e., natural variation in walking patterns) because of the fact that gait patterns are more invariant on a treadmill than over ground (Hollman et al. 2016). The different speeds minimize the contribution of intra-individual variability of performance. The features extracted from both systems indicate that the instrumentation error is acceptable for most of the gait variables. To develop from the results of Experiment 1, we conducted repeated with additional subject over ground (in laboratory) in a free condition. The accuracy of our system is comparable with that of MCS. As the laboratory space is limited to only few meters, we conducted Experiment 3 with young and older subjects in their home and find the results are also acceptable.

We analyse our results using various methods of correlation as each method has different strengths and weaknesses. ICCs are often thought to be more reliable at assessing correlations than Person's r and Spearman's rho test. Results need to be interpreted with caution as a high ICC does not necessarily mean good reliability, particularly in situations where there is a large variation of readings within the same subject. To address this, an absolute measure of reliability such as the coefficient of variation or limits of agreement (Bland and Altman 1986) is often used. The coefficient of variation is not affected by the presence of a heterogeneous sample such that a measurement that has a high ICC may not be reliable if the coefficient of variation is large. The determination of acceptable limits of the coefficient of variation is set depending on the level of agreement that the researcher aims to achieve when comparing groups or the outcomes of the intervention. As ICCs have limits in the accuracy they can achieve, we also use LCCs. Measuring using LCCs requires making less assumptions than that using ICC and identifies subtle deviations

in agreement between measured variables and reference criteria. We also use Pearson's correlation coefficients (r) to measure the linear strength of association between the IMU gait extracted features and MCS measurements. Pearson's correlations are a poor indicator of validity since they do not account for absolute agreement, but they indicate if measurements can be fixed with recalibration (Washabaugh et al. 2017). Bland-Altman plots are generated for IMU gait extracted and MCS measurements to visually display any systematic errors present in our IMU measurements.

There are a number of limitations to our study. We recruited a total of 48 young and older subjects where most did not have gait abnormality. A larger, more diverse population with multiple trails is needed that will include specific gait abnormality, children with gait pathology, severe Parkinsonian gait and other neurological disorder etc. IMU calibration is an essential part for automatic gait extraction features estimation. Although in our methods we try to minimize errors, as gait features are intrinsically variable from person to person, any such algorithm should involve a degree of calibration which we address. Individual quirks, heel strike, significant body up-down movement and other factors can also affect the results. There are several other possible sources of errors (S Flenniken et al. 2017) that may arise from the use of IMU sensors including errors of repeatability, stability and drift. Although IMU sensors performance has been ramped up dramatically, the errors in measurement are unavoidable, especially for miniature micro-electro-mechanical (MEMS) sensors. Future developments should focus on MEMS sensor error modelling and accommodation to further improve parameter estimation accuracy (Yang et al. 2012). Other possible areas of error may arise from frictional noise and the relative movement of clothing and shoes to the sensor. However, we compared our results to what is currently considered as gold standards MCS and Treadmill which show good accuracy making the effect of such errors acceptable.

The results from three experiments show that our proposed system provides acceptable results comparing with those of MCS and Treadmill and has the potential to be used in gait assessment and change monitoring for home and clinical use. Gait with slow velocity is common in older adults and an automatic system sensitive enough to detect gait features in these circumstances is required. Our low cost portable personalized proposed solution could bring out automatic gait features for monitoring longitudinal gait changes or abnormalities. In future work, we plan to use our automatic gait extracted features information to classify gait changes over time to identify abnormal gait patterns for the assessment of elderly fall risk, rehabitation and sports applications.

4.4. Conclusions

In the present work, two IMU sensors are placed at right and left metatarsal barefoot locations to collect accelerometer and gyroscope data. We design and develop an android app to collect real time synchronous data from both sensors. We propose a systematic method to extract automatic gait features for the gait assessment. We first apply the quaternion technique to raw data for estimating actual sensor orientation. We apply our proposed stride, stance, swing and step event detection technique and analysed for stride, step, cadence, step ratio, stance, and swing. We then estimate distance using double integration with drift removing from acceleration and analyzed for total velocity, distance and time. We apply our method for 10 young and 10 older subjects. Our results show that it is possible to extract GA features automatically in a clinical setting outside of a gait laboratory. This has the potential to make the evaluation of gait widely available in clinical practice rather than being limited to gait laboratories.

In biometrics and biomedical engineering, gait analysis has been used to characterize human locomotion and has many applications (Sadeghi et al. 2000; Bora et al. 2015b). This paper presented four gait asymmetry visualization approaches: 1) Real time dial visualization; 2) Visualization of individual leg time variation; 3) Visualization of both legs asymmetry; and 4) Boxplot-based visualization. Real time dial visualization showed the instantaneous gait asymmetry of both legs from distance and time of stride, step and swing phases of each gait cycle using a dial and an indicator. It also showed instantaneous distance and time of stride, step and swing values in a seven segment display. Individual leg variation visualization showed the variation in stride, stance and swing phases in time. Both legs asymmetry visualization showed the asymmetry between two legs for strides and steps. Boxplot-based visualization showed the overall stride, step, stance and swing phases distribution. These methods are user friendly and easy to interpret and have the potential of helping professionals detect and interpret gait asymmetry.

We develop an affordable, wireless, wearable, simple and easy to use automatic spatiotemporal gait features extraction system using IMU sensors that allows the subject to measure gait information in indoor and outdoor (open ground). We validate our IMU system with more generic variation of age and environment with a sample size of 900 strides. We apply ICC, LCC and Pearson's correlation to compare the levels of agreement for average spatiotemporal gait parameters obtained using IMU gait extracted features. We also perform *t*-test and generate

Bland-Altman plots. The results obtained from three experimental conditions demonstrate that our IMU gait extracted features are highly valid for spatiotemporal gait variables in young and older adults. The ICC, LCC and *r* values observed for the IMU system are comparable to MCS and Treadmill. These findings have meaningful implications for clinicians and researchers who use IMUs for evaluating and study gait abnormality. Our results show that our automatic IMU gait extraction features provide comprehensive spatiotemporal gait information in a clinical setting outside of a gait laboratory. This has the potential to make the evaluation of gait abnormality widely available in clinical practice rather than being limited to gait laboratories.

5. EVALUATION OF GAIT USING PROCRUSTES ANALYSIS AND EUCLIDEAN DISTANCE MATRIX ANALYSIS

The Chapter is organized in the following sections. Section 5.1 presents methods includes the participant selection, placing location, data collection, statistical shape analysis, understanding of shape, form and size, Procrustes analysis, and EDMA. Section 5.2 delivers the experimental results for 32 participants to demonstrate the proposed method. The discussions and conclusion are given in section 5.3 and 5.4.

5.1. Methods

5.1.1. Participants Selection

A convenience sample of 32 subjects are recruited: 12 healthy young subjects (9 male, mean age 25.4 years, standard deviation 4.64, range 19-35 years); 20 older adults (19 male, mean age 71.86 years, standard deviation 8.55, range 62-86 years). Among 12 young subjects, 10 are used for modelling while an additional 2 are used for validation. Young subjects are selected with no signs of gait, balance or walking abnormalities. Older adults from a care home are invited to participate. They are a group of patients chosen with some having a normal and others an abnormal gait. It is coincidental that the majority of subjects are male.

5.1.2. Sensor placing location

In this study, the sensors are placed at the base of the first metatarsal of both feet. This position is previously determined and validated for collecting data since this can achieve the best performance compared to other foot locations details presented in Chapter 3.

5.1.3. Data collection

The subjects perform a walk in a straight corridor comprising of 15 strides of normal forward walking, a turn-around and another 15 strides. Accelerometer and gyroscope data are collected by placing the sensors on right and left metatarsal foot locations of the barefoot and the procedure is described in Chapter 4. The gait time and distance based features of stride, stance, swing and step are also described in Chapter 4.

5.1.4. Statistical shape analysis

Statistical shape analysis is a type of geometrical analysis that involves a set of visual shapes in which statistics are measured to describe shape components of similar or different shapes. For example, the difference between male and female Gorilla skull shapes (Dryden and Mardia 1998). Some of the important aspects of shape analysis are to obtain a measure of distance between shapes, to estimate average shapes from a (possibly random) sample and to estimate shape variability in a sample (Dryden and Mardia 1998). Statistical shape analysis plays an important role in many kinds of biological studies (Kendall 1977; Bookstein 1978; Bookstein 1997; Kendall et al. 1999). Shape analysis is mainly automatic analysis of geometric shapes, for example using a computer to detect similarly shaped objects in a database or parts that fit together. For a computer to automatically analyze and process geometric shapes, the objects have to be represented in a digital form or mathematical representation. (Kendall 1977; Kendall 1984) and (Bookstein 1978; Bookstein 1997) are two of the early pioneers of the statistical theory of shape. Subsequently, developments have led to a deep differential geometric theory of shape spaces (Kendall et al. 1999), as well as practical statistical approaches to analysing objects using probability distributions of shape and likelihood based inference. In this research, Procrustes analysis and Euclidean distance matrix analysis (EDMA) have been investigated for gait analysis.

The method of superimposition, particularly the Procrustes superimposition, was originally developed and introduced to the biological sciences by famed anthropologist Franz Boaz and his student Eleanor Phelps (Lele and Richtsmeier 2001). Later, the idea of studying shape change using superimposition and deformation approaches has been seriously considered and further developed by many different researchers (Kendall 1984; Bookstein 1998; Dryden and Mardia 1998). Goodall reported Procrustes methods in the statistical analysis of shape (Goodall 1991). His methods are useful for estimating an average shape and for exploring the structure of shape variability in a dataset. Procrustes analysis has been used in a wide range of biological applications, for example assessing differences between Chinese and Caucasian head shapes (Ball et al. 2010) and assessing differences in body shape in horses (Druml et al. 2009). Therefore, Procrustes analysis can also be used for assessing of gait features shape changes.

Euclidean distance matrix analysis (EDMA) is applied for comparing two shapes using landmark data (Lele and Richtsmeier 1991). EDMA allows form variation or growth differences to be examined through the comparisons of ratios of landmarks of equivalent configurations. This

method can compare the form and/or growth of organisms that have been measured using two or three-dimensional coordinates. EDMA has been used to quantify form and growth differences for cebus apella skulls (Lele and Richtsmeier 1991), the cranial growth of squirrel monkeys (Corner and Richtsmeier 1992) and sexual dimorphism in macaques (Richtsmeier et al. 1993). Therefore, EDMA can also be used to quantify gait form differences for abnormal gait patterns.

5.1.5. Understanding of shape, form and size

Both *shape* and *form* consist of geometrical representation of an object and a set of points or landmarks can represent that information. A *form* change of an object occurs when differential change in magnitude occurs along various axes and there is difference in volume between the sphere surrounding the landmark in the reference form and the ellipsoid surrounding the landmark in the target form (Richtsmeier et al. 1992),. The relationship between shape, size and form changes is shown in Figure 5.1.

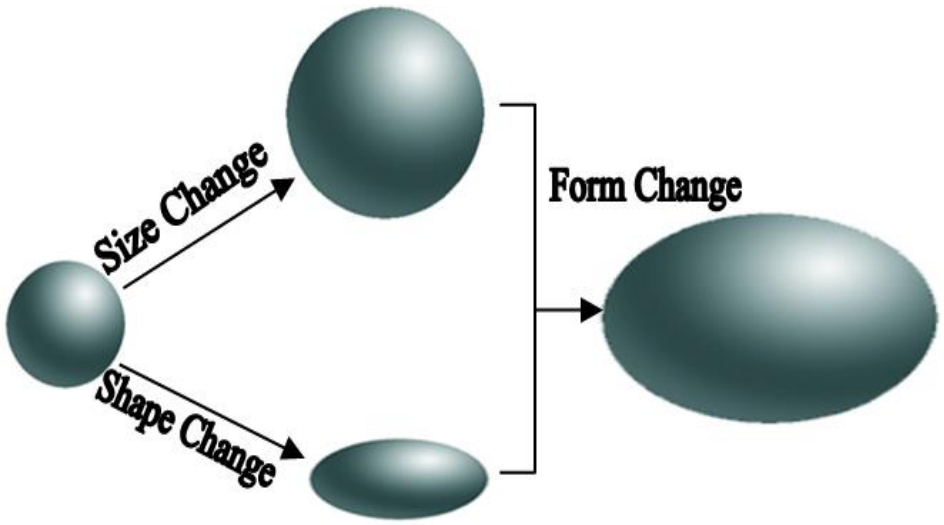

Figure 5.1: Geometric representation of form change relating with shape and size (Richtsmeier et al. 1992)

These landmarks remain invariant when an object is 1) moved within a given coordinate system (translation), 2) turned on any axis of a given coordinate system (rotation) and 3) flipped of a given coordinate system (reflection). For example, a triangle consists of three vertices. Considering those vertices as landmarks, the triangle can be rotated, translated or reflected to any arbitrary amount. Each such movement of the triangle results in changes in the coordinate locations of the three vertices, although no changes are made regarding the relative locations of the landmarks. As the triangle is moved, the coordinates of the vertices are translated, rotated or

reflected and a new set of coordinates is required to define the new location of the three landmarks. This means that the landmark coordinates matrix changes upon reflection, translation or rotation and that the landmark coordinate matrix is not invariant with respect to translation, rotation or reflection. In this research a total of eight gait features from the 13 extracted features used from right and left legs are considered as landmarks from 10 young and 20 older adult subjects

5.1.6. Procrustes analysis

Shape analysis is an important aspect of visualizing and understanding of shape information. The analysis of shape plays a vital role, not only in determining the differences between shape groups, but also in determining the location of differences among shapes. The form of statistical shape analysis used to analyse the distribution of a set of shapes in this work is Procrustes analysis (Gower and Dijksterhuis 2004). According to (Crosilla and Beinat 2002), Procrustes analysis is a set of mathematical least-squares tools to directly estimate and perform simultaneous similarity transformations among the model point coordinates matrices up to their maximal agreement. Procrustes analysis is a rigid shape analysis that uses translation, isotropic scaling and rotation to find the best fit between two or more landmarks shapes (Gower and Dijksterhuis 2004). It has variations and forms, of which are Orthogonal Procrustes analysis (OPA), Extended Orthogonal Procrustes analysis (EOPA), Weighted Extended Orthogonal Procrustes analysis (WEOPA), and Generalized Procrustes analysis (GPA) etc (Schonemann 1966; Schoenemann and Carroll 1970; Gower 1975; Goodall 1991). The former is a multivariate exploratory technique that involves transformations (i.e., translation, rotation, reflection, isotropic rescaling,) of individual data matrices to provide optimal comparability (Gower 1975) i.e. it is the evaluation of many sets of configurations which can be aligned to one target shape or aligned to each other. GPA is used in several domains. For example, it can be used in sensory analysis before a Preference Mapping to reduce the scale effects and to obtain a consensus configuration. It also allows a comparison the proximity between the terms that are used by different experts to describe products (Kristof and Wingersky 1971). On the other hand, OPA is used for matching two configurations (Ten Berge 1977).

Shapes and landmarks are two important concepts involved with Procrustes analysis. They have their own role in the process of aligning shapes. Dryden and Mardia define shape as the

geometrical information that remains when location, scale and rotational effects are filtered out from an object (Dryden and Mardia 1998). By this definition of shape, there exists transforms that allow the shape to move so that the differences may be removed between two shapes while proving the shape itself. The transforms used in aligning the shapes are; scaling, translation and rotation. They used the notation OPA as ordinary Procrustes analysis.

5.1.6.1. Graphical representation of Procrustes transformations

A representation of two configurations X and Y consisting of $n = 9$ landmarks on each object in $k = 2$ dimensional space can be seen in Figure 5.2(a). The landmarks are joined together by drawing lines between them to visualize the outline of two shape configurations. It can be seen that the two shapes are not aligned in the same way and they do not have the same origin. Their height and width are also different. The purpose of applying Procrustes analysis is to find the best fit between these two configurations. We can do this by superimposing the second configuration on to the first configuration and eliminating differences in scale and rotation. The result of the translation is shown in Figure 5.2 (b), Figure 5.2 (c) shows the result of scaling and the result of the rotation is shown in Figure 5.2 (d).

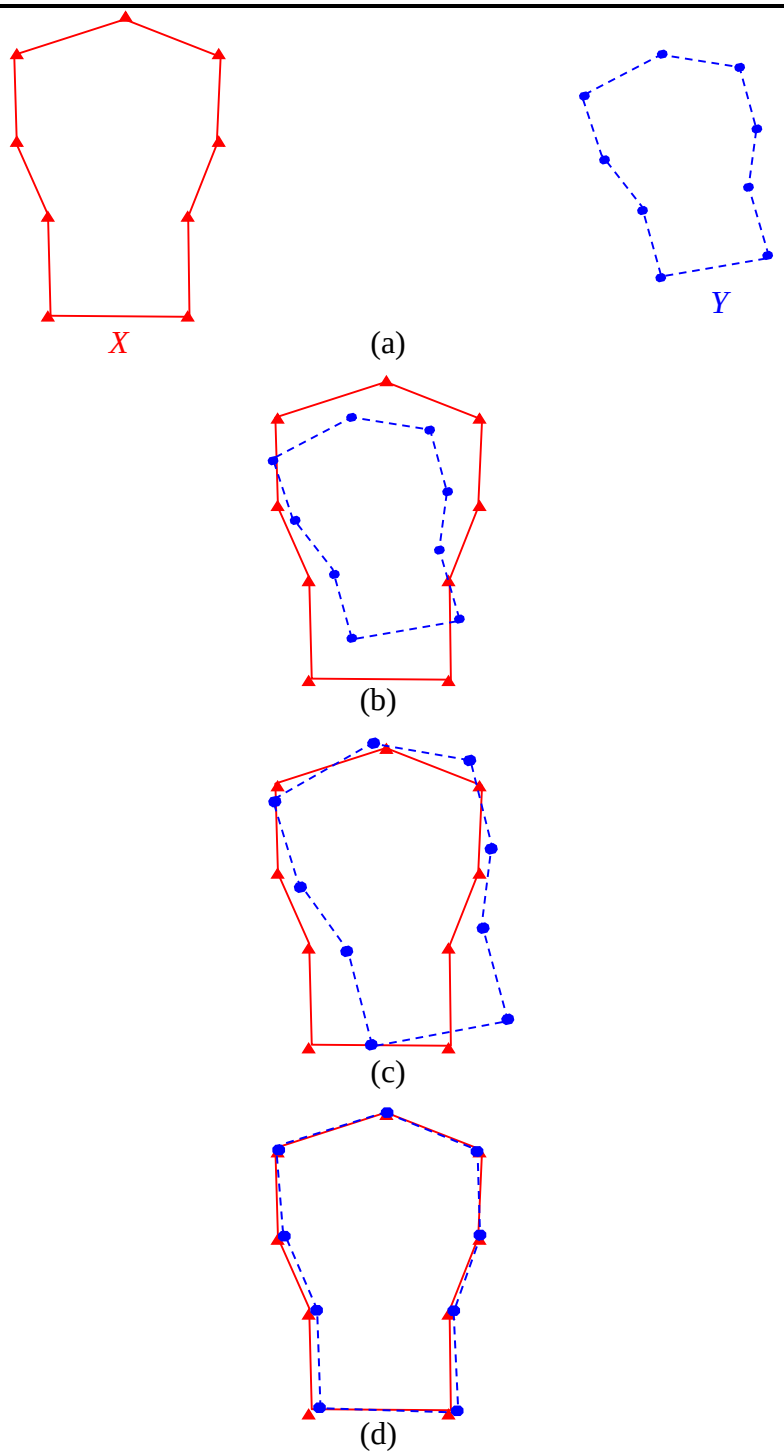

Figure 5.2: Removing variation due to differences in translation, scale and rotation (a) Original data of two configurations; (b) After translating the centroid of *X* to the centroid of *Y*; (c) After removing differences in scale; (d) After removing differences in rotation.

It is now important to understand mathematical formulae for these steps to implement this technique for object shape analysis.

5.1.6.2. Mathematical representation

Let X_i *(i=1,2,3,…,m)* be a series of *m* matrices that contain the coordinates of a set of *p* landmarks on the *m* shape configurations in *k* dimensions. The translation, rotation and scaling of a configuration can be described as (Gower 1975)

$$\hat{X}_i = c_i X_i O_i + j t_i^T \tag{5.1}$$

Where $\hat{X}_i$ gives the new coordinates of the landmarks in the configuration. O_i is the rotation matrix, c_i is the scaling factor, t_i is the translation vector and *j* is the unit vector. The superscript ^{T} indicates the transpose of the matrix. For GPA, the configurations are translated, rotated and scaled until the sum of the squares of the distances between the equivalent landmarks are minimized to give the best possible match between all configurations. The function to be minimized is thus

$$E \equiv \mathrm{tr}\left\{\sum_{i=1}^{m}\sum_{q=i+1}^{m}\left[\left(c_i X_i O_i + j t_i^T\right)-\left(c_q X_q O_q + j t_q^T\right)\right]^T\left[\left(c_i X_i O_i + j t_i^T\right)-\left(c_q X_q O_q + j t_q^T\right)\right]\right\} \tag{5.2}$$

The procedure can be described pictorially (Crosilla and Beinat 2002) as shown in Figure 5.3 where the individual configurations are translated, rotated and scaled so that they can be "superimposed" on each other to achieve a "best" fit.

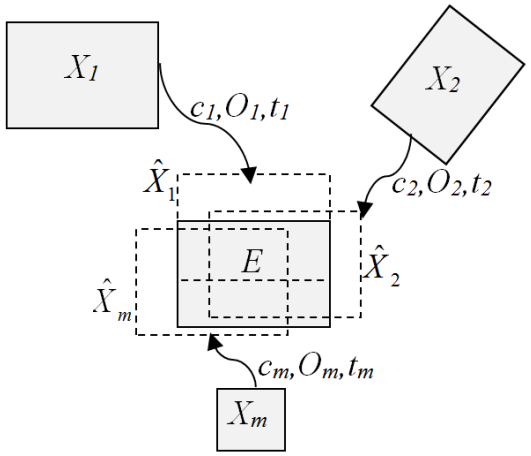

Figure 5.3: Concept of generalised Procrustes analysis

If the trivial solution found by setting all c_i to zero is excluded, another possible solution to the minimisation problem can be to select one configuration as the "norm" and scale all the other configurations relative to that one. However, this means that fitting X_1 to X_2 does not give an identical result to fitting X_2 to X_1. It is more satisfactory to estimate all c_i parameters such that

$$\sum_{i=1}^{m} c_i^2 \mathrm{tr}\left(X_i X_i^T\right) = \sum_{i=1}^{m} \mathrm{tr}\left(X_i X_i^T\right) \tag{5.3}$$

This means the sum of squares about the origin of the rotated, scaled and translated configurations is unchanged from the original value; in other words, some configurations are increased in size while others are reduced so that the overall sum remains the same.

$$\sum_{i=1}^{m} \sum_{q=i+1}^{m} \left\| \bar{X}_i - \bar{X}_q \right\| = \min \tag{5.4}$$

Where the operator $\|..\|$ represents normal vector space or norm and $\bar{X}$ is mean.

Let us consider the sum-of-squares between each cluster of points $P_i^{(q)}$ where $i=1,2,3,...m$ and their centroid is G_i which is summed over all P clusters. So the Euclidean distance between the pairs of points P_i and G_i is $\Delta(P_i^{(q)}, G_i)$. The mp lengths $\Delta(P_i^{(q)}, G_i)$ are termed residuals. The residual sum-of-squares R_s (Gower 1975) is therefore

$$R_s = \sum_{i=1}^{p} \sum_{q=1}^{m} \Delta^2(P_i^{(q)}, G_i) \tag{5.5}$$

because of the identity of different configurations

$$\sum_{u<v}^{m} \Delta^2(P_i^{(u)}, P_i^{(v)}) \equiv m \sum_{u=1}^{m} \Delta^2(P_i^{(u)}, G_i) \tag{5.6}$$

Now it is required to estimate the scaling factor c_i , the rotation matrix O_i and the translation vector t_i so that the residual sum-of-squares of equation (5.5) is minimized.

There is no unique solution for O_i as equation (5.2) is invariant to orthogonal rotations of the total system of pm points. A unique solution can be determined by referring all final co-

ordinates to the principal axes of the set of centroid points G_i where $i=1,2,3,....,m$. Equation (5.2) can therefore be minimized subject to the constraints of equation (5.3).

Every O_i (Gower 1975) is orthogonal can be represented by

$$\sum_{k=1}^{p} o_{uk}^{(i)} o_{vk}^{(i)} = \delta_{uv} \tag{5.7}$$

where δ_{uv} is the Kronecker-δ, for $u \leq v$ where $v=1,2,3,.....,p$

Associating with equation (5.3) the Lagrange multiplier μ and with equation (5.7) the $\frac{1}{2}mk(k+1)$ Lagrange $\lambda_{uv}^{(i)}$. Considering these as arranged in m symmetric matrices Λ_i where $i=1,2,3,....,m$ with general elements $\lambda_{uv}^{(i)}(u \neq v)$ and $2\lambda_{uv}^{(i)}$ on the diagonal. Thus finally we have to minimize

$$E + \mu(\sum_{i=1}^{m} c_i^2 \mathrm{tr}(X_i X_i^T) - \sum_{i=1}^{m} \mathrm{tr}(X_i X_i^T)) + \sum_{r=1}^{m}\sum_{i \leq q}^{k} \lambda_{iq}^{(r)} (\sum_{l=1}^{k} o_{il}^{(r)} o_{qk}^{(r)} - \delta_{iq}) \tag{5.8}$$

5.1.6.3. Translation

The only terms involving the translation matrix, t_i, occur in equation (5.2)

$$E_o \equiv \mathrm{tr}\left[(m-1)\left(c_i X_i O_i + j t_i^T\right)\left(c_i X_i O_i + j t_i^T\right)^T - 2\left\{ \sum_{j \neq i}^{m} \left(c_j X_j O_j + j t_j^T\right) t_i^T \right\} \right] \tag{5.9}$$

Now differentiating equation (3.9) (Gower 1975) with respect to the elements of row vector t_i gives $\frac{\partial E_o}{\partial t_i} \equiv pmt_i$ which is the vector of column sums $\sum_{i=1}^{m} jt_i$. So the minimum is $t_1=t_2= t_3.....= t_m$. It shows that all m configurations should be translated to have the same centroid. Thus the terms of equation (5.2) in t_i *(i= 1, 2, 3,...,m)* can be dropped from further consideration.

5.1.6.4. Rotation

Now differentiating equation (5.8) with respect to $o_{iq}^{(r)}$ (o_{iq} represents individual elements in O_i) gives

$$c_r\left\{c_1(X_r{}^T X_1 O_1)_{iq}+\cdots+c_{r-1}(X_r{}^T X_{r-1}O_{r-1})_{iq}+c_{r+1}(X_r{}^T X_{r+1}O_{r+1})_{iq}+\cdots+c_m(X_r{}^T X_m O_m)_{iq}\right\}$$
$$-\sum_{l\neq q}^{k}\lambda_{il}{}^{(r)}o_{il}{}^{(r)}-2\lambda_{iq}{}^{(r)}o_{iq}{}^{(r)}$$

(5.10)

Equating it to zero and expressing it in matrix terms gives (Gower 1975)

$$c_r X_r{}^T(mY-c_r X_r O_r)=\Lambda_r O_r \tag{5.11}$$

where $r=1,2,3,\ldots,m$ and $Y=\frac{1}{m}\sum_{i=1}^{m} c_i X_i O_i$ are the co-ordinates of the centroid of the group or consensus configuration after rotation and scaling. Post-multiplying by $O_r{}^T$ and rearranging gives

$$(c_r X_r{}^T Y)O_r{}^T=(c_r{}^2 X_r{}^T X_r+\Lambda_r)\Big/m \tag{5.12}$$

The singular value form of $c_r X_r{}^T Y$ is written as $U_r{}^T S_r V_r$ where U_r and V_r are orthogonal and S_r is diagonal. The right-hand-side of equation (5.12) is symmetric and thus equation (5.12) reduces to

$$O_r=U_r{}^T V_r \tag{5.13}$$

Therefore, the rotation is completed by multiplying $U_r{}^T V_r$ by the X_i matrix in order to align it with the $\overline{X}_i$ matrix. Thus $\left|X_r O_r-\overline{X}_r\right|$ is minimized for the value O_r.

5.1.6.5. Scale

Differentiating equation (5.9) with respect to c_i and equating the result to zero gives

$$(m-1)c_i\,\mathrm{tr}(X_i X_i^T)-\mathrm{tr}\left\{X_i O_i\sum_{\substack{l=1\\ l\neq i}}^{m} c_l O_l^T X_l^T\right\}+\mu c_i\,\mathrm{tr}(X_i X_i^T)=0 \tag{5.14}$$

or

$$(m-1)c_i\,\mathrm{tr}(X_i X_i^T)-\mathrm{tr}\left\{X_i O_i\sum_{l=1}^{m} c_l O_l^T X_l^T\right\}+c_i\,\mathrm{tr}(X_i X_i^T)+\mu c_i\,\mathrm{tr}(X_i X_i^T)=0 \tag{5.15}$$

Finally,

$$mc_i \mathrm{tr}(X_i X_i^T) - m\mathrm{tr}(X_i O_i Y^T) + \mu c_i \mathrm{tr}(X_i X_i^T) = 0 \tag{5.16}$$

Multiplying equation (5.16) by c_i and summing over $i=1, 2,3, \ldots, m$ and recalling the constraints of equation (5.4) yields

$$(m+\mu)\sum_{i=1}^{m} \mathrm{tr}(X_i X_i^T) = m^2 \mathrm{tr}(YY^T) \tag{5.17}$$

and hence

$$c_i = \frac{\mathrm{tr}(X_i O_i Y^T)\sum_{i=1}^{m}\mathrm{tr}(X_i X_i^T)}{m \ \ \mathrm{tr}(X_i X_i^T)\mathrm{tr}(YY^T)} \tag{5.18}$$

The alternative form can be written as

$$c^2_i = \frac{\mathrm{tr}(c_i X_i O_i Y^T)\sum_{i=1}^{m}\mathrm{tr}(X_i X_i^T)}{m \ \ \mathrm{tr}(X_i X_i^T)\mathrm{tr}(YY^T)} \tag{5.19}$$

Because Y itself involves the scaling factors, the above formulae do not give a direct method for calculating c_i, but have to be used iteratively. However, equation (5.16) is the same equation for determining c_i as when given X_i,O_i are to be scaled to fit *any* configuration Y and equations (5.18) and (5.19) still follow but with $tr(YY^T)$ replaced by $tr(\sum_{i=1}^{m} c_i X_i O_i Y^T)/m$.

Iterative procedures are used for the minimization process in GPA. The shapes are repeatedly scaled, rotated and translated until the sum-of-squares defining the distances between the equivalent landmarks on all shapes has been minimised.

5.1.6.6. Algorithm for GPA

The procedure to align the configurations using GPA is as follows:

1. Calculate the initial approximate mean with all centroids at the origin
2. Align all shapes to this mean:
    a. Calculate centroid for each shape

b. Translate each shape to origin (common centroid)

c. Scale each shape for best fit

d. Rotate each shape for best fit

3. Calculate new approximate mean from aligned shapes.

4. If the approximate mean from 3 differs by more than a set tolerance from the previous approximate mean, then repeat steps 2 and 3.

5.1.6.7. Algorithm for OPA

Ordinary Procrustes analysis is a special case of GPA where the number of configurations is two. The second configuration is translated, scaled and rotated to find the best match on the first configuration.

5.1.7. Normal mean gait shape estimation using Procrustes

In order to quantify and compare gait, a common procedure is to normalise the obtained gait features both in time and length. In total of eight gait features (stride length, stride time, stride velocity, step length, step time, step velocity, stance time, swing length, swing time and swing velocity) from right and left legs are presented in the Cartesian coordinate. The x and y axes represent the features of the right and left legs with the dimensionless numbers respectively. This two dimension Cartesian coordinate represents the shape based on gait features collected from both legs. For estimating NMGS using GPA, 10 young subjects gait information is used. GPA provides the least square correspondence of more than two data matrix configurations. Translation, rotation and scaling of a configuration can be described (Dryden and Mardia 1998) using equation (5.1). Using GPA, the configurations are translated, rotated and rescaled until the sum of the squares of the distances between the equivalent landmarks are minimized to give the best possible match between all configurations. The Procrustes superimposition computes a mean shape referred as NMGS for the young subjects based on gait features where scaling and reflection are not performed in this analysis. The shape of each subject's gait is defined by its Procrustes residuals which are the deviation of the landmarks from the NMGS.

5.1.8. Gait shape comparison

To quantify gait based on all gait features, RSD (Kendall 1984), RSSD (Le 2016), PSSD (Dryden and Mardia 1998) and RMSD (Dryden and Mardia 1998) are investigated. Riemannian geometry (Carmo 1992) studies higher dimensional space. A shortest curve between any pair of points on a curved surface is called a minimal geodesic. On some surfaces, there may be pairs of points which have more than one minimal geodesic between them (for example a sphere). The RSD gives a measure of the relationship between the curvature of a space and its shape. The RSD parameter has a value between 0 and $\pi/2$; the smaller this value, the smaller the difference between the gaits. The RSSD is the Riemannian distance between the size-and-shape of the configurations found by minimizing the Euclidean distance over rotations. The smaller the value is, the closer the configurations in size-and-shape distance. The PSSD is defined as the distance between two shapes as the closest distance between the fibers on the pre-shape sphere in a non-Euclidean shape metric space. This allows us to compare two configurations which are independent of position, scale and rotation. The small value means the small distance between them. The RMSD is another measure of size-and-shape differences between configurations where the value is estimated from the square root of ordinary Procrustes sum of squares divided by the number of landmarks and number of dimensions. The small value means the small deviation between the configurations. RSD, RSSD, PSSD and RMSD are estimated for distinguishing degree of abnormality of each gait compared to NMGS. Each gait is translated and rotated to find the best match with the NMGS using OPA and the distances are then estimated between the NMGS and each best match gait.

5.1.9. Euclidean distance matrix analysis

5.1.9.1. The perturbation model for landmarks

Suppose $n=9$ landmarks have been selected from the object in 2D, then the landmarks data matrix for one subject look as follows:

$$\begin{bmatrix} x_1 & y_1 \\ x_2 & y_2 \\ \dots & \dots \\ x_9 & y_9 \end{bmatrix}$$

where *x* and *y* denote the two-dimensional coordinates,

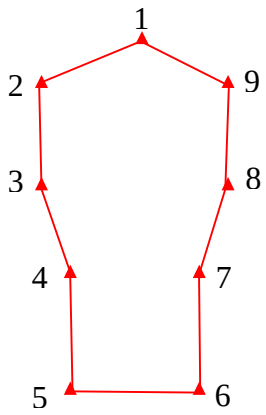

Figure 5.4: Diagram of an object indication the locations of 9 landmarks.

Assuming the configuration of these landmarks represents the form of a configuration as shown in Figure 5.4, the question is how to measure the variability among individuals that are represented by these two-dimensional landmark data. In statistical studies, when analysing landmark data, variability is particularly difficult to characterize, because data on an individual is collected in a coordinate system specific to the orientation of that individual during data collection. Sometimes it makes the problem statistically challenging. It is known that the general variance parameter is non-identifiable (Lele 1993; Lele and McCulloch 2002). For this analysis, a simple approach based on EDMA is used to estimate the parameters consistently.

Suppose K landmarks on a D-dimensional object are given. Then a matrix can be constructed of $K \times D$ whose j^{th} row consists of the D coordinates of the j^{th} landmark. Usually D is either 2 or 3 and K is assumed to be larger than D. All the information about the form of an object defined on the basis of landmark coordinates is summarized in the collection of all distances between pairs of landmarks, a matrix consisting of such a collection of distances are known as form matrix. The number of unique pair-wise linear distances in a form matrix is L where $L=K(K-1)/2$. X_i can be considered as an individual configuration and to denote the $K \times D$ matrix of coordinates for the i^{th} individual. A $K \times D$ matrix is designated M which describes the mean for the population of objects, where each row represents the D dimensional coordinates of a single landmark. The mean M is considered as the standard normal object, which is a mathematical construction based on a set of twenty normal objects in this research. No single

normal object is likely to be identical in form to the mean *M* and no two individuals are likely to be identical as normal objects also vary from person to person.

A graphical example of 9 landmark variations in normal objects can be seen from Figure 5.5. The variation is manifested as perturbation around the mean landmark configuration of *M*.

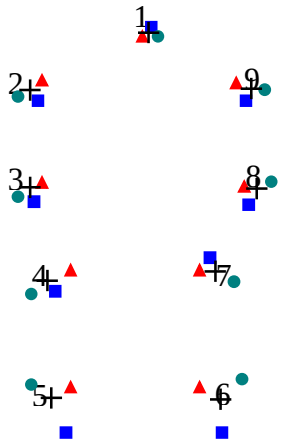

Figure 5.5: The landmarks for objects where individual differences in form originate. Plus signs (+) represent the mean configuration for a hypothetical standard object with nine landmarks. The triangles, rectangles and circles represent the landmark locations of different normal objects.

5.1.9.2. Perturbation Model

Landmarks data are commonly modelled using the perturbation model (Goodall 1991; Lele 1993) and it may be thought of as representing the following process. To generate a random geometrical object or equivalently, a *K* point configuration in *D* dimensional Euclidean space, nature first chooses a mean form (represented by matrix *M*) and perturbs the elements of this matrix by adding noise to this mean form according to a matrix-valued Gaussian distribution (Lele 1993). The *K* point configuration so obtained is then rotated and/or reflected by an unknown angle and translated by an unknown amount. Such perturbed, translated, rotated or reflected *K* point configurations generate our data.

The above description can be put in a mathematical form as follows. Let *M* denote the $K \times D$ landmark coordinate matrix corresponding to the mean form. Let E_i be the $K \times D$ matrix representing the error for the i^{th} individual and assume E_i is Gaussian with mean matrix 0 and variance-covariance matrix $\Sigma_K \otimes \Sigma_D$ where Σ_K is a $K \times K$ positive definite matrix representing

the variance among elements within the same column of E_i and Σ_D is a $D \times D$ positive definite matrix representing the variance among elements within the row of E_i. E_i also describes how X_i differs from mean M in the real data. The symbol $\otimes$ represents the Kronecker product. Σ_K describes the variances and covariances of the landmarks, while Σ_D describes the variances and covariances of the perturbation with respect to the real space coordinate axes. Let Γ_i be an $D \times D$ orthogonal matrix representing rotation and/or reflection of $(M + E_i)$ and t_i, a $K \times D$ matrix with identical rows representing translation. Then the landmark coordinate matrix corresponding to the i^{th} individual may be represented as $X_i = (M + E_i)\Gamma_i + t_i$. It then follows that

$$X_i \sim MN_{K \times D}(M\Gamma_i + t_i, \Sigma_K, \Gamma_i^T \Sigma_D \Gamma_i) \tag{5.20}$$

for $i=1,2,...,n$. Here "*MN*" stands for "matrix normal". Parameters of interest are (M, Σ_K, Σ_D) and (Γ_i, t_i) are the nuisance parameters. The details of these parameters are discussed in (Lele and Richtsmeier 1991).

5.1.9.3. Eliminating the nuisance parameters

Before estimating the mean form M and the variance-covariance matrix Σ_K and Σ_D, it is important to eliminate the nuisance parameters first. The data can be transferred in such a way that the distribution of the transformed data is independent of the nuisance parameters. Lele (Lele 1993) and Lele and McCulloch (Lele and McCulloch 2002) use a maximal invariant statistic $T(\cdot)$ to eliminate nuisance parameters. They define the maximal invariant as follows. Let S denote the space of all $K \times D$ matrices and let $T(\cdot)$ be a function defined on this space such that for X and X^* in S, $T(X) = T(X^*)$ if and only if X^* is just a rotation, translation, and/or reflection of X. Then $T(\cdot)$ is called a maximal invariant defined on the space S under the group of rotation, translation and reflection of X.

Let $H = I - \frac{1}{K}(1^T 1)$ where $I=(1,1,...,1)$ a $1 \times K$ row vector be a $K \times K$ centering matrix. Let $X^C = HX$, then the column of X^C sum to zero. The following theorem gives a maximal invariant of X, a $K \times D$ matrix of landmark coordinates.

Theorem 5.1. $T(X) = HXX^T H^T$ is a maximal invariant statistic, where X is a $K \times D$ matrix.

Proof:

1) $T(X)$ is invariant.

$$T(X\Gamma + t) = H(X\Gamma + t)(\Gamma^T X^T + t^T)H^T = HX\Gamma\Gamma^T H^T = T(X) \tag{5.22}$$

since *t* has identical rows and then *Ht* = 0.

2) $T(X)$ is maximal invariant.

To show that it is a maximal invariant, it is important to show that, given $T(X)$, it can be mapped object to a unique orbit in the original space. This can be proved using the fact that $T(X)$ is a centered inner product matrix and so there exists a unique (up to rotation, translation, reflection) mapping from the centered inner product matrix to a coordinate matrix (Lele 1991, 1993; Lele and McCulloch 2002). Furthermore, it follows from standard multivariave normal distribution theory (Arnold 1981) that if $\sum_D = I$

$B_i = T(X_i) = X_i^C (X_i^C)^T \sim \text{Wishart}_K(D, \Sigma_K^*, MM^T)$ that is, the random variables B_i s are $K \times K$ matrices and have a Wishart distribution independent of nuisance parameters, where $\Sigma_K^* = H\Sigma_K H^T$ is a $K \times K$ non-negative definite matrix of rank $K-1$ corresponding to the variance of the columns of X_i^C. Lele (Lele 1993) shows that Σ_K^* and $X_i^C (X_i^C)^T$ are identifiable and provides a consistent estimator of Σ_K^* and $X_i^C (X_i^C)^T$ based on the method of moments. It can be noted that $T(M) = M_i^C (M_i^C)^T = HMM^T H$ is a centered inner product matrix corresponding to the mean form *M*. The second point of the proof of Theorem 2.1 establishes that estimation of $M_i^C (M_i^C)^T$ are equivalent to estimating the mean form. In other words, given $M_i^C (M_i^C)^T$ one can construct *M* (up to translation, rotation and reflection).

5.1.9.4. The estimation of $M^C (M^C)^T$ and Σ_K^*

The following notations are used from (Lele and Richtsmeier 1991)

(i) $F(X) = [F_{lm}]_{\substack{l=1,2,\ldots,k \\ m=1,2,\ldots,k}}$ where F_{lm} is the Euclidean distance between landmarks l and m. Euclidean distance is the straight line distance between two points that can be measured by the ruler.

(ii) $Eu(x) = [F_{lm}^2] = [e_{lm}]$ denotes the matrix of squared distances.

(iii) $B(X) = M^C (M^C)^T$ denotes the centered inner product matrix.

(iv) Let $\sum_K = [\sigma_{lm}]_{\substack{l=1,2,\ldots,k \\ m=1,2,\ldots,k}}$ be the variance-covariance matrix and,

$Eu(M) = [\delta_{lm}]_{\substack{l=1,2,\ldots,k \\ m=1,2,\ldots,k}}$ be the Euclidean distance corresponding to the mean form M.

The following theorems lead to the consistent moment estimator for δ_{lm}'s. The proof follows from the consistency of the sample moments and the consistency of a continuous function of sample moments. The properties of non-central χ^2 distribution follow from (Welch 1972).

Theorem 5.2. $e_{l,m} \sim \phi_{lm} \chi_D^2 (\delta_{lm} / \phi_{lm})$ that is, squared Euclidean distances between pairs of landmarks have a non-central χ^2 distribution with D degrees of freedom, non-centrality parameter δ_{lm} and scaling parameter ϕ_{lm}, where $\phi_{lm} = \sigma_{ll} + \sigma_{mm} - 2\sigma_{lm}$.

Theorem 5.3. For a two-dimensional object,

$$E(e_{l,m}) = 2\phi_{l,m} + \delta_{l,m} = \alpha_1 \tag{5.23}$$

$$\mathrm{Var}(e_{l,m}) = 4\phi_{l,m}^2 + 4\delta_{l,m}\phi_{l,m} = \alpha_2 \tag{5.23}$$

and

$$\alpha_1 - \alpha_2 = (\delta_{l,m})^2 \tag{5.24}$$

We can then equate the sample moments to the population moments to obtain a moment estimator for δ_{lm}.

Theorem 5.4. Let e_{lm}^{i} denote the squared distance Euclidean distance between landmarks *l* and *m* in the *i*th object.

$$\text{Let } \bar{e}_{l,m} = \frac{1}{n}\sum_{i=1}^{n} e_{lm}^{i} \tag{5.25}$$

$$S^2(e_{l,m}) = \frac{1}{n}\sum_{i=1}^{n}(e_{lm}^{i} - \bar{e}_{l,m})^2 \tag{5.26}$$

and

$$\hat{S}_{l,m} = [(\bar{e}_{l,m})^2 - S^2(e_{l,m}))]^{1/2} \tag{5.27}$$

then as $n \to \infty, \hat{\delta}_{l,m} \to \delta_{l,m}$ in probability

We can now obtain the moment estimator of $\delta_{l,m}$ for three-dimensional objects.

Theorem 5.5.

$$E(e_{l,m}) = 3\phi_{l,m} + \delta_{l,m} = \beta_1 \tag{5.28}$$

$$\text{Var}(e_{l,m}) = 6\phi_{l,m}^2 + 4\delta_{l,m}\phi_{l,m} = \beta_2 \tag{5.29}$$

and

$$\beta_1^2 - \frac{3}{2}\beta_2 = (\delta_{l,m})^2 \tag{5.30}$$

Theorem 2.5. Using the same notation as in Theorem 5.4, and

$$\hat{S}_{l,m} = [(\bar{e}_{l,m})^2 - 1.5S^2(e_{l,m}))]^{1/2} \tag{5.31}$$

it follows that as $n \to \infty, \hat{\delta}_{l,m} \to \delta_{l,m}$ in probability.

Next theorem utilizes the estimators of $\delta_{l,m}$ to obtain a consistent estimator of the variance-covariance parameter Σ_K^*. The proof allows from Arnold (Arnold 1981) and consistency of moments and consistency of continuous function of moments from Theorem 5.1.

Theorem 5.6.

$E(B(X)) = D\Sigma_K^* + B(M)$ and $\hat{\Sigma}_K^* = \frac{1}{D}\left[\frac{1}{n}\sum_{i=1}^{n} B(X)\right] - B(M) \to \Sigma_K^*$ in probability

Following the theorems, the algorithm of obtaining and $\hat{M}$ and Σ_K^* can be shown as bellow:

Step1. Calculate $B(M) = -\frac{1}{2}H\{Eu(M)\}H$ where $H = I - 1/K(1^T 1)$ is a $K \times K$ symmetric matrix such that its diagonal entrees are *1-1/K* and off diagonal entrees are *–1/K*

Step2. Calculate the eigenvalues and eigenvectors of *B(M)*. Let the eigenvalues be $\lambda_1 > \lambda_2 > \cdots > \lambda_K$ and the corresponding eigenvectors be $h_1, h_2, \cdots, h_K$.

Step3. The estimator of the centered mean from $\hat{M}^C$ is given by:

For a two-dimensional object $\hat{M}^C = [\sqrt{\lambda_1 h_1}, \sqrt{\lambda_2 h_2}]$

For a three-dimensional object $\hat{M}^C = [\sqrt{\lambda_1 h_1}, \sqrt{\lambda_2 h_2}, \sqrt{\lambda_3 h_3}]$

Step4. The estimator of Σ_K^* is given by $\hat{\Sigma}_K^* = \frac{1}{D}\left[\frac{1}{n}\sum_{i=1}^{n} B(X)\right] - B(M) \to \Sigma_K^*$

This shows that $\Sigma_K^* = H\Sigma_K H^T$ is identifiable and estimable.

5.1.9.5. The estimation of Σ_K

However, it is our interest to estimate Σ_K. Unfortunately, mapping from Σ_K^* to Σ_K is non-unique because the centering matrix H is singular and hence it is not invertible (recall that $\Sigma_K^* = H\Sigma_K H^T$). To make this mapping unique, it is needed to impose conditions on Σ_K. Let *L* be a $(K-1)\times K$ matrix whose first column consists of -1 s and the rest of the matrix an identity matrix of

dimension $(K-1)\times(K-1)$. Let $\tilde{\Sigma}_K = L\Sigma_K L^T$. It should be noted that Σ_K is a symmetric $K\times K$ matrix of full rank *K* while $\tilde{\Sigma}_K$ is a $(K-1)\times(K-1)$ matrix of rank $(K-1)$. Lele and McCulloch (Lele and McCulloch 2002) give the conditions under which Σ_K is a unique transformation of $\tilde{\Sigma}_K$. Thus if $\tilde{\Sigma}_K$ is estimable, then Σ_K is also estimable.

5.1.10. Mean form and inter-feature distance estimation

EDMA for comparing two shapes using landmark data is a method for comparing the forms of organisms that are measured using two or three-dimensional coordinates of homologous landmarks. Homologous landmarks are those landmarks chosen to represent features on organisms that are similar due to a phylogenetic relationship. The organisms being compared thus share a common ancestor and the feature under study is present in all organisms under consideration due to each inheriting it from the common ancestor (Lele and Richtsmeier 2001). EDMA also allows form variation, shape or growth differences to examine through the comparisons of ratios of landmarks of equivalent configurations. (Lele and Richtsmeier 1991; Lele 1993; Lele and Cole III 1996; Lele 1999).

The gait features extracted from each subject consist of variation due to their different walking style, speed and body characteristics etc. This variation is manifested as perturbations around the mean gait configuration. These perturbations can vary in size and shape from feature to feature. Initially, the Euclidean distance between all possible pairs of features are estimated which is known as inter-feature distances (Lele 1993). This data is stored in an 8x8 matrix which is symmetric from the diagonal known as inter-feature distance matrix. The inter-feature distance matrix from all young subjects is then used to calculate the mean form matrix.

5.1.11. Form matrix and form difference matrix estimation

Suppose *A* is a matrix consisting of all possible pair-wise distances between landmarks.

$$FM(A) = \begin{bmatrix} 0 & d(1,2) & d(1,3) & \cdots & d(1,K) \\ d(2,1) & 0 & d(2,3) & \cdots & d(2,K) \\ \vdots & \vdots & \vdots & \vdots & \vdots \\ d(K,1) & d(K,2) & d(K,3) & \cdots & 0 \end{bmatrix} \tag{5.32}$$

where $d(i, j)$ denotes the Euclidean distance between landmarks *i* and *j*.

FM(*A*) is as the form matrix (*FM)* and returns all the relevant information about the form of an object as summarized by landmark coordinates.

Since *FM(A)* is systematic with diagonal elements zero, one can equivalently use a vector consisting of all the off-diagonal, upper entries of the matrix to represent *FM(A)*, of the form of the object *A*. The form of an object with *K* landmarks is then uniquely represented by a vector of *K(K-1)/2* distances between all possible pairs of landmarks. Equivalently, an object with *K* landmarks is represented by a point in the *L=K(K-1)/2* dimensional Euclidean space, which is called the form space (Lele and Richtsmeier 1991). The form space is a subset of the *L*-dimensional Euclidean space (Richtsmeier and Lele 1993).

For a form difference matrix, suppose the forms of two objects, *A* and *B*, each with *K* landmarks are to be compared. Following the ideas presented above, the forms of these two objects correspond to two points in an *L*-dimensional Euclidean space. If the forms are identical, these two points are the same. If the forms are similar (i.e. their spaces are the same) then these two points lie on a ray going through the origin. If neither of these conditions is true, then it can be concluded that the forms are different. There are several ways to describe this difference. An obvious description is the vector difference *F(B)-F(A)* where subtraction is done element-wise (i.e., for each individual linear distance). This representation defines the absolute difference between forms. Alternatively, to study the changed morphology relative to be initial morphology, Richtsmeier and Lele used the form difference matrix (*FDM)* (Lele 1991; Lele and Richtsmeier 1991) as following

$$FDM_{ij}(B, A) = \frac{FM_{ij}(B)}{FM_{ij}(A)} \text{ where } i, j = 1,2,\cdots,K \tag{5.33}$$

where *A* represents the form of the gait features each subject (including both young and older), *B* represents the mean form which is estimated from a set of 10 young subjects using EDMA. $FM_{ij}(B)$ represents the reference form which is the NMGF. $FM_{ij}(A)$ represents the real form measured from the individual. The ratios of corresponding linear distances from the two forms are calculated.

*FDM*s contain all the relevant information (as represented by the landmarks collected) regarding morphological distances between two forms (or sample of forms). Differences of form can reflect a simple difference in scaling of two forms (i.e. only in size), or a combination of difference in size and shape.

$FDM_{ij}(B,A)$ is then used to estimate the form difference from all young and older subjects. The variance and covariance are estimated for individual features. Two gait features have the same form if their Euclidean matrixes are identical. Two gait features also have the same form if the Euclidean matrix describing one form is a constant multiple of the Euclidean matrix describing the second form.

5.2. Experimental results

To verify the proposed gait quantification approach, we perform experiments to our collected gait features from young and older adult subjects. We also present detailed analysis on the experimental results using the statistical software R (Team 2017).

5.2.1. Data collection

A database is created for our experiment using the automatic gait feature extraction method presented in Chapter 4. The database consists of eight selected gait features among the 13 features extracted from right and left legs: include total distance (m), total time (s), velocity (m/s), swing length (m), swing velocity (m/s), stride length (m), stride time (s), stride velocity (m/s), step length (m), step time (s), step velocity (m/s), stance time (s), and swing time (s) for 12 young and 20 older subjects. Figure 5.6 shows the gait features arising from right and left legs in both young and older subjects. From our evaluation, we conclude that the first five features are redundant since they can be estimated from the rest eight features. Therefore, we use the last eight features as these are all an average reading from 30 strides. Eight features of all individual subjects are plotted and each of these points is notionally joined together to represent a shape.

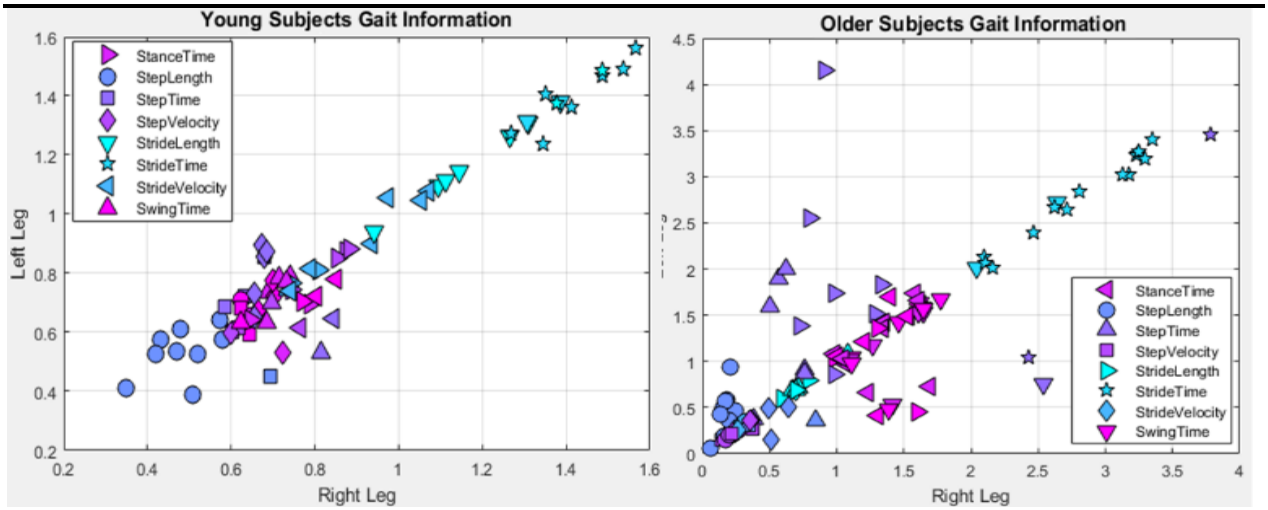

Figure 5.6: Gait features from young and older adults

Figure 5.6 shows that gait features of young subjects from the right and left legs are very similar, i.e., the features lying on or close to a diagonal 45^0 line indicative of equal features arising from the right and left legs. Conversely for the older subjects there is more variability in output of features from right and left legs. This results in a greater scatter in the output recorded, indicative of greater asymmetry shown in Figure 5.6. For this reason, we chose to perform our GPA on the young subjects who had a more normal gait than the older subjects with a view of developing a reference NMGS.

5.2.2. Estimating of mean normal gait shape

We perform the GPA on the features (shapes) derived from young subjects. To do this all 10 shapes of the young subjects obtained from both legs are plotted after GPA best fit alignment shown in Figure 5.7. This GPA translates and rotates each of the shapes to find the best fit. The mean of each shape of the features is then estimated and plotted generating the shape of NMGS shown in Figure 5.7 (black line).

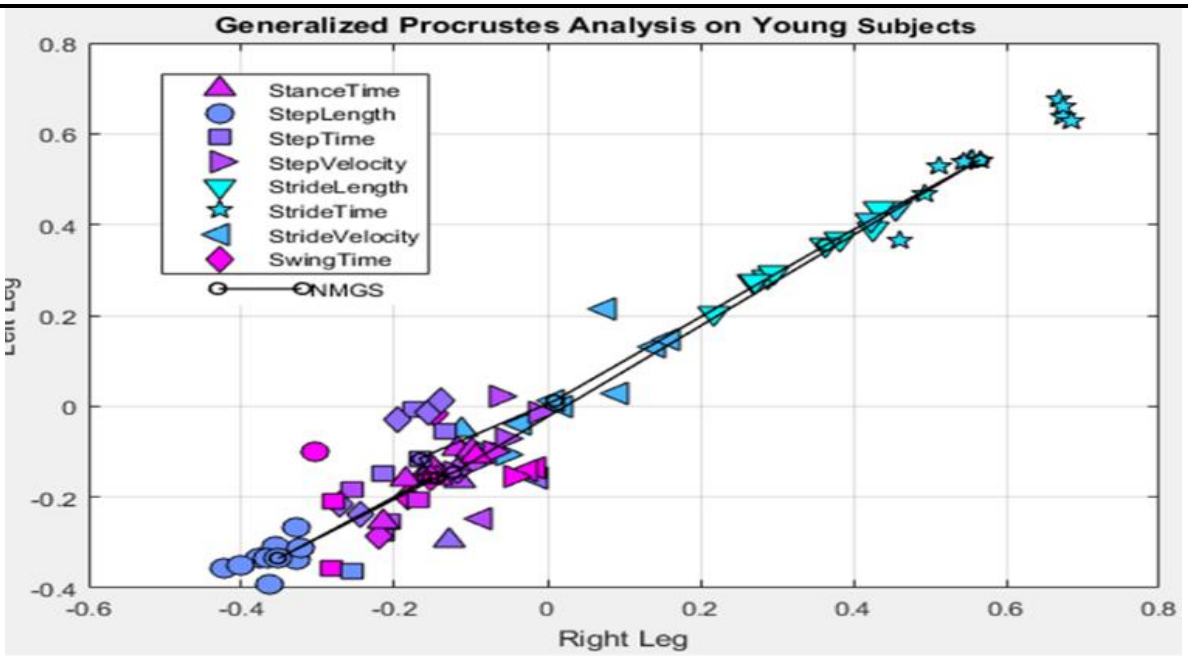

Figure 5.7: Gait features from young after GPA and the black line represents NMGS

Figure 5.7 shows that gait features and the MNGS obtained as the mean features from the individual young subjects are very close to the diagonal.

5.2.3. Gait quantification

Next, we determine the shape differences between each pair of shapes i.e. the MNGS with the individual gait shapes. To quantify a gait based on all gait features we use four shape comparison techniques. The RSD, RSSD, PSSD and RMSD are calculated and presented in Table 5.1. Results closer to 0 suggest a gait shape close to the NMGS gait.

TABLE 5.1
Gait Quantification Information

		RSD	RSSD	PSSD	RMSD
Young	1	0.129	0.152	0.129	0.054
	2	0.245	0.292	0.243	0.103
	3	0.304	0.364	0.299	0.129
	4	0.223	0.329	0.222	0.116
	5	0.367	0.467	0.359	0.165
	6	0.264	0.33	0.261	0.117
	7	0.204	0.237	0.202	0.084
	8	0.418	0.473	0.406	0.167
	9	0.38	0.441	0.371	0.156
	10	0.205	0.251	0.204	0.089
	11	0.270	0.324	0.267	0.156
	12	0.186	0.262	0.185	0.078

Older Adults	1	0.977	2.872	0.829	1.015
	2	0.922	1.885	0.797	0.666
	3	1.144	4.35	0.91	1.538
	4	0.905	1.79	0.786	0.633
	5	0.92	3.586	0.795	1.268
	6	0.886	3.104	0.775	1.097
	7	0.918	2.372	0.795	0.838
	8	0.874	1.711	0.767	0.605
	9	1.154	2.291	0.915	0.81
	10	0.959	3.417	0.819	1.208
	11	0.934	3.319	0.804	1.173
	12	1.058	3.755	0.872	1.328
	13	1.442	6.6	0.992	2.333
	14	1.018	2.989	0.851	1.057
	15	1.019	2.977	0.852	1.053
	16	1.173	5.084	0.922	1.798
	17	1.001	2.548	0.842	0.901
	18	0.94	1.848	0.807	0.653
	19	1.202	2.843	0.933	1.005
	20	1.01	3.809	0.847	1.347

Table 5.1 shows that variations of the distances of the young subjects are smaller than those of the older subjects. Therefore, Table 5.1 can help distinguishing different gait patterns in young and older adults.

We evaluate the data for statistical errors and assessed whether the estimated values are reasonable. A t-test comparing the mean values of RSD, RSSD, PSSD and RMSD values is carried out with a statistical significance level (alpha) of 0.05. The two sample unpaired *t*-test summary are given in Table 5.2.

TABLE 5.2: *T*-test for distances between MNGS and gaits

	MD	SD	*t*-value	*p*-value	df	95% Confidence Interval	
						Lower	Upper
Riemannian shape distance							
Young	0.274	0.092	9.441	0.000	9	0.208	0.340
Older Adults	1.023	0.140	32.708	0.000	19	0.957	1.088
Riemannian size-and-shape distance							
Young	0.334	0.106	9.979	0.000	9	0.258	0.409
Older Adults	3.158	1.199	11.775	0.000	19	2.596	3.719
Procrustes size-and-shape distance							
Young	0.270	0.088	9.706	0.000	9	0.207	0.332
Older Adults	0.846	0.061	61.831	0.000	19	0.817	0.874

Root mean square deviation							
Young	0.118	0.037	10.013	0.000	9	0.091	0.145
Older Adults	1.116	0.424	11.773	0.000	19	0.918	1.315

MD= Mean Difference

The t-tests indicate ($p<0.05$) that there is a significant mean difference between the gait of young and older subjects for RSD, RSSD, PSSD and RMSD values.

In order to study the variability in gait shapes we plot a box plot (Figure 5.8) and determine the range of results. From the box plot and *t*-test above, it is clearly seen that the mean values of RSD, RSSD, PSSD and RMSD of the normal young is significantly lower than those of older adults.

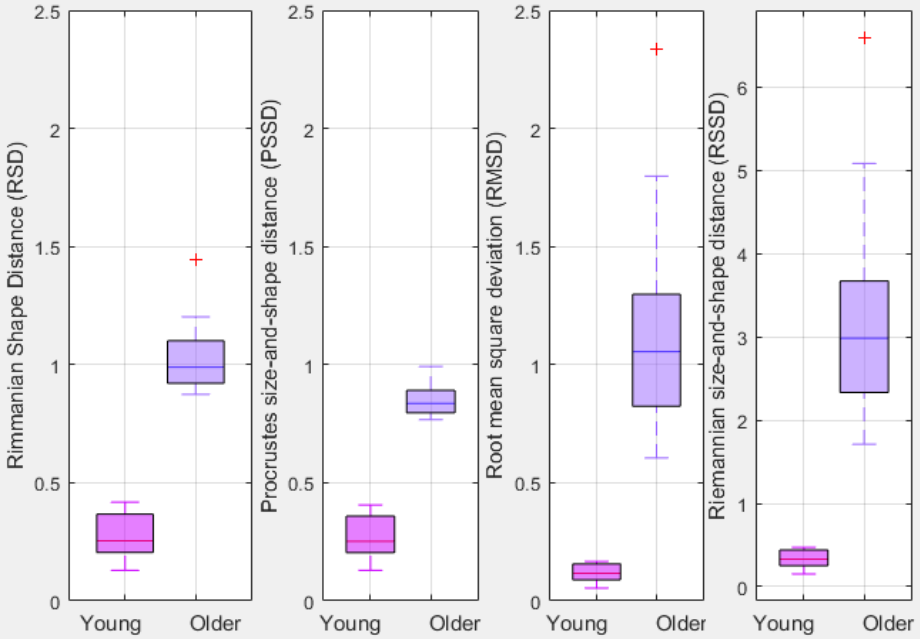

Figure 5.8: Boxplot of RSD, PSSD, RMSD and PSSD

Figure 5.8 shows that for young subjects, RSSD and RMSD are more consistent with less standard deviation (SD) than RSD and PSSD. For older subjects the opposite is identified with a wider SD for RSSD and RMSD than RSD and PSSD. The boxplot confirms the expected difference in gait shapes between young and older subjects. From Figure 5.8, we can observe that the RSSD provides the best indication among the four approaches since the variation of the older is large while the variation of the young is small. RMSD approach is the second best, followed by RSD and then PSSD. Next we determine what features of gait contribute to abnormality.

5.2.4. NMGF and inter-feature distance estimation

The mean form based on these normal gaits is estimated and is considered as the NMGF. The NMGF is estimated directly from the unit less feature coordinate data using EDMA, which is shown in Table 5.3.

TABLE 5.3: Normal Mean Gait Form (NMGF) Information

Index	Right	Left
F1	-0.48296	0.109081
F2	-0.77767	-0.09042
F3	-0.01428	0.002893
F4	0.489212	-0.05726
F5	0.192591	0.07357
F6	0.175095	-0.12865
F7	0.211629	0.007791
F8	0.206385	0.083

The Euclidean distance between all possible pairs of features are estimated from the NMGF for the inter-feature distances. This data is stored in an 8*8 matrix which is a symmetric matrix. Thus, Table 5.4 presents the lower triangular part of the matrix.

TABLE 5.4: Inter-feature distances

	F1	F2	F3	F4	F5	F6	F7	F8
F1	0							
F2	0.356	0						
F3	0.481	0.769	0					
F4	0.986	1.267	0.507	0				
F5	0.676	0.984	0.219	0.324	0			
F6	0.700	0.954	0.231	0.322	0.203	0		
F7	0.702	0.994	0.226	0.285	0.068	0.141	0	
F8	0.690	0.999	0.235	0.316	0.017	0.214	0.075	0

Each cell in Table 5.4 of the inter-feature distance matrix shows the distance in two-dimensions that does not require a coordinate system. For example, the cell, that contains the number 0.356 in the mean form matrix of the young subjects, represents the distance between features F1 and F2. This is the distance estimated directly from the feature coordinate data. The inter-feature distance of NMGF is used to estimate the form difference matrix between the NMGF and each gait to understand the degree of abnormality.

5.2.5. Form difference and form difference matrix between NMGF and each gait

Estimation of the FDM is carried out for all gaits relative to the NMGF. The sum of divergences to the median value for each feature is estimated considering the whole FDM matrix (Claude 2008). This is the matrix of the degree of abnormality where the higher the degree of difference the greater the abnormality. Lower values imply that the gait features of the individual are closer to the NMGF and conversely higher values mean that there is greater abnormality as there is greater deviation from the MNGF. To represent the degree of abnormality in a meaningful and easily interpretable way we propose a two dimensional plot to summarize, explore and interpret the FDM results. Figure 5.9 shows such a plot where the x axis represents individual gait features and the y axis represents the degree of abnormality in relation to the other features. The form difference for all eight gait features with respect to NMGF is plotted. For example, in Figure 5.9 feature 1 has the highest difference with feature 2 but is very close to features 3-8. This analysis is applied to a set of 32 gaits (12 young and 20 older).

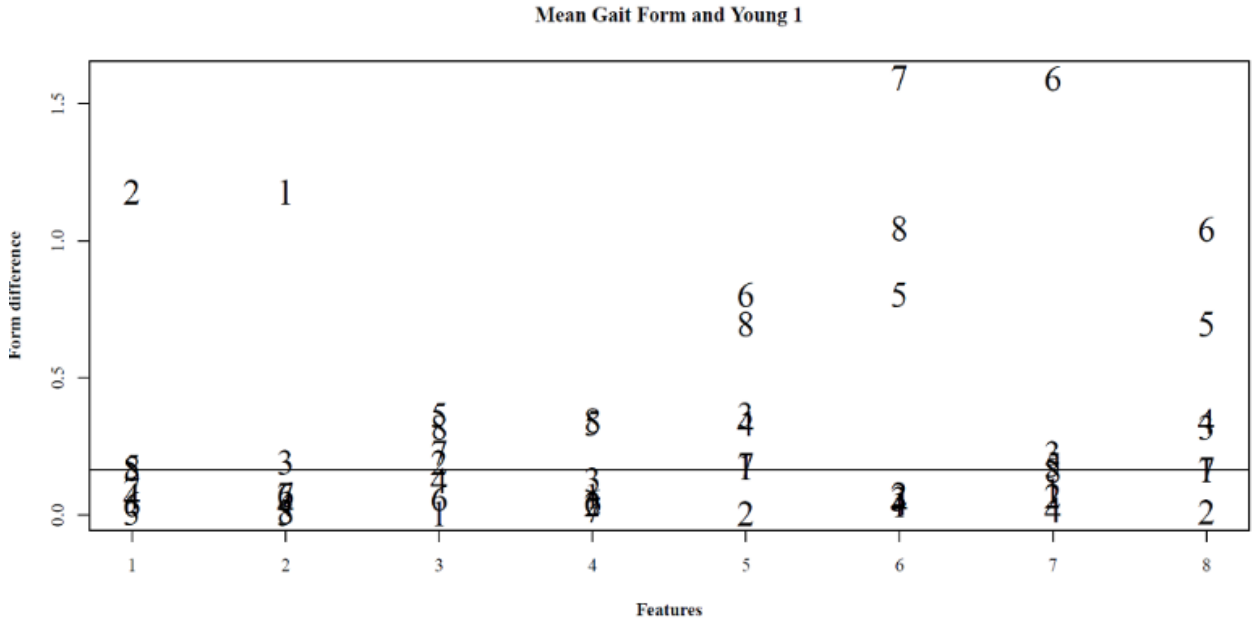

Figure 5.9: The degree of abnormality of Young Subject 1 with respect to the MNGF for all the eight gait features.

5.3. Discussion

This study demonstrates a comprehensive analysis of gait using Procrustes and EDMA methods. Procrustes is valuable in determining variation of gaits from NMGS while EDMA is useful in

determining the degree of abnormality of the gait feature. The data is collected from 12 young (10 for modelling and 2 for validation) and 20 older subjects. We obtain the results using eight gait features collected automatically from both right and left legs by adopting low cost IMU sensors synchronously. Generalized Procrustes analysis is used to estimate a standard normal mean gait shape (NMGS) for 10 young subjects which is our benchmark. Each gait feature of both young and older subjects is then converted to find the best match with the NMGS using ordinary Procrustes analysis. The shape distance between the NMGS and each gait shape is estimated using RSD, RSSD, PSSD and RMSD. In our results we have shown that a normal gait provides a set distribution of features. Any deviation from this distribution is identifiable as abnormal. This to our knowledge has not been done before. Although at this stage one cannot extrapolate this information to make accurate diagnoses, the ability to identify such subtle differences in gait may have the potential to support specific diagnoses as well as treatment. This new method is more comprehensive using a range of parameters that include eight features from each leg whereas other methods (Seliktar and Mizrahi 1986; Robinson et al. 1987; Vagenas and Hoshizaki 1992; Agrawal et al. 2009) often rely on single or a smaller number of features. We also introduce a morphological analysis to the evaluation of gait where one can see a pattern of gait and identify where changes occur in the gait pattern. Different parameters of gait indicate different type of gait abnormalities.

Although our results are encouraging, there are a number of limitations. The number of subjects is relatively small (32) and no steps are taken to ensure a random sample. Coincidentally there is a gender bias with most subjects being male. The aim of the study is to see whether a Procrustes method can be used to analyse gait and not to study gait differences between the genders. This gender bias is therefore unlikely to impact the value of our results and what they are trying to achieve. Other possible confounding factors are speed of walking as well as different height resulting in different gait parameters such as stride length. Our study was however intended to evaluate the normal baseline gait of our subjects only. The influence of these other factors will be studied in the future. Lastly, NMGS and NMGF are estimated using only 10 young subjects, while additional 2 young subjects are used for validation of our estimated NMGS and NMGF. There is the potential of a Type 1 error (false positive) in detecting an effect that is not there.

However, our work has established our method for gait evaluation. Future work is to establish a database with a larger number of subjects which stores more medical and physical information as well as longitudinal data across a longer period of time. Such longitudinal information will demonstrate the potential for using our method in monitoring response to treatment in patient with gait disorders.

Normal gait is not determined by time and distance travelled. It is determined by the degree of variation in the gait features. While the time and distance can be assessed relatively easily using visual observation the variation is more difficult to determine. The Procrustes analysis uses translation and rotation among all gait feature shapes to find the best fit to identify such variation. This normalization technique is used for a set of 10 normal young subjects to estimate the NMGS. In total 32 (12 young and 20 older) gaits are then translated and rotated according to the NMGS for the best fit. The RSD, RSSD, PSSD and RMSD distances between the NMGS and all gaits are then calculated. From Table 5.1 we can see that the highest and lowest of RSD, RSSD, PSSD and RMSD distances are found in Y8 (young 8) and Y1 for young subjects, O13 (older 13) and O8 for older subjects respectively. From the individual gait features, the highest and lowest travelled distance are found from Y5 and Y10, the highest and lowest time are found from Y4 and Y8. Interestingly, considering all gait features, the highest variation lies in Y8. This is demonstrated in the Procrustes shape obtained in Figure 5.10a. Although, other young subjects travelled distance and time are higher than Y8, based on the overall gait features, the shape difference between the MNGS, Y8 is the highest. Similar findings are also found for older subjects. The lowest and highest shape difference is found for O8 and O13 shown in Figure 5.10b.

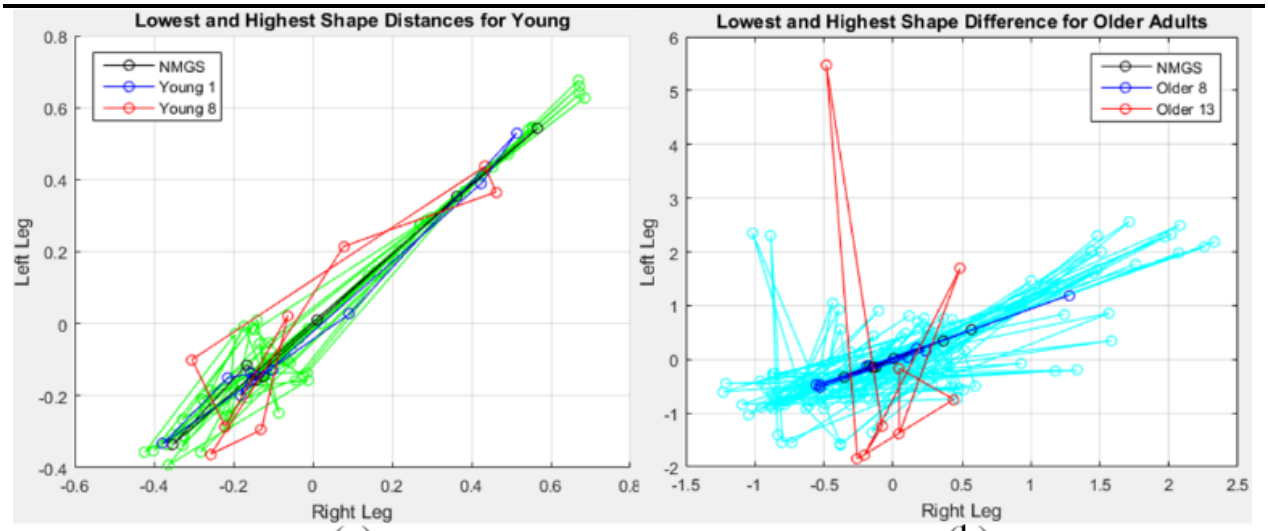

Figure 5.10: Lowest and highest shape differences from (a) young and (b) older subjects

Investigating the history of O13 helps explain the shape of the graph. In this case O13 had a stroke and numbness in the right leg. He is unable to move his right leg and used crutches for moving. Thus most of the movement during walking is covered by the left leg and crutches are used to keep body balance. In Figure 5.10b we can see that the normal left leg shows greater movement but the abnormal right leg has less movement detected. In the future we will investigate further the impact of specific diagnoses and patient health on these gait parameters by exploring gait patterns obtained in specific diagnoses such as Parkinsons disease, Stroke, and other conditions causing abnormal gaits.

A *t*-test and Boxplots using RSD, RSSD, PSSD and RMSD distances show that the gait of young are distinguishable from older. The standard deviations are close to the mean indicating that the gait data distribution from young subjects' is more consistent than that from older. The Box plots of the four different distance approaches, RSD, RSSD, PSSD and RMSD, show different distributions. The Box plots indicate that for young subjects RSSD and RMSD provides more consistent results with less standard deviation (SD) than RSD and PSSD. For older subjects the opposite is identified with a wider SD for RSSD and RMSD than RSD and PSSD. This difference is likely to arise as a consequence of the different mathematical formulas involved in calculating these measurements. In the future we will explore the reasons for this in more detail.

To fully understand the degree of gait abnormality for older subjects, we use EDMA to locate the specific feature of the gait contributing to the abnormality. The process starts with estimating a mean form from a set of normal young gaits called as NMGF. It is then used to

estimate the inter-feature distances that represents the distance between each features from one to another. The form difference matrix is then estimated between NMGF and all gaits. The form difference of Y1, Y8, O8 and O13 are shown in Figure 5.11. The details of the form difference matrix results are presented in the Appendix E.

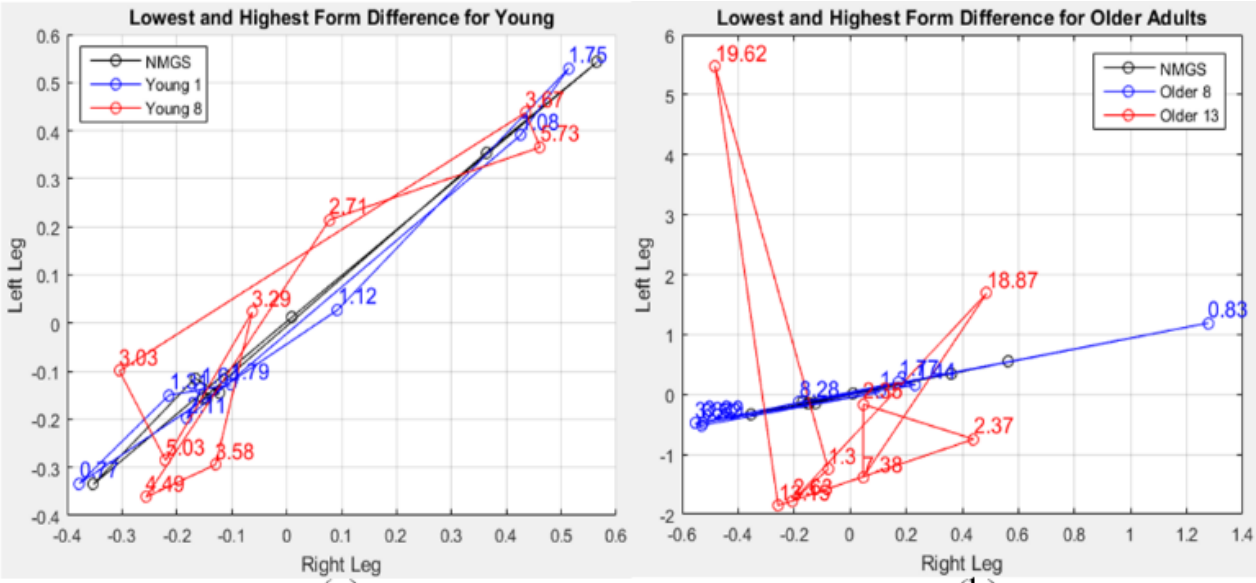

(a) (b)

Figure 5.11: Degree of abnormality from (a) young and (b) older adults

Gait quantification and evaluation is a challenging problem and has attracted growing interest. However, there is no baseline algorithm or standard acceptable commercially available automatic gait evaluation method for measuring and determining what factors affect gait performance. The commonly used approaches for quantification of gait are based on human observation and include scales such as the Gait Abnormality Rating Scale (Brach and VanSwearingen 2002), Figure of 8 Walk Test (Hess et al. 2010), Four Square Step Test (Duncan and Earhart 2013), The Functional Gait Assessment (Wrisley and Kumar 2010), Groningen Meander Walking Test (Bossers et al. 2014) and Berg Balance Scale (Berg et al. 1992). These approaches require clinician or expert help for gait assessment. Our method of gait evaluation is object, simple and user friendly. Our proposed gait evaluation method has two parts: we use 1) Procrustes for shape normalisation, 2) four techniques shown in Table 5.1 for gait quantification and 3) EDMA for identifying the degree of abnormality shown in Figures 5.10 and 5.11. Another advantage is that our proposed system is affordable and does not require laboratory setup.

With an aging population and the increase in chronic illness such as poor mobility and falls there is an increasing drive for new technologies to support treatment of patients in their own

home. Human gait becomes weak over time. Our proposed system can be used to monitor gait abnormality. This can apply to many diseases such as the slow, shuffling, festinant gait of Parkinson's disease, the hemiplegic gait of a stroke or the steppage gait seen in foot drop or myopathy. A series of gait feature measurements on a regular basis can identify the progression or recession of changes in gait pattern as well as response to treatment with rehabilitation for these types of diseases and more. Growing young adults particularly if they have physical disabilities may develop gait abnormalities during puberty growth spurts. The treatment for gait abnormality mainly depends on the severity and the potential growth of the patient and type of abnormality. Periodic monitoring is becoming essential to make sure that such gait abnormalities are not progressing. Our method of gait evaluation can be used for such longitudinal monitoring for these cases. The continuous monitoring is essential to determine any treatment regarding rehabilitation. Thus, our low cost gait evaluation system has the potential for widespread clinical use both at home and in a hospital setting. Using our methods, it is possible to identify where in the gait cycle the abnormality lies and this enables therapists to identify problems to address these timely and in a more specific way. In future works, we plan to use our gait evaluation information to classify gait changes over time to identify abnormal gait patterns for the assessment of elderly fall risk, rehabitation and sports applications.

5.4. Conclusion

We designed and implemented a system that is portable and can be used in both home and clinics without requiring access to a gait laboratory. We also designed and developed an android app to collect accelerometer and gyroscope data from multiple IMUs synchronously. We collected gait movement data from both right and left legs for 12 young and 20 older subjects using our developed system. The Procrustes and EDMA analysis are used for gait evaluation that provide a comprehensive interpretation of shape and form differences between individual gaits. This method creates a new way of gait quantification and provides information to distinguish young from older gaits taking the full features distribution into account rather than extracting specific length and time. Initially, GPA is used to normalize gait features from 10 young subjects and estimate the NMGS. Each gait is then translated and rotated to find the best fit with the NMGS using OPA. The shape distance between the NMGS and each gait are estimated using RSD, RSSD, PSSD and RMSD. The distance values for the young subjects are significantly lower than those for the older subjects. This suggests that the RSD, RSSD, PSSD and RMSD parameter may

be suitable for evaluating between young and older gait. A t-test is performed to provide statistical evidence that young gait is significantly different from older gaits. The distribution of the shape distances is presented in Boxplot. It shows that the data spread for young gait is very compact compared to that for the older gait. From the above scenario, it can be concluded that older gaits are distinguishable from the young gaits and assessing a number from individual gaits based on all gait features a value is obtained which indicates whether the assessed gait is normal or abnormal depending on their feature values. EDMA is used to estimate the degree of abnormality of individual features in a gait and visualize the feature in a gait. Initially NMGF and inter-feature distances are estimated from a set of 10 young subjects. Form difference is estimated between the NMGF and individual gaits. The degree of abnormality is then estimated for individual features and the result is plotted to visualize the feature in a gait. A conclusion is drawn from this analysis is that EDMA can help to estimate and visualize the position of the gait abnormality. The high value indicates the high degree of abnormality relative to the NMGF while the low value indicates low abnormality. Our method offers several advantages: 1) it is user friendly and is easy to set up and implement; 2) it does not require complex equipment with segmentation of body parts; 3) it is relatively inexpensive and therefore increases its affordability decreasing health inequality; and 4) its versatility increases its usability at home supporting inclusivity of patients who are home bound. Therefore, our method can help improve the accuracy of assessment and monitor the rehabilitation of patients with mobility problems.

6. CONCLUSION AND FUTURE WORKS

6.1. Conclusion

This thesis sought to develop an automatic gait analysis system suitable for use in homes and clinics environments. The recommended system needs to be customized and modified in future studies to understand of insight into effect of aging on gait and balance for therapeutic for planning, management, clinical decision making and rehabilitation.

6.2. Achievement of objectives

In this thesis eight objectives are set, five separate studies are conducted, and the results obtained from the studies are combined to address our primary objectives.

Objective 1:

Chapter 2 provides a review of prior studies in wearable sensors for gait analysis and identifies the shortcomings on previous gait analysis systems for home based users. A detailed research gap is described in Section 2.5. There are two main aspects of the research gaps in wearable sensor based gait analysis system. The first gap is related to practical aspects including cost, user acceptance, usability and privacy. The other gap is related to technical aspects described in Section 2.5.2. To overcome the practicality issues in terms of cost and acceptance and to extend the types of accuracy and reliability and improve in order to broaden the use of accurate quantitative gait monitoring in clinical application and research and to understand the gait and balance disorder deeply, an affordable automatic gait analysis system is required which can provide comprehensive gait information and allow to use in clinic or at home. It will also enable the identification of gait variables and changes, monitoring of gait and abnormal gait patterns of older people to reduce the potential for falling, support future falls risk management aiming to improve their quality of life.

Objective 2:

There are wearable wireless IMU sensors commercially used for health rehabilitation, movement monitoring, sports tracking or research. A wireless wearable Bluetooth, long autonomy, minimum consumption, multiple synchronised data transmission supported IMU sensor with low cost is important for our investigation. More specifically, since our later investigation is to

identify older adults gait pattern changes over long time, the IMU device is required to last approximately a week or more. Selecting a sensor should also have generic considerations such as protection from pressure, water and temperature, and the battery life etc. Based on the different aspect of our research and literatures, the MetaWearCPro sensor is selected for our research.

Once the sensor is selected, it is necessary to design the sensor protection system. Sensor protection is a very important infrastructure for lower limb gait analysis. The system will ensure that the sensor is protected from pressure, water and temperature etc. Due to damage of the protection system may directly affect the sensor output and its economic benefit. Therefore, casing damage is a serious problem to be considered during the design and development of the casing system, and in general, sensor casing damage are caused due to material stress factors, engineering technique factors and corrosion factors during body movement. Considering all issues, the sensor casing is designed and printed using 3d printer. A Velcro elastic belt and buckles are used to adjust and attach the sensor. Buckle and Elastic Belt: the buckle is sewn onto an elastic belt for fastening to Velcro; Bottom case keeps the sensor safe from pressure, temperature and water. Lock Open Edge which helps to open the cover from bottom case. Sensor Lock Mechanism: The four locks keep the sensor sideways movement and orientation. Cover Lock Mechanism which tightly locks with the case. Velcro-Elastic Joint: The elastic belt is sewed with Velcro. Velcro which adjusts and tighten when the sensor is attached.

The Android app is developed to collect real time data from the MetaWear sensor. The HTC M9 mobile phone which has BLE 4.1 is used to connect to multiple MetaWear Cpro sensors. This mobile phone supported up to 7 MetaWear Cpro devices and it is able to collect synchronous data. The app collected accelerometer and gyroscope data, and stored data on an external SD card as a csv file.

Objective 3:

The aim is to maximize the interpretable information for gait analysis. To achieve this, it is important to find the optimal sensor placement and the parameters that influence the extraction of automatic gait features. We investigated the effect of different anatomical foot locations on IMU sensor output. We selected a set of five anatomical foot locations covering most of the foot regions to place wearable wireless IMU sensors for data collection. We collected accelerometer and gyroscope data from 15 participants. Each participant performed a trial in a straight corridor comprising 25 strides of normal walking, a turn-around and another 25 strides. We also propose

an automatic gait features extraction method to analyze the data for stride number, distance, speed, length and period of stride, stance, and swing phases during walking. The highest accuracy for detecting stride number is in location 1 (first cuneiform) followed by location 5 (Achilles Tendon) and 4 (Talus). Location 1 is the closest to correlate estimate to the measured distance travelled. The accuracy of detecting number of strides on average is 95.47% from accelerometer data and 93.60% from gyroscope data and closest to the 60:40% split for average stance and swing for 15 subjects. To validate our results, using 10 young participants, we conducted trials using the Qualisys motion capture instrument and from our IMU sensor concurrently. The average accuracy of our result is 97.77% with 95% confidence interval 0.767 for Distance and 99.01% with 95% confidence interval 0.266 for Period.

Objective 4:

The aim is to assess the use of IMU sensors to identify gait asymmetry by extracting automatic gait features. The data are collected from 10 young and 10 older subjects. Each performed a trial in a straight corridor comprising 15 strides of normal walking, a turn around and another 15 strides. We analyse the data for total distance, total time, total velocity, stride, step, cadence, step ratio, stance, and swing. The accuracy of detecting the stride number using the proposed method is 100% for young and 92.67% for older subjects. The accuracy of estimating travelled distance using the proposed method for young subjects is 97.73% and 98.82% for right and left legs; and for the older, is 88.71% and 89.88% for right and left legs. The average travelled distance is 37.77 (95% CI ± 3.57) meters for young subjects and is 22.50 (95% CI ± 2.34) meters for older subjects. The average travelled time for young subjects is 51.85 (95% CI ± 3.08) seconds and for older subjects is 84.02 (95% CI ± 9.98) seconds. The results show that wearable sensors can be used for identifying gait asymmetry without the requirement and expense of an elaborate laboratory setup. This can serve as a tool in diagnosing gait abnormalities in individuals and opens the possibilities for home based self-gait asymmetry assessment.

Objective 5:

Visualization of gait asymmetry can provide added value in rehabilitation, clinics and sports. Common approaches for the quantification of gait asymmetry give the numerical values of parameters such as symmetry index, symmetry ratio, symmetry angle etc. It may be difficult for users to understand those numerical values. In order to conveniently use quantitative gait asymmetry monitoring for users, an affordable visualization tool is useful to provide a facility for

their use in clinic and at home. We investigate four approaches for monitoring gait asymmetry to provide automatic graphical visualizations of information about gait. The results show that affordable wearable IMUs can be used for objective gait asymmetry feature extraction without the requirement and expense of an elaborate laboratory setup. Our procedure significantly simplifies the monitoring protocols and opens possibilities for home based assessment and supports digital transformation strategies through the development of new technology.

Objective 6:

The assessment of gait features is important in treatment and rehabilitation of patients suffering from various conditions causing gait abnormalities. Currently such assessments depend on access to expensive complex equipment often based in gait laboratories. In order to increase the use of accurate quantitative gait monitoring in clinic and at home, a low cost gait assessment tool is required. The aims are to determine the concurrent validity of spatiotemporal IMU gait extracted features with MCS and Treadmill measurements in young and older adults and to compare the levels of agreement for average spatiotemporal gait parameters. 48 subjects (28 young and 20 older adults) participate in the study. We validate our system using three experiments; 1) Treadmill at various walking paces vs MCS, 2) Self-selected (free) walking vs MCS, and 3) Self-selected (free) walking vs Digital tape for distance. We apply ICC, LCC and r to measure the level of agreement between IMU gait extracted features and MCS measurements. The experimental results demonstrate that our IMU gait extracted features are highly valid for spatiotemporal gait variables in young and older adults. Experiment 1 shows that the relative accuracy of our IMU sensors is between 85.48%-99.96% for travel distance and 99.49%-99.97% for Time measurement. The level of agreement using ICC(2,1), LCC and r between IMU gait extracted features and MCS for each gait variable of distance and time at different speed levels from right and left legs from all subjects demonstrates excellent agreement is good (from 0.78-1). Experiment 2 shows the average accuracy is 97.57% with 95% confidence interval ±1.327 for the estimated distance and 99.01% with 95% confidence interval ±0.266 for the Time. Experiment 3, we validate our IMU system with more generic variation of age and environment with a sample size of 900 strides. The results show that the accuracy of detected stride and step number is achieves 100% excellent for young subjects. The accuracy of estimating travelled distance is 97.73% for right and 98.82% for left legs. The ratio of stance and swing is found closest to the 60:40% split for average stride, stance and swing. For older adults, the accuracy of detecting stride and step number is 92.67% and the accuracy of estimating the travelled distance is 88.71%

for right and 89.88% for left legs. We demonstrate that automatic gait features extraction can be done without the need to access an expensive gait laboratory. This can be the base of developing tools that can be used in the treatment, rehabilitation and self-assessment of gait at home.

Objective 7:

Objective assessment of gait is important in the treatment and rehabilitation of patients with different diseases. We propose a gait evaluation system using Procrustes and Euclidean distance matrix analysis. The data is collected from 12 young and 20 older subjects. We analyse the data collected from real world for stride, step, stance time and swing time. We validate our method with measurements of gait features. Our method is objective and simple. It has three parts: we use 1) Procrustes for shape normalisation, 2) four techniques shown in Table 5.1 for gait quantification and 3) EDMA for identifying the degree of abnormality shown in Figures 5.9 and 5.11. This method also provides information to distinguish young from older gaits taking the full features distribution into account rather than relying on individual parameters such as specific length and time. EDMA can help to estimate and visualize the position of the gait abnormality. Experimental results to demonstrate the performance of the proposed method.

Objective 8:

To increase accessibility to sophisticated gait assessment a major transformation strategy framework is necessary. We propose a digital transformation strategy framework for gait analysis based on the development and use of new technology, changes to value creation, structural change, affordability and sustainability. We use sensors to collect gait parameters. Via connectivity and cloud computing such information is analysed using machine learning techniques. This will enable a human (health care professionals, social carers and patients) computer interaction to support diagnosis and treatment of gait abnormalities. Therapists will be able to make complex assessments and patients will be able to monitor gait in their own home removing the need to attend hospitals or clinics. By using remote monitoring technology therapists, general practitioners and patients can use the same platform to monitor and make treatment decisions together. The details of this framework is described in Chapter 6.5.

6.3. Contributions

In order to address our primary objective, following engineering and clinical contributions are made.

6.3.1. Contribution in biomedical engineering

Gait Data Acquisition

- An Android app is developed to collect multiple IMUs data synchronously. The data can be stored in local storage or in the cloud.
- A sensor protection system (MetaWear casing, Velcro elastic belt, and buckles) is designed and developed to keep the sensor safe from pressure, water and temperature.
- Pre-processing methods are presented to clean-up and extract useful gait information from the recorded IMU sensor data including the spatiotemporal gait parameters.
- An engineering setup of the sensors in long open corridor and care home environment are shown and used to collect gait data from young and older adults.

Gait Data Analysis

It is shown how to use novel computational gait analysis algorithm and validate approaches to analyze high dimensional time-dependent gait data:

- A gait feature extraction method for finding the optimal location of placing IMU sensors on foot
- An automatic gait feature extraction method (a novel stride detection technique, a stance and swing detection technique, and a method for estimating travelled distance) to monitor gait asymmetry
- Four visualization approaches for monitoring gait asymmetry to provide automatic graphical visualizations of information about gait
- Concurrent validity of spatiotemporal IMU gait extracted features against MCS and Treadmill measurements in young and older adults and comparing the levels of agreement for average spatiotemporal gait parameters
- Gait evaluation method using Procrustes and Euclidean distance matrix analysis

6.3.2. Clinical contribution

Gait Data Acquisition

The presented automatic gait analysis system can be used in clinical settings as an alternative to currently used visual based observations or three dimensional motion capture system or pressure sensitive mats.

- Compared with the visual based observation assessments (details in Chapter 2), these conventional assessments are highly dependent on assessors' experience and judgment and such may not satisfy scientific criteria of reliability and validity which may affect the accuracy of diagnosis, follow-up and treatment.
- Compared with "gold standard" technologies such as three-dimensional kinematic analysis using a motion capture system, force plate and pressure activated sensors, these technologies are expensive, time consuming, limited to a single gait cycle and laboratory based which reduce their feasibility to be used in clinics.
- Compared with the pressure sensitive mat, it is not sensitive to foot placement and ground reaction force. These mats require the subjects to walk within the narrow width of the mat (88 cm), which is challenging for populations with vision impairment, stroke, Parkinson's or brain injuries.

Gait Data Analysis

The presented gait analysis tool can also help clinicians better interpret and analyze complicated gait data through the following applications:

- **A gait monitoring system:** The real time visualization of gait information and asymmetry can provide added value in rehabilitation, clinics and sports. The four visualization approaches (1) Real time dial visualization; 2) Visualization of individual leg time variation; 3) Visualization of both legs asymmetry; and 4) Boxplot-based visualization) are useful for people in health professionals as well as patient. Real time dial visualization showed the instantaneous gait asymmetry of both legs from distance and time of stride, step and swing phases of each gait cycle using a dial and an indicator. It also showed instantaneous distance and time of stride, step and swing values in a seven segment display. Individual leg variation visualization showed the variation in stride,

stance and swing phases in time. Both legs asymmetry visualization showed the asymmetry between two legs for strides and steps. Boxplot-based visualization showed the overall stride, step, stance and swing phases distribution. These approaches are user friendly and easy to interpret and have the potential of helping professionals detect and interpret gait associated abnormalities. This has the potential of a significant advance. As, gait asymmetry has been shown to be a determinant of recovery in patients suffering from several conditions with stroke (Hodt-Billington et al. 2008), lower limb amputations (Skinner and Effeney 1985), osteoarthritis (Shakoor et al. 2003) and cerebral palsy (Winiarski) such equipment may have a role in the evaluation of such patients. It can also be used to monitor patient progress in orthopedics and rehabilitation (Steultjens et al. 2000). Therefore, proposed real time dial based visualization tools offer an easy and user friendly way to visualize, monitor and rehabilitation of gait, and can be used for different applications at home as well as in clinics.

- **A gait evaluation system:** With an aging population and the increase in chronic illness such as poor mobility and falls there is an increasing drive for new technologies to support treatment of patients in their own home. Human gait becomes weak over time. Proposed gait evaluation system can be used to monitor gait abnormality. This can apply to many diseases such as the slow, shuffling, festinant gait of Parkinson's disease, the hemiplegic gait of a stroke or the steppage gait seen in foot drop or myopathy. A series of gait feature measurements on a regular basis can identify the progression or recession of changes in gait pattern as well as response to treatment with rehabilitation for these types of diseases and more. Growing young adults particularly if they have physical disabilities may develop gait abnormalities during puberty growth spurts. The treatment for gait abnormality mainly depends on the severity and the potential growth of the patient and type of abnormality. Periodic monitoring is becoming essential to make sure that such gait abnormalities are not progressing. Our method of gait evaluation can be used for such longitudinal monitoring for these cases. The continuous monitoring is essential to determine any treatment regarding rehabilitation. Thus, our low cost gait evaluation system has the potential for widespread clinical use both at home and in a hospital setting. Using our method, it is possible to identify where in the gait cycle the abnormality lies and this enables therapists to identify problems to address these timely and in a more specific way.

In general, the gait monitoring and diagnostic tools are potentially appropriate for frequent gait analysis in the home, i.e., without the need to visit a specialized gait clinic. It enables automated capture and analysis of gait for longitudinal monitoring.

6.4. Limitation

The ultimate goal of our research is to make the evaluation of gait widely available in diagnosing gait abnormalities in individuals and opens the possibilities for home based self-gait assessment aiming to identify long term gait changes and classify gait abnormalities. Home based monitoring, real-time identification of gait changes has many benefits such as early identification of potential fall risk and monitoring the progress of treatment outcomes. However, each of the five studies included in this thesis have limitations. The limitation of each studies are described details in each chapter Sections 3.3.2, 4.1.11, 4.2.5, 4.3.7 and 5.3.

6.5. Future work

The analysis and methods conducted in this thesis demonstrate a prototype for an automated gait analysis system which is designed to demonstrate feasibility for older adults to use in their home. Our future work therefore encompasses all essential steps required to transfer the developed prototype design to a real-world clinical application. Specifically, our future work will involve conducting a sizable number of clinical trials. Clinical trials will be used to gather information on how the tool actually performs for a range of rehabilitation applications. This would demonstrate acceptability to the clinicians and patients and also improve areas where problems are encountered. For instance, in order to explore burdens and problems that are specific to using such a technology in homes and residences, a future study will include making a series of experiments in older adults own homes or long-term care facilities where longitudinal monitoring of gait can be achieved over days, weeks or months. Furthermore, it is essential to provide education to understand the functionality of the system to healthcare providers (e.g. physical therapists) on appropriate use of the system. These two steps will make the prototype ready for market assessment and clinical use.

To increase sustainable accessibility of our developed gait assessment system a major digital transformation strategy is necessary. Therefore, we propose a digital transformation strategy framework based on our system and to use of new technology, changes to value creation,

structural change, affordability and sustainability. This will enable a human (healthcare professionals, social carers and patients) computer interaction to support diagnosis and treatment. Therapists will be able to make complex assessments and patients will be able to monitor gait at home. By using remote monitoring technology therapists, doctors and patients can use the same platform to monitor and make treatment decisions together. This will open opportunities for business companies to establish structures for the development and manufacture of equipment as well as opportunities for interaction with healthcare providers to improve the care of people with gait abnormalities.

Digital transformation drives a significant shift in the business operations, products, processes and organisational structure of a company facilitating its initiatives to make use of digital technologies (Matt et al. 2015). Digital transformation has revolutionized business models in a variety of industries. However, the adoption of digital services in healthcare has progressed at a relatively slow pace. Healthcare service providers are still in an experimental phase when it comes to offering digital services beyond traditional hospital based approaches. Therefore, the need for more profound transformation in healthcare systems has intensified in recent years due to social needs and technological developments (Barnett et al. 2011). On the one hand, the increasing demand for care challenges the sustainability of the current system due to the increase of an ageing population with complex health and social care needs (Lopreite and Mauro 2017). On the other hand, health economic studies point out that supply pressures also threaten the sustainability of healthcare systems (Lehoux et al. 2016). The challenge is of meeting increased demand while reducing the costs of healthcare systems. Digital transformation can play an important role driving the shaping of industry as digital services beyond the product itself are being integrated into the range of offerings that enables safer, accessible and more affordable healthcare systems (Agarwal et al. 2010). It has already been used on many fronts in healthcare, but products or services have mainly been targeted to professionals (e.g. electronic medical records) and are aligned with the prevailing logic in healthcare that focuses on ‘production of healthcare’ as opposed to producing health (Asch and Volpp 2012). Many digital health innovations aim to make healthcare more affordable through redesigning workflows or through automation of tasks previously conducted by health professionals, such as automatic image analysis. Together these innovations have become a phenomenon, referred to as the digital transformation or revolution of healthcare. This highlights expectations of the dramatic changes in the field of healthcare in the coming decades (Topol and Hill 2012).

6.5.1. Requirements of a digital transformation strategy framework for gait analysis

In this section, we address the requirements of a Digital Transformation Strategy Framework for Gait analysis by considering 1) affordability and portability; 2) reduction of inequality; 3) patient centred; 4) compatibility; 5) commercialisation.

6.5.1.1. Affordability and portability of personalized tools for healthcare

An important aspect of any new developments is a cost benefit analysis to ensure that any new developments offer good value for money. At present the detailed analysis of gait depends on expensive gait analysis equipment based in gait labs (Lipsitz et al. 2015; Mentiplay et al. 2015), which is financially unaffordable to the majority of patients. On the other hand, it requires patients to travel to the site where the equipment is based and therefore is not suitable for patients who have difficulty in travelling. Therefore, new affordable and portable products are needed to increase the availability to all patients. IMU has been used in several different spatiotemporal and kinematic assessments of gait. These include monitoring of post-operative gait abnormalities (Hanly et al. 2016), stride variability (Urbanek et al. 2017), measurement of gait asymmetry (Esser et al. 2012), fall-related gait characteristics measured on a treadmill in daily life (Rispens et al. 2016), nature of Parkinson gait (Okuda et al. 2016) and human walking foot trajectory (Kitagawa and Ogihara 2016). IMUs are relatively inexpensive with low power consumption which allows data collection over a long period of time where virtually an unlimited number of steps can be evaluated). Linking software with Bluetooth Low Energy based IMU technology, smart phones and tablets is a possible way of delivering gait analysis addressing issues of affordability and portability.

6.5.1.2. Reduction of health inequalities

Affordable portable equipment which is available to all helps address the social imperatives of reducing health inequalities and offers opportunities to those with mobility difficulty and unable to travel to hospital. The persistence of socioeconomic inequalities in health, even in the highly developed ‘welfare states’ of Western Europe, is one of the great challenges of public health (Mackenbach 2012). This includes three areas: 1) inequalities in access to material and immaterial resources that have not been eliminated by the welfare state, and are still substantial;

2) greater intergenerational mobility, i.e., the composition of lower socioeconomic groups has become more homogeneous with regard to personal characteristics associated with ill-health; and 3) change in epidemiological regime, in which consumption behaviour became the most important determinant of ill-health, increasing access to the marginal benefits of the immaterial resources by a higher social group (Mackenbach 2012).

6.5.1.3. Patient and user involvement

Patient-centered care, shared decision-making, patient participation and the recovery model are models of care which incorporate user involvement and patients' perspectives on their treatment and care (Storm and Edwards 2013). User involvement will increase influence of patients on decisions about their treatment, ensure that services are provided in accordance with patients' needs and enhance patients' control over their own healthcare (Borg et al. 2000). Technology needs to be acceptable to majority users (older people, caregivers, health professionals, community members). Barriers to the development and adoption of the technology need to be identified. To date no wearable systems have penetrated into clinical practice at scale (Kirtley 2006). There are various reasons that may contribute to this including poor tolerance of existing wearable devices, a lack of reliability of the information collected, very limited battery life and limited subsequent use of the data for clinical decision support. The inputs, requirements, issues, attitudes from the users need to be considered in relating with our innovative technology to conduct the design and technical choices while developing the proposed system. Public engagement events need to explore cross-cutting issues such as trustworthy data use and privacy.

6.5.1.4. Compatibility with other systems

Any systems that are developed need to be compatible with existing information technology systems (Drummond et al. 2015; Guthrie et al. 2015) to facilitate information collection, sharing and storing. The aim will be to facilitate information sharing with other systems used by other clinicians in NHS hospitals and GP surgeries. This will support integrated care by multi-professional and interdisciplinary specialists which is another aim in the NHS 5-year plan (England 2017a). The benefits of more coordinated care are several which include more efficiency with financial benefits in avoiding duplication/complications from missed treatments.

6.5.1.5. Market opportunity

The remote digital automatic gait assessment system we proposed offers a great market opportunity for equipment manufacturers, internet service providers and application developers. The digital smart objects are expected to reach 212 billion entities deployed globally with market forecast to exceed $7 trillion by the end of 2020 (Gantz and Reinsel 2012) and could generate up to $11.1 trillion a year in economic value by 2025 (Manyika et al. 2015). Considering the above aspects, an innovative digital strategy framework for gait analysis is proposed in the next section. We consider all above requirements in proposing the framework and demonstrate it through a pilot study.

6.5.2. Proposed digital transformation strategy framework for gait analysis

A major challenge for researchers and clinicians who address healthcare issues in the ageing population, is to monitor functioning, and to timely initiate interventions that aim to prevent loss of functional abilities to improve the quality of life of older people (Zijlstra and Aminian 2007). Gait assessment around the world urgently demands the transformation of gait assessment from a hospital or laboratory centered system to a person or home centered environment. Within this aim we have developed an automatic wearable multi-sensor IMU based system for gait analysis. This technology has the ability to make sophisticated real time assessments of various gait parameters. Information collected automatically is then uploaded to a cloud and using artificial intelligence (AI) this information can be analysed and subsequently accessed and shared by patients, care professionals including hospital specialists, general practitioners, therapists and social workers who can interact and decide on management plans. Figure 6.1 shows the proposed digital transformation strategy framework which consists of 1) human gait; 2) sensors; 3) connectivity; 4) cloud computing; 5) intelligence and 6) human computer interaction.

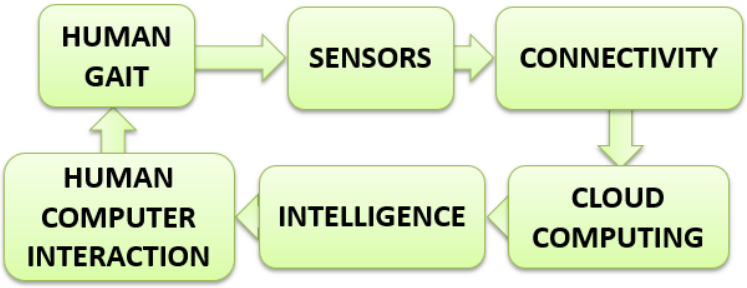

Figure 6.1: Proposed digital transformation strategy framework

The proposed framework will offer the ability to measure, infer and understand gait information to provide support and intervention through healthcare professionals. Human gait information will be collected using sensors and blend seamlessly from older adults in care homes or clinics, and the information is shared across platforms through connectivity, cloud computing and intelligence in order to develop a common operating picture for human computer interaction. Various sensors will be used for gait data collection. Sensors network technologies will be used for connectivity in which information and communication systems are invisibly embedded in the environment for automatic gait data collection. This generates enormous amounts of data which have to be stored, processed and presented in a seamless, efficient, and easily interpretable form. Cloud computing will provide the virtual infrastructure for such utility computing which integrates sensors, storage devices, analytics tools, visualization platforms and client delivery. AI and intelligent machine learning technologies will be used for information interpretation and generate assistive decision. Human computer interaction will provide a user-friendly interface for various users, e.g. healthcare professionals, patients, caregivers, etc. to manage, plan and treatment. The proposed digital transformation strategy framework is inspired by the Internet of Things (IoT) architecture (Gubbi et al. 2013). The detailed descriptions of Figure 6.1 are shown in the following subsections.

6.5.2.1. Human gait

The proposed digital transformation framework for gait analysis starts with understanding of human gait. Human gait is the systematic study of the way, the manor, the style of walking and the ability to maintain balance in an upright posture. Gait patterns are highly repeatable both within a subject and between subjects, but clearly each person has a unique walking style. Efficiency of walking depends on mobility of the joints, activity of the muscles, coordination and rhythm of the movements as well as the ability to smoothly move the center of gravity. This rhythmic locomotion is a series of rhythmic alternating movement of arms, legs, and trunk which create forward movement of the body (Murray 1967). The components of gait and balance are fundamental to physical function. Together, normal gait and balance enable ambulation, also known as mobility which is the primary mode of personal transport. Human gait analysis includes measureable parameters including spatiotemporal, kinematics, kinetics and dynamic and other features. Comprehensive gait parameters are shown in Figure 6.2.

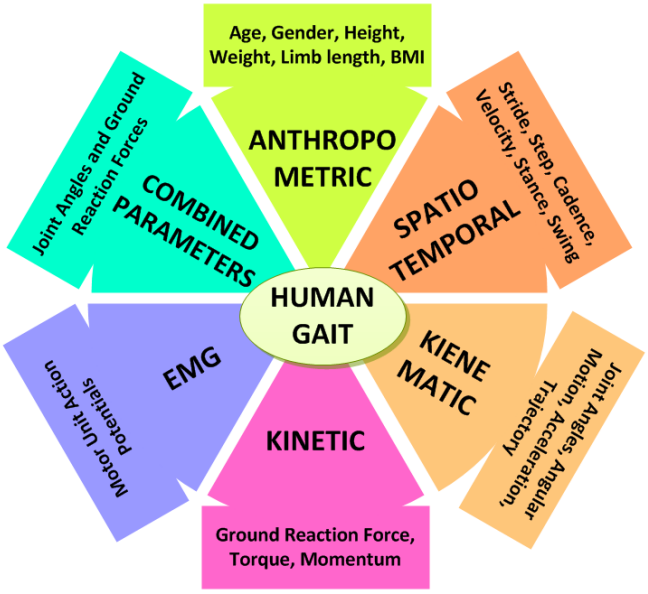

Figure 6.2: Gait parameters tree of human gait

Basic prerequisites for gait analysis are the assessment of spatiotemporal distance and time based gait parameters (e.g. stride, step, cadence, stance and swing) and the analysis of movements within subsequent stride cycles (Zijlstra and Hof 2003). The analysis of kinematic or physiologic signals (e.g. angle of joints such as trunk angle, hip angle, knee angle, ankle angle and foot) and kinetic signals (e.g. ground reaction force, muscle-tendon length, muscle moment arm and biofeedback) during subsequent stride cycles is also important for gait analysis where these parameters may contribute to development and/or progression of knee osteoarthritis (Hart et al. 2015). Gait analysis also includes EMG to record the electrical signals activating the muscle fibers, combined parameters (e.g. joint angles and ground reaction forces) and anthropometric information (e.g. age, gender, height, weight, limb length and body mass index) (Tasch et al. 2008).

6.5.2.2. Sensors

Clinical gait assessment is the process by which quantitative information is collected to aid in understanding the quality of patient's gait and balance abnormalities and in treatment decision-making. The details of sensors are discussed in Section 2.4.1. Conventionally, gait analysis is considered subjectively through visual observations but now with advanced technology, human gait analysis can be done objectively and empirically for the better quality of life. With the new technology for gait analysis, a variety of vision, wearable and ambient sensors are available

(Figure 6.3) and many of them are integrated into the garment's fabric, simultaneously collecting signals in a non-invasive and unobtrusive way.

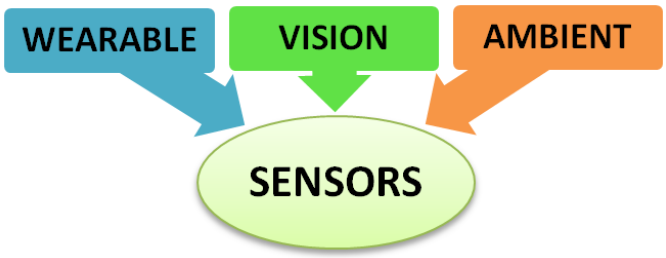

Figure 6.3: Sensors for gait data collection

Wearable, computer vision and ambient based solutions focus on gait analysis, motion analysis, posture analysis, proximity analysis, inactive detection, body shape and 3D head motion analysis (Yu 2008; Khan and Hoey 2017) have become a very active research area (Rafi et al. 2011). The details of sensor related issues are discussed in Sections 2.4.1 to 2.4.4. The collected data will be transferred to the needed locations through connectivity to be discussed in the next subsection.

6.5.2.3. Connectivity

The architecture and the platform of the sensor networks for gait analysis play a significant role for continuous monitoring of gait parameters especially of the older adults or chronic patient. The network should be selected based on cost, performance, ease of configuration, addition of extra sensor nodes, security, range and power consumption and other characteristics. Body area networks (BAN) are therefore designed to connect and operate sensors within, on or at close of human body (Lo et al. 2013; Akbar et al. 2017). It plays a unique role in health applications e.g. gait patterns (Jarchi et al. 2014), motor fluctuations gait assessment in Parkinson's patients (Cancela et al. 2014), balance and fall (Lai et al. 2014) in real time monitoring, decision making and therapeutic treatments (Poon et al. 2015). The IEEE wireless BAN standard (IEEE 804.15.6 TG6) (The Institute of Electrical and Electronics Engineers 2018) is formed in order to standardize the Physical Layer and Medium Access Control (MAC) protocols for short-range, low-power, and reliable wireless body sensors. Although BAN provide emerging research directions, however in the context of autonomic, context-aware, collaborative, and cloud-assisted of BAN are still challenging (Gravina et al. 2017). Other commercially available IoT wireless sensor network platforms are shown in Figure 6.4.

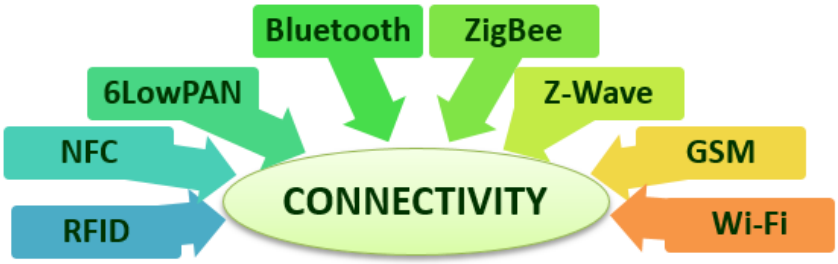

Figure 6.4: Connectivity for transferring sensor data to server through network

IoT was initially inspired by members of Radio Frequency Identification (RFID) community (Union 2005) for identifying of an object or person wirelessly using radio waves by browsing an internet address that corresponds to a particular RFID or Near Field Communication (NFC) (Want 2006). Clinical wireless devices used 6LowPAN/IEEE 802.15.4, Bluetooth, BLE (Bluetooth Low Energy), ZigBee, Z-wave and NFC for mobile-Health and electronic-Health applications (López et al. 2013). Mobile computing, medical sensors and communication technologies for healthcare services is a novel healthcare connectivity model that connects the 6LowPAN with evolving 4G (GSM) networks for future internet based health service (Islam et al. 2015). Wireless Fidelity (Wi-Fi), currently the most common standard used in homes and many businesses is 802.11n, which offers serious throughput in the range of hundreds of megabit per second, which is fine for file transfers, but may be too power-consuming for many IoT applications (Islam et al. 2015). The sensor connectivity architecture comprises of body worn sensors, vision and ambient sensors distributed in the environment. The software architecture and conceptual design for gait analysis platform along with the performance of the sensor network in terms of latencies and battery lifetime etc should be considered. The data from sensors will be stored in the cloud to be discussed in the next subsection.

6.5.2.4. Cloud computing

Cloud computing (CC) provides facilities for smart devices to send their data to the cloud, for big data to be processed in real-time, and eventually for end-users to benefit from the knowledge extracted from the collected big data (Al-Fuqaha et al. 2015). Providing high quality gait monitoring service by means of new technologies service based on personalized gait data is a challenging task comparing to traditional medical service within hospitals. Therefore, a CC platform based framework of gait analysis system will be designed to implement pervasive gait monitoring. Security needs to be considered to current connectivity and cloud support. There are still challenges for gait analysis applications such as 1) sensors node can be easily lost or

abducted as they are tiny in terms of size, 2) security solutions must be resource-efficient as sensors node have limited processing power, memory, and communication bandwidth. There are a lot of free and commercial cloud platforms and frameworks available to host IoT services (Al-Fuqaha et al. 2015). Therefore, during the architectural design physical security, network security, data protection, human engagements privacy, and services should be considered (Figure 6.5). The data stored at CC will be analysed using the intelligent approaches to be discussed in the next subsection.

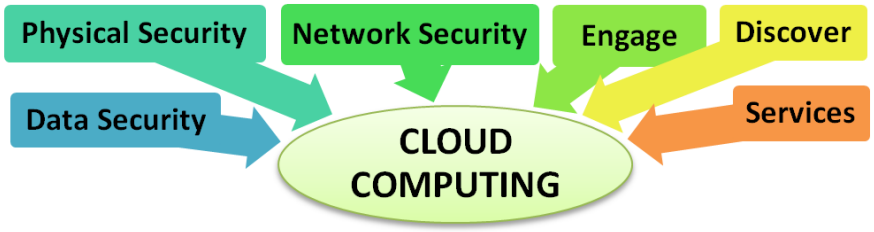

Figure 6.5: Cloud computing for servers hosted on the Internet to store, manage, and process data, provide security and safe communication

6.5.2.5. Intelligence

To promote sustainable development in gait analysis, the proposed digital strategy framework implies a global vision that adopts AI, big data, decision making, ontology, machine learning and intelligent dashboard presentation (Figure 6.6). The ageing issue is an aspect that researchers, business organizations, health professionals, patients and government should devote efforts in developing innovative gait analysis technology for people with gait abnormalities. Typical emerging optimization algorithms (such as evolutionary (Elkady and Abdelsalam 2016; Momete 2016), stochastic (Marti 2005; Faber and Behnke 2007) and combinatorial optimization (Denoyel et al. 2017)) and machine learning algorithms (such as unsupervised learning (Niebles et al. 2008), supervised learning (Williamson and Andrews 2000) and semi-supervised learning (Zhang et al. 2005)) will be explored. The results from intelligence will be presented to the users using human computer interaction to be discussed in the next subsection.

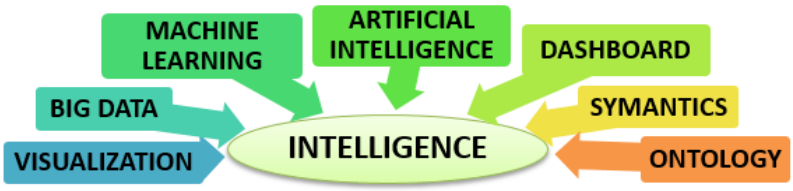

Figure 6.6: Intelligence

6.5.2.6. Human computer interaction

Human computer interaction will reduce the socioeconomic inequalities in healthcare (Mackenbach 2012). The information stored in the cloud is accessible to stake holders including patients' general practitioners, therapists, social carers and hospital specialists on a need to know basis (Figure 6.7).

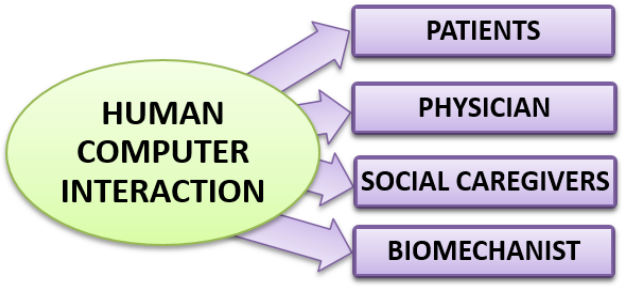

Figure 6.7: Human computer interaction

This will facilitate the interaction between the relevant members of the group who can make treatment recommendations and follow progress remotely. This will speed up considerable the assessment and treatment process as it removes the need for conventional medical and therapy consultation procedures often requiring the patients to attend pre booked clinics. This will also enable all stakeholders to see what each individual facilitating communication between members of the multidisciplinary team.

We describe the materials and methods of the proposed digital strategy framework. Based on this we describe the impact of the prosed digital strategy framework in the next subsections.

6.5.3. Impact of proposed digital strategy framework

The proposed digital transformation strategy framework requires the coming together of various components as shown in Figure 6.8. This will have an impact and require change across the whole spectrum of stakeholders. Health Professionals will need to look at new ways of working leading to different scenarios for consultations with more happening remotely. There will be different forms of communication between various professionals in hospital and in the community. Patients who are technology savvy will be able to participate more effectively with these new forms of treatment. As younger generations age it is likely that such technology will become more acceptable. Social carers will have the opportunity to interact with care professionals and carers with greater ease. Finally, such a strategy will offer several opportunities

to develop new business strategies and tap into new markets through interacting with users of this new technology.

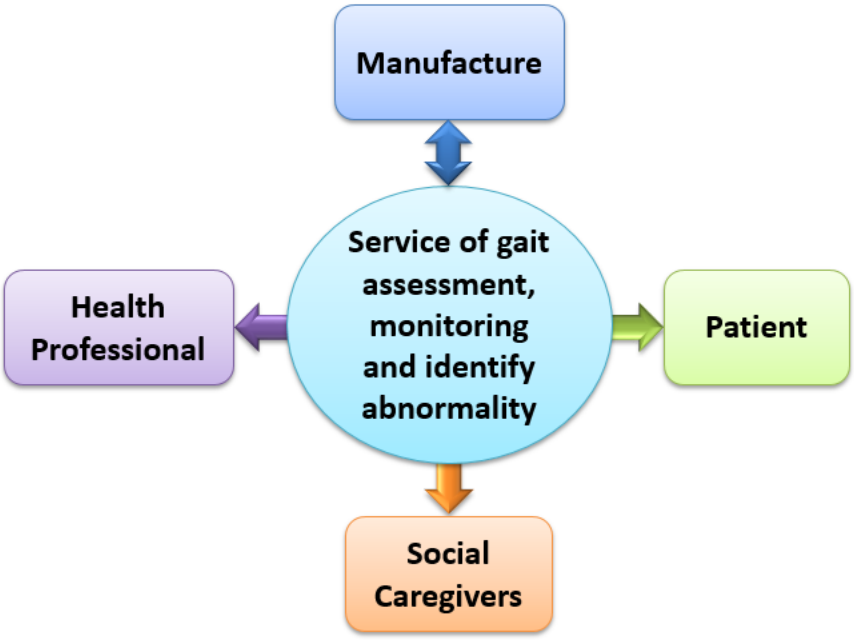

Figure 6.8: Impact analysis

6.5.3.1. Potential benefits

Most transformation initiatives fail due to their fragmented view and outdated theories of change that ignore the relationship aspects of organizations (Von Kutzschenbach and Brønn 2017). Therefore, a digital transformation strategy needs to be developed within the context of need. In order to implement and realize the benefits of digital transformation for gait analysis, we understand the consequences of the socio-technical change and identify the potential unintended consequences of the digital transformation. Figure 1 shows the components of such a strategy. The goals of such a transformation vary from a health sector perspective and a business perspective, while from a business, industry and IT perspective the strategy will focus on the development of new technologies and new equipment, from a healthcare perspective the strategy will need to be focused on the effective delivery of these new technologies. Both will need to address the organisational, staffing and leadership transformation to develop the strategy. Inevitably there will need to be a period of adjustment to the new technology and to recognise the opportunities this will present. It is therefore of vital importance that there is a close fit between the strategies of all stakeholders. There are several common aspects of developing such a strategy although the detail will inevitably differ. There needs to be a coming together of business and

health strategies to the point of effective diagnosis and treatment of gait disorders in patients in their own home.

From an industry perspective, there are various modes for the implementation of a Digital Transformation Framework. The basic requirements of such a strategy depends on the balancing of four transformation dimensions, the use of technologies, financial considerations, structural changes and changes to value creation. Although these basic tenants have been described as requirements for industry they also apply to health.

6.5.3.2. Structural change in healthcare

With different technologies in use and different forms of structural changes is often needed to provide an adequate basis for the new operations in digital transformation (Matt et al. 2015). The introduction of new technology needs to be accompanied by structural change to enable new ways of assessment and treatment. The care pathway for the assessment of patients with gait and mobility delivery of services is hospital centric and the aim should be to deliver the care currently delivered in hospital at home. A lot of work has been done in this regard already. However, patients needing access to specialist equipment still need to go to hospital or specialist centres for assessment. Here lies the potential for change in the digital transformation. While at present technology is used mostly for remote monitoring, the use of new technologies increases the possibilities of diagnosis and treatment of patients at home. Establishing a cloud will enable the upload of data remotely. This data can then be reviewed remotely by therapists, general practitioners, hospital specialists or tertiary centres and patients to coordinate management plans. The degree of change can vary with locality depending on the current infrastructure

6.5.3.3. Use of technologies

The use of technologies addresses a company's attitude towards new technologies as well as its ability to exploit these technologies which therefore contains the strategic role of IT for a company and its future technological ambition (Matt et al. 2015). This would be crucial for the development of a strategy. The take up of new technologies are slow and the successful implementation requires an understanding of attitude of stake holders to it. Localities need to decide whether they want to become leaders in the implementation of the new technology and models of care with the ability in setting new standards of care or stick with current models.

While being a leader can lead to advantages in setting one's own standards, it might be risky as it requires technological competence. This is the challenge that interested parties must address.

6.5.3.4. Financial considerations

Digital transformation offers great opportunities for healthcare and community care. Healthcare and manufacturing applications are projected to form the biggest economic impact. Healthcare applications such as mobile health and telecare that enable medical wellness, prevention, diagnosis, treatment and monitoring services are expected to create about $1.1–$2.5 trillion in growth annually by 2025 (Al-Fuqaha et al. 2015). Within this area of growth there remain financial pressures on the delivery of care due to increasing of aging population. Inevitably any developments need to take this into consideration. Financial pressures on delivering care can be a driver for change provided new care pathways can be delivered cost effectively and save money. Our proposed cost effective digital transformation strategy framework for gait analysis offers the ideal opportunity to develop in this context with benefit for all concerned.

6.5.3.5. Changes to value creation

From a business perspective, the use of new technologies often implies changes in value creation (Matt et al. 2015). The introduction of new technologies invariably results in a change of culture and the need to work in different ways. Introducing digital technology and treating patients in their own home requires different forms of funding and adjustments to commissioning of services. This may have to happen in parallel with more conventional ways of doing things. The technology must be user friendly and delivers on expectations. The changes also require management of this transition period to overcome barriers and scepticism. There are needs on acceptance of new forms of working to enable the new structure to work.

For our future research, we propose a digital transformation strategy framework of gait analysis for all stakeholders to develop the fertile area of gait analysis. We present an overview of technology we are developing to support this strategy. Applications in clinical diagnosis, geriatric care, sports, biometrics, rehabilitation, and industrial area are proposed separately. Available machine learning techniques are also presented with available datasets for gait analysis. The prospective opportunities in gait analysis are also discussed. A digital transformation of assessment of gait is a continuous complex undertaking requiring a change in the care pathway and the delivery of care. This needs to be managed carefully with good leadership. A half-hearted

approach may risk losing focus to overcome operational difficulties. The potential benefits are several, for example, 1) from a business perspective, increasing sales and productivity; and 2) from a health perspective, better and cost effective patient care delivered in the patient's home.

7. References

Achmad, W. and Bo-Suk, Y., 2007. Application of nonlinear feature extraction and support vector machines for fault diagnosis of induction motors. *Expert Systems with Applications*, 33 (241-250).

Afzal, M. R., Oh, M.-K., Lee, C.-H., Park, Y. S. and Yoon, J., 2015. A Portable Gait Asymmetry Rehabilitation System for Individuals with Stroke Using a Vibrotactile Feedback. *BioMed Research International*, 2015, 16.

Agarwal, R., Gao, G., DesRoches, C. and Jha, A. K., 2010. Research commentary—The digital transformation of healthcare: Current status and the road ahead. *Information Systems Research*, 21 (4), 796-809.

ageUK, 2015. Later Life in the United Kingdom.

Aging, N. I. O., January 2013. Falls And Older Adults: Causes And Risk Factors.

Agostini, V., Gastaldi, L., Rosso, V., Knaflitz, M. and Tadano, S., 2017. A Wearable Magneto-Inertial System for Gait Analysis (H-Gait): Validation on Normal Weight and Overweight/Obese Young Healthy Adults. *Sensors*, 17 (10), 2406.

Agostini, V., Knaflitz, M., Antenucci, L., Lisco, G., Gastaldi, L. and Tadano, S., 2015. Wearable sensors for gait analysis, *Medical Measurements and Applications (MeMeA), 2015 IEEE International Symposium on* (pp. 146-150).

Agrawal, V., Gailey, R., O'Toole, C., Gaunaurd, I. and Dowell, T., 2009. Symmetry in External Work (SEW): A Novel Method of Quantifying Gait Differences Between Prosthetic Feet. *Prosthetics and Orthotics International*, 33 (2), 148-156.

Ahmad A. Al-Hajji, March 2012. Rule-Based Expert System for Diagnosis and Symptom of Neurological Disorders "Neurologist Expert System (NES)", *Proceedings of First Taibah University International Conference on Computing and Information Technology (ICCIT)* (pp. 67-72). Saudi Arabia.

Akbar, M. S., Yu, H. and Cang, S., 2017. TMP: Tele-medicine protocol for slotted 802.15. 4 with duty-cycle optimization in wireless body area sensor networks. *IEEE Sensors Journal*, 17 (6), 1925-1936.

Al-Fuqaha, A., Guizani, M., Mohammadi, M., Aledhari, M. and Ayyash, M., 2015. Internet of things: A survey on enabling technologies, protocols, and applications. *IEEE Communications Surveys & Tutorials*, 17 (4), 2347-2376.

Alaqtash, M., Sarkodie-Gyan, T., Yu, H., Fuentes, O., Brower, R. and Abdelgawad, A., 2011. Automatic classification of pathological gait patterns using ground reaction forces and machine learning algorithms, *Engineering in Medicine and Biology Society, EMBC, 2011 Annual International Conference of the IEEE* (pp. 453-457): IEEE.

Albert, M. V., Kording, K., Herrmann, M. and Jayaraman, A., 2012. Fall classification by machine learning using mobile phones. *PLoS One*, 7 (5), e36556.

Allen, F. R., Ambikairajah, E., Lovell, N. H. and Celler, B. G., 2006. Classification of a known sequence of motions and postures from accelerometry data using adapted Gaussian mixture models. *Physiological measurement*, 27 (10), 935.

Allseits, E., Lučarević, J., Gailey, R., Agrawal, V., Gaunaurd, I. and Bennett, C., 2017. The development and concurrent validity of a real-time algorithm for temporal gait analysis using inertial measurement units. *Journal of biomechanics*, 55, 27-33.

Aminian, K., Robert, P., Jequier, E. and Schutz, Y., 1994. Estimation of speed and incline of walking using neural network, *Conference Proceedings. 10th Anniversary. IMTC/94. Advanced Technologies in I & M. 1994 IEEE Instrumentation and Measurement Technolgy Conference (Cat. No.94CH3424-9)* (pp. 160-162 vol.161).

Anon. , 2016. *Gyroscope- definition of gyroscope in English from the Oxford dictionary* [online]. Available from: http://www.oxforddictionaries.com/definition/english/gyroscope [Accessed 18/01/2016].

Anon. , 2017. STEADI Materials for Your Older Adult Patients | STEADI - Older Adult Fall Prevention | CDC Injury Center.

Anon. , Accessed on 27/01/2016. SparkFun Triple Axis Accelerometer, Gyrscope and Magnetometer.

Anwary, A. R., Yu, H. and Vassallo, M., 2018. An Automatic Gait Feature Extraction Method for Identifying Gait Asymmetry Using Wearable Sensors. *Sensors*, 18 (2), 676.

Apiletti, D. D. d. A. e. I., Politec. di Torino, Torino ; Baralis, E. ; Bruno, G. ; Cerquitelli, T., 2009. Real-Time Analysis of Physiological Data to Support Medical Applications. *Information Technology in Biomedicine*, 13 (3), 323-321.

Archer, K. R., Castillo, R. C., MacKenzie, E. J. and Bosse, M. J., 2006. Gait symmetry and walking speed analysis following lower-extremity trauma. *Physical therapy*, 86 (12), 1630.

Armand, S., Watelain, E., Roux, E., Mercier, M. and Lepoutre, F.-X., 2007. Linking clinical measurements and kinematic gait patterns of toe-walking using fuzzy decision trees. *Gait & posture*, 25 (3), 475-484.

Arnold, S. F., 1981. *The Theory of Linear Models and Multivariate Analysis*. New York: John Wiley and Sons.

Asch, D. A. and Volpp, K. G., 2012. What business are we in? The emergence of health as the business of health care. *New England Journal of Medicine*, 367 (10), 888-889.

Audigié, F., Pourcelot, P., Degueurce, C., Geiger, D. and Denoix, J. M., 2002. Fourier analysis of trunk displacements: a method to identify the lame limb in trotting horses. *Journal of Biomechanics*, 35 (9), 1173-1182.

Auvinet, E., Multon, F., Manning, V., Meunier, J. and Cobb, J. P., 2017. Validity and sensitivity of the longitudinal asymmetry index to detect gait asymmetry using Microsoft Kinect data. *Gait & Posture*, 51, 162-168.

Azevedo Coste, C., Sijobert, B., Pissard-Gibollet, R., Pasquier, M., Espiau, B. and Geny, C., 2014. Detection of freezing of gait in Parkinson disease: preliminary results. *Sensors*, 14 (4), 6819-6827.

Badesa, F. J., Morales, R., Garcia-Aracil, N., Sabater, J. M., Casals, A. and Zollo, L., 2014. Auto-adaptive robot-aided therapy using machine learning techniques. *Computer methods and programs in biomedicine*, 116 (2), 123-130.

Baker, R., 2006. Gait analysis methods in rehabilitation. *Journal of NeuroEngineering and Rehabilitation*, 3 (1), 4.

Balasubramanian, C. K., Neptune, R. R. and Kautz, S. A., 2009. Variability in spatiotemporal step characteristics and its relationship to walking performance post-stroke. *Gait & posture*, 29 (3), 408-414.

Ball, R., Shu, C., Xi, P., Rioux, M., Luximon, Y. and Molenbroek, J., 2010. A comparison between Chinese and Caucasian head shapes. *Applied Ergonomics*, 41 (6), 832-839.

Barnett, J., Vasileiou, K., Djemil, F., Brooks, L. and Young, T., 2011. Understanding innovators' experiences of barriers and facilitators in implementation and diffusion of healthcare service innovations: a qualitative study. *BMC Health Services Research*, 11 (1), 342.

Beauchet, O., Allali, G., Launay, C., Herrmann, F. and Annweiler, C., 2013. Gait variability at fast-pace walking speed: a biomarker of mild cognitive impairment? *The journal of nutrition, health & aging*, 17 (3), 235-239.

Beauchet, O., Herrmann, F. R., Grandjean, R., Dubost, V. and Allali, G., 2008. Concurrent validity of SMTEC® footswitches system for the measurement of temporal gait parameters. *Gait & posture*, 27 (1), 156-159.

Begg, R. and Kamruzzaman, J., 2005. A machine learning approach for automated recognition of movement patterns using basic, kinetic and kinematic gait data. *Journal of biomechanics*, 38 (3), 401-408.

Begg, R. K., Palaniswami, M. and Owen, B., 2005. Support vector machines for automated gait classification. *Biomedical Engineering, IEEE Transactions on*, 52 (5), 828-838.

Benedetti, M., Manca, M., Sicari, M., Ferraresi, G., Casadio, G., Buganè, F. and Leardini, A., 2011. Gait measures in patients with and without afo for equinus varus/drop foot, *Medical Measurements and Applications Proceedings (MeMeA), 2011 IEEE International Workshop on* (pp. 591-592): IEEE.

Benoussaad, M., Sijobert, B., Mombaur, K. and Azevedo Coste, C., 2015. Robust foot clearance estimation based on the integration of foot-mounted IMU acceleration data. *Sensors*, 16 (1), 12.

Berg, K. O., Wood-Dauphinee, S. L., Williams, J. I. and Maki, B., 1992. Measuring balance in the elderly: validation of an instrument. *Can J Public Health*, 83 (2), 7-11.

Bervet, K., Bessette, M., Godet, L. and Crétual, A., 2013. KeR-EGI, a new index of gait quantification based on electromyography. *Journal of Electromyography and Kinesiology*, 23 (4), 930-937.

Bianchi, V., Grossi, F., Matrella, G., Munari, I. D. and Ciampolini, P., 2008. Fall detection and gait analysis in a smart-home environment. *Gerontechnology*, 7 (2), 73.

Bilney, B., Morris, M. and Webster, K., 2003. Concurrent related validity of the GAITRite® walkway system for quantification of the spatial and temporal parameters of gait. *Gait & posture*, 17 (1), 68-74.

Bland, J. M. and Altman, D., 1986. Statistical methods for assessing agreement between two methods of clinical measurement. *The lancet*, 327 (8476), 307-310.

Bland, J. M. and Altman, D. G., 1999. Measuring agreement in method comparison studies. *Statistical methods in medical research*, 8 (2), 135-160.

Błażkiewicz, M., Wiszomirska, I. and Wit, A., 2014. Comparison of four methods of calculating the symmetry of spatial-temporal parameters of gait. *Acta of bioengineering and biomechanics*, 16 (1), 29--35.

Bloem, B. R., Gussekloo, J., Lagaay, A. M., Remarque, E. J., Haan, J. and Westendorp, R. G., 2000. Idiopathic senile gait disorders are signs of subclinical disease. *Journal of the American Geriatrics Society*, 48 (9), 1098-1101.

Böhm, H. and Döderlein, L., 2012. Gait asymmetries in children with cerebral palsy: Do they deteriorate with running? *Gait & Posture*, 35 (2), 322-327.

Bolink, S., van Laarhoven, S., Lipperts, M., Heyligers, I. and Grimm, B., 2012. Inertial sensor motion analysis of gait, sit–stand transfers and step-up transfers: differentiating knee patients from healthy controls. *Physiological measurement*, 33 (11), 1947.

Bookstein, F. L., 1978. *The measurement of biological shape and shape space change*. Vol. 24. New York: Springer-Verlag.

Bookstein, F. L., 1991. *Morphometric Tools for Landmark Data: Geometry and Biology*. Cambridge: Cambridge University Press.

Bookstein, F. L., 1997. Landmark methods for forms without landmarks: Morphometrics of group differences in outline shape. *Medical Image Analysis*, 1 (3), 225-243.

Bookstein, F. L., 1998. Features of deformation grids: an approach via singularity theory, *Proceedings of the Fourteenth Annual Symposium on Computational Geometry* (pp. 214-221). Minnesota: ACM.

Bora, N. M., Molke, G. V. and Munot, H. R., 2015a. Understanding human gait: A survey of traits for biometrics and biomedical applications. *International Conference on Energy Systems and Applications*. IEEE. 723-728.

Bora, N. M., Molke, G. V. and Munot, H. R., 2015b. Understanding human gait: A survey of traits for biometrics and biomedical applications, *2015 International Conference on Energy Systems and Applications* (pp. 723-728).

Borg, V., Kristensen, T. S. and Burr, H., 2000. Work environment and changes in self-rated health: a five year follow-up study. *Stress Medicine*, 16 (1), 37-47.

Bossers, W. J. R., van der Woude, L. H. V., Boersma, F., Scherder, E. J. A. and van Heuvelen, M. J. G., 2014. The Groningen Meander Walking Test: A Dynamic Walking Test for Older Adults With Dementia. *Physical Therapy*, 94 (2), 262-272.

Boutaayamou, M., Schwartz, C., Stamatakis, J., Denoël, V., Maquet, D., Forthomme, B., Croisier, J.-L., Macq, B., Verly, J. G., Garraux, G. and Brüls, O., 2015. Development and validation of an accelerometer-based method for quantifying gait events. *Medical Engineering & Physics*, 37 (2), 226-232.

Bouten, C. V., Sauren, A. A., Verduin, M. and Janssen, J. D., 1997. Effects of placement and orientation of body-fixed accelerometers on the assessment of energy expenditure during walking. *Med Biol Eng Comput*, 35 (1), 50-60.

Brach, J. S. and VanSwearingen, J. M., 2002. Physical Impairment and Disability: Relationship to Performance of Activities of Daily Living in Community-Dwelling Older Men. *Physical Therapy*, 82 (8), 752-761.

Brach, J. S. and VanSwearingen, J. M., 2013. Interventions to Improve Walking in Older Adults. *Current translational geriatrics and experimental gerontology reports*, 2 (4), 10.1007/s13670-13013-10059-13670.

Brajdic, A. and Harle, R., 2013. Walk detection and step counting on unconstrained smartphones. *Proceedings of the 2013 ACM international joint conference on Pervasive and ubiquitous computing*, Zurich, Switzerland. 2493449: ACM. 225-234.

Brandes, M., Zijlstra, W., Heikens, S., van Lummel, R. and Rosenbaum, D., 2006. Accelerometry based assessment of gait parameters in children. *Gait & Posture*, 24 (4), 482-486.

Brandstater, M. E., de Bruin, H., Gowland, C. and Clark, B. M., 1983. Hemiplegic gait: analysis of temporal variables. *Arch Phys Med Rehabil*, 64 (12), 583-587.

Bridenbaugh, S. A. and Kressig, R. W., 2011. Laboratory Review: The Role of Gait Analysis in Seniors' Mobility and Fall Prevention. *Gerontology*, 57 (3), 256-264.

Brink, H., 1993. Validity and reliability in qualitative research. *Curationis*, 16 (2), 35-38.

Burns, E. R., Stevens, J. A. and Lee, R., 2016. The direct costs of fatal and non-fatal falls among older adults—United States. *Journal of safety research*, 58, 99-103.

Cabral, S., Fernandes, R., Selbie, W. S., Moniz-Pereira, V. and Veloso, A. P., 2017. Inter-session agreement and reliability of the Global Gait Asymmetry index in healthy adults. *Gait & Posture*, 51, 20-24.

Caldas, R., Mundt, M., Potthast, W., Buarque, F. and Markert, B., 2017. A systematic review of gait analysis methods based on inertial sensors and adaptive algorithms. *Gait & Posture*.

Cancela, J., Pastorino, M., Arredondo, M. T., Nikita, K. S., Villagra, F. and Pastor, M. A., 2014. Feasibility study of a wearable system based on a wireless body area network for gait assessment in Parkinson's disease patients. *Sensors*, 14 (3), 4618-4633.

Carabello, R. J., Reid, K. F., Clark, D. J., Phillips, E. M. and Fielding, R. A., 2010. Lower extremity strength and power asymmetry assessment in healthy and mobility-limited populations: reliability and association with physical functioning. *Aging clinical and experimental research*, 22 (4), 324-329.

Carmo, M. d., 1992. *Riemannian Geometry*. Birkhäuser Basel, Englewoods Cliffs.

Carpes, F. P., Mota, C. B. and Faria, I. E., 2010. On the bilateral asymmetry during running and cycling – A review considering leg preference. *Physical Therapy in Sport,* 11 (4), 136-142.

Casamassima, F., Ferrari, A., Milosevic, B., Ginis, P., Farella, E. and Rocchi, L., 2014. A Wearable System for Gait Training in Subjects with Parkinson's Disease. *Sensors,* 14 (4), 6229.

Cavallo, F., Sabatini, A. M. and Genovese, V., 2005. A step toward GPS/INS personal navigation systems: real-time assessment of gait by foot inertial sensing, *Intelligent Robots and Systems, 2005.(IROS 2005). 2005 IEEE/RSJ International Conference on* (pp. 1187-1191): IEEE.

Chan, H., Yang, M., Wang, H., Zheng, H., McClean, S., Sterritt, R. and Mayagoitia, R. E., 2013. Assessing gait patterns of healthy adults climbing stairs employing machine learning techniques. *International Journal of Intelligent Systems,* 28 (3), 257-270.

Chatterji, S., Byles, J., Cutler, D., Seeman, T. and Verdes, E., 2015. Health, functioning, and disability in older adults—present status and future implications. *The Lancet,* 385 (9967), 563-575.

Chen, G., Patten, C., Kothari, D. H. and Zajac, F. E., 2005. Gait differences between individuals with post-stroke hemiparesis and non-disabled controls at matched speeds. *Gait & Posture,* 22 (1), 51-56.

Chen, S., 2013. Gait feature extraction from inertial body sensor networks for medical applications. *University of Virginia*.

Chen, S., Barth, A. T., Barth, J. T., Bennett, B. C., Brandt-Pearce, M., Broshek, D. K., Freeman, J. R., Samples, H. L. and Lach, J., 2012. Aiding diagnosis of normal pressure hydrocephalus with enhanced gait feature separability, *Proceedings of the conference on Wireless Health* (pp. 3): ACM.

Chen, S., Cunningham, C. L., Bennett, B. C. and Lach, J., 2011. Enabling longitudinal assessment of ankle-foot orthosis efficacy for children with cerebral palsy, *Proceedings of the 2nd Conference on Wireless Health* (pp. 4): ACM.

Chen, S., Lach, J., Lo, B. and Yang, G.-Z., 2016. Toward pervasive gait analysis with wearable sensors: A systematic review. *IEEE journal of biomedical and health informatics,* 20 (6), 1521-1537.

Chen, Y.-C. and Lin, Y.-W., 2010. Indoor RFID gait monitoring system for fall detection, *Aware Computing (ISAC), 2010 2nd International Symposium on* (pp. 207-212): IEEE.

Chizeck, H., 1997. Fuzzy model identification for classification of gait events in paraplegics. *IEEE Transactions on Fuzzy Systems,* 5 (4), 536-544.

Choi, J., Cho, J., Park, J., Eun, J. and Kim, M., 2008. An efficient gait phase detection device based on magnetic sensor array, *4th Kuala Lumpur International Conference on Biomedical Engineering 2008* (pp. 778-781): Springer.

Chon, Y., Talipov, E. and Cha, H., 2012. Autonomous management of everyday places for a personalized location provider. *IEEE Transactions on Systems, Man, and Cybernetics, Part C (Applications and Reviews),* 42 (4), 518-531.

Chung, P. C., Hsu, Y. L., Wang, C. Y., Lin, C. W., Wang, J. S. and Pai, M. C., 2012. Gait analysis for patients with Alzheimer'S disease using a triaxial accelerometer, *2012 IEEE International Symposium on Circuits and Systems* (pp. 1323-1326).

Claude, J., 2008. *Morphometrics with R*. New York: Springer-Verlag.

Cohen, H., Blatchly, C. A. and Gombash, L. L., 1993. A study of the clinical test of sensory interaction and balance. *Physical Therapy,* 73 (6), 346-351.

Cordero, A. F., Koopman, H. and Van Der Helm, F., 2004. Use of pressure insoles to calculate the complete ground reaction forces. *Journal of biomechanics*, 37 (9), 1427-1432.

Cornacchia, M., Ozcan, K., Zheng, Y. and Velipasalar, S., 2017. A Survey on Activity Detection and Classification Using Wearable Sensors. *IEEE Sensors Journal*, 17 (2), 386-403.

Corner, B. and Richtsmeier, J., 1992. Cranial growth in the squirrel monkey (Saimiri sciureus): a quantitative analysis using three dimensional coordinate data. *American Journal of Physical Anthropology*, 87, 67-81.

Crea, S., Cipriani, C., Donati, M., Carrozza, M. C. and Vitiello, N., 2015. Providing time-discrete gait information by wearable feedback apparatus for lower-limb amputees: usability and functional validation. *IEEE Transactions on Neural Systems and Rehabilitation Engineering*, 23 (2), 250-257.

Crenshaw, S. J. and Richards, J. G., 2006. A method for analyzing joint symmetry and normalcy, with an application to analyzing gait. *Gait & Posture*, 24 (4), 515-521.

Crosilla, F. and Beinat, A., 2002. Use of generalized Procrustes analysis for the photogrammetric block adjustment by independent models. *ISPRS Journal of Photogrammetry and Remote Sensing*, 53 (3), 195-209.

Cunha, U. V., 1998. Differential diagnosis of gait disorders in the elderly. *Geriatrics & Gerontology International*, 43, 33-42.

Cutter, G. R., Baier, M. L., Rudick, R. A., Cookfair, D. L., Fischer, J. S., Petkau, J., Syndulko, K., Weinshenker, B. G., Antel, J. P. and Confavreux, C., 1999. Development of a multiple sclerosis functional composite as a clinical trial outcome measure. *Brain*, 122 (5), 871-882.

Daby, S., Deepak S., T. and Michael, S., 2013. Mining of Sensor Data in Healthcare: A survey. *In:* Aggarwal, C., ed. *Managing and Mining Sensor Data*. Springer, 459-504.

De Ruyter, K. and Scholl, N., 1998. Positioning qualitative market research: reflections from theory and practice. *Qualitative market research: An international journal*, 1 (1), 7-14.

Deluzio, K. and Astephen, J., 2007. Biomechanical features of gait waveform data associated with knee osteoarthritis: an application of principal component analysis. *Gait & posture*, 25 (1), 86-93.

Denoyel, V., Alfandari, L. and Thiele, A., 2017. Optimizing healthcare network design under reference pricing and parameter uncertainty. *European Journal of Operational Research*, 263 (3), 996-1006.

Destelle, F., Ahmadi, A., O'Connor, N. E., Moran, K., Chatzitofis, A., Zarpalas, D. and Daras, P., 2014. Low-cost accurate skeleton tracking based on fusion of kinect and wearable inertial sensors, *Signal Processing Conference (EUSIPCO), 2014 Proceedings of the 22nd European* (pp. 371-375): IEEE.

DiBerardino III, L. A., Ragetly, C. A., Hong, S., Griffon, D. J. and Hsiao-Wecksler, E. T., 2012. Improving regions of deviation gait symmetry analysis with pointwise t tests. *Journal of applied biomechanics*, 28 (2), 210-214.

Domínguez, G., Cardiel, E., Arias, S. and Rogeli, P., 2013. A Digital Goniometer based on encoders for measuring knee-joint position in an orthosis, *Nature and Biologically Inspired Computing (NaBIC), 2013 World Congress on* (pp. 1-4): IEEE.

Donno, M., Palange, E., Di Nicola, F., Bucci, G. and Ciancetta, F., 2008. A new flexible optical fiber goniometer for dynamic angular measurements: Application to human joint movement monitoring. *IEEE Transactions on Instrumentation and Measurement*, 57 (8), 1614-1620.

Druml, T., Telalbasic, R. and Curik, I., 2009. Body shape analysis of Bosnian mountain horses using Procrustes statistics. *Italian Journal of Animal Science*, 8, 131-133.

Drummond, M. F., Sculpher, M. J., Claxton, K., Stoddart, G. L. and Torrance, G. W., 2015. *Methods for the economic evaluation of health care programmes*. Oxford university press.

Dryden, I. L. and Mardia, K. V., 1998. *Statistical Shape Analysis*. John Wiley & Sons, Chichester.

Duncan, R. P. and Earhart, G. M., 2013. Four square step test performance in people with Parkinson disease. *J Neurol Phys Ther*, 37 (1), 2-8.

Eakman, A. H., M.; Ager, S.; Buchanan, R.; Fee, N.; Gollick, S.; Michels, M.; Olson, L. Satterfield, K.; & Stevenson, K., 2002. Fall prevention in long-term care: An in-house interdisciplinary team approach. *Topics in Geriatric Rehabilitation*, 17 (3), 29 – 39.

Elkady, S. K. and Abdelsalam, H. M., 2016. A modified multi-objective particle swarm optimisation algorithm for healthcare facility planning. *International Journal of Business and Systems Research*, 10 (1), 1-22.

England, N., 2017a. Next steps on the NHS five year forward view: NHS England London.

England, P. H., 2017b. Falls and fracture consensus statement. Supporting commissioning for prevention.

Erni, T. and Colombo, G., 1998. Locomotor training in paraplegic patients: a new approach to assess changes in leg muscle EMG patterns. *Electroencephalography and Clinical Neurophysiology/Electromyography and Motor Control*, 109 (2), 135-139.

Eskofier, B. M., Federolf, P., Kugler, P. F. and Nigg, B. M., 2013. Marker-based classification of young–elderly gait pattern differences via direct PCA feature extraction and SVMs. *Computer Methods in Biomechanics and Biomedical Engineering*, 16 (4), 435-442.

Esser, P., Dawes, H., Collett, J. and Howells, K., 2013. Insights into gait disorders: Walking variability using phase plot analysis, Parkinson's disease. *Gait & Posture*, 38 (4), 648-652.

Esser, P., Howells, K., Dawes, H. and Collet, J., 2012. Gait asymmetry measurement (Vol. PCT/GB2012/051181): Google Patents: WO2012164262A2.

Faber, F. and Behnke, S., 2007. Stochastic optimization of bipedal walking using gyro feedback and phase resetting, *Humanoid Robots, 2007 7th IEEE-RAS International Conference on* (pp. 203-209): IEEE.

Fang, J., GU, Q.-t. and DING, T.-h., 2008. Dynamic zero velocity update for vehicle inertial navigation system [J]. *Journal of Chinese Inertial Technology*, 3, 004.

Feng, S. and Murray-Smith, R., 2014. Fusing Kinect sensor and inertial sensors with multi-rate Kalman filter.

Forczek, W. and Staszkiewicz, R., 2012. An Evaluation of Symmetry in the Lower Limb Joints During the Able-Bodied Gait of Women and Men. *Journal of Human Kinetics*, 35, 47-57.

Foster, R. C., Lanningham-Foster, L. M., Manohar, C., McCrady, S. K., Nysse, L. J., Kaufman, K. R., Padgett, D. J. and Levine, J. A., 2005. Precision and accuracy of an ankle-worn accelerometer-based pedometer in step counting and energy expenditure. *Preventive Medicine*, 41 (3–4), 778-783.

Foxlin, E., 2005. Pedestrian tracking with shoe-mounted inertial sensors. *IEEE Computer graphics and applications*, 25 (6), 38-46.

Fried, A., Cwikel, J., Ring, H. and Galinsky, D., 1990. ELGAM–-Extra-laboratory gait assessment method: Identification of risk factors for falls among the elderly at home. *International disability studies*, 12 (4), 161-164.

Frigo, C. and Crenna, P., 2009. Multichannel SEMG in clinical gait analysis: a review and state-of-the-art. *Clinical Biomechanics*, 24 (3), 236-245.

Gafurov, D. and Snekkenes, E., 2008. Towards understanding the uniqueness of gait biometric, *Automatic Face & Gesture Recognition, 2008. FG'08. 8th IEEE International Conference on* (pp. 1-8): IEEE.

Gantz, J. and Reinsel, D., 2012. The digital universe in 2020: Big data, bigger digital shadows, and biggest growth in the far east. *IDC iView: IDC Analyze the future*, 2007 (2012), 1-16.

Gemperle, F., Kasabach, C., Stivoric, J., Bauer, M. and Martin, R., 1998. Design for wearability, *Wearable Computers, 1998. Digest of Papers. Second International Symposium on* (pp. 116-122): IEEE.

Geurts, A. C., Mulder, T. W., Nienhuis, B. and Rijken, R. A., 1992. Postural reorganization following lower limb amputation. Possible motor and sensory determinants of recovery. *Scandinavian journal of rehabilitation medicine*, 24 (2), 83-90.

Ghoussayni, S., Stevens, C., Durham, S. and Ewins, D., 2004. Assessment and validation of a simple automated method for the detection of gait events and intervals. *Gait Posture*, 20 (3), 266-272.

Glonek, G. and Wojciechowski, A., 2016. Hybrid Method of Human Limb Joints Positioning—Hand Movement Case Study. *Information Technologies in Medicine*. Springer, 307-320.

Gong, J., Lach, J., Qi, Y. and Goldman, M. D., 2015. Causal analysis of inertial body sensors for enhancing gait assessment separability towards multiple sclerosis diagnosis, *Wearable and Implantable Body Sensor Networks (BSN), 2015 IEEE 12th International Conference on* (pp. 1-6): IEEE.

González, I., Fontecha, J., Hervás, R. and Bravo, J., 2015. An ambulatory system for gait monitoring based on wireless sensorized insoles. *Sensors*, 15 (7), 16589-16613.

Goodall, C., 1991. Procrustes methods in the statistical analysis of shape. *Journal Royal Statistical Society, Series B-Methodological*, 53 (2), 285-339.

Gouwanda, D. and Arosha, S., 2011. Identifying gait asymmetry using gyroscopes—A cross-correlation and Normalized Symmetry Index approach. *Journal of Biomechanics*, 44 (5), 972-978.

Gower, J. C., 1975. Generalized Procrustes analysis. *Psychometrika*, 40 (1), 33-51.

Gower, J. C. and Dijksterhuis, G. B., 2004. *Procrustes Problems*. Oxford University Press, Oxford.

Goyal, P., Ribeiro, V. J., Saran, H. and Kumar, A., 2011. Strap-down pedestrian dead-reckoning system, *Indoor Positioning and Indoor Navigation (IPIN), 2011 International Conference on* (pp. 1-7): IEEE.

Graham, D. L., Ferreira, H. A. and Freitas, P. P., 2004. Magnetoresistive-based biosensors and biochips. *TRENDS in Biotechnology*, 22 (9), 455-462.

Gravina, R., Alinia, P., Ghasemzadeh, H. and Fortino, G., 2017. Multi-sensor fusion in body sensor networks: State-of-the-art and research challenges. *Information Fusion*, 35, 68-80.

Greene, B. R., McGrath, D., O'Neill, R., O'Donovan, K. J., Burns, A. and Caulfield, B., 2010a. An adaptive gyroscope-based algorithm for temporal gait analysis. *Medical & biological engineering & computing*, 48 (12), 1251-1260.

Greene, B. R., O'Donovan, A., Romero-Ortuno, R., Cogan, L., Scanaill, C. N. and Kenny, R. A., 2010b. Quantitative Falls Risk Assessment Using the Timed Up and Go Test. *IEEE Transactions on Biomedical Engineering*, 57 (12), 2918-2926.

Gubbi, J., Buyya, R., Marusic, S. and Palaniswami, M., 2013. Internet of Things (IoT): A vision, architectural elements, and future directions. *Future generation computer systems*, 29 (7), 1645-1660.

Gunatilaka, A. H. and Baertlein, B. A., 2001. Feature-level and decision-level fusion of noncoincidently sampled sensors for land mine detection. *IEEE transactions on pattern analysis and machine intelligence*, 23 (6), 577-589.

Guo, Y., Zhao, G., Liu, Q., Mei, Z., Ivanov, K. and Wang, L., 2013. Balance and knee extensibility evaluation of hemiplegic gait using an inertial body sensor network. *Biomedical engineering online*, 12 (1), 83.

Guthrie, S., Bienkowska-Gibbs, T., Manville, C., Pollitt, A., Kirtley, A. and Wooding, S., 2015. The impact of the National Institute for Health Research Health Technology Assessment programme, 2003–13: a multimethod evaluation.

Hadi, B., Mobyen Uddin, A. and Amy, L., 2013. Data Mining for Wearable Sensors in Health Monitoring Systems: A Review of Recent Trends and Challenges. *Sensors*, 13, 17472-17500.

Hanly, R., Doyle, F., Whitehouse, S. and Timperley, A., 2016. OUTPATIENT 3-D GAIT ANALYSIS ONE YEAR AFTER THA USING A PORTABLE IMU SYSTEM. *Orthopaedic Proceedings*, 98-B (SUPP 11), 1-1.

Hart, H. F., Culvenor, A. G., Collins, N. J., Ackland, D. C., Cowan, S. M., Machotka, Z. and Crossley, K. M., 2015. Knee kinematics and joint moments during gait following anterior cruciate ligament reconstruction: a systematic review and meta-analysis. *Br J Sports Med*, bjsports-2015-094797.

Hasan, A. M., Samsudin, K., Ramli, A. R., Azmir, R. S. and Ismaeel, S. A., 2009. A review of navigation systems (integration and algorithms). *Australian journal of basic and applied sciences*, 3 (2), 943-959.

Hausdorff, J. M. and Alexander, N. B., 2005. *Gait disorders: evaluation and management*. Taylor & Francis US.

Hausdorff, J. M., Cudkowicz, M. E., Firtion, R., Wei, J. Y. and Goldberger, A. L., 1998. Gait variability and basal ganglia disorders: Stride-to-stride variations of gait cycle timing in parkinson's disease and Huntington's disease. *Movement disorders*, 13 (3), 428-437.

Hausdorff, J. M., Rios, D. A. and Edelberg, H. K., 2001. Gait variability and fall risk in community-living older adults: a 1-year prospective study. *Archives of Physical Medicine and Rehabilitation*, 82 (8), 1050-1056.

Healy, M. and Perry, C., 2000. Comprehensive criteria to judge validity and reliability of qualitative research within the realism paradigm. *Qualitative market research: An international journal*, 3 (3), 118-126.

Heck, A. and van Dongen, C., 2008. Gait analysis by high school students. *Physics Education*, 43 (3), 284.

Hegde, N., Bries, M. and Sazonov, E., 2016. A Comparative Review of Footwear-Based Wearable Systems. *Electronics*, 5 (3), 48.

HenkMuller, C. C., 2003. Personal position measurement using dead reckoning, *Proceedings of the Seventh IEEE International Symposium on Wearable Computers (ISWC03)* (Vol. 1530, pp. 17-00).

Herzog, W., Nigg, B. M., Read, L. J. and Olsson, E., 1989. Asymmetries in ground reaction force patterns in normal human gait. *Med Sci Sports Exerc*, 21 (1), 110-114.

Hess, R. J., Brach, J. S., Piva, S. R. and VanSwearingen, J. M., 2010. Walking Skill Can Be Assessed in Older Adults: Validity of the Figure-of-8 Walk Test. *Physical Therapy*, 90 (1), 89-99.

Hikihara, Y., Tanaka, C., Oshima, Y., Ohkawara, K., Ishikawa-Takata, K. and Tanaka, S., 2014. Prediction models discriminating between nonlocomotive and locomotive activities in children using a triaxial accelerometer with a gravity-removal physical activity classification algorithm. *PLoS One*, 9 (4), e94940.

Hodt-Billington, C., Helbostad, J. L. and Moe-Nilssen, R., 2008. Should trunk movement or footfall parameters quantify gait asymmetry in chronic stroke patients? *Gait Posture*, 27 (4), 552-558.

Hodt-Billington, C., Helbostad, J. L., Vervaat, W., Rognsvag, T. and Moe-Nilssen, R., 2011. Changes in gait symmetry, gait velocity and self-reported function following total hip replacement. *J Rehabil Med*, 43 (9), 787-793.

Hollman, J. H., Watkins, M. K., Imhoff, A. C., Braun, C. E., Akervik, K. A. and Ness, D. K., 2016. A comparison of variability in spatiotemporal gait parameters between treadmill and overground walking conditions. *Gait & posture*, 43, 204-209.

Holzreiter, S. H. and Köhle, M. E., 1993. Assessment of gait patterns using neural networks. *Journal of Biomechanics*, 26 (6), 645-651.

How, T. V., Chee, J., Wan, E. and Mihailidis, A., 2013. MyWalk: A mobile app for gait asymmetry rehabilitation in the community, *2013 7th International Conference on Pervasive Computing Technologies for Healthcare and Workshops* (pp. 73-76).

Howell, A. M., Kobayashi, T., Hayes, H. A., Foreman, K. B. and Bamberg, S. J. M., 2013. Kinetic gait analysis using a low-cost insole. *IEEE Transactions on Biomedical Engineering*, 60 (12), 3284-3290.

Hsu, Y.-L., Chung, P.-C., Wang, W.-H., Pai, M.-C., Wang, C.-Y., Lin, C.-W., Wu, H.-L. and Wang, J.-S., 2014. Gait and balance analysis for patients with Alzheimer's disease using an inertial-sensor-based wearable instrument. *IEEE journal of biomedical and health informatics*, 18 (6), 1822-1830.

IBM Corp, 2016. *IBM SPSS Statistics for Windows*. 24 [Armonk, NY: IBM Corp.

Igual, R., Medrano, C. and Plaza, I., 2013. Challenges, issues and trends in fall detection systems. *BioMedical Engineering OnLine*, 12 (1), 1-24.

Ihlen, E. A., Weiss, A., Beck, Y., Helbostad, J. L. and Hausdorff, J. M., 2016. A comparison study of local dynamic stability measures of daily life walking in older adult community-dwelling fallers and non-fallers. *Journal of biomechanics*, 49 (9), 1498-1503.

IJmker, T. and Lamoth, C. J., 2012. Gait and cognition: the relationship between gait stability and variability with executive function in persons with and without dementia. *Gait & posture*, 35 (1), 126-130.

Ilyas, M., Cho, K., Baeg, S.-H. and Park, S., 2016. Drift reduction in pedestrian navigation system by exploiting motion constraints and magnetic field. *Sensors*, 16 (9), 1455.

Inc, Y. L., 2015. *3-Space™ Wireless 2.4GHz DSSS* [online]. Available from: https://yostlabs.com/product/3-space-wireless-2-4ghz-dsss/ [Accessed 10/12/2015].

Instruments, T., Sensor Tag CC2650STK.

Intille, S. S., Lester, J., Sallis, J. F. and Duncan, G., 2012. New horizons in sensor development. *Med Sci Sports Exerc*, 44 (1 Suppl 1), S24-31.

Iosa, M., Fusco, A., Marchetti, F., Morone, G., Caltagirone, C., Paolucci, S. and Peppe, A., 2013. The Golden Ratio of Gait Harmony: Repetitive Proportions of Repetitive Gait Phases. *BioMed Research International*, 2013, 7.

Islam, S. R., Kwak, D., Kabir, M. H., Hossain, M. and Kwak, K.-S., 2015. The internet of things for health care: a comprehensive survey. *IEEE Access*, 3, 678-708.

Jarchi, D., Pope, J., Lee, T. K., Tamjidi, L., Mirzaei, A. and Sanei, S., 2018. A Review on Accelerometry Based Gait Analysis and Emerging Clinical Applications. *IEEE Reviews in Biomedical Engineering*.

Jarchi, D., Wong, C., Kwasnicki, R. M., Heller, B., Tew, G. A. and Yang, G.-Z., 2014. Gait parameter estimation from a miniaturized ear-worn sensor using singular spectrum analysis and longest common subsequence. *IEEE Transactions on Biomedical Engineering*, 61 (4), 1261-1273.

Jonathan Vespa, David M. Armstrong and Lauren Medina, 2018. Demographic Turning Points for the United States: Population Projections for 2020 to 2060 *Population Estimates and Projections*.

Judge, J. O., 2016. Gait Disorders in the Elderly. *MSD and the MSD Manuals* [online].

Kalkbrenner, C., Hacker, S., Algorri, M.-E. and Blechschmidt-Trapp, R., 2014. Motion Capturing with Inertial Measurement Units and Kinect, *Proceedings of the International Joint Conference on Biomedical Engineering Systems and Technologies-Volume 1* (pp. 120-126): SCITEPRESS-Science and Technology Publications, Lda.

Kalman, R. E., 1960. A new approach to linear filtering and prediction problems. *Journal of basic Engineering*, 82 (1), 35-45.

Kang, H. G. and Dingwell, J. B., 2008. Effects of walking speed, strength and range of motion on gait stability in healthy older adults. *Journal of biomechanics*, 41 (14), 2899-2905.

Karantonis, D. M., Narayanan, M. R., Mathie, M., Lovell, N. H. and Celler, B. G., 2006. Implementation of a real-time human movement classifier using a triaxial accelerometer for ambulatory monitoring. *IEEE transactions on information technology in biomedicine*, 10 (1), 156-167.

Kaufman, K. R., Miller, L. S. and Sutherland, D. H., 1996. Gait Asymmetry in Patients with Limb-Length Inequality. *Journal of Pediatric Orthopaedics*, 16 (2), 144-150.

Kavanagh, J. J., 2009. Lower trunk motion and speed-dependence during walking. *Journal of NeuroEngineering and Rehabilitation*, 6 (1), 9.

Kelly, H., 2000. Old Bailey Central Criminal Court London. *RV Saunders Google Scholar*.

Ken Ying-Kai Liao, Chuang-Chien Chiu and Shoou-Jeng Yeh, 2015. A Novel Approach for Classification of Congestive Heart Failure Using Relatively Short-term ECG Waveforms and SVM Classifier, *Proceedings of the International MultiConference of Engineers and Computer Scientists* (Vol. 1, pp. 47-50). Hong Kong.

Kendall, D. G., 1977. The diffusion of shape. *Advances in Applied Probability*, 9, 428–430.

Kendall, D. G., 1984. Shape manifolds, Procrustean metrics and complex projective spaces. *Bulletin of the London Mathematical Society*, 16 (2), 81-121.

Kendall, D. G., Barden, D., Carne, T. K. and Le, H., 1999. *Shape and Shape Theory*. Wiley, Chichester.

Khan, A. M., Young-Koo, L., Lee, S. Y. and Tae-Seong, K., 2010. A Triaxial Accelerometer-Based Physical-Activity Recognition via Augmented-Signal Features and a Hierarchical Recognizer. *Information Technology in Biomedicine, IEEE Transactions on*, 14 (5), 1166-1172.

Khan, S. S. and Hoey, J., 2017. Review of fall detection techniques: A data availability perspective. *Medical engineering & physics*, 39, 12-22.

Khandoker, A. H., Lai, D. T. H., Begg, R. K. and Palaniswami, M., 2007. Wavelet-based feature extraction for support vector machines for screening balance impairments in the elderly. *IEEE Trans Neural Syst Rehabil Eng*, 15 (4), 587-597.

Kim, J. W., Jang, H. J., Hwang, D.-H. and Park, C., 2004. A step, stride and heading determination for the pedestrian navigation system. *Positioning*, 1 (08), 0.

Kirtley, C., 2006. *Clinical gait analysis: theory and practice*. Elsevier Health Sciences.

Kitagawa, N. and Ogihara, N., 2016. Estimation of foot trajectory during human walking by a wearable inertial measurement unit mounted to the foot. *Gait Posture*, 45, 110-114.

Kramer, J. F., 1997. Accurate, rapid, reliable position sensing using multiple sensing technologies: Google Patents.

Kressig, R. W. and Beauchet, O., 2006. Guidelines for clinical applications of spatio-temporal gait analysis in older adults. *Aging clinical and experimental research*, 18 (2), 174-176.

Krigslund, R., Dosen, S., Popovski, P., Dideriksen, J. L., Pedersen, G. F. and Farina, D., 2013. A novel technology for motion capture using passive UHF RFID tags. *IEEE Transactions on Biomedical Engineering*, 60 (5), 1453-1457.

Krishnan, C., Washabaugh, E. P. and Seetharaman, Y., 2015. A low cost real-time motion tracking approach using webcam technology. *Journal of biomechanics*, 48 (3), 544-548.

Kristof, W. and Wingersky, B., 1971. Generalization of the orthogonal Procrustes rotation procedure to more than two matrices. *Proceedings of the 79th Annual Convention of the American Psychological Association*, 6, 89-90.

Kuipers, J., 2002. Quaternions and Rotation Sequences: A Primer with Applications to Orbits, Aerospace and Virtual Reality (p. 400): Princeton: Princeton University Press.[Links].

Kutilek, P., Socha, V., Viteckova, S. and Svoboda, Z., 2014. Quantification of gait asymmetry in patients with ankle foot orthoses based on hip–hip cyclograms. *Biocybernetics and Biomedical Engineering*, 34 (1), 46-52.

Lai, C.-F., Chen, M., Pan, J.-S., Youn, C.-H. and Chao, H.-C., 2014. A collaborative computing framework of cloud network and WBSN applied to fall detection and 3-D motion reconstruction. *IEEE journal of biomedical and health informatics*, 18 (2), 457-466.

Lai, D. T., Begg, R. K., Taylor, S. and Palaniswami, M., 2008. Detection of tripping gait patterns in the elderly using autoregressive features and support vector machines. *Journal of biomechanics*, 41 (8), 1762-1772.

Lan, K.-C. and Shih, W.-Y., 2013. On calibrating the sensor errors of a PDR-based indoor localization system. *Sensors*, 13 (4), 4781-4810.

Lapham, A. and Bartlett, R., 1995. The use of artificial intelligence in the analysis of sports performance: A review of applications in human gait analysis and future directions for sports biomechanics. *Journal of Sports Sciences*, 13 (3), 229-237.

Laroche, D., Tolambiya, A., Morisset, C., Maillefert, J., French, R. M., Ornetti, P. and Thomas, E., 2014. A classification study of kinematic gait trajectories in hip osteoarthritis. *Computers in biology and medicine*, 55, 42-48.

Larsen, P., Laessoe, U., Rasmussen, S., Graven-Nielsen, T., Berre Eriksen, C. and Elsoe, R., 2017. Asymmetry in gait pattern following tibial shaft fractures – a prospective one-year follow-up study of 49 patients. *Gait & Posture*, 51, 47-51.

Laskoski, G., Martins, L., Pichorim, S. and Abatti, P., 2009. Development of a telemetric goniometer, *World Congress on Medical Physics and Biomedical Engineering, September 7-12, 2009, Munich, Germany* (pp. 227-230): Springer.

Le, H., 2016. Mean size-and-shapes and mean shapes: a geometric point of view. *Advances in Applied Probability*, 27 (1), 44-55.

LeCompte, M. D. and Goetz, J. P., 1982. Problems of reliability and validity in ethnographic research. *Review of educational research*, 52 (1), 31-60.

Leddy, A. L., Crowner, B. E. and Earhart, G. M., 2011. Functional gait assessment and balance evaluation system test: reliability, validity, sensitivity, and specificity for identifying individuals with Parkinson disease who fall. *Physical Therapy*, 91 (1), 102.

Lee, H.-h., Choi, S. and Lee, M.-j., 2015. Step Detection Robust against the Dynamics of Smartphones. *Sensors*, 15 (10), 27230.

Lee, J. A., Cho, S. H., Lee, J. W., Lee, K. H. and Yang, H. K., 2007. Wearable Accelerometer System for Measuring the Temporal Parameters of Gait, *2007 29th Annual International Conference of the IEEE Engineering in Medicine and Biology Society* (pp. 483-486).

Lees, A., 2002. Technique analysis in sports: a critical review. *Journal of sports sciences*, 20 (10), 813-828.

Lehoux, P., Roncarolo, F., Rocha Oliveira, R. and Pacifico Silva, H., 2016. Medical innovation and the sustainability of health systems: A historical perspective on technological change in health. *Health Services Management Research*, 29 (4), 115-123.

Lele, S., 1991. Some comments on coordinate-free and scale-invariant methods in morphometrics. *American Journal of Physical Anthropology*, 85, 407-417.

Lele, S., 1993. Euclidean distance matrix analysis (EDMA): estimation of mean form and mean form difference. *Mathematical Geology*, 25 (5), 573-602.

Lele, S., 1999. Invariance and morphometrics: a critical appraisal of statistical techniques for landmark data. *In:* Chaplain, M. A. J., Singh, G. D. and McLachlan, J. C., eds. *On Growth and Forms: Spatio-temporal Pattern Formation in Biology.* Chichester: John Wiley and Sons Ltd, 325-336.

Lele, S. and Cole III, T. M., 1996. A new test for shape differences when variance-covariance matrices are unequal. *Journal of Human Evolution*, 31 (193-212).

Lele, S. and McCulloch, C., 2002. Invariance, identifiability, and morphometrics. *Journal of the American Statistical Association*, 97 (459), 796-804.

Lele, S. and Richtsmeier, J., 1991. Euclidean distance matrix analysis: a coordinate-free approach for comparing biological shapes using landmark data. *American Journal of Physical Anthropology*, 86 (3), 415-427.

Lele, S. and Richtsmeier, J., 2001. *An Invariant Approach to Statistical Analysis of Shapes*. First edition. London: Chapman and Hall-CRC Press.

Lewek, M. D., Bradley, C. E., Wutzke, C. J. and Zinder, S. M., 2014. The relationship between spatiotemporal gait asymmetry and balance in individuals with chronic stroke. *J Appl Biomech*, 30 (1), 31-36.

Li, Y., Ho, K. C. and Popescu, M., 2012. A microphone array system for automatic fall detection. *IEEE Trans Biomed Eng*, 59 (5), 1291-1301.

Liang, L., Popescu, M., Skubic, M. and Rantz, M., 2014. An automatic fall detection framework using data fusion of Doppler radar and motion sensor network, *Engineering in Medicine and Biology Society (EMBC), 2014 36th Annual International Conference of the IEEE* (pp. 5940-5943).

Liang, L., Popescu, M., Skubic, M., Rantz, M., Yardibi, T. and Cuddihy, P., 2011. Automatic fall detection based on Doppler radar motion signature, *Pervasive Computing Technologies for Healthcare (PervasiveHealth), 2011 5th International Conference on* (pp. 222-225).

Lin, L. I., 1989. A concordance correlation coefficient to evaluate reproducibility. *Biometrics*, 45 (1), 255-268.

Lincoln, L. S., Bamberg, S. J. M., Parsons, E., Salisbury, C. and Wheeler, J., 2012. An elastomeric insole for 3-axis ground reaction force measurement, *Biomedical Robotics and Biomechatronics (BioRob), 2012 4th IEEE RAS & EMBS International Conference on* (pp. 1512-1517): IEEE.

Lipsitz, L. A., Lough, M., Niemi, J., Travison, T., Howlett, H. and Manor, B., 2015. A shoe insole delivering subsensory vibratory noise improves balance and gait in healthy elderly people. *Archives of physical medicine and rehabilitation*, 96 (3), 432-439.

Liu, D.-X., Wu, X., Du, W., Wang, C. and Xu, T., 2016. Gait Phase Recognition for Lower-Limb Exoskeleton with Only Joint Angular Sensors. *Sensors*, 16 (10), 1579.

Llinas, J. and Hall, D. L., 1998. An introduction to multi-sensor data fusion, *Circuits and Systems, 1998. ISCAS'98. Proceedings of the 1998 IEEE International Symposium on* (Vol. 6, pp. 537-540): IEEE.

Lo, B., Thiemjarus, S., Panousopoulou, A. and Yang, G.-Z., 2013. Bioinspired design for body sensor networks [life sciences]. *IEEE Signal Processing Magazine*, 30 (1), 165-170.

López, P., Fernández, D., Jara, A. J. and Skarmeta, A. F., 2013. Survey of internet of things technologies for clinical environments, *Advanced Information Networking and Applications Workshops (WAINA), 2013 27th International Conference on* (pp. 1349-1354): IEEE.

Lopreite, M. and Mauro, M., 2017. The effects of population ageing on health care expenditure: a Bayesian VAR analysis using data from Italy. *Health policy*, 121 (6), 663-674.

Lovejoy, C. O., 1988. Evolution of human walking. *Scientific American*, 259 (5), 118-125.

Mackenbach, J. P., 2012. The persistence of health inequalities in modern welfare states: the explanation of a paradox. *Social science & medicine*, 75 (4), 761-769.

Madgwick, S., 2010. An efficient orientation filter for inertial and inertial/magnetic sensor arrays. *Report x-io and University of Bristol (UK)*, 25, 113-118.

Mahony, R., Hamel, T. and Pflimlin, J.-M., 2008. Nonlinear complementary filters on the special orthogonal group. *IEEE Transactions on automatic control*, 53 (5), 1203-1218.

Maki, B. E., 1997. Gait Changes in Older Adults: Predictors of Falls or Indicators of Fear? *Journal of the American Geriatrics Society*, 45 (3), 313-320.

Maki, H., Ogawa, H., Yonezawa, Y., Hahn, A. and Caldwell, W., 2012. A new ultrasonic stride length measuring system. *Biomedical sciences instrumentation*, 48, 282-287.

Manal, K. and Stanhope, S. J., 2004. A novel method for displaying gait and clinical movement analysis data. *Gait & Posture*, 20 (2), 222-226.

Manyika, J., Chui, M., Bisson, P., Woetzel, J., Dobbs, R., Bughin, J. and Aharon, D., 2015. Unlocking the Potential of the Internet of Things. *McKinsey Global Institute*.

Markowitz, J. and Herr, H., 2016. Human Leg Model Predicts Muscle Forces, States, and Energetics during Walking. *PLOS Computational Biology*, 12 (5), e1004912.

Marquis, S., Moore, M. M., Howieson, D. B., Sexton, G., Payami, H., Kaye, J. A. and Camicioli, R., 2002. Independent predictors of cognitive decline in healthy elderly persons. *Archives of neurology*, 59 (4), 601-606.

Marschollek, M., Wolf, K.-H., Gietzelt, M., Nemitz, G., Meyer zu Schwabedissen, H. and Haux, R., 2008. Assessing elderly persons' fall risk using spectral analysis on accelerometric data - a clinical evaluation study, *Engineering in Medicine and Biology Society, 2008. EMBS 2008. 30th Annual International Conference of the IEEE* (pp. 3682-3685).

Marti, K., 2005. *Stochastic optimization methods*. Vol. 2. Springer.

Mathias, S., Nayak, U. and Isaacs, B., 1986. Balance in elderly patients: the" get-up and go" test. *Archives of physical medicine and rehabilitation*, 67 (6), 387-389.

Matt, C., Hess, T. and Benlian, A., 2015. Digital transformation strategies. *Business & Information Systems Engineering*, 57 (5), 339-343.

Matthews, C. E., Hagströmer, M., Pober, D. M. and Bowles, H. R., 2012. Best practices for using physical activity monitors in population-based research. *Medicine and science in sports and exercise*, 44 (1 Suppl 1), S68-S76.

MbientLab, (accessed on 03/08/2016). https://mbientlab.com/docs/MetaWearCPSv0.5.pdf

Meijer, G. A., Westerterp, K. R., Verhoeven, F. M., Koper, H. B. and ten Hoor, F., 1991. Methods to assess physical activity with special reference to motion sensors and accelerometers. *IEEE Transactions on Biomedical Engineering*, 38 (3), 221-229.

Meng, X., Yu, H. and Tham, M. P., 2013. Gait phase detection in able-bodied subjects and dementia patients, *Engineering in Medicine and Biology Society (EMBC), 2013 35th Annual International Conference of the IEEE* (pp. 4907-4910): IEEE.

Mentiplay, B. F., Perraton, L. G., Bower, K. J., Pua, Y.-H., McGaw, R., Heywood, S. and Clark, R. A., 2015. Gait assessment using the Microsoft Xbox One Kinect: Concurrent validity and inter-day reliability of spatiotemporal and kinematic variables. *Journal of biomechanics*, 48 (10), 2166-2170.

Merryn, J. M., Adelle, C. F. C., Nigel, H. L. and Branko, G. C., 2004. Accelerometry: providing an integrated, practical method for long-term, ambulatory monitoring of human movement. *Physiological Measurement*, 25 (2), R1.

Michael and Whittle, 2002. *Gait Analysis: An Introduction*. Oxford: Butterworth Heinmann.

Michael Whittle, 2002. *Gait Analysis: An Introduction*. Oxford: Butterworth Heinmann.

Mikos, V., Heng, C. H., Tay, A., Chia, N. S. Y., Koh, K. M. L., Tan, D. M. L., Au, W. L. and Ieee, 2017. *Optimal Window Lengths, Features and Subsets Thereof for Freezing of Gait Classification*. New York: Ieee.

Miller, R. A., Thaut, M. H., McIntosh, G. C. and Rice, R. R., 1996. Components of EMG symmetry and variability in parkinsonian and healthy elderly gait. *Electroencephalogr Clin Neurophysiol*, 101 (1), 1-7.

Minetti, A. E., 2000. The three modes of terrestrial locomotion, *Biomechanics and Biology of Movement*. In Benno Maurus Nigg, Brian R. MacIntosh, Joachim Mester: Human Kinetics.

Mizell, D., 2003. Using gravity to estimate accelerometer orientation, *Proc. 7th IEEE Int. Symposium on Wearable Computers (ISWC 2003)* (Vol. 252): Citeseer.

Mladenov, M. and Mock, M., 2009. A step counter service for Java-enabled devices using a built-in accelerometer. *Proceedings of the 1st International Workshop on Context-Aware Middleware and Services: affiliated with the 4th International Conference on Communication System Software and Middleware (COMSWARE 2009)*, Dublin, Ireland. 1554235: ACM. 1-5.

Moeslund, T. B., Hilton, A. and Krüger, V., 2006. A survey of advances in vision-based human motion capture and analysis. *Computer Vision and Image Understanding*, 104 (2), 90-126.

Mohler, B. J., Thompson, W. B., Creem-Regehr, S. H., Pick, H. L. and Warren, W. H., 2007. Visual flow influences gait transition speed and preferred walking speed. *Experimental Brain Research*, 181 (2), 221-228.

Momete, D. C., 2016. Building a sustainable healthcare model: A cross-country analysis. *Sustainability*, 8 (9), 836.

Moncada-Torres, A., Leuenberger, K., Gonzenbach, R., Luft, A. and Gassert, R., 2014. Activity classification based on inertial and barometric pressure sensors at different anatomical locations. *Physiological measurement*, 35 (7), 1245.

Morrison, M. M., 1987. Inertial measurement unit: Google Patents.

Mukhopadhyay, S. C., 2015. Wearable Sensors for Human Activity Monitoring: A Review. *IEEE Sensors Journal*, 15 (3), 1321-1330.

Muro-de-la-Herran, A., Garcia-Zapirain, B. and Mendez-Zorrilla, A., 2014. Gait Analysis Methods: An Overview of Wearable and Non-Wearable Systems, Highlighting Clinical Applications. *Sensors*, 14 (2), 3362-3394.

Murray, M. P., 1967. Gait as a total pattern of movement: including a bibliography on gait. *American Journal of Physical Medicine & Rehabilitation*, 46 (1), 290-333.

Mussarat Yasmin, Muhammad Sharif and Sajjad Mohsin, 2013. Neural Networks in Medical Imaging Applications: A Survey. *World Applied Sciences Journal*, 22 (1), 85-96.

Najafi, B., Aminian, K., Paraschiv-Ionescu, A., Loew, F., Bula, C. J. and Robert, P., 2003. Ambulatory system for human motion analysis using a kinematic sensor: monitoring of daily physical activity in the elderly. *IEEE Transactions on biomedical Engineering*, 50 (6), 711-723.

Nam, Y. and Park, J. W., 2013. Child activity recognition based on cooperative fusion model of a triaxial accelerometer and a barometric pressure sensor. *IEEE journal of biomedical and health informatics*, 17 (2), 420-426.

Nations, U., 2013. World population ageing 2013, *New York, United Nations, Department of Economic and Social Affairs, Population Division*.

Niebles, J. C., Wang, H. and Fei-Fei, L., 2008. Unsupervised learning of human action categories using spatial-temporal words. *International journal of computer vision*, 79 (3), 299-318.

Novak, D., Reberšek, P., De Rossi, S. M. M., Donati, M., Podobnik, J., Beravs, T., Lenzi, T., Vitiello, N., Carrozza, M. C. and Munih, M., 2013. Automated detection of gait initiation and termination using wearable sensors. *Medical Engineering & Physics*, 35 (12), 1713-1720.

Nukala, B. T., Nakano, T., Rodriguez, A., Tsay, J., Lopez, J., Nguyen, T. Q., Zupancic, S. and Lie, D. Y., 2016. Real-time classification of patients with balance disorders vs. normal subjects using a low-cost small wireless wearable gait sensor. *Biosensors*, 6 (4), 58.

O'Donovan, K. J., Kamnik, R., O'Keeffe, D. T. and Lyons, G. M., 2007. An inertial and magnetic sensor based technique for joint angle measurement. *Journal of biomechanics*, 40 (12), 2604-2611.

Okuda, S., Takano, S., Ueno, M., Hara, Y., Chida, Y., Ikkaku, T., Kanda, F. and Toda, T., 2016. Gait analysis of patients with Parkinson's disease using a portable triaxial accelerometer. *Neurology and Clinical Neuroscience*, 4 (3), 93-97.

Oppenheim, A. V., and R.W. Schafer, 1989. *Discrete-Time Signal Processing*. Englewood Cliffs, NJ: Prentice Hall.

Orfanidis, S. J., 1996. *Introduction to Signal Processing*. Englewood Cliffs, New Jersey: Prentice-Hall.

Organization, W. H., 2007. WHO global report on falls prevention in older age. *WHo Global report on falls Prevention in older Age* [online].

Otero, M., 2005. Application of a continuous wave radar for human gait recognition, *Signal Processing, Sensor Fusion, and Target Recognition XIV* (Vol. 5809, pp. 538-549): International Society for Optics and Photonics.

Paranietharan, D. N., 2017. WHO | Bangladesh. *WHO* [online].

Park, Y. S., Lim, Y. T., Koh, K., Kim, J. M., Kwon, H. J., Yang, J. S. and Shim, J. K., 2016. Association of spinal deformity and pelvic tilt with gait asymmetry in adolescent idiopathic scoliosis patients: Investigation of ground reaction force. *Clinical Biomechanics*, 36, 52-57.

Patel, S., Park, H., Bonato, P., Chan, L. and Rodgers, M., 2012. A review of wearable sensors and systems with application in rehabilitation. *Journal of neuroengineering and rehabilitation*, 9 (1), 21.

Patterson, K. K., Gage, W. H., Brooks, D., Black, S. E. and McIlroy, W. E., 2010. Evaluation of gait symmetry after stroke: a comparison of current methods and recommendations for standardization. *Gait & posture*, 31 (2), 241-246.

Patterson, K. K., Parafianowicz, I., Danells, C. J., Closson, V., Verrier, M. C., Staines, W. R., Black, S. E. and McIlroy, W. E., 2008. Gait Asymmetry in Community-Ambulating Stroke Survivors. *Archives of Physical Medicine and Rehabilitation*, 89 (2), 304-310.

Patterson, M., Delahunt, E., Sweeney, K. and Caulfield, B., 2014. An Ambulatory Method of Identifying Anterior Cruciate Ligament Reconstructed Gait Patterns. *Sensors*, 14 (1), 887.

Plasqui, G. and Westerterp, K. R., 2007. Physical activity assessment with accelerometers: an evaluation against doubly labeled water. *Obesity (Silver Spring)*, 15 (10), 2371-2379.

Plotnik, M., Dagan, Y., Gurevich, T., Giladi, N. and Hausdorff, J. M., 2011. Effects of cognitive function on gait and dual tasking abilities in patients with Parkinson's disease suffering from motor response fluctuations. *Experimental Brain Research*, 208 (2), 169-179.

Plotnik, M., Giladi, N., Balash, Y., Peretz, C. and Hausdorff, J. M., 2005. Is freezing of gait in Parkinson's disease related to asymmetric motor function? *Annals of Neurology*, 57 (5), 656-663.

Plotnik, M., Giladi, N. and Hausdorff, J. M., 2007. A new measure for quantifying the bilateral coordination of human gait: effects of aging and Parkinson's disease. *Experimental brain research*, 181 (4), 561-570.

Pogorelc, B., Bosnić, Z. and Gams, M., 2012. Automatic recognition of gait-related health problems in the elderly using machine learning. *Multimedia Tools and Applications*, 58 (2), 333-354.

Polk, J. D., Stumpf, R. M. and Rosengren, K. S., 2017. Limb dominance, foot orientation and functional asymmetry during walking gait. *Gait & Posture*, 52, 140-146.

Poon, C. C., Lo, B. P., Yuce, M. R., Alomainy, A. and Hao, Y., 2015. Body sensor networks: In the era of big data and beyond. *IEEE reviews in biomedical engineering*, 8, 4-16.

Popescu, M., Yun, L., Skubic, M. and Rantz, M., 2008. An acoustic fall detector system that uses sound height information to reduce the false alarm rate, *Engineering in Medicine and Biology Society, 2008. EMBS 2008. 30th Annual International Conference of the IEEE* (pp. 4628-4631).

Pourcelot, P., Audigie, F., Degueurce, C., Denoix, J. M. and Geiger, D., 1997. Kinematic symmetry index: a method for quantifying the horse locomotion symmetry using kinematic data. *Vet Res*, 28 (6), 525-538.

Prevention, C. f. D. C. a., 2015. *Web-based Injury Statistics Query and Reporting System (WISQARS). Available from: http://www.cdc.gov/injury/wisqars Accessed December 23, 2015*.

Qualisys Motion Capture, *https://www.qualisys.com/* [online]. Available from: 04/08/2017].

R Development Core Team, 2018. R: A Language and Environment for Statistical Computing. R Foundation for Statistical Computing, Vienna, Austria.

R. Craven and P. Bruno, 1986. Teach the elderly to prevent falls. *Journal of Gerontology Nursing*, 12, 27 – 33.

Rabiner, L. and Juang, B., 1986. An introduction to hidden Markov models. *IEEE ASSp Magazine*, 3, 4-16.

Rafi, M., Hamid, M. E., Khan, M. S. and Wahidabanu, R., 2011. A parametric approach to gait signature extraction for human motion identification. *International Journal of Image Processing (IJIP)*, 5 (2), 185.

Rainoldi, A., Melchiorri, G. and Caruso, I., 2004. A method for positioning electrodes during surface EMG recordings in lower limb muscles. *Journal of neuroscience methods*, 134 (1), 37-43.

Rebula, J. R., Ojeda, L. V., Adamczyk, P. G. and Kuo, A. D., 2013. Measurement of foot placement and its variability with inertial sensors. *Gait & Posture*, 38 (4), 974-980.

Ribeiro, J., De Castro, J. and Freire, J., 2001. New Improvements in the Digital Double Integration Filtering Method to Measure Displacements Using Accelerometers, *Proceedings-SPIE the International Society for Optical Engineering* (Vol. 1, pp. 538-542): International Society for Optical Engineering; 1999.

Richtsmeier, J., Cheverud, J., Danahey, S., Corner, B. and Lele, S., 1993. Sexual dimorphism of ontogeny in the crab-eating macaque (Macaca fascicularis). *Journal of Human Evolution*, 25, 1-30.

Richtsmeier, J. T., Cheverud, J. and Lele, S. R., 1992. Advances in Anthropological Morphometrics. *Annual Reviews in Anthropology*, 21, 283-305.

Richtsmeier, J. T. and Lele, S., 1993. A coordinate free approach to the analysis of growth patterns: Models and theoretical considerations. *Biological Reviews*, 68, 381-411.

Rispens, S. M., Van Dieën, J. H., Van Schooten, K. S., Cofré Lizama, L. E., Daffertshofer, A., Beek, P. J. and Pijnappels, M., 2016. Fall-related gait characteristics on the treadmill and in daily life. *Journal of NeuroEngineering and Rehabilitation*, 13 (1), 1-9.

Robinson, R., Herzog, W. and Nigg, B., 1987. Use of force platform variables to quantify the effects of chiropractic manipulation on gait symmetry. *Journal of manipulative and physiological therapeutics*, 10 (4), 172-176.

Rodríguez-Martín, D., Pérez-López, C., Samà, A., Cabestany, J. and Català, A., 2013. A Wearable Inertial Measurement Unit for Long-Term Monitoring in the Dependency Care Area. *Sensors*, 13 (10), 14079.

Rosa, M. D., Scientifico-Tecnologico, P., m.dirosa@inrca.it, Stara, V., Scientifico-Tecnologico, P., v.stara@inrca.it, Rossi, L., Scientifico-Tecnologico, P., l.rossi@inrca.it, Breuil, F., Lluch, C.-A. d. E., fbreuil@cetemmsa.com, Reixach, E., Lluch, C.-A. d. E., Paredes, J. G., planta, U. A. d. B. s. E. d. E.-., juan.garcia.paredes@uab.cat, Burkard, S., GmbH&Co, S. T. and s.burkard@springtechno.com, 2015. A Wireless Sensor Insole to Collect and Analyse Gait Data in Real Environment: The WIISEL Project. *Ambient Assisted Living*, 71-80.

Rösevall, J., Rusu, C., Talavera, G., Carrabina, J., Garcia, J., Carenas, C., Breuil, F., Reixach, E., Torrent, M., Burkard, S. and Colitti, W., 2014. A wireless sensor insole for collecting gait data. *Stud Health Technol Inform*, 200, 176-178.

S Flenniken, W., H Wall, J. and M Bevly, D., 2017. *Characterization of Various IMU Error Sources and the Effect on Navigation Performance*.

Sadeghi, H., 2003. Local or global asymmetry in gait of people without impairments. *Gait Posture*, 17 (3), 197-204.

Sadeghi, H., Allard, P., Prince, F. and Labelle, H., 2000. Symmetry and limb dominance in able-bodied gait: a review. *Gait & Posture*, 12 (1), 34-45.

Salzman, B., 2010. Gait and balance disorders in older adults. *The Journal of American Family Physician*, 82 (1), 61-68.

Sant'Anna, A., Salarian, A. and Wickstrom, N., 2011. A new measure of movement symmetry in early Parkinson's disease patients using symbolic processing of inertial sensor data. *IEEE Trans Biomed Eng*, 58 (7), 2127-2135.

Sant'Anna, A., Salarian, A. and Wickstrom, N., 2011. A new measure of movement symmetry in early Parkinson's disease patients using symbolic processing of inertial sensor data. *IEEE Transactions on biomedical engineering*, 58 (7), 2127-2135.

Sazonov, E. S., Fulk, G., Hill, J., Schutz, Y. and Browning, R., 2011. Monitoring of Posture Allocations and Activities by a Shoe-Based Wearable Sensor. *IEEE Transactions on Biomedical Engineering*, 58 (4), 983-990.

Schepers, H. M., Van Asseldonk, E. H., Buurke, J. H. and Veltink, P. H., 2009. Ambulatory estimation of center of mass displacement during walking. *IEEE Transactions on Biomedical Engineering*, 56 (4), 1189-1195.

Schoenemann, P. H. and Carroll, R., 1970. Fitting one matrix to another under choice of a central dilation and a rigid motion. *Psychometrika*, 35 (2), 245-255.

Schonemann, P. H., 1966. A generalized solution of the orthogonal Procrustes problem. *Psychometrika*, 31, 1-10.

Scilingo, E. P., Lorussi, F., Mazzoldi, A. and De Rossi, D., 2003. Strain-sensing fabrics for wearable kinaesthetic-like systems. *IEEE sensors journal*, 3 (4), 460-467.

Seel, T., Raisch, J. and Schauer, T., 2014. IMU-Based Joint Angle Measurement for Gait Analysis. *Sensors*, 14 (4), 6891.

Seliktar, R. and Mizrahi, J., 1986. Some gait characteristics of below-knee amputees and their reflection on the ground reaction forces. *Eng Med*, 15 (1), 27-34.

Shakoor, N., Hurwitz, D. E., Block, J. A., Shott, S. and Case, J. P., 2003. Asymmetric knee loading in advanced unilateral hip osteoarthritis. *Arthritis Rheum*, 48 (6), 1556-15561.

Shaltis, P. A., Reisner, A. and Asada, H. H., 2006. Wearable, cuff-less PPG-based blood pressure monitor with novel height sensor, *Engineering in Medicine and Biology Society, 2006. EMBS'06. 28th Annual International Conference of the IEEE* (pp. 908-911): IEEE.

Shelat, A. M., 2/3/2015. *Evidence-Based Physical Diagnosis, 3rd Edition* [online]. U.S. National Library of Medicine: Available from: https://www.nlm.nih.gov/medlineplus/ency/article/003199.htm [Accessed 30/06/2016].

Shorter, K. A., Polk, J. D., Rosengren, K. S. and Hsiao-Wecksler, E. T., 2008. A new approach to detecting asymmetries in gait. *Clinical Biomechanics*, 23 (4), 459-467.

Shrout, P. E. and Fleiss, J. L., 1979. Intraclass correlations: uses in assessing rater reliability. *Psychological bulletin*, 86 (2), 420.

Shumway-Cook, A. and Horak, F. B., 1986. Assessing the influence of sensory interaction on balance: suggestion from the field. *Physical therapy*, 66 (10), 1548-1550.

Skinner, H. B. and Effeney, D. J., 1985. Gait analysis in amputees. *American journal of physical medicine*, 64 (2), 82-89.

Slifka, L. D., 2004. *An accelerometer based approach to measuring displacement of a vehicle body*. University of Michigan–Dearborn.

Snijders, A. H., van de Warrenburg, B. P., Giladi, N. and Bloem, B. R., Neurological gait disorders in elderly people: clinical approach and classification. *The Lancet Neurology*, 6 (1), 63-74.

SolidWorks, I., 2002. Solidworks corporation. *Concord, MA*.

Song, Y., Shin, S., Kim, S., Lee, D. and Lee, K. H., 2007. Speed Estimation From a Tri-axial Accelerometer Using Neural Networks, *2007 29th Annual International Conference of the IEEE Engineering in Medicine and Biology Society* (pp. 3224-3227).

Starlino, 2009. A Guide to using IMU (Accelerometer and Gyroscope Devices) in Embedded Applications.

Steultjens, M. P. M., Dekker, J., Baar, M. E. v., Oostendorp, R. A. B. and Bijlsma, J. W. J., 2000. Range of joint motion and disability in patients with osteoarthritis of the knee or hip. *Rheumatology*, 39 (9), 955-961.

Storm, M. and Edwards, A., 2013. Models of user involvement in the mental health context: intentions and implementation challenges. *Psychiatric Quarterly*, 84 (3), 313-327.

Su, B. L., Song, R., Guo, L. Y. and Yen, C. W., 2015. Characterizing gait asymmetry via frequency sub-band components of the ground reaction force. *Biomedical Signal Processing and Control*, 18, 56-60.

Su, F.-C. and Wu, W.-L., 2000. Design and testing of a genetic algorithm neural network in the assessment of gait patterns. *Medical engineering and Physics*, 22 (1), 67-74.

Sukumar, C. F. P. and Hazas, M., 2012. Tutorial: implementation of a pedestrian tracker using foot-mounted inertial sensors. *IEEE Pervasive Computing*.

Tahir Khan, R. G., August 2012. Gait alterations associated with diabetic neuropathy | Lower Extremity Review Magazine.

Tannous, H., Istrate, D., Benlarbi-Delai, A., Sarrazin, J., Gamet, D., Ho Ba Tho, M. C. and Dao, T. T., 2016. A new multi-sensor fusion scheme to improve the accuracy of knee flexion kinematics for functional rehabilitation movements. *Sensors*, 16 (11), 1914.

Tao, W., Liu, T., Zheng, R. and Feng, H., 2012. Gait analysis using wearable sensors. *Sensors*, 12 (2), 2255-2283.

Tasch, U., Moubarak, P., Tang, W., Zhu, L., Lovering, R., Roche, J. and Bloch, R., 2008. An Instrument That Simultaneously Measures Spatiotemporal Gait Parameters and Ground Reaction Forces of Locomoting Rats, *ASME 2008 9th Biennial Conference on*

Engineering Systems Design and Analysis (pp. 45-49): American Society of Mechanical Engineers.

Team, R. D. C., 2017. *R: A Language and Environment for Statistical Computing*.

Ten Berge, J. M. F., 1977. Orthogonal Procrustes rotation for two or more matrices. *Psychometrika*, 42, 267-276.

Terrier, P. and Schutz, Y., 2005. How useful is satellite positioning system (GPS) to track gait parameters? A review. *Journal of neuroengineering and rehabilitation*, 2 (1), 28.

The Institute of Electrical and Electronics Engineers, I., 2018. *IEEE 804.15.6 Standard on Wireless Body Area Networks* [online]. Available from: http://www.ieee802.org/15/pub/TG6.html [Accessed 01/08/2018].

The MathWorks Inc, 2016. *Find local maxima-MATLAB findpeaks, MathWorks United Kingdom* [online]. Available from: https://uk.mathworks.com/help/signal/ref/findpeaks.html [Accessed 14/12/2016].

Thi Hong Nhan Vua, Namkyu Parka, Yang Koo Leeb, Yongmi Leeb, Jong Yun Leec and Keun Ho Ryub, 2010. Online discovery of Heart Rate Variability patterns in mobile healthcare services. *Journal of Systems and Software*, 83, 1930-1940.

Thingstad, P., Egerton, T., Ihlen, E. F., Taraldsen, K., Moe-Nilssen, R. and Helbostad, J. L., 2015. Identification of gait domains and key gait variables following hip fracture. *BMC geriatrics*, 15 (1), 150.

Thong, Y. K., Woolfson, M. S., Crowe, J. A., Hayes-Gill, B. R. and Jones, D. A., 2004. Numerical double integration of acceleration measurements in noise. *Measurement*, 36 (1), 73-92.

Tian, Y., Meng, X., Tao, D., Liu, D. and Feng, C., 2015. Upper limb motion tracking with the integration of IMU and Kinect. *Neurocomputing*, 159, 207-218.

Tinetti, M. E., 1986. Performance-oriented assessment of mobility problems in elderly patients. *Journal of the American Geriatrics Society*, 34 (2), 119-126.

Tinetti, M. E., Williams, T. F. and Mayewski, R., 1986. Fall risk index for elderly patients based on number of chronic disabilities. *The American journal of medicine*, 80 (3), 429-434.

Tognetti, A., Bartalesi, R., Lorussi, F. and De Rossi, D., 2007. Body segment position reconstruction and posture classification by smart textiles. *Transactions of the Institute of Measurement and Control*, 29 (3-4), 215-253.

Tognetti, A., Lorussi, F., Carbonaro, N. and De Rossi, D., 2015. Wearable goniometer and accelerometer sensory fusion for knee joint angle measurement in daily life. *Sensors*, 15 (11), 28435-28455.

Tong, K. and Granat, M. H., 1999. A practical gait analysis system using gyroscopes. *Medical engineering and physics*, 21 (2), 87-94.

Topol, E. J. and Hill, D., 2012. *The creative destruction of medicine: How the digital revolution will create better health care*. Basic Books New York.

Trueblood, P. and Rubenstein, L., 1991. Assessment of instability and gait in elderly persons. *Comprehensive therapy*, 17 (8), 20-29.

Truong, P., Lee, J., Kwon, A.-R. and Jeong, G.-M., 2016. Stride Counting in Human Walking and Walking Distance Estimation Using Insole Sensors. *Sensors*, 16 (6), 823.

Tunca, C., Pehlivan, N., Ak, N., Arnrich, B., Salur, G. and Ersoy, C., 2017. Inertial sensor-based robust gait analysis in non-hospital settings for neurological disorders. *Sensors*, 17 (4), 825.

Union, I. T., 2005. ITU Internet Reports. The Internet of Things: 7th Edition.

Urbanek, J. K., Harezlak, J., Glynn, N. W., Harris, T., Crainiceanu, C. and Zipunnikov, V., 2017. Stride variability measures derived from wrist- and hip-worn accelerometers. *Gait & Posture*, 52, 217-223.

Vagenas, G. and Hoshizaki, B., 1992. A Multivariable Analysis of Lower Extremity Kinematic Asymmetry in Running. *International Journal of Sport Biomechanics*, 8 (1), 11-29.

van der Linde, H., Hofstad, C. J., Geurts, A. C., Postema, K., Geertzen, J. H. and van Limbeek, J., 2004. A systematic literature review of the effect of different prosthetic components on human functioning with a lower-limb prosthesis. *J Rehabil Res Dev*, 41 (4), 555-570.

van Nuenen, B. F. L., Esselink, R. A. J., Munneke, M., Speelman, J. D., van Laar, T. and Bloem, B. R., 2008. Postoperative gait deterioration after bilateral subthalamic nucleus stimulation in Parkinson's disease. *Movement Disorders*, 23 (16), 2404-2406.

Vander Linden, D. W., 1996. Shumway-Cook A, Wollacott MH. Motor Control: Theory and Practical Applications. Baltimore, Md:: Williams and Wilkins Inc; 1995. Hardcover, 475 pp, $43. *Journal of Neurologic Physical Therapy*, 20 (1), 64-65.

VanSwearingen, J. M., Paschal, K. A., Bonino, P. and Yang, J.-F., 1996. The modified Gait Abnormality Rating Scale for recognizing the risk of recurrent falls in community-dwelling elderly adults. *Physical Therapy*, 76 (9), 994-1002.

Verghese, J., Wang, C., Lipton, R. B., Holtzer, R. and Xue, X., 2007. Quantitative gait dysfunction and risk of cognitive decline and dementia. *Journal of Neurology, Neurosurgery & Psychiatry*, 78 (9), 929-935.

Vili, P., Peter, K., Bruno, S. and Ivan, R., 2002. Decision trees: an overview and their use in medicine. *Journal of Medical Systems*, 26 (5), 445-463.

Von Kutzschenbach, M. and Brønn, C., 2017. Education for managing digital transformation: a feedback systems approach. *J Syst Cybernet Informat JSCI*, 15 (2), 14-19.

Wagner, M., Slijepcevic, D., Horsak, B., Rind, A., Zeppelzauer, M. and Aigner, W., 2018. KAVAGait: Knowledge-assisted visual analytics for clinical gait analysis. *IEEE Transactions on Visualization and Computer Graphics*.

Wahab, Y. and Bakar, N. A., 2011. Gait analysis measurement for sport application based on ultrasonic system. *2011 IEEE 15th International Symposium on Consumer Electronics (ISCE)*, 14-17 June 2011. 20-24.

Wall, J. C. and Turnbull, G. I., 1986. Gait asymmetries in residual hemiplegia. *Archives of Physical Medicine and Rehabilitation*, 67 (8), 550-553.

Wang, Y., Xu, J., Xu, X., Wu, X., Pottie, G. and Kasier, W., 2013. Inertial sensor based motion trajectory visualization and quantitative quality assessment of hemiparetic gait, *Proceedings of the 8th International Conference on Body Area Networks* (pp. 169-172): ICST (Institute for Computer Sciences, Social-Informatics and Telecommunications Engineering).

Want, R., 2006. An Introduction to RFID Technology. the IEEE CS and IEEE ComSoc.

Washabaugh, E. P., Kalyanaraman, T., Adamczyk, P. G., Claflin, E. S. and Krishnan, C., 2017. Validity and repeatability of inertial measurement units for measuring gait parameters. *Gait & posture*, 55, 87-93.

Wei, W., Honggang, W., M, H., Dongming, P., H, S. and HH, C., 2011. Secure Stochastic ECG Signals Based on Gaussian Mixture Model for Healthcare Systems *IEEE Systems Journal*, 5 (4), 564-573.

Weisstein, E. W., 2004. Newton-cotes formulas. *MathWorld* [online].

Welch, B., 1972. Distributions in Statistics: Continuous Univariate Distributions. *Journal of the Royal Statistical Society: Series A (General)*, 135 (3), 433-433.

Welch, G. and Foxlin, E., 2002. Motion tracking: no silver bullet, but a respectable arsenal. *IEEE Computer Graphics and Applications*, 22 (6), 24-38.

Welfare, A. I. o. H. a., 2017. Older Australia at a glance.

Westbrook, M., 1994. Accelerometers (pp. 150-174): Institute of Physics Publishers: Bristol, UK.

Whitney, J., Close, J. C., Jackson, S. H. and Lord, S. R., 2012. Understanding risk of falls in people with cognitive impairment living in residential care. *Journal of the American Medical Directors Association*, 13 (6), 535-540.

Williams, A. J., Peterson, D. S. and Earhart, G. M., 2013. Gait coordination in Parkinson disease: Effects of step length and cadence manipulations. *Gait & Posture*, 38 (2), 340-344.

Williamson, R. and Andrews, B. J., 2000. Gait event detection for FES using accelerometers and supervised machine learning. *IEEE Transactions on Rehabilitation Engineering*, 8 (3), 312-319.

Winiarski, S., Are there asymmetry indices reliable indicator of gait performance? *Gait & Posture*, 30, S143-S144.

Wolfson, L., 2001. Gait and balance dysfunction: a model of the interaction of age and disease. *Neuroscientist*, 7 (2), 178-183.

Wolfson, L., Whipple, R., Amerman, P. and Tobin, J. N., 1990. Gait assessment in the elderly: a gait abnormality rating scale and its relation to falls. *Journal of Gerontology*, 45 (1), M12-M19.

Wood, L. B. and Asada, H. H., 2007. Low variance adaptive filter for cancelling motion artifact in wearable photoplethysmogram sensor signals, *Engineering in Medicine and Biology Society, 2007. EMBS 2007. 29th Annual International Conference of the IEEE* (pp. 652-655): IEEE.

Wrisley, D. M. and Kumar, N. A., 2010. Functional gait assessment: concurrent, discriminative, and predictive validity in community-dwelling older adults. *Phys Ther*, 90 (5), 761-773.

Wu, J., Wang, J. and Liu, L., 2007. Feature extraction via KPCA for classification of gait patterns. *Human movement science*, 26 (3), 393-411.

Wu, Q., Zhang, Y. D., Tao, W. and Amin, M. G., 2015. Radar-based fall detection based on Doppler time–frequency signatures for assisted living. *IET Radar, Sonar & Navigation*, 9 (2), 164-172.

Yang, C.-C. and Hsu, Y.-L., 2010. A Review of Accelerometry-Based Wearable Motion Detectors for Physical Activity Monitoring. *Sensors*, 10 (8), 7772.

Yang, S., Laudanski, A. and Li, Q., 2012. Inertial sensors in estimating walking speed and inclination: an evaluation of sensor error models. *Medical & biological engineering & computing*, 50 (4), 383-393.

Yi, H., Ye, L. and Shu-Di, B., 2012. Fall detection by built-in tri-accelerometer of smartphone, *Biomedical and Health Informatics (BHI), 2012 IEEE-EMBS International Conference on* (pp. 184-187).

Yogev, G., Plotnik, M., Peretz, C., Giladi, N. and Hausdorff, J. M., 2007. Gait asymmetry in patients with Parkinson's disease and elderly fallers: when does the bilateral coordination of gait require attention? *Experimental Brain Research*, 177 (3), 336-346.

Yu, X., 2008. Approaches and principles of fall detection for elderly and patient, *e-health Networking, Applications and Services, 2008. HealthCom 2008. 10th International Conference on* (pp. 42-47): IEEE.

Yun, X. and Bachmann, E. R., 2006. Design, implementation, and experimental results of a quaternion-based Kalman filter for human body motion tracking. *IEEE transactions on Robotics*, 22 (6), 1216-1227.

Zammit, G. V., Menz, H. B. and Munteanu, S. E., 2010. Reliability of the TekScan MatScan® system for the measurement of plantar forces and pressures during barefoot level walking in healthy adults. *Journal of foot and ankle research*, 3 (1), 11.

Zeni, J. A. and Higginson, J. S., 2010. Gait parameters and stride-to-stride variability during familiarization to walking on a split-belt treadmill. *Clinical Biomechanics*, 25 (4), 383-386.

Zhang, D., Gatica-Perez, D., Bengio, S. and McCowan, I., 2005. Semi-supervised adapted hmms for unusual event detection, *Computer Vision and Pattern Recognition, 2005. CVPR 2005. IEEE Computer Society Conference on* (Vol. 1, pp. 611-618): IEEE.

Zhang, J., Lockhart, T. E. and Soangra, R., 2014. Classifying lower extremity muscle fatigue during walking using machine learning and inertial sensors. *Annals of biomedical engineering*, 42 (3), 600-612.

Zhi, R., 2016. A Drift Eliminated Attitude & Position Estimation Algorithm In 3D.

Zhu, C. and Sheng, W., 2009. Multi-sensor fusion for human daily activity recognition in robot-assisted living, *Proceedings of the 4th ACM/IEEE international conference on Human robot interaction* (pp. 303-304): ACM.

Zifchock, R. A., Davis, I., Higginson, J. and Royer, T., 2008. The symmetry angle: a novel, robust method of quantifying asymmetry. *Gait & posture*, 27 (4), 622-627.

Zijlstra, W. and Aminian, K., 2007. Mobility assessment in older people: new possibilities and challenges. *European Journal of Ageing*, 4 (1), 3-12.

Zijlstra, W. and Hof, A. L., 2003. Assessment of spatio-temporal gait parameters from trunk accelerations during human walking. *Gait Posture*, 18.

Appendix A

Certificates for completed online modules

blank

EPIGEUM

Bournemouth University

Certificate

This is to certify that Md. Anwary !

Successfully Completed the Course

'Ethics 1: Good Research Practice'

as part of the Epigeum Online Course

Young Adult Participant Information Sheet

Project Title An intelligent multi-sensor based personalized risk assessment system of elderly fall

Aim of the Research

This research will investigate on how to predict and identify real time elderly fall based on longitudinal gait pattern and physical information. The research will also compare how different a person's gait and physical condition from a normal person result a fall based on gait pattern and vital physical information to provide real time necessary interventions. The aim of this research is to develop a real time based automatic elderly fall detection system. The system will perform fall risk assessment based on user's inertial, gait and physical information through sensors. It will also provide risk notification in order to reduce the potential risk associated with fall so that elderly people could lead quality of life. The system will be designed in a way that will not affect the normal daily activities of the user. It will provide an early warning to the user when an abnormality over a period of time is found.

Invitation

You are invited to participate in this research project. Before you decide for participation, it is important for you to understand why the research is being done and what it will involve. Please take time to read the following information carefully and consult it with others if you wish. Ask me if there is anything which is not clear or if you would like more information. Take time to decide whether or not you wish to participate.

Why have I been chosen?

You are chosen for this research because you are a person in the age range of 20 to 39 (or 40) with acting ability and considered as a young adult. A group of 5 to 10 young adult will be selected for data collection. Your participation will actively promote the research progress.

Do I have to take part?

Your decision to participate in this study is entirely voluntary and you may decide at any time to withdraw from the study. You will be able to withdraw up to the point of anonymisation when your identity will no longer be identifiable. You do not need to explain your reason. If you do decide to participate you will be given this information sheet to keep (and be asked to sign a consent form).

What will happen if I take part, and what do I have to do?

You are expected to participate with others. You will be asked to wear user friendly Inertial Measurement Unit (IMU) sensors like wrist watch. You will then be asked to walk 10 steps and turn around and walk another 10 steps for up to 4 times. You will also be asked to act like different kinds of pretend falling. We will record this information of walking and falling pattern for the research.

What are the benefits (if any) of taking part?

We will show our sincere gratitude for your participation. You will also be a part of contributing to the knowledge of this research area.

Will I be recorded, and how will the recorded media be used?
This research will not involve producing recorded media.

What are the risks (if any) of taking part?
A data collector with a nurse will be present during the data collection. It may take around 20 to 30 minutes for collecting your data. There is no side effect of IMU sensors.

How will information about me be used?
The collected data will be stored securely and will be used only for the purpose of this research study. The data will be completely anonymised before it appears in any type of publication. No other use will be made of them without your written permission and no one outside the project will be allowed access to the original data.

Who will have access to information about be?
Your confidentiality will be safeguarded during and after the study. Only the research team will have access to your data. The data will be stored securely in softcopy.

Who is funding this research?
This Research Project is funded by the Erasmus Mundus FUSION project, www.fusion-edu.eu.

What if there is a problem?
If you have a concern about any aspect of this study, you may wish to speak to the researcher who will do their best to answer your questions. You can contact with the researcher Md. Arif Reza Anwary, ROOM P319, Poole House, Talbot Campus, Fern Barrow, Poole, BH12 5BB, manwary@bournemouth.ac.uk and a local address will be provided to you before data collection.

If you remain unhappy about the research and/wish to raise a complaint about any aspect of the way that you have been approached or treated during the research, please write to my supervisor Professor Hongnian Yu yuh@bournemouth.ac.uk Or Professor Matt Bentley who is the deputy dean of Research and Professional Practice and independent to this study. His email account is mbentley@bournemouth.ac.uk

You can also contact with Dr. Azizur Rab, Karim Pharmacy, Chawk Bazar, Dhaka, Bangladesh. Mobile:+8801711604363

Finally
Thank you for taking time to read through the information. If you decide to participate in this project you will be given a copy of the Participant Agreement Form and, you can sign and keep a record with you.

Young Adult Participant Agreement Form

Project Title: **An intelligent multi-sensor based personalized risk assessment system of elderly fall**

Bournemouth University

Name and contact details of researcher:

Md. Arif Reza Anwary
ROOM P319, Poole House, Talbot Campus, Fern Barrow, Poole. BH12 5BB
manwary@bournemouth.ac.uk

Please tick box if you agree with the statement:

1.	I confirm that I have read and understood the participant information sheet for the above research project and have had the opportunity to ask questions	☐
2.	I understand that I am free to withdraw at any time up to the point where the data are processed and become anonymous, so my identity cannot be determined	☐
3.	I understand that data collected about me will not be revealed at any time. I understand that my name will not be linked with the research materials	☐
4.	I give permission for members of the research team to use my identifiable information for the purposes of this research project if it is needed	☐

_____	_____	_____
Name of Participant	Date	Signature

_____	_____	_____
Name of Researcher	Date	Signature

Elderly Participant Information Sheet

Project Title An intelligent multi-sensor based personalized risk assessment system of elderly fall

Aim of the Research

This research will investigate how to predict and identify real time elderly fall based on longitudinal gait pattern and physical information. The research will also compare how different a person's gait and physical condition from a normal person could result in a fall based on gait pattern and vital physical information in order to provide real time necessary interventions. The aim of this research is to develop a real time based automatic elderly fall detection system. The system will perform a fall risk assessment based on users' inertial, gait and physical information through sensors. It will also provide risk notification in order to reduce the potential risk associated with a fall so that elderly people could lead a better quality of life. The system will be designed in a way that will not affect the normal daily activities of the user. It will provide an early warning to the user when an abnormality over a period of time is found.

Invitation

You are invited to participate in this research project. Before you decide to participate, it is important for you to understand why the research is being done and what it will involve. Please take time to read the following information carefully and consult with others if you wish. Ask me if there is anything which is not clear or if you would like more information. Take time to decide whether or not you wish to participate.

Why have I been chosen?

You have been chosen for this research because you are over 65 years old and considered as an elderly person. Three groups: 1. One group with elderly participants with previous fall history, 2. One group of elderly participants with no fall history and 3. One group of young adults. Each group will consist of 5 to 10 participants for data collection. The elderly participants will be selected from an elderly care home for long term monitoring. Your participation will actively promote the research progress.

Do I have to take part?

Your decision to participate in this study is entirely voluntary and you may decide at any time to withdraw from the study. You will be able to withdraw up to the point of anonymization when your identity will no longer be identifiable. You do not need to explain your reason. If you do decide to participate you will be given this information sheet to keep (and be asked to sign a consent form).

What will happen if I take part, and what do I have to do?

You are expected to participate in this research with others. You will be asked to wear user friendly Inertial Measurement Unit (IMU) sensors like wrist watch. You will then be asked to walk 10 steps and turn around and walk another 10 steps for up to 4 times. Your medical information (Electrocardiogram (ECG), Oxygen saturation (SpO2), Pulse rate (PR), Respiratory rate (RR), Blood pressure (BP), and other medical history suggested by healthcare professional (like diabetes, tranquilizer, cardiac and hypertensive etc) will also be recorded with the help of a

nurse. Each session may take up to 30 minutes. Your data will be collected every Monday and Thursday for three months from the starting date. Another three months of data will be collected subsequently.

What are the benefits (if any) of taking part?
There are no specific benefit to take part in this research however you will be contributing to increased knowledge in this research area. We will be sincerely grateful for your contribution.

Will I be recorded, and how will the recorded media be used?
This research will not involve producing any recorded media.

What are the risks (if any) of taking part?
A data collector with a nurse will be present during the data collection. It may take around 20 to 30 minutes to collect your data. There are no side effects of IMU sensors.

How will information about me be used?
The collected data will be stored securely and will be used only for the purpose of this research study. The data will be completely anonymised before it appears in any type of publication. No other use will be made of them without your written permission and no one outside the project will be allowed access to the original data.

Who will have access to information about be?
Your confidentiality will be safeguarded during and after the study. Only the research team will have access to your data. The data will be stored securely in softcopy.

Who is funding this research?
This Research Project is funded by the Erasmus Mundus FUSION project, www.fusion-edu.eu.

What if there is a problem?
If you have a concern about any aspect of this study, you may wish to speak to the researcher who will do the best to answer your questions. You can contact the researcher Md. Arif Reza Anwary, ROOM P319, Poole House, Talbot Campus, Fern Barrow, Poole, BH12 5BB, manwary@bournemouth.ac.uk and a local address will be provided to you before data collection.
If you remain unhappy about the research and/wish to raise a complaint about any aspect of the way that you have been approached or treated during the research, please write to researcher supervisor Professor Hongnian Yu yuh@bournemouth.ac.uk Or Professor Matt Bentley who is the deputy dean of Research and Professional Practice and is independent to this study. His email account is mbentley@bournemouth.ac.uk

You can also contact with Dr. Azizur Rab, Karim Pharmacy, Chawk Bazar, Dhaka, Bangladesh. Mobile:+8801711604363

Finally
Thank you for taking time to read through the information. If you decide to participate in this project you will be given a copy of the Participant Agreement Form and, you can sign and keep a record with you.

Elderly Participant Agreement Form

Project Title: **An intelligent multi-sensor based personalized risk assessment system of elderly fall**

Bournemouth University

Name and contact details of researcher:

Md. Arif Reza Anwary
ROOM P319, Poole House, Talbot Campus, Fern Barrow, Poole. BH12 5BB
manwary@bournemouth.ac.uk

Please tick box if you agree with the statement:

1.	I confirm that I have read and understood the participant information sheet for the above research project and have had the opportunity to ask questions	☐
2.	I understand that I am free to withdraw up at any time to the point where the data are processed and become anonymous, so my identity cannot be determined	☐
3.	I understand that data collected about me during this study will be anonymised and my identity will not be revealed at any time. I understand that my name will not be linked with the research materials	☐
4.	I give permission for members of the research team to use my identifiable information for the purposes of this research project if it is needed	☐

_____	_____	_____
Name of Participant	Date	Signature

_____	_____	_____
Name of Researcher	Date	Signature

Appendix B

1. Participant 1

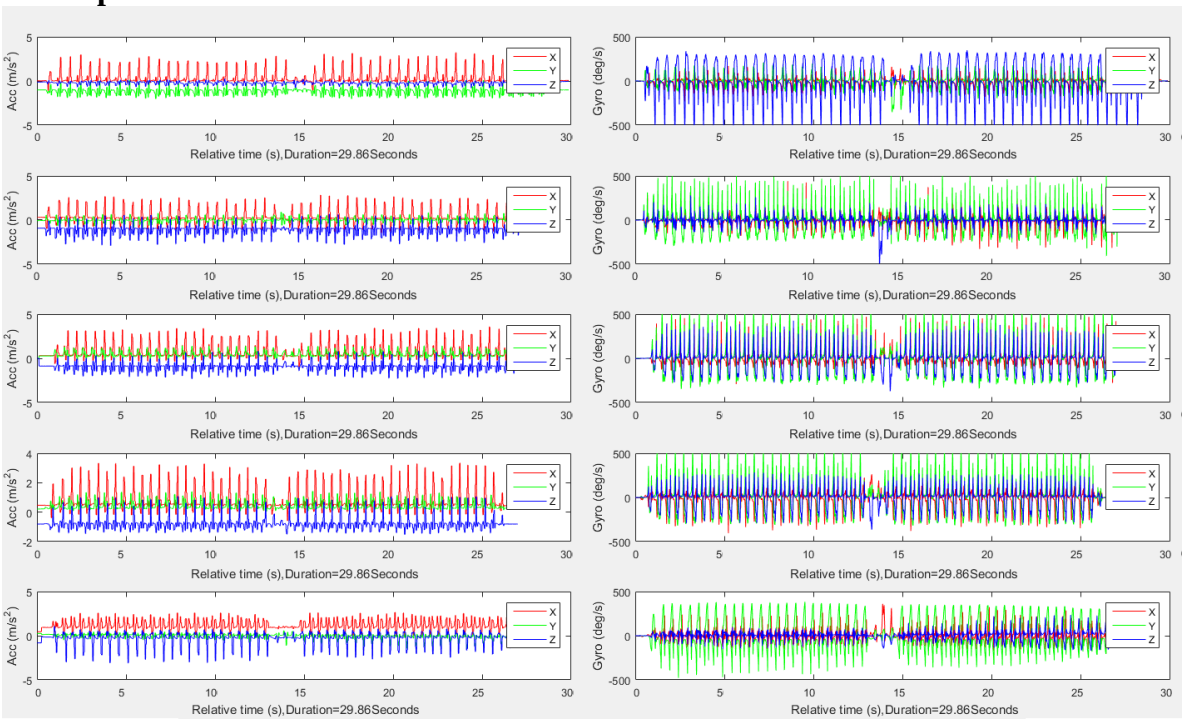

TABLE 1.1. Stride number estimation

Sensor Location	$StrideNumber_{Acc}$	*Accuracy*	$StrideNumber_{Gyr}$	*Accuracy*
1	48	96%	50	100%
2	43	86%	46	92%
3	48	96%	49	98%
4	48	96%	48	96%
5	50	100%	50	100%

TABLE 1.2. Distance and speed estimation

Sensor Location	Real* (m)	Estimated* (m)	Accuracy(%)	Period(s)	Speed (m/s)
1	60.96	60.38	99.05	29.86	2.02
2	60.96	55.11	90.40	29.86	1.85
3	60.96	68.24	88.06	29.86	2.29
4	60.96	40.46	66.37	29.86	1.35
5	60.96	61.35	99.36	29.86	2.05

* Distance

TABLE 1.3. Stride, Stance and Swing information

Sensor Location	Average Stride		Average Stance			Average Swing		
	Length (m)	Period (s)	Length (m)	Period (s)	% of Stride	Length (m)	Period (s)	% of Stride
1	1.099	0.514	0.626	0.264	56.954	0.473	0.250	43.046
2	1.639	0.510	0.574	0.189	35.036	1.065	0.320	64.964
3	0.744	0.567	0.377	0.298	50.652	0.367	0.269	49.348
4	0.927	0.478	0.414	0.271	44.626	0.513	0.207	55.364
5	0.977	0.462	0.590	0.263	60.313	0.388	0.199	39.697

2. Participant 2

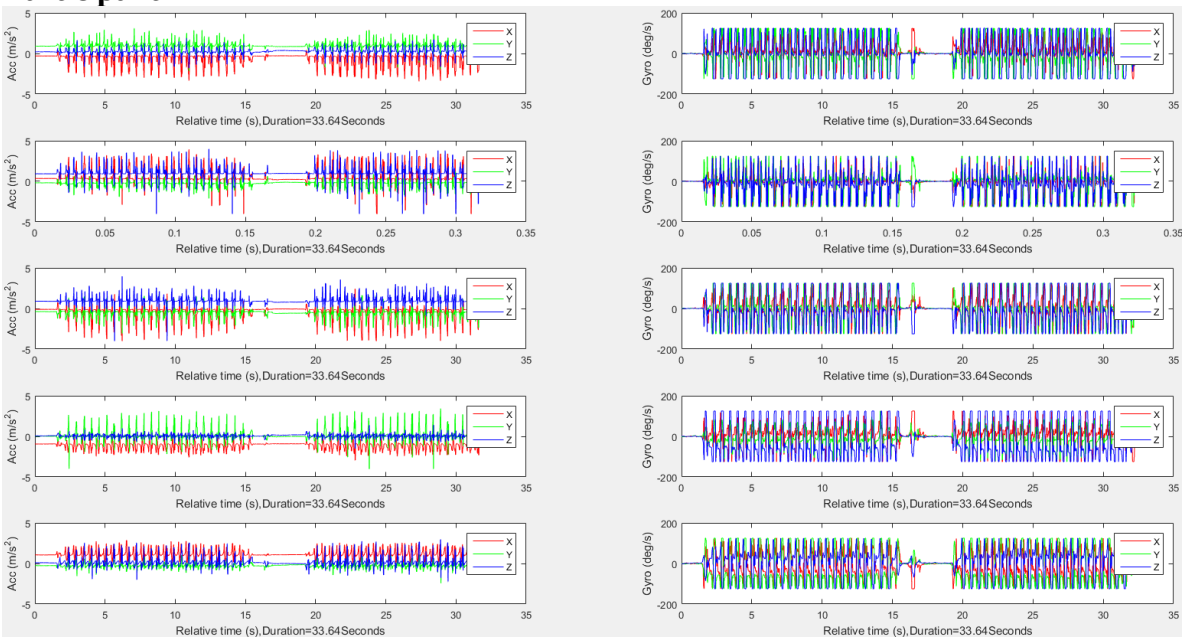

TABLE 2.1. Stride number estimation

Sensor Location	$StrideNumber_{Acc}$	*Accuracy*	$StrideNumber_{Gyr}$	*Accuracy*
1	49	98%	48	96%
2	41	82%	44	88%
3	34	68%	35	70%
4	42	84%	38	76%
5	45	90%	46	92%

TABLE 2.2. Distance and speed estimation

Sensor Location	Real* (m)	Estimated* (m)	Accuracy(%)	Period(s)	Speed (m/s)
1	64.00	59.59	93.11	45.60	1.31
2	64.00	58.98	92.15	45.60	1.29
3	64.00	70.72	89.50	45.60	1.55
4	64.00	47.26	73.84	45.60	1.04
5	64.00	60.99	95.30	45.60	1.34

* Distance

TABLE 2.3. Stride, Stance and Swing information

Sensor Location	Average Stride		Average Stance			Average Swing		
	Length (m)	Period (s)	Length (m)	Period (s)	% of Stride	Length (m)	Period (s)	% of Stride
1	1.201	0.492	0.654	0.262	54.455	0.547	0.230	45.545
2	0.688	0.295	0.328	0.148	46.802	0.366	0.147	52.326
3	0.815	0.268	0.356	0.110	42.086	0.472	0.158	56.319
4	0.645	0.288	0.288	0.131	43.876	0.362	0.158	55.349
5	1.204	0.422	0.611	0.217	49.834	0.604	0.205	49.252

3. Participant 3

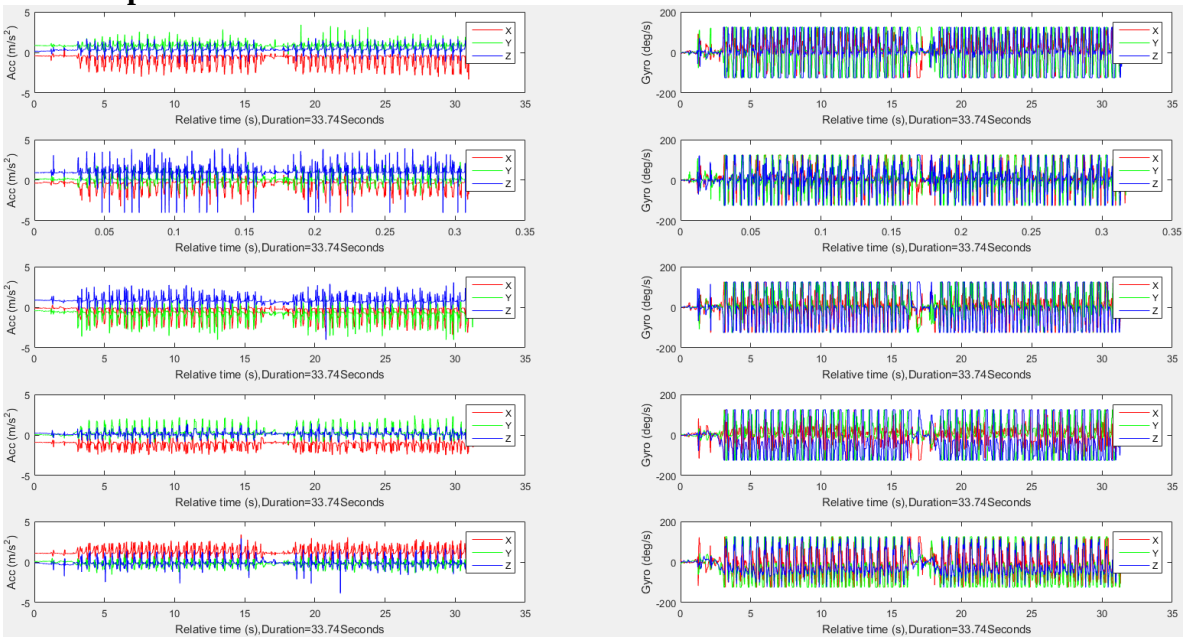

TABLE 3.1. Stride number estimation

Sensor Location	$StrideNumber_{Acc}$	*Accuracy*	$StrideNumber_{Gyr}$	*Accuracy*
1	48	96%	49	98%
2	51	98%	46	92%
3	49	98%	48	96%
4	46	92%	48	96%
5	40	80%	37	74%

TABLE 3.2. Distance and speed estimation

Sensor Location	**Real* (m)**	**Estimated* (m)**	**Accuracy(%)**	**Period(s)**	**Speed (m/s)**
1	67.20	64.20	95.54	59.20	1.08
2	67.20	60.97	90.72	59.20	1.03
3	67.20	58.46	86.99	59.20	0.99
4	67.20	52.35	77.90	59.20	0.88
5	67.20	64.05	95.31	59.20	1.08

* Distance

TABLE 3.3. Stride, Stance and Swing information

Sensor Location	**Average Stride**		**Average Stance**			**Average Swing**		
	Length (m)	**Period (s)**	**Length (m)**	**Period (s)**	**% of Stride**	**Length (m)**	**Period (s)**	**% of Stride**
1	1.190	0.597	0.890	0.309	74.790	0.300	0.288	25.210
2	0.230	0.531	0.180	0.288	59.130	0.366	0.243	21.739
3	0.290	0.266	0.155	0.134	62.759	0.472	0.132	46.552
4	0.074	0.552	0.054	0.261	389.189	0.362	0.291	27.027
5	0.405	0.600	0.204	0.304	49.136	0.604	0.296	49.630

4. Participant 4

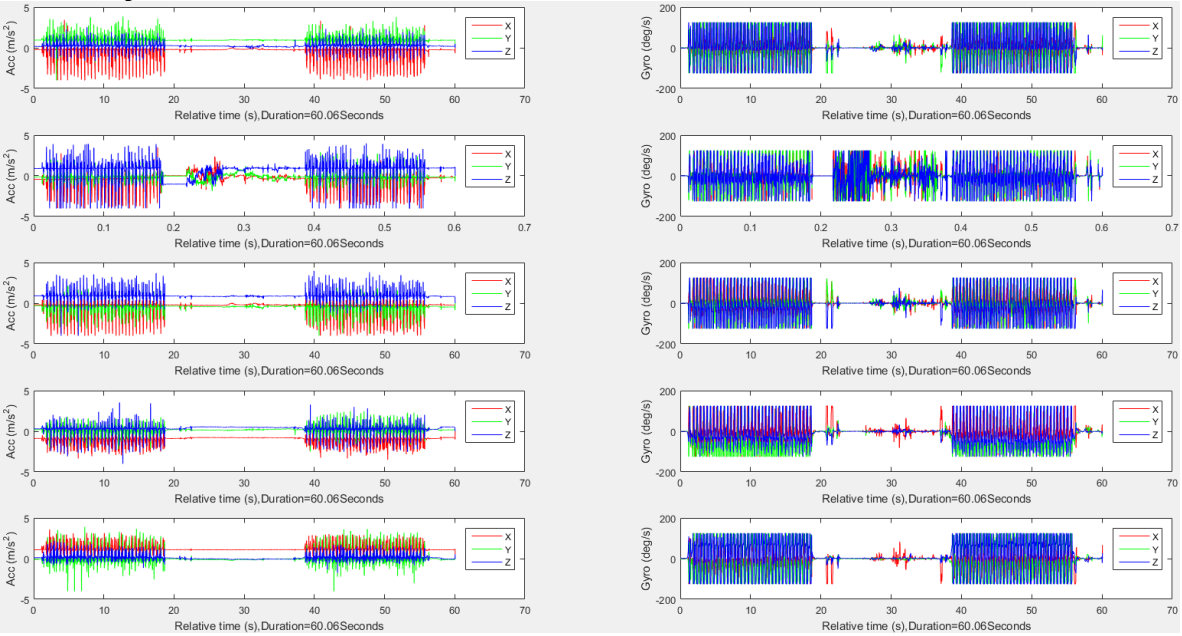

TABLE 4.1. Stride number estimation

Sensor Location	$StrideNumber_{Acc}$	*Accuracy*	$StrideNumber_{Gyr}$	*Accuracy*
1	50	100%	49	98%
2	51	98%	50	100%
3	49	98%	47	94%
4	49	98%	49	98%
5	49	98%	44	88%

TABLE 4.2. Distance and speed estimation

Sensor Location	**Real* (m)**	**Estimated* (m)**	**Accuracy(%)**	**Period(s)**	**Speed (m/s)**
1	58.40	58.27	99.77	33.16	1.76
2	58.40	62.56	92.87	33.16	1.89
3	58.40	59.56	98.01	33.16	1.80
4	58.40	60.61	96.21	33.16	1.83
5	58.40	51.72	88.56	33.16	1.56

* Distance

TABLE 4.3. Stride, Stance and Swing information

Sensor Location	**Average Stride**		**Average Stance**			**Average Swing**		
	Length (m)	**Period (s)**	**Length (m)**	**Period (s)**	**% of Stride**	**Length (m)**	**Period (s)**	**% of Stride**
1	1.169	0.525	0.705	0.264	60.308	0.464	0.261	39.692
2	1.572	0.516	0.795	0.261	76.718	0.366	0.256	49.427
3	1.591	0.524	0.844	0.264	70.333	0.472	0.260	46.952
4	0.828	0.532	0.423	0.265	56.280	0.362	0.267	48.913
5	1.928	0.513	0.972	0.258	68.672	0.604	0.255	49.585

5. Participant 5

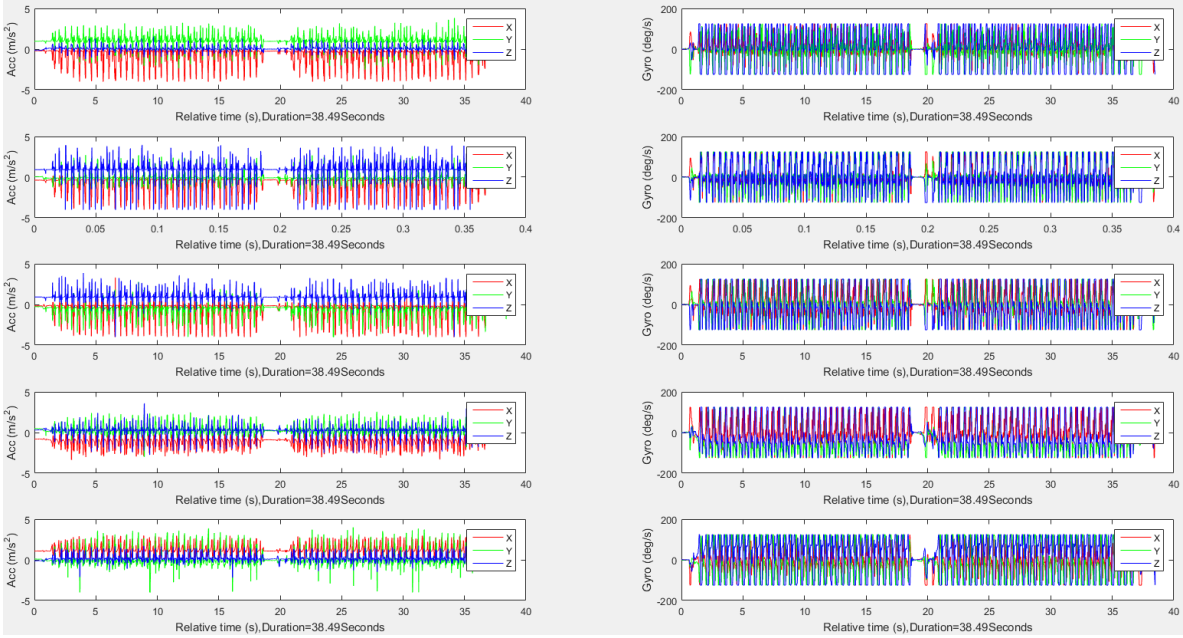

TABLE 5.1. Stride number estimation

Sensor Location	$StrideNumber_{Acc}$	*Accuracy*	$StrideNumber_{Gyr}$	*Accuracy*
1	48	96%	44	88%
2	47	94%	47	94%
3	48	96%	47	94%
4	48	96%	44	88%
5	46	92%	47	94%

TABLE 5.2. Distance and speed estimation

Sensor Location	**Real* (m)**	**Estimated* (m)**	**Accuracy(%)**	**Period(s)**	**Speed (m/s)**
1	61.60	62.45	98.62	45.16	0.63
2	61.60	62.56	98.43	45.16	0.64
3	61.60	58.84	95.52	45.16	0.62
4	61.60	52.79	85.71	45.16	0.62
5	61.60	59.69	96.90	45.16	0.62

* Distance

TABLE 5.3. Stride, Stance and Swing information

Sensor Location	**Average Stride**		**Average Stance**			**Average Swing**		
	Length (m)	**Period (s)**	**Length (m)**	**Period (s)**	**% of Stride**	**Length (m)**	**Period (s)**	**% of Stride**
1	0.870	0.512	0.526	0.259	60.460	0.344	0.253	39.540
2	1.120	0.489	0.583	0.245	67.321	0.366	0.244	47.946
3	0.705	0.480	0.355	0.239	33.050	0.472	0.241	49.645
4	1.140	0.477	0.583	0.243	68.246	0.362	0.234	48.860
5	0.859	0.491	0.438	0.248	29.686	0.604	0.243	49.010

6. Participant 6

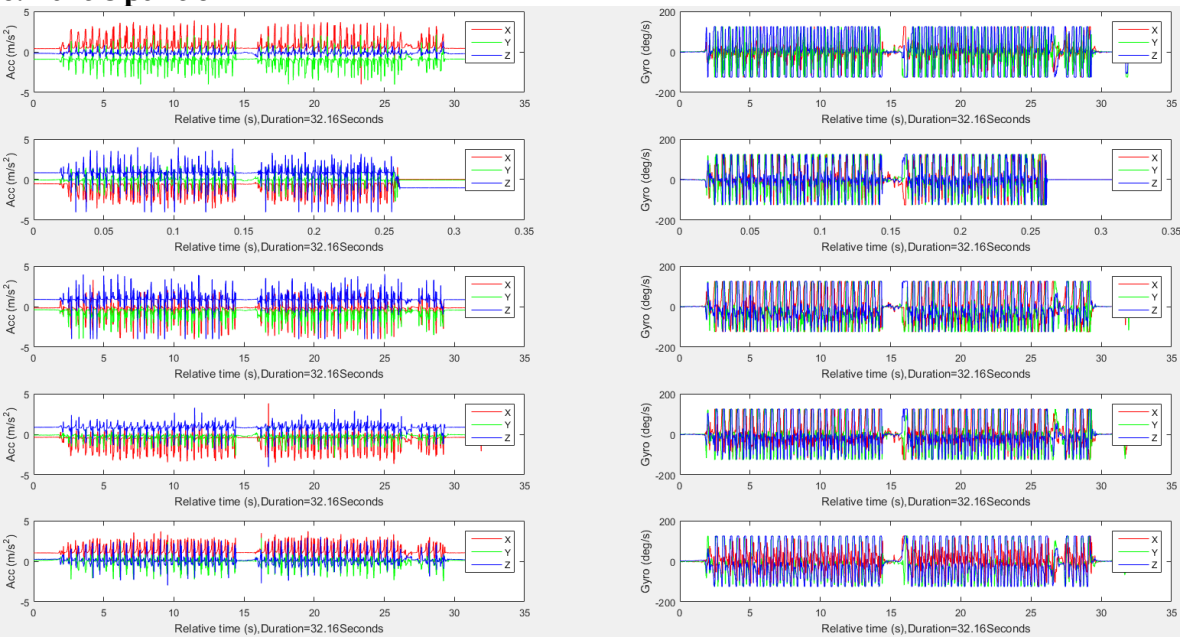

TABLE 6.1. Stride number estimation

Sensor Location	$StrideNumber_{Acc}$	*Accuracy*	$StrideNumber_{Gyr}$	*Accuracy*
1	48	96%	45	90%
2	45	90%	46	92%
3	45	90%	46	92%
4	47	94%	46	92%
5	47	94%	47	94%

TABLE 6.2. Distance and speed estimation

Sensor Location	**Real* (m)**	**Estimated* (m)**	**Accuracy(%)**	**Period(s)**	**Speed (m/s)**
1	56.08	59.56	93.79	37.21	1.60
2	56.08	62.56	88.44	37.21	1.68
3	56.08	51.12	91.15	37.21	1.37
4	56.08	59.69	93.56	37.21	1.60
5	56.08	51.94	92.61	37.21	1.40

* Distance

TABLE 6.3. Stride, Stance and Swing information

Sensor Location	**Average Stride**		**Average Stance**			**Average Swing**		
	Length (m)	**Period (s)**	**Length (m)**	**Period (s)**	**% of Stride**	**Length (m)**	**Period (s)**	**% of Stride**
1	0.435	0.731	0.317	0.361	72.874	0.118	0.370	27.126
2	1.807	0.722	0.892	0.354	79.745	0.366	0.367	50.636
3	1.715	0.689	0.812	0.327	72.478	0.472	0.361	52.653
4	1.304	0.659	0.661	0.337	72.239	0.362	0.322	49.310
5	1.667	0.601	0.766	0.285	63.767	0.604	0.316	54.049

7. Participant 7

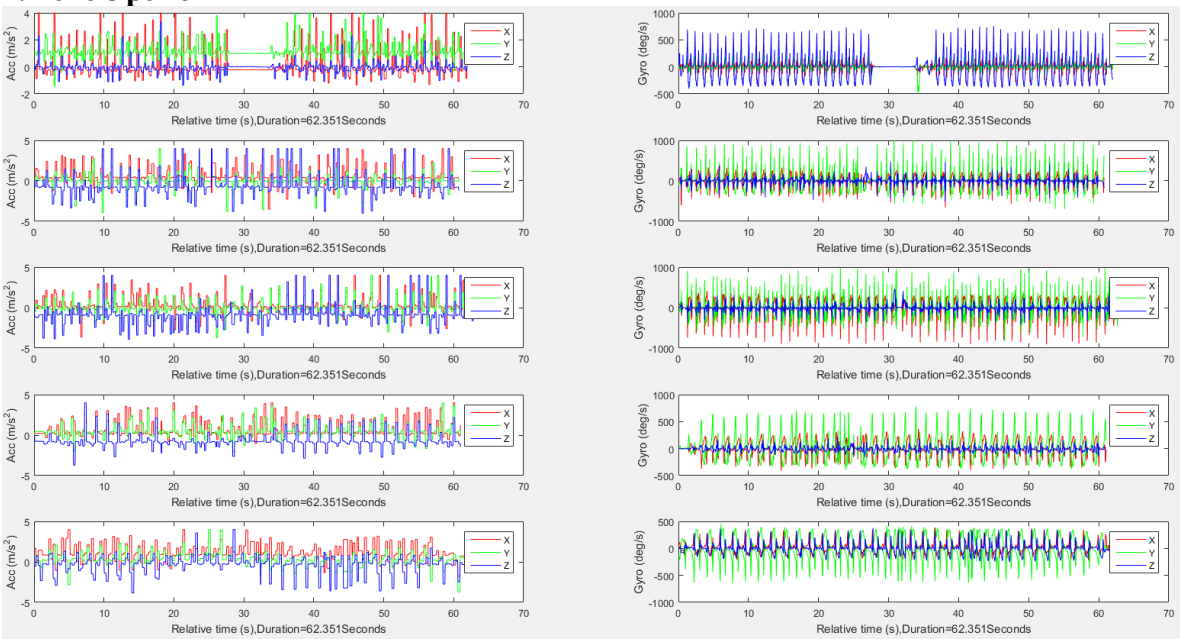

TABLE 7.1. Stride number estimation

Sensor Location	$StrideNumber_{Acc}$	*Accuracy*	$StrideNumber_{Gyr}$	*Accuracy*
1	47	94%	44	88%
2	42	84%	45	90%
3	42	84%	45	90%
4	46	92%	47	94%
5	47	94%	46	92%

TABLE 7.2. Distance and speed estimation

Sensor Location	**Real* (m)**	**Estimated* (m)**	**Accuracy(%)**	**Period(s)**	**Speed (m/s)**
1	50.59	51.94	97.34	33.57	1.55
2	50.59	62.56	76.33	33.57	1.86
3	50.59	45.74	90.40	33.57	1.36
4	50.59	59.69	82.01	33.57	1.78
5	50.59	59.56	82.27	33.57	1.77

* Distance

TABLE 7.3. Stride, Stance and Swing information

Sensor Location	**Average Stride**		**Average Stance**			**Average Swing**		
	Length (m)	**Period (s)**	**Length (m)**	**Period (s)**	**% of Stride**	**Length (m)**	**Period (s)**	**% of Stride**
1	0.887	0.681	0.451	0.340	50.846	0.436	0.341	49.154
2	1.250	0.653	0.603	0.304	70.720	0.366	0.349	51.760
3	1.099	0.643	0.551	0.318	57.052	0.472	0.324	49.864
4	0.792	0.682	0.394	0.341	54.293	0.362	0.341	50.253
5	0.872	0.620	0.403	0.300	30.734	0.604	0.320	53.784

8. Participant 8

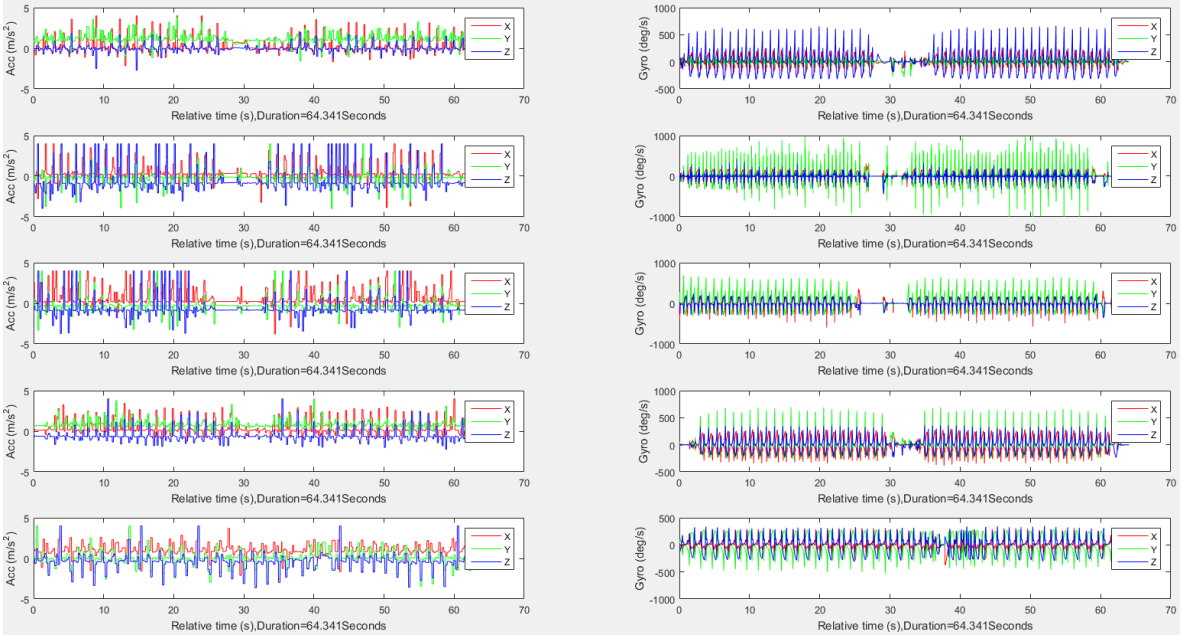

TABLE 8.1. Stride number estimation

Sensor Location	$StrideNumber_{Acc}$	*Accuracy*	$StrideNumber_{Gyr}$	*Accuracy*
1	48	96%	41	82%
2	44	88%	47	94%
3	41	82%	46	92%
4	49	98%	48	96%
5	48	96%	48	96%

TABLE 8.2. Distance and speed estimation

Sensor Location	**Real* (m)**	**Estimated* (m)**	**Accuracy(%)**	**Period(s)**	**Speed (m/s)**
1	45.45	51.12	87.53	31.62	1.62
2	45.45	62.56	62.34	31.62	1.98
3	45.45	59.56	68.96	31.62	1.88
4	45.45	59.69	68.66	31.62	1.89
5	45.45	51.94	85.73	31.62	1.64

* Distance

TABLE 8.3. Stride, Stance and Swing information

Sensor Location	**Average Stride**		**Average Stance**			**Average Swing**		
	Length (m)	**Period (s)**	**Length (m)**	**Period (s)**	**% of Stride**	**Length (m)**	**Period (s)**	**% of Stride**
1	1.203	0.697	0.684	0.335	56.858	0.519	0.361	43.142
2	1.979	0.668	0.870	0.305	81.506	0.366	0.363	56.038
3	1.852	0.652	0.828	0.307	74.514	0.472	0.344	55.292
4	1.633	0.691	0.837	0.343	77.832	0.362	0.348	48.745
5	1.883	0.633	0.830	0.294	67.924	0.604	0.339	55.921

9. Participant 9

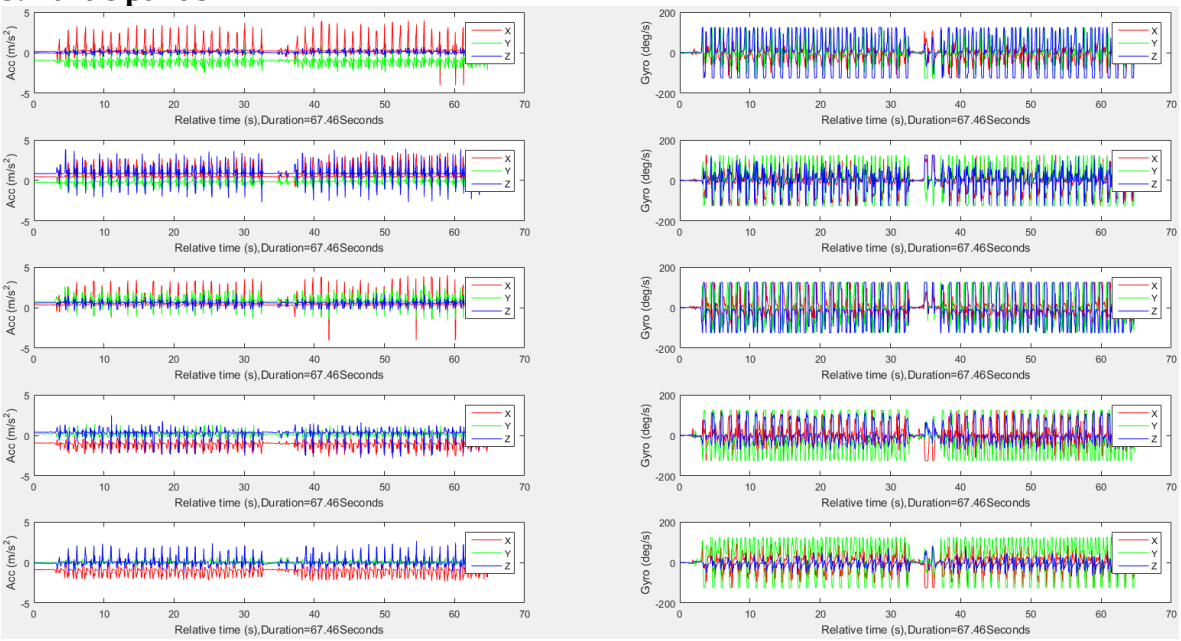

TABLE 9.1. Stride number estimation

Sensor Location	$StrideNumber_{Acc}$	*Accuracy*	$StrideNumber_{Gyr}$	*Accuracy*
1	48	96%	44	88%
2	46	92%	45	90%
3	44	88%	46	92%
4	47	94%	46	92%
5	50	100%	48	96%

TABLE 9.2. Distance and speed estimation

Sensor Location	**Real* (m)**	**Estimated* (m)**	**Accuracy(%)**	**Period(s)**	**Speed (m/s)**
1	51.20	51.12	99.84	42.18	1.21
2	51.20	62.56	77.80	42.18	1.48
3	51.20	59.56	83.67	42.18	1.41
4	51.20	59.69	83.41	42.18	1.42
5	51.20	51.94	98.56	42.18	1.23

* Distance

TABLE 9.3. Stride, Stance and Swing information

Sensor Location	**Average Stride**		**Average Stance**			**Average Swing**		
	Length (m)	**Period (s)**	**Length (m)**	**Period (s)**	**% of Stride**	**Length (m)**	**Period (s)**	**% of Stride**
1	1.140	0.675	0.596	0.334	52.281	0.544	0.341	47.719
2	1.449	0.675	0.699	0.292	74.741	0.366	0.332	51.760
3	1.633	0.675	0.798	0.322	71.096	0.472	0.330	51.133
4	0.954	0.675	0.476	0.304	62.055	0.362	0.313	50.105
5	1.168	0.675	0.534	0.290	48.288	0.604	0.326	54.281

10. Participant 10

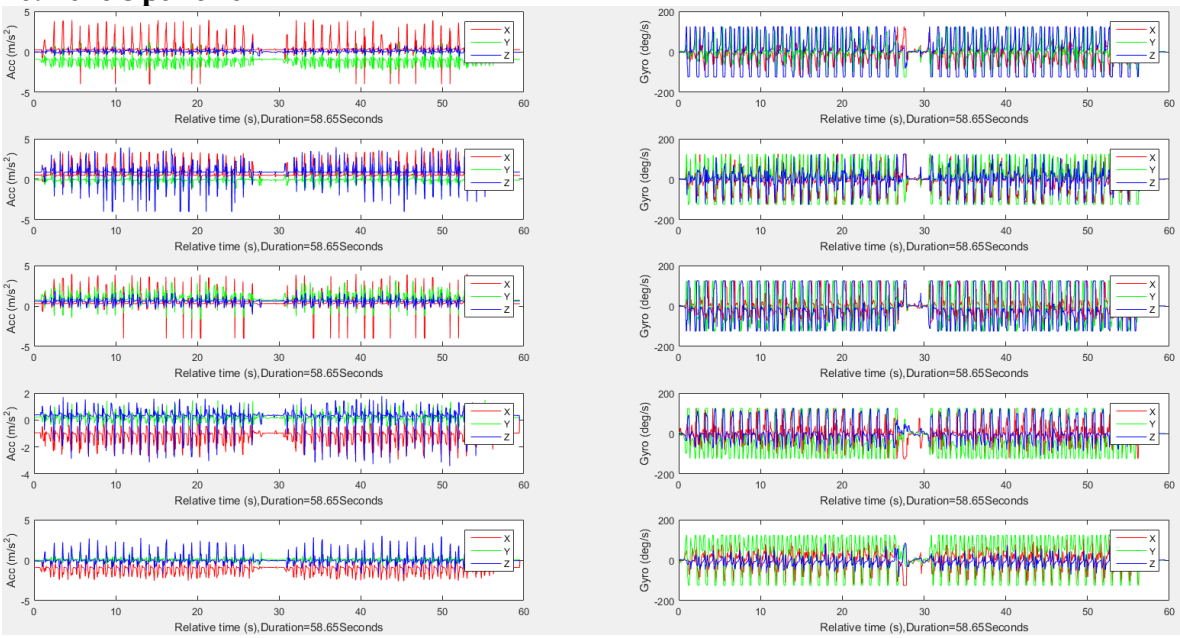

TABLE 10.1. Stride number estimation

Sensor Location	$StrideNumber_{Acc}$	*Accuracy*	$StrideNumber_{Gyr}$	*Accuracy*
1	45	90%	41	82%
2	42	84%	42	84%
3	42	84%	44	88%
4	45	90%	46	92%
5	46	92%	48	96%

TABLE 10.2. Distance and speed estimation

Sensor Location	**Real* (m)**	**Estimated* (m)**	**Accuracy(%)**	**Period(s)**	**Speed (m/s)**
1	54.86	51.12	93.18	38.61	1.32
2	54.86	62.56	85.96	38.61	1.62
3	54.86	59.56	91.43	38.61	1.54
4	54.86	59.69	91.19	38.61	1.55
5	54.86	51.94	94.67	38.61	1.35

* Distance

TABLE 10.3. Stride, Stance and Swing information

Sensor Location	**Average Stride**		**Average Stance**			**Average Swing**		
	Length (m)	**Period (s)**	**Length (m)**	**Period (s)**	**% of Stride**	**Length (m)**	**Period (s)**	**% of Stride**
1	1.054	0.577	0.629	0.298	59.677	0.425	0.279	40.323
2	0.774	0.419	0.383	0.196	52.713	0.366	0.222	50.517
3	0.763	0.448	0.358	0.210	38.139	0.472	0.238	53.080
4	0.848	0.564	0.472	0.314	57.311	0.362	0.250	44.340
5	1.040	0.460	0.522	0.238	41.923	0.604	0.222	49.808

11. Participant 11

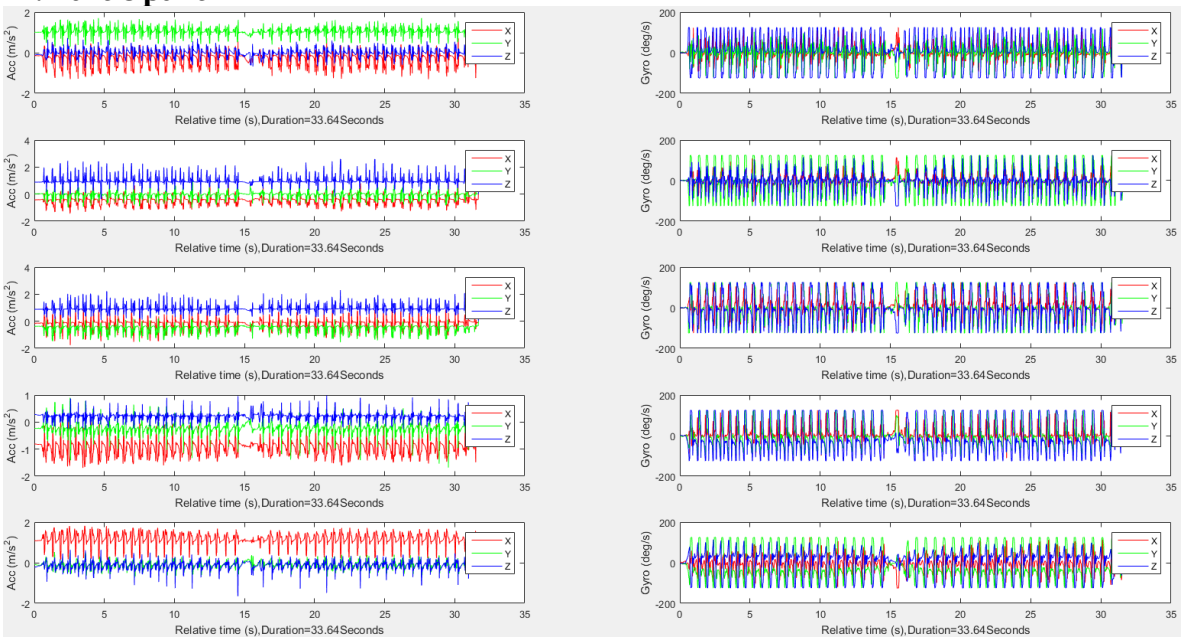

TABLE 11.1. Stride number estimation

Sensor Location	$StrideNumber_{Acc}$	*Accuracy*	$StrideNumber_{Gyr}$	*Accuracy*
1	50	100%	50	100%
2	51	98%	52	96%
3	52	96%	53	94%
4	53	94%	46	92%
5	53	94%	49	98%

TABLE 11.2. Distance and speed estimation

Sensor Location	**Real* (m)**	**Estimated* (m)**	**Accuracy(%)**	**Period(s)**	**Speed (m/s)**
1	55.62	59.56	92.92	45.61	1.31
2	55.62	62.56	87.52	45.61	1.37
3	55.62	51.12	91.90	45.61	1.12
4	55.62	59.69	92.68	45.61	1.31
5	55.62	51.94	93.37	45.61	1.14

* Distance

TABLE 11.3. Stride, Stance and Swing information

Sensor Location	**Average Stride**		**Average Stance**			**Average Swing**		
	Length (m)	**Period (s)**	**Length (m)**	**Period (s)**	**% of Stride**	**Length (m)**	**Period (s)**	**% of Stride**
1	1.018	0.406	0.597	0.227	58.644	0.421	0.179	41.356
2	0.738	0.406	0.364	0.209	50.407	0.366	0.197	50.678
3	0.688	0.295	0.328	0.148	31.395	0.472	0.147	52.326
4	0.834	0.431	0.495	0.253	56.595	0.362	0.178	40.647
5	1.204	0.422	0.611	0.217	49.834	0.604	0.205	49.252

12. Participant 12

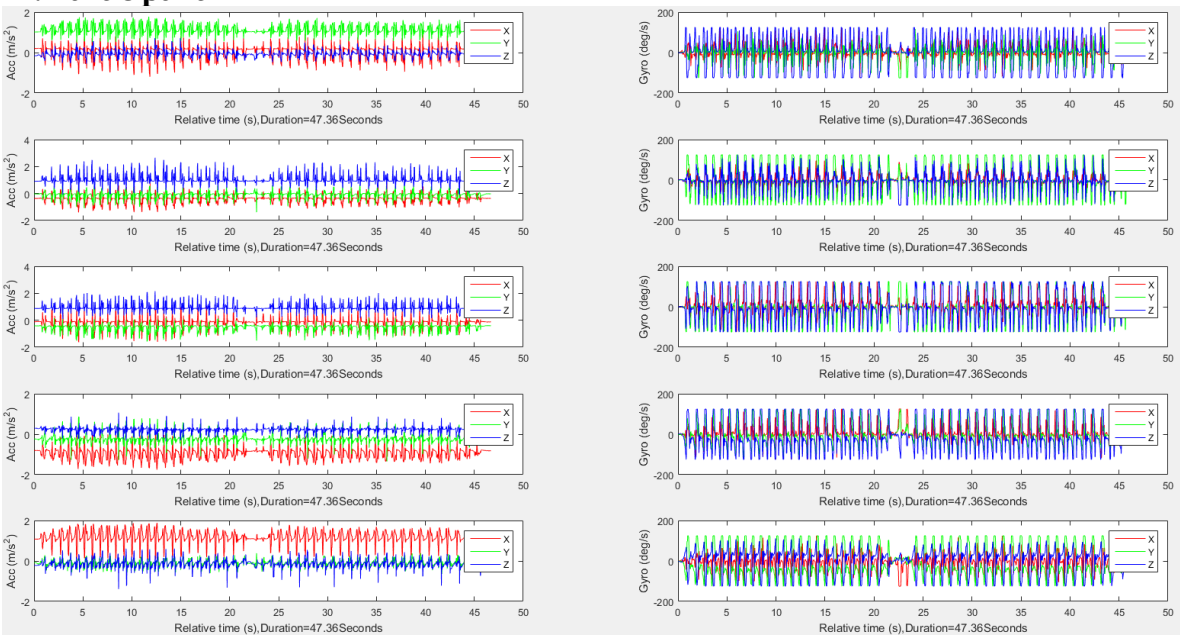

TABLE 12.1. Stride number estimation

Sensor Location	$StrideNumber_{Acc}$	*Accuracy*	$StrideNumber_{Gyr}$	*Accuracy*
1	48	96%	49	98%
2	47	94%	49	98%
3	46	92%	49	98%
4	49	98%	49	98%
5	49	98%	46	92%

TABLE 12.2. Distance and speed estimation

Sensor Location	**Real* (m)**	**Estimated* (m)**	**Accuracy(%)**	**Period(s)**	**Speed (m/s)**
1	68.43	62.56	91.43	46.19	1.35
2	68.43	51.94	75.90	46.19	1.12
3	68.43	51.12	74.70	46.19	1.11
4	68.43	59.69	87.23	46.19	1.29
5	68.43	59.56	87.04	46.19	1.29

* Distance

TABLE 12.3. Stride, Stance and Swing information

Sensor Location	**Average Stride**		**Average Stance**			**Average Swing**		
	Length (m)	**Period (s)**	**Length (m)**	**Period (s)**	**% of Stride**	**Length (m)**	**Period (s)**	**% of Stride**
1	1.705	0.480	0.991	0.259	58.123	0.714	0.222	41.877
2	2.489	0.440	1.493	0.253	85.295	0.366	0.187	40.016
3	2.644	0.370	1.534	0.211	82.148	0.472	0.160	41.982
4	1.661	0.491	0.847	0.248	78.206	0.362	0.243	49.007
5	1.793	0.481	0.945	0.254	66.313	0.604	0.227	47.295

13. Participant 13

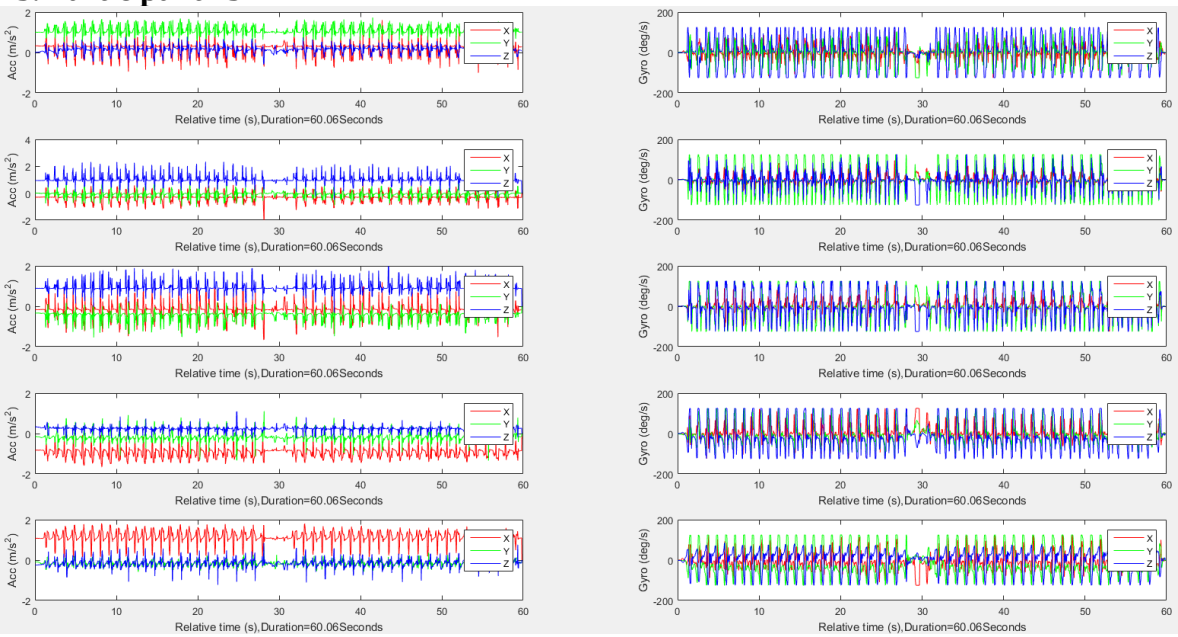

TABLE 13.1. Stride number estimation

Sensor Location	$StrideNumber_{Acc}$	*Accuracy*	$StrideNumber_{Gyr}$	*Accuracy*
1	49	98%	50	100%
2	47	94%	47	94%
3	46	92%	47	94%
4	48	96%	49	98%
5	47	94%	48	96%

TABLE 13.2. Distance and speed estimation

Sensor Location	**Real* (m)**	**Estimated* (m)**	**Accuracy(%)**	**Period(s)**	**Speed (m/s)**
1	63.44	59.69	94.09	38.64	1.54
2	63.44	62.56	98.62	38.64	1.62
3	63.44	51.12	80.58	38.64	1.32
4	63.44	59.56	93.88	38.64	1.54
5	63.44	51.94	81.87	38.64	1.34

* Distance

TABLE 13.3. Stride, Stance and Swing information

Sensor Location	**Average Stride**		**Average Stance**			**Average Swing**		
	Length (m)	**Period (s)**	**Length (m)**	**Period (s)**	**% of Stride**	**Length (m)**	**Period (s)**	**% of Stride**
1	0.904	0.294	0.603	0.169	66.704	0.301	0.125	33.296
2	0.454	0.253	0.243	0.137	19.383	0.366	0.116	46.476
3	0.579	0.292	0.245	0.117	18.480	0.472	0.175	57.686
4	0.858	0.285	0.424	0.141	57.809	0.362	0.145	50.583
5	0.756	0.288	0.427	0.164	20.106	0.604	0.125	43.519

14. Participant 14

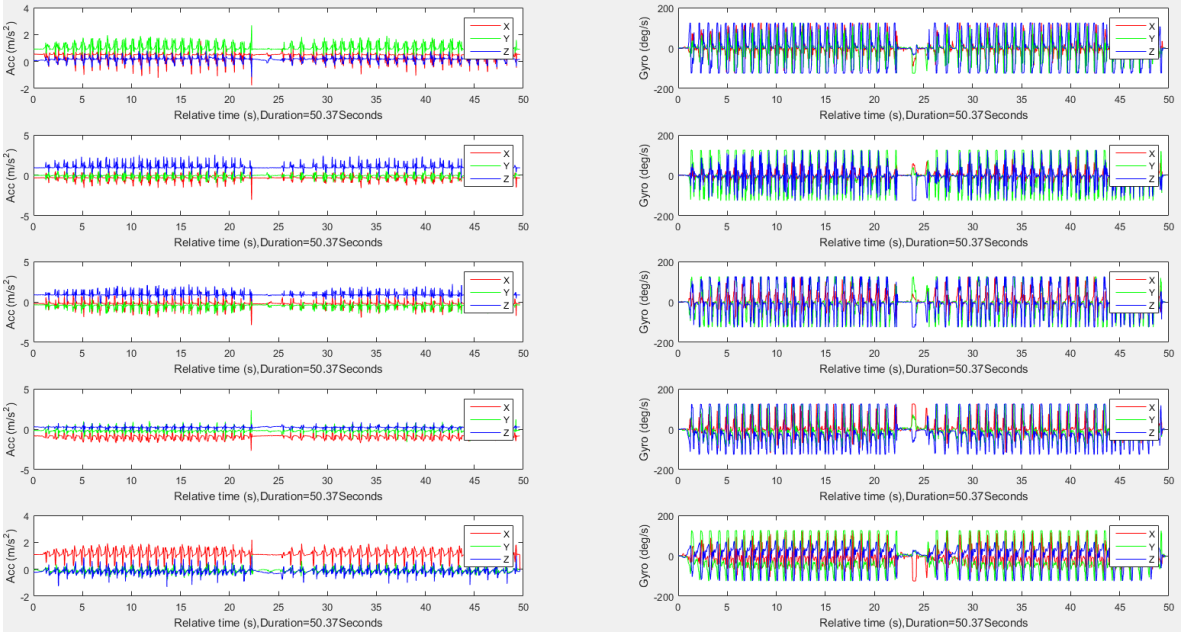

TABLE 14.1. Stride number estimation

Sensor Location	$StrideNumber_{Acc}$	*Accuracy*	$StrideNumber_{Gyr}$	*Accuracy*
1	45	90%	42	84%
2	39	78%	43	86%
3	39	78%	40	80%
4	37	74%	44	88%
5	42	84%	45	90%

TABLE 14.2. Distance and speed estimation

Sensor Location	**Real* (m)**	**Estimated* (m)**	**Accuracy(%)**	**Period(s)**	**Speed (m/s)**
1	62.76	62.56	99.69	43.29	1.45
2	62.76	59.56	94.90	43.29	1.38
3	62.76	51.12	81.45	43.29	1.18
4	62.76	59.69	95.11	43.29	1.38
5	62.76	51.94	82.75	43.29	1.20

* Distance

TABLE 14.3. Stride, Stance and Swing information

Sensor Location	**Average Stride**		**Average Stance**			**Average Swing**		
	Length (m)	**Period (s)**	**Length (m)**	**Period (s)**	**% of Stride**	**Length (m)**	**Period (s)**	**% of Stride**
1	1.053	0.416	0.576	0.231	54.701	0.477	0.185	45.299
2	1.492	0.403	0.856	0.219	75.469	0.366	0.184	42.627
3	1.243	0.407	0.718	0.231	62.027	0.472	0.176	42.237
4	0.632	0.408	0.363	0.228	42.722	0.362	0.179	42.563
5	1.016	0.418	0.579	0.240	40.551	0.604	0.179	43.012

15. Participant 15

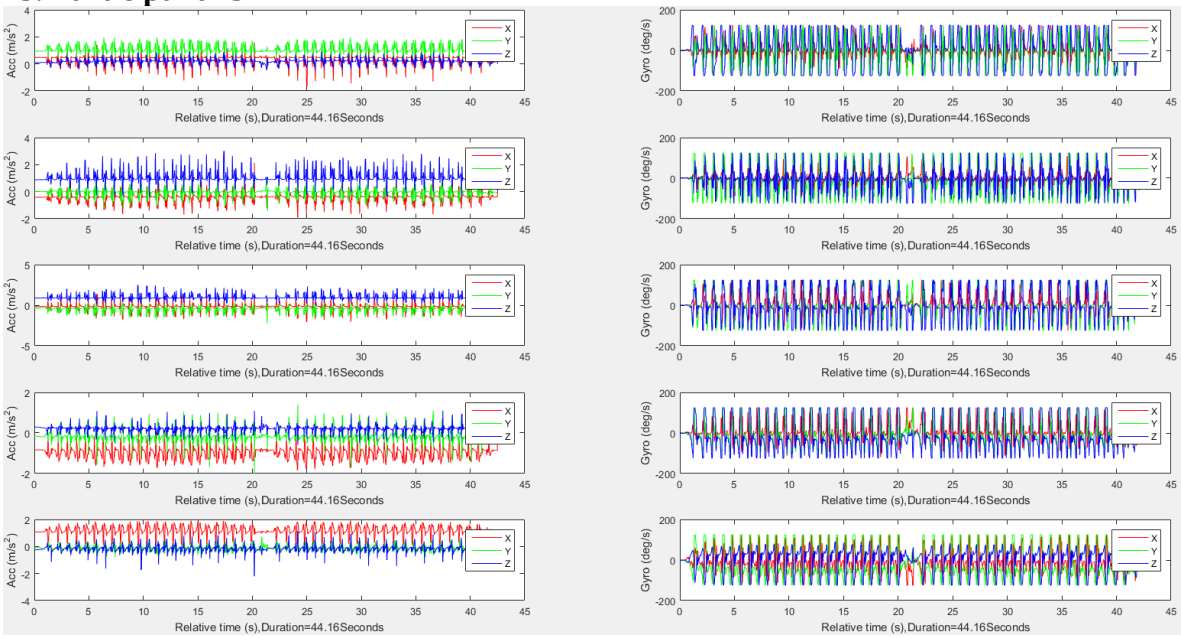

TABLE 15.1. Stride number estimation

Sensor Location	$StrideNumber_{Acc}$	*Accuracy*	$StrideNumber_{Gyr}$	*Accuracy*
1	50	100%	50	100%
2	40	80%	44	88%
3	49	98%	48	96%
4	51	98%	50	100%
5	50	100%	48	96%

TABLE 15.2. Distance and speed estimation

Sensor Location	**Real* (m)**	**Estimated* (m)**	**Accuracy(%)**	**Period(s)**	**Speed (m/s)**
1	67.54	62.56	92.63	48.37	1.29
2	67.54	51.94	76.90	48.37	1.07
3	67.54	51.12	75.69	48.37	1.06
4	67.54	59.56	88.18	48.37	1.23
5	67.54	59.69	88.38	48.37	1.23

* Distance

TABLE 15.3. Stride, Stance and Swing information

Sensor Location	**Average Stride**		**Average Stance**			**Average Swing**		
	Length (m)	**Period (s)**	**Length (m)**	**Period (s)**	**% of Stride**	**Length (m)**	**Period (s)**	**% of Stride**
1	1.632	0.451	0.895	0.231	54.841	0.737	0.220	45.159
2	1.885	0.427	1.025	0.220	80.584	0.366	0.206	45.623
3	2.403	0.436	0.958	0.178	80.358	0.472	0.258	60.133
4	1.431	0.467	0.754	0.241	74.703	0.362	0.226	47.310
5	1.570	0.460	0.885	0.257	61.529	0.604	0.204	43.631

Appendix C

1: Young Participant 1

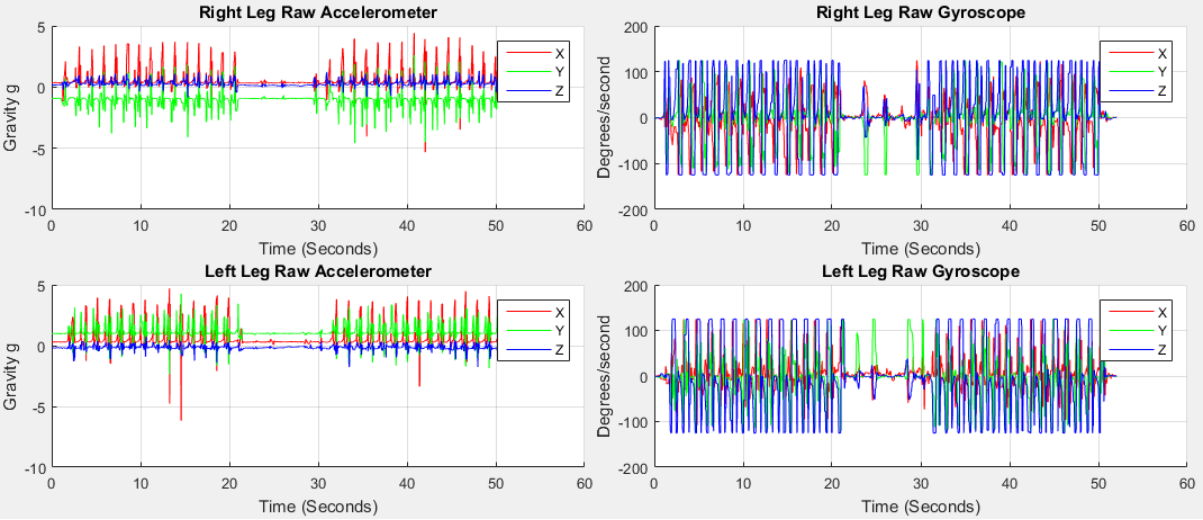

Figure 1.1: Accelerometer and gyroscope data from right and left legs

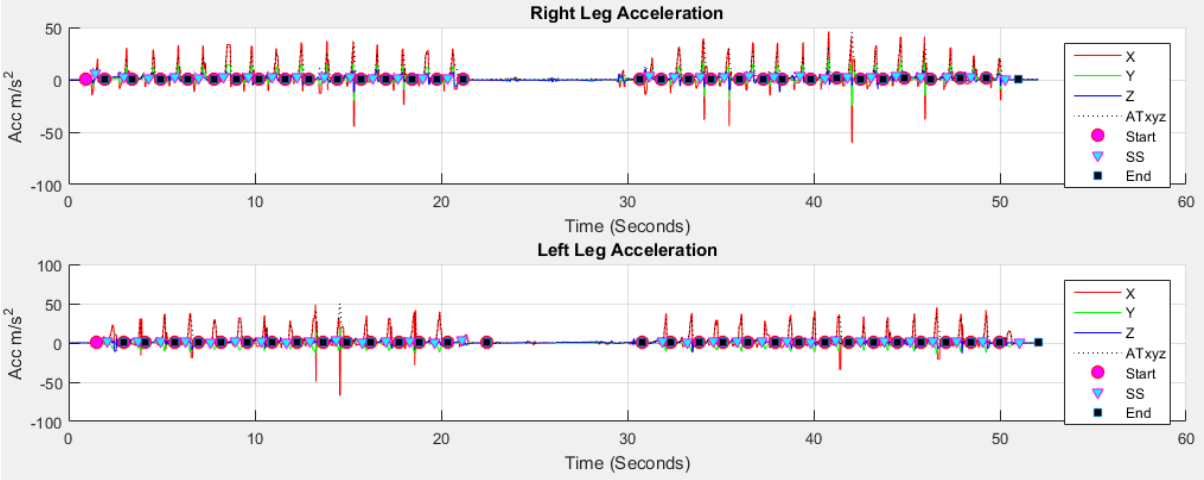

Figure 1.2: Result of stride, stance and swing event detection using proposed method

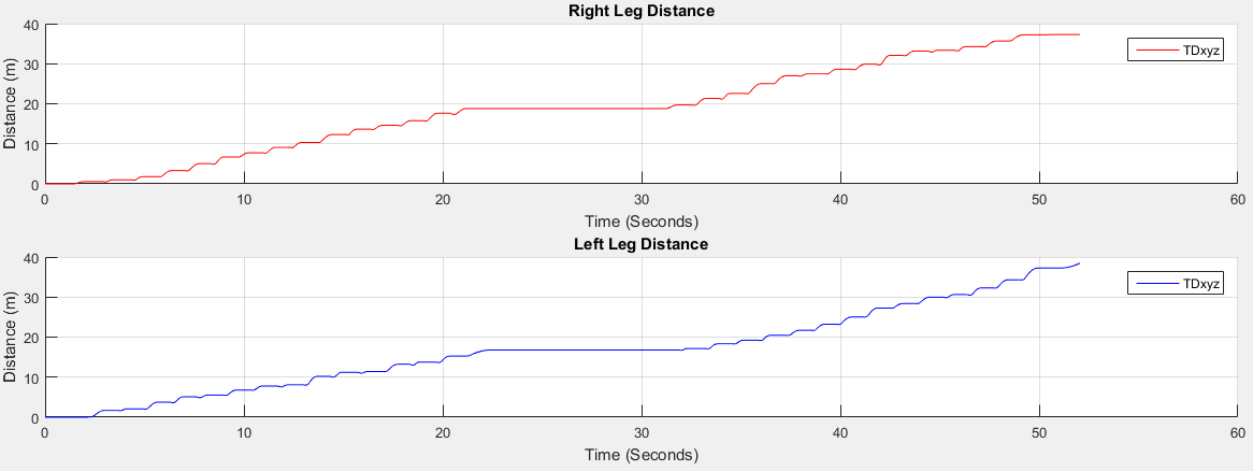

Figure 1.3: Result of distance estimation using proposed method

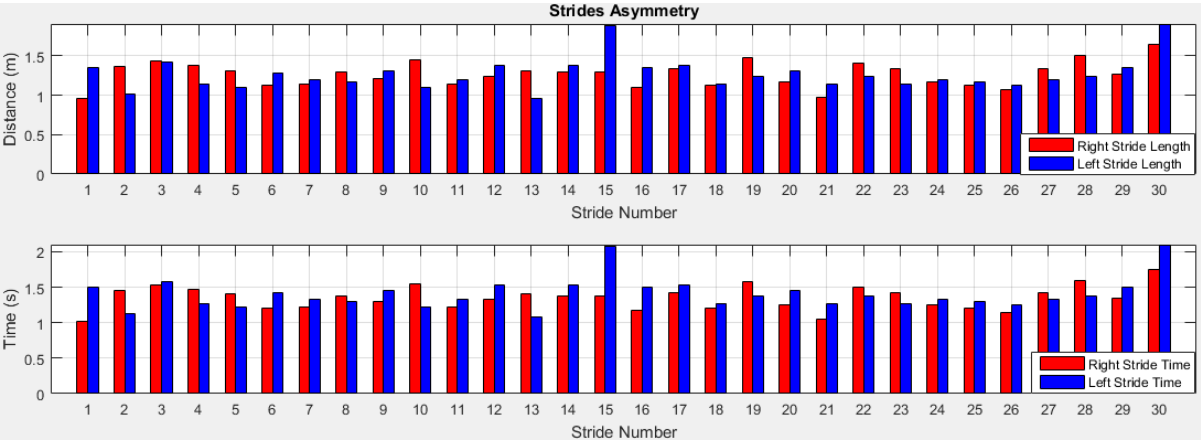

Figure 1.4: Stride asymmetry estimation of right and left legs

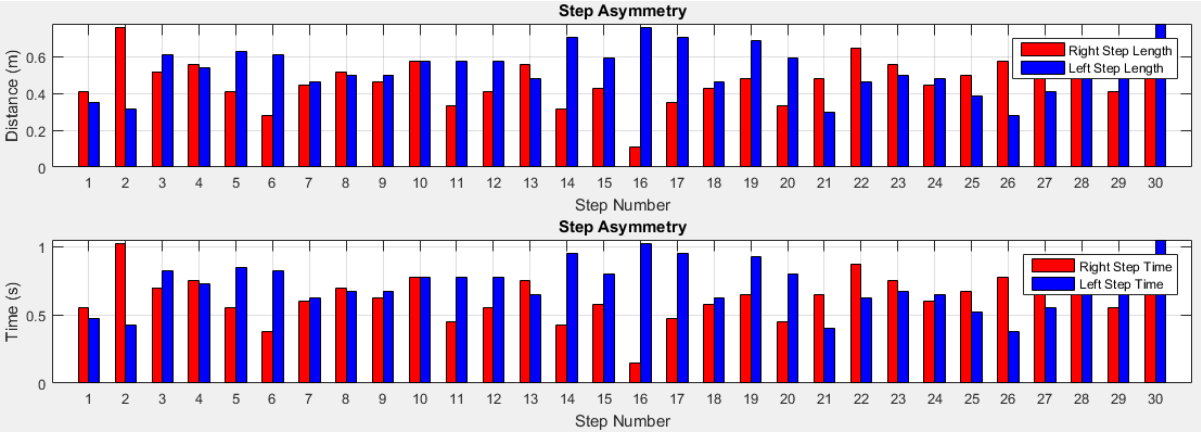

Figure 1.5: Step asymmetry estimation of right and left legs

2: Young Participant 2

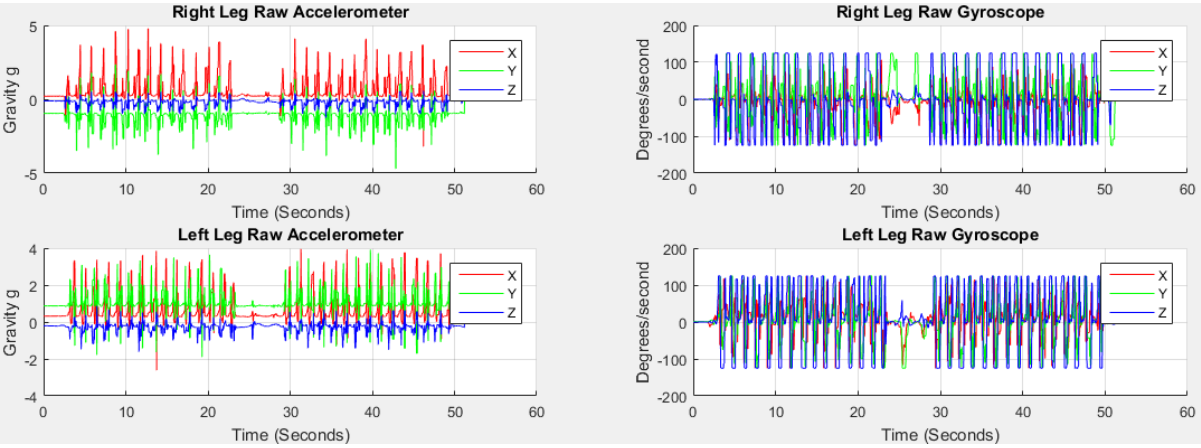

Figure 2.1: Accelerometer and gyroscope data from right and left legs

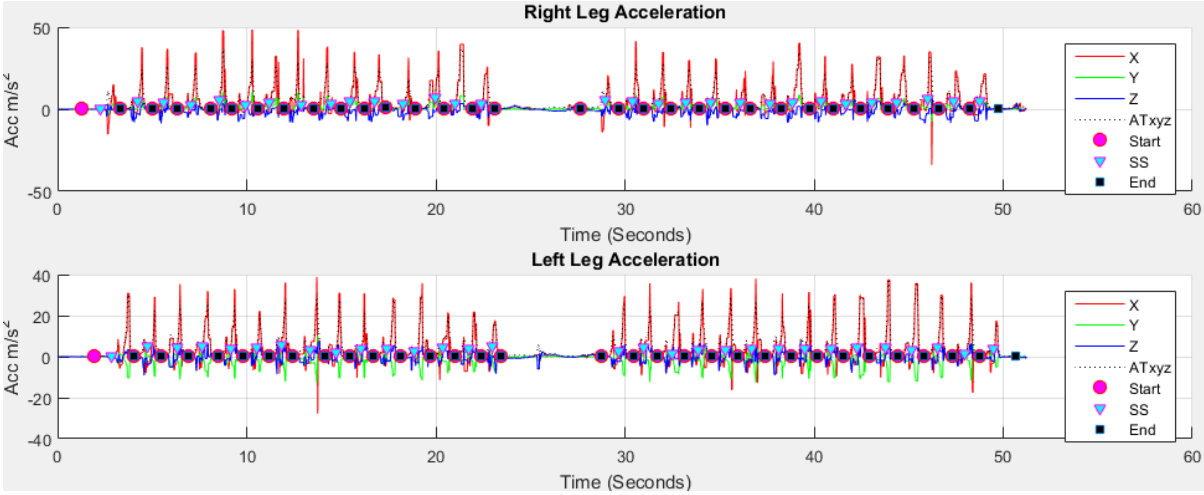

Figure 2.2:Result of stride, stance and swing event detection using proposed method

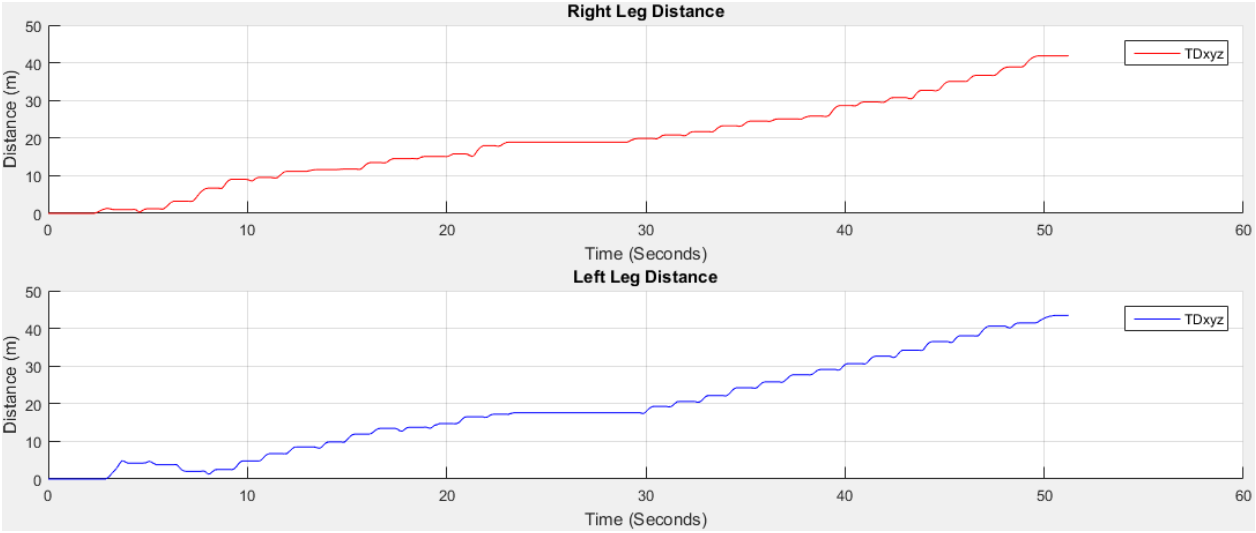

Figure 2.3: Result of distance estimation using proposed method

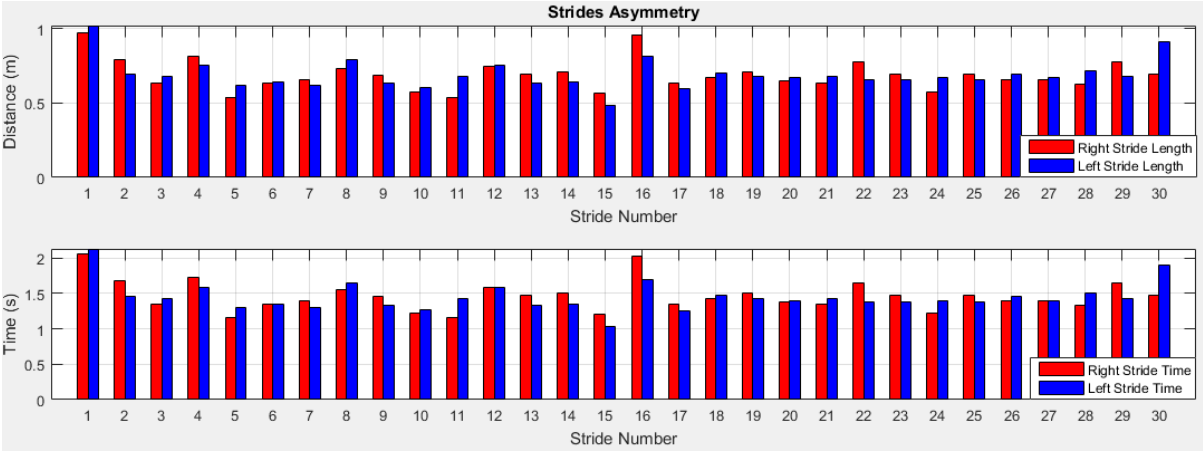

Figure 2.4: Stride asymmetry estimation of right and left legs

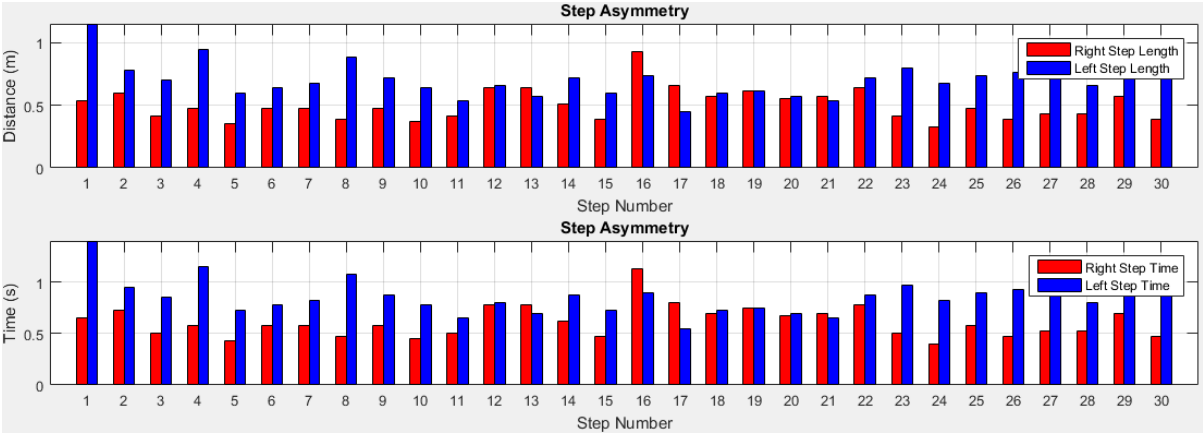

Figure 2.5: Step asymmetry estimation of right and left legs

3: Young Participant 3

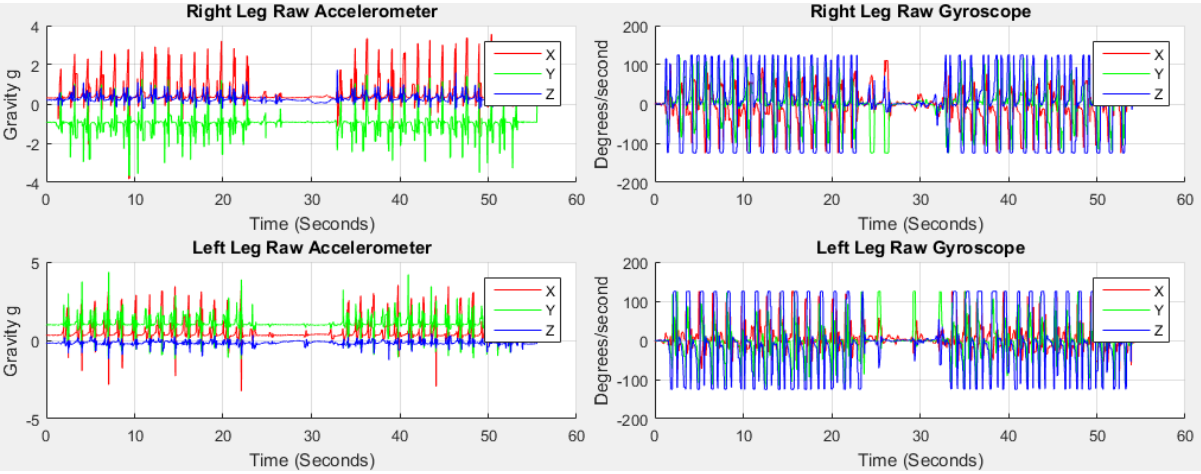

Figure 3.1: Accelerometer and gyroscope data from right and left legs

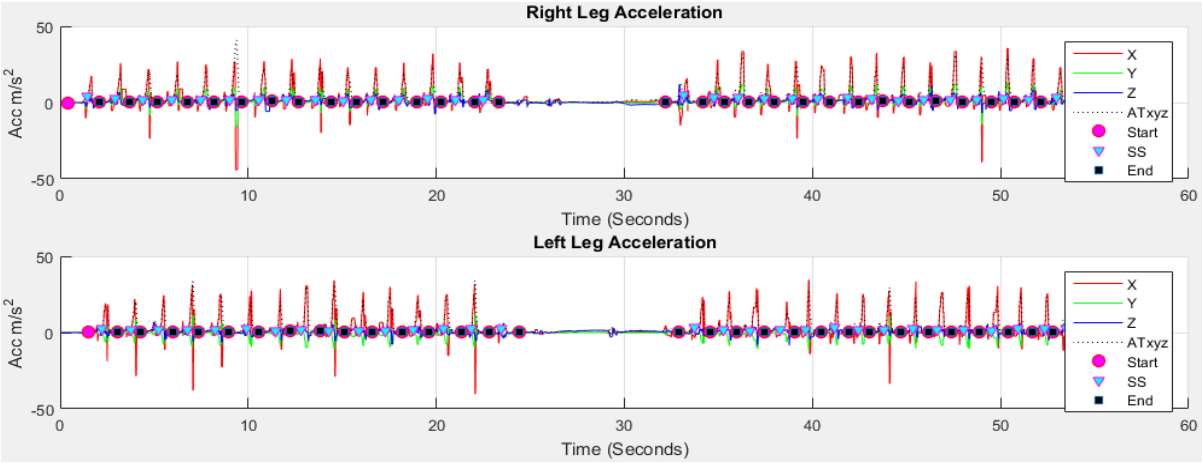

Figure 3.2: Result of stride, stance and swing event detection using proposed method

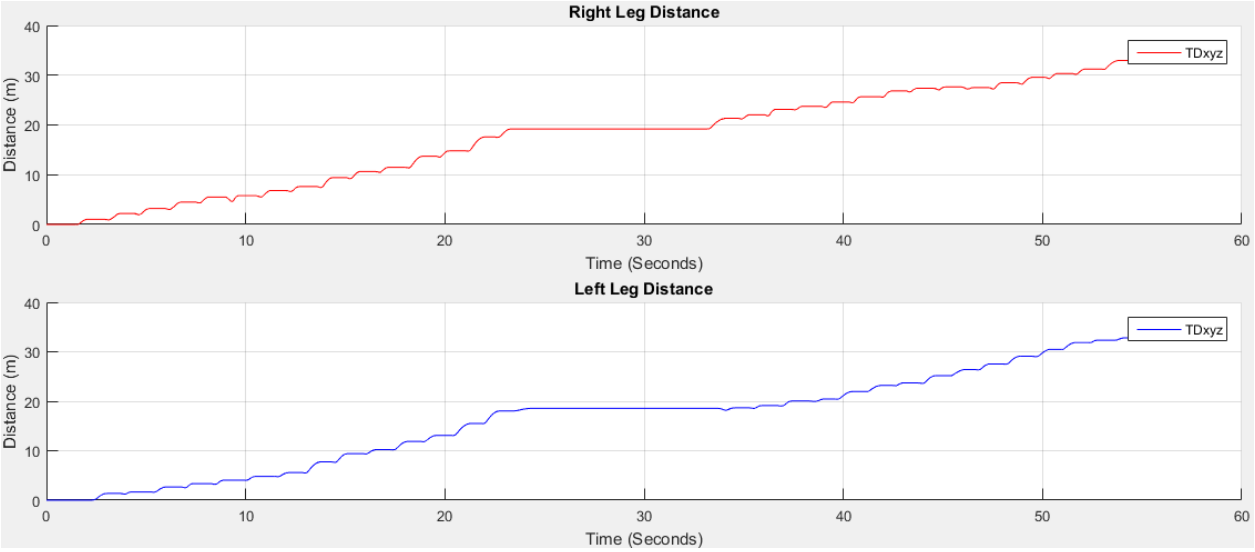

Figure 3.3: Result of distance estimation using proposed method

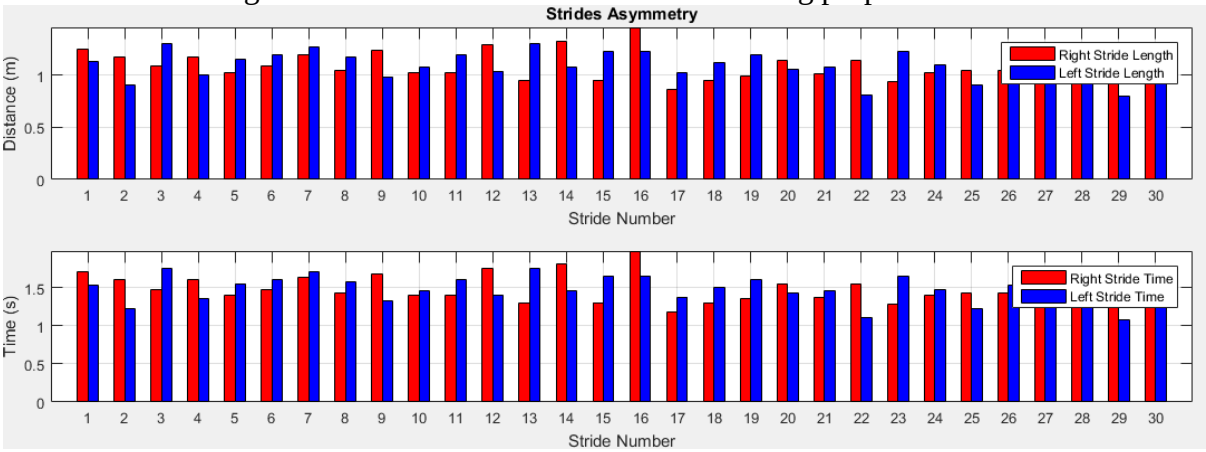

Figure 3.4: Stride asymmetry estimation of right and left legs

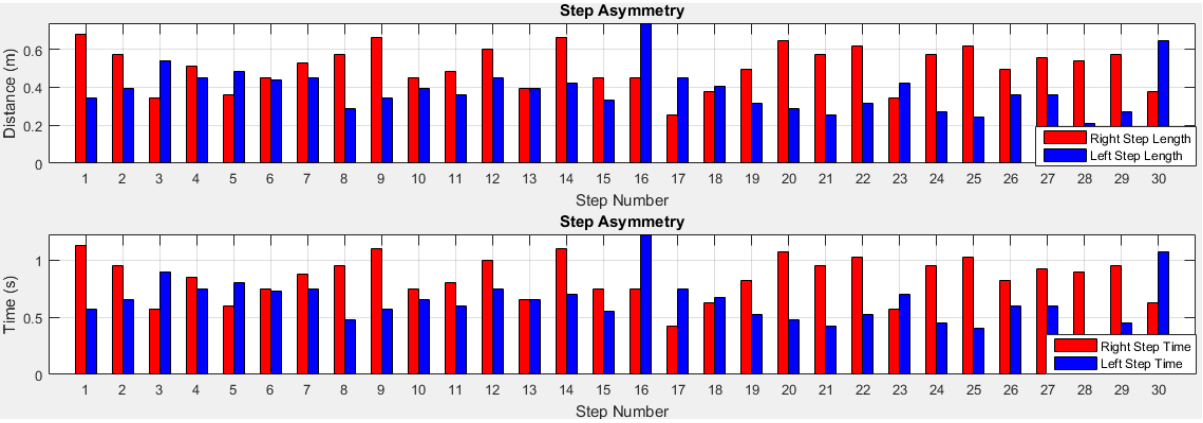

Figure 3.5: Step asymmetry estimation of right and left legs

4: Young Participant 4

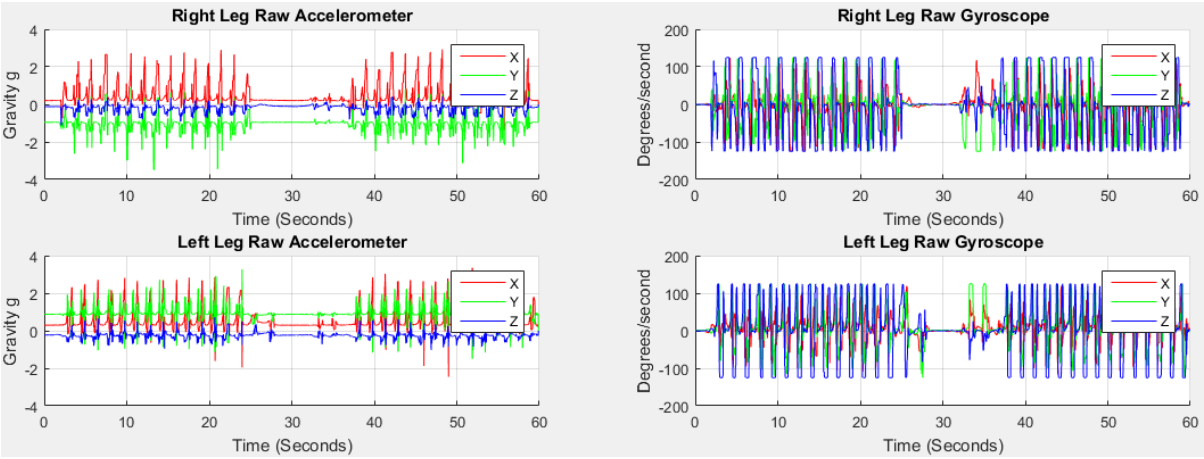

Figure 4.1: Accelerometer and gyroscope data from right and left legs

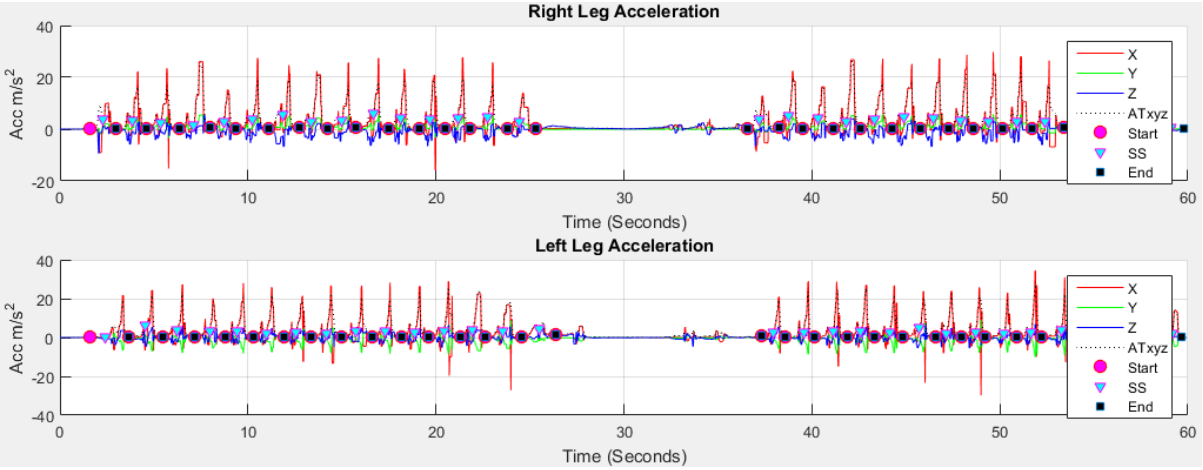

Figure 4.2: Result of stride, stance and swing event detection using proposed method

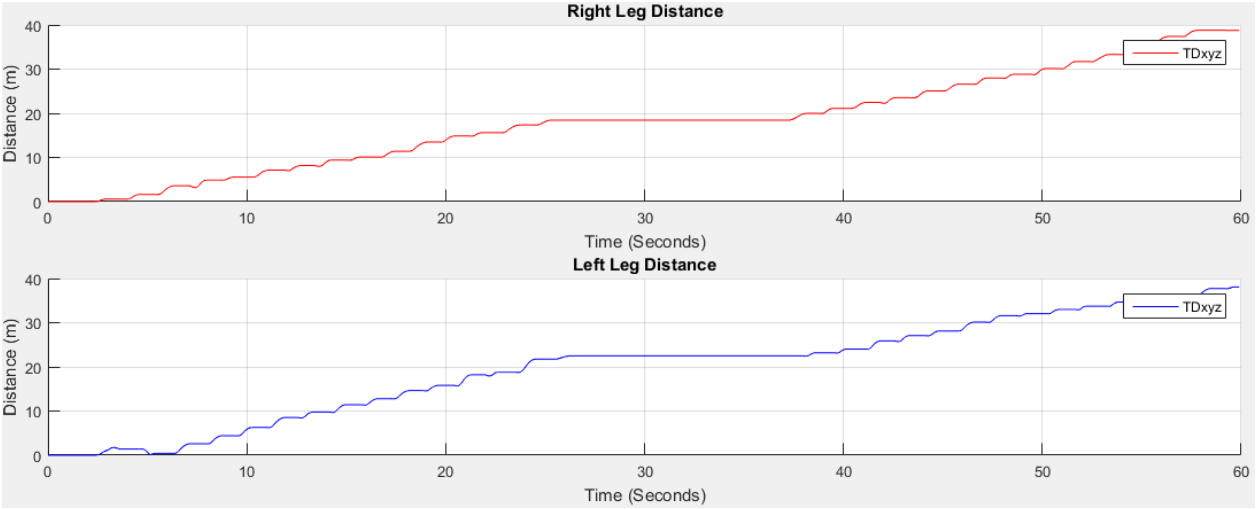

Figure 4.3: Result of distance estimation using proposed method

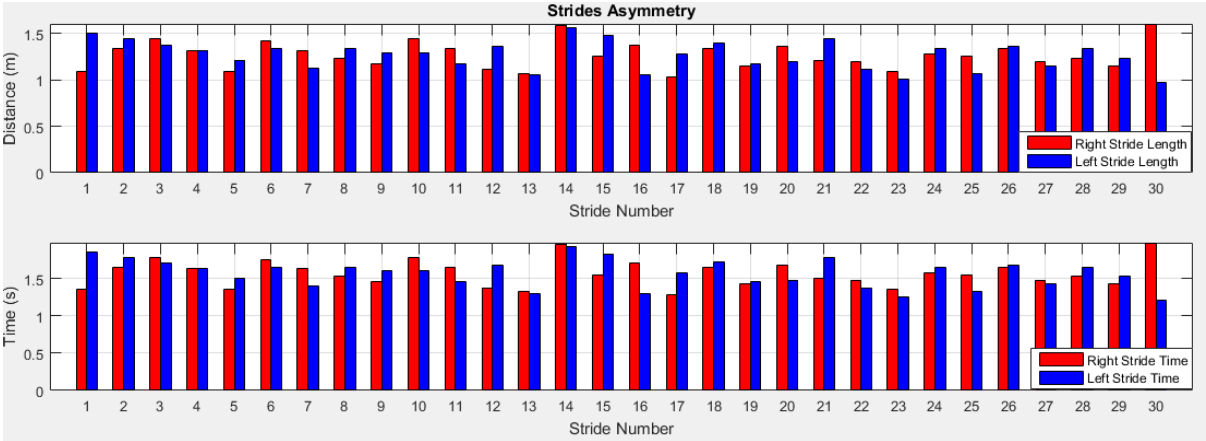

Figure 4.4: Stride asymmetry estimation of right and left legs

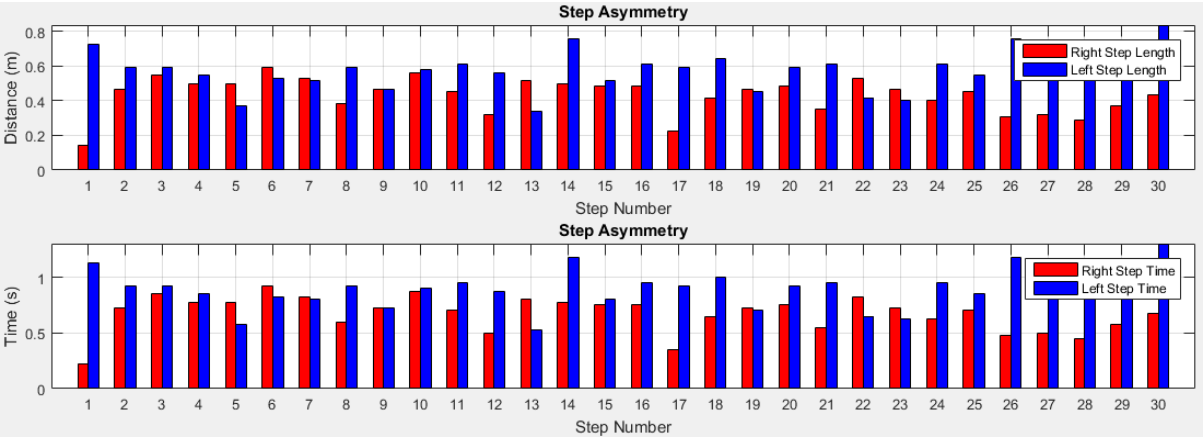

Figure 4.5: Step asymmetry estimation of right and left legs

5: Young Participant 5

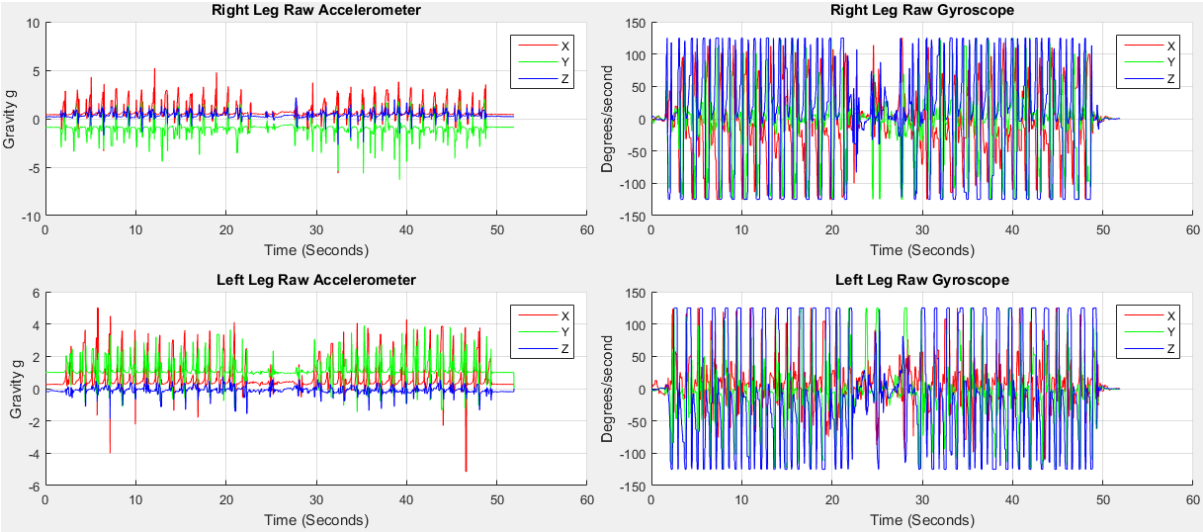

Figure 5.1: Accelerometer and gyroscope data from right and left legs

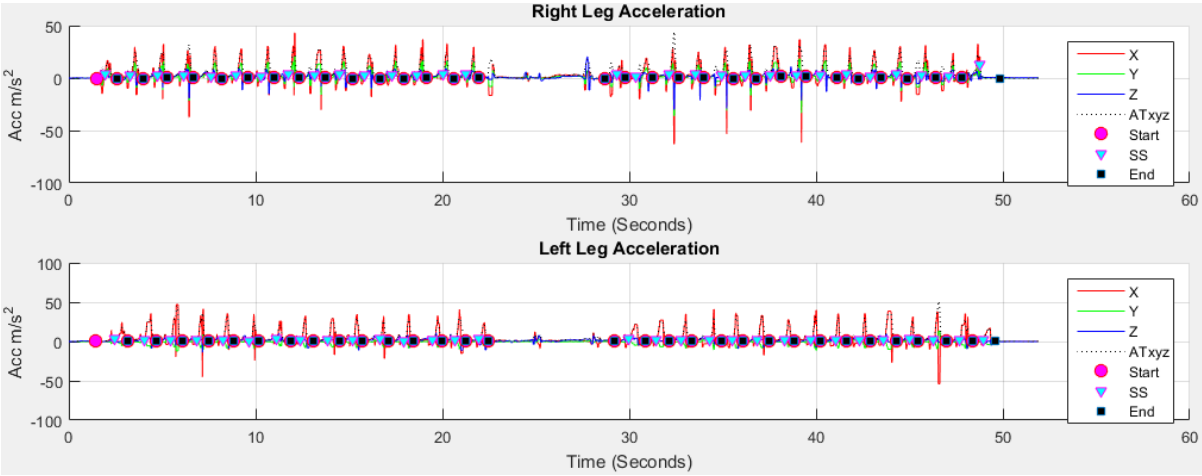

Figure 5.2: Result of stride, stance and swing event detection using proposed method

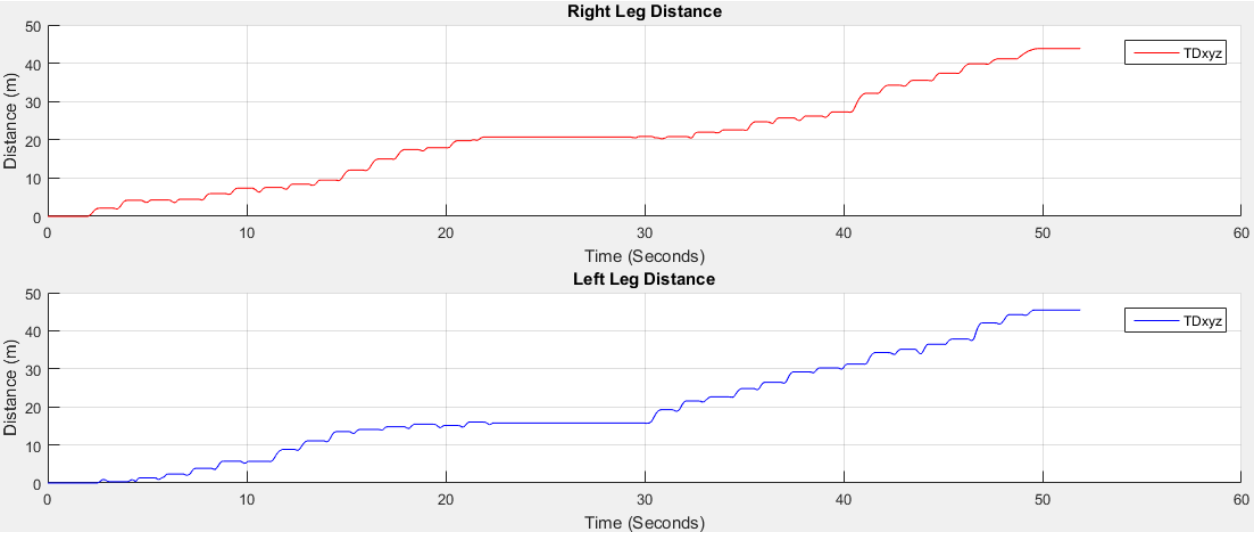

Figure 5.3: Result of distance estimation using proposed method

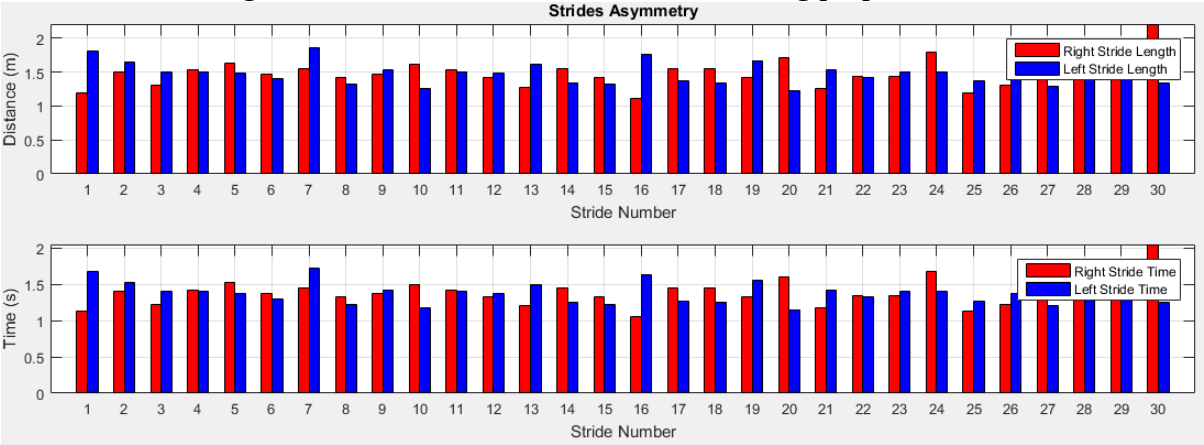

Figure 5.4: Stride asymmetry estimation of right and left legs

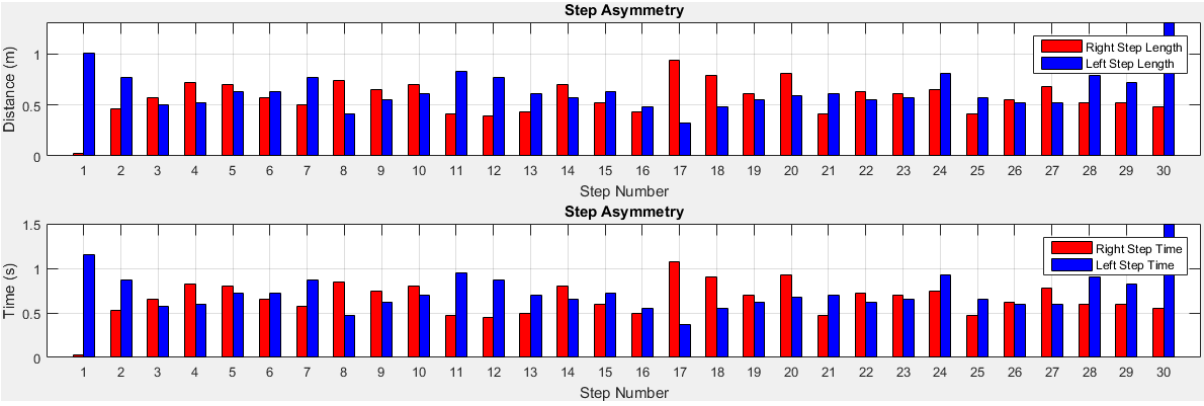

Figure 5.5: Step asymmetry estimation of right and left legs

6: Young Participant 6

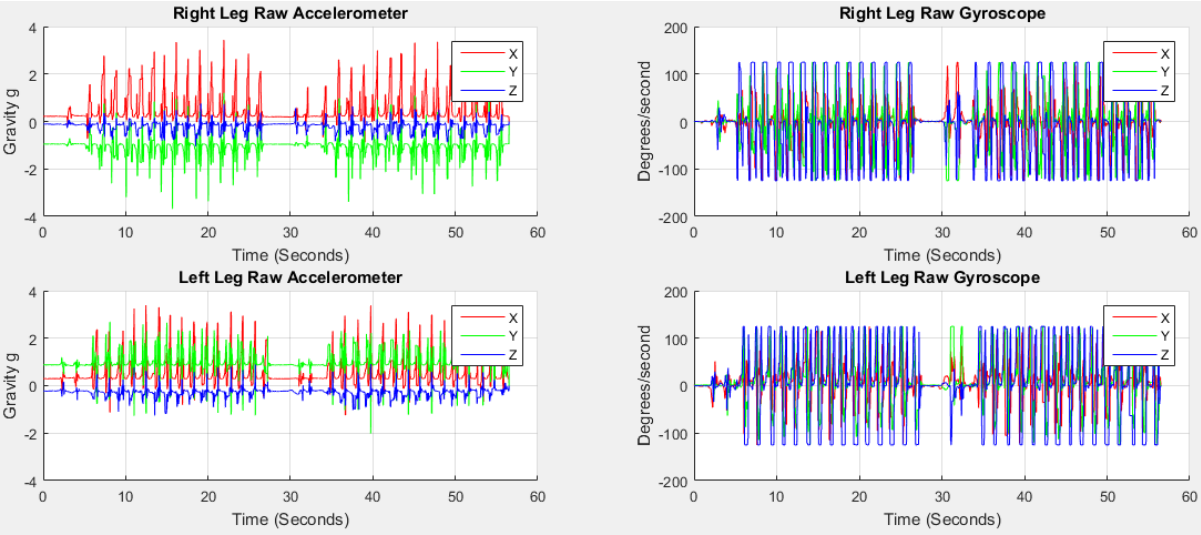

Figure 6.1: Accelerometer and gyroscope data from right and left legs

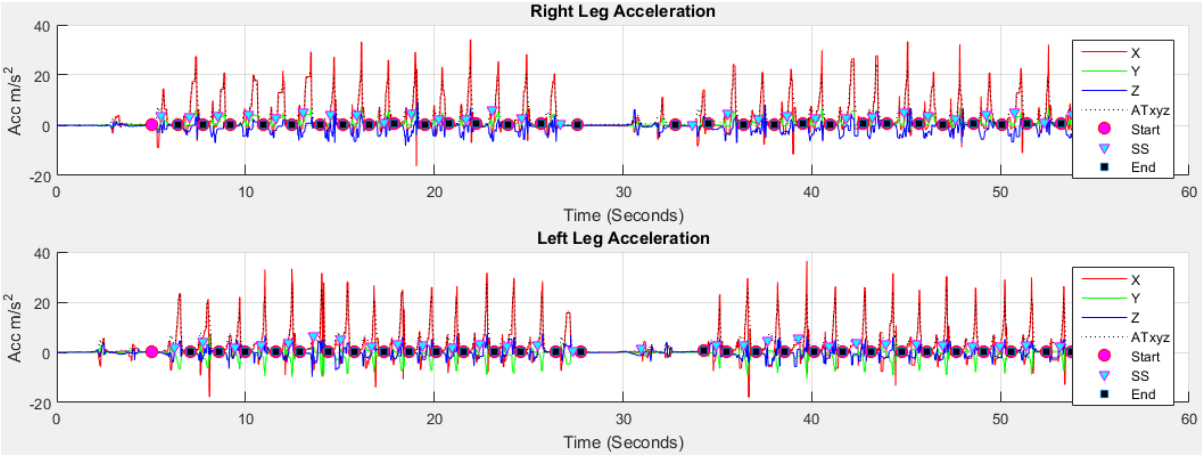

Figure 6.2: Result of stride, stance and swing event detection using proposed method

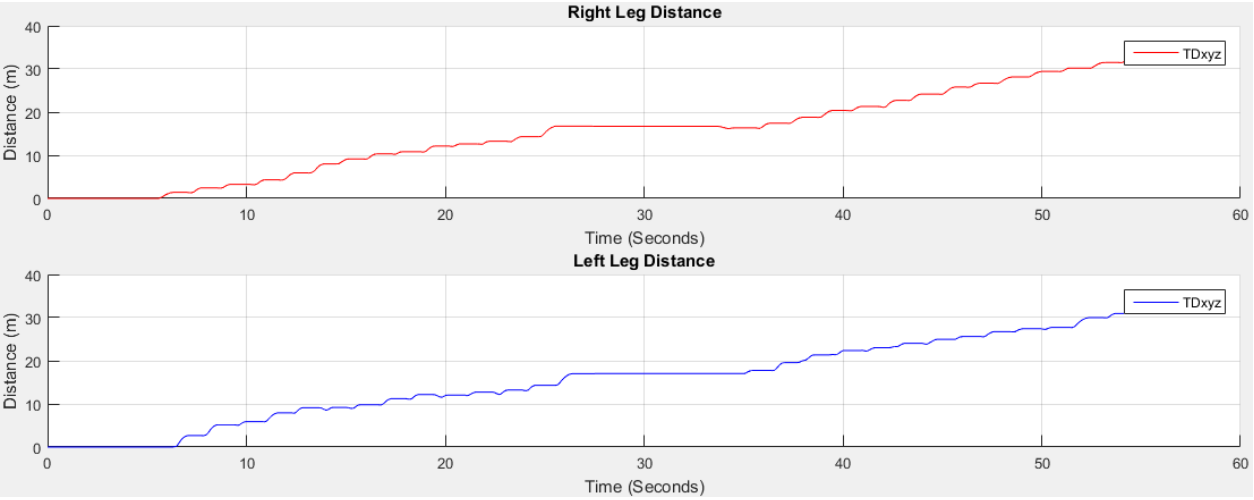

Figure 6.3: Result of distance estimation using proposed method

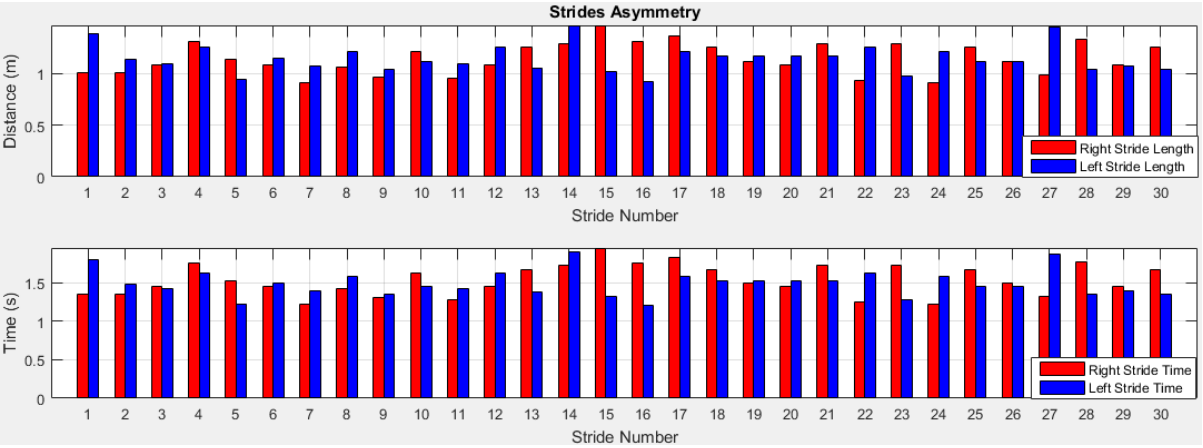

Figure 6.4: Stride asymmetry estimation of right and left legs

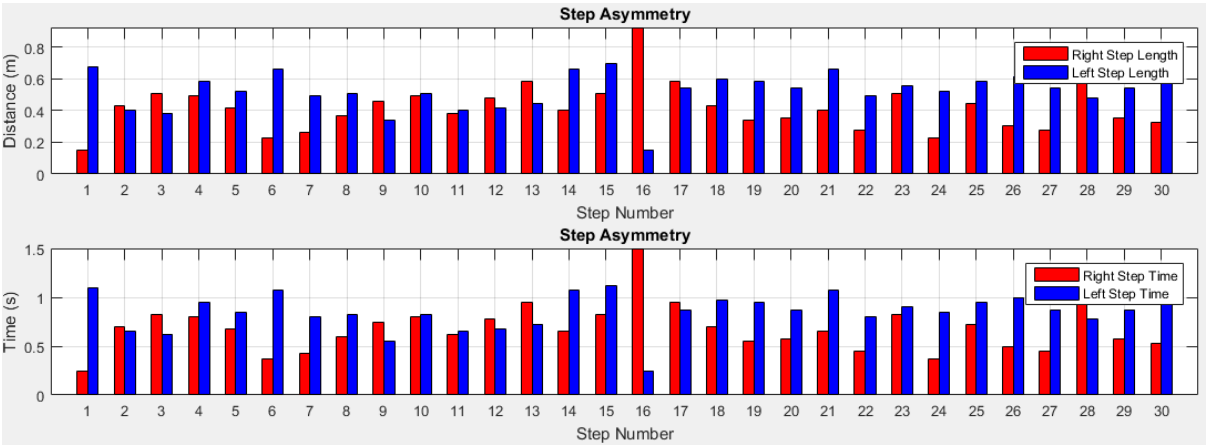

Figure 6.5: Step asymmetry estimation of right and left legs

7: Young Participant 7

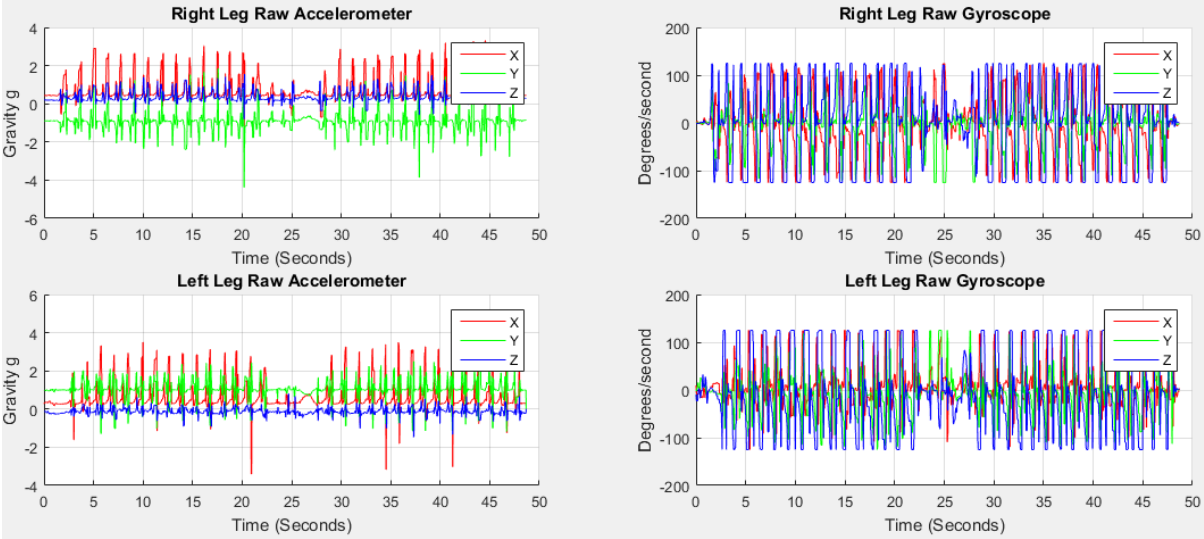

Figure 7.1: Accelerometer and gyroscope data from right and left legs

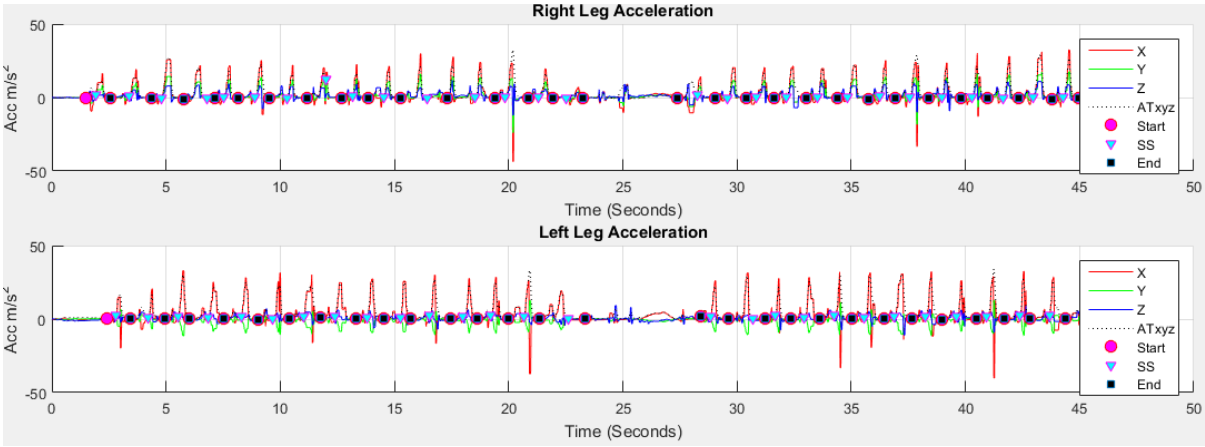

Figure 7.2: Result of stride, stance and swing event detection using proposed method

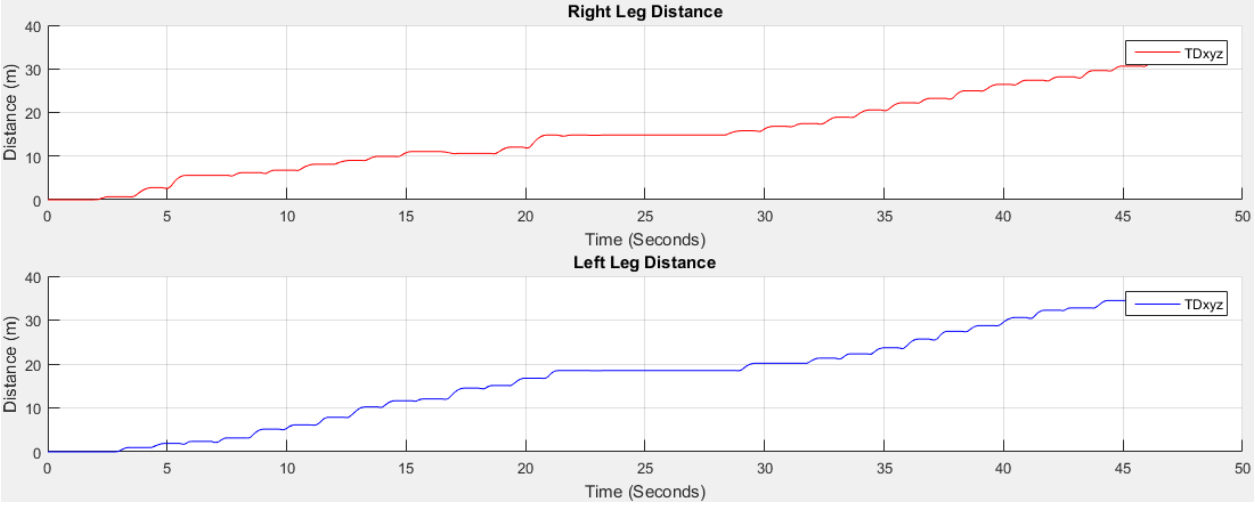

Figure 7.3: Result of distance estimation using proposed method

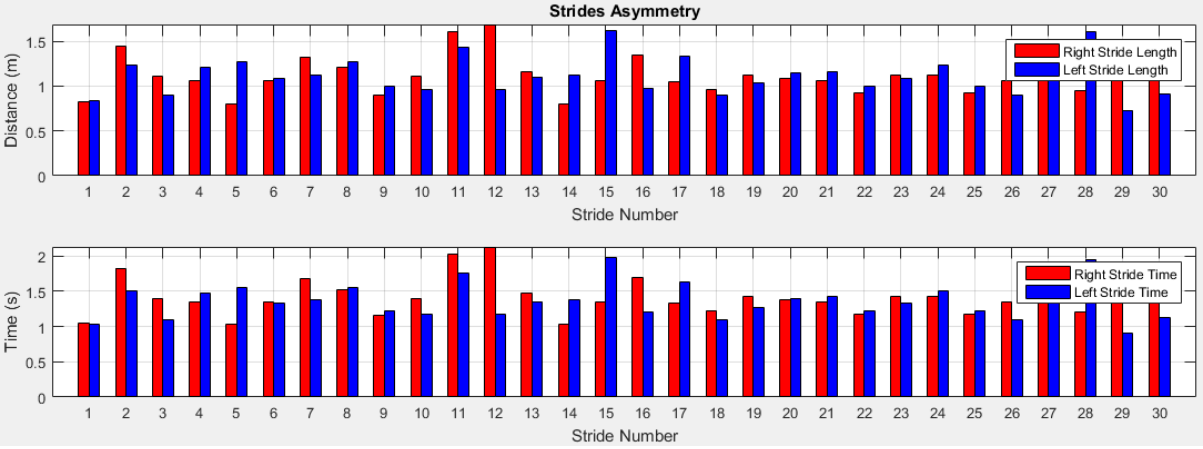

Figure 7.4: Stride asymmetry estimation of right and left legs

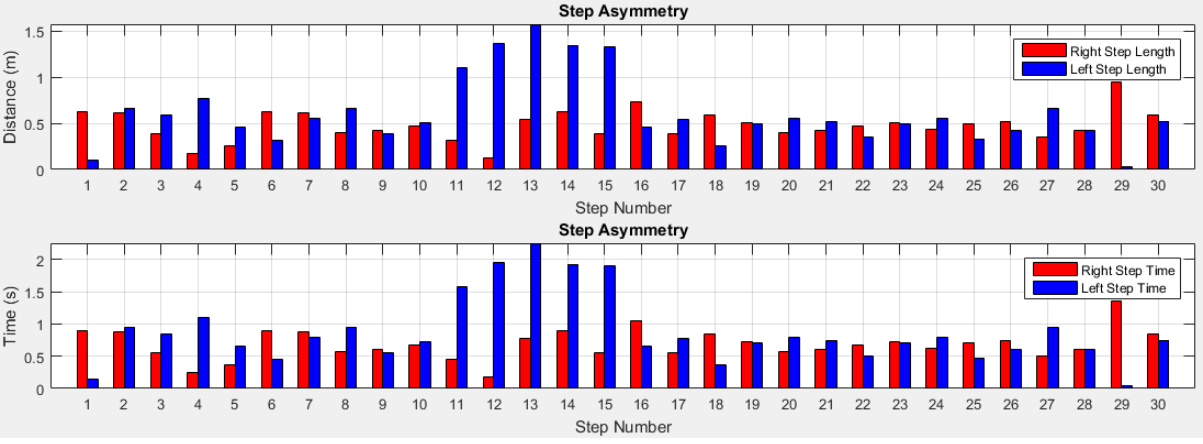

Figure 7.5: Step asymmetry estimation of right and left legs

8: Young Participant 8

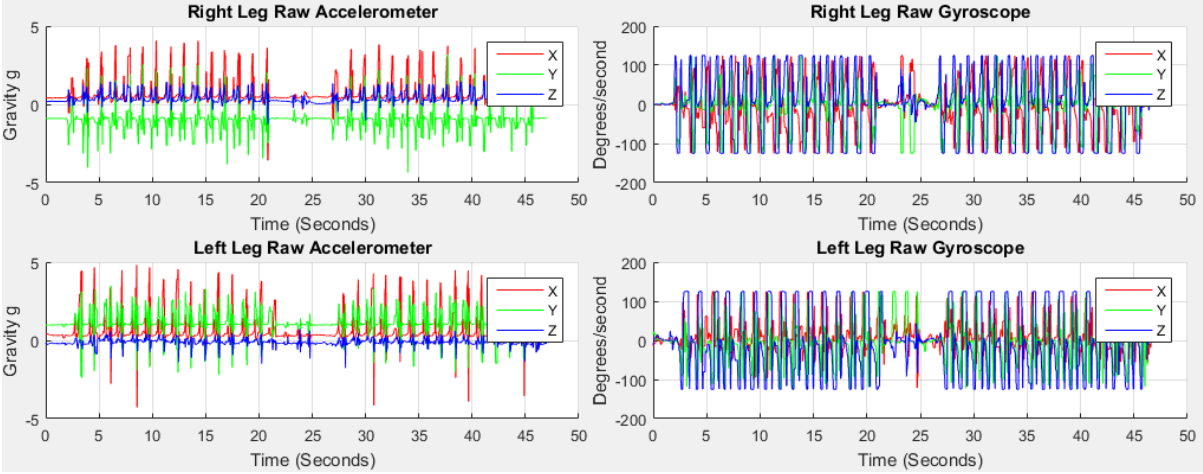

Figure 8.1: Accelerometer and gyroscope data from right and left legs

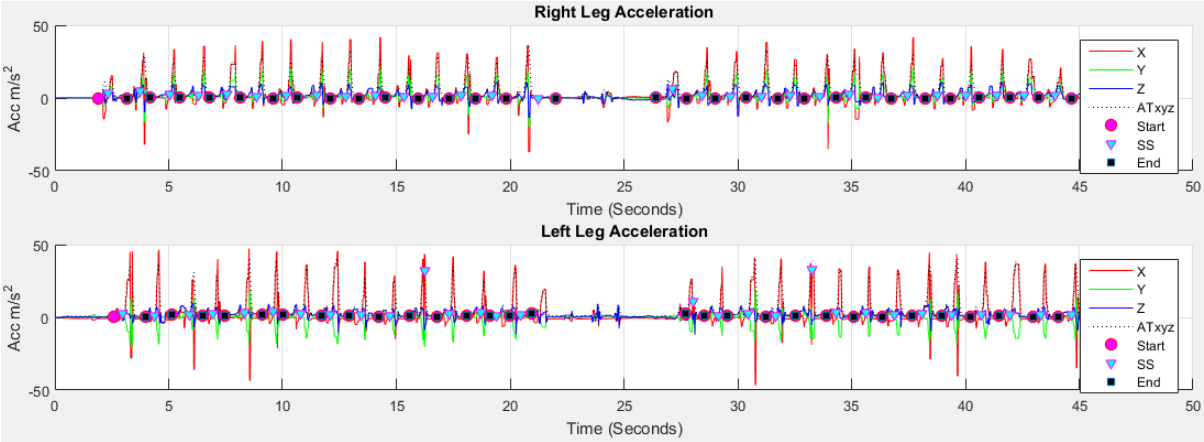

Figure 8.2: Result of stride, stance and swing event detection using proposed method

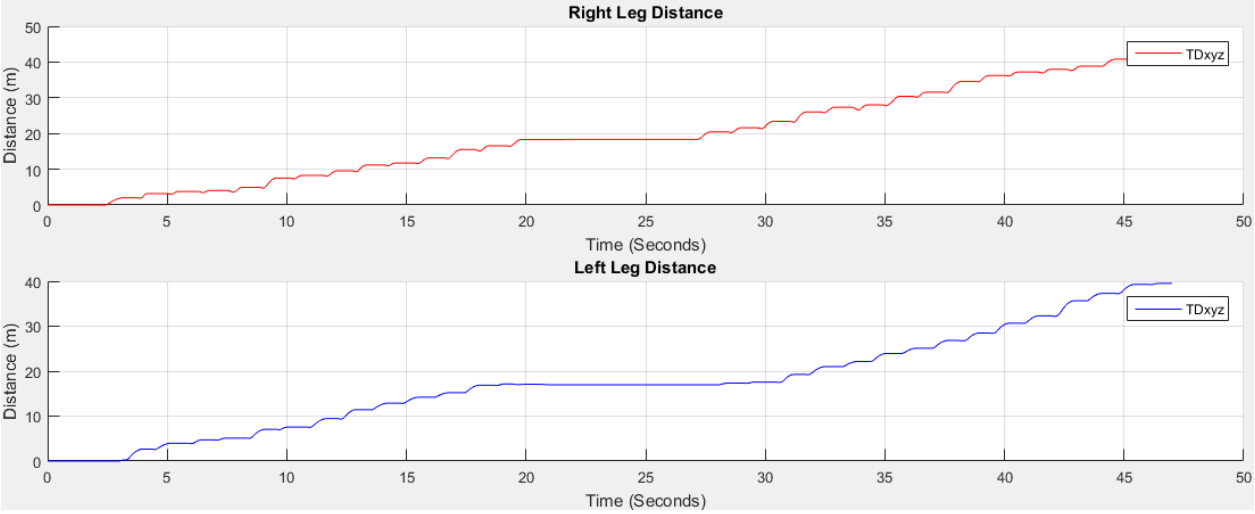

Figure 8.3: Result of distance estimation using proposed method

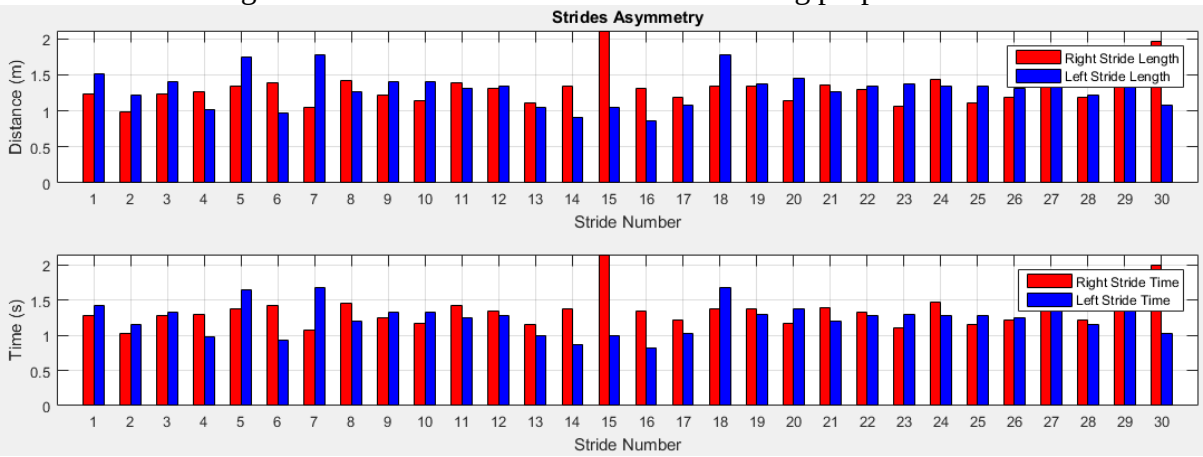

Figure 8.4: Stride asymmetry estimation of right and left legs

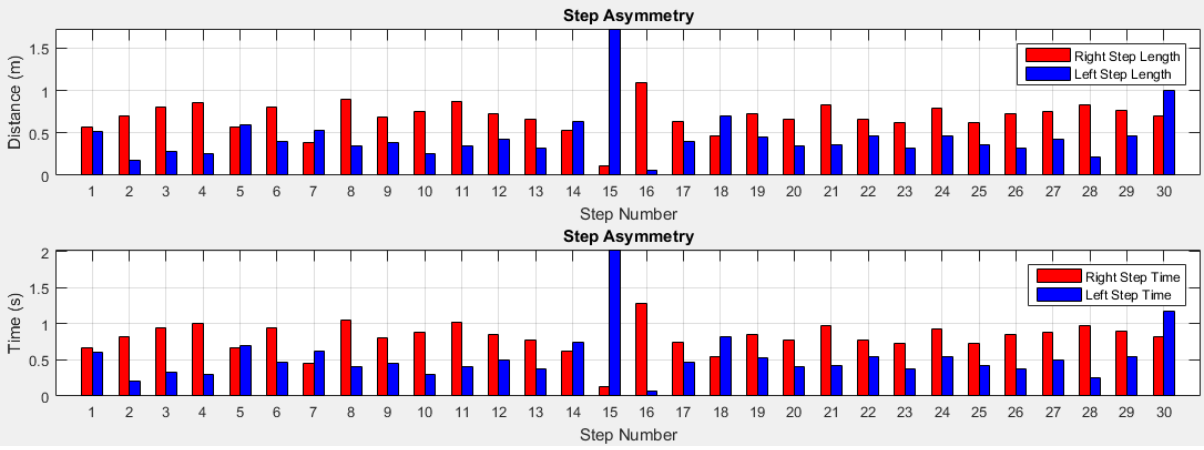

Figure 8.5: Step asymmetry estimation of right and left legs

9: Young Participant 9

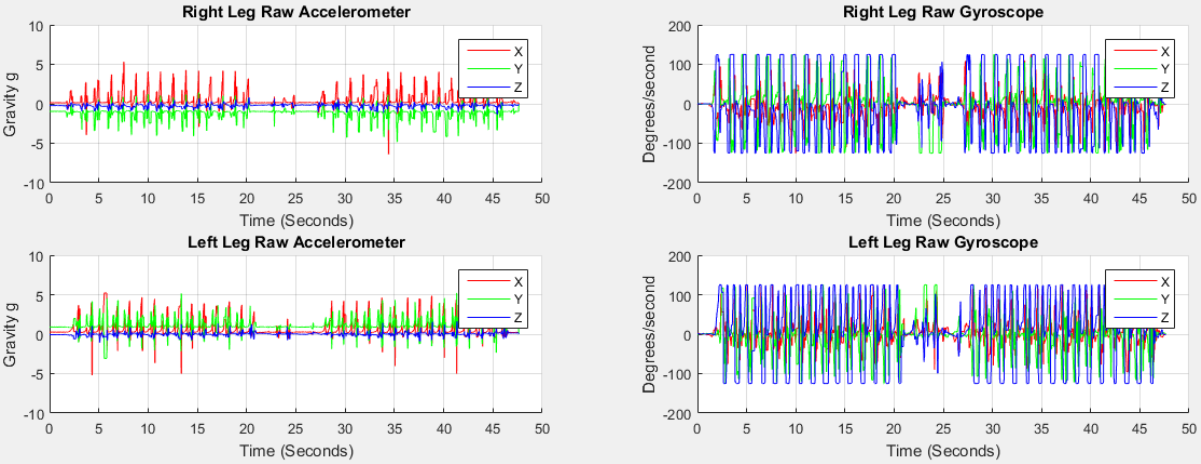

Figure 9.1: Accelerometer and gyroscope data from right and left legs

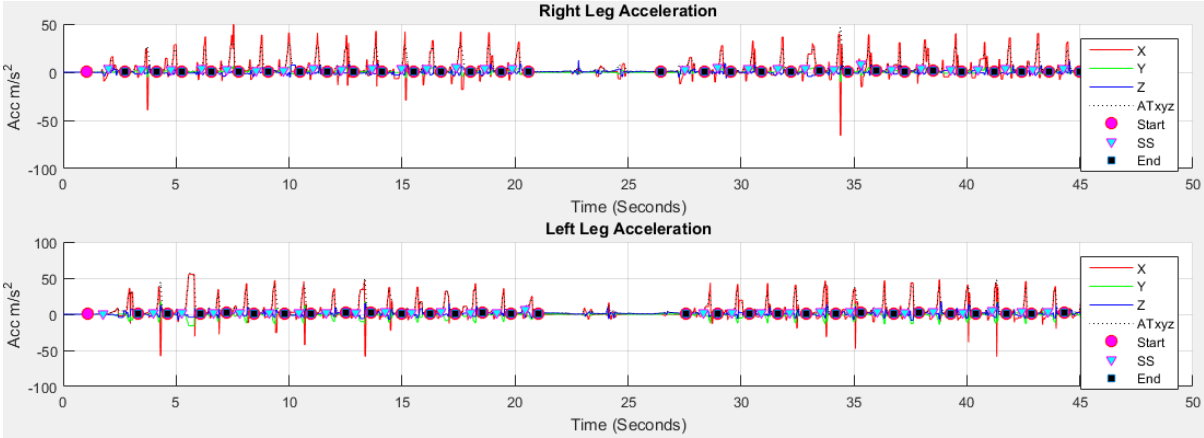

Figure 9.2: Result of stride, stance and swing event detection using proposed method

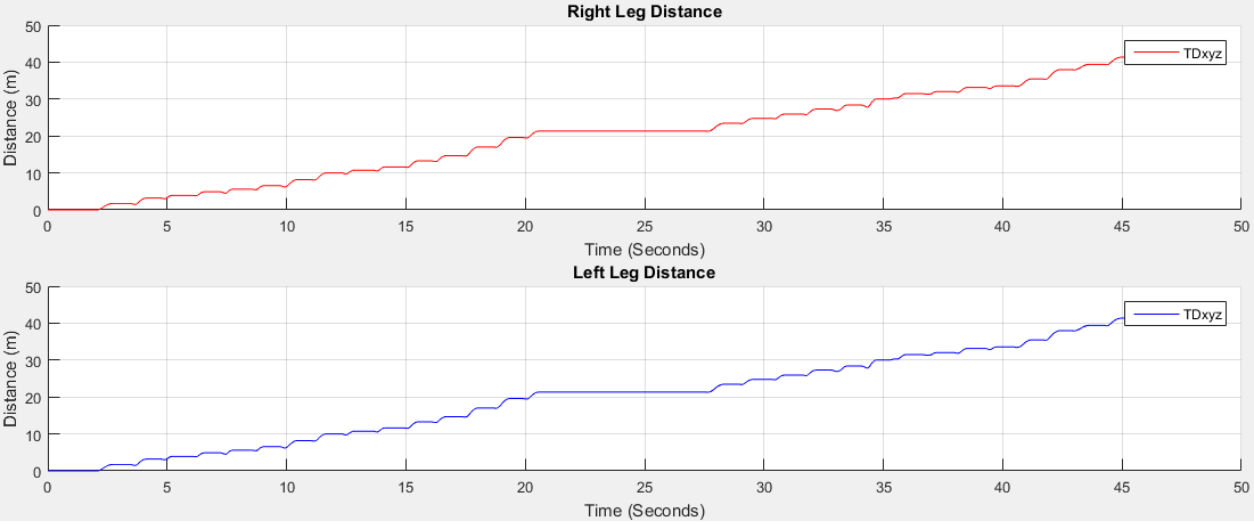

Figure 9.3: Result of distance estimation using proposed method

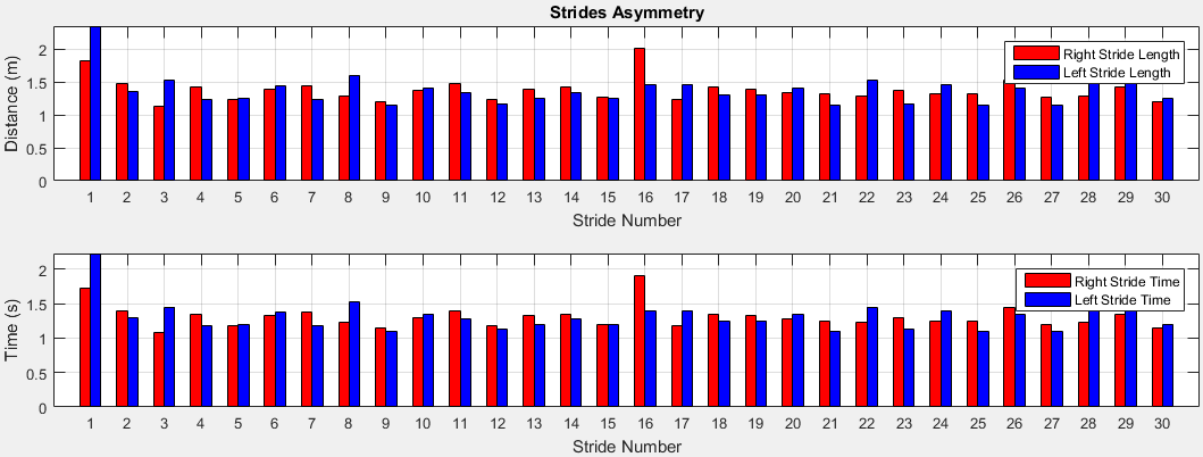

Figure 9.4: Stride asymmetry estimation of right and left legs

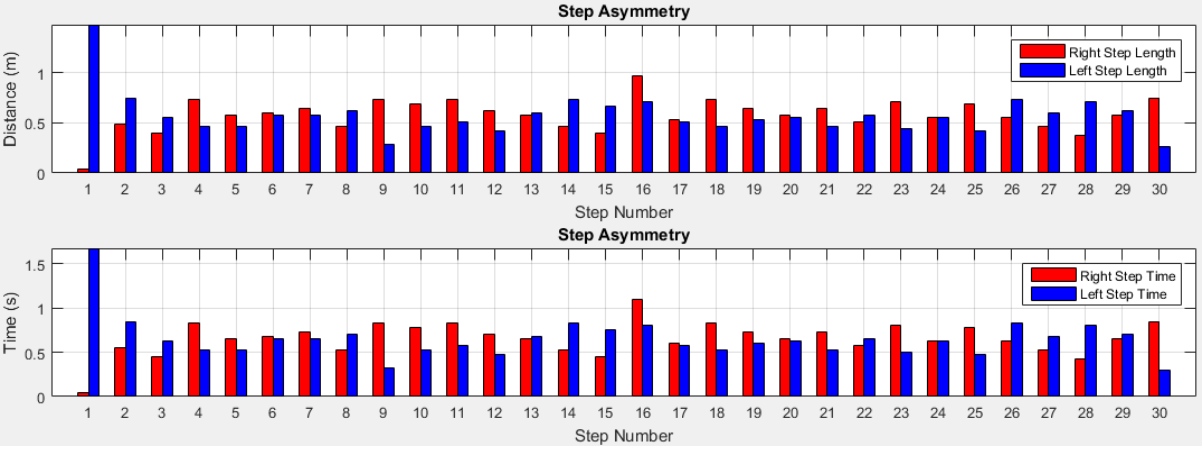

Figure 9.5: Step asymmetry estimation of right and left legs

10: Young Participant 10

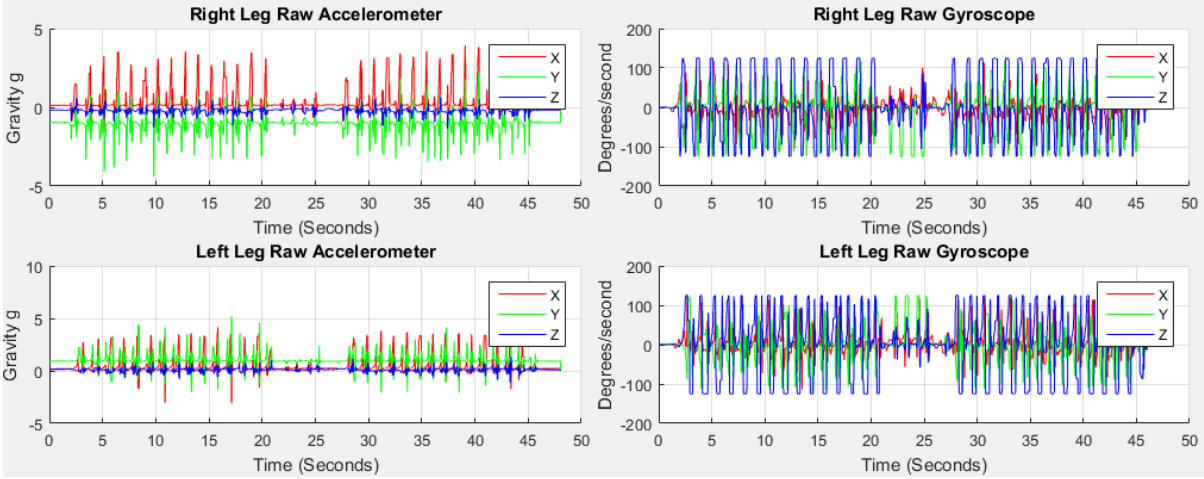

Figure 10.1: Accelerometer and gyroscope data from right and left legs

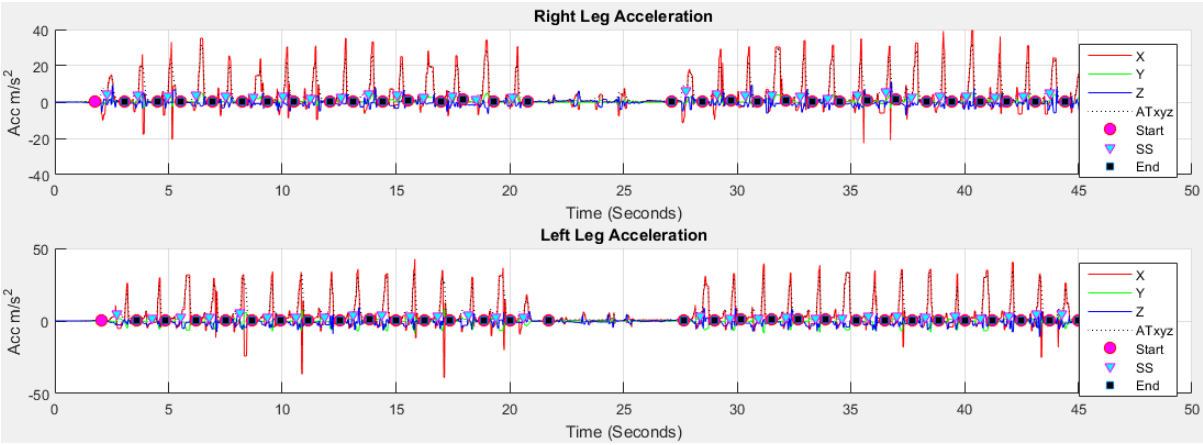

Figure 10.2: Result of stride, stance and swing event detection using proposed method

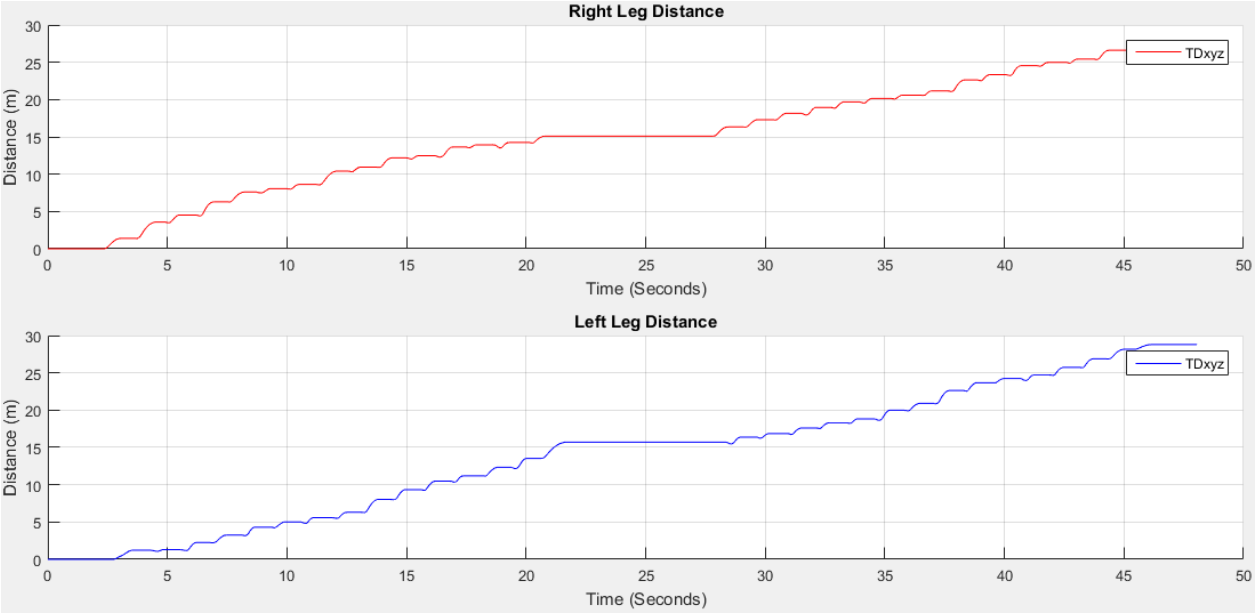

Figure 10.3: Result of distance estimation using proposed method

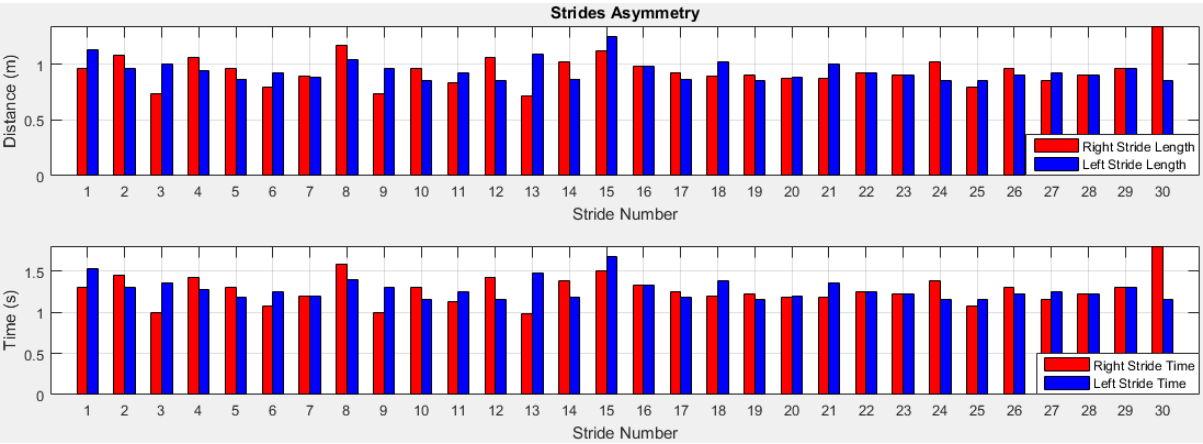

Figure 10.4: Stride asymmetry estimation of right and left legs

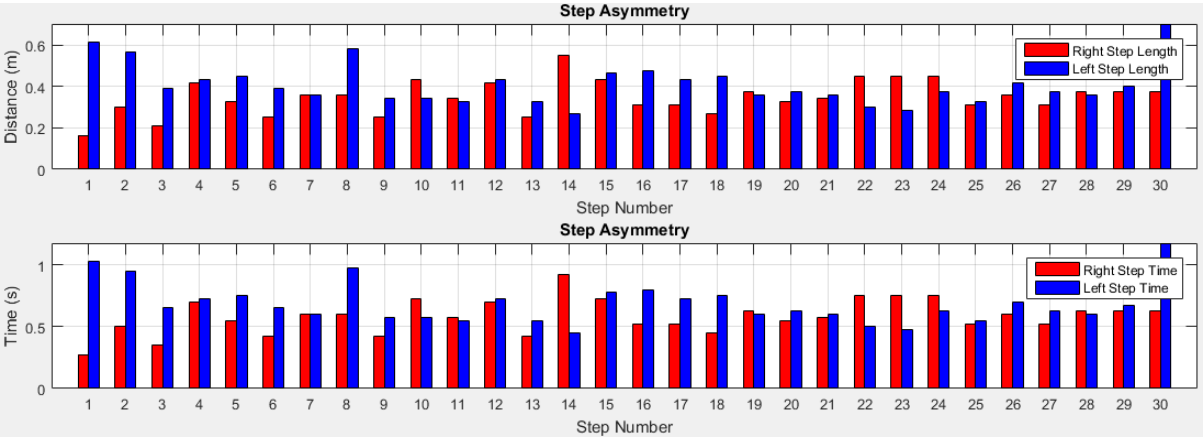

Figure 10.5: Step asymmetry estimation of right and left legs

1:Elderly Participant 1

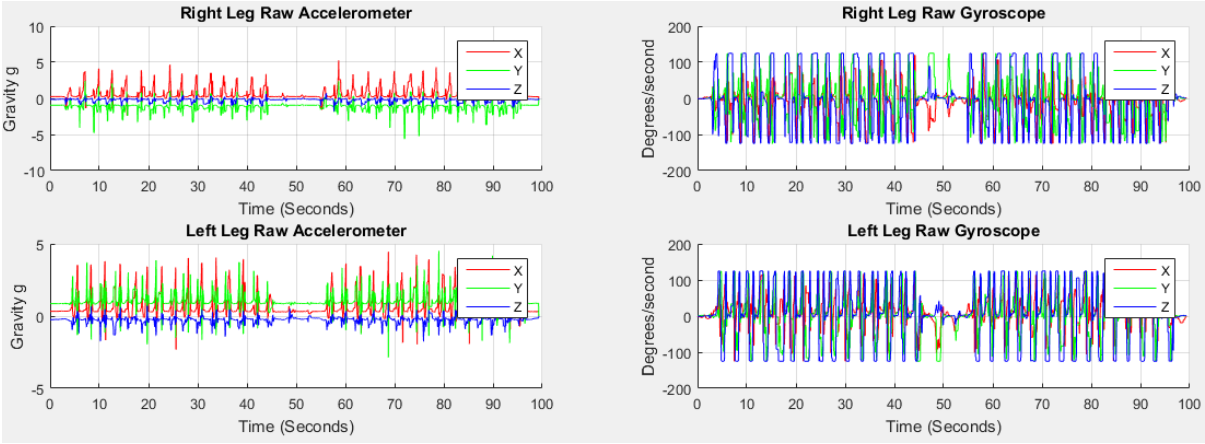

Figure 1.1: Accelerometer and gyroscope data from right and left foots

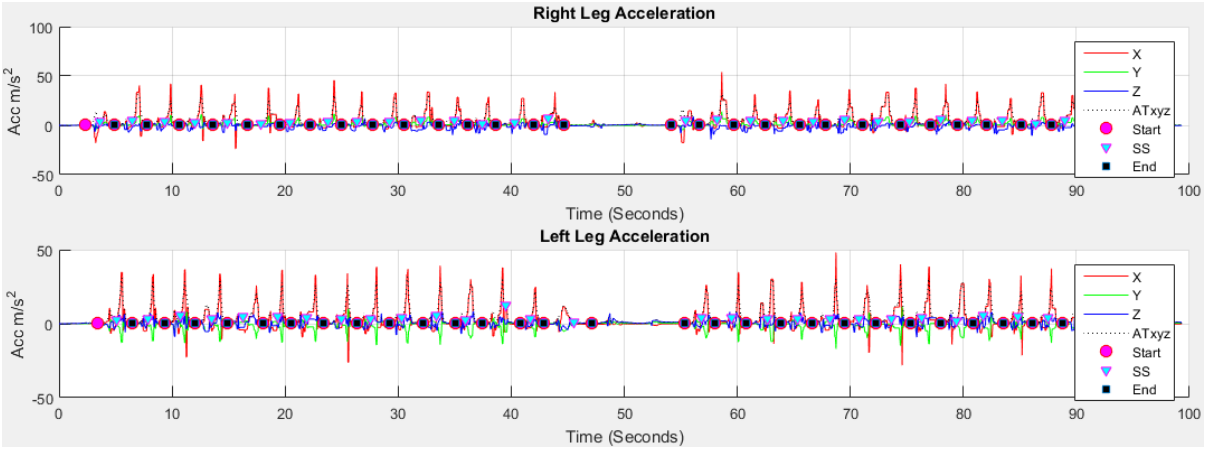

Figure 1.2: Result of stride, stance and swing event detection using proposed method

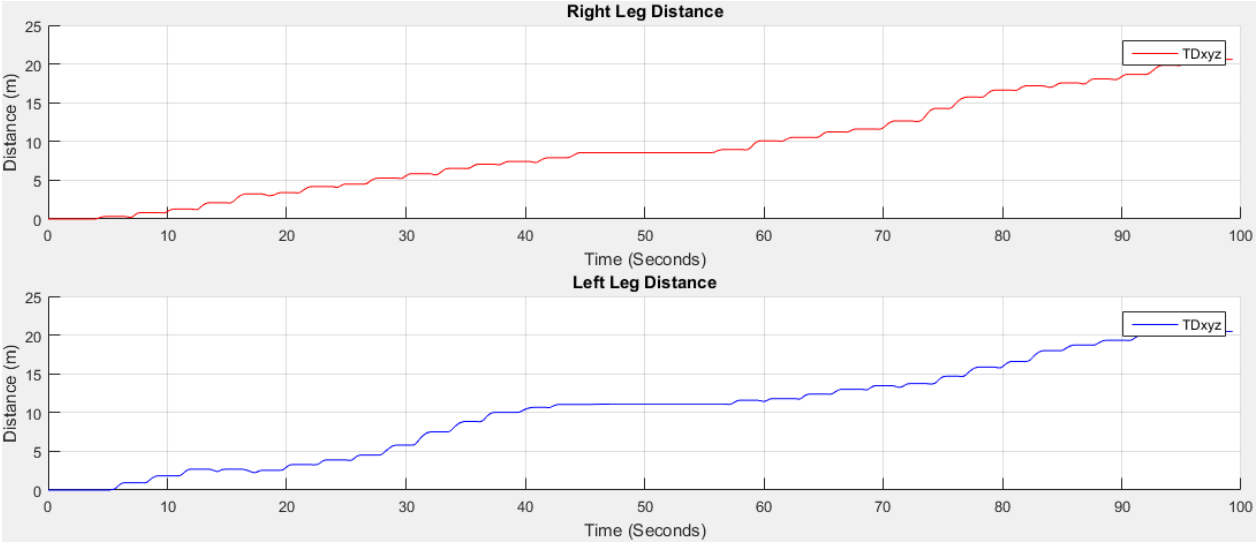

Figure 1.3: Result of distance estimation using proposed method

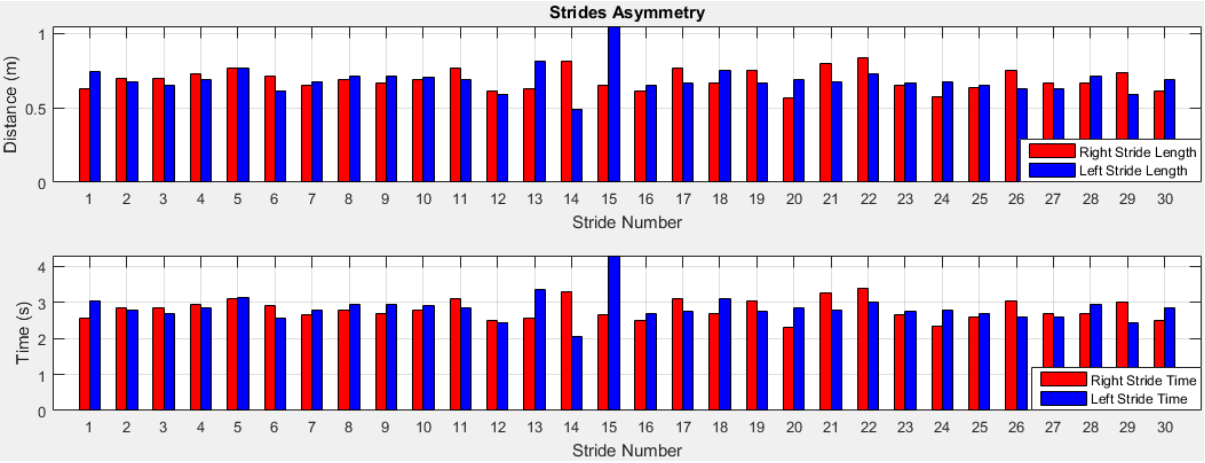

Figure 1.4: Stride asymmetry estimation of right and left legs

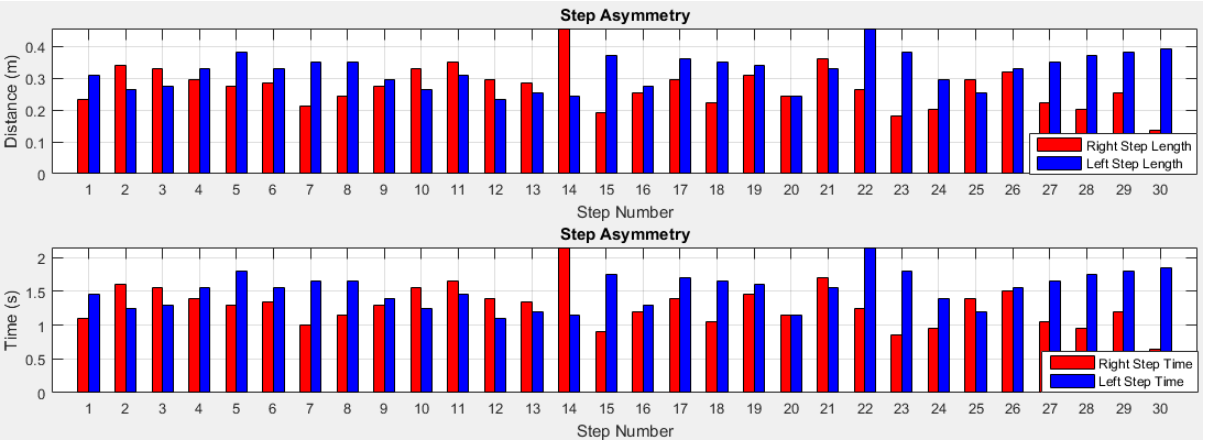

Figure 1.5: Step asymmetry estimation of right and left legs

2: Elderly Participant 2

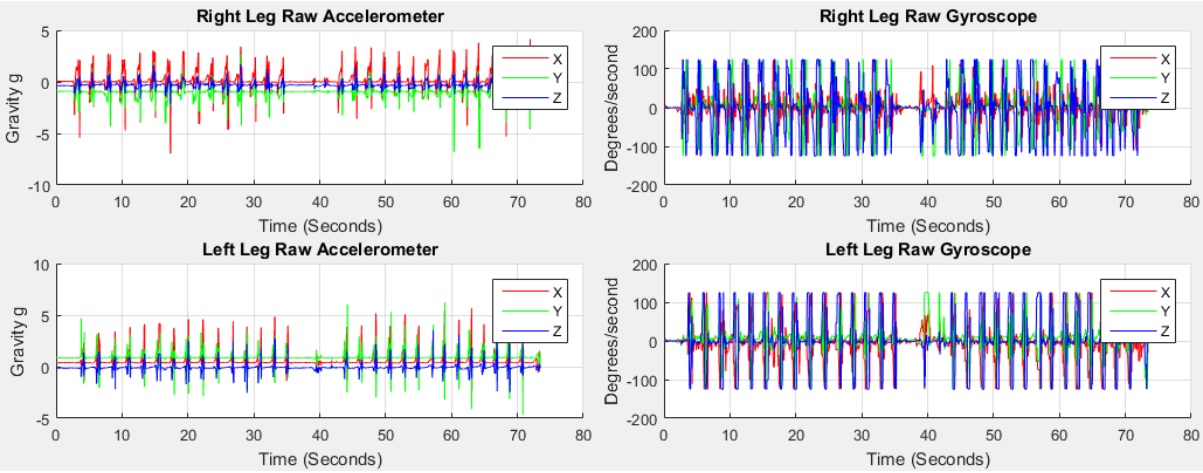

Figure 2.1: Accelerometer and gyroscope data from right and left legs

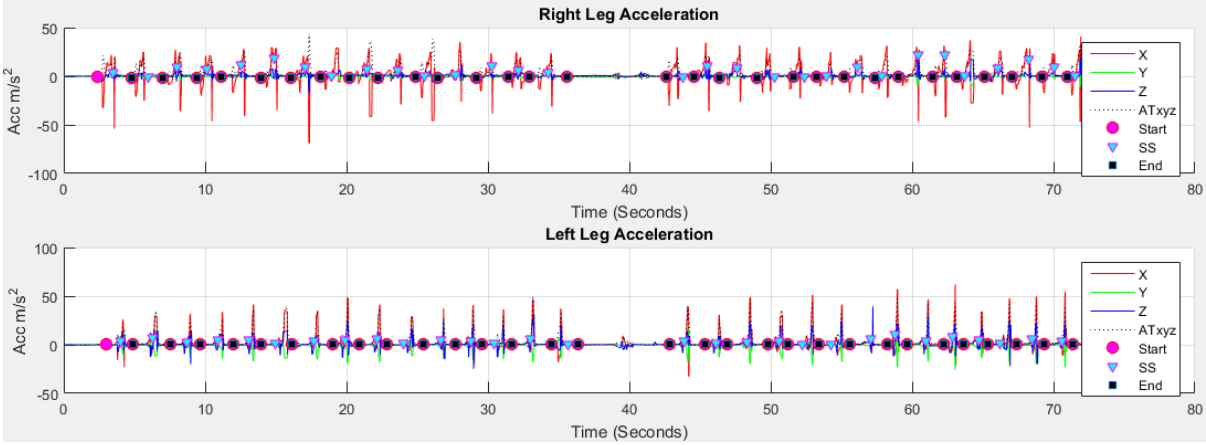

Figure 2.2: Result of stride, stance and swing event detection using proposed method

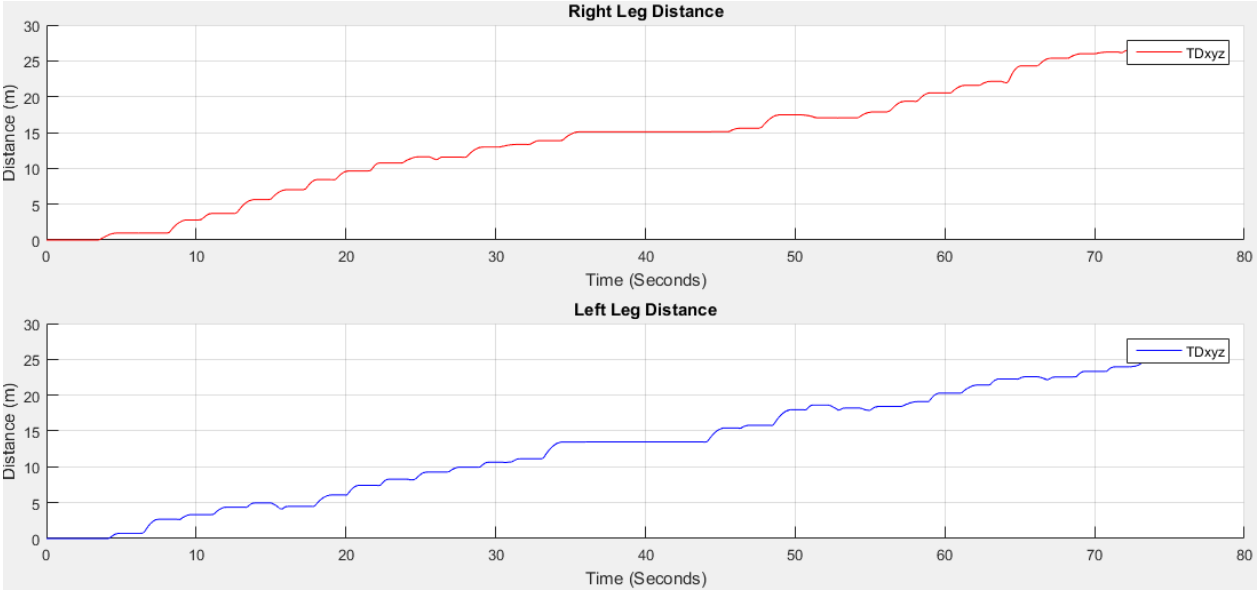

Figure 2.3: Result of distance estimation using proposed method

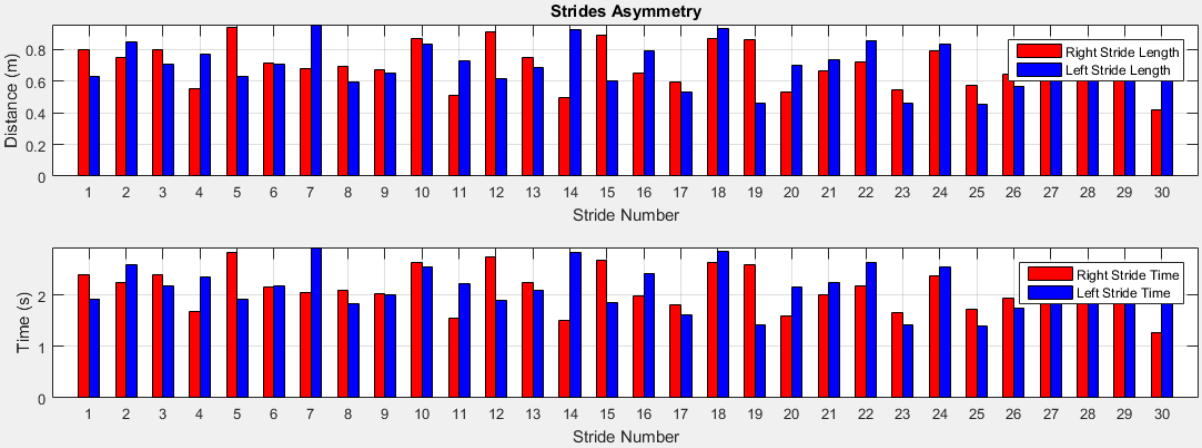

Figure 2.4: Stride asymmetry estimation of right and left legs

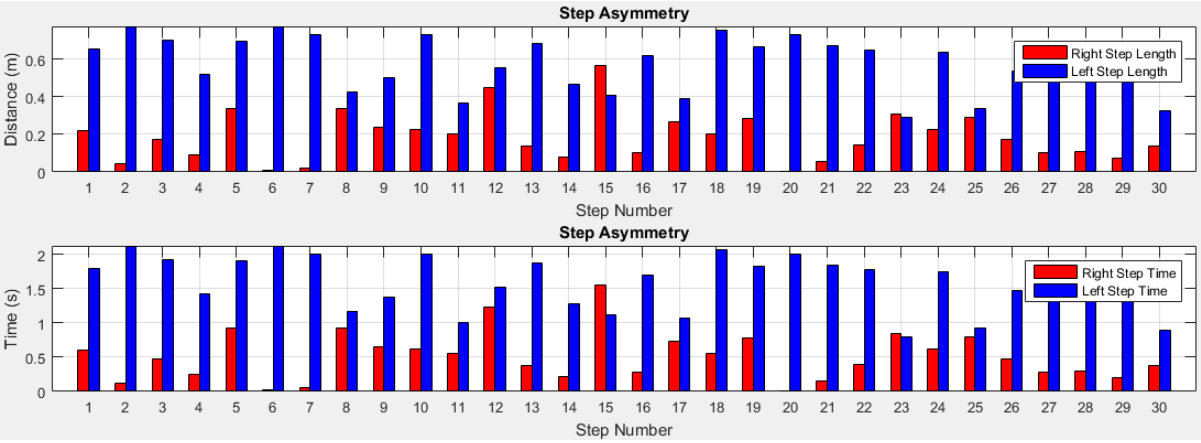

Figure 2.5: Step asymmetry estimation of right and left legs

3: Elderly Participant 3

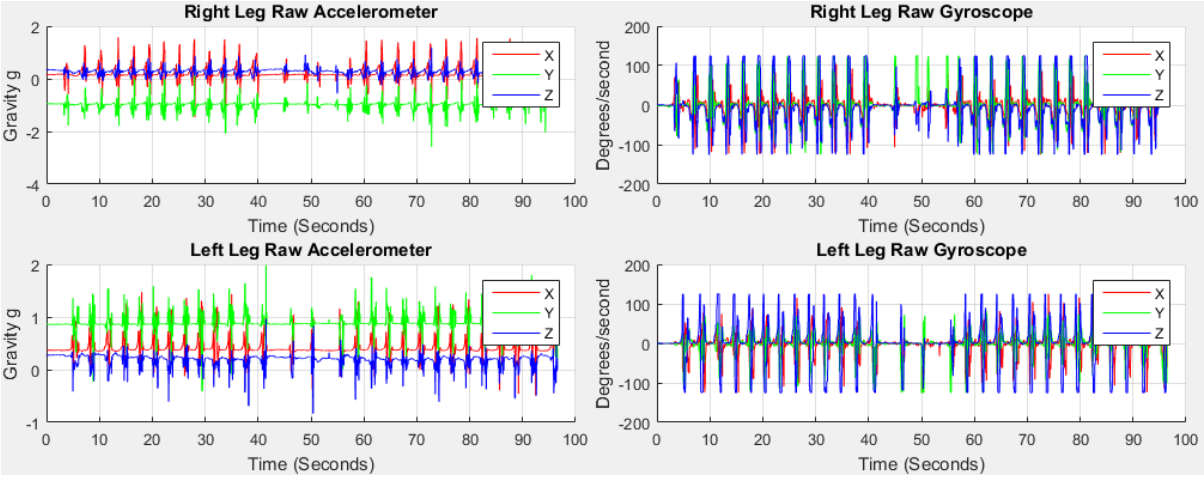

Figure 3.1: Accelerometer and gyroscope data from right and left legs

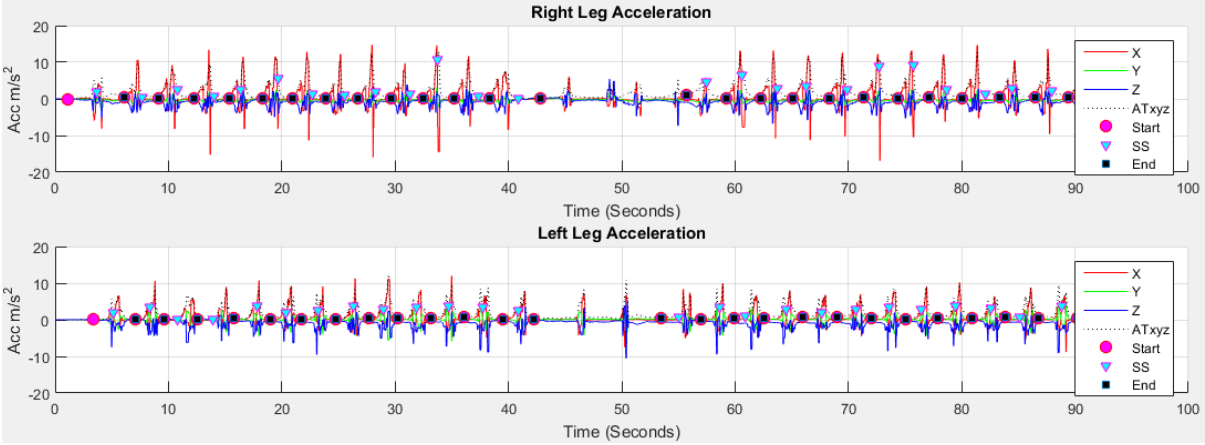

Figure 3.2: Result of stride, stance and swing event detection using proposed method

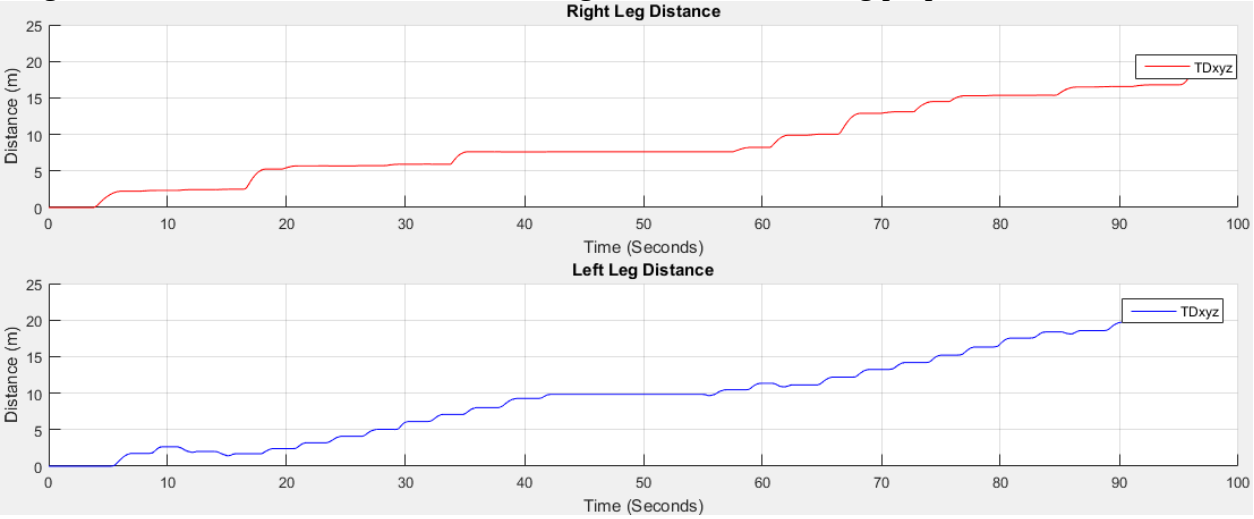

Figure 3.3: Result of distance estimation using proposed method

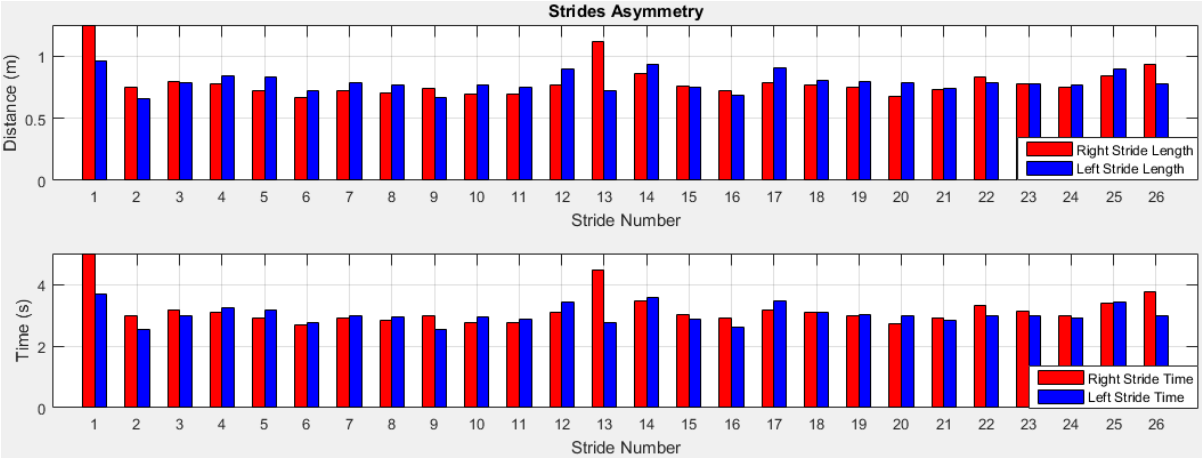

Figure 3.4: Stride asymmetry estimation of right and left legs

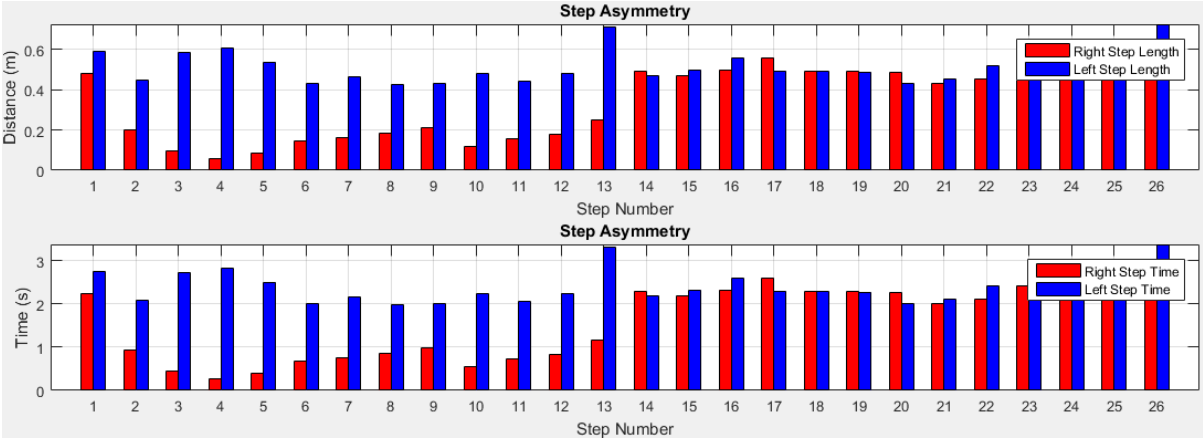

Figure 3.5: Step asymmetry estimation of right and left legs

4: Elderly Participant 4

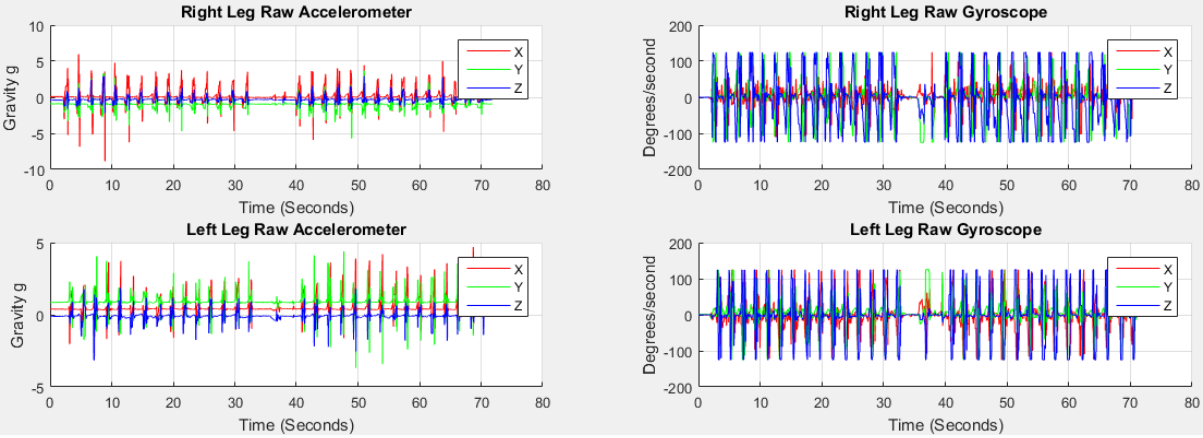

Figure 4.1: Accelerometer and gyroscope data from right and left legs

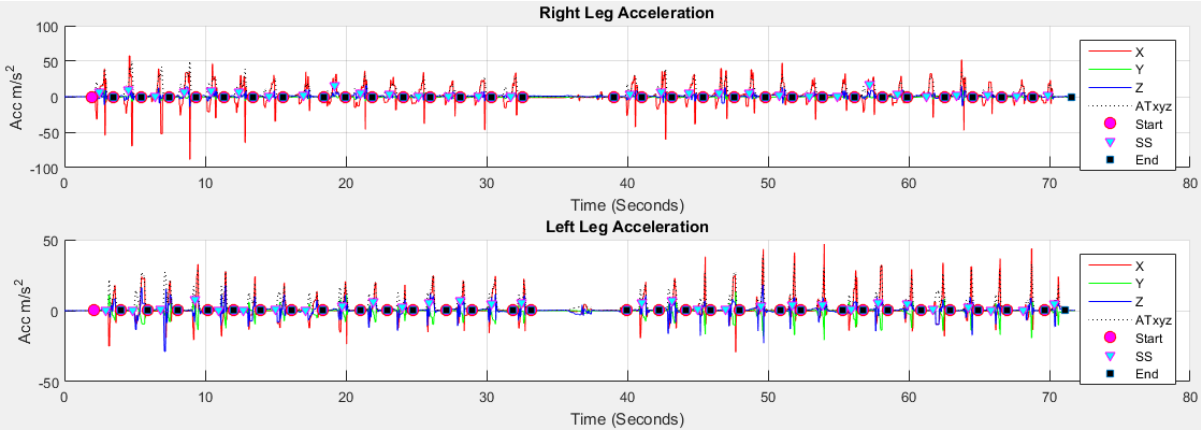

Figure 4.2: Result of stride, stance and swing event detection using proposed method

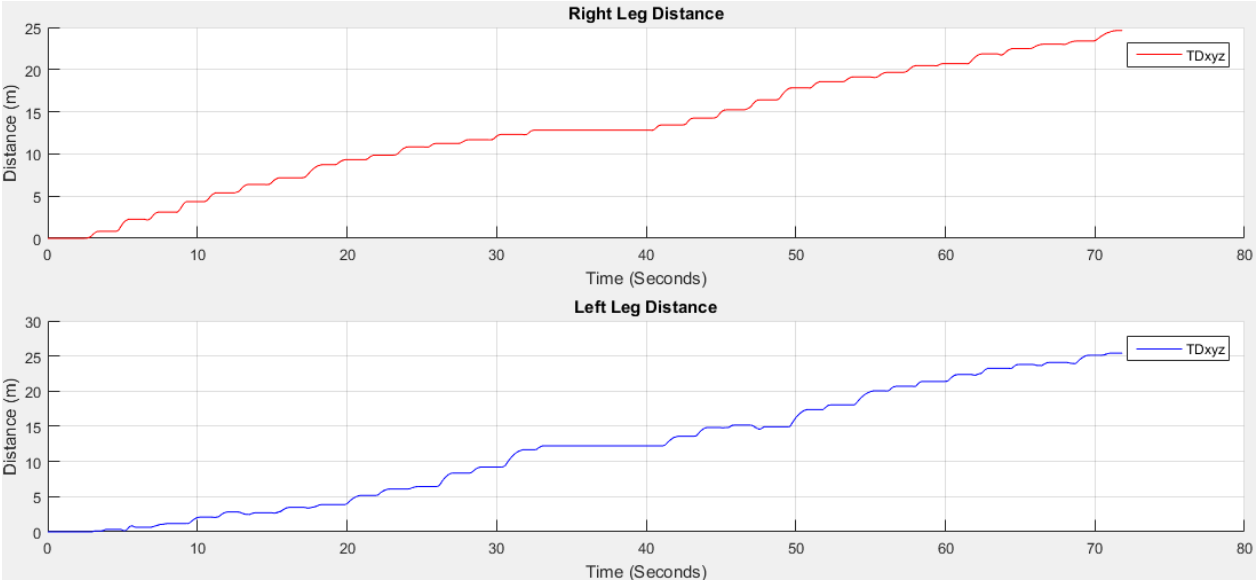

Figure 4.3: Result of distance estimation using proposed method

Figure 4.4: Stride asymmetry estimation of right and left legs

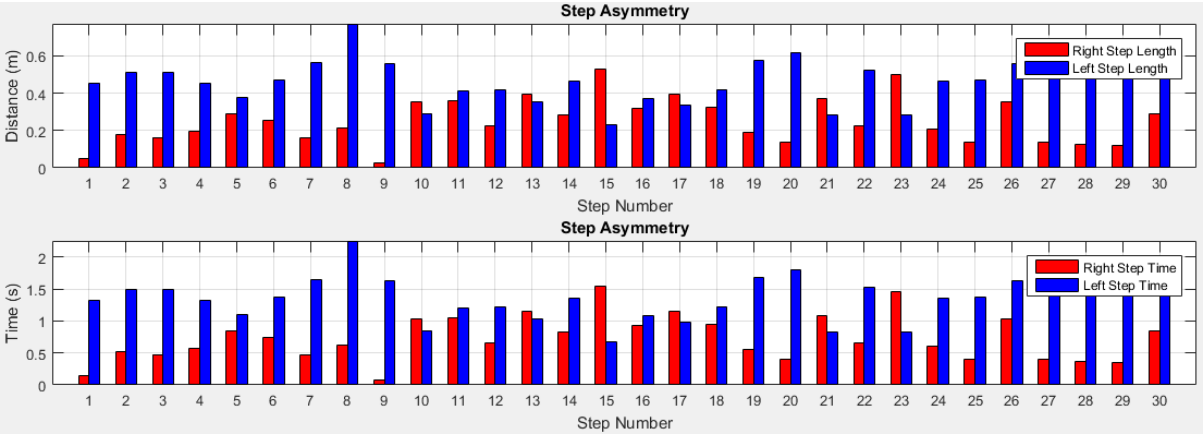

Figure 4.5: Step asymmetry estimation of right and left legs

5: Elderly Participant 5

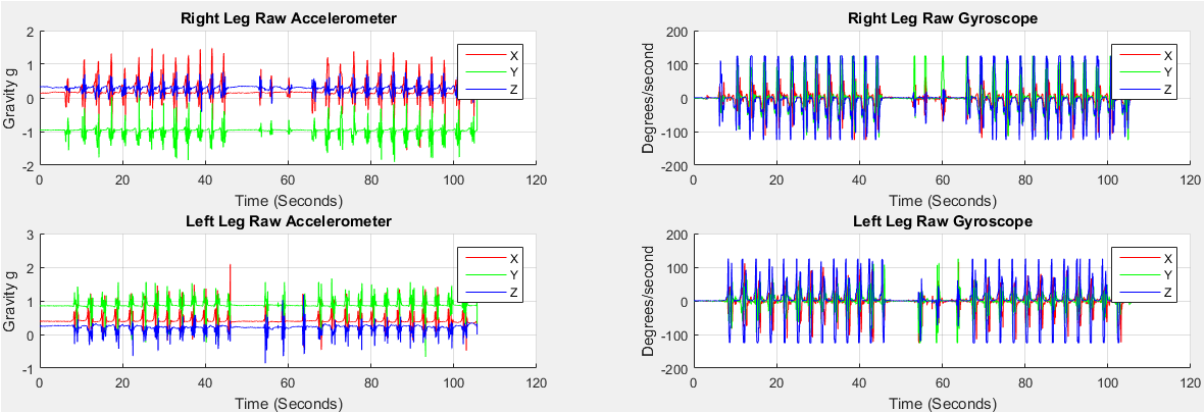

Figure 5.1: Accelerometer and gyroscope data from right and left legs

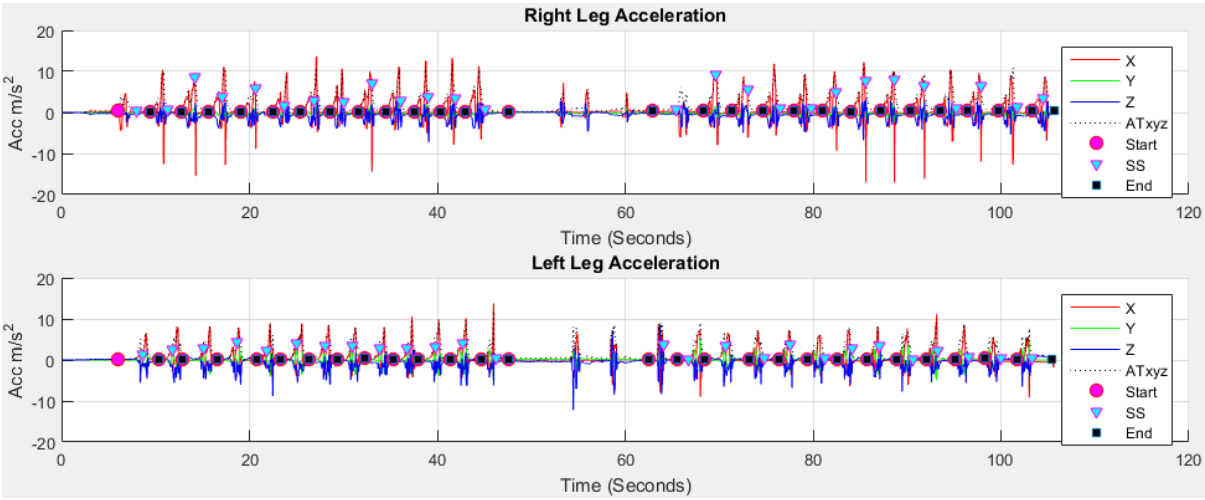

Figure 5.2: Result of stride, stance and swing event detection using proposed method

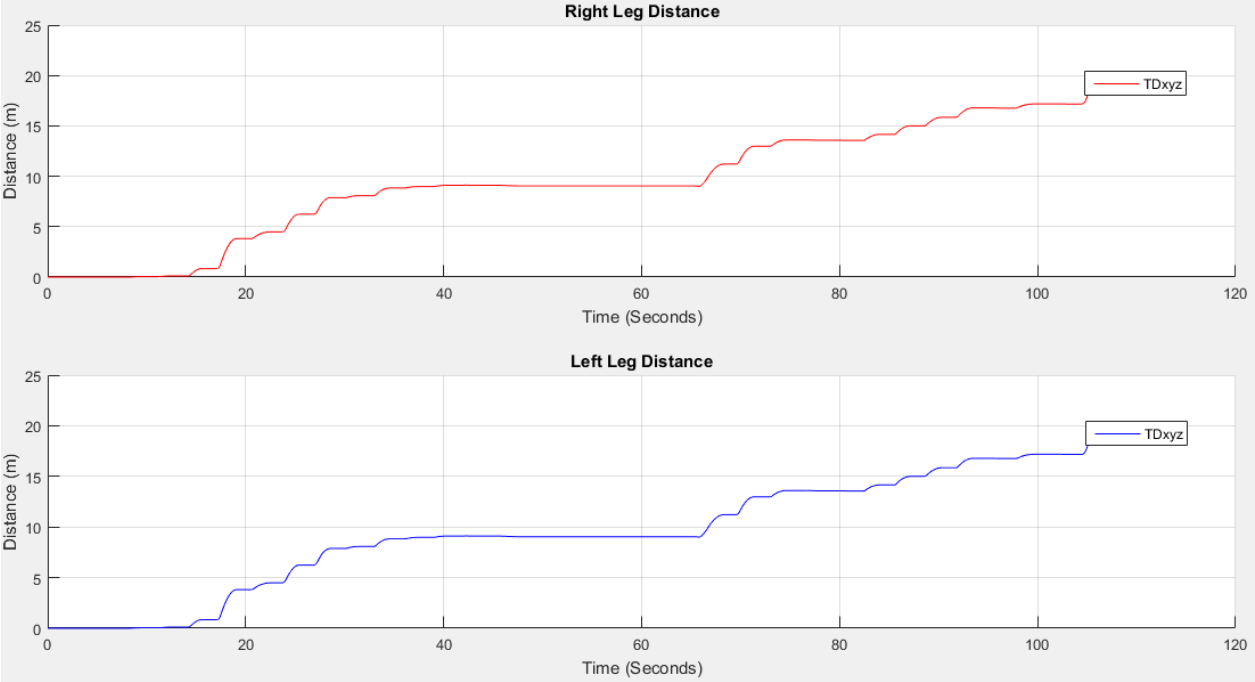

Figure 5.3: Result of distance estimation using proposed method

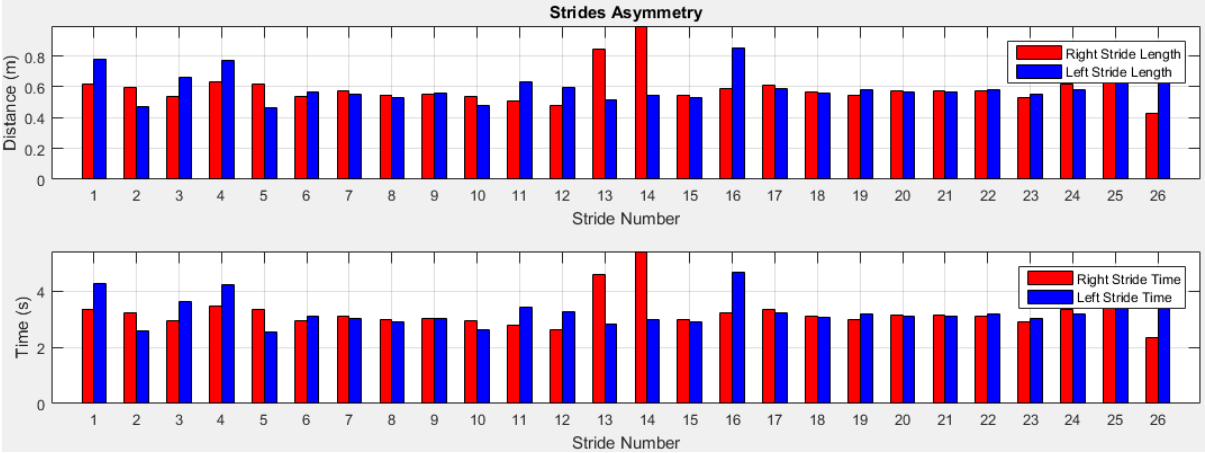

Figure 5.4: Stride asymmetry estimation of right and left legs

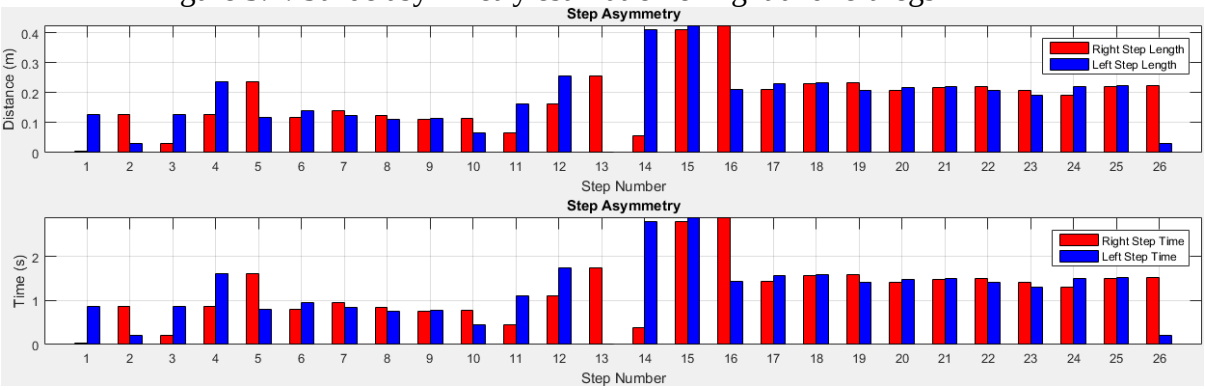

Figure 5.5: Step asymmetry estimation of right and left legs

6: Elderly Participant 6

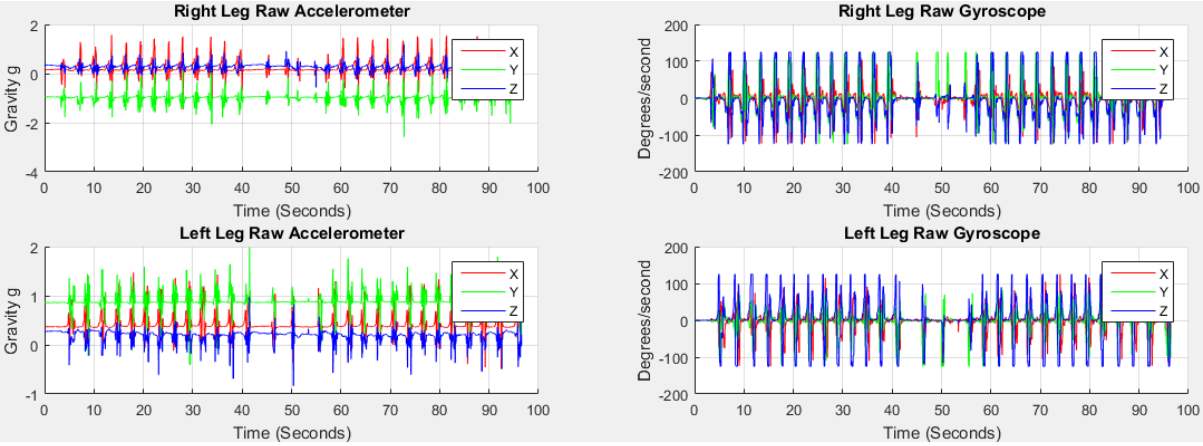

Figure 6.1: Accelerometer and gyroscope data from right and left legs

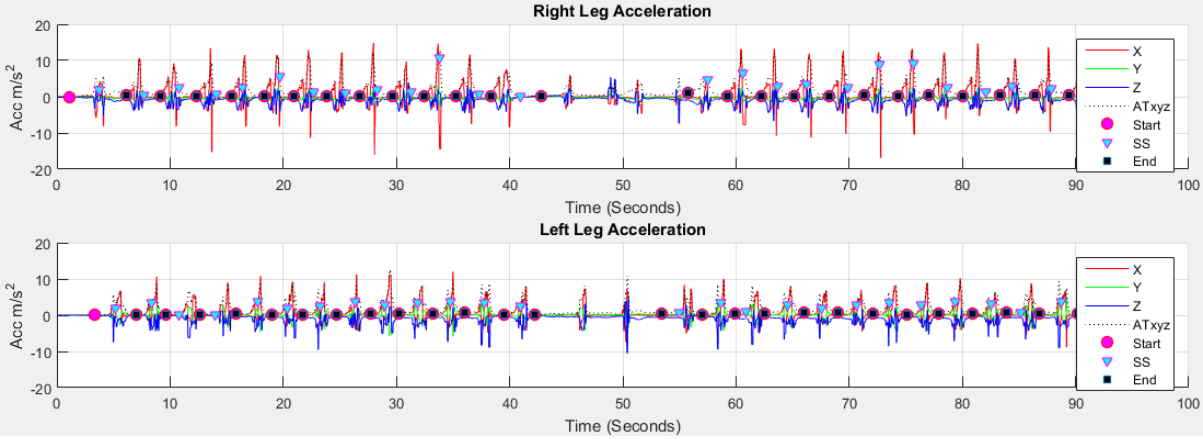

Figure 6.2: Result of stride, stance and swing event detection using proposed method

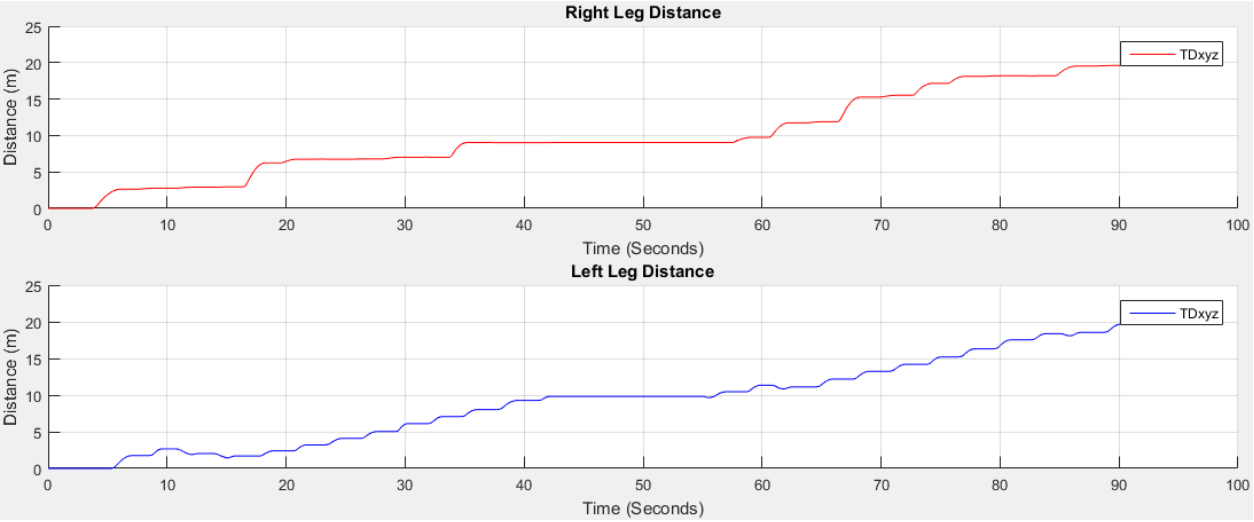

Figure 6.3: Result of distance estimation using proposed method

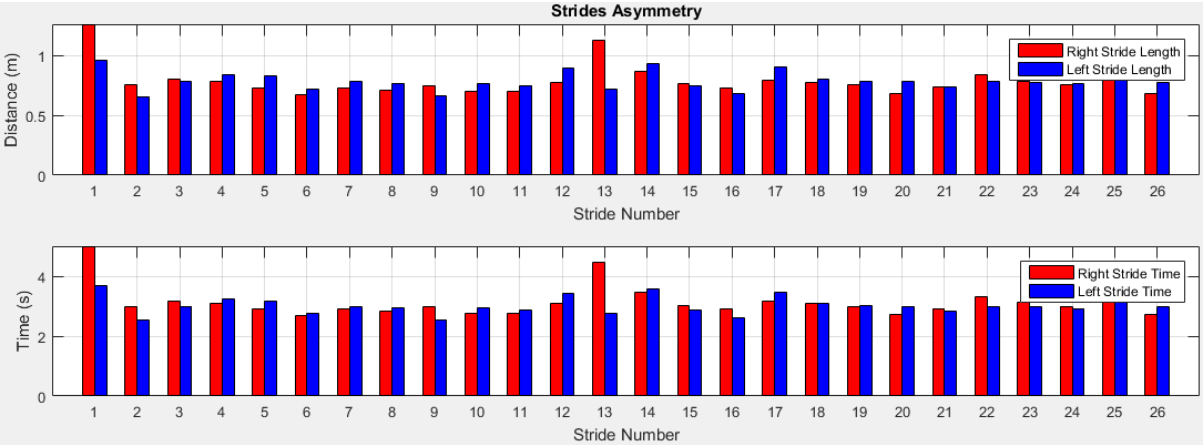

Figure 6.4: Stride asymmetry estimation of right and left legs

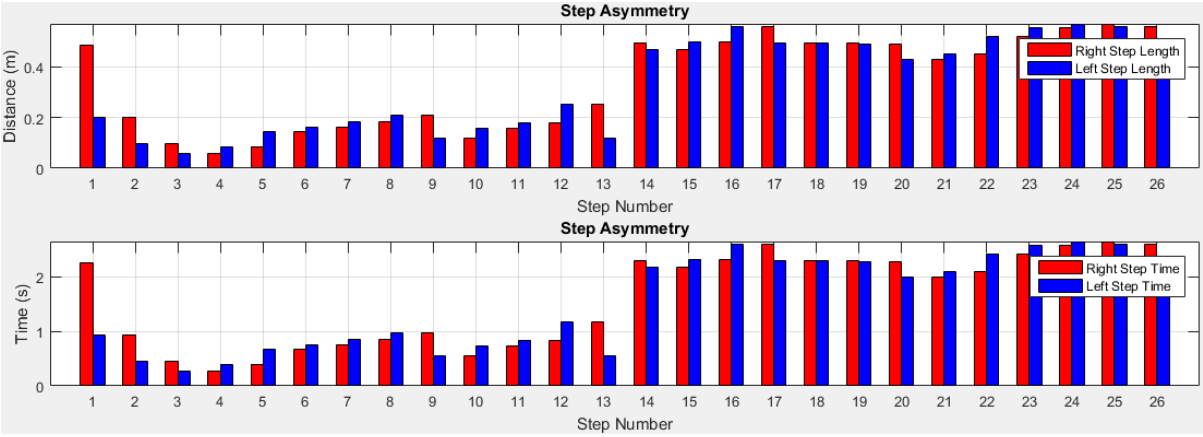

Figure 6.5: Step asymmetry estimation of right and left legs

7: Elderly Participant 7

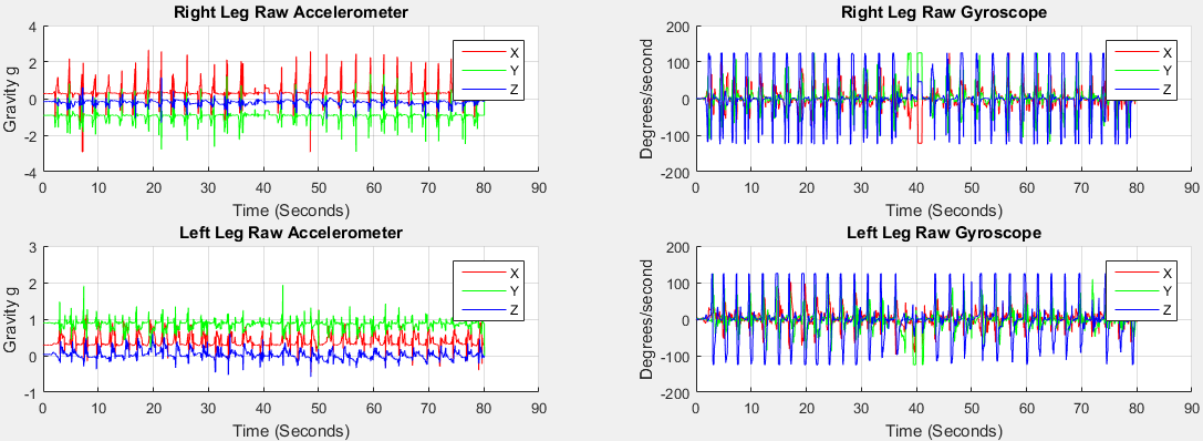

Figure 7.1: Accelerometer and gyroscope data from right and left legs

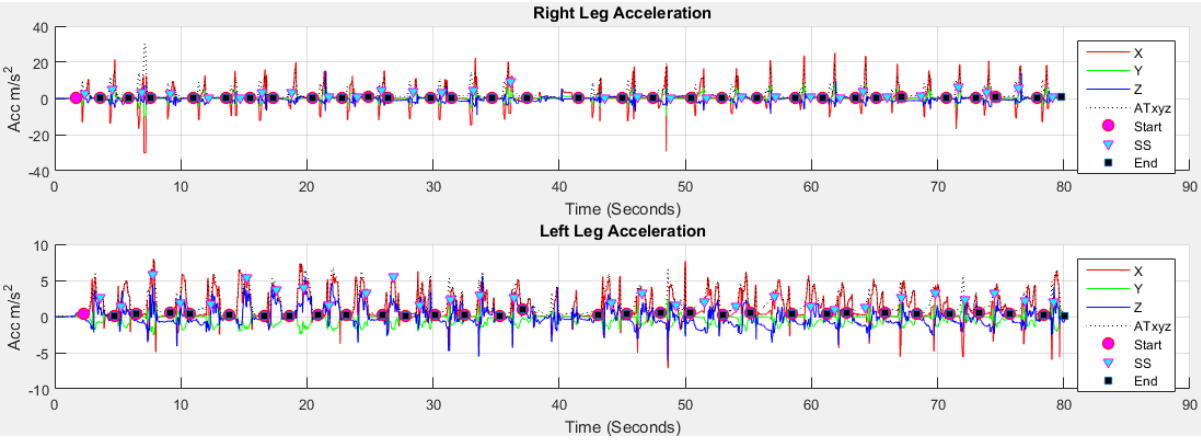

Figure 7.2: Result of stride, stance and swing event detection using proposed method

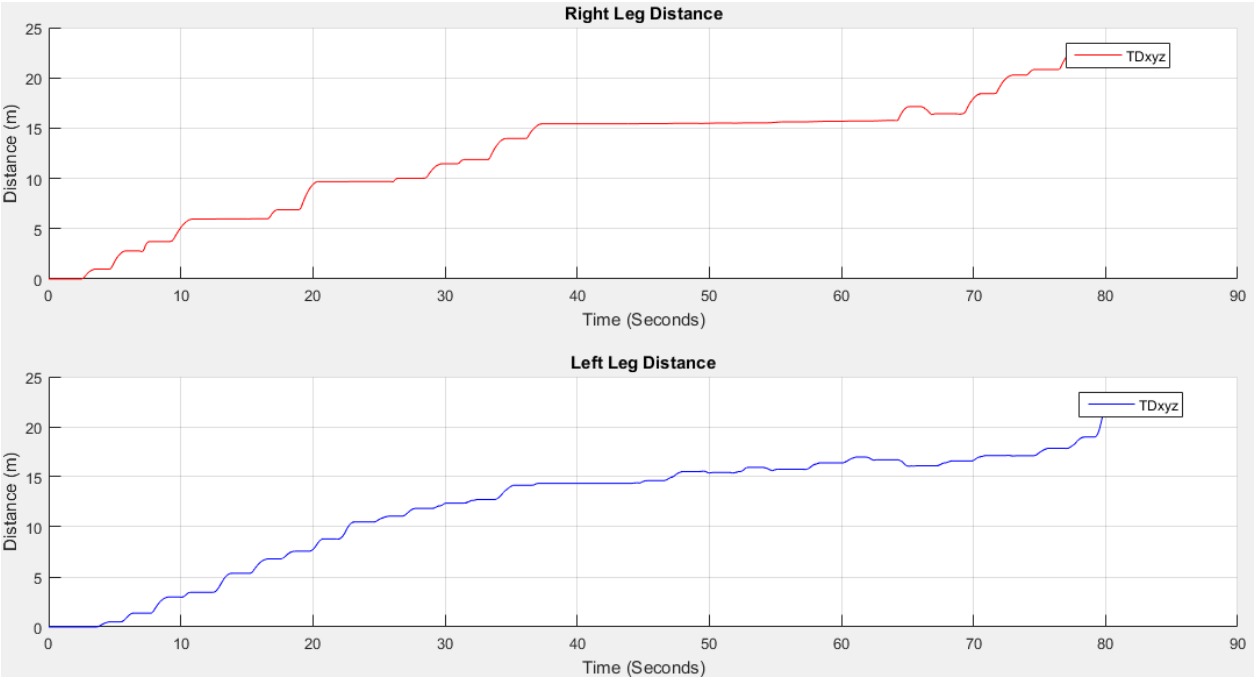

Figure 7.3: Result of distance estimation using proposed method

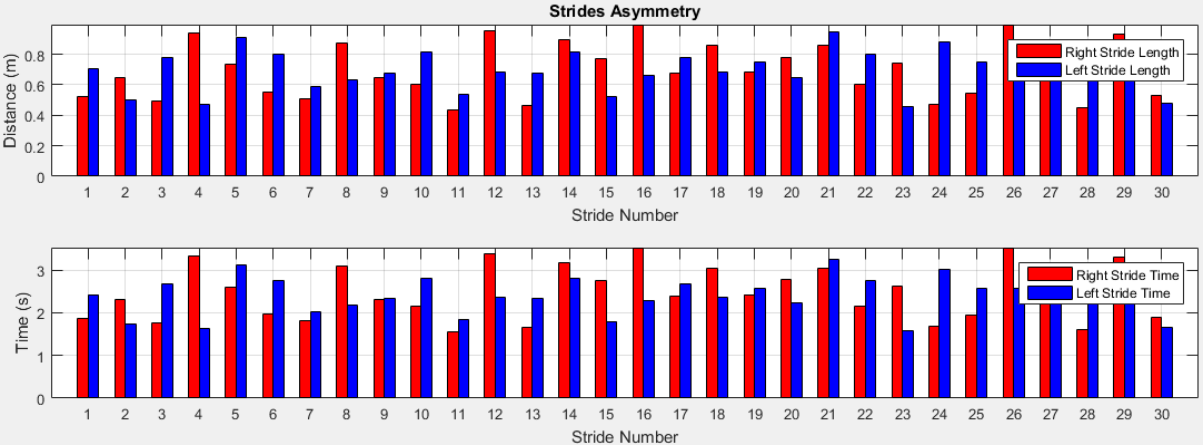

Figure 7.4: Stride asymmetry estimation of right and left legs

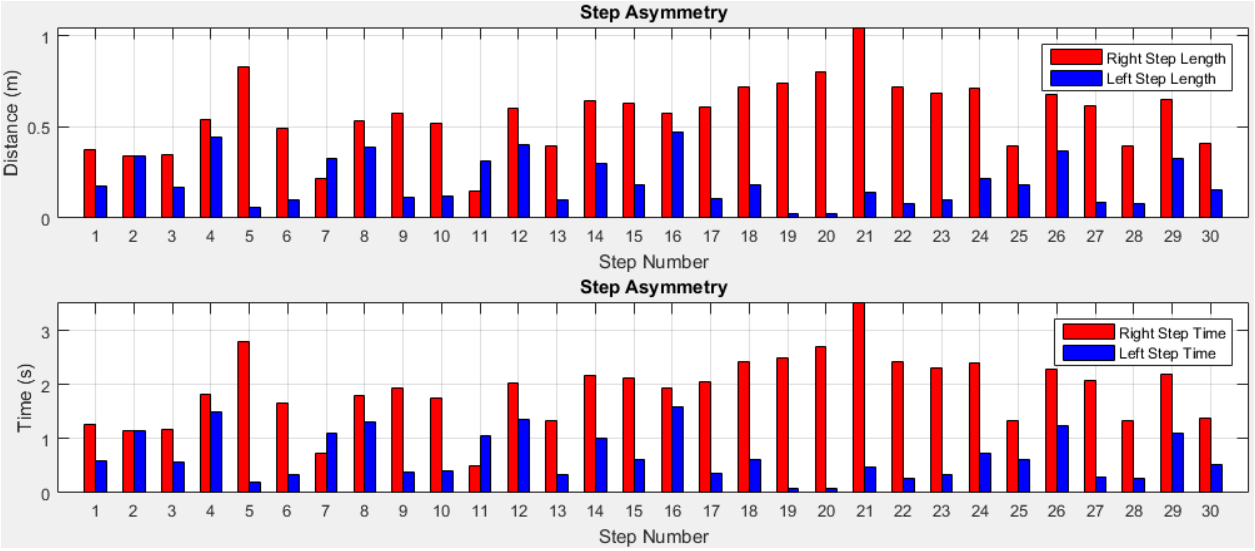

Figure 7.5: Step asymmetry estimation of right and left legs

8: Elderly Participant 8

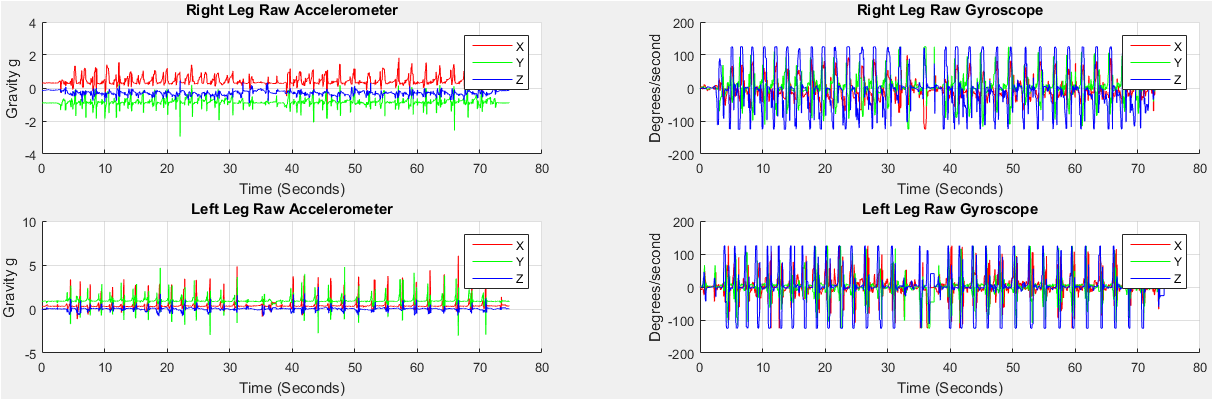

Figure 8.1: Accelerometer and gyroscope data from right and left legs

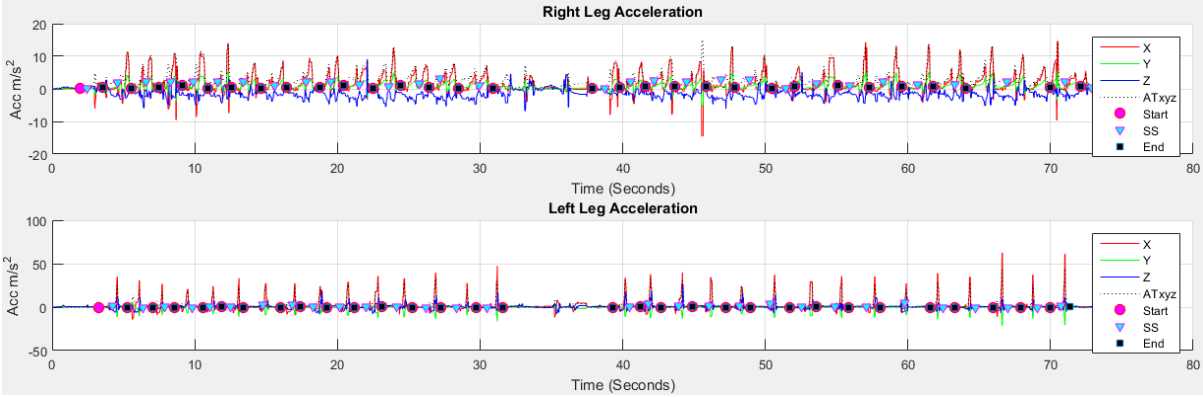

Figure 8.2: Result of stride, stance and swing event detection using proposed method

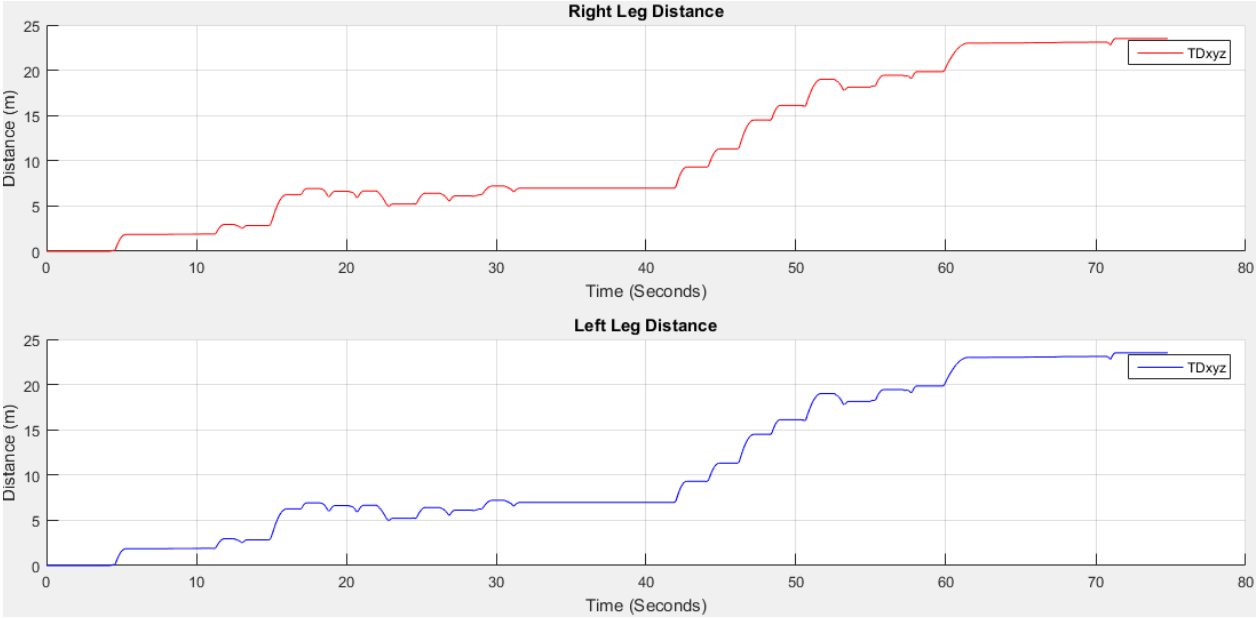

Figure 8.3: Result of distance estimation using proposed method

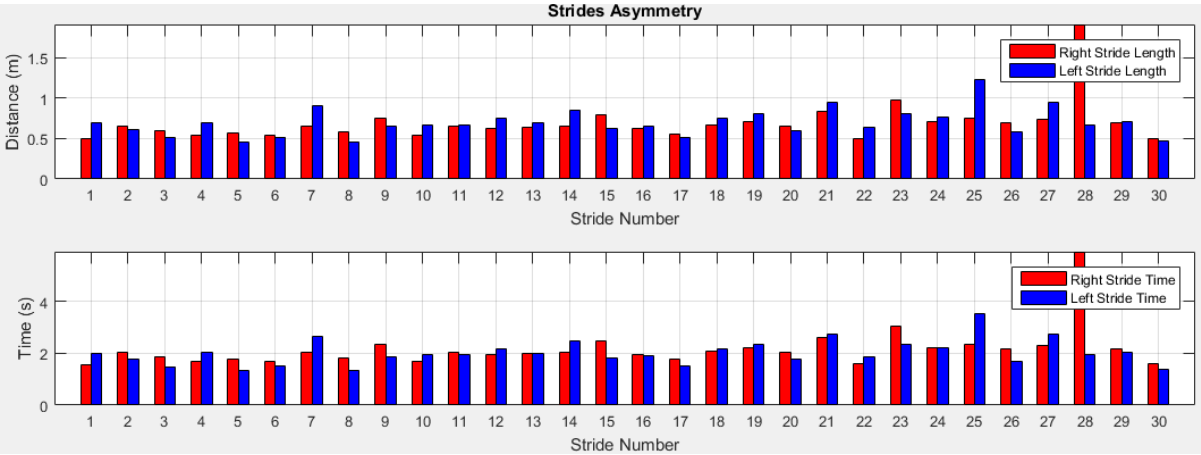

Figure 8.4: Stride asymmetry estimation of right and left legs

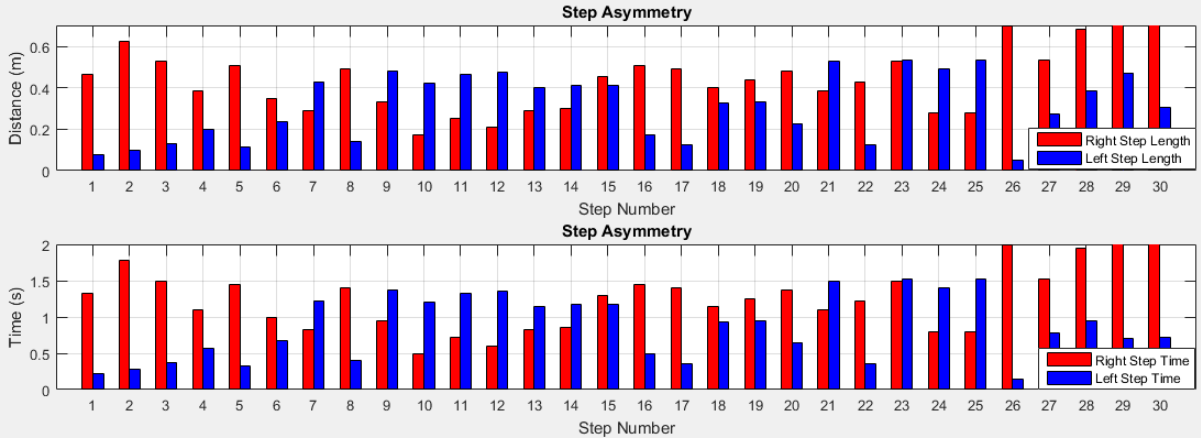

Figure 8.5: Step asymmetry estimation of right and left legs

9: Elderly Participant 9

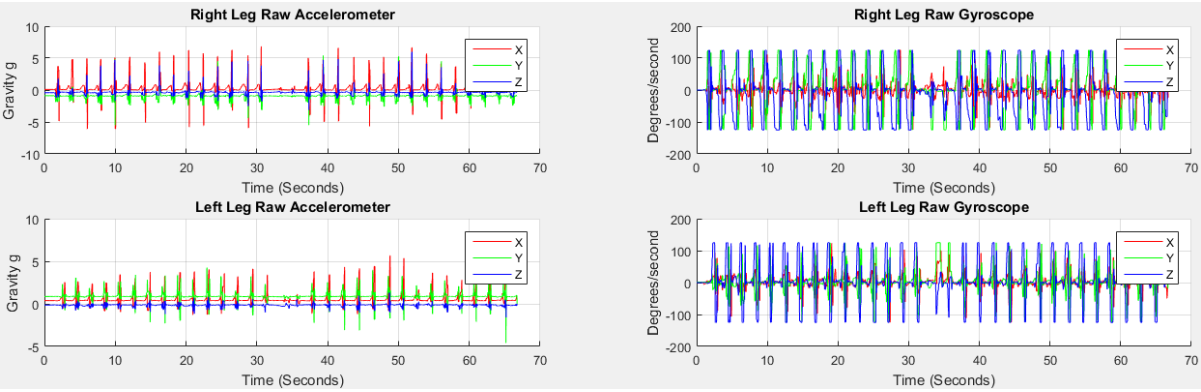

Figure 9.1: Accelerometer and gyroscope data from right and left legs

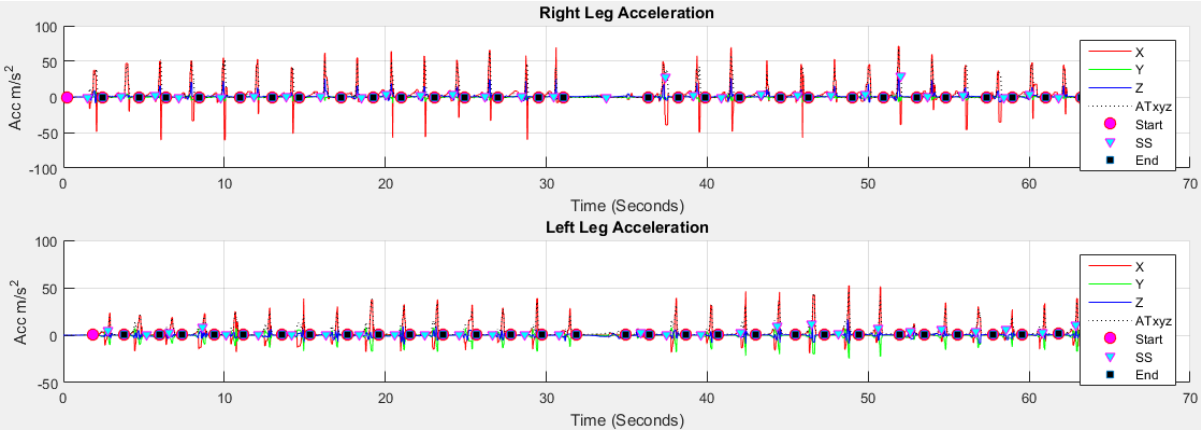

Figure 9.2: Result of stride, stance and swing event detection using proposed method

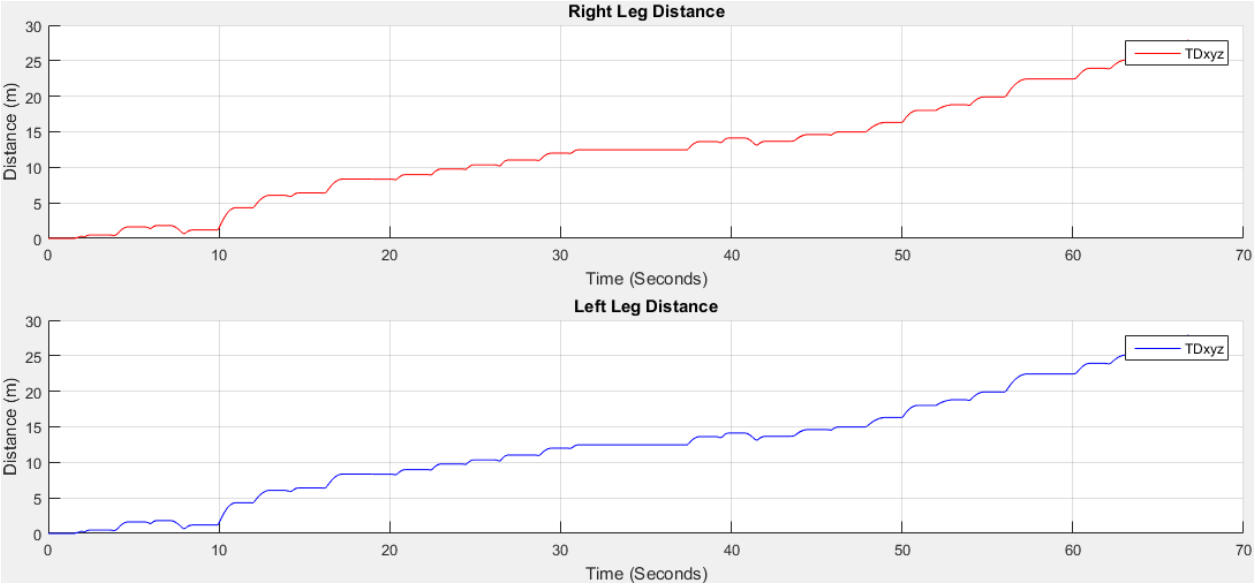

Figure 9.3: Result of distance estimation using proposed method

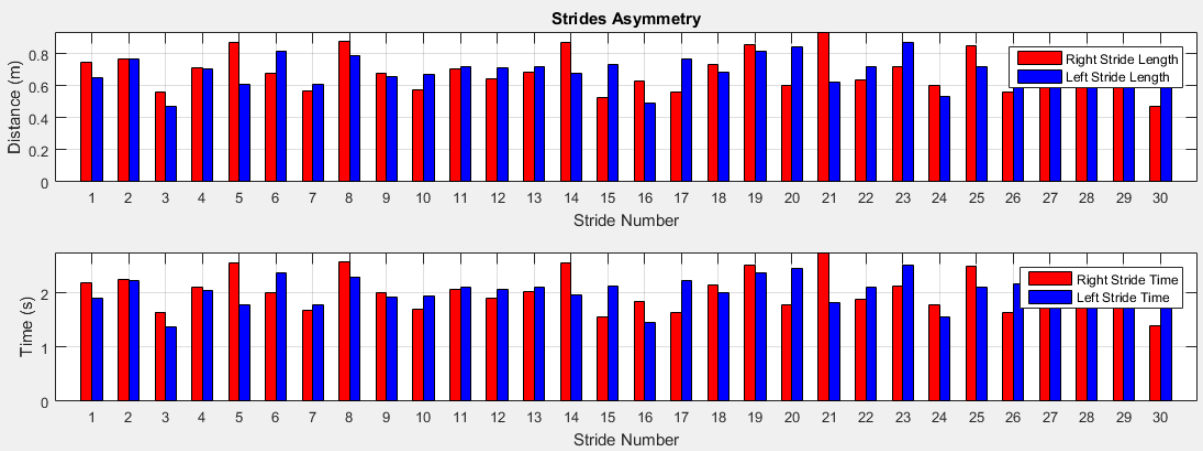

Figure 9.4: Stride asymmetry estimation of right and left legs

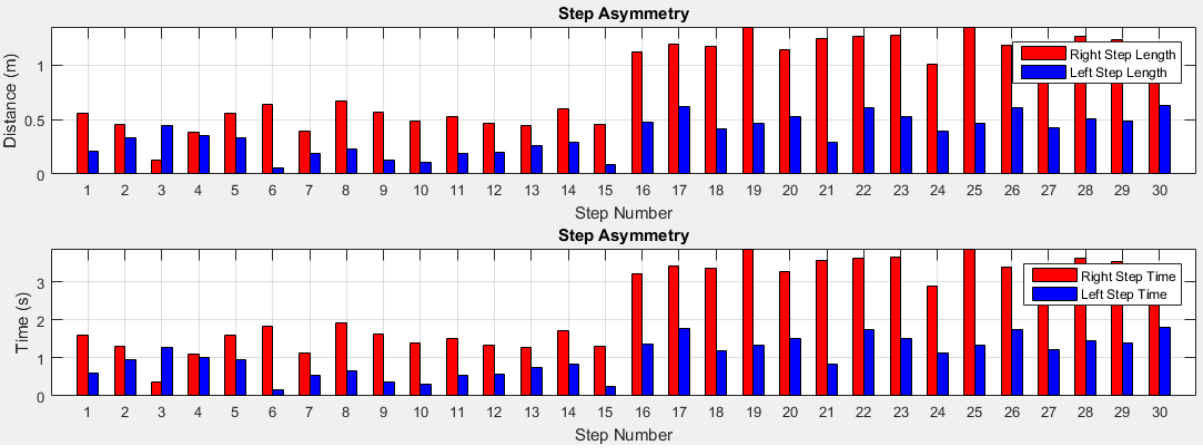

Figure 9.5: Step asymmetry estimation of right and left legs

10: Elderly Participant 10

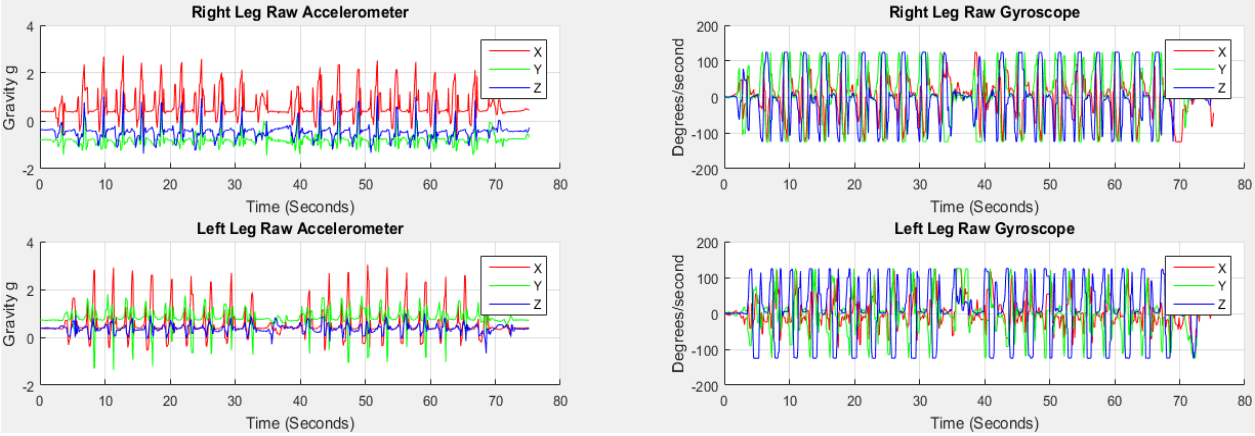

Figure 10.1: Accelerometer and gyroscope data from right and left legs

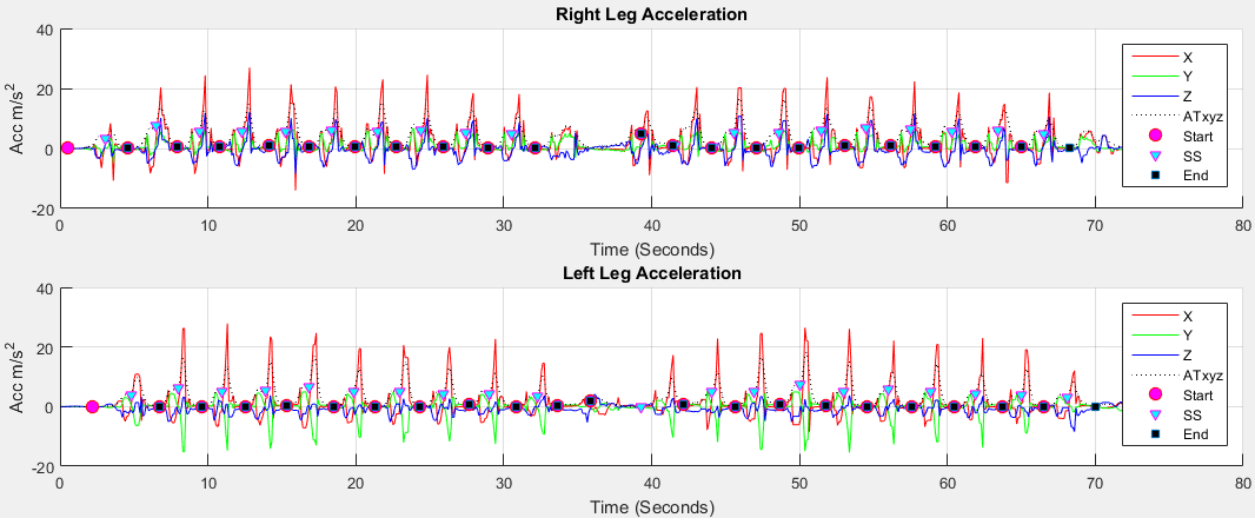

Figure 10.2: Result of stride, stance and swing event detection using proposed method

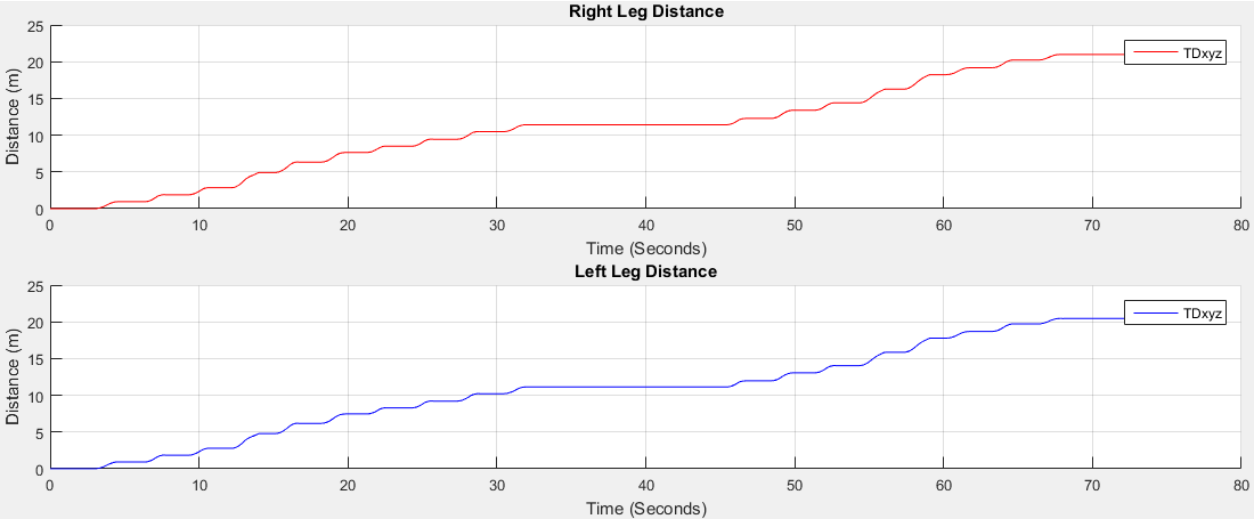

Figure 10.3: Result of distance estimation using proposed method

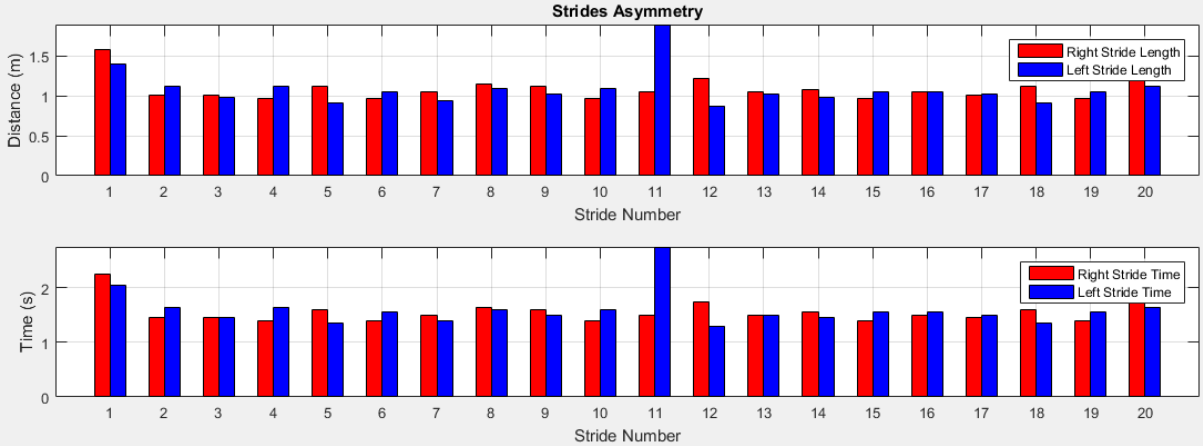

Figure 10.4: Stride asymmetry estimation of right and left legs

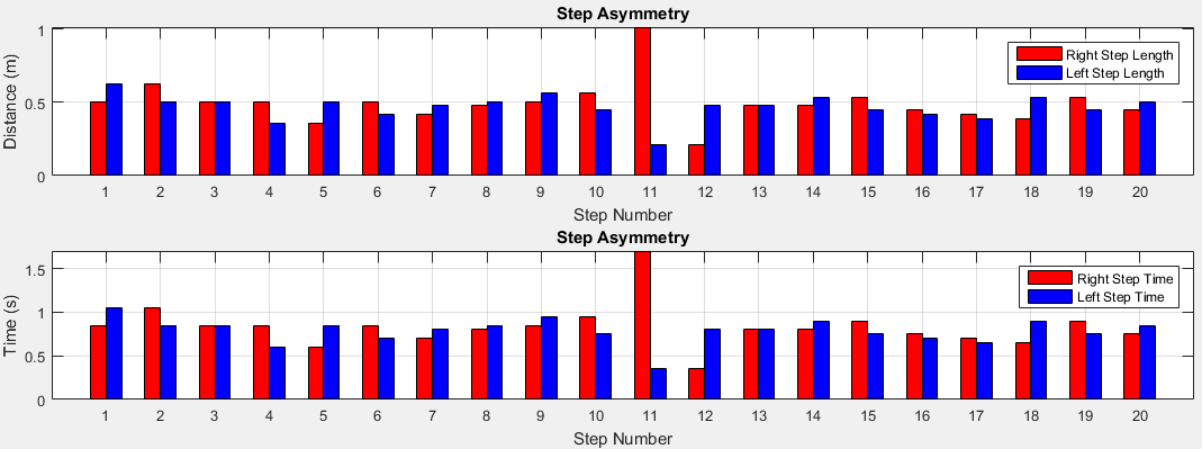

Figure 10.5: Step asymmetry estimation of right and left legs

Young Participant 1	Age	Height (m)	Weight (Kg)	Gender
	23.0000	1.6500	60.0000	Male

Total Time (s)	52.0500				
	Actual	**Right Leg**	**Accuracy**	**Left Leg**	**Accuracy**
Total Distance (m)	38.6600	37.2979	96.4767	38.5012	99.5892
Estimated Velocity (m/s)	0.7427	0.7166	96.4767	0.7397	99.5892
Detected Stride Number	30.0000	30.0000	100.0000	30.0000	100.0000
Detected Step Number	30.0000	30.0000	100.0000	30.0000	100.0000

	Right					**Left**				
Gait Features	**Mean**	**StaDev**	**Variance**	**MinRange**	**MaxRange**	**Mean**	**StaDev**	**Variance**	**MinRange**	**MaxRange**
Stride Length (m)	1.2656	0.1588	0.0252	0.9540	1.6456	1.2665	0.2036	0.0415	0.9631	1.9032
Stride Time (s)	1.3523	0.1666	0.0277	1.0255	1.7508	1.4065	0.2221	0.0493	1.0755	2.1010
Stride Velocity (m/s)	0.9359	0.9359	0.9359			0.9005	0.9005	0.9005		
Cadence (step/min)	34.5821					34.5821				
Step Speed (m/s)	0.9359	0.9535	0.9092			0.9005	0.9168	0.8404		
Step length (m)	0.4688	0.1279	0.0164	0.1115	0.7617	0.5357	0.1314	0.0173	0.2787	0.7803
Step time(s)	0.6311	0.1722	0.0297	0.1501	1.0255	0.7212	0.1769	0.0313	0.3752	1.0505
Step Ratio (Step length/cadence)	0.01					0.01				
Stance Time (s)	0.6887	0.1510	0.0221			0.7337	0.1314	0.0163		
Swing Length (m)	1.2510	0.5693	0.3241			1.2917	0.6358	0.4042		
Swing Time (s)	0.6637	0.1115	0.0131			0.6728	0.1755	0.0308		
Swing Velocity (m/s)	1.8850	1.8830	1.8830			1.9463	1.9158	1.9158		

Young Participant 2	Age	Height (m)	Weight (Kg)	Gender
	19.0000	1.1700	55.0000	Female

Total Time (s)	51.2250				
	Actual	**Right Leg**	**Accuracy**	**Left Leg**	**Accuracy**
Total Distance (m)	42.0600	41.8235	99.4378	43.4401	96.7187
Estimated Velocity (m/s)	0.8211	0.8165	99.4378	0.8480	96.7187
Detected Stride Number	30.0000	30.0000	100.0000	30.0000	100.0000
Detected Step Number	30.0000	30.0000	100.0000	30.0000	100.0000

	Right					**Left**				
Gait Features	**Mean**	**StaDev**	**Variance**	**MinRange**	**MaxRange**	**Mean**	**StaDev**	**Variance**	**MinRange**	**MaxRange**
Stride Length (m)	0.6894	0.1029	0.0106	0.5389	0.9701	0.6893	0.0975	0.0095	0.4854	1.0193
Stride Time (s)	1.4649	0.2148	0.0462	1.1506	2.0510	1.4457	0.2009	0.0404	1.0255	2.1260
Stride Velocity (m/s)	0.4706	0.4706	0.4706			0.4768	0.4768	0.4768		
Cadence (step/min)	35.13					35.13				
Step Speed (m/s)	0.4706	0.4788	0.2293			0.4768	0.4852	0.2354		
Step length (m)	0.5032	0.1258	0.0158	0.3286	0.9242	0.6996	0.1368	0.0187	0.4518	1.1501
Step time(s)	0.6128	0.1532	0.0235	0.4002	1.1255	0.8521	0.1666	0.0277	0.5503	1.4007
Step Ratio (Step length/cadence)	0.01					0.01				
Stance Time (s)	0.7270	0.2032	0.0413			0.7204	0.0890	0.0079		
Swing Length (m)	1.4004	0.8569	0.7343			1.4550	1.0381	1.0776		
Swing Time (s)	0.7379	0.1442	0.0208			0.7254	0.1441	0.0208		
Swing Velocity (m/s)	1.8980	1.8980	1.8980			1.9719	2.0059	2.0059		

Young Participant 3	Age	Height (m)	Weight (Kg)	Gender
	23.0000	1.7200	63.0000	Male

Total Time (s)	55.5250				
	Actual	**Right Leg**	**Accuracy**	**Left Leg**	**Accuracy**
Total Distance (m)	33.3800	32.9581	98.7360	32.8014	98.2667
Estimated Velocity (m/s)	0.6012	0.5936	98.7360	0.5908	98.2667
Detected Stride Number	30.0000	30.0000	100.0000	30.0000	100.0000
Detected Step Number	30.0000	30.0000	100.0000	30.0000	100.0000

	Right					**Left**				
Gait Features	**Mean**	**StaDev**	**Variance**	**MinRange**	**MaxRange**	**Mean**	**StaDev**	**Variance**	**MinRange**	**MaxRange**
Stride Length (m)	1.0946	0.1369	0.0188	0.8612	1.4603	1.0944	0.1328	0.0176	0.7952	1.3064
Stride Time (s)	1.4873	0.1829	0.0335	1.1755	1.9759	1.4707	0.1754	0.0308	1.0755	1.7508
Stride Velocity (m/s)	0.7359	0.7359	0.7359			0.7441	0.7441	0.7441		
Cadence (step/min)	32.41					32.41				
Step Speed (m/s)	0.7359	0.7485	0.5603			0.7441	0.7570	0.5731		
Step length (m)	0.5067	0.1101	0.0121	0.2556	0.6766	0.3874	0.1145	0.0131	0.2105	0.7368
Step time(s)	0.8429	0.1831	0.0335	0.4252	1.1255	0.6445	0.1904	0.0363	0.3502	1.2256
Step Ratio (Step length/cadence)	0.01					0.01				
Stance Time (s)	0.7879	0.1227	0.0150			0.6961	0.1387	0.0192		
Swing Length (m)	1.1076	0.5979	0.3574			1.0975	0.6184	0.3825		
Swing Time (s)	0.6995	0.1300	0.0169			0.7745	0.1389	0.0193		
Swing Velocity (m/s)	1.5834	1.5834	1.5834			1.5690	1.4170	1.4170		

Young Participant 4	Age	Height (m)	Weight (Kg)	Gender
	25.0000	1.5500	63.0000	Male

Total Time (s)	59.9000				
	Actual	**Right Leg**	**Accuracy**	**Left Leg**	**Accuracy**
Total Distance (m)	38.5800	38.7624	99.5271	38.0767	98.6954
Estimated Velocity (m/s)	0.6441	0.6471	99.5271	0.6357	98.6954
Detected Stride Number	30.0000	30.0000	100.0000	30.0000	100.0000
Detected Step Number	30.0000	30.0000	100.0000	30.0000	100.0000

	Right					**Left**				
Gait Features	**Mean**	**StaDev**	**Variance**	**MinRange**	**MaxRange**	**Mean**	**StaDev**	**Variance**	**MinRange**	**MaxRange**
Stride Length (m)	1.2661	0.1447	0.0209	1.0277	1.6032	1.2661	0.1546	0.0239	0.9671	1.5638
Stride Time (s)	1.5657	0.1761	0.0310	1.2755	1.9758	1.5640	0.1879	0.0353	1.2005	1.9258
Stride Velocity (m/s)	0.8087	0.8087	0.8087			0.8095	0.8095	0.8095		
Cadence (step/min)	30.05					30.05				
Step Speed (m/s)	0.8087	0.8218	0.6754			0.8095	0.8227	0.6768		
Step length (m)	0.4328	0.1033	0.0107	0.1450	0.5960	0.5756	0.1141	0.0130	0.3383	0.8376
Step time(s)	0.6719	0.1604	0.0257	0.2251	0.9254	0.8937	0.1771	0.0314	0.5252	1.3005
Step Ratio (Step length/cadence)	0.01					0.01				
Stance Time (s)	0.7153	0.1611	0.0260			0.7845	0.1296	0.0168		
Swing Length (m)	1.2961	0.4891	0.2393			1.2750	0.7640	0.5837		
Swing Time (s)	0.8504	0.1279	0.0163			0.7795	0.1601	0.0256		
Swing Velocity (m/s)	1.5241	1.5241	1.5241			1.4993	1.6356	1.6356		

Young Participant 5	Age	Height (m)	Weight (Kg)	Gender
	26.0000	1.6500	61.0000	Male

Total Time (s)	51.9000				
	Actual	**Right Leg**	**Accuracy**	**Left Leg**	**Accuracy**
Total Distance (m)	45.3600	43.8421	96.6537	45.4254	99.8559
Estimated Velocity (m/s)	0.8740	0.8447	96.6537	0.8752	99.8559
Detected Stride Number	30.0000	30.0000	100.0000	30.0000	100.0000
Detected Step Number	30.0000	30.0000	100.0000	30.0000	100.0000

	Right					**Left**				
Gait Features	**Mean**	**StaDev**	**Variance**	**MinRange**	**MaxRange**	**Mean**	**StaDev**	**Variance**	**MinRange**	**MaxRange**
Stride Length (m)	1.4856	0.2062	0.0425	1.1190	2.2107	1.4855	0.1590	0.0253	1.2348	1.8660
Stride Time (s)	1.3865	0.1890	0.0357	1.0505	2.0510	1.3790	0.1449	0.0210	1.1506	1.7258
Stride Velocity (m/s)	1.0715	1.0715	1.0715			1.0772	1.0772	1.0772		
Cadence (step/min)	34.68					34.68				
Step Speed (m/s)	1.0715	1.0912	1.1907			1.0772	1.0971	1.2037		
Step length (m)	0.5727	0.1710	0.0292	0.0219	0.9400	0.6405	0.1883	0.0355	0.3279	1.3116
Step time(s)	0.6553	0.1957	0.0383	0.0250	1.0755	0.7329	0.2155	0.0464	0.3752	1.5007
Step Ratio (Step length/cadence)	0.01					0.01				
Stance Time (s)	0.7420	0.1313	0.0172			0.7879	0.1266	0.0160		
Swing Length (m)	1.4712	1.0718	1.1487			1.5330	1.1008	1.2118		
Swing Time (s)	0.6445	0.1366	0.0187			0.5911	0.0980	0.0096		
Swing Velocity (m/s)	2.2827	2.2827	2.2827			2.3786	2.5933	2.5933		

Young Participant 6	Age	Height (m)	Weight (Kg)	Gender
	25.0000	1.7200	60.0000	Male

Total Time (s)	56.5250				
	Actual	**Right Leg**	**Accuracy**	**Left Leg**	**Accuracy**
Total Distance (m)	34.8600	34.9764	99.6662	35.4092	98.4245
Estimated Velocity (m/s)	0.6167	0.6188	99.6662	0.6264	98.4245
Detected Stride Number	30.0000	30.0000	100.0000	30.0000	100.0000
Detected Step Number	30.0000	30.0000	100.0000	30.0000	100.0000

	Right					**Left**				
Gait Features	**Mean**	**StaDev**	**Variance**	**MinRange**	**MaxRange**	**Mean**	**StaDev**	**Variance**	**MinRange**	**MaxRange**
Stride Length (m)	1.1437	0.1515	0.0230	0.9089	1.4580	1.1431	0.1315	0.0173	0.9169	1.4631
Stride Time (s)	1.5357	0.2002	0.0401	1.2255	1.9509	1.4907	0.1686	0.0284	1.2005	1.9008
Stride Velocity (m/s)	0.7447	0.7447	0.7447			0.7669	0.7669	0.7669		
Cadence (step/min)	38.14					38.14				
Step Speed (m/s)	0.7447	0.7571	0.5732			0.7669	0.7800	0.6083		
Step length (m)	0.4190	0.1484	0.0220	0.1542	0.9255	0.5280	0.1197	0.0143	0.1542	0.7095
Step time(s)	0.6795	0.2406	0.0579	0.2501	1.5007	0.8562	0.1940	0.0376	0.2501	1.1505
Step Ratio (Step length/cadence)	0.01					0.01				
Stance Time (s)	0.7328	0.1617	0.0262			0.7695	0.1000	0.0100		
Swing Length (m)	1.1707	0.5774	0.3334			1.1844	0.8454	0.7148		
Swing Time (s)	0.8029	0.1236	0.0153			0.7212	0.1451	0.0211		
Swing Velocity (m/s)	1.4582	1.4582	1.4582			1.4752	1.6423	1.6423		

Young Participant 7	Age	Height (m)	Weight (Kg)	Gender
	29.0000	1.6500	62.0000	Male

Total Time (s)	48.6750				
	Actual	**Right Leg**	**Accuracy**	**Left Leg**	**Accuracy**
Total Distance (m)	33.9800	32.8346	96.6292	34.3799	98.8230
Estimated Velocity (m/s)	0.6981	0.6746	96.6292	0.7063	98.8230
Detected Stride Number	30.0000	30.0000	100.0000	30.0000	100.0000
Detected Step Number	30.0000	30.0000	100.0000	30.0000	100.0000

	Right					**Left**				
Gait Features	**Mean**	**StaDev**	**Variance**	**MinRange**	**MaxRange**	**Mean**	**StaDev**	**Variance**	**MinRange**	**MaxRange**
Stride Length (m)	1.1133	0.2098	0.0440	0.8028	1.6860	1.1126	0.2106	0.0443	0.7283	1.6230
Stride Time (s)	1.4124	0.2615	0.0684	1.0255	2.1261	1.3624	0.2531	0.0641	0.9005	1.9760
Stride Velocity (m/s)	0.7882	0.7882	0.7882			0.8166	0.8166	0.8166		
Cadence (step/min)	36.98					36.98				
Step Speed (m/s)	0.7882	0.8024	0.6439			0.8166	0.8319	0.6921		
Step length (m)	0.4784	0.1638	0.0268	0.1222	0.9429	0.6112	0.3713	0.1379	0.0349	1.5715
Step time(s)	0.6854	0.2347	0.0551	0.1751	1.3507	0.8754	0.5319	0.2829	0.0500	2.2512
Step Ratio (Step length/cadence)	0.01					0.01				
Stance Time (s)	0.6428	0.2228	0.0496			0.6595	0.2127	0.0452		
Swing Length (m)	1.0983	0.7311	0.5344			1.1511	0.7527	0.5666		
Swing Time (s)	0.7696	0.1448	0.0210			0.7029	0.1485	0.0221		
Swing Velocity (m/s)	1.4271	1.4271	1.4271			1.4957	1.6377	1.6377		

Young Participant 8	Age	Height (m)	Weight (Kg)	Gender
	20.0000	1.5700	59.0000	Male

Total Time (s)	47.0000				
	Actual	**Right Leg**	**Accuracy**	**Left Leg**	**Accuracy**
Total Distance (m)	40.0400	40.8586	97.9555	39.5247	98.7130
Estimated Velocity (m/s)	0.8519	0.8693	97.9555	0.8410	98.7130
Detected Stride Number	30.0000	30.0000	100.0000	30.0000	100.0000
Detected Step Number	30.0000	30.0000	100.0000	30.0000	100.0000

	Right					**Left**				
Gait Features	**Mean**	**StaDev**	**Variance**	**MinRange**	**MaxRange**	**Mean**	**StaDev**	**Variance**	**MinRange**	**MaxRange**
Stride Length (m)	1.3106	0.2313	0.0535	0.9942	2.1126	1.3086	0.2375	0.0564	0.8622	1.7784
Stride Time (s)	1.3440	0.2328	0.0542	1.0255	2.1511	1.2398	0.2205	0.0486	0.8254	1.6759
Stride Velocity (m/s)	0.9751	0.9751	0.9751			1.0555	1.0555	1.0555		
Cadence (step/min)	38.29					38.29				
Step Speed (m/s)	0.9751	0.9936	0.9873			1.0555	1.0772	1.1604		
Step length (m)	0.6933	0.1765	0.0312	0.1065	1.0868	0.4518	0.2975	0.0885	0.0639	1.7260
Step time(s)	0.8138	0.2072	0.0429	0.1251	1.2757	0.5303	0.3492	0.1219	0.0750	2.0261
Step Ratio (Step length/cadence)	0.01					0.01				
Stance Time (s)	0.7221	0.2019	0.0408			0.5311	0.1529	0.0234		
Swing Length (m)	1.3743	0.7833	0.6135			1.3201	0.8302	0.6893		
Swing Time (s)	0.6220	0.1006	0.0101			0.7087	0.1698	0.0288		
Swing Velocity (m/s)	2.2095	2.2095	2.2095			2.1224	1.8627	1.8627		

Young Participant 9	Age	Height (m)	Weight (Kg)	Gender
	28.0000	1.7100	63.0000	Male

Total Time (s)	47.6250				
	Actual	**Right Leg**	**Accuracy**	**Left Leg**	**Accuracy**
Total Distance (m)	42.0600	41.9621	99.7673	41.7334	99.2236
Estimated Velocity (m/s)	0.8831	0.8811	99.7673	0.8763	99.2236
Detected Stride Number	30.0000	30.0000	100.0000	30.0000	100.0000
Detected Step Number	30.0000	30.0000	100.0000	30.0000	100.0000

			Right						**Left**	
Gait Features	**Mean**	**StaDev**	**Variance**	**MinRange**	**MaxRange**	**Mean**	**StaDev**	**Variance**	**MinRange**	**MaxRange**
Stride Length (m)	1.3761	0.1767	0.0312	1.1266	2.0118	1.3762	0.2322	0.0539	1.1476	2.3485
Stride Time (s)	1.3082	0.1648	0.0271	1.0756	1.9010	1.3149	0.2176	0.0474	1.1006	2.2262
Stride Velocity (m/s)	1.0519	1.0519	1.0519			1.0467	1.0467	1.0467		
Cadence (step/min)	37.79					37.79				
Step Speed (m/s)	1.0519	1.0724	1.1500			1.0467	1.0670	1.1384		
Step length (m)	0.5795	0.1636	0.0268	0.0442	0.9720	0.5758	0.2088	0.0436	0.2651	1.4801
Step time(s)	0.6562	0.1853	0.0343	0.0500	1.1006	0.6520	0.2364	0.0559	0.3002	1.6759
Step Ratio (Step length/cadence)	0.01					0.01				
Stance Time (s)	0.6862	0.1366	0.0187			0.6345	0.1044	0.0109		
Swing Length (m)	1.4099	0.5759	0.3317			1.3937	2.3612	5.5754		
Swing Time (s)	0.6220	0.1019	0.0104			0.6804	0.1955	0.0382		
Swing Velocity (m/s)	2.2667	2.2667	2.2667			2.2407	2.0485	2.0485		

Young Participant 10	Age	Height (m)	Weight (Kg)	Gender
	35.0000	1.7500	73.0000	Male

Total Time (s)	48.0500				
	Actual	**Right Leg**	**Accuracy**	**Left Leg**	**Accuracy**
Total Distance (m)	28.7600	26.5916	92.4603	28.7914	99.8909
Estimated Velocity (m/s)	0.5985	0.5534	92.4603	0.5992	99.8909
Detected Stride Number	30.0000	30.0000	100.0000	30.0000	100.0000
Detected Step Number	30.0000	30.0000	100.0000	30.0000	100.0000

	Right					**Left**				
Gait Features	**Mean**	**StaDev**	**Variance**	**MinRange**	**MaxRange**	**Mean**	**StaDev**	**Variance**	**MinRange**	**MaxRange**
Stride Length (m)	0.9404	0.1343	0.0180	0.7181	1.3416	0.9404	0.0938	0.0088	0.8487	1.2447
Stride Time (s)	1.2698	0.1778	0.0316	0.9755	1.8009	1.2723	0.1244	0.0155	1.1506	1.6759
Stride Velocity (m/s)	0.7406	0.7406	0.7406			0.7391	0.7391	0.7391		
Cadence (step/min)	37.46					37.46				
Step Speed (m/s)	0.7406	0.7555	0.5707			0.7391	0.7540	0.5685		
Step length (m)	0.3498	0.0818	0.0067	0.1647	0.5539	0.4102	0.0994	0.0099	0.2695	0.7037
Step time(s)	0.5845	0.1366	0.0187	0.2751	0.9255	0.6854	0.1661	0.0276	0.4502	1.1756
Step Ratio (Step length/cadence)	0.01					0.01				
Stance Time (s)	0.6462	0.1190	0.0142			0.6412	0.0909	0.0083		
Swing Length (m)	0.8935	0.5170	0.2673			0.9670	0.4313	0.1860		
Swing Time (s)	0.6237	0.1275	0.0163			0.6312	0.1292	0.0167		
Swing Velocity (m/s)	1.4327	1.4327	1.4327			1.5506	1.5322	1.5322		

Elderly Participant 1	Age	Height (m)	Weight (Kg)	Gender						
	67.0000	1.5700	68.0000	Male						
Total Time (s)	99.3000									
	Actual	**Right Leg**	**Accuracy**	**Left Leg**	**Accuracy**					
Total Distance (m)	21.0300	20.5910	97.9123	20.4708	97.3409					
Estimated Velocity (m/s)	0.2118	0.2074	97.9123	0.2062	97.3409					
Detected Stride Number	30.0000	30.0000	100.0000	30.0000	100.0000					
Detected Step Number	30.0000	30.0000	100.0000	30.0000	100.0000					
	Right					**Left**				
Gait Features	**Mean**	**StaDev**	**Variance**	**MinRange**	**MaxRange**	**Mean**	**StaDev**	**Variance**	**MinRange**	**MaxRange**
Stride Length (m)	0.6889	0.0702	0.0049	0.5630	0.8382	0.6891	0.0902	0.0081	0.4931	1.0478
Stride Time (s)	2.8047	0.2805	0.0787	2.3012	3.4017	2.8464	0.3660	0.1340	2.0510	4.3022
Stride Velocity (m/s)	0.2456	0.2456	0.2456			0.2421	0.2421	0.2421		
Cadence (step/min)	11.13					11.13				
Step Speed (m/s)	0.2456	0.2501	0.0625			0.2421	0.2464	0.0607		
Step length (m)	0.2719	0.0643	0.0041	0.1377	0.4556	0.3221	0.0541	0.0029	0.2331	0.4556
Step time(s)	1.2840	0.3037	0.0922	0.6503	2.1511	1.5208	0.2556	0.0653	1.1006	2.1511
Step Ratio (Step length/cadence)	0.02					0.02				
Stance Time (s)	1.3457	0.2315	0.0535			1.4274	0.3481	0.1216		
Swing Length (m)	0.6896	0.3485	0.1215			0.6853	0.4392	0.1929		
Swing Time (s)	1.4591	0.2341	0.0549			1.4194	0.2071	0.0418		
Swing Velocity (m/s)	0.4726	0.4717	0.4717			0.4688	0.4831	0.4831		

Elderly Participant 2	Age	Height (m)	Weight (Kg)	Gender
	63.0000	1.7300	62.0000	Female

Total Time (s)	73.4500				
	Actual	**Right Leg**	**Accuracy**	**Left Leg**	**Accuracy**
Total Distance (m)	26.8200	26.4892	98.7666	25.2723	94.2292
Estimated Velocity (m/s)	0.3651	0.3606	98.7666	0.3441	94.2292
Detected Stride Number	30.0000	30.0000	100.0000	30.0000	100.0000
Detected Step Number	30.0000	30.0000	100.0000	30.0000	100.0000

	Right					**Left**				
Gait Features	**Mean**	**StaDev**	**Variance**	**MinRange**	**MaxRange**	**Mean**	**StaDev**	**Variance**	**MinRange**	**MaxRange**
Stride Length (m)	0.6929	0.1353	0.0183	0.4184	0.9373	0.6930	0.1357	0.0184	0.4527	0.9548
Stride Time (s)	2.0957	0.4044	0.1635	1.2754	2.8260	2.1307	0.4124	0.1701	1.4005	2.9260
Stride Velocity (m/s)	0.3306	0.3306	0.3306			0.3253	0.3253	0.3253		
Cadence (step/min)	24.50					24.50				
Step Speed (m/s)	0.3306	0.3346	0.1120			0.3253	0.3291	0.1083		
Step length (m)	0.1820	0.1408	0.0198	-0.1461	0.5662	0.5832	0.1458	0.0212	0.2922	0.7762
Step time(s)	0.4985	0.3856	0.1487	-0.4001	1.5505	1.5972	0.3992	0.1594	0.8003	2.1257
Step Ratio (Step length/cadence)	0.02					0.02				
Stance Time (s)	0.9853	0.2655	0.0705			1.0870	0.2469	0.0609		
Swing Length (m)	0.8820	0.6585	0.4336			0.8433	0.6916	0.4783		
Swing Time (s)	1.1104	0.2307	0.0532			1.0437	0.2568	0.0659		
Swing Velocity (m/s)	0.7943	0.7943	0.7943			0.7595	0.8080	0.8080		

Elderly Participant 3	Age	Height (m)	Weight (Kg)	Gender
	86.0000	1.4200	64.0000	Male

Total Time (s)	96.5750				
	Actual	**Right Leg**	**Accuracy**	**Left Leg**	**Accuracy**
Total Distance (m)	20.7000	20.8989	99.0393	20.6760	99.8842
Estimated Velocity (m/s)	0.2143	0.2164	99.0393	0.2141	99.8842
Detected Stride Number	26.0000	26.0000	100.0000	26.0000	100.0000
Detected Step Number	26.0000	26.0000	100.0000	26.0000	100.0000

	Right					**Left**				
Gait Features	**Mean**	**StaDev**	**Variance**	**MinRange**	**MaxRange**	**Mean**	**StaDev**	**Variance**	**MinRange**	**MaxRange**
Stride Length (m)	0.7901	0.1315	0.0173	0.6653	1.2490	0.7898	0.0780	0.0061	0.6586	0.9616
Stride Time (s)	3.1729	0.5238	0.2744	2.6757	5.0013	3.0239	0.2961	0.0877	2.5257	3.6760
Stride Velocity (m/s)	0.2490	0.2490	0.2490			0.2612	0.2612	0.2612		
Cadence (step/min)	18.63					18.63				
Step Speed (m/s)	0.2490	0.2510	0.0630			0.2612	0.2634	0.0694		
Step length (m)	-0.1633	0.3575	0.1278	-0.5682	0.4824	0.1952	0.3440	0.1183	-0.2519	0.7236
Step time(s)	-0.7617	1.6678	2.7816	-2.6507	2.2506	0.9108	1.6050	2.5759	-1.1753	3.3759
Step Ratio (Step length/cadence)	0.01					0.01				
Stance Time (s)	1.6427	0.4033	0.1626			1.5292	0.2439	0.0595		
Swing Length (m)	0.8025	1.1141	1.2413			0.7953	0.5205	0.2709		
Swing Time (s)	1.5302	0.3247	0.1054			1.4946	0.2224	0.0494		
Swing Velocity (m/s)	0.5244	0.5244	0.5244			0.5198	0.5321	0.5321		

Elderly Participant 4	Age	Height (m)	Weight (Kg)	Gender
	73.0000	1.4400	65.0000	Male

Total Time (s)	71.8250				
	Actual	**Right Leg**	**Accuracy**	**Left Leg**	**Accuracy**
Total Distance (m)	24.6000	24.6303	99.8769	25.4147	96.6884
Estimated Velocity (m/s)	0.3425	0.3429	99.8769	0.3538	96.6884
Detected Stride Number	30.0000	30.0000	100.0000	30.0000	100.0000
Detected Step Number	30.0000	30.0000	100.0000	30.0000	100.0000

	Right					**Left**				
Gait Features	**Mean**	**StaDev**	**Variance**	**MinRange**	**MaxRange**	**Mean**	**StaDev**	**Variance**	**MinRange**	**MaxRange**
Stride Length (m)	0.6929	0.0989	0.0098	0.4836	0.9506	0.6928	0.1469	0.0216	0.4318	0.9990
Stride Time (s)	2.1032	0.2967	0.0881	1.4755	2.8760	2.0716	0.4340	0.1883	1.3005	2.9760
Stride Velocity (m/s)	0.3295	0.3295	0.3295			0.3344	0.3344	0.3344		
Cadence (step/min)	25.06					25.06				
Step Speed (m/s)	0.3295	0.3334	0.1112			0.3344	0.3385	0.1146		
Step length (m)	0.2484	0.1259	0.0158	-0.0257	0.5311	0.4720	0.1252	0.0157	0.2313	0.7709
Step time(s)	0.7253	0.3675	0.1351	-0.0750	1.5505	1.3780	0.3655	0.1336	0.6752	2.2508
Step Ratio (Step length/cadence)	0.01					0.01				
Stance Time (s)	1.1029	0.1900	0.0361			1.0204	0.2560	0.0655		
Swing Length (m)	0.8217	0.3438	0.1182			0.8482	0.6649	0.4421		
Swing Time (s)	1.0003	0.2136	0.0456			1.0512	0.2618	0.0685		
Swing Velocity (m/s)	0.8214	0.8214	0.8214			0.8479	0.8069	0.8069		

Elderly Participant 5	Age	Height (m)	Weight (Kg)	Gender
	75.0000	1.3200	62.0000	Male

Total Time (s)	105.6250				
	Actual	**Right Leg**	**Accuracy**	**Left Leg**	**Accuracy**
Total Distance (m)	15.5000	20.1874	69.7587	19.0633	77.0108
Estimated Velocity (m/s)	0.1467	0.1911	69.7587	0.1805	77.0108
Detected Stride Number	26.0000	26.0000	100.0000	26.0000	100.0000
Detected Step Number	26.0000	26.0000	100.0000	26.0000	100.0000

	Right					**Left**				
Gait Features	**Mean**	**StaDev**	**Variance**	**MinRange**	**MaxRange**	**Mean**	**StaDev**	**Variance**	**MinRange**	**MaxRange**
Stride Length (m)	0.5917	0.1095	0.0120	0.4283	0.9947	0.5917	0.0937	0.0088	0.4640	0.8545
Stride Time (s)	3.2383	0.5948	0.3538	2.3506	5.4263	3.2460	0.5103	0.2604	2.5506	4.6761
Stride Velocity (m/s)	0.1827	0.1827	0.1827			0.1823	0.1823	0.1823		
Cadence (step/min)	17.04					17.04				
Step Speed (m/s)	0.1827	0.1842	0.0339			0.1823	0.1837	0.0338		
Step length (m)	-0.0557	0.2005	0.0402	-0.4257	0.2569	0.0546	0.2006	0.0402	-0.2569	0.4257
Step time(s)	-0.3799	1.3664	1.8669	-2.9007	1.7504	0.3722	1.3671	1.8689	-1.7504	2.9007
Step Ratio (Step length/cadence)	0.003					0.003				
Stance Time (s)	1.6196	0.3026	0.0916			1.6292	0.3636	0.1322		
Swing Length (m)	0.7756	0.9104	0.8289			0.7327	0.8279	0.6855		
Swing Time (s)	1.6187	0.4003	0.1602			1.6167	0.2991	0.0895		
Swing Velocity (m/s)	0.4791	0.4791	0.4791			0.4527	0.4532	0.4532		

Elderly Participant 6	Age	Height (m)	Weight (Kg)	Gender
	62.0000	1.6800	59.0000	Male

Total Time (s)	96.5750				
	Actual	**Right Leg**	**Accuracy**	**Left Leg**	**Accuracy**
Total Distance (m)	20.7000	20.7377	99.8179	20.6760	99.8842
Estimated Velocity (m/s)	0.2143	0.2147	99.8179	0.2141	99.8842
Detected Stride Number	26.0000	26.0000	100.0000	26.0000	100.0000
Detected Step Number	26.0000	26.0000	100.0000	26.0000	100.0000

	Right					**Left**				
Gait Features	**Mean**	**StaDev**	**Variance**	**MinRange**	**MaxRange**	**Mean**	**StaDev**	**Variance**	**MinRange**	**MaxRange**
Stride Length (m)	0.7900	0.1314	0.0173	0.6737	1.2648	0.7898	0.0780	0.0061	0.6586	0.9616
Stride Time (s)	3.1335	0.5171	0.2674	2.6757	5.0013	3.0239	0.2961	0.0877	2.5257	3.6760
Stride Velocity (m/s)	0.2521	0.2521	0.2521			0.2612	0.2612	0.2612		
Cadence (step/min)	18.63					18.63				
Step Speed (m/s)	0.2521	0.2542	0.0646			0.2612	0.2634	0.0694		
Step length (m)	-0.1633	0.3575	0.1278	-0.5682	0.4824	0.1868	0.3330	0.1109	-0.2519	0.5682
Step time(s)	-0.7617	1.6678	2.7816	-2.6507	2.2506	0.8714	1.5538	2.4142	-1.1753	2.6507
Step Ratio (Step length/cadence)	0.01					0.01				
Stance Time (s)	1.6091	0.3821	0.1460			1.5292	0.2439	0.0595		
Swing Length (m)	0.7961	1.0520	1.1068			0.7953	0.5205	0.2709		
Swing Time (s)	1.5244	0.3275	0.1072			1.4946	0.2224	0.0494		
Swing Velocity (m/s)	0.5223	0.5223	0.5223			0.5217	0.5321	0.5321		

Elderly Participant 7	Age	Height (m)	Weight (Kg)	Gender
	71.0000	1.6500	64.0000	Male

Total Time (s)	80.1000				
	Actual	**Right Leg**	**Accuracy**	**Left Leg**	**Accuracy**
Total Distance (m)	23.7700	22.9554	96.5728	23.2947	98.0005
Estimated Velocity (m/s)	0.2968	0.2866	96.5728	0.2908	98.0005
Detected Stride Number	30.0000	30.0000	100.0000	30.0000	100.0000
Detected Step Number	30.0000	30.0000	100.0000	30.0000	100.0000

	Right					**Left**				
Gait Features	**Mean**	**StaDev**	**Variance**	**MinRange**	**MaxRange**	**Mean**	**StaDev**	**Variance**	**MinRange**	**MaxRange**
Stride Length (m)	0.6941	0.1794	0.0322	0.4334	0.9947	0.6939	0.1307	0.0171	0.4543	0.9453
Stride Time (s)	2.4683	0.6315	0.3988	1.5505	3.5261	2.3932	0.4462	0.1991	1.5755	3.2510
Stride Velocity (m/s)	0.2812	0.2812	0.2812			0.2899	0.2899	0.2899		
Cadence (step/min)	21.47					21.47				
Step Speed (m/s)	0.2812	0.2841	0.0807			0.2899	0.2930	0.0859		
Step length (m)	0.1680	0.1747	0.0305	-0.2152	0.4750	0.5645	0.1912	0.0365	0.1484	1.0464
Step time(s)	0.5660	0.5888	0.3467	-0.7252	1.6005	1.9023	0.6442	0.4150	0.5002	3.5261
Step Ratio (Step length/cadence)	0.02					0.02				
Stance Time (s)	1.2662	0.3561	0.1268			1.1787	0.2943	0.0866		
Swing Length (m)	0.7653	0.9251	0.8558			0.7766	0.8934	0.7981		
Swing Time (s)	1.2020	0.3521	0.1240			1.2145	0.2146	0.0460		
Swing Velocity (m/s)	0.6366	0.6366	0.6366			0.6460	0.6394	0.6394		

Elderly Participant 8	Age	Height (m)	Weight (Kg)	Gender
	67.0000	1.5800	60.0000	Male

Total Time (s)	74.8000				
	Actual	**Right Leg**	**Accuracy**	**Left Leg**	**Accuracy**
Total Distance (m)	26.2100	26.8913	97.4006	23.5050	89.6797
Estimated Velocity (m/s)	0.3504	0.3595	97.4006	0.3142	89.6797
Detected Stride Number	30.0000	30.0000	100.0000	30.0000	100.0000
Detected Step Number	30.0000	30.0000	100.0000	30.0000	100.0000

	Right					**Left**				
Gait Features	**Mean**	**StaDev**	**Variance**	**MinRange**	**MaxRange**	**Mean**	**StaDev**	**Variance**	**MinRange**	**MaxRange**
Stride Length (m)	0.6932	0.2528	0.0639	0.4953	1.9081	0.6926	0.1675	0.0280	0.4538	1.2217
Stride Time (s)	2.1599	0.7787	0.6064	1.5505	5.9020	2.0098	0.4799	0.2303	1.3254	3.5262
Stride Velocity (m/s)	0.3209	0.3209	0.3209			0.3446	0.3446	0.3446		
Cadence (step/min)	24.06					24.06				
Step Speed (m/s)	0.3209	0.3247	0.1054			0.3446	0.3489	0.1218		
Step length (m)	0.3444	0.3203	0.1026	-0.7536	0.7010	0.3124	0.1583	0.0251	0.0526	0.5345
Step time(s)	0.9828	0.9140	0.8354	-2.1507	2.0007	0.8604	0.4435	0.1967	0.1501	1.5255
Step Ratio (Step length/cadence)	0.01					0.01				
Stance Time (s)	1.0495	0.4316	0.1863			1.0278	0.2793	0.0780		
Swing Length (m)	0.8962	1.3252	1.7561			0.7856	1.2665	1.6041		
Swing Time (s)	1.1104	0.4352	0.1894			0.9820	0.2690	0.0724		
Swing Velocity (m/s)	0.8071	0.8071	0.8071			0.7075	0.8000	0.8000		

Elderly Participant 9	Age	Height (m)	Weight (Kg)	Gender
	63.0000	1.2700	62.0000	Female

Total Time (s)	66.7500				
	Actual	**Right Leg**	**Accuracy**	**Left Leg**	**Accuracy**
Total Distance (m)	23.2600	27.9676	79.7611	22.9786	98.7900
Estimated Velocity (m/s)	0.3485	0.4190	79.7611	0.3442	98.7900
Detected Stride Number	30.0000	30.0000	100.0000	30.0000	100.0000
Detected Step Number	30.0000	30.0000	100.0000	30.0000	100.0000

	Right					**Left**				
Gait Features	**Mean**	**StaDev**	**Variance**	**MinRange**	**MaxRange**	**Mean**	**StaDev**	**Variance**	**MinRange**	**MaxRange**
Stride Length (m)	0.6927	0.1188	0.0141	0.4727	0.9368	0.6926	0.0968	0.0094	0.4697	0.8697
Stride Time (s)	2.0408	0.3457	0.1195	1.4005	2.7510	2.0166	0.2782	0.0774	1.3755	2.5259
Stride Velocity (m/s)	0.3394	0.3394	0.3394			0.3434	0.3434	0.3434		
Cadence (step/min)	26.99					26.99				
Step Speed (m/s)	0.3394	0.3436	0.1181			0.3434	0.3478	0.1209		
Step length (m)	0.8462	0.3802	0.1445	0.1307	1.3508	0.3622	0.1700	0.0289	0.0610	0.6275
Step time(s)	2.4284	1.0910	1.1903	0.3751	3.8765	1.0396	0.4878	0.2380	0.1751	1.8007
Step Ratio (Step length/cadence)	0.03					0.01				
Stance Time (s)	1.0621	0.2186	0.0478			0.9837	0.2181	0.0475		
Swing Length (m)	0.9328	0.8875	0.7877			0.7679	1.2501	1.5628		
Swing Time (s)	0.9787	0.2440	0.0595			1.0329	0.2003	0.0401		
Swing Velocity (m/s)	0.9531	0.9531	0.9531			0.7846	0.7434	0.7434		

Elderly Participant 10	Age	Height (m)	Weight (Kg)	Gender
	67.0000	1.5700	68.0000	Male

Total Time (s)	37.6000				
	Actual	**Right Leg**	**Accuracy**	**Left Leg**	**Accuracy**
Total Distance (m)	22.3500	10.7724	48.1985	10.5724	47.3039
Estimated Velocity (m/s)	0.5944	0.2865	48.1985	0.2812	47.3039
Detected Stride Number	20.0000	20.0000	100.0000	20.0000	100.0000
Detected Step Number	20.0000	20.0000	100.0000	20.0000	100.0000

	Right					**Left**				
Gait Features	**Mean**	**StaDev**	**Variance**	**MinRange**	**MaxRange**	**Mean**	**StaDev**	**Variance**	**MinRange**	**MaxRange**
Stride Length (m)	1.0824	0.1372	0.0188	0.7758	1.4777	1.0842	0.2780	0.0773	0.9227	2.1188
Stride Time (s)	1.5170	0.1860	0.0346	1.1015	2.0527	1.5996	0.4074	0.1659	1.4019	3.1542
Stride Velocity (m/s)	0.7135	0.7135	0.7135			0.6778	0.6617	0.6617		
Cadence (step/min)	31.91					31.91				
Step Speed (m/s)	0.7135	0.7379	0.5444			0.6778	0.6826	0.4659		
Step length (m)	0.4955	0.1494	0.0223	0.2083	1.0119	0.4896	0.0870	0.0076	-0.6250	-0.2083
Step time(s)	0.8336	0.2513	0.0631	0.3505	1.7023	0.8236	0.1463	0.0214	-1.0514	-0.3505
Step Ratio (Step length/cadence)	0.01					0.01				
Stance Time (s)	0.8186	0.2151	0.0462			0.7911	0.2637	0.0696		
Swing Length (m)	0.5294	0.2644	0.0699			0.5929	0.5208	0.2712		
Swing Time (s)	0.6984	0.2642	0.0698			0.8486	0.1604	0.0257		
Swing Velocity (m/s)	0.7579	0.7579	0.7579			0.8489	0.6986	0.6986		

Appendix D

Stride No	Participant 1: Treadmill speed 0.6 m/s							
	Qualisys				IMU			
	Right Leg		Left Leg		Right Leg		Left Leg	
	Distance (m)	Period (s)	Distance (m)	Period (s)	Distance(m)	Period(s)	Distance(m)	Period(s)
1	1.235	1.480	1.203	1.450	1.248	1.404	1.080	1.279
2	1.153	1.425	1.070	1.490	1.165	1.193	0.854	1.368
3	1.165	1.575	1.153	1.425	1.177	1.377	1.071	1.180
4	1.137	1.870	1.052	1.615	1.149	1.712	0.800	1.448
5	1.126	1.220	1.087	1.465	1.138	1.369	0.966	1.352
6	1.186	1.795	1.085	1.505	1.198	1.673	1.088	1.432
7	1.141	1.180	1.126	2.000	1.152	1.337	1.078	1.973
8	1.123	1.585	1.049	1.090	1.134	1.731	0.892	1.208
9	1.048	1.600	1.034	2.015	1.058	1.603	1.112	1.838
10	1.040	1.705	0.951	1.245	1.050	1.638	0.684	1.524
11	1.044	2.310	0.930	1.615	1.054	2.205	0.882	1.547
12	1.101	1.645	1.002	1.795	1.112	1.501	0.863	1.742
13	1.039	1.695	1.014	1.635	1.049	1.705	0.865	1.558
14	1.083	1.150	1.050	1.815	1.094	1.214	1.074	1.833
15	1.147	2.380	1.086	1.630	1.158	2.355	1.089	1.593
16	1.107	1.060	1.088	1.835	1.118	1.295	1.348	1.810
17	1.079	2.240	1.063	2.040	1.090	2.078	0.950	1.822
18	1.204	1.820	1.037	1.375	1.216	1.743	0.793	1.673
19	1.046	1.085	1.029	2.180	1.056	1.402	1.197	2.005
20	1.031	1.630	1.038	1.130	1.042	1.743	0.830	1.260
21	1.029	1.340	1.062	1.445	1.040	1.383	1.154	1.764
22	1.088	1.435	1.023	1.535	1.099	1.437	0.919	1.363
23	1.069	1.890	1.053	1.360	1.080	1.779	1.213	1.403
24	1.059	1.580	1.093	1.480	1.069	1.646	1.203	1.627
25	1.054	1.540	1.072	1.520	1.064	1.322	1.191	1.524
26	1.104	1.540	1.112	1.480	1.116	1.755	0.964	1.501
27	1.069	1.890	1.053	1.360	1.080	1.700	1.315	1.570
28	1.059	1.580	1.093	1.480	1.069	1.626	1.115	1.615
29	1.054	1.540	1.072	1.520	1.064	1.486	1.189	1.455
30	1.104	1.540	1.112	1.480	1.116	1.673	1.009	1.547

	Participant 1: Treadmill speed 1.0 m/s							
	Qualisys				IMU			
	Right Leg		Left Leg		Right Leg		Left Leg	
	Distance (m)	Period (s)	Distance (m)	Period (s)	Distance(m)	Period(s)	Distance(m)	Period(s)
1	0.864	0.950	0.854	0.860	0.944	0.923	0.768	0.745
2	0.897	0.925	0.819	0.915	0.781	0.900	0.739	0.689
3	0.887	0.890	0.826	0.875	1.100	0.811	1.005	1.067
4	0.882	0.985	0.804	1.035	1.049	0.889	0.714	0.811
5	0.891	0.745	0.856	0.880	0.790	1.045	0.704	1.067
6	0.824	0.910	0.835	0.850	0.704	0.967	0.940	0.978
7	0.902	1.030	0.890	1.015	0.928	0.968	0.746	0.811
8	0.927	0.895	0.878	0.820	1.215	1.167	1.103	1.012
9	0.897	0.910	0.843	0.875	0.602	0.845	0.915	1.123
10	0.931	0.935	0.892	0.895	0.776	0.878	1.041	1.134
11	0.933	0.820	0.895	0.960	0.830	0.789	0.598	1.023
12	0.943	1.000	0.939	0.895	0.971	1.145	0.716	0.667
13	0.956	0.785	0.899	0.935	1.007	0.878	0.808	0.656

14	0.948	1.035	0.905	0.905	0.833	1.034	0.673	0.945
15	0.961	0.790	0.915	0.905	0.789	0.634	0.657	0.967
16	0.956	1.105	0.915	0.975	1.185	1.112	0.946	1.089
17	0.963	0.805	0.956	0.945	0.990	0.978	0.803	0.823
18	0.944	1.065	0.901	0.950	0.719	1.000	0.706	1.056
19	0.946	0.915	0.931	0.905	0.714	0.923	0.973	0.978
20	0.965	0.785	0.928	0.915	0.810	0.900	0.640	0.800
21	0.975	1.020	0.967	0.910	0.961	0.923	1.246	1.025
22	0.975	0.810	0.975	0.905	0.839	0.978	0.918	0.700
23	0.984	1.150	0.966	0.945	0.849	0.900	0.855	0.656
24	0.988	0.895	0.950	0.965	0.886	0.945	0.773	1.123
25	0.959	0.810	0.918	0.935	0.948	0.945	0.630	0.967
26	0.923	1.065	0.908	0.945	0.844	0.911	0.790	0.967
27	0.946	0.825	0.915	0.950	0.858	0.978	0.994	1.134
28	0.959	1.110	0.912	0.935	0.805	0.934	0.746	0.789
29	1.002	1.110	0.952	1.030	1.182	1.012	0.997	0.956
30	0.860	1.110	0.855	1.030	0.813	0.923	0.768	0.950

	Participant 1: Treadmill speed 1.4 m/s							
	Qualisys				IMU			
	Right Leg		Left Leg		Right Leg		Left Leg	
	Distance (m)	Period (s)	Distance (m)	Period (s)	Distance(m)	Period(s)	Distance(m)	Period(s)
1	1.097	0.770	1.112	0.680	1.157	0.778	0.822	0.623
2	1.172	0.795	1.107	0.750	1.375	0.811	0.973	0.856
3	1.145	0.625	1.118	0.735	0.946	0.723	0.896	0.645
4	1.133	0.845	1.125	0.720	1.235	0.767	0.969	0.834
5	1.148	0.690	1.087	0.765	1.103	0.689	1.061	0.634
6	1.102	0.855	1.024	0.765	0.908	0.789	0.891	0.867
7	1.059	0.680	0.991	0.765	1.239	0.822	0.994	0.723
8	1.055	0.835	1.044	0.760	0.814	0.789	0.827	0.645
9	1.115	0.850	1.106	0.820	1.035	0.878	1.127	0.867
10	1.104	0.720	1.087	0.835	1.099	0.912	1.064	0.745
11	1.087	0.885	1.033	0.830	1.155	1.078	0.815	1.067
12	1.069	0.725	1.056	0.790	0.874	0.511	0.987	0.734
13	1.047	0.890	1.037	0.785	0.892	1.078	1.023	0.700
14	1.084	0.730	1.110	0.810	1.234	0.845	1.267	0.889
15	1.091	0.855	1.113	0.785	0.944	0.567	1.287	0.945
16	1.157	0.755	1.128	0.810	1.192	0.797	0.994	0.667
17	1.112	0.785	1.087	0.840	1.343	0.889	1.154	0.856
18	1.108	0.825	1.094	0.780	1.086	0.756	1.153	0.889
19	1.093	0.855	1.135	0.820	0.796	0.856	0.982	0.700
20	1.172	0.765	1.176	0.805	1.145	0.778	1.054	0.678
21	1.126	0.935	1.079	0.820	1.262	0.823	1.113	0.900
22	1.090	0.690	1.052	0.810	0.914	0.567	1.017	0.856
23	1.114	0.860	1.062	0.840	0.907	1.112	1.146	0.811
24	1.072	0.900	1.111	0.865	0.875	0.789	1.310	0.867
25	1.140	0.840	1.107	0.890	1.416	1.003	1.204	0.900
26	1.115	0.855	1.082	0.845	1.383	0.778	1.199	1.089
27	1.089	0.940	1.090	0.850	1.290	0.912	0.909	0.811
28	1.135	0.820	1.124	0.835	1.133	0.789	0.926	0.778
29	1.172	0.775	1.153	0.795	1.164	0.511	1.448	0.745
30	1.200	0.775	1.171	0.850	1.030	0.511	1.448	0.745

	Participant 1: Treadmill speed 1.8 m/s							
	Qualisys				IMU			
	Right Leg		Left Leg		Right Leg		Left Leg	
	Distance (m)	Period (s)	Distance (m)	Period (s)	Distance(m)	Period(s)	Distance(m)	Period(s)
1	1.189	0.675	1.167	0.775	1.194	0.912	1.085	0.611
2	1.237	0.750	1.238	0.720	1.000	0.611	1.057	0.656
3	1.258	0.670	1.218	0.695	1.522	0.700	1.478	0.734
4	1.206	0.735	1.208	0.680	1.457	0.845	1.242	0.734
5	1.238	0.710	1.229	0.720	1.169	0.678	1.476	0.834
6	1.230	0.680	1.217	0.690	1.130	0.689	1.096	0.600
7	1.247	0.700	1.244	0.695	1.253	0.667	1.400	0.834
8	1.261	0.725	1.235	0.690	1.206	0.734	1.116	0.734
9	1.209	0.650	1.178	0.700	1.073	0.678	1.091	0.611
10	1.265	0.665	1.237	0.665	1.054	0.723	1.003	0.578
11	1.280	0.665	1.222	0.660	1.205	0.634	1.189	0.745
12	1.257	0.680	1.217	0.685	1.209	0.589	1.108	0.667
13	1.145	0.695	1.121	0.685	1.426	0.767	1.205	0.589
14	1.212	0.640	1.226	0.680	0.936	0.734	1.174	0.867
15	1.282	0.675	1.267	0.680	1.192	0.567	1.284	0.793
16	1.256	0.670	1.214	0.660	1.245	0.789	1.307	0.756
17	1.233	0.655	1.251	0.660	1.040	0.645	1.550	0.723
18	1.280	0.705	1.265	0.670	1.075	0.678	1.529	0.700
19	1.333	0.695	1.292	0.685	1.143	0.711	1.003	0.789
20	1.331	0.730	1.311	0.715	1.039	0.778	1.275	0.623
21	1.253	0.670	1.244	0.725	1.540	0.689	1.149	0.656
22	1.270	0.695	1.255	0.675	1.061	0.678	0.961	0.623
23	1.267	0.710	1.261	0.695	1.290	0.745	1.203	0.856
24	1.260	0.785	1.243	0.720	1.177	0.700	0.952	0.667
25	1.312	0.645	1.299	0.715	1.280	0.600	1.430	0.623
26	1.283	0.755	1.250	0.725	1.294	0.823	1.336	0.889
27	1.260	0.640	1.286	0.700	1.462	0.634	1.379	0.723
28	1.292	0.735	1.267	0.700	1.201	0.700	1.524	0.611
29	1.236	0.760	1.242	0.705	1.357	0.778	1.453	0.700
30	1.278	0.850	1.271	0.725	1.169	0.656	1.470	0.700

	Participant 1: Treadmill speed 2.0 m/s							
	Qualisys				IMU			
	Right Leg		Left Leg		Right Leg		Left Leg	
	Distance (m)	Period (s)	Distance (m)	Period (s)	Distance(m)	Period(s)	Distance(m)	Period(s)
1	1.311	0.655	1.339	0.650	1.179	0.623	1.253	0.623
2	1.321	0.675	1.207	0.675	1.232	0.656	1.471	0.723
3	1.328	0.650	1.285	0.665	1.407	0.689	1.083	0.656
4	1.278	0.685	1.295	0.655	1.330	0.689	1.171	0.578
5	1.302	0.645	1.327	0.655	1.094	0.567	1.392	0.856
6	1.338	0.720	1.327	0.675	1.096	0.634	1.191	0.511
7	1.400	0.650	1.339	0.675	1.510	0.789	1.131	0.634
8	1.424	0.690	1.271	0.695	1.626	0.800	1.282	0.989
9	1.399	0.705	1.330	0.680	1.211	0.645	1.040	0.511
10	1.426	0.695	1.325	0.710	1.454	0.689	1.202	0.789
11	1.402	0.695	1.320	0.695	1.693	0.723	1.053	0.611
12	1.460	0.675	1.427	0.675	1.482	0.678	1.460	0.945

13	1.441	0.645	1.383	0.685	1.582	0.645	1.322	0.743
14	1.412	0.705	1.409	0.695	1.560	0.767	1.492	0.789
15	1.385	0.665	1.350	0.650	1.155	0.667	1.091	0.578
16	1.372	0.710	1.322	0.705	1.161	0.700	1.451	0.711
17	1.344	0.695	1.292	0.705	1.327	0.623	1.013	0.700
18	1.304	0.735	1.307	0.700	1.432	0.745	1.456	0.734
19	1.284	0.665	1.259	0.700	1.329	0.711	1.425	0.723
20	1.313	0.705	1.342	0.690	1.324	0.734	1.523	0.734
21	1.301	0.685	1.317	0.695	1.376	0.700	1.416	0.934
22	1.312	0.690	1.276	0.695	1.312	0.711	1.047	0.600
23	1.364	0.710	1.346	0.695	1.343	0.700	1.243	0.600
24	1.359	0.670	1.344	0.710	1.244	0.756	1.158	0.611
25	1.373	0.720	1.385	0.690	1.223	0.623	1.620	0.823
26	1.347	0.690	1.298	0.725	1.270	0.689	1.080	0.634
27	1.320	0.650	1.281	0.670	1.319	0.667	1.206	0.545
28	1.305	0.695	1.283	0.645	1.229	0.723	1.005	0.556
29	1.340	0.695	1.339	0.685	1.254	0.667	1.246	0.611
30	1.353	0.695	1.366	0.685	1.330	0.667	1.212	0.611

	Participant 1: Treadmill speed 2.2 m/s							
	Qualisys				IMU			
	Right Leg		Left Leg		Right Leg		Left Leg	
	Distance (m)	Period (s)	Distance (m)	Period (s)	Distance(m)	Period(s)	Distance(m)	Period(s)
1	1.407	0.655	1.400	0.685	1.297	0.556	1.377	0.567
2	1.495	0.635	1.447	0.625	1.490	0.634	1.703	0.900
3	1.343	0.730	1.380	0.660	1.358	0.556	1.297	0.623
4	1.422	0.610	1.411	0.665	1.631	0.856	1.282	0.567
5	1.420	0.630	1.417	0.610	1.160	0.589	1.387	0.623
6	1.473	0.640	1.412	0.635	1.529	0.934	1.390	0.656
7	1.426	0.630	1.399	0.655	1.615	0.738	1.551	0.634
8	1.410	0.655	1.386	0.655	1.688	0.623	1.462	0.611
9	1.362	0.645	1.395	0.625	1.619	0.634	1.527	0.689
10	1.356	0.620	1.398	0.625	1.360	0.689	1.422	0.812
11	1.369	0.655	1.370	0.635	1.313	0.545	1.154	0.656
12	1.393	0.645	1.385	0.660	1.408	0.734	1.351	0.634
13	1.435	0.645	1.424	0.655	1.393	0.534	1.673	0.767
14	1.416	0.655	1.451	0.650	1.274	0.756	1.669	0.711
15	1.410	0.670	1.428	0.640	1.295	0.689	1.169	0.611
16	1.427	0.635	1.354	0.635	1.211	0.567	1.289	0.545
17	1.343	0.630	1.300	0.665	1.419	0.723	1.300	0.645
18	1.386	0.690	1.371	0.675	1.108	0.600	1.466	0.800
19	1.413	0.605	1.364	0.670	1.398	0.734	1.361	0.511
20	1.411	0.680	1.413	0.635	1.396	0.611	1.635	0.789
21	1.450	0.675	1.444	0.655	1.457	0.789	1.373	0.545
22	1.530	0.660	1.462	0.675	1.276	0.511	1.663	0.867
23	1.472	0.635	1.490	0.645	1.497	0.912	1.378	0.511
24	1.451	0.645	1.514	0.645	1.450	0.656	1.534	0.934
25	1.626	0.655	1.593	0.665	1.358	0.623	1.455	0.545
26	1.642	0.665	1.625	0.655	1.614	0.511	1.329	0.545
27	1.629	0.670	1.608	0.645	1.404	0.645	1.641	0.723
28	1.517	0.635	1.519	0.635	1.243	0.711	1.320	0.667
29	1.473	0.710	1.551	0.710	1.309	0.667	1.602	0.634
30	1.571	0.710	1.541	0.710	1.309	0.667	1.506	0.700

	Participant 1: Treadmill speed 2.5 m/s							
	Qualisys				IMU			
	Right Leg		Left Leg		Right Leg		Left Leg	
	Distance (m)	Period (s)	Distance (m)	Period (s)	Distance(m)	Period(s)	Distance(m)	Period(s)
1	1.611	0.580	1.601	0.595	1.346	0.445	1.654	0.734
2	1.551	0.650	1.533	0.625	1.534	0.578	1.792	0.623
3	1.535	0.595	1.550	0.605	1.506	0.623	1.780	0.656
4	1.563	0.590	1.558	0.620	1.672	0.667	1.320	0.589
5	1.507	0.620	1.538	0.595	1.751	0.689	1.544	0.645
6	1.606	0.625	1.513	0.635	1.416	0.511	1.457	0.611
7	1.571	0.595	1.539	0.595	1.625	0.700	1.381	0.589
8	1.573	0.620	1.556	0.630	1.848	0.812	1.623	0.678
9	1.558	0.615	1.548	0.615	1.296	0.611	1.322	0.600
10	1.504	0.615	1.529	0.605	1.318	0.378	1.251	0.623
11	1.575	0.580	1.541	0.605	1.680	0.611	1.591	0.578
12	1.579	0.620	1.569	0.605	1.665	0.667	1.641	0.634
13	1.601	0.570	1.538	0.595	1.424	0.567	1.756	0.578
14	1.511	0.640	1.505	0.605	1.777	0.800	1.683	0.656
15	1.660	0.585	1.608	0.590	1.845	0.623	1.783	0.578
16	1.609	0.630	1.616	0.580	1.851	0.600	1.726	0.611
17	1.459	0.570	1.525	0.595	1.429	0.389	1.290	0.600
18	1.430	0.590	1.411	0.615	1.473	0.656	1.442	0.623
19	1.485	0.655	1.463	0.600	1.390	0.578	1.604	0.623
20	1.604	0.560	1.493	0.610	1.721	0.778	1.487	0.589
21	1.458	0.615	1.511	0.610	1.328	0.656	1.218	0.578
22	1.497	0.640	1.499	0.615	1.332	0.434	1.308	0.645
23	1.546	0.595	1.467	0.615	1.456	0.478	1.429	0.634
24	1.496	0.615	1.440	0.605	1.685	0.723	1.277	0.623
25	1.450	0.600	1.357	0.600	1.700	0.623	1.539	0.600
26	1.492	0.595	1.418	0.600	1.434	0.545	1.607	0.611
27	1.464	0.620	1.426	0.600	1.736	0.878	1.167	0.600
28	1.493	0.595	1.443	0.625	1.359	0.578	1.465	0.611
29	1.512	0.630	1.446	0.660	1.283	0.422	1.249	0.600
30	1.453	0.630	1.453	0.660	1.205	0.434	1.691	0.689

Stride No	Participant 2: Treadmill speed 0.6 m/s							
	Qualisys				IMU			
	Right Leg		Left Leg		Right Leg		Left Leg	
	Distance (m)	Period (s)	Distance (m)	Period (s)	Distance(m)	Period(s)	Distance(m)	Period(s)
1	0.660	0.945	0.933	0.716	0.723	0.945	0.971	0.736
2	0.799	0.947	0.766	1.092	0.798	0.950	0.763	1.087
3	0.923	1.084	0.894	0.964	0.921	1.087	0.890	1.031
4	0.939	1.003	0.929	1.050	0.942	1.003	0.886	1.036
5	0.827	1.040	0.868	1.330	0.829	1.074	0.873	1.328
6	0.831	1.202	0.755	0.917	0.838	1.202	0.849	0.935
7	0.697	0.871	0.779	1.058	0.698	0.874	0.787	1.055
8	0.729	1.224	0.627	1.070	0.719	1.221	0.629	1.071
9	0.668	1.096	0.735	1.257	0.723	1.114	0.755	1.281
10	0.541	1.196	0.546	1.149	0.558	1.190	0.551	1.149

11	0.472	1.202	0.521	1.188	0.473	1.197	0.521	1.190
12	0.446	1.038	0.538	1.292	0.461	1.050	0.543	1.276
13	0.632	1.228	0.519	0.948	0.635	1.220	0.576	0.968
14	0.565	0.961	0.566	1.151	0.574	0.965	0.575	1.148
15	0.528	1.078	0.500	1.109	0.537	1.081	0.490	1.096
16	0.602	1.076	0.584	1.062	0.606	1.076	0.676	1.062
17	0.697	1.078	0.591	1.074	0.697	1.078	0.626	1.077
18	0.702	1.234	0.688	1.233	0.693	1.217	0.663	1.230
19	0.652	1.210	0.700	1.711	0.744	1.209	0.759	1.659
20	0.622	1.252	0.660	0.759	0.607	1.249	0.636	0.772
21	0.480	0.945	0.557	1.074	0.489	0.950	0.563	1.073
22	0.583	1.076	0.528	1.025	0.590	1.073	0.532	1.029
23	0.653	0.971	0.720	1.064	1.013	0.971	0.721	1.082
24	0.584	1.136	0.597	1.153	0.581	1.090	0.597	1.146
25	0.601	1.164	0.553	1.186	0.614	1.165	0.559	1.183
26	0.567	1.064	0.574	0.962	0.566	1.065	0.563	0.957
27	0.680	1.182	0.608	1.257	0.668	1.167	0.604	1.251
28	0.722	1.140	0.656	1.546	0.714	1.136	0.672	1.546
29	0.638	1.140	0.626	0.740	0.663	1.140	0.664	0.742
30	0.714	1.140	0.611	0.740	0.718	1.132	0.625	0.763

	Participant 2: Treadmill speed 1.0 m/s							
	Qualisys				IMU			
	Right Leg		Left Leg		Right Leg		Left Leg	
	Distance (m)	Period (s)	Distance (m)	Period (s)	Distance(m)	Period(s)	Distance(m)	Period(s)
1	0.880	1.125	0.785	1.030	0.893	1.145	0.788	1.057
2	0.848	1.465	0.804	1.215	0.842	1.458	0.799	1.216
3	0.803	0.930	0.856	1.320	0.760	0.934	0.854	1.312
4	0.833	1.205	0.793	1.030	0.845	1.205	0.808	1.032
5	0.891	1.170	0.837	1.370	0.905	1.174	0.810	1.359
6	0.903	1.195	0.906	1.025	0.944	1.195	0.936	1.030
7	0.856	1.140	0.908	1.195	0.854	1.138	0.905	1.147
8	0.879	1.130	0.912	1.045	0.878	1.129	0.887	1.048
9	0.928	1.155	0.990	1.215	1.047	1.156	1.005	1.243
10	0.953	1.145	0.974	1.075	0.945	1.143	0.944	1.077
11	1.055	1.145	1.021	1.305	1.048	1.146	1.026	1.307
12	1.114	1.145	1.126	1.140	1.131	1.151	1.119	1.134
13	1.084	1.120	1.135	1.110	1.084	1.128	1.134	1.104
14	1.085	1.095	1.105	1.045	1.040	1.092	1.085	1.042
15	1.144	1.205	1.099	1.045	1.144	1.200	1.111	1.056
16	1.134	1.040	1.119	1.020	1.069	1.040	1.101	0.995
17	1.208	0.905	1.142	1.050	1.186	0.907	1.140	1.072
18	1.254	1.125	1.222	1.145	1.224	1.116	1.213	1.121
19	1.244	0.995	1.276	1.045	1.297	1.006	1.308	1.044
20	1.325	1.060	1.332	1.035	1.304	1.056	1.263	1.047
21	1.378	1.075	1.367	0.930	1.369	1.076	1.362	0.933
22	1.353	0.995	1.349	1.135	1.334	0.995	1.310	1.122
23	1.421	1.115	1.389	1.100	1.445	1.119	1.392	1.102
24	1.448	1.100	1.363	1.020	1.439	1.091	1.222	1.012
25	1.360	0.985	1.338	1.100	1.298	1.000	1.321	1.100
26	1.303	1.115	1.379	0.985	1.149	1.124	1.337	0.985
27	1.343	0.920	1.343	0.995	1.202	0.920	1.313	0.974
28	1.362	1.030	1.392	1.015	1.310	1.026	1.383	1.017

29	1.366	0.990	1.366	1.075	1.366	0.990	1.347	1.071
30	1.411	0.990	1.392	1.075	1.388	0.987	1.368	1.070

	Participant 2: Treadmill speed 1.4 m/s							
	Qualisys				IMU			
	Right Leg		Left Leg		Right Leg		Left Leg	
	Distance (m)	Period (s)	Distance (m)	Period (s)	Distance(m)	Period(s)	Distance(m)	Period(s)
1	1.011	1.050	1.041	0.830	1.013	1.049	1.051	0.832
2	1.061	0.755	1.051	0.815	1.082	0.766	1.029	0.808
3	1.077	0.855	1.094	0.895	1.051	0.854	1.025	0.896
4	1.119	0.840	1.091	0.785	1.036	0.831	1.091	0.787
5	1.080	0.830	1.099	0.950	1.059	0.839	1.099	0.949
6	1.156	0.945	1.128	0.795	1.145	0.941	1.123	0.799
7	1.084	0.775	1.111	0.840	1.057	0.785	1.107	0.833
8	1.054	0.895	1.071	0.900	1.052	0.895	1.067	0.892
9	1.083	0.880	1.065	0.930	1.084	0.885	1.115	0.935
10	1.074	0.865	1.075	0.855	1.069	0.865	1.034	0.843
11	1.113	0.820	1.085	0.745	1.102	0.820	1.043	0.768
12	1.084	0.785	1.105	0.835	1.055	0.787	1.086	0.838
13	1.159	0.825	1.133	0.850	1.147	0.827	1.131	0.861
14	1.244	0.860	1.236	0.880	1.191	0.868	1.224	0.877
15	1.264	0.885	1.216	0.770	1.076	0.884	1.158	0.777
16	1.198	0.900	1.159	0.865	1.174	0.900	1.115	0.846
17	1.235	0.740	1.188	0.765	1.235	0.745	1.048	0.792
18	1.254	0.730	1.199	0.735	1.248	0.732	1.157	0.737
19	1.236	0.785	1.252	0.805	1.234	0.791	1.239	0.815
20	1.274	0.785	1.303	0.825	1.235	0.776	1.294	0.822
21	1.313	0.810	1.365	0.740	1.297	0.812	1.308	0.740
22	1.256	0.850	1.298	0.885	1.173	0.850	1.277	0.885
23	1.256	0.765	1.212	0.780	1.244	0.769	1.197	0.782
24	1.230	0.770	1.268	0.805	1.067	0.770	1.087	0.804
25	1.267	0.835	1.278	0.875	1.228	0.850	1.180	0.878
26	1.226	0.895	1.191	0.800	1.132	0.894	1.176	0.804
27	1.149	0.770	1.139	0.835	1.121	0.769	1.063	0.816
28	1.124	0.920	1.134	0.830	1.102	0.922	1.129	0.829
29	1.156	0.795	1.200	0.895	1.142	0.796	1.218	0.896
30	1.183	0.795	1.235	0.895	1.092	0.795	1.244	0.896

	Participant 2: Treadmill speed 1.8 m/s							
	Qualisys				IMU			
	Right Leg		Left Leg		Right Leg		Left Leg	
	Distance (m)	Period (s)	Distance (m)	Period (s)	Distance(m)	Period(s)	Distance(m)	Period(s)
1	0.986	0.710	1.063	0.780	0.975	0.712	1.045	0.796
2	0.960	0.730	1.044	0.705	0.957	0.732	1.044	0.713
3	0.958	0.720	1.022	0.655	0.830	0.713	1.014	0.655
4	0.980	0.675	1.024	0.710	0.972	0.692	0.982	0.709
5	0.964	0.700	1.039	0.675	0.943	0.694	1.007	0.676
6	0.973	0.805	1.060	0.730	0.973	0.805	1.033	0.731
7	1.012	0.680	1.055	0.735	0.959	0.680	1.040	0.732
8	1.012	0.665	1.053	0.705	0.970	0.679	1.052	0.705
9	1.006	0.685	1.044	0.720	0.920	0.686	0.997	0.717
10	1.023	0.715	1.099	0.715	1.022	0.699	1.098	0.723

11	1.061	0.720	1.098	0.655	1.056	0.721	1.087	0.657
12	1.027	0.670	1.083	0.710	1.026	0.727	1.070	0.715
13	1.048	0.685	1.107	0.715	1.023	0.680	1.071	0.716
14	1.025	0.740	1.121	0.755	1.010	0.740	1.104	0.752
15	0.994	0.815	1.083	0.720	0.886	0.798	1.042	0.709
16	0.997	0.615	1.069	0.705	0.954	0.627	1.031	0.705
17	1.039	0.740	1.105	0.690	1.003	0.746	1.091	0.695
18	1.043	0.690	1.099	0.705	1.040	0.679	1.080	0.703
19	1.008	0.720	1.110	0.700	1.040	0.721	1.095	0.700
20	1.013	0.715	1.082	0.685	1.006	0.716	1.082	0.685
21	1.054	0.660	1.098	0.675	1.036	0.660	1.078	0.676
22	1.028	0.705	1.102	0.720	0.995	0.705	1.070	0.710
23	1.010	0.670	1.101	0.680	1.000	0.674	1.101	0.683
24	1.027	0.710	1.089	0.720	0.898	0.710	1.024	0.716
25	0.993	0.695	1.073	0.700	0.995	0.696	1.029	0.705
26	0.976	0.690	1.047	0.640	0.920	0.685	1.018	0.663
27	0.960	0.690	1.052	0.760	0.927	0.691	1.051	0.753
28	0.931	0.715	1.024	0.635	0.920	0.716	0.976	0.638
29	0.935	0.675	0.990	0.705	0.929	0.679	0.976	0.703
30	0.945	0.675	0.987	0.705	0.906	0.676	0.903	0.705

	Participant 2: Treadmill speed 2.0 m/s							
	Qualisys				IMU			
	Right Leg		Left Leg		Right Leg		Left Leg	
	Distance (m)	Period (s)	Distance (m)	Period (s)	Distance(m)	Period(s)	Distance(m)	Period(s)
1	1.165	0.670	1.167	0.700	1.175	0.679	1.192	0.700
2	1.150	0.665	1.163	0.695	1.143	0.665	1.055	0.679
3	1.203	0.690	1.206	0.665	1.188	0.688	1.153	0.662
4	1.258	0.715	1.199	0.705	1.159	0.713	1.204	0.706
5	1.311	0.650	1.285	0.680	1.251	0.686	1.132	0.667
6	1.397	0.655	1.313	0.650	1.397	0.721	1.203	0.634
7	1.443	0.705	1.385	0.685	1.442	0.705	1.342	0.685
8	1.465	0.665	1.429	0.650	1.429	0.662	1.230	0.650
9	1.403	0.680	1.349	0.695	1.360	0.681	1.313	0.699
10	1.274	0.705	1.191	0.715	1.187	0.707	1.143	0.714
11	1.279	0.675	1.298	0.685	1.279	0.677	1.299	0.698
12	1.338	0.755	1.345	0.635	1.231	0.730	1.350	0.641
13	1.360	0.580	1.332	0.665	1.322	0.574	1.329	0.665
14	1.397	0.665	1.360	0.695	1.406	0.706	1.347	0.695
15	1.391	0.675	1.369	0.690	1.372	0.675	1.317	0.687
16	1.443	0.695	1.448	0.690	1.329	0.695	1.240	0.685
17	1.473	0.695	1.410	0.665	1.432	0.686	1.376	0.670
18	1.460	0.650	1.445	0.670	1.424	0.651	1.418	0.668
19	1.507	0.725	1.485	0.715	1.379	0.723	1.484	0.715
20	1.553	0.650	1.530	0.665	1.545	0.650	1.456	0.670
21	1.510	0.710	1.490	0.675	1.510	0.711	1.416	0.675
22	1.539	0.710	1.539	0.665	1.496	0.740	1.460	0.675
23	1.586	0.690	1.549	0.765	1.398	0.703	1.469	0.763
24	1.601	0.660	1.566	0.640	1.535	0.660	1.545	0.658
25	1.573	0.635	1.556	0.650	1.450	0.634	1.543	0.651
26	1.555	0.680	1.539	0.660	1.543	0.667	1.538	0.658
27	1.559	0.670	1.540	0.710	1.465	0.669	1.466	0.708
28	1.557	0.690	1.558	0.645	1.428	0.686	1.508	0.664

29	1.542	0.860	1.559	0.745	1.472	0.848	1.341	0.742
30	1.562	0.860	1.572	0.745	1.560	0.851	1.455	0.740

	Participant 2: Treadmill speed 2.2 m/s							
	Qualisys				IMU			
	Right Leg		Left Leg		Right Leg		Left Leg	
	Distance (m)	Period (s)	Distance (m)	Period (s)	Distance(m)	Period(s)	Distance(m)	Period(s)
1	1.389	0.690	1.376	0.615	1.348	0.690	1.355	0.617
2	1.397	0.655	1.410	0.670	1.391	0.659	1.245	0.670
3	1.356	0.645	1.343	0.640	1.311	0.645	1.335	0.631
4	1.394	0.620	1.380	0.660	1.297	0.636	1.375	0.661
5	1.435	0.645	1.428	0.610	1.400	0.639	1.426	0.614
6	1.477	0.615	1.471	0.630	1.467	0.643	1.468	0.635
7	1.512	0.645	1.514	0.635	1.501	0.663	1.506	0.635
8	1.513	0.640	1.501	0.630	1.492	0.643	1.476	0.630
9	1.506	0.605	1.499	0.635	1.489	0.584	1.447	0.636
10	1.586	0.670	1.550	0.650	1.543	0.669	1.498	0.651
11	1.499	0.660	1.496	0.655	1.434	0.657	1.443	0.656
12	1.410	0.615	1.413	0.605	1.331	0.616	1.247	0.608
13	1.413	0.630	1.431	0.665	1.404	0.638	1.421	0.662
14	1.434	0.635	1.443	0.655	1.418	0.634	1.345	0.650
15	1.392	0.680	1.423	0.650	1.307	0.676	1.385	0.659
16	1.479	0.670	1.413	0.690	1.448	0.671	1.410	0.693
17	1.427	0.665	1.376	0.630	1.399	0.678	1.348	0.637
18	1.405	0.615	1.425	0.610	1.399	0.617	1.375	0.610
19	1.495	0.675	1.512	0.700	1.416	0.668	1.322	0.694
20	1.481	0.695	1.514	0.675	1.407	0.695	1.509	0.676
21	1.478	0.635	1.468	0.640	1.474	0.692	1.456	0.632
22	1.522	0.665	1.536	0.690	1.497	0.654	1.524	0.693
23	1.548	0.665	1.545	0.655	1.445	0.644	1.390	0.653
24	1.551	0.645	1.520	0.615	1.544	0.645	1.409	0.618
25	1.569	0.630	1.528	0.680	1.567	0.631	1.495	0.683
26	1.561	0.690	1.554	0.660	1.492	0.695	1.514	0.660
27	1.588	0.635	1.556	0.605	1.527	0.632	1.551	0.608
28	1.643	0.670	1.610	0.725	1.640	0.683	1.464	0.725
29	1.579	0.650	1.577	0.620	1.537	0.652	1.569	0.626
30	1.567	0.690	1.555	0.620	1.566	0.694	1.395	0.619

	Participant 2: Treadmill speed 2.5 m/s							
	Qualisys				IMU			
	Right Leg		Left Leg		Right Leg		Left Leg	
	Distance (m)	Period (s)	Distance (m)	Period (s)	Distance(m)	Period(s)	Distance(m)	Period(s)
1	1.411	0.615	1.385	0.655	1.343	0.590	1.347	0.648
2	1.401	0.610	1.404	0.600	1.375	0.612	1.380	0.600
3	1.414	0.590	1.423	0.610	1.340	0.589	1.394	0.611
4	1.384	0.610	1.375	0.575	1.268	0.610	1.362	0.576
5	1.355	0.605	1.351	0.625	1.355	0.605	1.303	0.606
6	1.389	0.605	1.395	0.620	1.389	0.610	1.311	0.611
7	1.408	0.610	1.399	0.610	1.283	0.597	1.244	0.585
8	1.416	0.595	1.411	0.575	1.399	0.594	1.377	0.576
9	1.410	0.630	1.414	0.655	1.408	0.626	1.366	0.653
10	1.397	0.620	1.397	0.600	1.405	0.630	1.383	0.600

11	1.390	0.600	1.353	0.610	1.239	0.600	1.283	0.610
12	1.368	0.615	1.388	0.610	1.258	0.603	1.214	0.610
13	1.399	0.615	1.417	0.625	1.286	0.617	1.401	0.625
14	1.458	0.620	1.420	0.595	1.413	0.620	1.404	0.583
15	1.446	0.605	1.442	0.605	1.269	0.600	1.422	0.608
16	1.452	0.625	1.464	0.620	1.447	0.626	1.450	0.640
17	1.416	0.605	1.426	0.615	1.348	0.603	1.379	0.622
18	1.461	0.610	1.466	0.625	1.445	0.610	1.457	0.647
19	1.477	0.615	1.456	0.605	1.392	0.615	1.431	0.602
20	1.455	0.620	1.485	0.625	1.459	0.626	1.453	0.625
21	1.474	0.615	1.490	0.600	1.362	0.611	1.467	0.601
22	1.517	0.610	1.509	0.635	1.477	0.606	1.439	0.633
23	1.521	0.615	1.523	0.600	1.495	0.617	1.476	0.601
24	1.554	0.630	1.538	0.640	1.472	0.630	1.531	0.636
25	1.522	0.580	1.483	0.570	1.455	0.578	1.425	0.576
26	1.469	0.595	1.437	0.620	1.466	0.603	1.426	0.620
27	1.460	0.630	1.504	0.605	1.210	0.626	1.358	0.608
28	1.488	0.640	1.510	0.640	1.474	0.633	1.465	0.641
29	1.490	0.620	1.470	0.600	1.456	0.621	1.289	0.604
30	1.457	0.630	1.419	0.610	1.345	0.623	1.386	0.614

Stride No	Participant 3: Treadmill speed 0.6 m/s							
	Qualisys				IMU			
	Right Leg		Left Leg		Right Leg		Left Leg	
	Distance (m)	Period (s)	Distance (m)	Period (s)	Distance(m)	Period(s)	Distance(m)	Period(s)
1	1.162	1.900	1.162	2.045	1.160	1.885	1.193	1.993
2	1.280	1.825	1.280	2.065	1.210	1.850	1.309	2.066
3	1.223	2.210	1.223	1.985	1.210	2.213	1.257	1.996
4	1.301	2.105	1.301	1.910	1.301	2.100	1.306	1.907
5	1.277	2.015	1.277	2.140	1.294	2.022	1.275	2.148
6	1.274	2.140	1.274	2.265	1.200	2.130	1.255	2.256
7	1.290	1.995	1.290	1.765	1.186	1.998	1.105	1.772
8	1.365	2.025	1.365	2.105	1.364	2.029	1.333	2.105
9	1.412	2.075	1.412	2.160	1.412	2.074	1.354	2.157
10	1.393	1.955	1.393	1.980	1.433	1.955	1.387	1.981
11	1.439	1.935	1.439	1.585	1.429	1.976	1.438	1.598
12	1.513	2.010	1.513	2.295	1.510	2.028	1.514	2.252
13	1.585	2.250	1.585	2.210	1.587	2.246	1.573	2.215
14	1.504	2.375	1.504	2.325	1.447	2.364	1.491	2.324
15	1.378	2.095	1.378	1.695	1.397	2.108	1.377	1.722
16	1.303	1.750	1.303	2.560	1.303	1.783	1.283	2.530
17	1.307	2.275	1.307	1.810	1.311	2.259	1.387	1.810
18	1.434	2.185	1.434	2.280	1.434	2.198	1.499	2.281
19	1.388	2.090	1.388	2.105	1.615	2.091	1.387	2.104
20	1.340	2.030	1.340	1.880	1.362	2.022	1.338	1.901
21	1.383	1.670	1.383	2.120	1.389	1.707	1.341	2.110
22	1.396	2.050	1.396	2.310	1.396	2.083	1.386	2.309
23	1.304	2.670	1.304	2.135	1.347	2.651	1.432	2.159
24	1.239	1.865	1.239	2.145	1.261	1.894	1.173	2.147
25	1.187	2.115	1.187	1.900	1.208	2.115	1.031	1.900
26	1.201	1.980	1.201	2.230	1.200	1.995	1.245	2.218
27	1.158	2.245	1.158	1.910	1.373	2.227	1.195	1.942

28	1.261	1.855	1.261	1.825	1.281	1.877	1.378	1.862
29	1.342	2.210	1.342	2.570	1.350	2.211	1.348	2.486
30	1.305	2.210	1.305	2.570	1.355	2.210	1.337	2.504

	Participant 3: Treadmill speed 1.0 m/s							
	Qualisys				IMU			
	Right Leg		Left Leg		Right Leg		Left Leg	
	Distance (m)	Period (s)	Distance (m)	Period (s)	Distance(m)	Period(s)	Distance(m)	Period(s)
1	0.909	0.920	0.860	0.980	0.904	0.922	0.928	0.983
2	0.927	1.040	0.965	0.935	0.928	1.040	0.965	0.935
3	0.959	1.015	0.974	1.020	1.004	1.020	1.012	1.024
4	0.999	1.120	1.017	1.055	0.999	1.117	1.085	1.066
5	1.031	0.985	1.078	1.020	1.116	0.986	1.194	1.020
6	1.112	1.050	1.139	1.145	1.160	1.050	1.144	1.127
7	1.131	1.030	1.090	1.020	1.169	1.031	1.063	1.019
8	1.115	1.130	1.108	1.095	1.137	1.125	1.122	1.096
9	1.113	0.945	1.121	0.990	1.127	0.947	1.082	0.980
10	1.137	1.045	1.140	1.060	1.140	1.040	1.139	1.052
11	1.169	1.010	1.158	0.895	1.268	1.010	1.204	0.898
12	1.204	1.025	1.152	1.025	1.198	1.025	1.141	1.008
13	1.162	0.990	1.137	1.025	1.135	0.990	1.122	0.974
14	1.202	0.960	1.168	1.170	1.266	0.969	1.158	1.169
15	1.245	1.295	1.221	0.975	1.192	1.263	1.303	0.984
16	1.135	0.940	1.150	1.155	1.129	0.948	1.161	1.150
17	1.128	1.115	1.104	0.890	1.275	1.117	1.108	0.892
18	1.061	1.000	1.064	1.065	1.058	1.000	1.060	1.056
19	1.027	1.035	1.051	1.110	1.015	1.033	1.019	1.107
20	1.032	1.020	1.000	1.095	1.034	1.020	0.987	1.083
21	1.006	1.085	0.940	1.025	1.092	1.091	0.972	1.026
22	0.967	1.090	0.951	0.930	0.967	1.090	0.975	0.932
23	0.963	1.070	0.960	1.085	0.954	1.070	0.964	1.086
24	0.998	1.115	0.978	1.100	1.019	1.123	1.029	1.123
25	0.957	1.010	0.952	1.245	0.983	1.011	0.929	1.245
26	0.951	1.030	0.950	1.050	0.950	1.033	0.965	1.051
27	0.949	1.200	0.957	0.895	0.949	1.196	0.958	0.899
28	0.947	1.060	0.971	1.295	0.919	1.050	1.056	1.297
29	0.975	1.010	0.973	0.910	0.960	1.010	1.031	0.916
30	0.994	1.160	1.017	1.080	0.900	1.156	1.011	1.045

	Participant 3: Treadmill speed 1.4 m/s							
	Qualisys				IMU			
	Right Leg		Left Leg		Right Leg		Left Leg	
	Distance (m)	Period (s)	Distance (m)	Period (s)	Distance(m)	Period(s)	Distance(m)	Period(s)
1	1.032	0.900	1.014	0.930	1.017	0.904	1.004	0.894
2	1.139	0.995	1.122	1.010	1.143	1.001	1.040	0.978
3	1.186	0.875	1.204	0.910	1.166	0.875	1.170	0.910
4	1.195	1.010	1.219	0.890	1.176	0.999	1.190	0.891
5	1.193	0.885	1.207	0.965	1.179	0.892	1.204	0.966
6	1.275	1.010	1.285	0.945	1.270	1.010	1.283	0.942
7	1.278	0.985	1.292	0.965	1.298	0.984	1.307	0.973
8	1.367	0.970	1.371	0.920	1.364	0.969	1.431	0.928
9	1.409	0.975	1.367	1.010	1.420	1.006	1.367	1.007

10	1.408	0.950	1.386	0.955	1.401	0.945	1.385	0.956
11	1.424	0.975	1.409	1.120	1.366	0.972	1.364	1.107
12	1.392	0.990	1.405	0.855	1.392	1.018	1.405	0.859
13	1.380	1.020	1.379	0.995	1.266	1.018	1.378	0.992
14	1.381	1.010	1.382	1.000	1.313	1.011	1.371	1.009
15	1.404	0.955	1.411	0.985	1.235	0.955	1.399	0.984
16	1.413	1.000	1.423	1.005	1.391	1.003	1.506	1.069
17	1.401	1.000	1.379	1.010	1.392	0.989	1.374	0.994
18	1.408	0.965	1.385	0.945	1.458	0.971	1.373	0.935
19	1.335	1.025	1.358	0.995	1.317	1.018	1.373	1.000
20	1.399	0.945	1.417	0.985	1.433	0.947	1.417	1.006
21	1.353	0.985	1.395	0.985	1.355	0.985	1.398	0.985
22	1.443	0.955	1.449	0.930	1.444	0.948	1.412	0.930
23	1.461	1.005	1.472	1.050	1.499	1.005	1.466	1.048
24	1.494	1.000	1.505	1.010	1.521	1.000	1.507	1.010
25	1.444	0.995	1.442	0.940	1.451	0.996	1.501	0.949
26	1.470	1.015	1.501	1.010	1.478	1.017	1.500	1.009
27	1.466	0.960	1.512	1.065	1.454	0.957	1.494	1.000
28	1.452	0.990	1.461	0.920	1.454	0.996	1.558	0.926
29	1.568	0.975	1.556	1.150	1.552	0.974	1.477	1.134
30	1.526	1.030	1.534	1.000	1.523	1.027	1.569	1.004

	Participant 3: Treadmill speed 1.8 m/s							
	Qualisys				IMU			
	Right Leg		Left Leg		Right Leg		Left Leg	
	Distance (m)	Period (s)	Distance (m)	Period (s)	Distance(m)	Period(s)	Distance(m)	Period(s)
1	1.795	0.845	1.283	0.930	1.795	0.838	1.289	0.930
2	1.336	0.875	1.406	0.920	1.511	0.876	1.491	0.919
3	1.426	0.880	1.424	0.830	1.569	0.881	1.424	0.830
4	1.368	0.890	1.384	0.850	1.453	0.890	1.369	0.848
5	1.339	0.830	1.397	0.935	1.339	0.825	1.376	0.911
6	1.381	0.890	1.441	0.800	1.384	0.891	1.433	0.786
7	1.445	0.870	1.455	0.935	1.407	0.874	1.537	0.964
8	1.434	0.850	1.457	0.785	1.368	0.845	1.276	0.776
9	1.436	0.845	1.474	0.915	1.297	0.841	1.299	0.914
10	1.477	0.845	1.542	0.850	1.419	0.850	1.543	0.895
11	1.522	0.855	1.543	0.765	1.519	0.855	1.530	0.769
12	1.537	0.745	1.557	0.915	1.399	0.747	1.521	0.877
13	1.537	0.920	1.565	0.805	1.537	0.928	1.568	0.806
14	1.563	0.845	1.585	0.805	1.557	0.848	1.569	0.805
15	1.543	0.850	1.536	0.920	1.522	0.828	1.374	0.907
16	1.532	0.835	1.583	0.760	1.510	0.835	1.666	0.850
17	1.509	0.870	1.588	0.885	1.510	0.876	1.588	0.884
18	1.534	0.840	1.585	0.840	1.535	0.845	1.565	0.827
19	1.551	0.875	1.605	0.910	1.472	0.872	1.598	0.907
20	1.610	0.830	1.648	0.810	1.575	0.831	1.594	0.810
21	1.552	0.795	1.612	0.825	1.515	0.795	1.605	0.823
22	1.610	0.860	1.706	0.855	1.508	0.848	1.638	0.855
23	1.698	0.865	1.705	0.870	1.763	0.879	1.703	0.870
24	1.631	0.860	1.606	0.805	1.631	0.857	1.592	0.802
25	1.551	0.850	1.609	0.935	1.566	0.855	1.711	0.937
26	1.595	0.885	1.588	0.870	1.516	0.884	1.583	0.857
27	1.576	0.855	1.617	0.855	1.576	0.866	1.650	0.869

28	1.592	0.815	1.605	0.825	1.593	0.821	1.608	0.826
29	1.595	0.820	1.607	0.840	1.546	0.799	1.590	0.836
30	1.652	0.820	1.530	0.840	1.547	0.818	1.529	0.840

	Participant 3: Treadmill speed 2.0 m/s							
	Qualisys				IMU			
	Right Leg		Left Leg		Right Leg		Left Leg	
	Distance (m)	Period (s)	Distance (m)	Period (s)	Distance(m)	Period(s)	Distance(m)	Period(s)
1	1.442	0.750	1.448	0.795	1.429	0.751	1.448	0.792
2	1.577	0.830	1.539	0.765	1.554	0.830	1.545	0.767
3	1.551	0.755	1.530	0.820	1.531	0.756	1.564	0.820
4	1.521	0.800	1.573	0.780	1.496	0.803	1.553	0.773
5	1.518	0.790	1.527	0.805	1.517	0.790	1.536	0.807
6	1.523	0.785	1.539	0.790	1.525	0.792	1.601	0.792
7	1.523	0.820	1.498	0.795	1.447	0.809	1.567	0.834
8	1.573	0.735	1.574	0.790	1.557	0.735	1.572	0.802
9	1.567	0.850	1.549	0.750	1.583	0.847	1.498	0.751
10	1.485	0.745	1.497	0.765	1.484	0.747	1.410	0.755
11	1.506	0.745	1.549	0.745	1.503	0.745	1.539	0.745
12	1.583	0.715	1.599	0.765	1.532	0.718	1.465	0.766
13	1.644	0.785	1.636	0.760	1.626	0.784	1.530	0.751
14	1.691	0.780	1.684	0.775	1.694	0.796	1.684	0.776
15	1.680	0.750	1.666	0.850	1.676	0.752	1.615	0.843
16	1.614	0.840	1.642	0.750	1.635	0.840	1.637	0.750
17	1.657	0.790	1.668	0.775	1.658	0.786	1.633	0.771
18	1.589	0.755	1.583	0.775	1.616	0.762	1.560	0.771
19	1.594	0.785	1.591	0.790	1.594	0.786	1.572	0.793
20	1.584	0.800	1.608	0.805	1.648	0.798	1.609	0.807
21	1.591	0.785	1.661	0.775	1.586	0.786	1.631	0.764
22	1.569	0.790	1.612	0.795	1.567	0.790	1.617	0.798
23	1.649	0.800	1.665	0.785	1.618	0.794	1.680	0.786
24	1.652	0.780	1.672	0.760	1.653	0.783	1.653	0.760
25	1.565	0.755	1.610	0.810	1.564	0.754	1.616	0.810
26	1.522	0.780	1.554	0.775	1.404	0.780	1.557	0.774
27	1.528	0.730	1.530	0.690	1.488	0.732	1.528	0.690
28	1.496	0.795	1.486	0.830	1.445	0.795	1.511	0.820
29	1.425	0.800	1.467	0.870	1.378	0.798	1.442	0.868
30	1.433	0.800	1.465	0.870	1.430	0.797	1.402	0.853

	Participant 3: Treadmill speed 2.2 m/s							
	Qualisys				IMU			
	Right Leg		Left Leg		Right Leg		Left Leg	
	Distance (m)	Period (s)	Distance (m)	Period (s)	Distance(m)	Period(s)	Distance(m)	Period(s)
1	1.515	0.760	1.552	0.730	1.480	0.763	1.397	0.728
2	1.547	0.690	1.552	0.710	1.527	0.691	1.554	0.717
3	1.549	0.740	1.558	0.750	1.533	0.740	1.554	0.746
4	1.613	0.715	1.593	0.700	1.610	0.721	1.583	0.699
5	1.656	0.730	1.628	0.730	1.596	0.724	1.616	0.722
6	1.632	0.770	1.595	0.770	1.634	0.787	1.560	0.764
7	1.530	0.715	1.545	0.725	1.435	0.715	1.534	0.733
8	1.533	0.750	1.540	0.735	1.516	0.748	1.516	0.739
9	1.553	0.705	1.542	0.725	1.553	0.713	1.494	0.724

10	1.535	0.755	1.499	0.720	1.479	0.755	1.496	0.731
11	1.570	0.710	1.524	0.725	1.465	0.709	1.503	0.723
12	1.581	0.700	1.542	0.710	1.573	0.704	1.538	0.713
13	1.654	0.740	1.686	0.755	1.649	0.737	1.639	0.756
14	1.627	0.725	1.628	0.730	1.679	0.732	1.629	0.731
15	1.685	0.725	1.644	0.745	1.682	0.725	1.634	0.741
16	1.634	0.800	1.579	0.735	1.674	0.801	1.575	0.736
17	1.596	0.720	1.621	0.725	1.601	0.720	1.629	0.740
18	1.608	0.695	1.577	0.745	1.580	0.693	1.585	0.747
19	1.643	0.760	1.634	0.690	1.620	0.751	1.620	0.691
20	1.709	0.730	1.691	0.745	1.708	0.730	1.687	0.745
21	1.727	0.745	1.726	0.780	1.747	0.752	1.697	0.759
22	1.695	0.710	1.636	0.715	1.709	0.716	1.643	0.721
23	1.621	0.760	1.607	0.715	1.622	0.759	1.598	0.714
24	1.651	0.715	1.633	0.720	1.651	0.716	1.646	0.721
25	1.654	0.710	1.656	0.780	1.620	0.705	1.665	0.783
26	1.666	0.715	1.646	0.690	1.569	0.715	1.642	0.695
27	1.666	0.780	1.622	0.740	1.637	0.780	1.601	0.737
28	1.631	0.700	1.615	0.725	1.607	0.701	1.611	0.714
29	1.611	0.815	1.635	0.730	1.607	0.814	1.681	0.731
30	1.740	0.815	1.739	0.730	1.735	0.815	1.684	0.725

	Participant 3: Treadmill speed 2.5 m/s							
	Qualisys				IMU			
	Right Leg		Left Leg		Right Leg		Left Leg	
	Distance (m)	Period (s)	Distance (m)	Period (s)	Distance(m)	Period(s)	Distance(m)	Period(s)
1	1.842	0.715	1.864	0.670	1.842	0.715	1.863	0.671
2	1.833	0.670	1.836	0.690	1.833	0.669	1.753	0.689
3	1.775	0.730	1.778	0.710	1.776	0.731	1.778	0.715
4	1.694	0.660	1.702	0.695	1.691	0.658	1.673	0.696
5	1.622	0.705	1.626	0.690	1.618	0.706	1.623	0.690
6	1.607	0.695	1.639	0.680	1.604	0.695	1.636	0.680
7	1.658	0.690	1.622	0.680	1.655	0.689	1.622	0.681
8	1.609	0.650	1.600	0.640	1.608	0.650	1.589	0.640
9	1.582	0.620	1.544	0.655	1.581	0.620	1.544	0.655
10	1.593	0.705	1.543	0.690	1.593	0.705	1.543	0.687
11	1.656	0.675	1.628	0.660	1.656	0.672	1.627	0.659
12	1.643	0.675	1.578	0.675	1.642	0.675	1.586	0.675
13	1.645	0.615	1.577	0.625	1.645	0.616	1.561	0.624
14	1.713	0.685	1.652	0.690	1.722	0.686	1.652	0.690
15	1.751	0.685	1.693	0.665	1.747	0.685	1.660	0.663
16	1.773	0.670	1.708	0.655	1.781	0.671	1.709	0.655
17	1.669	0.605	1.695	0.630	1.666	0.605	1.697	0.630
18	1.630	0.645	1.632	0.660	1.611	0.645	1.631	0.660
19	1.659	0.650	1.646	0.645	1.647	0.650	1.634	0.643
20	1.647	0.645	1.640	0.620	1.639	0.643	1.631	0.613
21	1.629	0.625	1.629	0.635	1.721	0.671	1.630	0.650
22	1.657	0.620	1.627	0.635	1.657	0.625	1.625	0.635
23	1.590	0.635	1.600	0.615	1.596	0.637	1.600	0.616
24	1.609	0.635	1.635	0.625	1.606	0.633	1.634	0.625
25	1.639	0.610	1.590	0.620	1.645	0.615	1.598	0.621
26	1.622	0.615	1.608	0.620	1.621	0.615	1.610	0.622
27	1.657	0.655	1.680	0.675	1.653	0.652	1.674	0.675

28	1.712	0.685	1.716	0.690	1.708	0.685	1.704	0.689
29	1.752	0.800	1.719	0.690	1.739	0.795	1.712	0.690
30	1.721	0.800	1.556	0.690	2.300	0.823	2.106	1.816

Stride No	Participant 4: Treadmill speed 0.6 m/s							
	Qualisys				IMU			
	Right Leg		Left Leg		Right Leg		Left Leg	
	Distance (m)	Period (s)	Distance (m)	Period (s)	Distance(m)	Period(s)	Distance(m)	Period(s)
1	1.625	2.510	1.628	2.485	1.630	2.495	1.627	2.480
2	1.721	2.495	1.681	2.350	1.735	2.612	1.846	2.413
3	1.693	3.435	1.656	3.010	1.745	3.393	1.664	2.959
4	1.599	3.895	1.514	3.680	2.035	3.865	1.619	3.660
5	1.653	3.715	1.592	3.900	1.706	3.732	1.520	3.878
6	1.649	4.485	1.656	4.270	1.748	4.456	1.648	4.083
7	1.654	2.980	1.526	3.310	2.542	2.980	1.548	3.415
8	1.804	2.890	1.586	2.860	1.826	2.894	1.585	2.859
9	1.905	3.430	1.898	3.365	1.931	3.405	1.891	3.341
10	1.697	3.695	1.693	3.335	1.688	3.607	1.646	3.232
11	1.635	2.925	1.782	3.325	1.638	2.944	1.922	3.313
12	1.794	3.065	1.763	3.115	1.916	3.121	1.884	3.085
13	1.806	3.710	1.760	2.990	1.833	3.709	1.763	2.979
14	1.918	2.585	1.764	3.410	2.158	2.723	1.922	3.409
15	1.454	2.960	1.495	2.980	1.455	2.943	1.654	2.981
16	1.556	3.050	1.415	3.110	1.766	3.064	1.345	3.004
17	1.558	2.830	1.539	2.815	1.584	2.828	1.605	2.837
18	1.615	2.620	1.612	2.650	1.642	2.598	1.701	2.683
19	1.706	2.540	1.660	2.820	1.795	2.553	1.671	2.830
20	1.643	2.470	1.592	2.335	1.658	2.447	1.664	2.396
21	1.503	1.875	1.565	1.905	1.638	1.888	1.588	1.945
22	1.670	1.850	1.711	2.430	1.690	1.850	1.890	2.458
23	1.772	3.080	1.806	2.380	1.818	3.029	1.839	2.397
24	1.686	2.450	1.886	2.600	1.685	2.426	1.846	2.545
25	1.863	2.240	1.917	2.365	1.854	2.284	1.907	2.358
26	1.841	2.145	1.897	2.155	2.084	2.164	1.881	2.155
27	1.777	2.410	1.976	2.035	1.673	2.407	1.990	2.068
28	1.457	1.835	1.590	2.170	1.537	1.852	1.653	2.181
29	1.608	2.040	1.596	2.135	1.593	2.037	1.613	2.136
30	1.691	2.040	1.772	1.915	1.658	2.038	1.792	1.922

	Participant 4: Treadmill speed 1.0 m/s							
	Qualisys				IMU			
	Right Leg		Left Leg		Right Leg		Left Leg	
	Distance (m)	Period (s)	Distance (m)	Period (s)	Distance(m)	Period(s)	Distance(m)	Period(s)
1	1.190	1.400	1.123	1.460	1.192	1.400	1.149	1.447
2	1.273	1.050	1.226	0.995	1.297	1.076	1.296	1.033
3	1.276	1.310	1.254	1.265	1.272	1.301	1.220	1.264
4	1.318	1.390	1.303	1.255	1.322	1.384	1.320	1.255
5	1.303	1.235	1.323	1.295	1.266	1.241	1.310	1.296
6	1.262	1.195	1.279	1.225	1.195	1.197	1.251	1.226
7	1.288	1.245	1.258	1.540	1.287	1.246	1.173	1.524
8	1.359	1.450	1.311	1.395	1.305	1.446	1.302	1.387
9	1.082	1.370	1.073	1.040	1.077	1.337	1.056	1.048

10	0.945	1.165	0.955	1.240	0.940	1.166	0.914	1.247
11	1.004	1.150	0.969	1.460	1.003	1.150	1.005	1.462
12	1.105	1.405	1.013	0.980	1.197	1.405	1.014	0.985
13	1.093	1.035	1.090	1.260	1.072	1.042	1.086	1.260
14	1.136	1.350	1.104	1.160	1.018	1.338	1.049	1.172
15	1.250	0.995	1.240	1.385	1.212	1.020	1.222	1.385
16	1.327	1.480	1.300	1.090	1.122	1.466	1.139	1.096
17	1.170	0.950	1.178	1.140	1.063	0.994	1.176	1.144
18	1.204	1.135	1.106	1.400	1.145	1.151	1.091	1.400
19	1.348	1.455	1.244	1.155	1.214	1.448	1.421	1.174
20	1.300	0.940	1.316	1.005	1.267	0.946	1.254	1.039
21	1.364	1.205	1.342	1.255	1.363	1.206	1.212	1.248
22	1.351	1.245	1.338	1.245	1.343	1.236	1.131	1.252
23	1.308	1.220	1.309	1.170	1.293	1.220	1.223	1.195
24	1.362	1.415	1.326	1.190	1.293	1.415	1.319	1.188
25	1.350	1.245	1.371	1.215	1.136	1.244	1.350	1.216
26	1.369	1.270	1.379	1.265	1.173	1.268	1.377	1.259
27	1.341	0.930	1.362	1.180	1.276	0.940	1.250	1.183
28	1.370	1.195	1.340	1.300	1.322	1.203	1.323	1.291
29	1.277	1.575	1.368	1.260	1.149	1.530	1.173	1.249
30	1.260	1.575	1.290	1.260	1.248	1.503	1.284	1.260

	Participant 4: Treadmill speed 1.4 m/s							
	Qualisys				IMU			
	Right Leg		Left Leg		Right Leg		Left Leg	
	Distance (m)	Period (s)	Distance (m)	Period (s)	Distance(m)	Period(s)	Distance(m)	Period(s)
1	1.429	0.950	1.448	0.805	1.468	0.937	1.522	0.822
2	1.421	0.870	1.375	0.925	1.423	0.869	1.524	0.934
3	1.330	0.905	1.326	0.945	1.466	0.907	1.594	0.953
4	1.330	0.855	1.295	0.880	1.683	0.907	1.461	0.878
5	1.353	0.895	1.399	0.835	1.461	0.900	1.462	0.824
6	1.455	0.945	1.451	0.975	1.466	0.942	1.551	0.974
7	1.373	0.920	1.248	0.810	1.495	0.920	1.312	0.810
8	1.210	0.805	1.228	0.890	1.267	0.809	1.436	0.885
9	1.215	0.865	1.208	0.915	1.329	0.833	1.226	0.903
10	1.282	0.885	1.273	0.825	1.342	0.878	1.289	0.823
11	1.321	0.840	1.337	0.850	1.525	0.838	1.337	0.835
12	1.380	0.945	1.370	0.930	1.525	0.931	1.358	0.912
13	1.341	0.965	1.275	0.940	1.453	0.960	1.335	0.936
14	1.237	0.795	1.210	0.860	1.440	0.833	1.222	0.861
15	1.222	0.870	1.239	0.875	1.238	0.838	1.371	0.879
16	1.219	0.830	1.201	0.810	1.351	0.831	1.207	0.807
17	1.172	0.885	1.198	0.935	1.321	0.884	1.279	0.935
18	1.179	0.870	1.191	0.865	1.265	0.870	1.191	0.862
19	1.177	0.840	1.177	0.850	1.229	0.840	1.273	0.853
20	1.135	0.840	1.215	0.870	1.371	0.860	1.382	0.886
21	1.236	0.945	1.268	0.860	1.334	0.945	1.326	0.842
22	1.217	0.865	1.174	0.850	1.221	0.865	1.299	0.857
23	1.152	0.925	1.162	0.890	1.287	0.940	1.222	0.889
24	1.138	0.850	1.152	0.870	1.265	0.851	1.121	0.869
25	1.124	0.880	1.139	0.875	1.138	0.876	1.223	0.873
26	1.119	0.960	1.133	0.885	1.304	0.946	1.236	0.890
27	1.118	0.835	1.120	0.960	1.353	0.853	1.126	0.956

28	1.073	0.840	1.072	0.855	1.075	0.835	1.309	0.906
29	1.100	0.935	1.150	0.910	1.116	0.962	1.158	0.904
30	1.110	0.935	1.012	0.910	1.125	0.935	1.220	0.911

	Participant 4: Treadmill speed 1.8 m/s							
	Qualisys				IMU			
	Right Leg		Left Leg		Right Leg		Left Leg	
	Distance (m)	Period (s)	Distance (m)	Period (s)	Distance(m)	Period(s)	Distance(m)	Period(s)
1	1.246	0.795	1.264	0.790	1.246	0.790	1.264	0.787
2	1.304	0.755	1.298	0.745	1.503	0.764	1.300	0.749
3	1.345	0.755	1.351	0.790	1.407	0.755	1.357	0.790
4	1.351	0.755	1.404	0.750	1.372	0.761	1.446	0.750
5	1.392	0.745	1.406	0.755	1.501	0.745	1.412	0.755
6	1.396	0.845	1.436	0.765	1.507	0.845	1.509	0.765
7	1.393	0.695	1.435	0.755	1.610	0.696	1.442	0.755
8	1.413	0.750	1.475	0.740	1.520	0.750	1.609	0.740
9	1.426	0.735	1.435	0.765	1.595	0.744	1.463	0.765
10	1.440	0.805	1.501	0.770	1.480	0.805	1.501	0.770
11	1.423	0.765	1.454	0.730	1.481	0.762	1.460	0.728
12	1.446	0.720	1.464	0.750	1.475	0.720	1.469	0.751
13	1.464	0.750	1.502	0.745	1.552	0.773	1.507	0.745
14	1.434	0.760	1.517	0.775	1.498	0.760	1.530	0.775
15	1.307	0.825	1.426	0.820	1.341	0.824	1.434	0.821
16	1.242	0.740	1.272	0.760	1.313	0.740	1.269	0.757
17	1.300	0.785	1.311	0.790	1.308	0.785	1.316	0.788
18	1.284	0.765	1.315	0.760	1.305	0.767	1.352	0.759
19	1.291	0.760	1.310	0.735	1.303	0.762	1.325	0.735
20	1.313	0.770	1.329	0.765	1.387	0.768	1.360	0.765
21	1.318	0.750	1.335	0.750	1.404	0.750	1.336	0.750
22	1.357	0.750	1.375	0.775	1.417	0.750	1.381	0.773
23	1.310	0.785	1.361	0.785	1.331	0.785	1.380	0.783
24	1.368	0.740	1.370	0.745	1.370	0.740	1.384	0.744
25	1.375	0.750	1.383	0.730	1.376	0.749	1.393	0.730
26	1.408	0.735	1.404	0.770	1.409	0.735	1.548	0.768
27	1.400	0.790	1.429	0.745	1.511	0.790	1.430	0.743
28	1.410	0.780	1.398	0.780	1.510	0.780	1.418	0.780
29	1.451	0.735	1.450	0.870	1.453	0.735	1.460	0.869
30	1.489	0.735	1.133	0.870	1.590	0.736	1.143	0.870

	Participant 4: Treadmill speed 2.0 m/s							
	Qualisys				IMU			
	Right Leg		Left Leg		Right Leg		Left Leg	
	Distance (m)	Period (s)	Distance (m)	Period (s)	Distance(m)	Period(s)	Distance(m)	Period(s)
1	1.438	0.565	1.499	0.765	1.464	0.569	1.533	0.758
2	1.326	0.705	1.401	0.760	1.357	0.705	1.469	0.760
3	1.288	0.720	1.354	0.725	1.288	0.674	1.415	0.727
4	1.380	0.760	1.439	0.780	1.407	0.754	1.479	0.785
5	1.417	0.750	1.460	0.760	1.870	0.752	1.495	0.751
6	1.408	0.775	1.443	0.745	1.562	0.770	1.497	0.754
7	1.397	0.715	1.430	0.710	1.402	0.717	1.608	0.702
8	1.390	0.715	1.403	0.685	1.691	0.764	1.489	0.686
9	1.459	0.690	1.457	0.755	1.647	0.647	1.547	0.756

10	1.448	0.775	1.453	0.765	1.461	0.757	1.493	0.765
11	1.463	0.740	1.511	0.725	1.485	0.740	1.528	0.726
12	1.464	0.785	1.485	0.770	1.526	0.775	1.824	0.770
13	1.435	0.795	1.501	0.765	1.651	0.802	1.568	0.769
14	1.432	0.680	1.448	0.735	1.647	0.687	1.455	0.730
15	1.503	0.750	1.515	0.725	1.550	0.738	1.559	0.739
16	1.518	0.725	1.567	0.730	1.663	0.738	1.598	0.730
17	1.530	0.745	1.567	0.710	1.556	0.749	1.788	0.710
18	1.541	0.675	1.552	0.690	1.631	0.675	1.820	0.691
19	1.535	0.685	1.569	0.715	1.751	0.700	1.660	0.715
20	1.449	0.765	1.451	0.735	1.483	0.748	1.530	0.724
21	1.431	0.710	1.469	0.760	1.517	0.743	1.728	0.760
22	1.411	0.745	1.481	0.720	1.431	0.745	1.542	0.749
23	1.480	0.735	1.482	0.715	1.474	0.710	1.531	0.713
24	1.465	0.685	1.527	0.695	1.560	0.666	1.656	0.709
25	1.483	0.720	1.507	0.745	1.532	0.719	1.537	0.739
26	1.478	0.735	1.510	0.725	1.600	0.726	1.556	0.722
27	1.462	0.745	1.506	0.710	1.488	0.743	1.594	0.711
28	1.489	0.700	1.520	0.730	1.530	0.700	1.562	0.734
29	1.477	0.740	1.505	0.745	1.619	0.742	1.961	0.747
30	1.495	0.710	1.080	0.745	1.681	0.707	1.286	0.748

	Participant 4: Treadmill speed 2.2 m/s							
	Qualisys				IMU			
	Right Leg		Left Leg		Right Leg		Left Leg	
	Distance (m)	Period (s)	Distance (m)	Period (s)	Distance(m)	Period(s)	Distance(m)	Period(s)
1	1.625	0.730	1.621	0.745	1.679	0.730	1.710	0.744
2	1.558	0.725	1.610	0.705	1.581	0.725	1.669	0.706
3	1.589	0.735	1.623	0.745	1.595	0.734	1.626	0.746
4	1.563	0.725	1.619	0.745	1.578	0.726	1.632	0.746
5	1.620	0.780	1.671	0.725	1.615	0.771	1.672	0.725
6	1.589	0.700	1.611	0.730	1.594	0.700	1.618	0.730
7	1.593	0.685	1.620	0.710	1.593	0.668	1.649	0.710
8	1.665	0.740	1.737	0.730	1.671	0.739	1.861	0.730
9	1.691	0.755	1.718	0.740	1.864	0.749	1.721	0.740
10	1.666	0.740	1.690	0.715	1.755	0.740	1.716	0.717
11	1.689	0.720	1.723	0.720	1.752	0.725	1.765	0.721
12	1.722	0.695	1.746	0.750	1.724	0.687	1.765	0.752
13	1.610	0.750	1.667	0.725	1.612	0.750	1.808	0.722
14	1.634	0.715	1.674	0.735	1.634	0.715	1.764	0.735
15	1.631	0.725	1.672	0.720	1.659	0.725	1.824	0.720
16	1.600	0.765	1.630	0.735	1.926	0.767	1.651	0.735
17	1.541	0.710	1.579	0.710	1.541	0.710	1.604	0.712
18	1.564	0.705	1.585	0.735	1.694	0.705	1.601	0.733
19	1.555	0.745	1.582	0.730	1.573	0.745	1.696	0.730
20	1.583	0.715	1.585	0.730	1.838	0.724	1.585	0.728
21	1.558	0.720	1.591	0.715	1.566	0.720	1.671	0.717
22	1.573	0.725	1.606	0.700	1.626	0.725	1.766	0.701
23	1.595	0.720	1.625	0.760	1.597	0.719	1.662	0.760
24	1.561	0.755	1.628	0.715	1.836	0.755	1.629	0.715
25	1.601	0.715	1.603	0.715	1.612	0.714	1.604	0.715
26	1.569	0.705	1.616	0.715	1.577	0.705	1.649	0.717
27	1.621	0.730	1.656	0.745	1.645	0.731	1.667	0.745

28	1.611	0.745	1.683	0.750	1.611	0.745	1.712	0.750
29	1.598	0.770	1.642	0.855	1.642	0.770	1.655	0.852
30	1.646	0.770	1.028	0.855	1.649	0.770	1.044	0.855

	Participant 4: Treadmill speed 2.5 m/s							
	Qualisys				IMU			
	Right Leg		Left Leg		Right Leg		Left Leg	
	Distance (m)	Period (s)	Distance (m)	Period (s)	Distance(m)	Period(s)	Distance(m)	Period(s)
1	1.428	0.670	1.458	0.685	1.560	0.695	1.401	0.673
2	1.483	0.705	1.461	0.695	1.444	0.705	1.461	0.695
3	1.490	0.685	1.474	0.695	1.760	0.688	1.436	0.687
4	1.546	0.715	1.538	0.705	1.676	0.714	1.537	0.696
5	1.516	0.685	1.503	0.680	1.765	0.684	1.565	0.683
6	1.586	0.690	1.577	0.685	1.770	0.696	1.566	0.655
7	1.599	0.670	1.603	0.680	1.839	0.678	1.699	0.682
8	1.630	0.685	1.620	0.690	1.635	0.685	1.751	0.690
9	1.690	0.685	1.685	0.685	1.907	0.682	1.923	0.684
10	1.655	0.675	1.676	0.685	1.790	0.676	1.769	0.685
11	1.723	0.680	1.715	0.680	1.725	0.681	1.825	0.680
12	1.705	0.685	1.719	0.665	1.706	0.689	1.676	0.665
13	1.824	0.700	1.786	0.660	1.818	0.695	1.603	0.660
14	1.863	0.630	1.855	0.675	1.858	0.633	1.852	0.680
15	1.861	0.685	1.891	0.675	1.861	0.675	1.742	0.670
16	1.839	0.690	1.912	0.700	1.970	0.686	1.904	0.703
17	1.608	0.685	1.757	0.685	1.685	0.685	1.759	0.682
18	1.614	0.680	1.586	0.670	1.646	0.680	1.593	0.671
19	1.655	0.660	1.618	0.665	1.596	0.653	1.620	0.666
20	1.706	0.680	1.690	0.665	1.889	0.682	1.728	0.671
21	1.745	0.650	1.701	0.695	1.629	0.645	1.726	0.693
22	1.726	0.700	1.770	0.675	1.829	0.706	1.829	0.674
23	1.731	0.670	1.725	0.635	1.672	0.662	1.731	0.635
24	1.775	0.655	1.752	0.675	1.826	0.655	1.748	0.677
25	1.829	0.655	1.830	0.660	1.950	0.657	1.830	0.661
26	1.859	0.680	1.861	0.680	1.866	0.679	1.919	0.680
27	1.842	0.695	1.876	0.680	1.957	0.692	2.102	0.680
28	1.800	0.665	1.800	0.705	1.937	0.671	1.900	0.705
29	1.776	0.680	1.795	0.690	1.795	0.661	1.803	0.690
30	1.834	0.680	1.806	0.690	1.912	0.668	1.838	0.689

Stride No	Participant 5: Treadmill speed 0.6 m/s							
	Qualisys				IMU			
	Right Leg		Left Leg		Right Leg		Left Leg	
	Distance (m)	Period (s)	Distance (m)	Period (s)	Distance(m)	Period(s)	Distance(m)	Period(s)
1	0.402	0.825	0.399	0.885	0.414	0.824	0.395	0.885
2	0.417	0.965	0.400	0.890	0.428	0.965	0.387	0.889
3	0.431	0.835	0.416	0.825	0.434	0.836	0.423	0.836
4	0.459	0.830	0.434	0.855	0.458	0.830	0.434	0.855
5	0.466	0.785	0.452	0.860	0.462	0.785	0.402	0.853
6	0.483	0.870	0.470	0.790	0.469	0.868	0.461	0.801
7	0.498	0.865	0.500	0.800	0.497	0.865	0.488	0.798
8	0.496	0.825	0.504	0.885	0.477	0.828	0.496	0.885
9	0.521	0.805	0.527	0.805	0.509	0.810	0.515	0.810

10	0.542	0.850	0.541	0.835	0.527	0.850	0.504	0.835
11	0.557	0.815	0.550	0.845	0.554	0.817	0.544	0.838
12	0.546	0.850	0.555	0.870	0.536	0.850	0.595	0.901
13	0.540	0.840	0.564	0.825	0.536	0.841	0.562	0.801
14	0.546	0.880	0.541	0.870	0.540	0.880	0.513	0.870
15	0.515	0.865	0.534	0.905	0.500	0.865	0.491	0.904
16	0.522	0.910	0.521	0.900	0.518	0.910	0.520	0.907
17	0.521	0.930	0.517	0.940	0.505	0.942	0.516	0.940
18	0.528	0.820	0.521	0.855	0.500	0.811	0.469	0.851
19	0.550	0.930	0.538	0.875	0.544	0.943	0.552	0.895
20	0.561	0.830	0.556	0.920	0.550	0.830	0.541	0.915
21	0.575	0.920	0.551	0.820	0.539	0.920	0.548	0.821
22	0.580	0.805	0.566	0.670	0.574	0.806	0.552	0.670
23	0.562	0.780	0.581	0.945	0.546	0.783	0.580	0.936
24	0.548	0.920	0.542	0.900	0.535	0.920	0.529	0.915
25	0.503	0.880	0.532	0.750	0.496	0.879	0.531	0.757
26	0.483	0.825	0.502	0.950	0.463	0.825	0.481	0.919
27	0.484	0.820	0.502	0.785	0.484	0.825	0.503	0.787
28	0.505	0.830	0.482	0.845	0.504	0.828	0.479	0.843
29	0.513	0.825	0.515	0.865	0.499	0.815	0.505	0.865
30	0.526	0.900	0.506	0.765	0.526	0.903	0.510	0.782

	Participant 5: Treadmill speed 1.0 m/s							
	Qualisys				IMU			
	Right Leg		Left Leg		Right Leg		Left Leg	
	Distance (m)	Period (s)	Distance (m)	Period (s)	Distance(m)	Period(s)	Distance(m)	Period(s)
1	0.656	0.710	0.670	0.665	0.663	0.746	0.637	0.667
2	0.629	0.655	0.648	0.685	0.602	0.654	0.643	0.685
3	0.555	0.650	0.545	0.620	0.528	0.650	0.523	0.618
4	0.579	0.620	0.576	0.685	0.539	0.618	0.563	0.685
5	0.584	0.620	0.604	0.630	0.582	0.622	0.571	0.630
6	0.624	0.635	0.626	0.615	0.544	0.635	0.613	0.619
7	0.642	0.655	0.654	0.640	0.590	0.654	0.578	0.640
8	0.647	0.630	0.654	0.665	0.635	0.633	0.643	0.663
9	0.646	0.645	0.655	0.625	0.645	0.649	0.641	0.626
10	0.644	0.610	0.643	0.615	0.602	0.609	0.602	0.615
11	0.650	0.650	0.664	0.655	0.645	0.650	0.612	0.646
12	0.652	0.650	0.661	0.610	0.651	0.652	0.654	0.612
13	0.653	0.615	0.652	0.660	0.620	0.617	0.618	0.659
14	0.629	0.685	0.633	0.680	0.624	0.679	0.628	0.680
15	0.620	0.675	0.631	0.660	0.615	0.674	0.622	0.648
16	0.623	0.630	0.618	0.615	0.631	0.631	0.615	0.644
17	0.630	0.665	0.635	0.690	0.613	0.665	0.631	0.689
18	0.640	0.665	0.652	0.640	0.624	0.672	0.651	0.645
19	0.644	0.655	0.653	0.675	0.635	0.655	0.622	0.670
20	0.649	0.655	0.661	0.615	0.635	0.653	0.590	0.617
21	0.661	0.645	0.660	0.665	0.641	0.645	0.659	0.664
22	0.669	0.635	0.659	0.605	0.663	0.635	0.647	0.605
23	0.677	0.645	0.665	0.670	0.663	0.645	0.662	0.670
24	0.682	0.615	0.671	0.635	0.649	0.615	0.669	0.635
25	0.670	0.650	0.669	0.625	0.666	0.651	0.668	0.626
26	0.689	0.620	0.676	0.640	0.688	0.620	0.646	0.629
27	0.674	0.625	0.669	0.635	0.652	0.624	0.667	0.636

28	0.674	0.620	0.663	0.615	0.660	0.624	0.663	0.617
29	0.651	0.640	0.658	0.605	0.644	0.637	0.621	0.603
30	0.656	0.625	0.579	0.660	0.617	0.624	0.569	0.658

	Participant 5: Treadmill speed 1.4 m/s							
	Qualisys				IMU			
	Right Leg		Left Leg		Right Leg		Left Leg	
	Distance (m)	Period (s)	Distance (m)	Period (s)	Distance(m)	Period(s)	Distance(m)	Period(s)
1	0.806	0.605	0.771	0.595	0.793	0.605	0.769	0.598
2	0.823	0.565	0.832	0.595	0.803	0.561	0.827	0.594
3	0.835	0.620	0.833	0.590	0.830	0.620	0.802	0.599
4	0.848	0.570	0.849	0.615	0.818	0.571	0.841	0.614
5	0.826	0.640	0.863	0.610	0.820	0.640	0.862	0.611
6	0.835	0.600	0.852	0.595	0.832	0.606	0.808	0.598
7	0.822	0.615	0.854	0.610	0.816	0.613	0.741	0.609
8	0.814	0.595	0.825	0.605	0.810	0.597	0.812	0.606
9	0.806	0.605	0.827	0.605	0.804	0.605	0.782	0.619
10	0.794	0.600	0.814	0.615	0.782	0.602	0.814	0.606
11	0.785	0.620	0.797	0.585	0.765	0.617	0.769	0.588
12	0.788	0.600	0.813	0.625	0.736	0.602	0.751	0.622
13	0.782	0.595	0.786	0.600	0.780	0.593	0.773	0.600
14	0.795	0.625	0.796	0.615	0.757	0.622	0.792	0.621
15	0.849	0.600	0.842	0.630	0.841	0.604	0.808	0.643
16	0.888	0.585	0.887	0.570	0.877	0.585	0.844	0.570
17	0.877	0.645	0.897	0.600	0.834	0.644	0.836	0.600
18	0.858	0.585	0.866	0.645	0.857	0.585	0.815	0.646
19	0.859	0.625	0.875	0.610	0.858	0.625	0.743	0.610
20	0.878	0.605	0.876	0.600	0.853	0.610	0.833	0.600
21	0.869	0.610	0.873	0.620	0.863	0.609	0.851	0.614
22	0.871	0.615	0.869	0.565	0.872	0.616	0.819	0.573
23	0.861	0.580	0.856	0.580	0.838	0.579	0.807	0.579
24	0.862	0.570	0.849	0.565	0.827	0.570	0.841	0.565
25	0.853	0.580	0.845	0.620	0.802	0.578	0.807	0.617
26	0.853	0.595	0.837	0.600	0.800	0.598	0.820	0.604
27	0.865	0.615	0.847	0.550	0.832	0.624	0.814	0.558
28	0.850	0.580	0.858	0.585	0.826	0.580	0.829	0.583
29	0.876	0.580	0.858	0.620	0.866	0.579	0.826	0.619
30	0.889	0.580	0.816	0.620	0.881	0.561	0.742	0.616

	Participant 5: Treadmill speed 1.8 m/s							
	Qualisys				IMU			
	Right Leg		Left Leg		Right Leg		Left Leg	
	Distance (m)	Period (s)	Distance (m)	Period (s)	Distance(m)	Period(s)	Distance(m)	Period(s)
1	0.982	0.570	0.939	0.540	0.989	0.581	0.906	0.541
2	0.978	0.540	0.959	0.550	0.978	0.542	0.793	0.550
3	0.945	0.570	0.949	0.565	0.897	0.573	0.828	0.566
4	0.946	0.550	0.956	0.545	0.849	0.547	0.929	0.543
5	0.920	0.520	0.926	0.530	0.919	0.524	0.904	0.533
6	0.841	0.545	0.822	0.560	0.855	0.543	0.790	0.559
7	0.788	0.560	0.722	0.515	0.770	0.555	0.706	0.514
8	0.846	0.555	0.837	0.565	0.842	0.556	0.834	0.566
9	0.859	0.575	0.878	0.565	0.836	0.583	0.818	0.573

10	0.886	0.565	0.877	0.550	0.880	0.565	0.858	0.550
11	0.945	0.560	0.930	0.585	0.862	0.560	0.903	0.585
12	0.999	0.545	0.983	0.570	0.952	0.552	0.882	0.574
13	1.041	0.560	1.032	0.510	0.918	0.559	0.994	0.509
14	1.075	0.570	1.060	0.600	1.074	0.570	0.959	0.597
15	1.083	0.565	1.074	0.575	1.071	0.565	1.044	0.578
16	1.061	0.545	1.048	0.565	1.057	0.547	1.018	0.567
17	1.041	0.555	1.047	0.530	1.030	0.554	1.025	0.529
18	1.065	0.600	1.076	0.550	1.037	0.600	0.959	0.550
19	1.089	0.560	1.100	0.595	1.078	0.567	1.099	0.597
20	1.099	0.570	1.141	0.570	1.047	0.570	1.111	0.578
21	1.108	0.570	1.100	0.590	1.082	0.565	1.068	0.589
22	1.092	0.535	1.082	0.560	1.050	0.547	1.010	0.570
23	1.091	0.580	1.087	0.540	1.042	0.580	0.909	0.540
24	1.095	0.560	1.082	0.540	1.049	0.562	1.067	0.541
25	1.075	0.565	1.090	0.565	1.070	0.560	1.084	0.563
26	1.061	0.575	1.075	0.570	0.995	0.576	1.034	0.579
27	1.050	0.560	1.070	0.605	1.023	0.561	1.042	0.595
28	1.075	0.560	1.095	0.565	1.067	0.559	0.964	0.566
29	1.078	0.570	1.095	0.550	1.076	0.571	1.094	0.553
30	1.082	0.570	1.064	0.550	1.036	0.574	1.007	0.556

	Participant 5: Treadmill speed 2.0 m/s							
	Qualisys				IMU			
	Right Leg		Left Leg		Right Leg		Left Leg	
	Distance (m)	Period (s)	Distance (m)	Period (s)	Distance(m)	Period(s)	Distance(m)	Period(s)
1	1.273	0.550	1.295	0.560	1.217	0.551	1.274	0.561
2	1.250	0.565	1.277	0.590	1.149	0.568	1.267	0.590
3	1.255	0.550	1.269	0.515	1.239	0.546	1.087	0.515
4	1.200	0.570	1.237	0.605	1.189	0.570	1.236	0.603
5	1.183	0.535	1.221	0.530	1.183	0.536	1.209	0.531
6	1.109	0.550	1.102	0.525	1.129	0.554	1.097	0.530
7	1.031	0.525	1.070	0.535	1.009	0.525	1.058	0.535
8	1.038	0.550	1.058	0.560	1.058	0.554	0.993	0.552
9	1.027	0.575	1.071	0.560	1.007	0.574	1.027	0.564
10	1.015	0.540	1.035	0.570	1.015	0.541	1.012	0.571
11	0.948	0.590	0.992	0.565	0.986	0.590	0.989	0.567
12	0.946	0.555	0.945	0.575	0.945	0.553	0.939	0.572
13	0.877	0.570	0.897	0.565	0.884	0.570	0.892	0.564
14	0.954	0.560	0.976	0.555	0.904	0.560	0.948	0.557
15	1.053	0.555	1.075	0.545	1.052	0.555	1.073	0.546
16	1.112	0.555	1.123	0.570	1.105	0.555	1.103	0.564
17	1.091	0.550	1.145	0.560	1.089	0.551	1.144	0.561
18	1.083	0.605	1.113	0.565	1.099	0.604	1.113	0.565
19	1.120	0.515	1.142	0.540	1.105	0.516	1.138	0.541
20	1.146	0.565	1.159	0.535	1.146	0.565	1.120	0.541
21	1.151	0.545	1.174	0.565	1.136	0.542	1.121	0.552
22	1.144	0.560	1.192	0.560	1.104	0.560	1.177	0.560
23	1.157	0.580	1.195	0.575	1.239	0.581	1.202	0.579
24	1.174	0.545	1.205	0.570	1.149	0.546	1.184	0.569
25	1.175	0.580	1.205	0.570	1.172	0.580	1.101	0.571
26	1.195	0.565	1.226	0.575	1.180	0.567	1.096	0.575
27	1.143	0.570	1.197	0.565	1.142	0.570	1.153	0.569

28	1.158	0.585	1.210	0.565	1.156	0.585	1.192	0.562
29	1.207	0.535	1.260	0.685	1.151	0.527	1.231	0.653
30	1.252	0.535	1.023	0.685	1.086	0.533	0.959	0.680

	Participant 5: Treadmill speed 2.2 m/s							
	Qualisys				IMU			
	Right Leg		Left Leg		Right Leg		Left Leg	
	Distance (m)	Period (s)	Distance (m)	Period (s)	Distance(m)	Period(s)	Distance(m)	Period(s)
1	1.096	0.535	1.164	0.530	1.094	0.537	1.164	0.540
2	1.135	0.550	1.174	0.575	1.092	0.551	1.087	0.575
3	1.116	0.550	1.172	0.550	1.101	0.553	1.164	0.553
4	1.163	0.560	1.219	0.575	1.144	0.559	1.201	0.575
5	1.240	0.530	1.274	0.550	1.174	0.533	1.253	0.545
6	1.261	0.570	1.284	0.555	1.256	0.571	1.167	0.556
7	1.254	0.540	1.286	0.530	1.254	0.541	1.225	0.532
8	1.223	0.585	1.250	0.600	1.147	0.576	1.251	0.600
9	1.192	0.520	1.255	0.495	1.189	0.524	1.219	0.496
10	1.197	0.580	1.200	0.560	1.111	0.579	1.164	0.561
11	1.187	0.510	1.224	0.540	1.174	0.511	1.176	0.540
12	1.205	0.550	1.212	0.555	1.203	0.552	1.208	0.554
13	1.165	0.570	1.237	0.555	1.195	0.571	1.151	0.547
14	1.197	0.570	1.276	0.570	1.156	0.566	1.284	0.579
15	1.259	0.570	1.329	0.560	1.199	0.571	1.329	0.560
16	1.262	0.540	1.297	0.540	1.116	0.541	1.247	0.542
17	1.274	0.580	1.311	0.625	1.231	0.580	1.292	0.624
18	1.282	0.545	1.324	0.515	1.208	0.550	1.320	0.521
19	1.267	0.565	1.281	0.555	1.157	0.567	1.227	0.557
20	1.244	0.565	1.281	0.580	1.240	0.565	1.235	0.580
21	1.251	0.555	1.271	0.565	1.144	0.559	1.241	0.564
22	1.247	0.560	1.242	0.525	1.239	0.557	1.172	0.527
23	1.241	0.555	1.235	0.575	1.188	0.557	1.055	0.567
24	1.277	0.580	1.260	0.570	1.185	0.579	1.240	0.570
25	1.250	0.550	1.264	0.560	1.179	0.550	1.232	0.555
26	1.282	0.560	1.265	0.570	1.279	0.561	1.263	0.574
27	1.237	0.580	1.279	0.560	1.143	0.580	1.278	0.562
28	1.240	0.550	1.249	0.560	1.240	0.550	1.240	0.557
29	1.247	0.560	1.249	0.680	1.182	0.558	1.248	0.671
30	1.247	0.560	0.959	0.680	1.134	0.522	0.950	0.678

	Participant 5: Treadmill speed 2.5 m/s							
	Qualisys				IMU			
	Right Leg		Left Leg		Right Leg		Left Leg	
	Distance (m)	Period (s)	Distance (m)	Period (s)	Distance(m)	Period(s)	Distance(m)	Period(s)
1	1.379	0.545	1.414	0.560	1.378	0.554	1.399	0.573
2	1.366	0.530	1.418	0.505	1.325	0.533	1.407	0.506
3	1.322	0.565	1.392	0.550	1.322	0.562	1.362	0.595
4	1.334	0.530	1.356	0.555	1.325	0.532	1.356	0.556
5	1.291	0.525	1.352	0.515	1.269	0.529	1.361	0.545
6	1.278	0.540	1.324	0.530	1.266	0.540	1.310	0.531
7	1.262	0.550	1.345	0.570	1.215	0.550	1.232	0.571
8	1.267	0.520	1.330	0.525	1.242	0.523	1.329	0.526
9	1.252	0.550	1.324	0.520	1.242	0.550	1.320	0.520

10	1.285	0.525	1.320	0.555	1.256	0.525	1.306	0.556
11	1.274	0.580	1.353	0.555	1.161	0.580	1.344	0.555
12	1.291	0.555	1.338	0.535	1.271	0.567	1.286	0.529
13	1.279	0.505	1.340	0.565	1.210	0.494	1.335	0.570
14	1.230	0.530	1.316	0.500	1.230	0.532	1.284	0.499
15	1.239	0.540	1.273	0.540	1.191	0.536	1.249	0.542
16	1.285	0.565	1.283	0.560	1.281	0.565	1.262	0.558
17	1.317	0.535	1.330	0.550	1.248	0.531	1.309	0.553
18	1.343	0.535	1.387	0.545	1.264	0.535	1.384	0.543
19	1.376	0.565	1.404	0.535	1.358	0.565	1.393	0.534
20	1.395	0.540	1.433	0.550	1.313	0.540	1.400	0.551
21	1.400	0.530	1.448	0.540	1.308	0.533	1.439	0.546
22	1.413	0.565	1.477	0.545	1.407	0.563	1.301	0.544
23	1.405	0.535	1.468	0.550	1.387	0.536	1.459	0.545
24	1.419	0.535	1.473	0.535	1.410	0.533	1.457	0.536
25	1.406	0.550	1.455	0.540	1.377	0.550	1.358	0.539
26	1.416	0.540	1.425	0.535	1.412	0.540	1.377	0.535
27	1.419	0.550	1.462	0.550	1.364	0.548	1.394	0.550
28	1.404	0.525	1.448	0.545	1.395	0.526	1.428	0.545
29	1.371	0.425	1.418	0.650	1.309	0.431	1.413	0.616
30	1.319	0.425	1.056	0.650	1.147	0.437	1.055	0.589

Stride No	Participant 6: Treadmill speed 0.6 m/s							
	Qualisys				IMU			
	Right Leg		Left Leg		Right Leg		Left Leg	
	Distance (m)	Period (s)	Distance (m)	Period (s)	Distance(m)	Period(s)	Distance(m)	Period(s)
1	0.388	0.940	0.377	0.900	0.387	0.942	0.374	0.888
2	0.376	0.940	0.366	0.980	0.367	0.937	0.376	0.986
3	0.364	0.840	0.353	0.880	0.361	0.838	0.356	0.895
4	0.362	0.955	0.407	0.880	0.370	0.952	0.362	0.870
5	0.492	0.825	0.556	0.865	0.496	0.836	0.559	0.869
6	0.583	0.790	0.646	0.760	0.582	0.789	0.644	0.759
7	0.617	0.800	0.650	0.835	0.616	0.802	0.635	0.850
8	0.647	0.845	0.657	0.825	0.656	0.846	0.656	0.828
9	0.635	0.840	0.634	0.830	0.624	0.803	0.588	0.821
10	0.632	0.835	0.608	0.850	0.629	0.836	0.547	0.835
11	0.605	0.855	0.571	0.830	0.530	0.854	0.570	0.832
12	0.578	0.870	0.552	0.855	0.575	0.887	0.491	0.873
13	0.550	0.860	0.542	0.845	0.545	0.856	0.532	0.844
14	0.543	0.865	0.537	0.875	0.542	0.865	0.498	0.885
15	0.536	0.875	0.540	0.885	0.535	0.884	0.539	0.885
16	0.537	0.880	0.541	0.855	0.522	0.863	0.508	0.837
17	0.534	0.865	0.535	0.870	0.526	0.866	0.537	0.880
18	0.540	0.820	0.527	0.855	0.518	0.820	0.484	0.857
19	0.531	0.840	0.523	0.860	0.529	0.852	0.506	0.860
20	0.522	0.825	0.533	0.820	0.488	0.828	0.525	0.827
21	0.522	0.830	0.525	0.840	0.518	0.830	0.488	0.837
22	0.518	0.835	0.516	0.795	0.516	0.838	0.485	0.795
23	0.512	0.845	0.506	0.865	0.502	0.845	0.488	0.860
24	0.502	0.825	0.491	0.840	0.471	0.827	0.487	0.841
25	0.490	0.885	0.478	0.860	0.472	0.882	0.429	0.854
26	0.469	0.815	0.465	0.840	0.460	0.833	0.459	0.852

27	0.452	0.865	0.457	0.850	0.417	0.868	0.413	0.855
28	0.438	0.840	0.442	0.860	0.433	0.826	0.382	0.841
29	0.421	0.810	0.436	0.840	0.411	0.820	0.410	0.844
30	0.418	0.810	0.383	0.840	0.413	0.812	0.372	0.844

	Participant 6: Treadmill speed 1.0 m/s							
	Qualisys				IMU			
	Right Leg		Left Leg		Right Leg		Left Leg	
	Distance (m)	Period (s)	Distance (m)	Period (s)	Distance(m)	Period(s)	Distance(m)	Period(s)
1	1.799	1.455	1.636	1.465	1.770	1.437	1.672	1.467
2	1.682	1.865	1.653	1.565	1.681	1.798	1.729	1.555
3	1.676	1.140	1.658	1.500	1.640	1.144	1.648	1.500
4	1.565	1.460	1.564	1.600	1.598	1.474	1.569	1.595
5	1.551	1.995	1.612	1.430	1.546	1.961	1.597	1.431
6	1.481	1.135	1.591	1.425	1.454	1.169	1.557	1.426
7	1.464	1.395	1.555	1.640	1.482	1.416	1.555	1.682
8	1.602	1.620	1.546	1.520	1.586	1.619	1.535	1.491
9	1.477	2.085	1.540	1.635	1.561	2.027	1.532	1.635
10	1.528	1.125	1.607	1.460	1.948	1.144	1.605	1.466
11	1.518	2.170	1.497	1.655	1.534	2.133	1.474	1.658
12	1.524	1.645	1.495	1.665	1.525	1.645	1.465	1.663
13	1.445	1.585	1.427	1.625	1.450	1.589	1.440	1.625
14	1.397	1.590	1.392	1.740	1.397	1.591	1.399	1.728
15	1.395	1.135	1.386	1.480	1.372	1.176	1.421	1.487
16	1.402	1.545	1.337	1.610	1.415	1.551	1.476	1.614
17	1.382	1.585	1.379	1.585	1.421	1.574	1.369	1.585
18	1.242	1.510	1.303	1.620	1.436	1.511	1.353	1.621
19	1.345	1.985	1.434	1.395	1.326	1.971	1.428	1.400
20	1.421	1.440	1.502	1.510	1.406	1.441	1.537	1.510
21	1.330	1.245	1.400	1.525	1.279	1.301	1.349	1.523
22	1.391	1.250	1.404	1.375	1.383	1.257	1.368	1.375
23	1.333	1.305	1.412	1.475	1.359	1.306	1.403	1.476
24	1.422	1.775	1.501	1.350	1.425	1.735	1.463	1.350
25	1.467	1.415	1.551	1.375	1.437	1.416	1.428	1.379
26	1.465	1.250	1.606	1.410	1.451	1.280	1.587	1.410
27	1.534	1.275	1.555	1.270	1.525	1.287	1.467	1.270
28	1.520	1.205	1.480	1.330	1.520	1.211	1.494	1.329
29	1.551	1.160	1.650	1.295	1.545	1.162	1.635	1.289
30	1.602	1.160	1.158	1.295	1.525	1.161	1.170	1.282

	Participant 6: Treadmill speed 1.4 m/s							
	Qualisys				IMU			
	Right Leg		Left Leg		Right Leg		Left Leg	
	Distance (m)	Period (s)	Distance (m)	Period (s)	Distance(m)	Period(s)	Distance(m)	Period(s)
1	1.190	0.835	1.152	0.875	1.184	0.836	1.147	0.876
2	1.198	0.850	1.214	0.810	1.197	0.850	1.166	0.816
3	1.174	0.800	1.196	0.795	1.186	0.802	1.157	0.798
4	1.171	0.775	1.204	0.855	1.162	0.779	1.196	0.855
5	1.185	0.825	1.195	0.770	1.156	0.824	1.139	0.771
6	1.134	0.835	1.185	0.860	1.126	0.835	1.072	0.860
7	1.180	0.845	1.140	0.830	1.167	0.845	1.064	0.830
8	1.129	0.825	1.179	0.840	1.128	0.825	1.159	0.822

9	1.147	0.840	1.197	0.870	1.135	0.844	1.254	0.890
10	1.134	0.830	1.145	0.795	1.132	0.830	1.145	0.797
11	1.143	0.805	1.174	0.805	1.134	0.806	1.115	0.809
12	1.118	0.810	1.151	0.795	1.123	0.813	1.145	0.799
13	1.156	0.795	1.158	0.770	1.038	0.792	1.115	0.770
14	1.162	0.775	1.146	0.795	1.156	0.776	1.127	0.795
15	1.068	0.840	1.096	0.825	1.110	0.840	1.095	0.830
16	1.113	0.790	1.121	0.810	1.106	0.786	1.106	0.806
17	1.152	0.800	1.121	0.795	1.087	0.800	1.113	0.798
18	1.101	0.805	1.119	0.795	1.092	0.807	1.109	0.795
19	1.103	0.795	1.102	0.815	1.101	0.786	1.015	0.803
20	1.124	0.810	1.101	0.825	1.119	0.819	1.058	0.847
21	1.150	0.845	1.135	0.825	1.158	0.848	1.126	0.827
22	1.083	0.775	1.097	0.790	1.052	0.775	1.075	0.789
23	1.102	0.810	1.110	0.800	1.090	0.810	1.092	0.800
24	1.086	0.805	1.125	0.820	1.069	0.802	1.128	0.820
25	1.129	0.820	1.127	0.755	1.108	0.823	1.095	0.755
26	1.125	0.775	1.136	0.795	1.124	0.787	1.135	0.803
27	1.028	0.785	1.122	0.780	1.054	0.785	1.043	0.781
28	1.092	0.785	1.150	0.765	1.037	0.785	1.146	0.765
29	1.102	0.765	1.146	0.815	1.030	0.739	1.123	0.787
30	1.131	0.765	0.769	0.815	1.123	0.746	0.606	0.812

	Participant 6: Treadmill speed 1.8 m/s							
	Qualisys				IMU			
	Right Leg		Left Leg		Right Leg		Left Leg	
	Distance (m)	Period (s)	Distance (m)	Period (s)	Distance(m)	Period(s)	Distance(m)	Period(s)
1	1.205	0.700	1.220	0.690	1.169	0.692	1.225	0.692
2	1.181	0.705	1.226	0.665	1.179	0.748	1.182	0.671
3	1.197	0.690	1.200	0.715	1.163	0.669	1.136	0.705
4	1.219	0.680	1.242	0.690	1.141	0.682	1.198	0.714
5	1.226	0.675	1.264	0.670	1.199	0.676	1.248	0.671
6	1.206	0.685	1.256	0.670	1.172	0.683	1.255	0.669
7	1.266	0.705	1.299	0.685	1.201	0.707	1.291	0.686
8	1.282	0.650	1.307	0.660	1.257	0.643	1.295	0.657
9	1.260	0.660	1.315	0.655	1.222	0.661	1.305	0.655
10	1.240	0.695	1.332	0.690	1.186	0.713	1.356	0.717
11	1.272	0.660	1.290	0.650	1.270	0.663	1.285	0.651
12	1.256	0.680	1.288	0.660	1.209	0.682	1.284	0.661
13	1.226	0.630	1.324	0.680	1.057	0.630	1.221	0.641
14	1.264	0.670	1.323	0.670	1.211	0.667	1.454	0.689
15	1.240	0.695	1.292	0.645	1.056	0.659	1.233	0.646
16	1.218	0.640	1.235	0.700	1.149	0.642	1.183	0.686
17	1.202	0.685	1.221	0.675	1.173	0.638	1.008	0.674
18	1.217	0.670	1.205	0.650	1.216	0.666	1.168	0.667
19	1.174	0.685	1.188	0.720	1.173	0.685	1.086	0.720
20	1.189	0.675	1.183	0.670	1.184	0.676	1.181	0.669
21	1.236	0.680	1.194	0.685	1.176	0.678	1.186	0.683
22	1.170	0.690	1.208	0.665	1.055	0.685	1.184	0.665
23	1.222	0.670	1.221	0.690	1.157	0.657	1.217	0.681
24	1.217	0.675	1.227	0.670	1.196	0.673	1.126	0.668
25	1.228	0.655	1.229	0.645	1.184	0.672	1.228	0.658
26	1.177	0.670	1.225	0.665	1.175	0.686	1.149	0.655

27	1.207	0.650	1.224	0.670	1.082	0.642	1.165	0.668
28	1.144	0.660	1.193	0.655	1.058	0.651	1.173	0.658
29	1.194	0.675	1.179	0.805	1.193	0.672	1.001	0.771
30	1.099	0.675	0.735	0.805	1.009	0.672	0.711	0.792

	Participant 6: Treadmill speed 2.0 m/s							
	Qualisys				IMU			
	Right Leg		Left Leg		Right Leg		Left Leg	
	Distance (m)	Period (s)	Distance (m)	Period (s)	Distance(m)	Period(s)	Distance(m)	Period(s)
1	1.235	0.635	1.230	0.640	1.238	0.636	1.222	0.632
2	1.255	0.660	1.265	0.670	1.194	0.660	1.264	0.667
3	1.277	0.650	1.298	0.635	1.271	0.651	1.268	0.646
4	1.307	0.650	1.307	0.635	1.257	0.652	1.200	0.639
5	1.273	0.655	1.268	0.675	1.239	0.660	1.262	0.697
6	1.275	0.670	1.292	0.650	1.255	0.649	1.164	0.649
7	1.305	0.605	1.289	0.645	1.238	0.605	1.273	0.644
8	1.303	0.635	1.297	0.635	1.247	0.634	1.272	0.630
9	1.285	0.645	1.337	0.605	1.285	0.641	1.336	0.607
10	1.306	0.635	1.340	0.645	1.305	0.641	1.164	0.647
11	1.286	0.615	1.332	0.625	1.270	0.615	1.324	0.614
12	1.296	0.635	1.332	0.645	1.283	0.635	1.324	0.646
13	1.240	0.640	1.249	0.605	1.202	0.640	1.057	0.608
14	1.269	0.650	1.242	0.645	1.149	0.650	1.129	0.645
15	1.293	0.605	1.270	0.655	1.242	0.606	1.245	0.661
16	1.288	0.620	1.321	0.600	1.249	0.621	1.262	0.601
17	1.316	0.650	1.282	0.645	1.222	0.650	1.257	0.644
18	1.308	0.615	1.342	0.630	1.158	0.619	1.337	0.628
19	1.334	0.655	1.336	0.645	1.308	0.657	1.293	0.647
20	1.285	0.630	1.334	0.630	1.249	0.624	1.231	0.626
21	1.243	0.650	1.212	0.640	1.008	0.650	1.189	0.640
22	1.261	0.640	1.217	0.635	1.206	0.640	1.109	0.646
23	1.245	0.635	1.233	0.640	1.245	0.638	1.222	0.643
24	1.253	0.615	1.243	0.635	1.230	0.619	1.189	0.635
25	1.225	0.635	1.186	0.615	1.198	0.633	1.178	0.616
26	1.240	0.630	1.223	0.645	1.206	0.631	1.142	0.645
27	1.248	0.635	1.219	0.625	1.110	0.633	1.129	0.624
28	1.269	0.635	1.315	0.645	1.211	0.634	1.297	0.645
29	1.236	0.630	1.274	0.615	1.140	0.626	1.188	0.615
30	1.232	0.630	1.114	0.640	1.207	0.609	1.075	0.627

	Participant 6: Treadmill speed 2.2 m/s							
	Qualisys				IMU			
	Right Leg		Left Leg		Right Leg		Left Leg	
	Distance (m)	Period (s)	Distance (m)	Period (s)	Distance(m)	Period(s)	Distance(m)	Period(s)
1	1.298	0.715	1.304	0.650	1.246	0.715	1.291	0.651
2	1.345	0.680	1.341	0.630	1.327	0.679	1.269	0.629
3	1.429	0.635	1.392	0.665	1.372	0.636	1.366	0.669
4	1.417	0.650	1.430	0.650	1.406	0.648	1.422	0.657
5	1.415	0.610	1.388	0.610	1.369	0.612	1.243	0.609
6	1.438	0.650	1.438	0.645	1.248	0.650	1.426	0.646
7	1.454	0.620	1.437	0.610	1.448	0.623	1.394	0.618
8	1.410	0.610	1.428	0.640	1.299	0.610	1.410	0.640

9	1.382	0.635	1.434	0.630	1.357	0.646	1.384	0.634
10	1.370	0.655	1.428	0.650	1.329	0.650	1.352	0.650
11	1.377	0.630	1.426	0.635	1.361	0.630	1.418	0.629
12	1.379	0.640	1.416	0.615	1.305	0.640	1.411	0.629
13	1.413	0.610	1.418	0.645	1.325	0.610	1.349	0.641
14	1.386	0.660	1.452	0.665	1.385	0.664	1.204	0.663
15	1.364	0.620	1.426	0.610	1.255	0.620	1.403	0.607
16	1.333	0.635	1.385	0.635	1.322	0.635	1.356	0.631
17	1.323	0.640	1.376	0.620	1.288	0.640	1.374	0.620
18	1.319	0.625	1.391	0.605	1.281	0.625	1.381	0.609
19	1.397	0.640	1.368	0.660	1.369	0.616	1.329	0.660
20	1.411	0.625	1.467	0.620	1.322	0.618	1.440	0.625
21	1.385	0.635	1.457	0.615	1.385	0.659	1.427	0.614
22	1.413	0.615	1.430	0.640	1.362	0.595	1.354	0.640
23	1.481	0.630	1.499	0.630	1.290	0.637	1.469	0.632
24	1.495	0.610	1.507	0.610	1.403	0.617	1.502	0.609
25	1.442	0.630	1.480	0.625	1.164	0.629	1.338	0.634
26	1.373	0.620	1.401	0.625	1.345	0.620	1.348	0.625
27	1.380	0.625	1.365	0.620	1.360	0.625	1.365	0.623
28	1.399	0.615	1.401	0.605	1.297	0.615	1.348	0.602
29	1.372	0.615	1.350	0.625	1.305	0.609	1.277	0.630
30	1.421	0.625	0.831	0.740	1.378	0.602	0.816	0.738

	Participant 6: Treadmill speed 2.5 m/s							
	Qualisys				IMU			
	Right Leg		Left Leg		Right Leg		Left Leg	
	Distance (m)	Period (s)	Distance (m)	Period (s)	Distance(m)	Period(s)	Distance(m)	Period(s)
1	1.459	0.605	1.469	0.550	1.415	0.605	1.348	0.554
2	1.456	0.615	1.482	0.610	1.450	0.618	1.461	0.612
3	1.470	0.620	1.504	0.595	1.384	0.618	1.482	0.595
4	1.511	0.600	1.553	0.635	1.452	0.600	1.467	0.637
5	1.511	0.610	1.526	0.575	1.409	0.610	1.500	0.576
6	1.510	0.615	1.503	0.645	1.468	0.616	1.411	0.644
7	1.478	0.615	1.494	0.625	1.230	0.610	1.472	0.625
8	1.490	0.610	1.510	0.590	1.449	0.611	1.426	0.596
9	1.517	0.630	1.531	0.620	1.497	0.630	1.386	0.619
10	1.498	0.620	1.520	0.620	1.412	0.619	1.511	0.619
11	1.558	0.600	1.549	0.625	1.543	0.612	1.540	0.631
12	1.517	0.650	1.521	0.625	1.505	0.640	1.499	0.624
13	1.540	0.610	1.553	0.595	1.424	0.622	1.495	0.595
14	1.517	0.610	1.537	0.645	1.257	0.609	1.527	0.644
15	1.531	0.625	1.586	0.615	1.419	0.625	1.542	0.616
16	1.542	0.630	1.523	0.630	1.373	0.634	1.517	0.630
17	1.521	0.590	1.547	0.595	1.518	0.590	1.411	0.595
18	1.594	0.625	1.579	0.630	1.583	0.622	1.342	0.629
19	1.575	0.620	1.584	0.605	1.512	0.620	1.577	0.606
20	1.570	0.615	1.559	0.620	1.569	0.615	1.499	0.620
21	1.589	0.655	1.585	0.630	1.536	0.655	1.534	0.630
22	1.584	0.625	1.629	0.635	1.489	0.624	1.625	0.632
23	1.642	0.615	1.681	0.620	1.461	0.615	1.683	0.622
24	1.649	0.605	1.658	0.635	1.643	0.605	1.656	0.635
25	1.531	0.630	1.610	0.605	1.527	0.630	1.582	0.605
26	1.571	0.615	1.615	0.625	1.416	0.617	1.514	0.625

27	1.558	0.645	1.585	0.635	1.548	0.645	1.584	0.632
28	1.582	0.625	1.642	0.640	1.471	0.626	1.641	0.640
29	1.635	0.610	1.642	0.590	1.591	0.609	1.562	0.588
30	1.681	0.610	1.096	0.680	1.626	0.607	1.081	0.672

Stride No	Participant 7: Treadmill speed 0.6 m/s							
	Qualisys				IMU			
	Right Leg		Left Leg		Right Leg		Left Leg	
	Distance (m)	Period (s)	Distance (m)	Period (s)	Distance(m)	Period(s)	Distance(m)	Period(s)
1	2.623	3.135	2.444	2.775	2.391	3.111	2.430	2.677
2	1.695	2.710	1.710	4.055	1.737	2.694	2.007	3.942
3	1.806	3.160	1.755	1.830	1.724	3.133	1.768	1.840
4	1.740	3.290	1.594	4.000	1.750	3.154	1.592	3.987
5	1.423	2.315	1.864	2.455	1.447	2.284	1.826	2.473
6	1.821	2.650	2.227	2.765	2.262	2.662	2.296	2.827
7	2.134	2.755	2.146	2.760	2.151	2.755	2.028	2.760
8	1.795	2.755	1.769	1.960	2.206	2.769	1.773	2.025
9	1.677	2.470	1.652	1.865	1.692	2.476	2.456	1.926
10	1.659	3.010	1.264	1.845	1.659	3.000	1.272	1.859
11	1.325	2.195	1.058	2.840	1.446	2.195	1.061	2.831
12	1.233	2.770	1.420	2.260	2.469	2.770	1.419	2.272
13	1.352	2.620	1.102	2.520	1.705	2.620	1.105	2.525
14	0.908	2.270	0.938	2.865	1.071	2.273	0.943	2.864
15	0.949	2.615	1.625	3.545	0.978	2.601	1.676	3.525
16	1.449	3.205	1.503	3.630	1.486	3.205	1.493	3.433
17	1.535	2.155	1.847	2.395	1.638	2.176	1.801	2.409
18	1.606	1.790	2.010	2.555	1.701	1.833	1.982	2.513
19	1.712	2.645	2.074	2.685	1.975	2.579	1.998	2.686
20	1.575	3.665	1.578	2.400	1.723	3.635	1.653	2.419
21	1.423	2.180	1.677	2.305	1.444	2.209	1.631	2.300
22	1.411	1.875	1.547	2.530	1.508	1.910	1.556	2.590
23	1.580	3.290	1.682	2.495	1.648	3.271	1.614	2.461
24	1.614	1.930	1.570	2.350	1.889	1.962	1.558	2.336
25	1.325	3.055	1.194	2.645	1.329	3.020	1.200	2.681
26	1.125	1.780	1.037	2.315	1.154	1.802	1.037	2.315
27	0.997	2.020	0.842	2.385	1.026	2.103	1.012	2.388
28	1.201	1.935	1.574	2.130	1.719	1.937	1.603	2.134
29	1.724	2.400	2.041	2.370	1.735	2.396	2.018	2.370
30	1.812	2.400	1.000	2.370	2.307	2.357	0.065	2.367

	Participant 7: Treadmill speed 1.0 m/s							
	Qualisys				IMU			
	Right Leg		Left Leg		Right Leg		Left Leg	
	Distance (m)	Period (s)	Distance (m)	Period (s)	Distance(m)	Period(s)	Distance(m)	Period(s)
1	1.292	1.320	1.264	1.335	1.294	1.318	1.244	1.317
2	1.406	1.330	1.343	1.285	1.448	1.357	1.295	1.286
3	1.492	1.490	1.506	1.090	1.518	1.484	1.493	1.091
4	1.587	1.075	1.472	1.505	1.581	1.074	1.423	1.427
5	1.211	1.310	1.328	1.150	1.392	1.356	1.383	1.188
6	1.274	1.235	1.354	1.410	1.279	1.241	1.405	1.410
7	1.370	1.300	1.384	1.100	1.369	1.281	1.387	1.119
8	1.313	1.550	1.338	1.465	1.341	1.545	1.317	1.465

9	1.353	1.065	1.402	1.305	1.345	1.068	1.421	1.355
10	1.574	1.215	1.594	1.215	1.577	1.219	1.479	1.196
11	1.700	1.335	1.828	1.365	1.664	1.336	1.811	1.359
12	1.461	1.315	1.532	1.140	1.447	1.254	1.523	1.149
13	1.634	1.135	1.561	1.355	1.613	1.162	1.561	1.355
14	1.484	1.820	1.448	1.330	1.468	1.696	1.469	1.330
15	1.180	1.340	1.187	1.535	1.183	1.341	1.169	1.482
16	0.933	1.070	0.939	1.110	0.952	1.071	0.923	1.136
17	1.041	1.345	1.032	1.565	1.020	1.358	1.136	1.568
18	0.940	1.355	0.996	1.090	0.972	1.355	0.978	1.091
19	1.033	1.530	0.923	1.505	1.028	1.529	0.951	1.429
20	1.109	1.185	1.202	1.420	1.106	1.167	1.215	1.421
21	1.285	1.250	1.192	1.285	1.298	1.274	1.137	1.249
22	1.347	1.675	1.349	1.060	1.269	1.669	1.355	1.227
23	1.312	1.320	1.320	1.695	1.312	1.323	1.306	1.661
24	1.203	1.070	1.202	1.380	1.206	1.076	1.132	1.380
25	1.333	1.380	1.337	1.070	1.337	1.380	1.314	1.072
26	1.319	1.345	1.359	1.390	1.296	1.306	1.363	1.397
27	1.325	1.340	1.312	1.250	1.325	1.340	1.314	1.270
28	1.365	1.295	1.320	1.585	1.348	1.293	1.291	1.576
29	1.368	1.430	1.351	1.385	1.368	1.431	1.352	1.386
30	1.613	1.430	1.388	1.385	1.576	1.430	1.399	1.387

	Participant 7: Treadmill speed 1.4 m/s							
	Qualisys				IMU			
	Right Leg		Left Leg		Right Leg		Left Leg	
	Distance (m)	Period (s)	Distance (m)	Period (s)	Distance(m)	Period(s)	Distance(m)	Period(s)
1	1.170	1.175	1.272	0.965	1.138	1.166	1.272	0.967
2	1.438	0.985	1.439	1.105	1.503	1.011	1.384	1.125
3	1.476	1.130	1.490	1.185	1.572	1.135	1.499	1.179
4	1.465	1.140	1.391	1.130	1.465	1.137	1.279	1.125
5	1.273	1.100	1.289	1.070	1.263	1.101	1.297	1.074
6	1.457	1.115	1.387	1.110	1.464	1.118	1.373	1.115
7	1.311	1.250	1.295	1.120	1.285	1.230	1.258	1.119
8	1.260	0.905	1.230	0.915	1.257	0.918	1.223	0.910
9	1.196	1.105	1.203	1.095	1.195	1.106	1.227	1.142
10	1.269	1.025	1.270	1.160	1.236	1.006	1.260	1.151
11	1.408	1.070	1.307	1.045	1.411	1.068	1.307	1.017
12	1.395	1.060	1.311	1.130	1.383	1.061	1.292	1.130
13	1.399	1.035	1.300	1.045	1.272	1.019	1.290	1.038
14	1.564	1.205	1.573	1.010	1.562	1.186	1.514	1.011
15	1.783	0.955	1.784	0.950	1.805	0.963	1.783	0.953
16	1.627	1.035	1.614	1.195	1.604	1.037	1.508	1.190
17	1.620	1.225	1.622	1.105	1.585	1.228	1.636	1.149
18	1.534	1.050	1.443	1.045	1.520	1.043	1.403	1.037
19	1.588	0.965	1.611	1.110	1.408	0.932	1.607	1.132
20	1.654	1.135	1.551	0.995	1.600	1.139	1.314	0.992
21	1.649	0.950	1.697	1.075	1.619	0.951	1.673	1.085
22	1.624	1.140	1.723	1.055	1.558	1.134	1.675	1.054
23	1.649	1.030	1.707	1.000	1.652	1.030	1.694	1.001
24	1.734	1.085	1.741	1.085	1.732	1.085	1.680	1.111
25	1.601	1.025	1.749	1.020	1.589	1.025	1.747	1.024
26	1.618	0.940	1.715	1.025	1.614	0.935	1.551	1.028

27	1.652	1.100	1.586	1.125	1.652	1.100	1.571	1.124
28	1.525	1.045	1.571	1.030	1.532	1.050	1.311	1.016
29	1.535	1.070	1.523	1.065	1.461	1.070	1.470	1.092
30	1.501	1.070	1.457	1.065	1.500	1.071	1.441	1.072

	Participant 7: Treadmill speed 1.8 m/s							
	Qualisys				IMU			
	Right Leg		Left Leg		Right Leg		Left Leg	
	Distance (m)	Period (s)	Distance (m)	Period (s)	Distance(m)	Period(s)	Distance(m)	Period(s)
1	1.084	0.845	1.048	0.490	1.083	0.843	1.048	0.496
2	1.233	0.855	0.990	0.835	1.211	0.857	1.063	0.835
3	1.590	0.885	1.395	0.900	1.420	0.875	1.337	0.898
4	1.473	0.875	1.475	0.825	1.451	0.885	1.457	0.833
5	1.479	0.865	1.410	0.905	1.447	0.865	1.374	0.896
6	1.536	0.860	1.432	0.880	1.516	0.861	1.435	0.887
7	1.423	0.890	1.484	0.905	1.422	0.893	1.473	0.905
8	1.350	0.910	1.351	0.895	1.271	0.910	1.333	0.895
9	1.413	0.885	1.416	0.825	1.401	0.885	1.312	0.825
10	1.479	0.870	1.459	0.935	1.476	0.872	1.328	0.933
11	1.468	0.890	1.420	0.850	1.387	0.891	1.418	0.852
12	1.751	0.865	1.538	0.885	1.654	0.830	1.508	0.880
13	1.838	0.875	1.771	0.915	1.838	0.882	1.732	0.913
14	1.776	0.900	1.794	0.895	1.571	0.900	1.726	0.896
15	1.504	0.935	1.594	0.910	1.475	0.935	1.567	0.911
16	1.476	0.860	1.400	0.890	1.477	0.862	1.406	0.892
17	1.538	0.985	1.509	0.885	1.522	0.985	1.491	0.885
18	1.573	0.840	1.518	0.885	1.553	0.849	1.533	0.886
19	1.635	0.850	1.558	0.885	1.609	0.851	1.505	0.881
20	1.710	0.875	1.592	0.835	1.706	0.875	1.590	0.846
21	1.730	0.845	1.640	0.890	1.706	0.848	1.623	0.890
22	1.717	0.905	1.719	0.895	1.565	0.899	1.602	0.894
23	1.692	0.905	1.627	0.845	1.596	0.905	1.622	0.847
24	1.780	0.960	1.724	0.960	1.738	0.957	1.707	0.957
25	1.790	0.815	1.718	0.860	1.742	0.815	1.675	0.831
26	1.881	0.870	1.782	0.890	1.866	0.871	1.728	0.890
27	1.974	1.020	1.974	0.930	1.948	1.019	1.964	0.940
28	1.811	0.835	1.947	0.905	1.674	0.836	1.917	0.908
29	1.985	0.980	1.843	0.890	1.951	0.976	1.841	0.891
30	1.432	0.980	2.014	0.890	1.396	0.976	2.005	0.891

	Participant 7: Treadmill speed 2.0 m/s							
	Qualisys				IMU			
	Right Leg		Left Leg		Right Leg		Left Leg	
	Distance (m)	Period (s)	Distance (m)	Period (s)	Distance(m)	Period(s)	Distance(m)	Period(s)
1	1.585	0.815	1.578	0.845	1.536	0.821	1.618	0.846
2	1.638	0.835	1.618	0.850	1.607	0.835	1.521	0.850
3	1.774	0.870	1.777	0.765	1.687	0.882	1.775	0.763
4	1.759	0.920	1.667	0.970	1.641	0.919	1.664	0.983
5	1.690	0.835	1.761	0.870	1.654	0.839	1.735	0.870
6	1.619	0.890	1.699	0.900	1.445	0.890	1.611	0.898
7	1.649	0.860	1.705	0.840	1.631	0.864	1.691	0.819
8	1.606	0.935	1.614	0.890	1.583	0.935	1.569	0.899

9	1.600	0.920	1.713	0.920	1.591	0.922	1.680	0.921
10	1.644	0.835	1.676	0.905	1.567	0.847	1.583	0.904
11	1.658	0.885	1.675	0.880	1.590	0.887	1.598	0.883
12	1.768	0.990	1.782	0.925	1.718	0.992	1.720	0.955
13	1.743	0.835	1.827	0.910	1.615	0.825	1.790	0.908
14	1.628	0.870	1.629	0.875	1.594	0.869	1.585	0.853
15	1.523	0.915	1.519	0.845	1.372	0.915	1.465	0.855
16	1.645	0.870	1.609	0.885	1.631	0.834	1.578	0.882
17	1.771	0.860	1.831	0.885	1.718	0.856	1.783	0.854
18	1.703	0.850	1.693	0.855	1.702	0.876	1.524	0.813
19	1.645	0.875	1.626	0.835	1.645	0.868	1.571	0.830
20	1.610	0.855	1.606	0.900	1.600	0.854	1.532	0.898
21	1.628	0.840	1.661	0.850	1.553	0.869	1.646	0.860
22	1.677	0.885	1.703	0.840	1.577	0.864	1.702	0.831
23	1.749	0.865	1.861	0.850	1.617	0.865	1.820	0.852
24	1.758	0.800	1.794	0.890	1.655	0.803	1.671	0.891
25	1.783	0.875	1.812	0.795	1.699	0.875	1.670	0.797
26	1.788	0.810	1.827	0.865	1.788	0.809	1.807	0.860
27	1.832	0.860	1.888	0.880	1.824	0.857	1.877	0.878
28	1.837	0.920	1.884	0.825	1.832	0.929	1.882	0.841
29	1.845	0.440	1.943	0.870	1.744	0.462	1.933	0.869
30	1.367	0.440	2.205	0.870	1.338	0.485	2.113	0.869

	Participant 7: Treadmill speed 2.2 m/s							
	Qualisys				IMU			
	Right Leg		Left Leg		Right Leg		Left Leg	
	Distance (m)	Period (s)	Distance (m)	Period (s)	Distance(m)	Period(s)	Distance(m)	Period(s)
1	1.654	0.835	1.669	0.855	1.646	0.807	1.598	0.854
2	1.698	0.795	1.676	0.775	1.693	0.798	1.575	0.776
3	1.790	0.815	1.755	0.790	1.747	0.816	1.752	0.792
4	1.895	0.815	1.806	0.835	1.863	0.814	1.758	0.834
5	1.790	0.810	1.791	0.790	1.733	0.817	1.771	0.793
6	1.689	0.835	1.720	0.895	1.688	0.834	1.719	0.884
7	1.666	0.830	1.586	0.810	1.653	0.834	1.581	0.818
8	1.677	0.845	1.608	0.815	1.638	0.843	1.588	0.815
9	1.747	0.835	1.670	0.865	1.736	0.835	1.658	0.865
10	1.816	0.795	1.788	0.795	1.779	0.796	1.779	0.799
11	1.882	0.815	1.829	0.790	1.825	0.817	1.737	0.798
12	2.023	0.790	1.956	0.820	1.995	0.790	1.876	0.820
13	2.008	0.840	1.920	0.860	1.994	0.840	1.859	0.859
14	1.927	0.835	1.937	0.805	1.864	0.834	1.910	0.802
15	1.865	0.880	1.849	0.885	1.847	0.880	1.849	0.885
16	2.005	0.810	1.942	0.845	1.982	0.812	1.892	0.844
17	1.971	0.865	1.891	0.860	1.971	0.865	1.891	0.861
18	1.807	0.835	1.720	0.810	1.765	0.836	1.679	0.813
19	1.785	0.820	1.699	0.790	1.780	0.822	1.581	0.791
20	1.851	0.855	1.827	0.895	1.785	0.855	1.776	0.895
21	1.973	0.835	1.948	0.775	1.909	0.835	1.859	0.778
22	2.041	0.840	1.977	0.835	2.022	0.840	1.909	0.835
23	2.121	0.890	2.024	0.905	2.090	0.897	2.097	0.901
24	2.031	0.865	2.007	0.875	1.984	0.869	1.991	0.876
25	1.914	0.800	1.868	0.870	1.757	0.810	1.949	0.871
26	1.874	0.850	1.767	0.830	1.846	0.850	1.767	0.827

27	1.803	0.880	1.786	0.800	1.738	0.878	1.835	0.801
28	1.897	0.805	1.883	0.900	1.863	0.808	1.890	0.898
29	1.970	1.065	1.881	0.700	1.772	1.056	2.011	0.720
30	1.833	1.065	1.735	0.700	1.682	1.057	1.789	0.709

	Participant 7: Treadmill speed 2.5 m/s							
	Qualisys				IMU			
	Right Leg		Left Leg		Right Leg		Left Leg	
	Distance (m)	Period (s)	Distance (m)	Period (s)	Distance(m)	Period(s)	Distance(m)	Period(s)
1	1.769	0.785	1.839	0.765	1.589	0.779	1.804	0.762
2	1.827	0.780	1.873	0.800	1.632	0.772	1.866	0.776
3	1.894	0.800	1.970	0.795	1.853	0.821	1.961	0.796
4	1.962	0.775	1.988	0.775	1.907	0.774	1.969	0.754
5	1.847	0.805	1.831	0.795	1.823	0.805	1.813	0.800
6	1.740	0.745	1.828	0.790	1.740	0.761	1.699	0.790
7	1.735	0.780	1.852	0.760	1.688	0.779	1.758	0.760
8	1.724	0.775	1.864	0.785	1.724	0.774	1.826	0.784
9	1.856	0.785	1.864	0.780	1.808	0.756	1.822	0.786
10	1.892	0.765	1.999	0.775	1.842	0.779	1.914	0.777
11	1.831	0.790	1.894	0.750	1.813	0.789	1.806	0.752
12	1.971	0.785	2.079	0.800	1.932	0.790	1.987	0.794
13	2.102	0.765	2.217	0.770	2.040	0.765	2.072	0.769
14	2.019	0.825	2.153	0.800	1.877	0.824	2.108	0.801
15	1.894	0.780	1.994	0.760	1.879	0.782	1.921	0.760
16	1.795	0.780	1.839	0.810	1.649	0.785	1.790	0.810
17	1.662	0.775	1.754	0.810	1.612	0.777	1.713	0.810
18	1.757	0.800	1.797	0.750	1.745	0.801	1.772	0.755
19	1.812	0.740	1.924	0.745	1.700	0.741	1.858	0.746
20	1.896	0.750	2.040	0.800	1.886	0.753	2.030	0.800
21	1.974	0.795	1.999	0.770	1.948	0.763	1.960	0.766
22	1.998	0.770	2.087	0.775	1.853	0.771	1.986	0.775
23	1.841	0.780	1.963	0.765	1.828	0.813	1.819	0.767
24	1.769	0.765	1.830	0.775	1.757	0.764	1.731	0.774
25	1.780	0.715	1.873	0.735	1.779	0.716	1.836	0.737
26	1.782	0.805	1.828	0.785	1.756	0.805	1.605	0.785
27	1.960	0.725	2.047	0.745	1.959	0.699	2.016	0.740
28	1.917	0.785	2.005	0.765	1.913	0.785	2.001	0.765
29	1.985	0.530	2.030	0.680	1.985	0.541	1.970	0.695
30	2.982	0.530	1.476	0.680	2.776	0.598	1.411	0.682

Stride No	Participant 8: Treadmill speed 0.6 m/s							
	Qualisys				IMU			
	Right Leg		Left Leg		Right Leg		Left Leg	
	Distance (m)	Period (s)	Distance (m)	Period (s)	Distance(m)	Period(s)	Distance(m)	Period(s)
1	0.681	0.905	0.667	0.970	0.664	0.907	0.606	0.971
2	0.672	0.930	0.665	0.870	0.669	0.933	0.659	0.872
3	0.657	0.920	0.645	1.040	0.657	0.925	0.637	1.015
4	0.655	1.000	0.647	0.995	0.639	1.000	0.647	0.998
5	0.647	1.045	0.629	1.050	0.639	1.045	0.624	1.031
6	0.642	1.050	0.629	1.020	0.627	1.049	0.629	1.030
7	0.648	1.015	0.639	1.125	0.587	1.013	0.580	1.124
8	0.653	1.100	0.634	1.130	0.646	1.101	0.629	1.130

9	0.650	1.175	0.633	1.035	0.725	1.194	0.599	1.035
10	0.653	1.060	0.636	1.130	0.653	1.062	0.641	1.127
11	0.639	1.105	0.639	1.140	0.646	1.105	0.620	1.138
12	0.635	0.990	0.652	1.035	0.650	0.990	0.658	1.090
13	0.635	1.085	0.655	1.015	0.647	1.089	0.654	1.015
14	0.645	1.070	0.658	1.100	0.648	1.069	0.657	1.099
15	0.664	1.070	0.660	1.095	0.750	1.071	0.643	1.089
16	0.684	1.100	0.682	1.080	0.800	1.102	0.692	1.097
17	0.667	1.120	0.678	1.050	0.669	1.119	0.731	1.062
18	0.653	1.045	0.666	1.090	0.666	1.047	0.668	1.091
19	0.664	1.015	0.665	1.070	0.665	1.023	0.669	1.070
20	0.653	1.125	0.646	1.145	0.897	1.132	0.650	1.144
21	0.626	1.225	0.631	1.285	1.045	1.221	0.646	1.277
22	0.634	1.035	0.632	1.200	1.187	1.036	0.662	1.197
23	0.646	1.420	0.673	1.080	0.841	1.417	1.185	1.082
24	0.639	0.985	0.650	1.235	0.758	0.988	0.729	1.235
25	0.645	1.360	0.650	1.170	0.743	1.291	0.659	1.163
26	0.643	1.105	0.636	1.090	0.787	1.105	0.711	1.082
27	0.633	1.085	0.648	1.085	1.472	1.101	0.723	1.080
28	0.628	1.045	0.642	1.100	0.630	1.050	0.653	1.104
29	0.631	1.105	0.644	1.020	0.632	1.094	0.687	1.029
30	0.634	1.130	0.652	1.020	0.642	1.118	0.673	1.028

	Participant 8: Treadmill speed 1.0 m/s							
	Qualisys				IMU			
	Right Leg		Left Leg		Right Leg		Left Leg	
	Distance (m)	Period (s)	Distance (m)	Period (s)	Distance(m)	Period(s)	Distance(m)	Period(s)
1	0.592	0.925	0.594	0.465	0.592	0.924	0.593	0.470
2	0.596	0.765	0.602	0.855	0.574	0.770	0.595	0.854
3	0.500	0.840	0.549	0.755	0.469	0.839	0.552	0.766
4	0.531	0.800	0.541	0.800	0.523	0.795	0.529	0.795
5	0.605	0.830	0.570	0.905	0.605	0.832	0.564	0.907
6	0.774	0.790	0.664	0.710	0.760	0.795	0.658	0.711
7	0.946	0.785	0.820	0.835	0.941	0.784	0.819	0.828
8	0.935	0.800	0.892	0.840	0.904	0.803	0.883	0.841
9	0.896	0.800	0.884	0.740	0.891	0.806	0.866	0.744
10	0.875	0.800	0.890	0.825	0.830	0.801	0.863	0.822
11	0.849	0.795	0.850	0.730	0.778	0.783	0.833	0.733
12	0.834	0.770	0.820	0.810	0.830	0.774	0.807	0.801
13	0.764	0.875	0.818	0.755	0.762	0.869	0.815	0.755
14	0.705	0.755	0.742	0.845	0.704	0.754	0.734	0.880
15	0.782	0.845	0.726	0.845	0.785	0.846	0.688	0.840
16	0.875	0.910	0.821	0.790	0.804	0.898	0.779	0.807
17	0.845	0.775	0.861	0.830	0.802	0.780	0.857	0.829
18	0.722	0.800	0.744	0.875	0.652	0.805	0.742	0.873
19	0.724	0.815	0.693	0.840	0.723	0.813	0.687	0.837
20	0.700	0.835	0.681	0.795	0.698	0.842	0.680	0.809
21	0.679	0.770	0.667	0.785	0.650	0.767	0.663	0.782
22	0.647	0.810	0.620	0.860	0.647	0.812	0.618	0.863
23	0.706	0.780	0.587	0.700	0.665	0.780	0.587	0.699
24	1.008	0.685	0.841	0.805	0.971	0.687	0.805	0.793
25	1.009	0.770	1.013	0.710	1.009	0.766	0.939	0.713
26	1.021	0.715	1.018	0.695	1.019	0.718	0.883	0.703

27	1.012	0.720	1.039	0.700	0.978	0.720	0.959	0.701
28	0.980	0.695	1.011	0.805	0.886	0.696	0.962	0.801
29	0.931	0.820	1.007	0.670	0.922	0.817	0.939	0.672
30	0.856	0.820	0.689	0.670	0.775	0.818	0.678	0.682

	Participant 8: Treadmill speed 1.4 m/s							
	Qualisys				IMU			
	Right Leg		Left Leg		Right Leg		Left Leg	
	Distance (m)	Period (s)	Distance (m)	Period (s)	Distance(m)	Period(s)	Distance(m)	Period(s)
1	0.893	0.635	0.874	0.585	0.855	0.642	0.877	0.595
2	0.912	0.680	0.915	0.670	0.909	0.680	0.852	0.670
3	0.967	0.655	0.942	0.660	0.964	0.655	0.900	0.662
4	1.006	0.695	0.992	0.710	0.996	0.695	0.915	0.706
5	0.961	0.655	0.995	0.685	0.936	0.656	0.962	0.700
6	1.008	0.690	0.982	0.655	0.995	0.691	0.972	0.661
7	0.967	0.685	0.955	0.665	0.901	0.685	0.947	0.657
8	0.963	0.640	0.948	0.660	0.941	0.640	0.939	0.664
9	0.901	0.680	0.939	0.660	0.884	0.677	0.915	0.660
10	0.837	0.600	0.885	0.650	0.818	0.604	0.834	0.648
11	0.780	0.640	0.834	0.620	0.749	0.644	0.833	0.620
12	0.738	0.635	0.775	0.605	0.597	0.627	0.750	0.608
13	0.741	0.635	0.742	0.635	0.736	0.635	0.636	0.640
14	0.778	0.625	0.704	0.620	0.775	0.625	0.699	0.621
15	0.874	0.645	0.816	0.660	0.856	0.642	0.778	0.664
16	0.930	0.640	0.905	0.675	0.899	0.640	0.859	0.656
17	0.923	0.635	0.952	0.625	0.913	0.633	0.879	0.625
18	0.927	0.665	0.964	0.690	0.835	0.672	0.963	0.686
19	1.006	0.635	0.950	0.625	0.932	0.635	0.948	0.639
20	0.972	0.635	0.981	0.645	0.969	0.635	0.872	0.636
21	0.939	0.615	0.945	0.610	0.930	0.612	0.911	0.611
22	0.939	0.675	0.936	0.655	0.938	0.678	0.849	0.654
23	0.911	0.640	0.900	0.585	0.861	0.627	0.884	0.592
24	0.934	0.655	0.928	0.695	0.930	0.657	0.898	0.687
25	0.935	0.655	0.941	0.630	0.933	0.656	0.924	0.636
26	0.875	0.605	0.922	0.635	0.868	0.605	0.900	0.636
27	0.890	0.685	0.878	0.680	0.811	0.685	0.823	0.673
28	0.874	0.630	0.863	0.615	0.814	0.630	0.829	0.618
29	0.945	0.655	0.893	0.665	0.944	0.671	0.880	0.658
30	0.945	0.655	0.962	0.665	0.922	0.656	0.956	0.679

	Participant 8: Treadmill speed 1.8 m/s							
	Qualisys				IMU			
	Right Leg		Left Leg		Right Leg		Left Leg	
	Distance (m)	Period (s)	Distance (m)	Period (s)	Distance(m)	Period(s)	Distance(m)	Period(s)
1	1.175	0.595	1.238	0.605	1.162	0.597	1.235	0.608
2	1.220	0.605	1.234	0.615	1.182	0.605	1.180	0.611
3	1.171	0.600	1.237	0.590	1.156	0.604	1.208	0.594
4	1.223	0.615	1.272	0.615	1.176	0.615	1.227	0.614
5	1.160	0.620	1.216	0.585	1.120	0.620	1.076	0.590
6	1.206	0.585	1.232	0.670	1.140	0.585	1.183	0.665
7	1.157	0.645	1.197	0.620	1.083	0.645	1.065	0.620
8	1.127	0.585	1.163	0.570	1.124	0.596	1.158	0.571

9	1.121	0.620	1.122	0.575	1.106	0.619	1.119	0.577
10	1.100	0.550	1.148	0.585	0.966	0.551	1.047	0.580
11	1.299	0.585	1.300	0.605	1.270	0.585	1.298	0.605
12	1.137	0.640	1.217	0.600	1.041	0.640	1.209	0.608
13	1.064	0.560	1.120	0.585	1.018	0.569	0.995	0.585
14	1.156	0.570	1.114	0.540	1.108	0.574	1.111	0.546
15	1.088	0.565	1.022	0.625	0.996	0.567	0.981	0.625
16	1.060	0.625	0.989	0.580	1.060	0.624	0.935	0.575
17	1.104	0.590	1.148	0.630	1.097	0.591	1.112	0.637
18	1.134	0.630	1.160	0.590	1.129	0.630	1.086	0.590
19	1.180	0.595	1.152	0.620	1.138	0.594	1.092	0.620
20	1.174	0.600	1.123	0.625	1.170	0.599	1.118	0.617
21	1.079	0.600	1.062	0.555	1.071	0.604	0.931	0.556
22	1.044	0.640	0.985	0.660	1.043	0.636	0.969	0.656
23	1.004	0.615	1.057	0.620	0.990	0.616	0.976	0.620
24	1.047	0.595	1.049	0.560	0.983	0.599	1.049	0.564
25	0.944	0.625	0.899	0.650	0.909	0.622	0.885	0.648
26	0.846	0.625	0.822	0.600	0.831	0.625	0.772	0.604
27	0.857	0.595	0.832	0.670	0.798	0.596	0.829	0.670
28	0.757	0.620	0.800	0.580	0.704	0.622	0.791	0.589
29	1.026	0.625	0.990	0.675	0.994	0.625	0.960	0.675
30	1.009	0.625	1.006	0.675	0.924	0.625	1.003	0.661

	Participant 8: Treadmill speed 2.0 m/s							
	Qualisys				IMU			
	Right Leg		Left Leg		Right Leg		Left Leg	
	Distance (m)	Period (s)	Distance (m)	Period (s)	Distance(m)	Period(s)	Distance(m)	Period(s)
1	1.467	0.665	1.456	0.585	1.466	0.663	1.303	0.575
2	1.382	0.610	1.430	0.595	1.375	0.609	1.330	0.602
3	1.455	0.565	1.383	0.650	1.453	0.577	1.361	0.653
4	1.475	0.680	1.537	0.610	1.440	0.680	1.496	0.610
5	1.454	0.660	1.522	0.650	1.382	0.666	1.521	0.650
6	1.485	0.650	1.479	0.675	1.412	0.659	1.401	0.675
7	1.328	0.615	1.460	0.710	1.230	0.612	1.353	0.708
8	1.252	0.665	1.340	0.595	1.142	0.665	1.273	0.602
9	1.253	0.635	1.287	0.645	1.252	0.635	1.285	0.649
10	1.058	0.650	1.168	0.685	0.951	0.650	1.166	0.681
11	1.057	0.635	1.115	0.565	1.031	0.645	1.092	0.578
12	1.147	0.630	1.089	0.690	1.141	0.630	1.032	0.682
13	1.197	0.685	1.201	0.655	1.098	0.685	1.196	0.656
14	1.328	0.675	1.258	0.705	1.271	0.673	1.208	0.706
15	1.333	0.645	1.307	0.610	1.324	0.654	1.261	0.612
16	1.279	0.665	1.324	0.675	1.267	0.664	1.322	0.675
17	1.370	0.630	1.388	0.610	1.292	0.630	1.367	0.613
18	1.496	0.640	1.358	0.630	1.474	0.641	1.355	0.630
19	1.537	0.655	1.338	0.625	1.526	0.656	1.335	0.627
20	1.461	0.595	1.427	0.640	1.447	0.635	1.316	0.640
21	1.415	0.685	1.390	0.660	1.366	0.681	1.262	0.659
22	1.458	0.605	1.365	0.645	1.455	0.599	1.320	0.646
23	1.474	0.625	1.406	0.635	1.416	0.631	1.387	0.632
24	1.360	0.650	1.379	0.615	1.358	0.651	1.284	0.615
25	1.253	0.685	1.283	0.680	1.250	0.685	1.277	0.683
26	1.006	0.645	1.148	0.665	1.006	0.667	1.080	0.664

27	0.946	0.655	0.888	0.625	0.933	0.649	0.853	0.624
28	0.962	0.670	0.903	0.690	0.930	0.664	0.843	0.688
29	0.983	0.640	1.033	0.650	0.958	0.647	0.995	0.657
30	1.059	0.650	0.988	0.650	1.043	0.653	0.968	0.652

	Participant 8: Treadmill speed 2.2 m/s							
	Qualisys				IMU			
	Right Leg		Left Leg		Right Leg		Left Leg	
	Distance (m)	Period (s)	Distance (m)	Period (s)	Distance(m)	Period(s)	Distance(m)	Period(s)
1	1.220	0.600	1.280	0.530	1.200	0.615	1.258	0.534
2	1.257	0.575	1.252	0.610	1.250	0.575	1.225	0.613
3	1.286	0.555	1.279	0.560	1.285	0.555	1.252	0.560
4	1.343	0.580	1.350	0.575	1.303	0.583	1.310	0.581
5	1.262	0.585	1.311	0.570	1.230	0.577	1.220	0.570
6	1.265	0.580	1.237	0.590	1.257	0.580	1.227	0.590
7	1.354	0.580	1.295	0.560	1.335	0.580	1.291	0.550
8	1.302	0.560	1.313	0.580	1.296	0.556	1.252	0.580
9	1.306	0.590	1.276	0.580	1.282	0.594	1.260	0.584
10	1.330	0.565	1.246	0.560	1.252	0.565	1.228	0.559
11	1.360	0.580	1.313	0.575	1.357	0.581	1.306	0.580
12	1.331	0.595	1.370	0.580	1.253	0.593	1.362	0.580
13	1.301	0.570	1.339	0.600	1.299	0.570	1.337	0.601
14	1.315	0.575	1.237	0.580	1.296	0.575	1.167	0.579
15	1.250	0.590	1.221	0.575	1.233	0.590	1.075	0.574
16	1.259	0.570	1.219	0.575	1.236	0.570	1.222	0.582
17	1.257	0.570	1.229	0.575	1.228	0.568	1.161	0.575
18	1.214	0.570	1.158	0.575	1.209	0.571	1.120	0.575
19	1.135	0.580	1.163	0.570	1.135	0.582	1.180	0.587
20	1.231	0.605	1.236	0.620	1.230	0.605	1.167	0.609
21	1.305	0.580	1.336	0.615	1.291	0.575	1.312	0.590
22	1.238	0.615	1.309	0.565	1.236	0.614	1.289	0.570
23	1.303	0.590	1.204	0.585	1.285	0.587	1.139	0.586
24	1.360	0.590	1.298	0.610	1.358	0.591	1.230	0.610
25	1.359	0.610	1.367	0.645	1.314	0.601	1.249	0.635
26	1.371	0.630	1.389	0.590	1.348	0.624	1.339	0.588
27	1.319	0.620	1.393	0.640	1.308	0.617	1.390	0.635
28	1.327	0.635	1.370	0.615	1.326	0.632	1.340	0.610
29	1.406	0.600	1.384	0.605	1.384	0.597	1.291	0.604
30	1.352	0.640	1.390	0.605	1.326	0.640	1.309	0.605

	Participant 8: Treadmill speed 2.5 m/s							
	Qualisys				IMU			
	Right Leg		Left Leg		Right Leg		Left Leg	
	Distance (m)	Period (s)	Distance (m)	Period (s)	Distance(m)	Period(s)	Distance(m)	Period(s)
1	1.190	0.550	1.311	0.530	1.178	0.547	1.226	0.530
2	1.343	0.530	1.298	0.585	1.325	0.531	1.285	0.588
3	1.331	0.565	1.370	0.545	1.330	0.555	1.351	0.540
4	1.470	0.555	1.414	0.560	1.410	0.555	1.298	0.561
5	1.371	0.570	1.419	0.545	1.346	0.579	1.260	0.546
6	1.351	0.555	1.407	0.590	1.152	0.555	1.334	0.588
7	1.446	0.560	1.450	0.545	1.439	0.563	1.296	0.549
8	1.448	0.580	1.459	0.585	1.253	0.577	1.456	0.583

9	1.452	0.550	1.446	0.560	1.262	0.551	1.440	0.573
10	1.406	0.555	1.438	0.540	1.238	0.552	1.434	0.539
11	1.397	0.575	1.374	0.575	1.310	0.574	1.340	0.574
12	1.201	0.570	1.348	0.555	1.109	0.571	1.338	0.556
13	1.308	0.545	1.331	0.570	1.267	0.547	1.207	0.569
14	1.362	0.585	1.342	0.545	1.362	0.585	1.107	0.546
15	1.359	0.550	1.388	0.575	1.285	0.552	1.372	0.564
16	1.462	0.530	1.469	0.535	1.449	0.530	1.346	0.536
17	1.436	0.595	1.496	0.595	1.301	0.595	1.313	0.595
18	1.499	0.550	1.484	0.575	1.493	0.551	1.470	0.575
19	1.473	0.580	1.500	0.545	1.415	0.577	1.465	0.542
20	1.526	0.560	1.502	0.560	1.443	0.566	1.438	0.562
21	1.415	0.555	1.525	0.550	1.320	0.555	1.513	0.546
22	1.564	0.560	1.567	0.560	1.508	0.566	1.566	0.560
23	1.520	0.555	1.497	0.560	1.475	0.555	1.470	0.563
24	1.466	0.550	1.534	0.545	1.355	0.550	1.407	0.545
25	1.453	0.555	1.520	0.580	1.413	0.555	1.323	0.576
26	1.481	0.545	1.470	0.525	1.470	0.546	1.448	0.525
27	1.281	0.560	1.314	0.555	1.155	0.561	1.282	0.556
28	1.224	0.535	1.278	0.535	1.123	0.536	1.225	0.536
29	1.298	0.550	1.223	0.690	1.120	0.550	1.063	0.665
30	1.293	0.550	1.349	0.690	1.216	0.548	1.190	0.682

Table 1: IMU gait extracted features accuracy with Qualisys and Treadmill (0.6 m/s)

	Treadmill Speed = 0.6 m/s																	
Subjects	QUALISYS						IMU						Accuracy (%)					
	Right Leg			Left Leg			Right Leg			Left Leg			Right Leg			Left Leg		
	D(	T(	S(	D(	T(	S(	D(	T(	S(	D(	T(	S(	D(	T(	S(	D(	T(	S(
1	26.	38.	0.6	25.	37.	0.6	26.	38.	0.6	24.	37.	0.6	98.	99.	98.	96.	99.	96.
2	19.	32.	0.6	19.	32.	0.6	20.	32.	0.6	20.	32.	0.6	96.	99.	96.	97.	99.	98.
3	31.	49.	0.6	31.	50.	0.6	32.	49.	0.6	31.	50.	0.6	99.	99.	99.	99.	99.	99.
4	40.	67.	0.6	40.	67.	0.6	42.	67.	0.6	41.	67.	0.6	94.	99.	94.	97.	99.	97.
5	15.	25.	0.6	15.	25.	0.6	15.	25.	0.5	15.	25.	0.5	98.	99.	98.	98.	99.	97.
6	15.	25.	0.6	15.	25.	0.6	15.	25.	0.5	14.	25.	0.5	97.	99.	97.	95.	99.	95.
7	36.	61.	0.6	38.	62.	0.6	40.	61.	0.6	38.	62.	0.6	89.	99.	89.	99.	99.	99.
8	19.	32.	0.6	19.	32.	0.6	22.	32.	0.6	20.	32.	0.6	85.	99.	85.	96.	99.	96.

D=Distance, T=Time, S=Speed

Table 2: IMU gait extracted features accuracy with Qualisys and Treadmill (1.0 m/s)

	Treadmill Speed = 1.0 m/s																	
Subject	QUALISYS						IMU						Accuracy (%)					
	Right Leg			Left Leg			Right Leg			Left Leg			Right Leg			Left Leg		
	D(	T(	S(	D(	T(	S(	D(	T(	S(	D(	T(	S(	D(	T(	S(	D(	T(	S(
1	27.	28.	0.9	27.	27.	0.9	26.	28.	0.9	24.	27.	0.9	95.	99.	95.	92.	99.	92.
2	34.	32.	1.0	34.	32.	1.0	33.	32.	1.0	33.	32.	1.0	98.	99.	98.	98.	99.	98.
3	31.	31.	1.0	31.	31.	1.0	31.	31.	1.0	31.	31.	1.0	98.	99.	98.	98.	99.	97.
4	37.	37.	1.0	37.	37.	1.0	36.	37.	0.9	36.	37.	0.9	95.	99.	96.	97.	99.	97.
5	19.	19.	1.0	19.	19.	1.0	18.	19.	0.9	18.	19.	0.9	97.	99.	97.	97.	99.	97.
6	44.	44.	1.0	44.	44.	1.0	45.	44.	1.0	44.	44.	1.0	98.	99.	98.	99.	99.	99.
7	39.	39.	1.0	39.	39.	1.0	39.	39.	1.0	39.	39.	0.9	99.	99.	99.	99.	99.	99.
8	23.	23.	1.0	23.	23.	1.0	23.	23.	0.9	22.	23.	0.9	96.	99.	96.	97.	99.	96.

D=Distance, T=Time, S=Speed

Table 3: IMU gait extracted features accuracy with Qualisys and Treadmill (1.4 m/s)

	Treadmill Speed = 1.4 m/s																	
Subjects	QUALISYS						IMU						Accuracy (%)					
	Right Leg			Left Leg			Right Leg			Left Leg			Right Leg			Left Leg		
	D(	T(	S(	D(	T(	S(	D(	T(	S(	D(	T(	S(	D(	T(	S(	D(	T(	S(
1	33.	24.	1.3	32.	24.	1.3	32.	23.	1.3	32.	24.	1.3	98.	99.	99.	97.	99.	97.
2	35.	25.	1.4	35.	25.	1.4	33.	25.	1.3	34.	25.	1.3	96.	99.	96.	97.	99.	97.
3	41.	29.	1.4	41.	29.	1.4	40.	29.	1.3	41.	29.	1.4	99.	99.	98.	99.	99.	99.
4	37.	26.	1.4	37.	26.	1.4	40.	26.	1.5	39.	26.	1.5	91.	99.	91.	93.	99.	93.
5	25.	18.	1.4	25.	18.	1.4	24.	18.	1.3	24.	18.	1.3	97.	99.	97.	95.	99.	95.
6	33.	24.	1.4	34.	24.	1.4	33.	24.	1.3	33.	24.	1.3	98.	99.	98.	97.	99.	97.
7	44.	32.	1.4	44.	32.	1.4	44.	32.	1.3	43.	32.	1.3	98.	99.	99.	97.	99.	96.
8	27.	19.	1.4	27.	19.	1.4	26.	19.	1.3	26.	19.	1.3	96.	99.	96.	96.	99.	96.

D=Distance, T=Time, S=Speed

Table 4: IMU gait extracted features accuracy with Qualisys and Treadmill (1.8 m/s)

	Treadmill Speed = 1.8 m/s

Subjects	QUALISYS						IMU						Accuracy (%)					
	Right Leg			Left Leg			Right Leg			Left Leg			Right Leg			Left Leg		
	D(	T(	S(	D(	T(	S(	D(	T(	S(	D(	T(	S(	D(	T(	S(	D(	T(s	S(
1	37.	21.	1.7	37.	20.	1.7	36.	21.	1.7	37.	21.	1.7	96.	99.	96.	99.	98.	99.
2	29.	21.	1.4	32.	21.	1.5	29.	21.	1.3	31.	21.	1.4	97.	99.	96.	97.	99.	97.
3	45.	25.	1.8	46.	25.	1.8	45.	25.	1.7	45.	25.	1.7	98.	99.	99.	99.	99.	98.
4	41.	22.	1.8	41.	23.	1.8	43.	22.	1.8	42.	23.	1.8	95.	99.	95.	98.	99.	98.
5	30.	16.	1.8	30.	16.	1.8	29.	16.	1.7	28.	16.	1.7	97.	99.	96.	94.	99.	94.
6	36.	20.	1.8	36.	20.	1.8	34.	20.	1.7	35.	20.	1.7	95.	99.	96.	96.	99.	97.
7	48.	26.	1.8	47.	26.	1.8	46.	26.	1.7	46.	26.	1.7	96.	99.	97.	98.	99.	98.
8	32.	18.	1.8	32.	18.	1.8	31.	18.	1.7	31.	18.	1.7	96.	99.	96.	96.	100	96.

D=Distance, T=Time, S=Speed

Table 5: IMU gait extracted features accuracy with Qualisys and Treadmill (2.0 m/s)

	Treadmill Speed = 2.0 m/s																	
Subjects	QUALISYS						IMU						Accuracy (%)					
	Right Leg			Left Leg			Right Leg			Left Leg			Right Leg			Left Leg		
	D(	T(	S(	D(	T(	S(	D(	T(	S(	D(	T(	S(	D(	T(	S(	D(	T(	S(
1	40.	20.	1.9	39.	20.	1.9	40.	20.	1.9	37.	20.	1.8	98.	99.	98.	95.	99.	94.
2	42.	20.	2.0	42.	20.	2.0	41.	20.	1.9	40.	20.	1.9	96.	99.	95.	95.	99.	95.
3	46.	23.	2.0	47.	23.	2.0	46.	23.	1.9	46.	23.	1.9	99.	99.	99.	99.	99.	99.
4	43.	21.	2.0	44.	22.	2.0	46.	21.	2.1	47.	22.	2.1	93.	99.	92.	92.	99.	92.
5	33.	16.	2.0	34.	17.	2.0	33.	16.	1.9	33.	17.	1.9	98.	99.	98.	97.	99.	97.
6	38.	19.	2.0	38.	19.	2.0	36.	19.	1.9	36.	19.	1.9	95.	99.	96.	95.	99.	95.
7	50.	25.	2.0	52.	26.	2.0	48.	25.	1.9	50.	26.	1.9	96.	99.	96.	97.	99.	97.
8	38.	19.	2.0	38.	19.	2.0	37.	19.	1.9	37.	19.	1.9	97.	99.	96.	96.	99.	96.

D=Distance, T=Time, S=Speed

Table 6: IMU gait extracted features accuracy with Qualisys and Treadmill (2.2 m/s)

	Treadmill Speed = 2.2 m/s																	
Subjects	QUALISYS						IMU						Accuracy (%)					
	Right Leg			Left Leg			Right Leg			Left Leg			Right Leg			Left Leg		
	D(	T(	S(	D(	T(	S(	D(	T(	S(	D(	T(	S(	D(	T(	S(	D(	T(	S(
1	43.	19.	2.2	43.	19.	2.2	41.	19.	2.0	43.	20.	2.1	96.	98.	94.	99.	97.	97.
2	44.	19.	2.2	44.	19.	2.2	43.	19.	2.2	42.	19.	2.2	97.	99.	97.	96.	99.	96.
3	48.	22.	2.2	48.	21.	2.2	48.	22.	2.1	47.	21.	2.1	98.	99.	98.	99.	99.	99.
4	48.	21.	2.2	48.	22.	2.2	49.	21.	2.2	49.	22.	2.2	96.	99.	96.	97.	99.	97.
5	36.	16.	2.2	37.	16.	2.2	35.	16.	2.1	36.	16.	2.1	96.	99.	96.	97.	99.	97.
6	41.	19.	2.2	41.	19.	2.2	39.	18.	2.1	40.	19.	2.1	95.	99.	95.	96.	99.	96.
7	56.	25.	2.2	54.	24.	2.2	54.	25.	2.1	53.	24.	2.1	97.	99.	97.	98.	99.	98.
8	38.	17.	2.2	38.	17.	2.2	38.	17.	2.1	37.	17.	2.1	98.	99.	98.	96.	99.	96.

D=Distance, T=Time, S=Speed

Table 7: IMU gait extracted features accuracy with Qualisys and Treadmill (2.5 m/s)

	Treadmill Speed = 2.5 m/s					
Subj ects	QUALISYS		IMU		Accuracy (%)	
	Right Leg	Left Leg	Right Leg	Left Leg	Right Leg	Left Leg

	D(	T(	S(	D(	T(	S(	D(	T(	S(	D(	T(	S(	D(	T(	S(	D(	T(s	S(
1	45.	18.	2.5	45.	18.	2.4	46.	18.	2.5	45.	18.	2.4	99.	98.	98.	99.	98.	98.
2	43.	18.	2.3	43.	18.	2.3	41.	18.	2.2	41.	18.	2.2	95.	99.	95.	96.	99.	96.
3	50.	20.	2.5	49.	19.	2.5	50.	20.	2.5	49.	20.	2.3	98.	99.	99.	99.	94.	95.
4	50.	20.	2.5	51.	20.	2.5	53.	20.	2.6	51.	20.	2.5	95.	99.	95.	98.	99.	98.
5	40.	16.	2.5	41.	16.	2.5	38.	16.	2.4	40.	16.	2.4	97.	99.	96.	97.	99.	97.
6	46.	18.	2.5	46.	18.	2.5	44.	18.	2.3	44.	18.	2.4	95.	99.	95.	96.	100	96.
7	56.	22.	2.5	57.	23.	2.5	55.	22.	2.4	55.	23.	2.4	97.	99.	96.	96.	99.	96.
8	41.	16.	2.5	42.	17.	2.5	39.	16.	2.3	40.	16.	2.3	94.	99.	94.	94.	99.	94.

D=Distance, T=Time, S=Speed

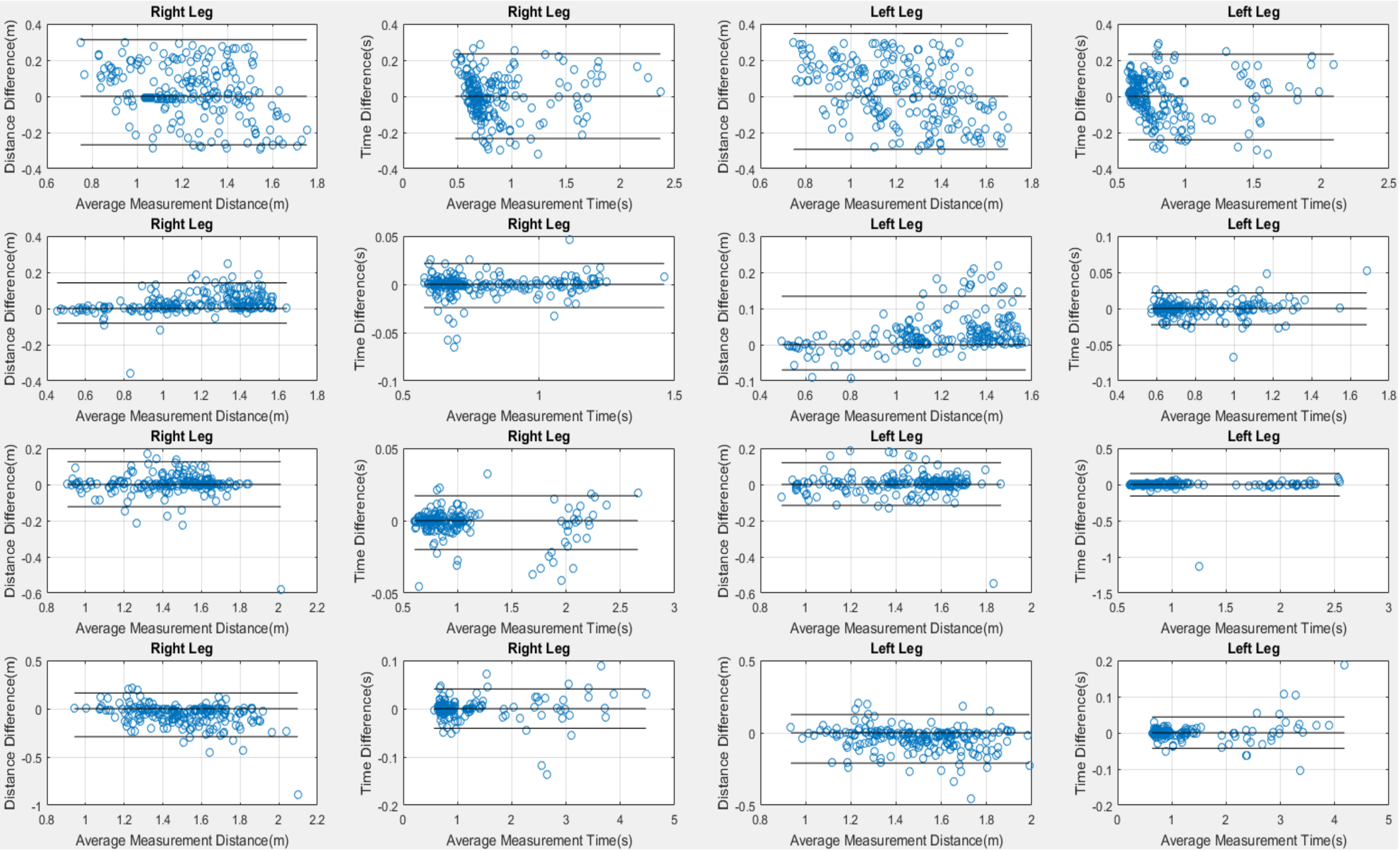

Figure 7: Bland-Altman plots for validity of distance and time measured for right and left legs with IMU and Qualisys from subject 1 to 4

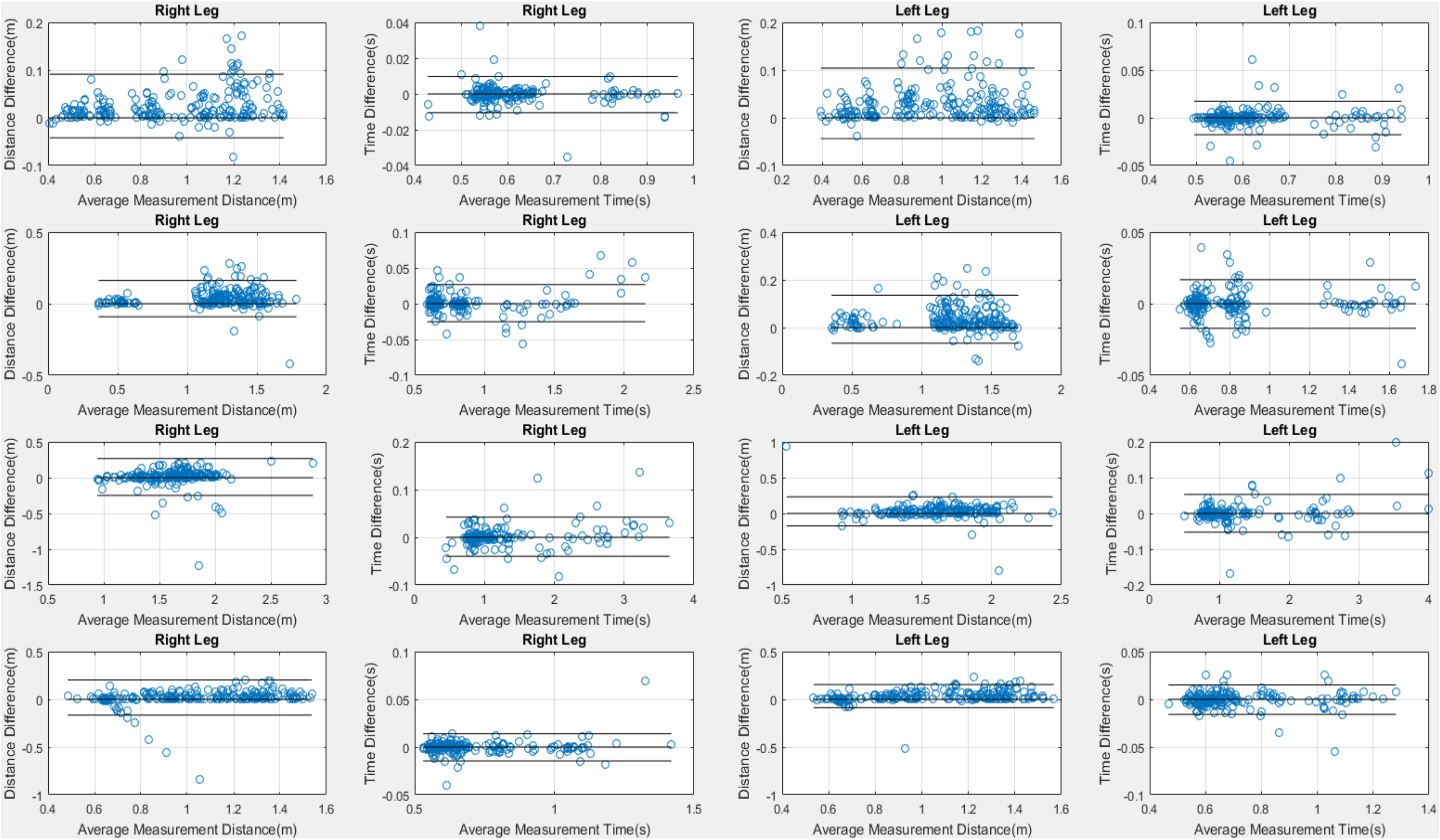

Figure 8: Bland-Altman plots for validity of distance and time measured for right and left legs with IMU and Qualisys from subject 5 to 8

Appendix E

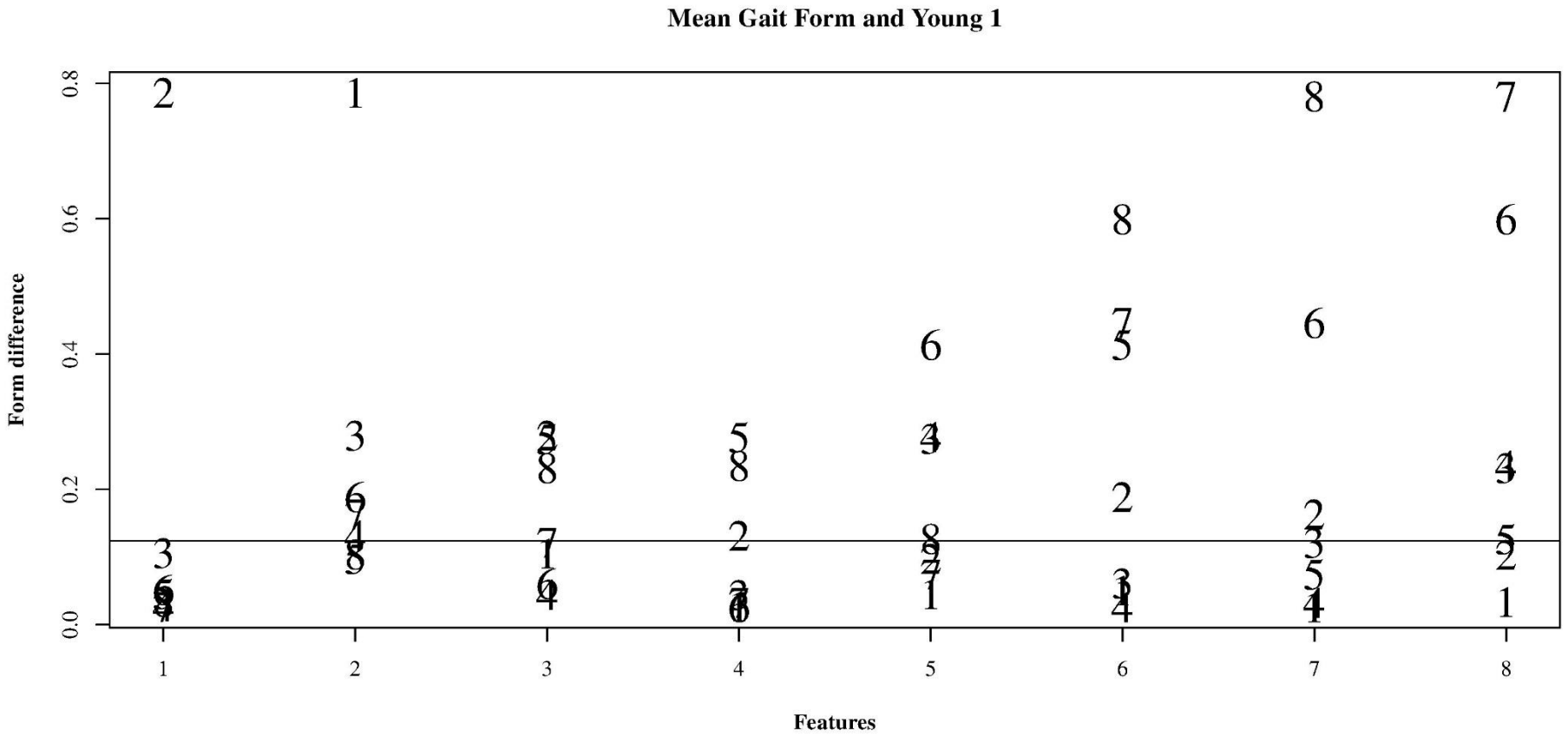
Mean Gait Form and Young 1
Form difference
0.0
0.2
0.4
0.6
0.8
1
2
3
4
5
6
7
8
Features

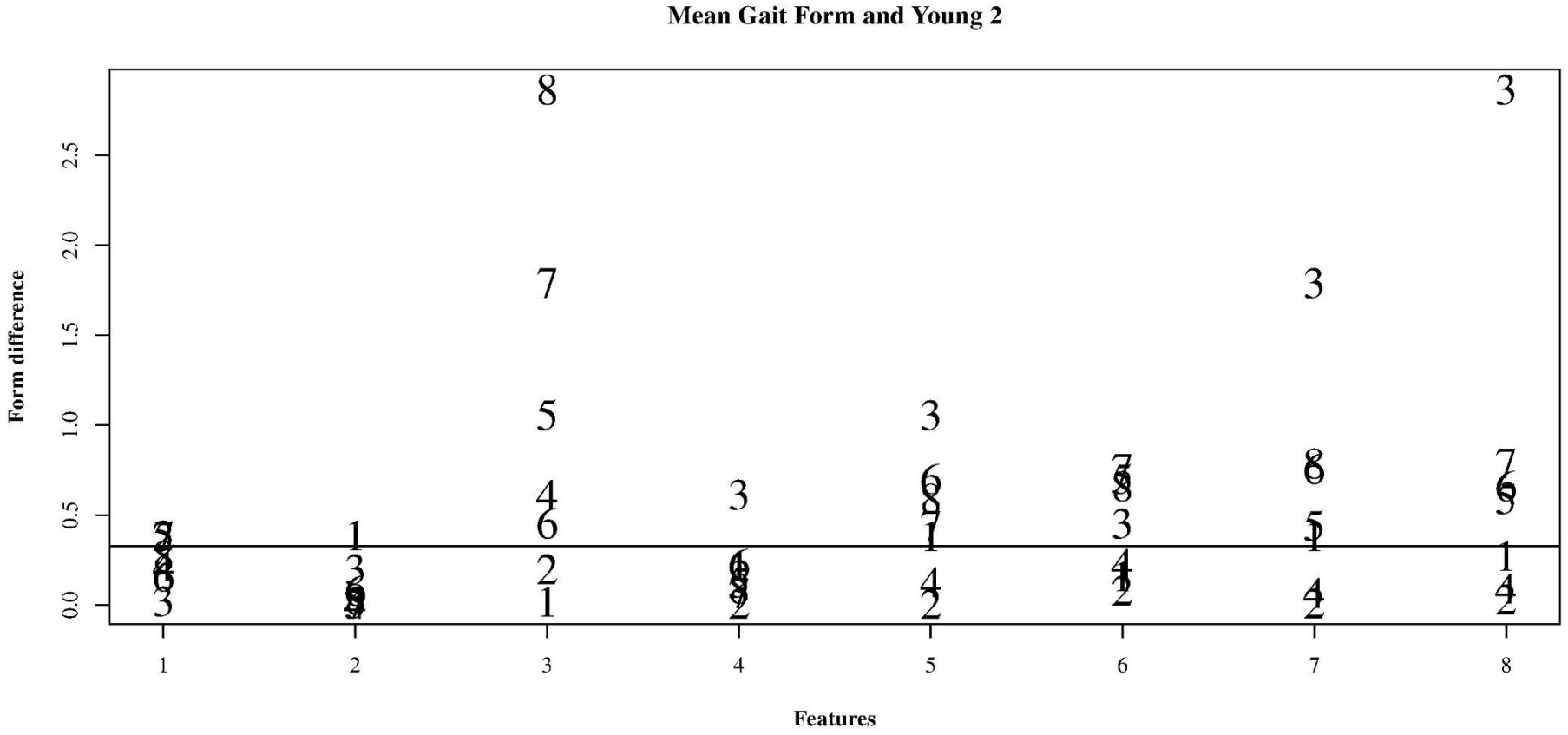
Mean Gait Form and Young 2
Form difference
0.0
0.5
1.0
1.5
2.0
2.5
1
2
3
4
5
6
7
8
Features

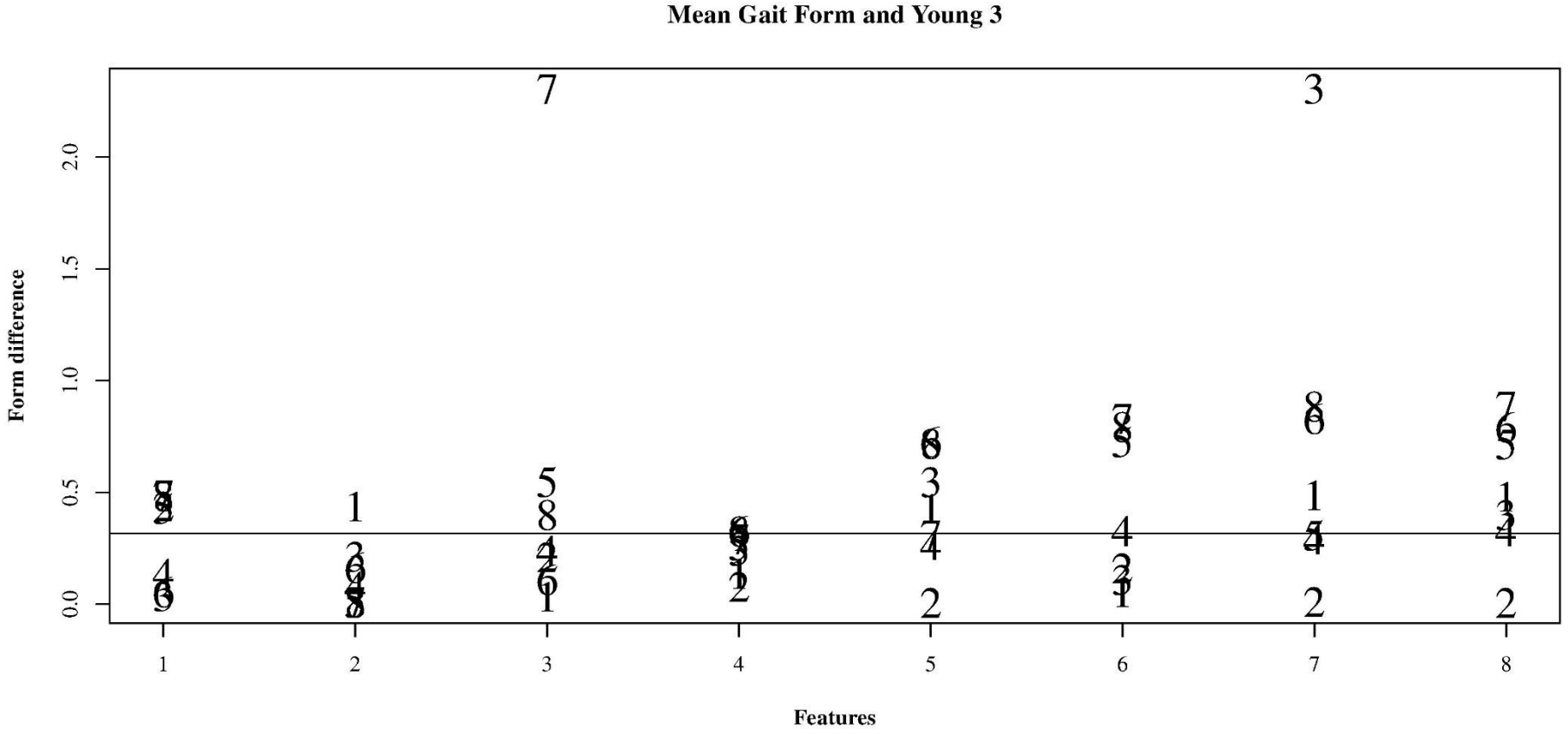
Mean Gait Form and Young 3
Form difference
0.0
0.5
1.0
1.5
2.0
1
2
3
4
5
6
7
8
Features

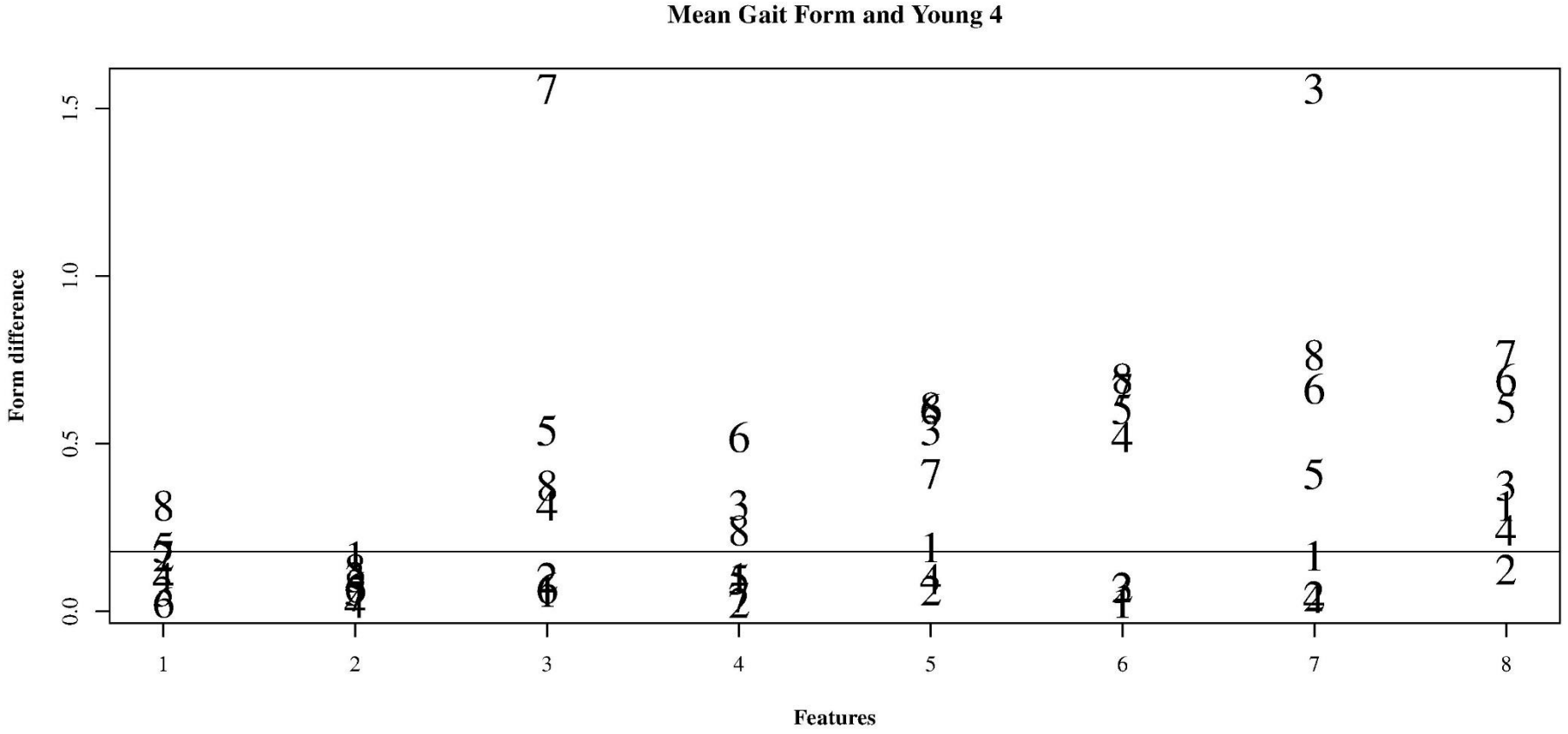
Mean Gait Form and Young 4
Form difference
0.0
0.5
1.0
1.5
1
2
3
4
5
6
7
8
Features

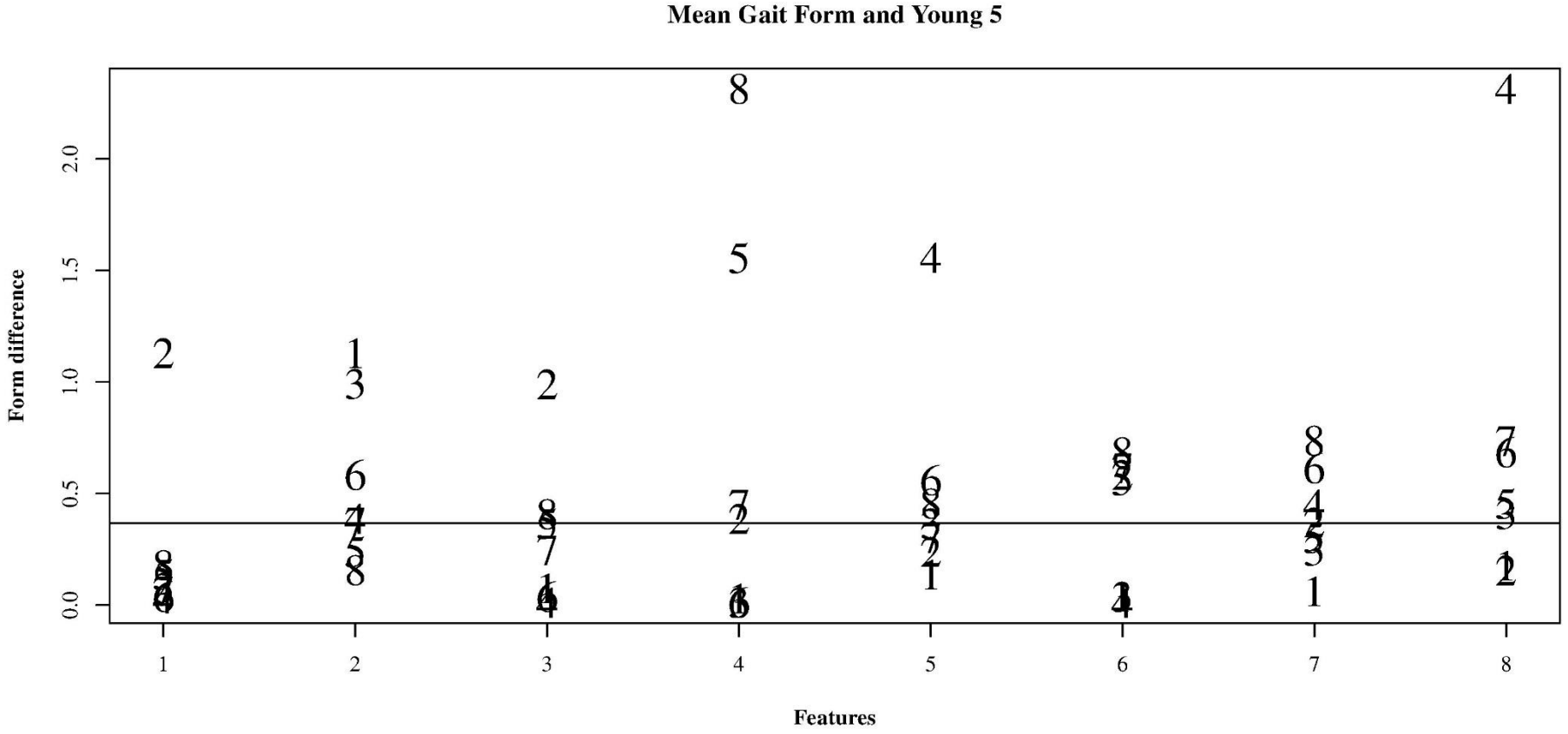
Mean Gait Form and Young 5
Form difference
0.0
0.5
1.0
1.5
2.0
1
2
3
4
5
6
7
8
Features

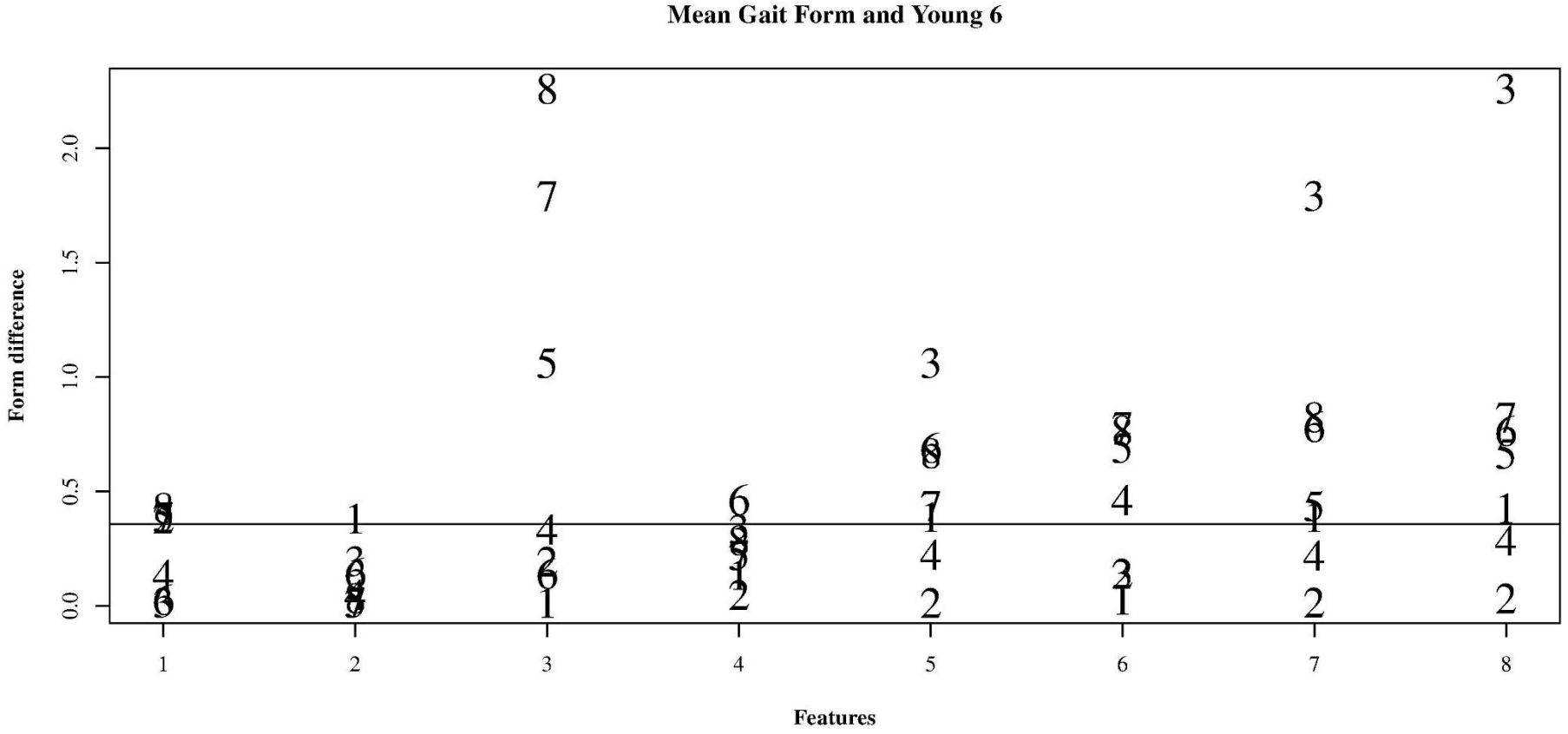
Mean Gait Form and Young 6
Form difference
0.0
0.5
1.0
1.5
2.0
1
2
3
4
5
6
7
8
Features

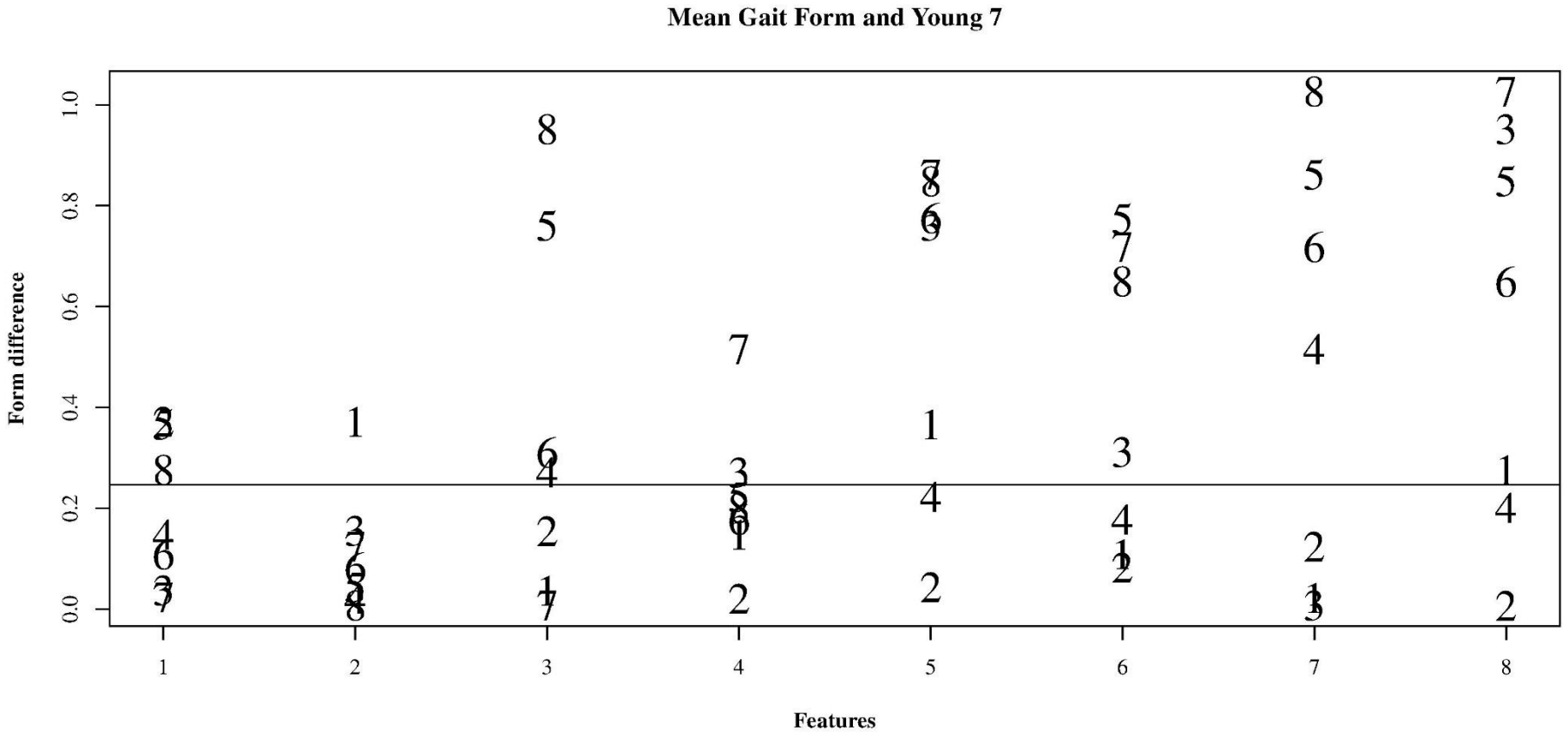
Mean Gait Form and Young 7
Form difference
0.0
0.2
0.4
0.6
0.8
1.0
1
2
3
4
5
6
7
8
Features

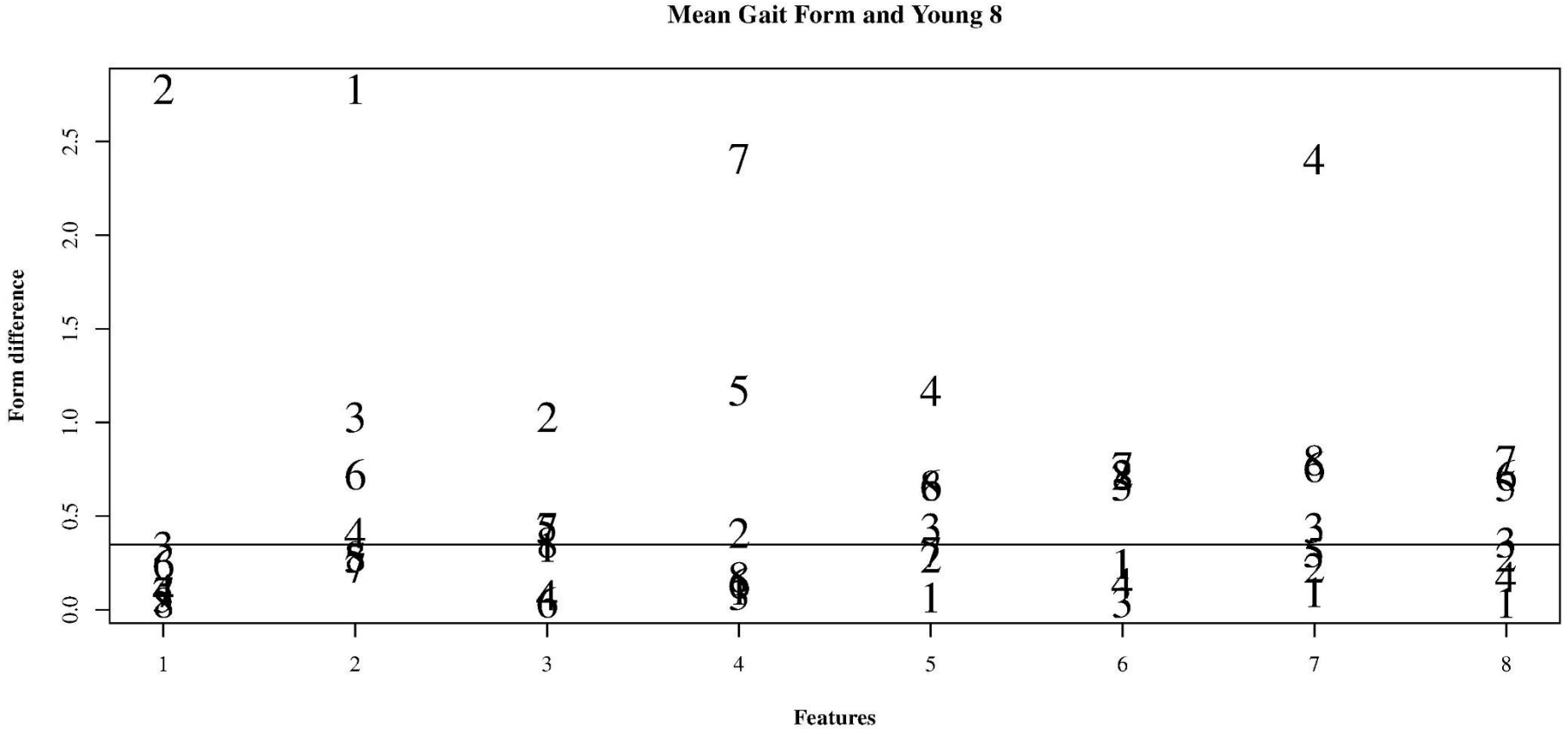
Mean Gait Form and Young 8
Form difference
0.0
0.5
1.0
1.5
2.0
2.5
1
2
3
4
5
6
7
8
Features

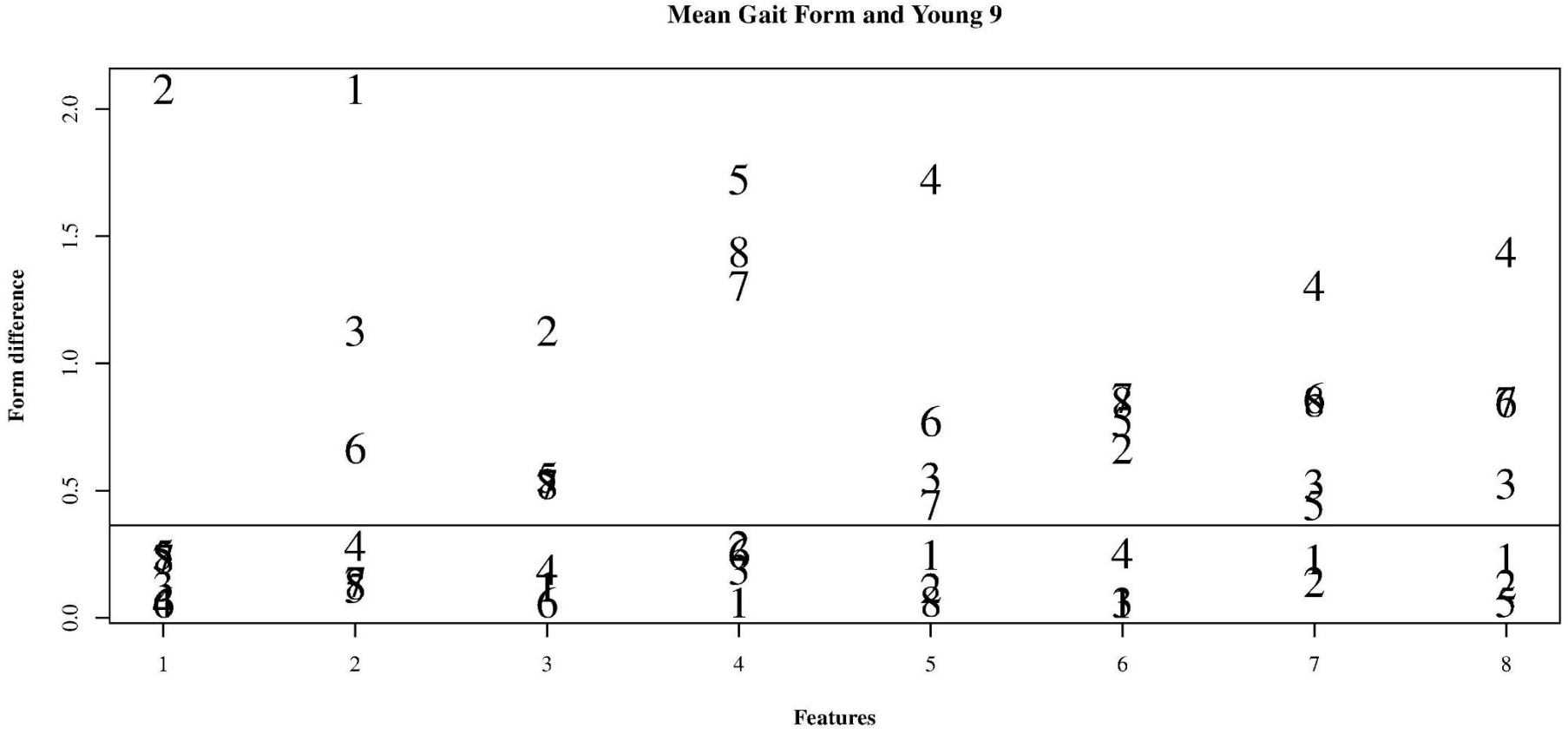
Mean Gait Form and Young 9
Form difference
0.0
0.5
1.0
1.5
2.0
1
2
3
4
5
6
7
8
Features

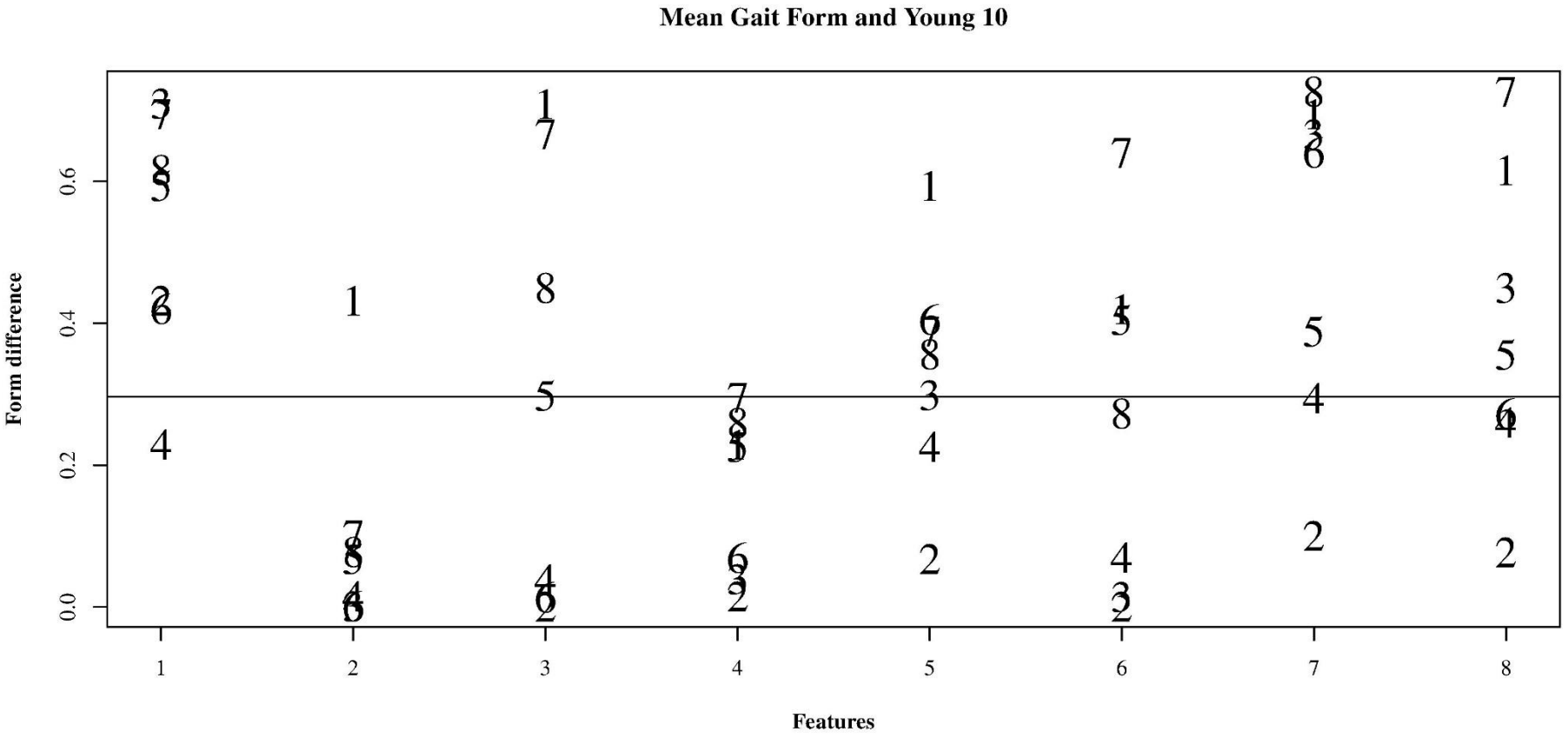
Mean Gait Form and Young 10
Form difference
0.0
0.2
0.4
0.6
1
2
3
4
5
6
7
8
Features

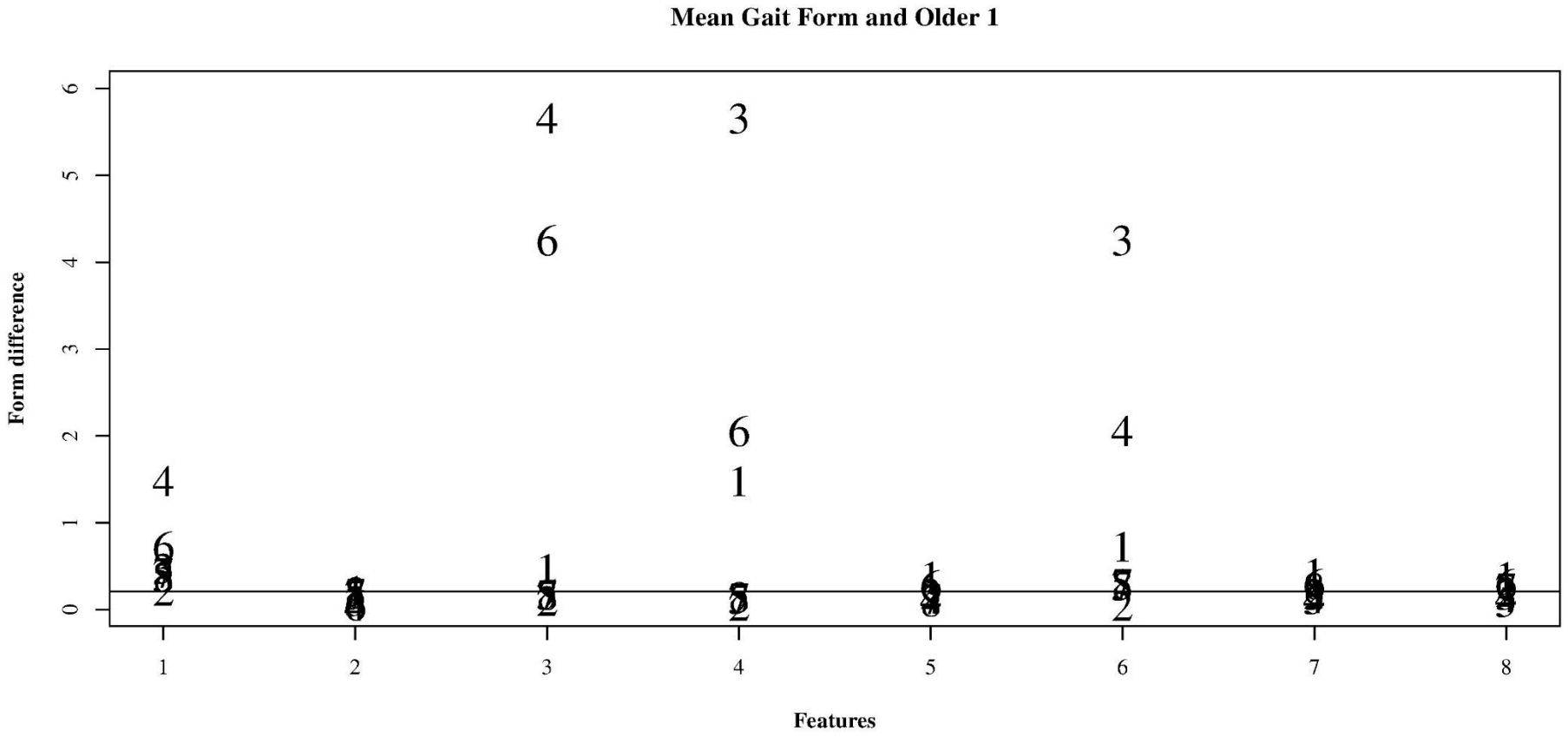
Mean Gait Form and Older 1
Form difference
0
1
2
3
4
5
6
1
2
3
4
5
6
7
8
Features

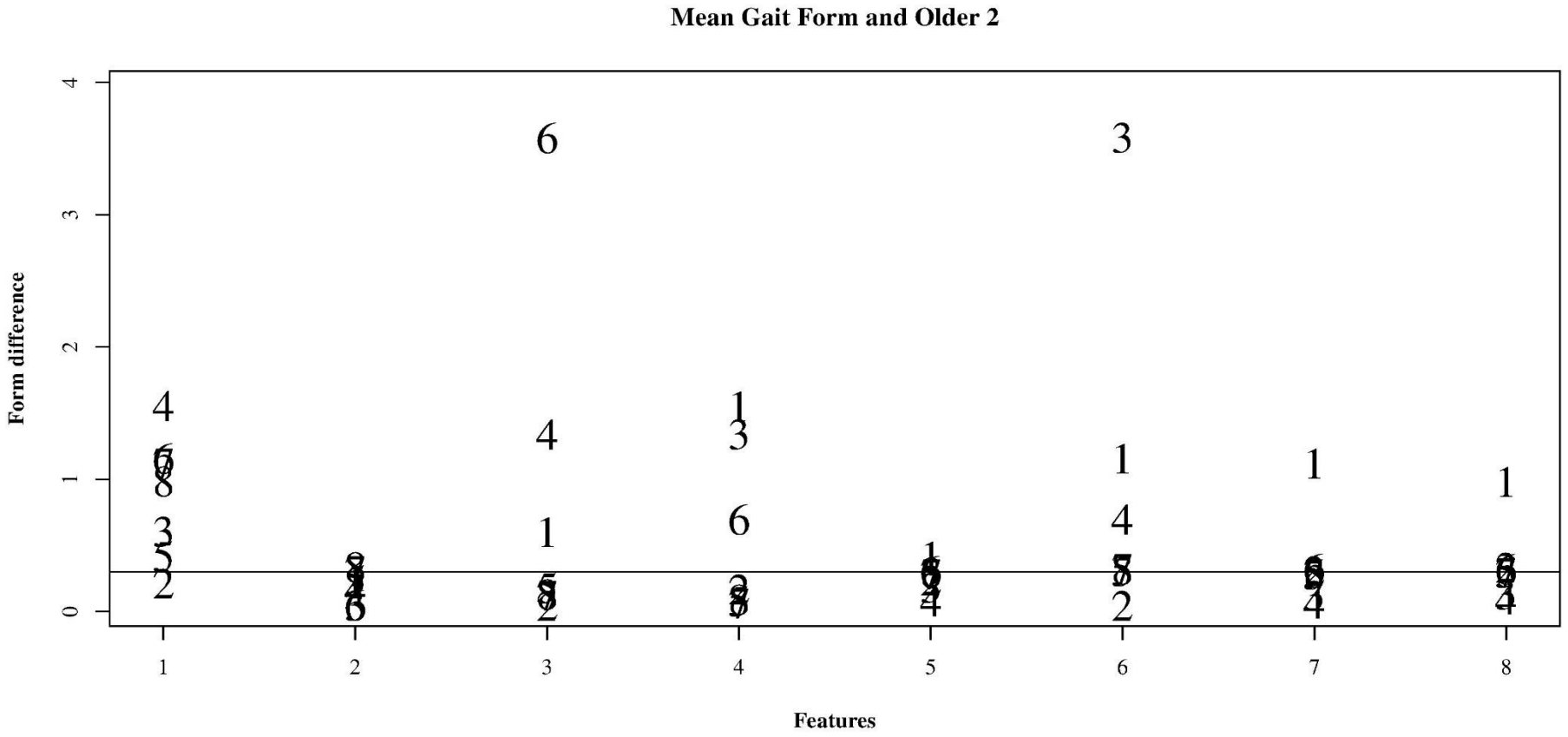
Mean Gait Form and Older 2
Form difference
0
1
2
3
4
1
2
3
4
5
6
7
8
Features

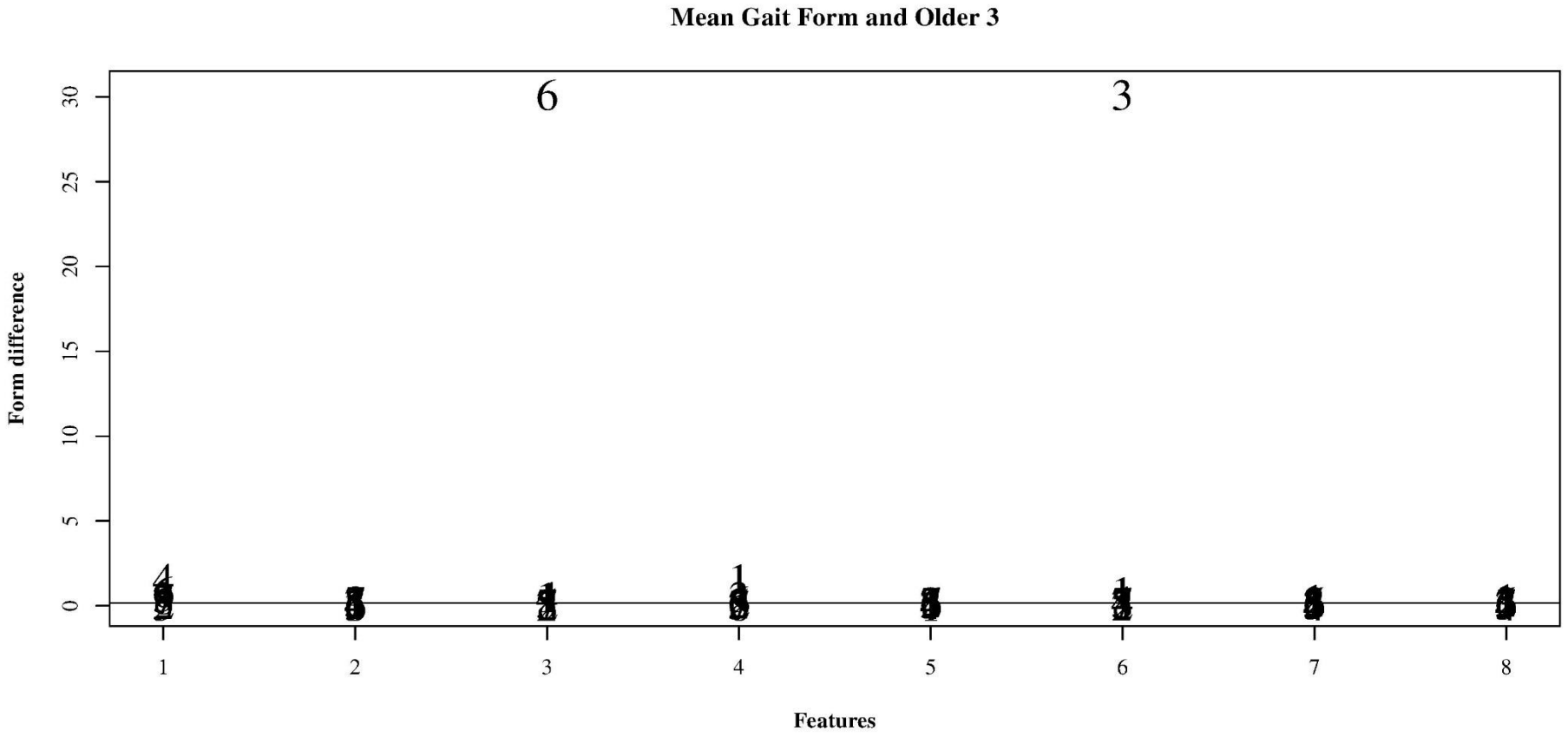
Mean Gait Form and Older 3
Form difference
0
5
10
15
20
25
30
6
3
1
2
3
4
5
6
7
8
Features

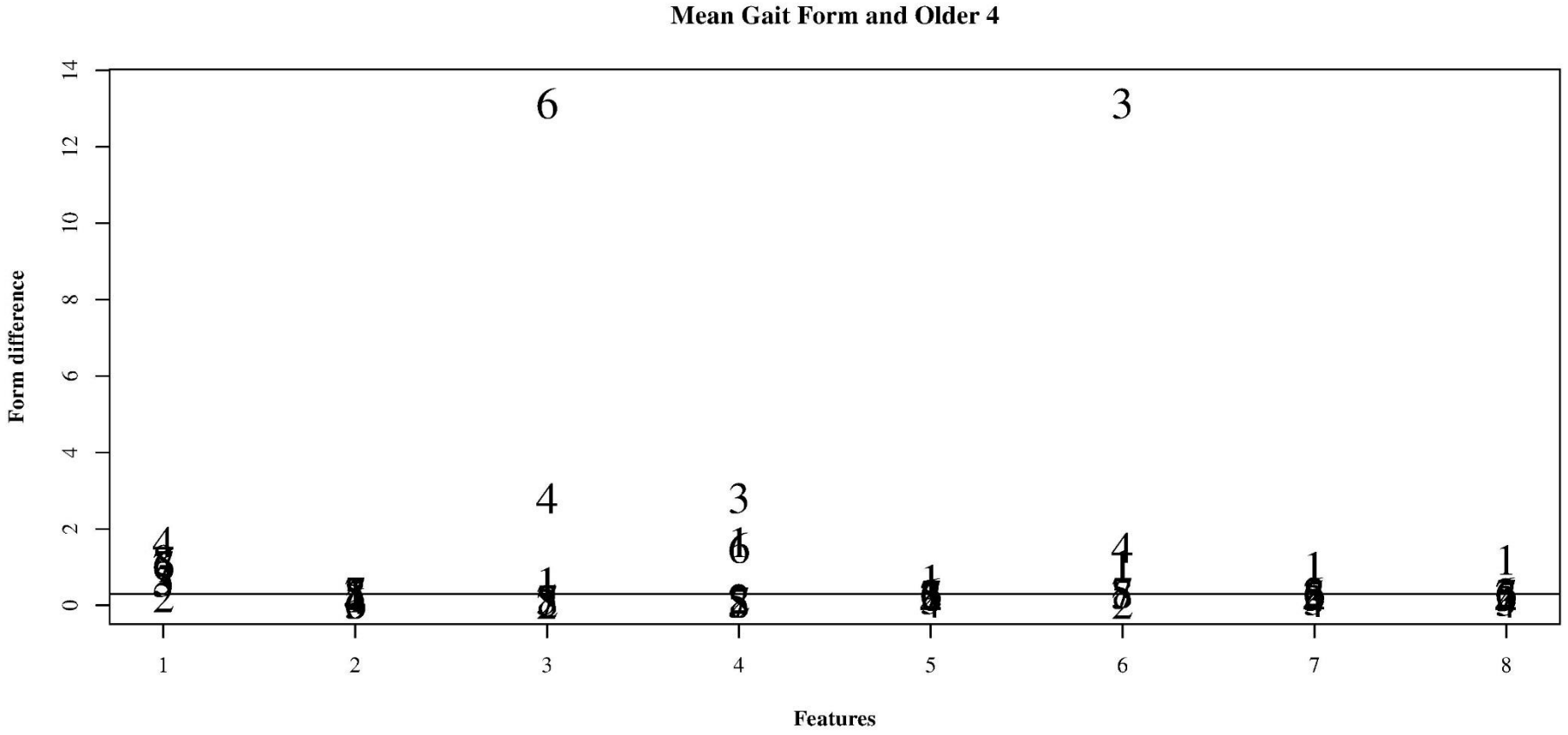
Mean Gait Form and Older 4
Form difference
0
2
4
6
8
10
12
14
1
2
3
4
5
6
7
8
Features

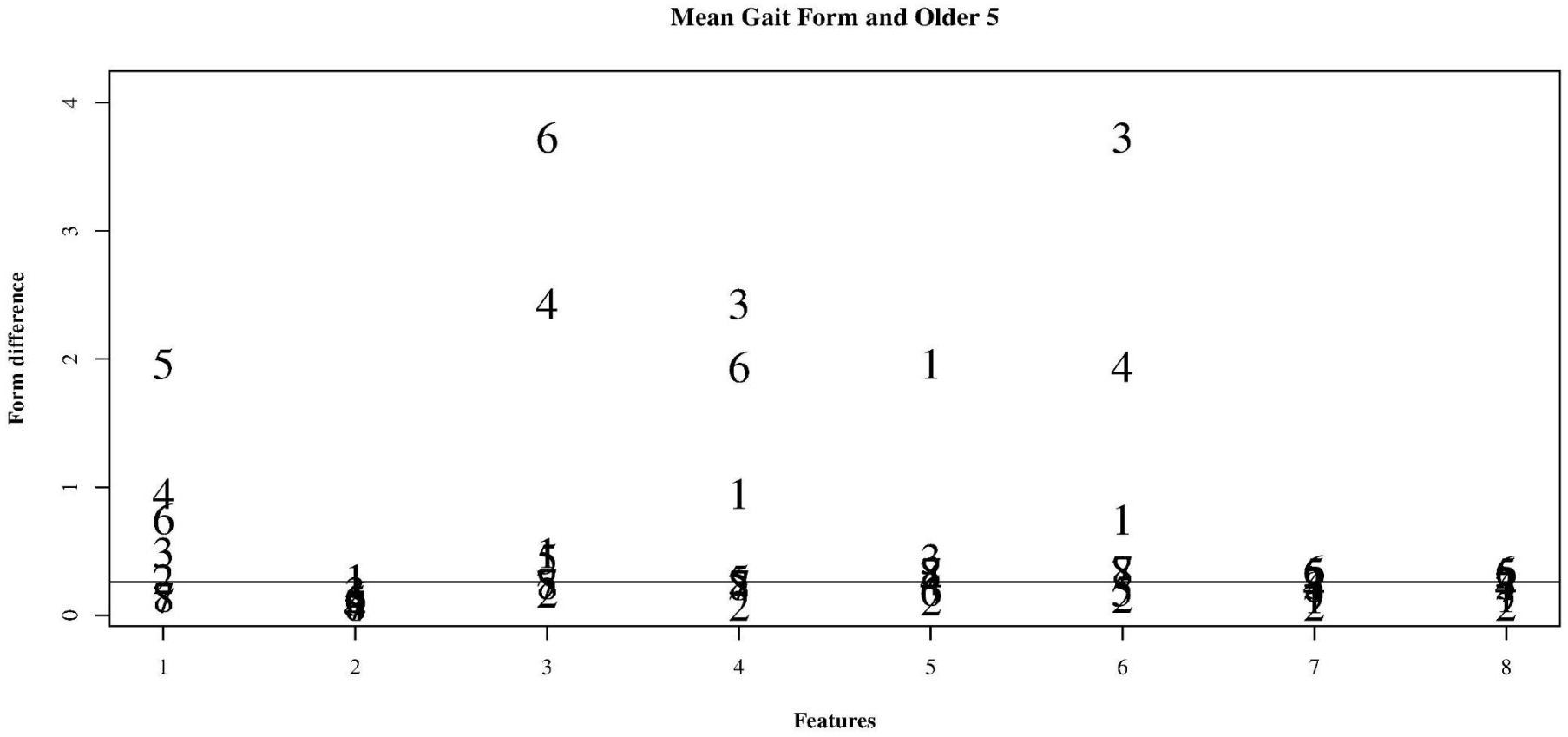
Mean Gait Form and Older 5
Form difference
0
1
2
3
4
1
2
3
4
5
6
7
8
Features

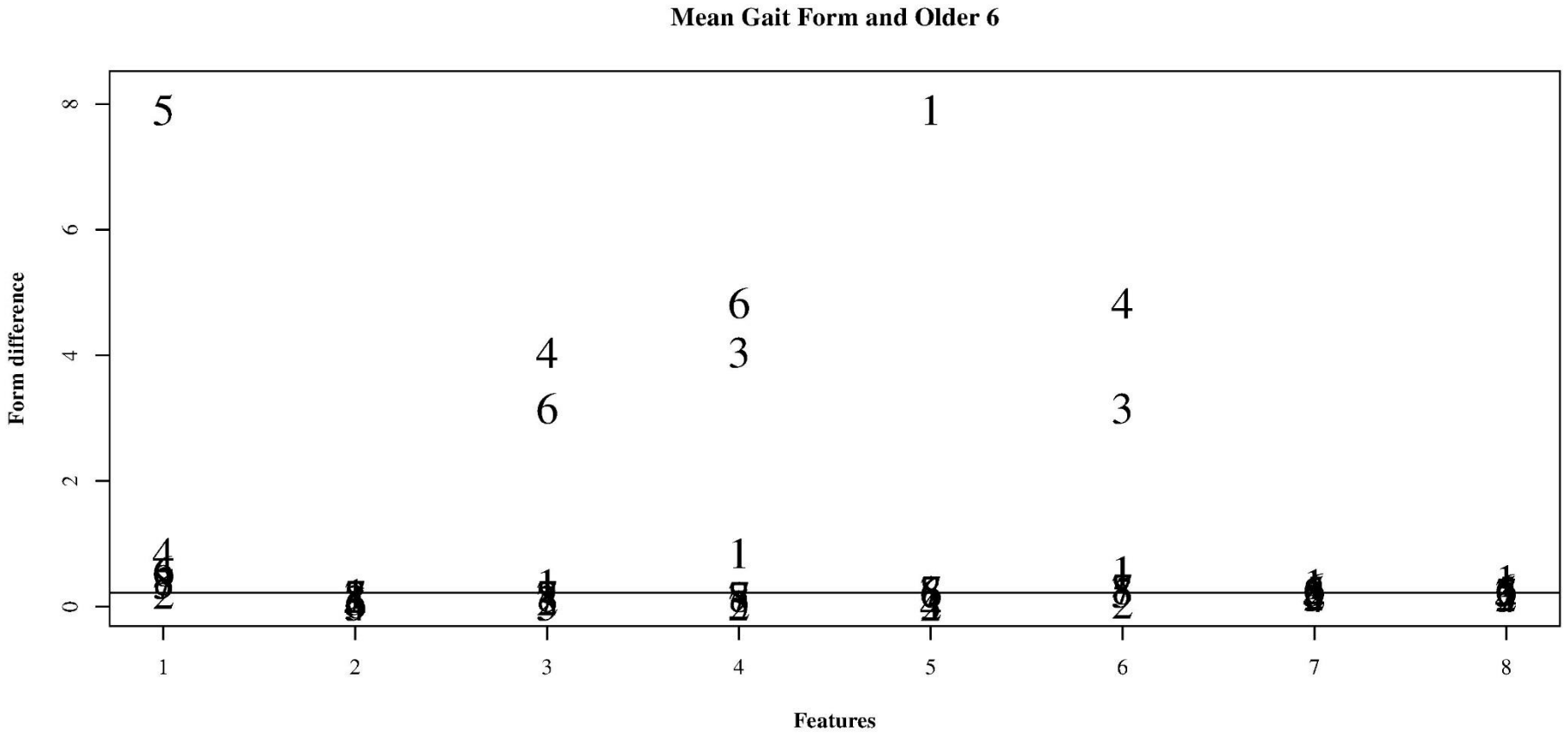
Mean Gait Form and Older 6
Form difference
0
2
4
6
8
1
2
3
4
5
6
7
8
Features

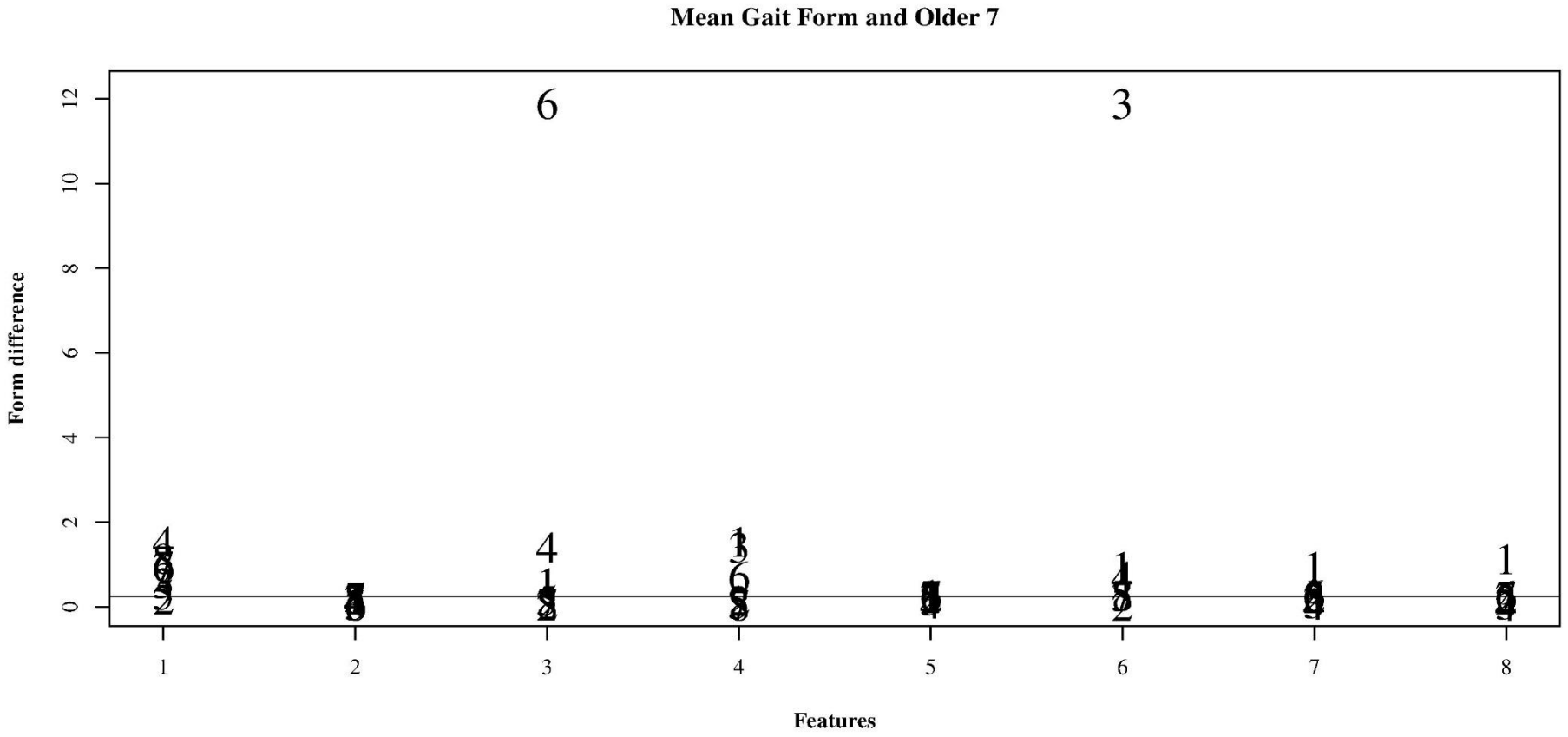
Mean Gait Form and Older 7
Form difference
0
2
4
6
8
10
12
1
2
3
4
5
6
7
8
Features

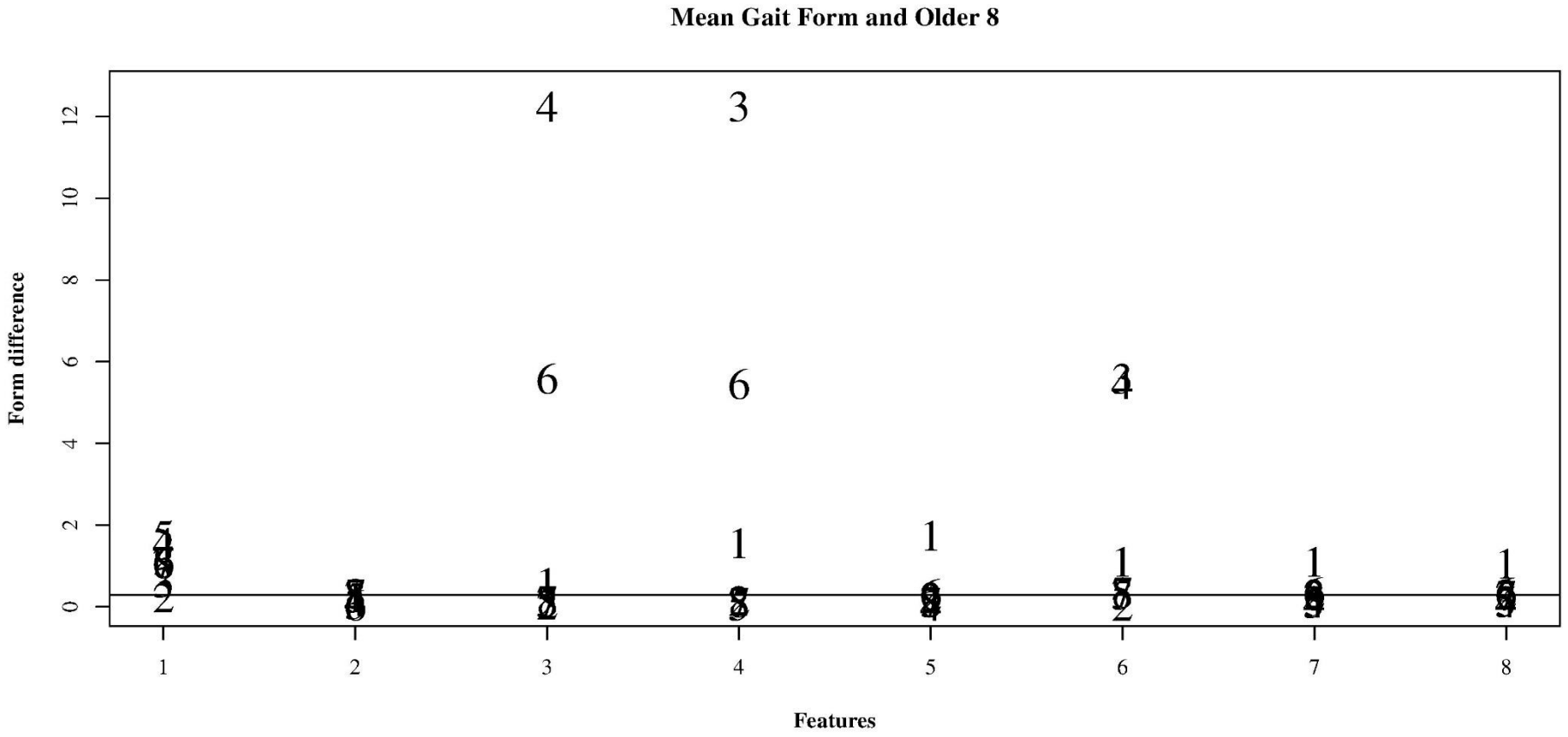
Mean Gait Form and Older 8
Form difference
0
2
4
6
8
10
12
1
2
3
4
5
6
7
8
Features

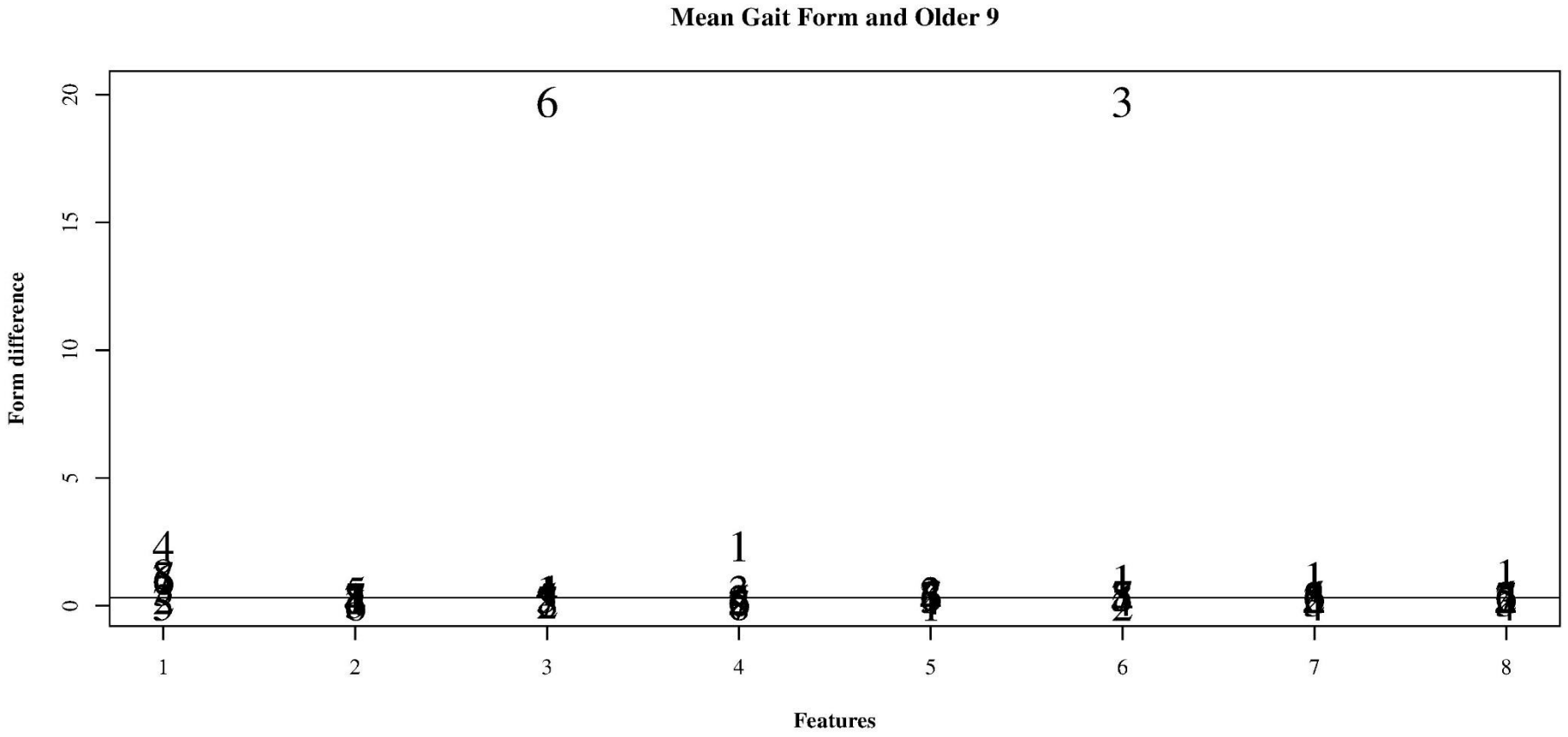
Mean Gait Form and Older 9
Form difference
0
5
10
15
20
1
2
3
4
5
6
7
8
Features

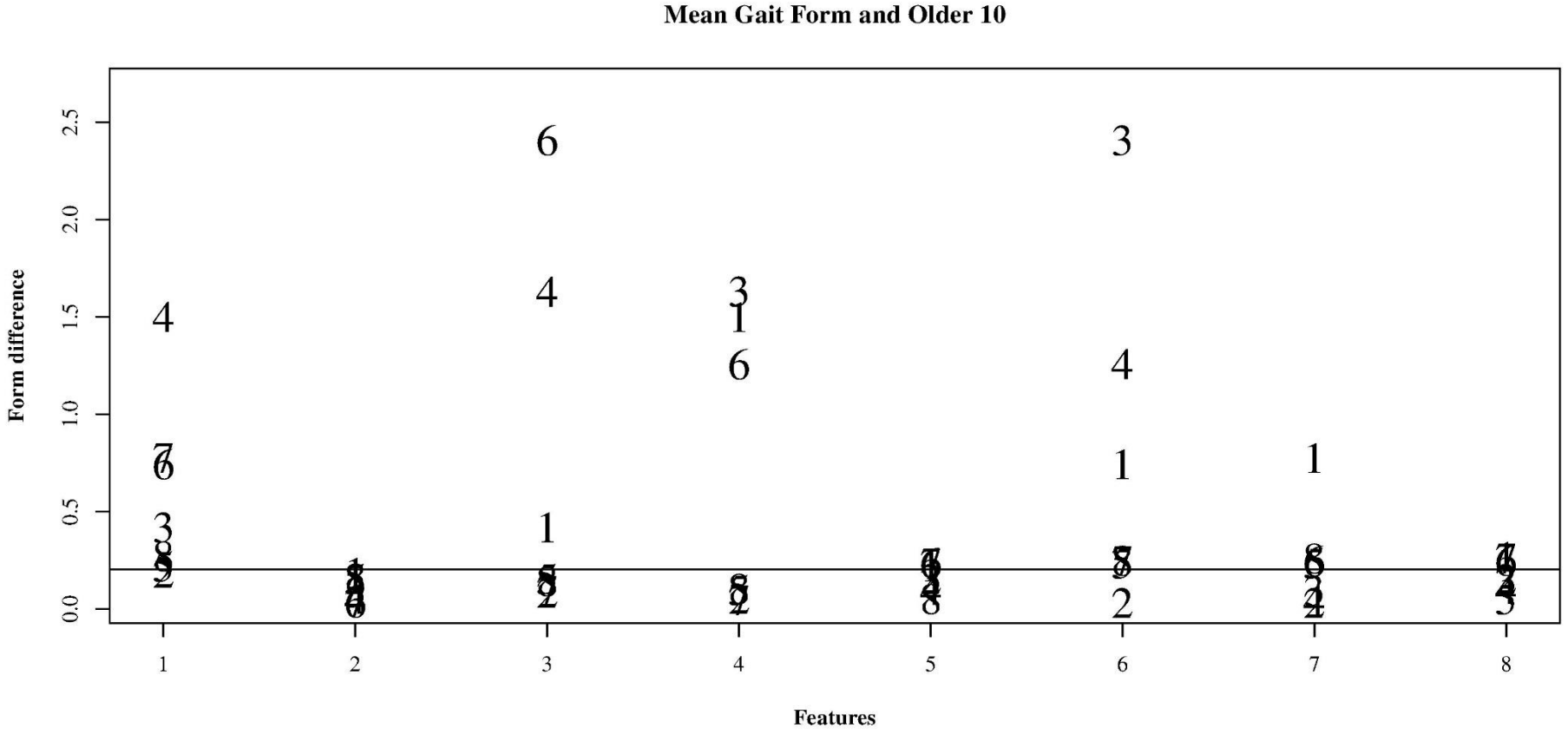
Mean Gait Form and Older 10
Form difference
0.0
0.5
1.0
1.5
2.0
2.5
1
2
3
4
5
6
7
8
Features

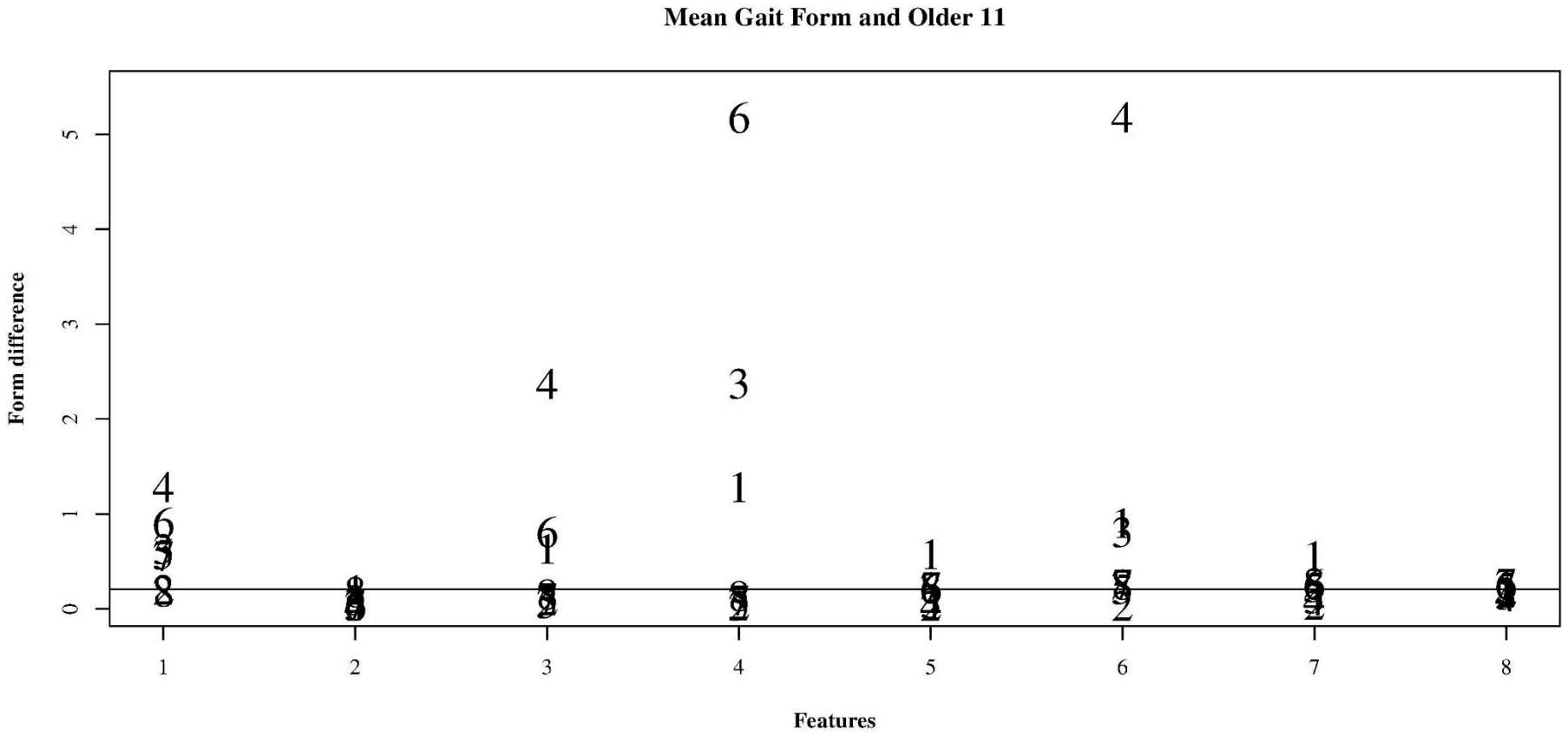
Mean Gait Form and Older 11
Form difference
0
1
2
3
4
5
1
2
3
4
5
6
7
8
Features

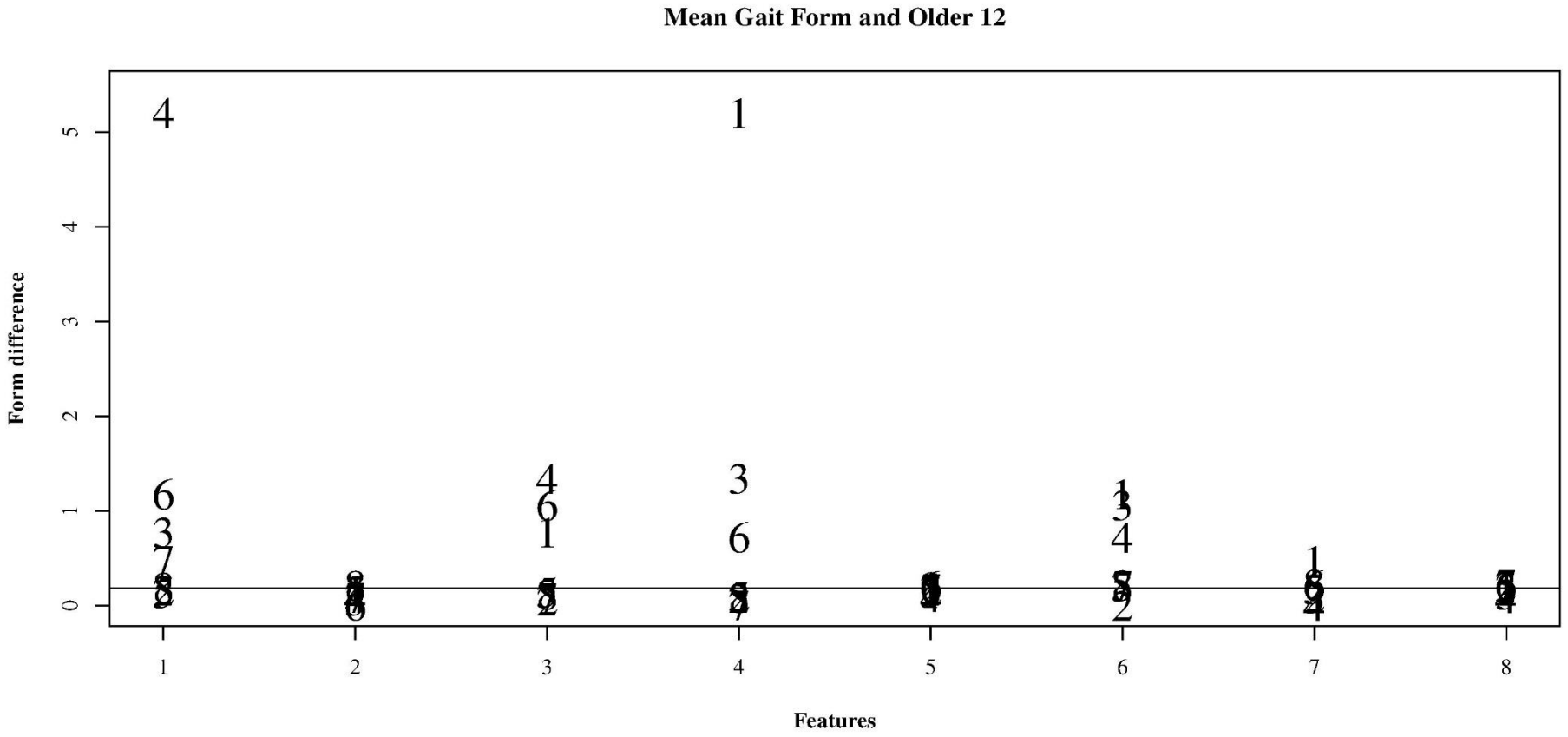
Mean Gait Form and Older 12
Form difference
0
1
2
3
4
5
1
2
3
4
5
6
7
8
Features

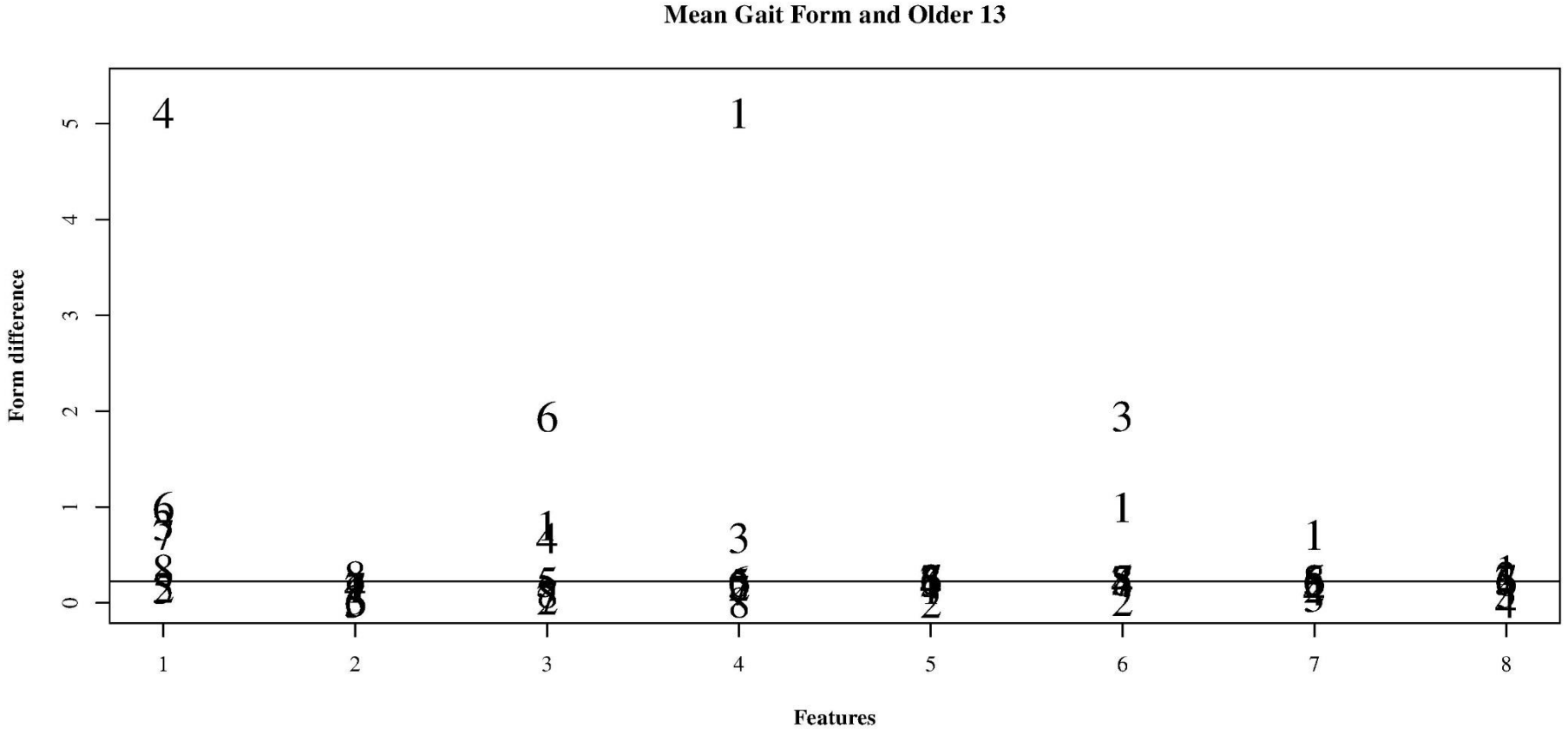
Mean Gait Form and Older 13
Form difference
0
1
2
3
4
5
1
2
3
4
5
6
7
8
Features

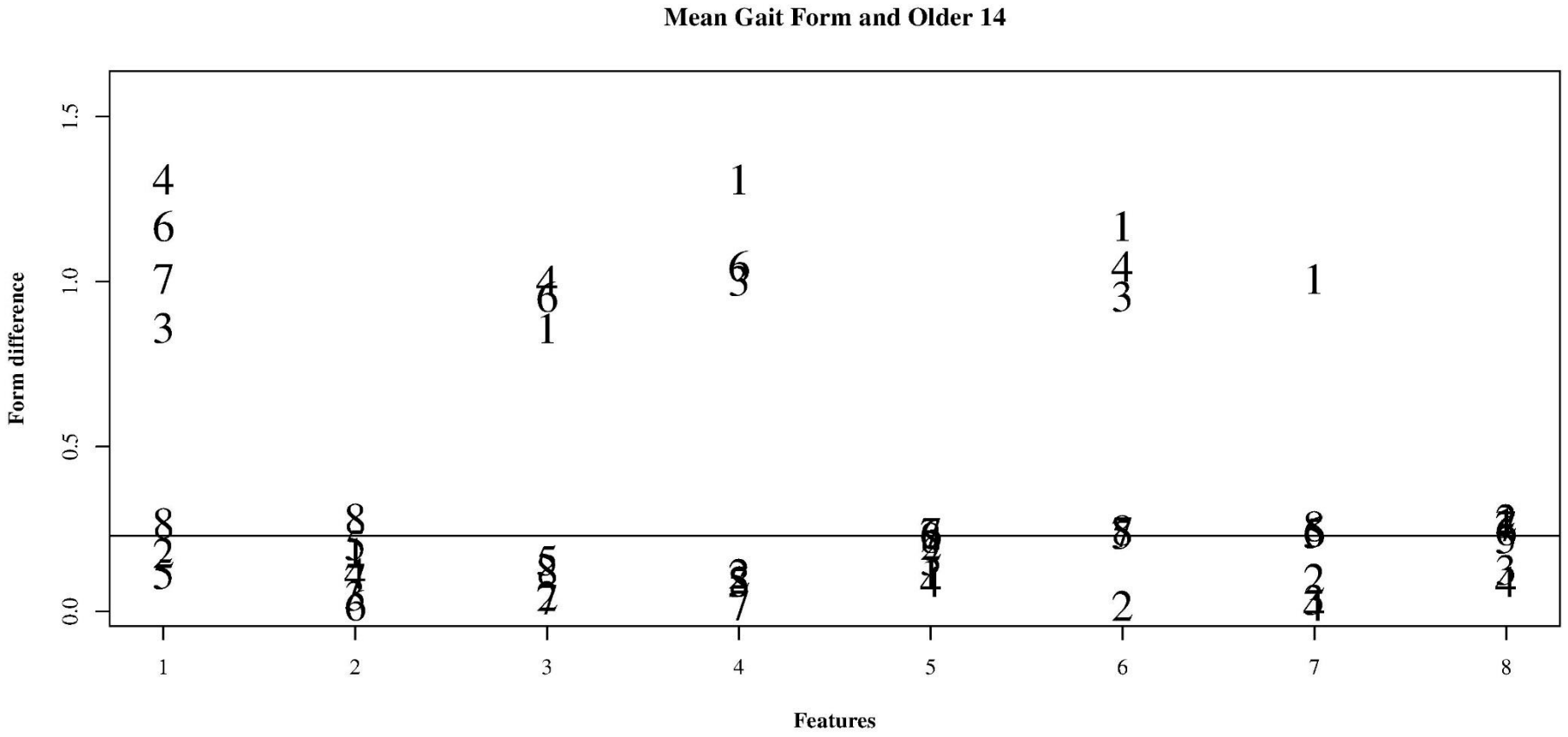
Mean Gait Form and Older 14
Form difference
0.0
0.5
1.0
1.5
1
2
3
4
5
6
7
8
Features

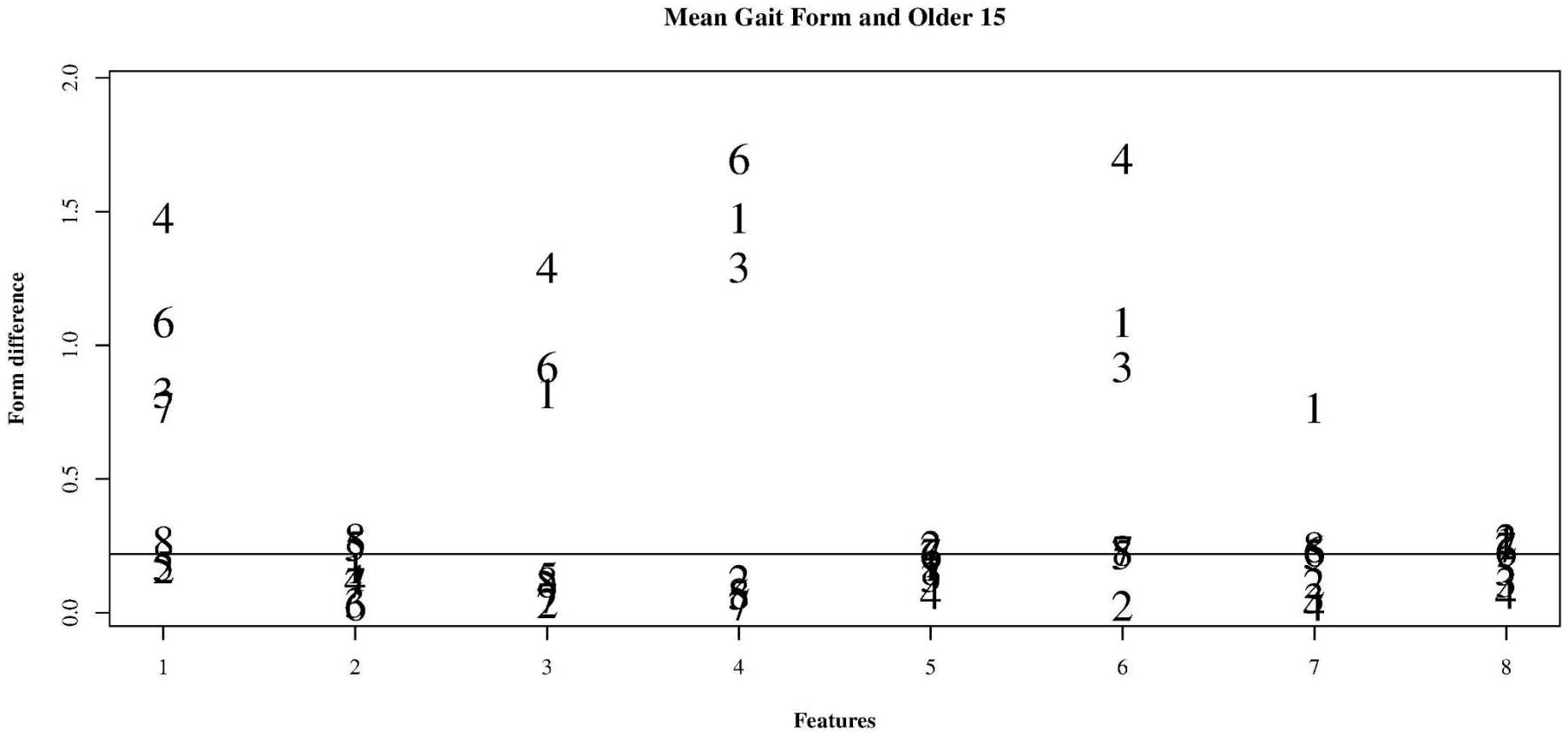
Mean Gait Form and Older 15
Form difference
0.0
0.5
1.0
1.5
2.0
1
2
3
4
5
6
7
8
Features

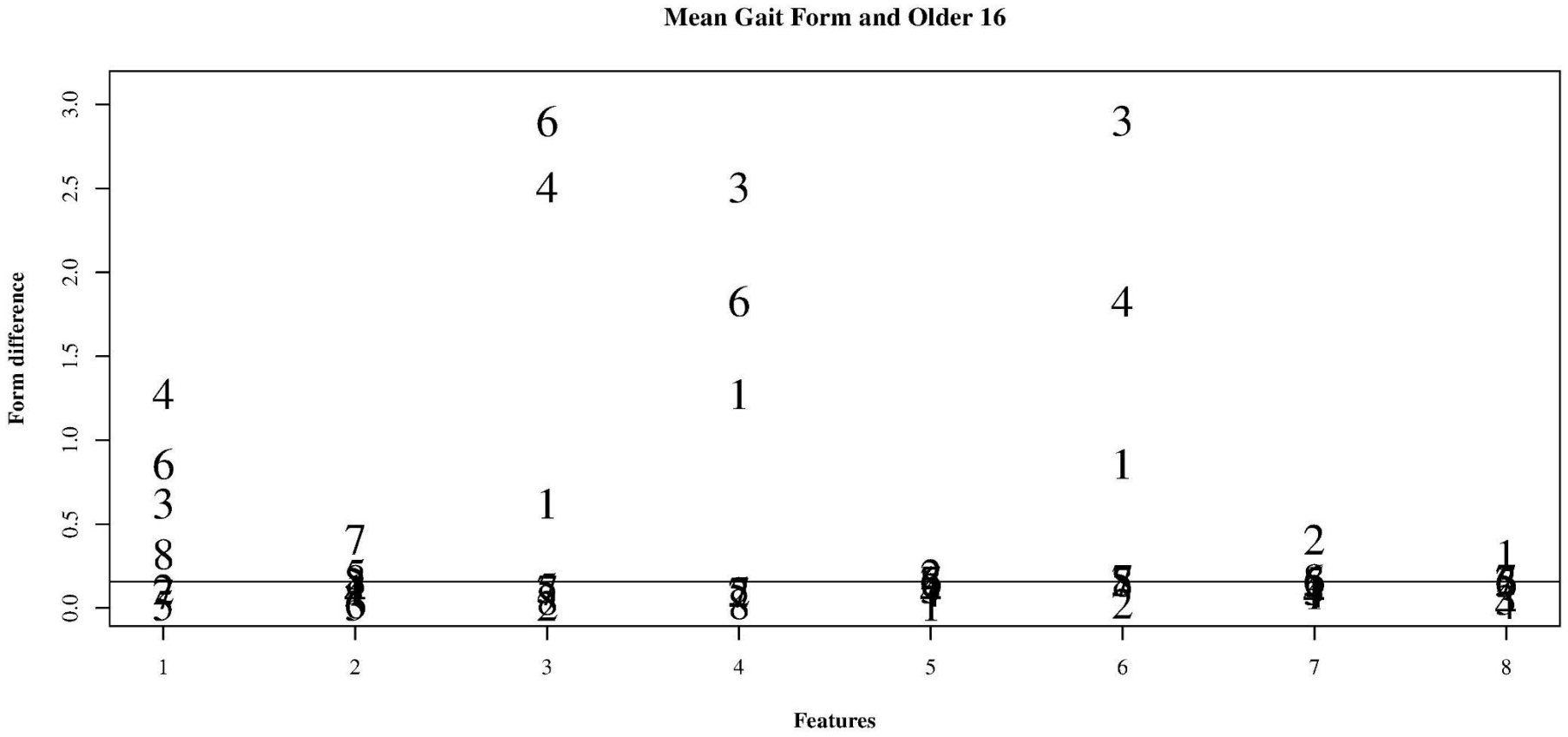
Mean Gait Form and Older 16
Form difference
0.0
0.5
1.0
1.5
2.0
2.5
3.0
1
2
3
4
5
6
7
8
Features

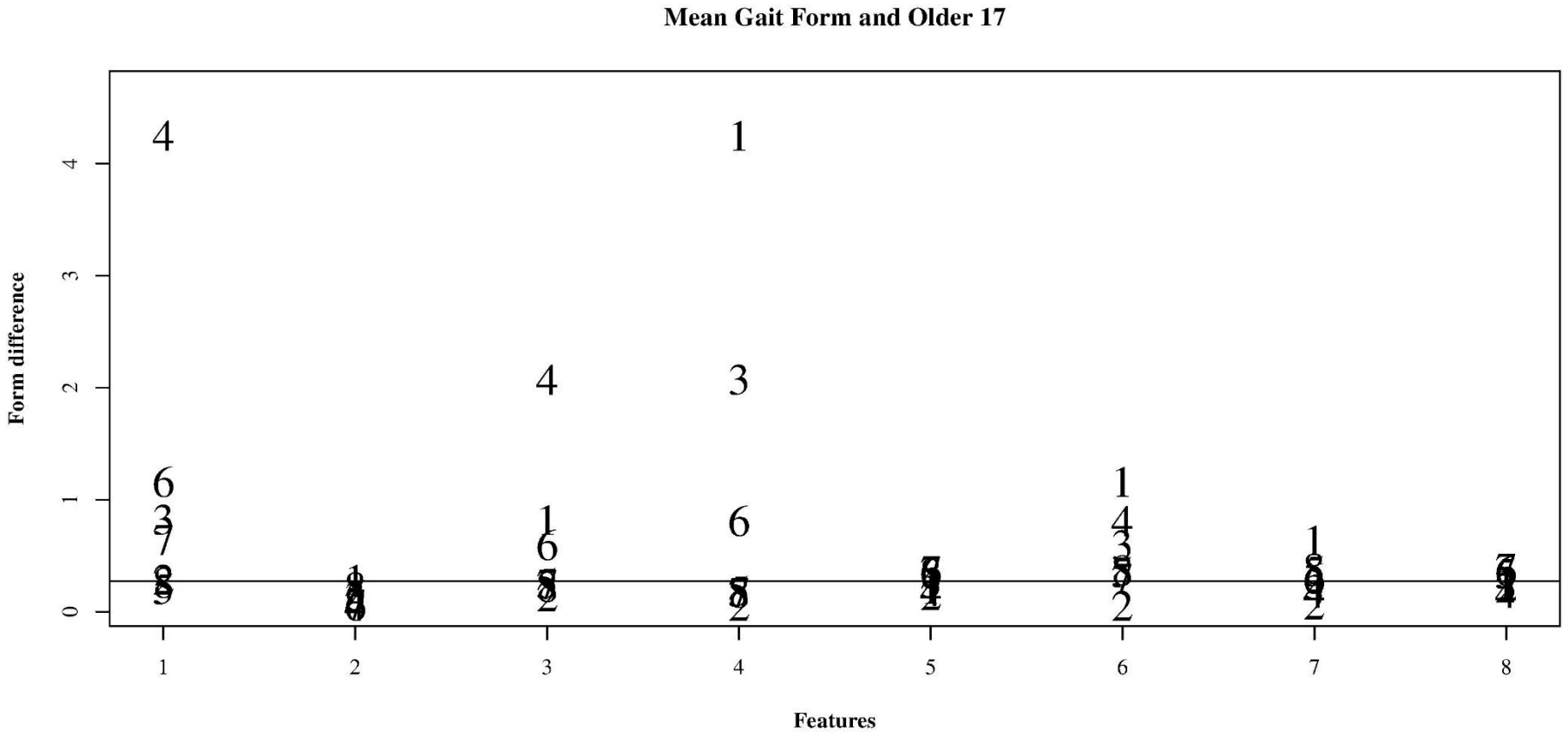
Mean Gait Form and Older 17
Form difference
0
1
2
3
4
1
2
3
4
5
6
7
8
Features

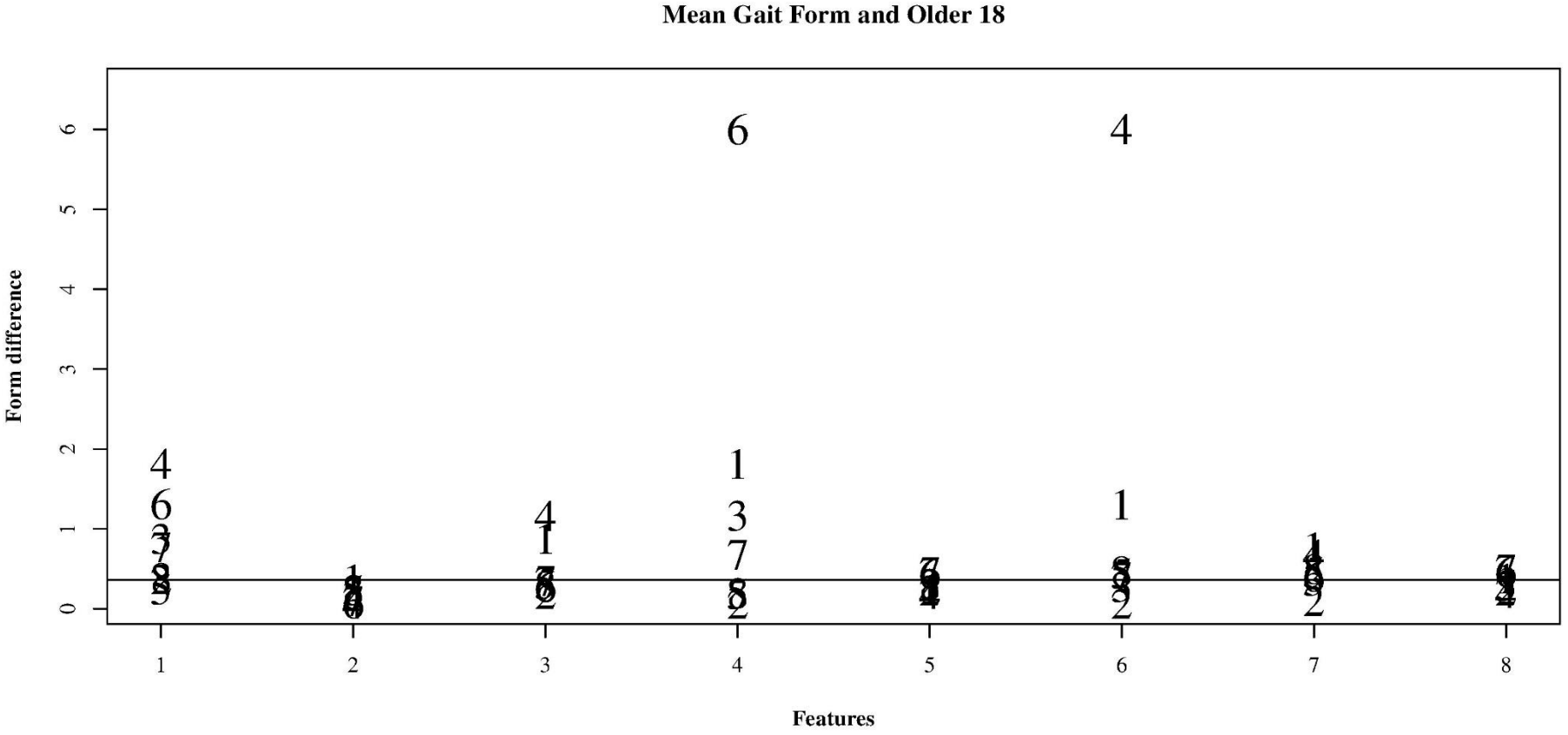
Mean Gait Form and Older 18
Form difference
0
1
2
3
4
5
6
Features
1
2
3
4
5
6
7
8

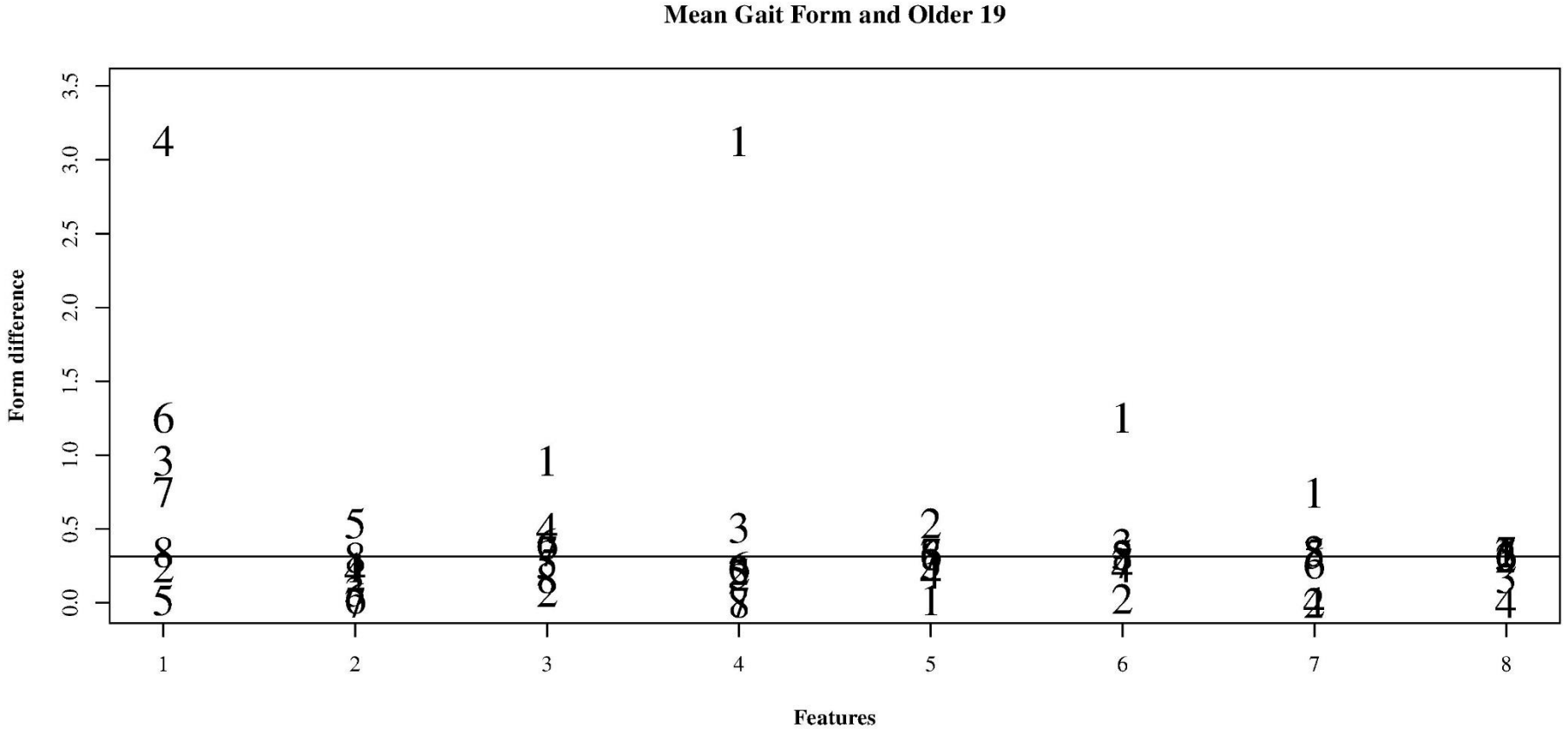
Mean Gait Form and Older 19
Form difference
0.0
0.5
1.0
1.5
2.0
2.5
3.0
3.5
1
2
3
4
5
6
7
8
Features

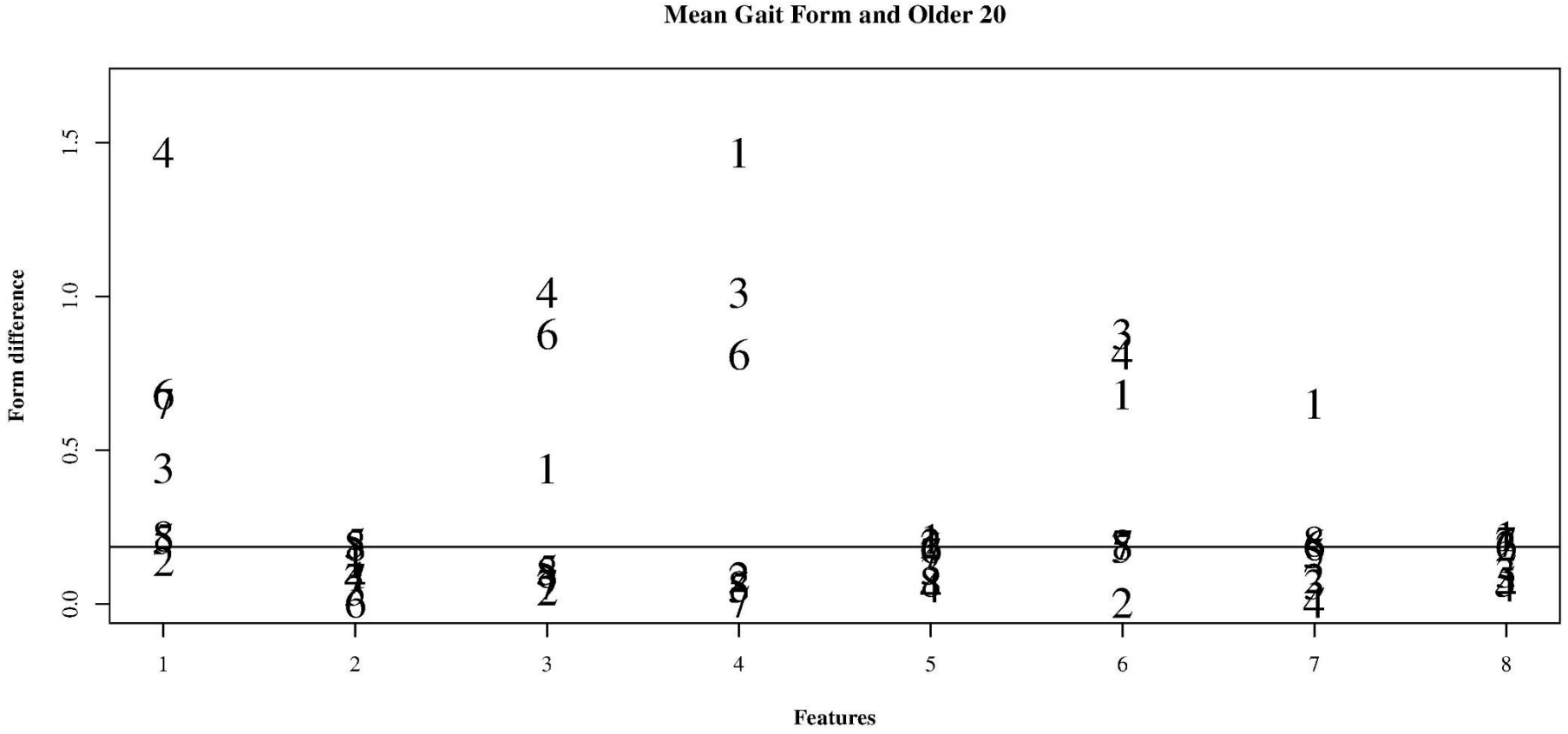
Mean Gait Form and Older 20
Form difference
0.0
0.5
1.0
1.5
1
2
3
4
5
6
7
8
Features